The Role of SNPs in the Management of Cancer in the Broader Population



Isaac Kitchen-Smith

Linacre College

University of Oxford

A thesis submitted for the degree of

Doctor of Philosophy in Clinical Medicine

Michaelmas 2020

Acknowledgements

I would like to express my gratitude to my supervisors, Professor Gareth Bond and Professor Sarah Blagden, who guided me throughout this project. I would like to thank the team members of both lab groups whose insights and advice were invaluable throughout my studies. In particular I would like to thank Dr Ping Zhang who I collaborated with closely on my projects and who was always available to provide knowledge and feedback. I would also like to thank my friends and family who supported me at all times.

Abstract

Heterogeneity is a pervasive concept in oncology and underpins many of the biggest challenges facing the field. Patients presenting with tumours which appear similar on the surface, can respond very differently to clinical management. Novel methods are urgently required to understand heterogeneity in cancer and to translate this information into the clinic. Studies of twins and familial cancer syndromes have indicated that a substantial proportion of cancers could be heritable but that rare, highly penetrant germline mutations cannot explain this phenomenon. The remaining 'missing heritability' is likely to be explained by common, less penetrant variants including Single Nucleotide Polymorphisms (SNPs). SNPs can associate with differential disease risk, with response to therapy and with the development and behaviour of tumours. Moreover, there is associative evidence that SNPs can inform drug response. However, a key blockade to the clinical translation of promising SNPs is the difficulty in elucidating the mechanistic function of susceptibility loci. In this thesis, we address this challenge by investigating the effect of p53 pathway SNPs on tumours and unpicking the molecular mechanisms underpinning these effects.

In Chapter Two, we experimentally model a SNP found in a p53 response element which associates with Testicular Germ Cell Tumours with one of the highest odds ratios identified for a cancer-risk SNP to date. This SNP leads us to uncover a novel, pro-tumour, negative feedback loop which is driven by the ability of wild-type p53 to upregulate KITLG expression. Moreover, we demonstrate that inhibition of this axis combined with p53 activation has a synergistic effect on cell death and could be a therapeutic opportunity for refractory TGCT. In Chapter Three, we employ high-throughput omics technologies and data mining to establish the molecular mechanisms underpinning the synergistic effect on cell death in TGCT cells while in Chapter Four, we leverage multi-omics datasets to identify possible repurposing opportunities for this combinatorial therapy. Our work in TGCT highlighted a novel therapeutic strategy to reactivate wild-type p53 by inhibiting oncogenic axis driven by p53 target genes. In Chapter Four we investigate whether other p53 target-genes could have pro-survival function in cancer types which infrequently mutate TP53. In Chapter Five, we highlight that the p53 pathway is enriched for genes which harbour pleitropic SNPs and focus on a partiuclar SNP in the TP53 polyadenylation signal. We provide evidence for its long-lasting effects on tumours and shed light on the molecular mechanisms which could underpin these effects.

The analyses presented in this thesis support previous publications indicating that common germline genetics could inform management of heterogeneity in cancer. We provide proof-of-principle that cancer-risk SNPs can uncover novel cancer biology which can in turn shape therapeutic design.

Contents

List of Figures **xi**

List of Tables **xv**

List of Abbreviations **xvii**

1 Introduction **1**

1.1 The 'War on Cancer' . . . 2
1.2 Heterogeneity amongst cancer patients . . . 3
1.3 Conventional Drug Discovery is Failing . . . 4
1.4 Germline Variants and the Management of Cancer . . . 6
1.5 Genome Wide Association Studies . . . 7
1.5.1 Population Stratification . . . 8
1.5.2 Pharmacogenomics . . . 10
1.5.3 Therapeutic Design . . . 10
1.6 Challenges in Harnessing susceptibly loci for the management of cancer 11
1.7 The P53 Pathway is enriched for cancer-susceptibility loci . . . 12
1.7.1 TP53 encodes the p53 transcription factor . . . 13
1.7.2 p53 activity is negatively regulated by MDM2 . . . 14
1.7.3 p53 integrates cellular stress signals . . . 14
1.7.4 The refined model of p53 activation . . . 16
1.7.5 p53 promotes cell cycle arrest, apoptosis and cellular senescence 16
1.7.6 The p53 network is highly complex . . . 16
1.7.7 The p53 network is widely inactivated in cancer . . . 17
1.7.8 Some cancer-susceptibility loci in the p53 pathway are mechanistically understood . . . 18
1.8 Aims . . . 18

2 The p53/KITLG/KIT axis promotes cell survival in TGCT and represents a therapeutic opportunity for a repurposed combination strategy **21**

2.1 Abstract . . . 22
2.2 Introduction . . . 23

2.2.1 Single nucleotide polymorphisms in P53 response elements can influence cancer risk . . . 23
2.2.2 KITLG is the ligand for the oncogenic c-KIT receptor which triggers pro-survival signalling . . . 24
2.2.3 C-KIT is a pro-survival receptor tyrosine kinase . . . 26
2.2.4 The KITLG-p53RE-SNP is associated with Testicular Germ Cell Tumours . . . 27
2.2.5 KITLG/c-KIT signalling is important for normal development of the testes . . . 29
2.2.6 Upregulation of KITLG expression could facilitate the early steps in TGCT development . . . 29
2.2.7 P53 upregulates KITLG in an allelic-specific manner . . . 31
2.3 Results . . . 33
2.3.1 C-KIT promotes survival, proliferation and migration in two TGCT cell-lines . . . 33
2.3.2 The p53/KITLG/KIT axis regulates cell survival, proliferation and migration and chemosensitivity in TGCT . . . 36
2.3.3 Pharmacological inhibition of the p53/KITLG/KIT axis and p53 activation have a synergistic effect on cell death . . . 47
2.3.4 The combination of Dasatinib and Doxorubicin represents a novel, repurposing therapy for refractory TGCT . . . 57
2.4 Discussion . . . 61
2.4.1 Summary . . . 61
2.4.2 Platinum-Resistant TGCT is an increasingly urgent and unmet clinical need . . . 61
2.4.3 Cancer-susceptibility loci may provide insights into chemoresistance . . . 62
2.4.4 The emerging pro-survival role of p53 . . . 63
2.4.5 Polymorphic p53 response elements and disease . . . 64
2.4.6 Estimating and predicting synergistic drug combinations . . . 66

3 Investigating the mechanism of the synergy between inhibition of p53-mediated KITLG/KIT signalling and p53 activation in TGCT 70
3.1 Abstract . . . 71
3.2 Introduction . . . 72
3.2.1 Proof-of-mechanism is important for improving the approval rate of novel therapies . . . 72
3.2.2 Downstream signalling from KITLG/KIT is complex and can vary between tissues . . . 72

3.2.3 P53 can mediate both extrinsic and intrinsic apoptosis pathways 76
3.2.4 Hypothetical integration points between KITLG/KIT and p53 signaling . . . 77
3.2.5 Multi-omics data for uncovering novel cancer biology . . . 78
3.3 Results . . . 80
3.3.1 The synergy between Dasatinib and Nutlin-3a is dependent on p53 . . . 80
3.3.2 Investigating the role of p53 activity in the synergy between KIT inhibition and p53 activation . . . 82
3.3.3 Investigating the mechanism of signal transduction from KITLG/KIT in TGCT . . . 98
3.3.4 Clinically relevant gene modules in TGCT are enriched for PI3K/AKT/mTOR genes . . . 106
3.3.5 PI3K/AKT/mTOR is a potential therapeutic target in TGCT 114
3.3.6 BCL2 family factors integrate signals from pro-survival KITLG/KIT and apoptotic p53 signalling . . . 120
3.4 Discussion . . . 129
3.4.1 KITLG/KIT does not regulate p53 expression levels or transcriptional activity . . . 130
3.4.2 Signalling from p53 and KITLG/KIT could integrate through control of mitochondrial apoptosis . . . 131
3.4.3 PI3K/AKT/mTOR signalling is key to pro-survival signalling from KITLG/KIT in TGCT . . . 134
3.4.4 AKT inhibitors as promising anti-cancer therapies . . . 136

4 Identifying novel, druggable inhibitors of the p53-apoptotic response in the p53 network 138
4.1 Abstract . . . 139
4.2 Introduction . . . 140
4.2.1 The activity of wild-type p53 in cancer is clinically relevant . 140
4.2.2 KITLG/c-KIT signalling is key in the development of multiple tissues . . . 140
4.2.3 Tissue specificity of TP53 target-genes . . . 141
4.3 Results . . . 144
4.3.1 The p53 pathway in human cancer . . . 144
4.3.2 KITLG/KIT alterations in human cancer . . . 151
4.3.3 P53 target-gene expression accurately predicts the tissue of origin of tumours . . . 169
4.3.4 Identifying p53 inhibitors using pharmacogenomics . . . 175

4.3.5 Exploring the role of pro-survival p53-target genes in human tumours . . . 179
4.4 Discussion . . . 186
4.4.1 Co-modulation of KITLG/KIT and p53 signalling could have therapeutic benefit in Skin Cutaneous Melanoma . . . 186
4.4.2 KITLG/KIT signalling could inhibit the p53-apoptotic response in TP53 wild-type Colon Adenocarcinoma . . . 189
4.4.3 CPE and PARD6G could represent cancer-type specific, druggable inhibitors of p53-mediated tumour-suppression . . . 191
4.4.4 The importance of context . . . 194

5 A highly pleiotropic cancer-risk SNP in the p53 pathway could have clinical impact for multiple cancer types 197
5.1 Abstract . . . 198
5.2 Introduction . . . 199
5.2.1 Pleiotropic factors underpin multiple distinct traits . . . 199
5.2.2 SNP-level Pleiotropy has biological and clinical implications 200
5.2.3 Pleiotropy is prevalent in cancer . . . 200
5.3 Results . . . 203
5.3.1 Cancer-associated SNPs are enriched for pleiotropy compared to SNPs associated with other diseases . . . 203
5.3.2 The p53 pathway is enriched for SNPs associated with multiple cancer-types . . . 206
5.3.3 The TP53-PAS-SNP can have long-lasting associations in tumours . . . 210
5.3.4 The TP53-PAS-SNP inhibits mutant p53 . . . 219
5.3.5 Insights into the mechanism of the TP53-PAS-SNP . . . 224
5.3.6 Modest reductions in p53 expression associate with reduced sensitivity to many anti-cancer compounds . . . 229
5.4 Discussion . . . 236
5.4.1 Summary . . . 236
5.4.2 The mechanism of the TP53-PAS-SNP . . . 236
5.4.3 Potential clinical impact of the TP53-PAS-SNP . . . 239
5.4.4 Implications of the interplay between germline and somatic genetics . . . 240

6 Discussion **243**
6.1 Summary . . . 243
6.2 Novel approaches to therapeutically target the p53 pathway in cancer 245
6.3 High-throughput identification of functional cancer-SNPs is required for clinical translation . . . 248
6.4 Practical and ethical challenges of the clinical translation of common germline variants . . . 251
6.5 Conclusion . . . 254

7 Materials and Methods **255**
7.1 P53 pathway gene set . . . 256
7.2 Omics analyses . . . 256
7.2.1 RNA-seq . . . 256
7.2.2 Proteomics . . . 258
7.2.3 Sample Preparation . . . 258
7.2.4 Pathway Enrichment Analysis . . . 258
7.3 Data Mining . . . 260
7.3.1 The Cancer Genome Atlas (TCGA) . . . 260
7.3.2 Weighted Gene Co-expression Network Analysis . . . 262
7.3.3 Genomics of Drug Sensitivity in Cancer (GDSC) . . . 263
7.3.4 Gene Expression Omnibus . . . 264
7.3.5 GWAS Datasets . . . 264
7.3.6 Druggable Genome . . . 265
7.3.7 STRING Protein-Protein Interactions . . . 265
7.4 Statistical Analyses . . . 266
7.4.1 Machine Learning . . . 266
7.5 Experimental Techniques . . . 267
7.5.1 CRISPR-Cas9 Genome Editing . . . 267
7.5.2 Cell culture and their treatments . . . 268
7.5.3 Drug screening . . . 268
7.5.4 IC50 and combination index CI analyses . . . 268
7.5.5 In vivo study . . . 269
7.5.6 SDS-PAGE and western blotting . . . 269
7.5.7 RNA isolation, cDNA synthesis and qRT-PCR . . . 270
7.5.8 MTT assay . . . 270
7.5.9 Cell proliferation and migration . . . 270
7.5.10 Phospho-kinase assay . . . 271

Appendices

A Supplementary Figures **273**
A.1 The p53/KITLG/KIT axis promotes cell survival in TGCT and represents a therapeutic opportunity for a repurposed combination strategy 274
A.2 Investigating the mechanism of the synergy between inhibition of the p53/KITLG/KIT axis and p53 activation in TGCT 276
A.3 Identifying novel, druggable negative-feedback loops in the p53 network 278
A.4 A highly pleiotropic cancer-risk SNP in the p53 pathway could have clinical impact for multiple cancer types 288
A.5 Materials and Methods 291

B Supplementary Methods **292**
B.1 RNA-sequencing 292
B.1.1 Overview of methodology 292
B.1.2 Additional details regarding differential gene analysis 293
B.2 WGCNA 294
B.2.1 Network Construction 294
B.2.2 Eigengene Calculation and Correlation with Traits 295
B.3 GISTIC scores 296
B.4 Random Forest ML 296

C Supplementary Tables **298**

References **379**

List of Figures

1.1 Mortality and Incidence Rates in the UK 3
1.2 Heterogeneity in Cancer 5
1.3 Germline Variants 8
1.4 Clinical Application of SNPs 9
1.5 Molecular Mechanisms of SNPs 13
1.6 P53 Structure and Mutations 15
1.7 The p53 Network 19

2.1 SNPs in p53RE's 25
2.2 KITLG and c-KIT 28
2.3 KITLG and TGCT 30
2.4 C-KIT promotes cell survival, proliferation and migration 34
2.5 Deletion of the KITLG-p53RE reduces KITLG expression 38
2.6 Deletion of the KITLG-p53RE reduces cell proliferation and migration and sensitizes to p53 activation 41
2.7 Knocking-in the KITLG-p53RE restores the p53/KITLG/KIT axis 44
2.8 High-throughput drug screen and Topoisomerase inhibitors 46
2.9 Dasatinib in TGCT cells 49
2.10 C-KIT inhibition synergises with p53 activation 54
2.11 C-KIT inhibition synergises with p53 activation in platinum-resistant TGCT 56
2.12 C-KIT inhibition and Doxorubicin synergises in refractory TGCT . 60
2.13 TGCT is an early onset cancer 62
2.14 A model for identifying contextual synergistic drug combinations . . 67

3.1 Downstream signalling from KITLG/KIT 73
3.2 Extrinsic and intrinsic apoptosis 77
3.3 Hypothetical Integration Points between p53-mediated KITLG/KIT and the p53-apoptotic response 80
3.4 Introduction to RNA-seq and Proteomics data 85
3.5 Inducible p53 target-genes 88
3.6 Genetic inhibition of p53/KITLG/KIT axis and p53 target-genes . 90

3.7 Pharmacological inhibition of KITLG/KIT and p53 target-genes . . 91
3.8 SFN and p53 S392 are regulated by KITLG/KIT 96
3.9 Genetic inhibition reduces expression of PI3K/AKT/mTOR components 101
3.10 Effect of genetic inhibition of KITLG/KIT on PTMs 103
3.11 Pharmacological inhibition of KITLG/KIT reduces expression of PI3K/AKT/mTOR components 106
3.12 Introduction to WGCNA 108
3.13 Blue and Green modules associate with higher disease stage and progression 110
3.14 Blue and Green modules are enriched for PI3K/AKT/mTOR factors and associate with faster progression 113
3.15 Inhibition of AKT synergises with p53 activation in a KITLG-p53RE dependent manner 118
3.16 High KITLG expression associates with reduced sensitivity to PI3K/AKT/mTOR inhibitors 119
3.17 Dasatinib and Nutlin-3a regulate different pro-apoptotic BCL2 factors 127
3.18 BCL2 pro/anti ratios regulate chemosensitivity and disease progression 130
3.19 Model of integration points between KITLG/KIT and the p53-apoptotic response 133

4.1 p53 autoregulatory loops 141
4.2 KITLG/KIT signalling in other tissues 143
4.3 TP53 mutation and deletion in human tumours 145
4.4 TP53 alterations reduce expresison of p53 target genes and increase GI 148
4.5 TP53 alterations associate with poorer prognosis 149
4.6 The KITLG-p53RE-SNP risk allele associates with faster progression in TGCT 153
4.7 KITLG/KIT alterations in human cancer 156
4.8 Oncogenic KIT mutations in melanoma 160
4.9 KITLG/KIT inhibition synergises with p53 activation in melanoma 163
4.10 Colon cancer is enriched for KITLG gain 167
4.11 The expression of p53 target-genes exhibits tissue-specificity 172
4.12 The direct p53 inhibitor, MDM2, is frequently over-expressed in cancer and associates with poor prognosis 174
4.13 Identifying pro-survival p53-target genes 179
4.14 Pro-survival p53-target genes in human tumours 183
4.15 CPE and PARD6G associate with poor prognosis in KIRC and DLBC respectively 185
4.16 KITLG/KIT signalling in melanoma 190

4.17 Future experiments to confirm the roles of p53 and KITLG/KIT signalling in TP53WT SKCM and COAD 192

5.1 Pleiotropy can be on gene and SNP levels 201
5.2 Cancer-associated SNPs exhibit pleiotropy 206
5.3 Identifying multi-cancer SNPs using the GWAS catalog 209
5.4 P53 pathway CAGs are enriched for multi-cancer SNPs 209
5.5 The TP53-PAS-SNP minor allele associates with reduced p53 expression and poorer outcome after tumour development 214
5.6 The impact of the TP53-PAS-SNP may be stronger in cancer-types which low TP53 mutation frequency 218
5.7 Haploid isogenic cell models of the TP53-PAS-SNP 220
5.8 The TP53-PAS-SNP minor allele affects the TP53Mutant transcriptome 224
5.9 The TP53-PAS-SNP minor allele could induce a an APA event . . . 232
5.10 Extension of the p53 3'UTR could enhance miRNA-mediated regulation 234
5.11 Modest reductions in p53 expression associate with reduced sensitivity to anti-cancer compounds 235
5.12 Model for the TP53-PAS-SNP on p53 expression 238
5.13 Methods of reactivating p53 240
5.14 Clinical value of germline-somatic interactions 242

6.1 A model for high-throughput identification and study of functional SNPs 252

7.1 Processing of transcriptomic data 257
7.2 Processing of PTM data 259
7.3 Classification of TCGA tumours by TP53 status 261
7.4 Pre-processing of TGCT transcriptomic data for WGCNA 263

A.1 Conservation of the KITLG p53RE 274
A.2 CRISPR-Cas9 for SusaCR and GH cells 274
A.3 CRISPR-Cas9 for 2102EP 275
A.4 GS vs MM scatterplots 276
A.5 Module Adjacency 276
A.6 Methods for identifying module hub genes 277
A.7 Multivariate Cox Regression for KIT mutation, KITLG and KIT expression in TP53WT SKCM 278
A.8 Multivariate Cox Regression for SKCM with clinical factors 279
A.9 Multivariate Cox Regression for primary SKCM with clinical factors 280
A.10 Multivariate Cox Regression for metastatic SKCM with clinical factors 281
A.11 KITLG-p53RE-SNP and KITLG expression in melanoma 281

A.12 Multivariate Cox Regression for KITLG, KIT and MDM2 expression in TP53-NF COAD 282
A.13 Multivariate Cox Regression for TP53WT-NOLOSS COAD with clinical factors 283
A.14 Highly expressed p53 target-genes vary between cancer-types 283
A.15 Random Forest *mtry* optimization 284
A.16 Random Forest error vs trees 284
A.17 Expression of 51 target genes against sensitivity to 26 compounds . 285
A.18 Identifying high confidence inhibitor genes 286
A.19 Validation of inhibitor genes in GDSC2 286
A.20 High CPE associates with faster progression in KIRC 287
A.21 High PARD6G expression associates with shorter OS in DLBC . . . 287
A.22 TP53-PAS-SNP eQTL associations in GTEx 289
A.23 Expression of miR-6788 and miR-6812 in cancer 290
A.24 Estimating variance in transcriptomics 291

List of Tables

2.1 Table of GWAS associations of three SNPs, highly linked with KITLG-p53RE-SNP, with TGCT risk. Reported odds ratios are per alele. 31

3.1 A table of p53 transcriptional cofactors derived from a literature search. 96
3.2 Summary of the 19 BCL2 family factors which were expressed in TERA1 cells. 124

4.1 Output from the tdAUC for SKCM. Two model were compared, the clinical only model and the full model featuring clinical factors plus KITLG expression, KIT expression and KIT mutation status. AUC generated every 12months 159
4.2 Output from the tdAUC for COAD. Two model were compared, the clinical only model and the full model featuring clinical factors plus KITLG expression. AUC generated every 3months. 168
4.3 Performance summary of the Random Forest model used to classify tumours into 14 classes based on the expression of 170 p53 target genes. 171

5.1 The eight SNPs from the GWAS catalog which map to p53 pathway genes and associate with multiple cancer types. 210

C.1 Table of p53 target genes validated by Fischer 2017. Each gene has been classified as pro-survival, anti-survival or Other based on the literature. 298
C.2 Table of p53 pathway genes including p53 targets from C.1 and pathway genes annotated by KEGG, PANTHER and BIOCARTA. 307
C.3 The compounds used as part of the Oncology drug screen comparing KITLG p53RE +/+ and -/- TERA1 and TERA2 cells. 317
C.4 The 227 p53 target genes found to be inducible by Nutlin-3a in TERA1 cells. 325
C.5 The overlapping significant genes between the Combo vs Nutlin-3a contrast and Combo vs Dasatinib (CSTs). 334

C.6 Hub genes for the Blue and Green Modules identified by WGCNA. 338
C.7 Results of linear regressions between KITLG expression and IC50s for inhibitors of the PI3K/AKT/mTOR and ERK/MAPK pathways for TP53 WT and Mutant cell lines in the GDSC datasets. 341
C.8 Risk allele frequencies for the KITLG-p53RE-SNP for each TCGA study where data genotyping data was available. Cases are also split into TP53 WT and TP53 Mutant. 352
C.9 Associations of known COAD driver gene mutations with TP53 status in COAD samples from TCGA. 355
C.10 Results of linear regressions between expression of each p53 pathway gene and Nutlin-3a IC50 for TP53 WT and TP53 MUTLOSS cell lines in GDSC1. 357
C.11 The 26 compounds in GDSC1 for which TP53 wild-type cell lines are more sensitive compared to TP53 Mutants and for which high wild-type TP53 expression associates with high sensitivity. 359
C.12 Results of enrichment analysis to determine cancer types enriched for TP53WT NOLOSS status compared to NF status. 361
C.13 Summary of associations between the TP53-PAS-SNP and cancer in GWAS. 362
C.14 Details of the 17 putative TP53 PAS sites identified using PolyA_DB.v3.2. 366
C.15 Summary of miRNAs which were predicted to bind the extended p53 3'UTR and of those which have previously been linked to p53 regulation in a way which may be impaired or enhanced by the TP53-PAS-SNP. 367
C.16 Table of datasets generated within this thesis or used in this thesis. 371
C.17 Table of R packages used for data analysis in this thesis. 372
C.18 Table of oligos used in this thesis. 374
C.19 Table of cell lines used in this thesis. 376
C.20 Table of compounds used in this thesis. 377
C.21 Table of software used in this study. 378

List of Abbreviations

RTK . . . . . Receptor Tyrosine Kinase.

CML . . . . . Chronic Myeloid Leukemia.

GIST . . . . . Gastrointestinal Stromal Tumours.

GBM . . . . . Glioblastoma

CNS . . . . . Central Nervous System

TP53 . . . . . Tumour Protein 53

PTEN . . . . . Phosphatase and Tensin Homolog

KRAS . . . . . Kirsten Rat Sarcoma Viral Oncogene Homolog

BRCA1 . . . . Breast Cancer Type 1 Susceptibility Protein

BRCA2 . . . . Breast Cancer Type 2 Susceptibility Protein

SNP . . . . . Single Nucleotide Polymorphism

GWAS . . . . . Genome Wide Association Study

WGS . . . . . Whole Genome Sequencing

PRS . . . . . Polygenic Risk Scores

CLL . . . . . Chronic lymphocytic leukaemia

LD . . . . . Linkage Disequilibrium

miRNA . . . . micro Ribonucleic Acid

eQTL . . . . . Expression Quantitative Trait Loci

eSNP . . . . . Expression SNP. A SNP in an eQTL locus

mRNA . . . . Messenger Ribonucleic Acid

TAD . . . . . Transactivation Domain of p53

DBD . . . . . DNA Binding Domain of p53

OD . . . . . Oligomerisation/Tetramerization Domain of p53

PTM . . . . . Post-Translational Modification

p53-RE . . . . p53 Response Element

MDM2 . . . . Mouse Double Minute 2 homolog
KEGG . . . . . Kyoto Encyclopedia of Genes and Genomes
PANTHER . . Protein Analysis Through Evolutionary Relationships
LOF . . . . . Loss of Function Mutations
GOF . . . . . Gain of Function Mutations
DN . . . . . Dominant-Negative Mutations
KITLG . . . . KIT Ligand
3'UTR . . . . . 3' Untranslated Region
TGCT . . . . . Testicular Germ Cell Tumour
LFS . . . . . Li-Fraumeni Syndrome
PWM . . . . . Position Weight Matrix
RTK . . . . . Receptor Tyrosine Kinase
CRC . . . . . Colorectal Cancer
PGC . . . . . Primordial Germ Cell
CRISPR . . . Clustered Regularly Interspaced Short Palindromic Repeats
HDR . . . . . Homology-Directed Repair
siRNA . . . . . small interfering RNA
MTT . . . . . 3-(4,5-dimethylthiazol-2-yl)-2,5-diphenyltetrazolium bromide
IC50 . . . . . Half Maximal Inhibitory Concentration
sgRNA . . . . Guide RNA
PCR . . . . . Polymerase Chain Reaction
qRT-PCR . . . Quantitative Reverse Transcription Polymerase Chain Reaction
DMSO . . . . . Dimethyl sulfoxide
BEP . . . . . Bleomycin, Etoposide and Platinum
CPT . . . . . Camptothecin
CI . . . . . Combination Index
DRI . . . . . Dose Reduction Index
FA . . . . . Fraction Affected
MMR . . . . . Mismatch Repair
CAG . . . . . Cancer-Associated Gene
MuSyC . . . . Multi-dimensional Synergy of Combinations

MSP . . . . . Multiplicative Survival Principle

DEP . . . . . Dose Equivalence Principle

ORR . . . . . Objective Response Rate

SFK . . . . . SRC Family Kinases

MOMP . . . . Mitochondrial Outer Membrane Permeabilization

TCGA . . . . . The Cancer Genome Atlas

GDSC . . . . . Genomics of Drug Sensitivity

FDR . . . . . False Discovery Rate

DEG . . . . . Differentially Expressed Gene

RPKM . . . . Reads Per Kilobase of transcript, per Million mapped reads

EMT . . . . . Epithelial Mesenchymal Transition

CST . . . . . Combination Specific Transcript

WGCNA . . . Weighted Gene Co-expression Network Analysis

GS . . . . . Gene Significance score

MM . . . . . Module Membership score

PPI . . . . . Protein-Protein Interactions

LOH . . . . . Loss of Heterozygosity

TP53-NF . . . TP53 Non-Functional

GI . . . . . Genomic Instability

PFI . . . . . Progression Free Survival

OS . . . . . Overall Survival

SKCM . . . . . Skin Cutaneous Melanoma

COAD . . . . . Colon Adenocarcinoma

AUC . . . . . Area Under the Curve

tdAUC . . . . time dependent AUC

CMS . . . . . Consensus Molecular Subtype

MSI/S . . . . . Micro-satellite instability/stable

CNS . . . . . Central Nervous System

RF . . . . . Random Forest

CPE . . . . . Carboxypeptidase E

PARD6G . . . Par-6 Family Cell Polarity Regulator Gamma

KIRC . . . . . Kidney Renal Clear Cell Carcinoma

DLBC . . . . . Diffuse large B-cell lymphoma

PheWAS . . . Phenome Wide Association Studies

PDP-SNP . . Pan-Domain Pleiotropic SNP

Intra-DP-SNP Intra-Domain Pleiotropic SNP

Inter-DP-SNP Inter-Domain Pleiotropic SNP

CAG . . . . . Cancer-Associated Gene

PAS . . . . . Polyadenylation Signal

MAF . . . . . Minor Allele Frequency

H.MAF L.MUT High MAF and Low TP53 Mutation Frequency

L.MAF H.MUT Low MAF and High TP53 Mutation Frequency

CPSF . . . . . Cleavage and Polyadenylation Specificity Factor

APA . . . . . Alternative Polyadenylation

RED . . . . . Relative Expression Difference

PCAWG . . . Pan-Cancer Analysis of Whole Genomes

SILCAC . . . . Stable Isotope Labeling with Amino acids in Cell culture

FPKM . . . . Fragments Per Kilobase of transcript per Million mapped reads

1 Introduction

Contents

1.1 The 'War on Cancer' 2
1.2 Heterogeneity amongst cancer patients 3
1.3 Conventional Drug Discovery is Failing 4
1.4 Germline Variants and the Management of Cancer . . 6
1.5 Genome Wide Association Studies 7
1.5.1 Population Stratification 8
1.5.2 Pharmacogenomics 10
1.5.3 Therapeutic Design 10
1.6 Challenges in Harnessing susceptibly loci for the management of cancer 11
1.7 The P53 Pathway is enriched for cancer-susceptibility loci 12
1.7.1 TP53 encodes the p53 transcription factor 13
1.7.2 p53 activity is negatively regulated by MDM2 14
1.7.3 p53 integrates cellular stress signals 14
1.7.4 The refined model of p53 activation 16
1.7.5 p53 promotes cell cycle arrest, apoptosis and cellular senescence 16
1.7.6 The p53 network is highly complex 16
1.7.7 The p53 network is widely inactivated in cancer 17
1.7.8 Some cancer-susceptibility loci in the p53 pathway are mechanistically understood 18
1.8 Aims 18

1.1 The 'War on Cancer'

'Cancer' is an umbrella term for a very large constellation of distinct diseases which can affect any tissue in the body and are characterised by rapid proliferation of abnormal cells. Cells become cancerous when genetic, molecular and biochemical changes free the cell from mechanisms which restrict proliferation. Cancer accounts for the second largest number of deaths worldwide and in 2018 alone, it was the leading cause for almost 10 million deaths (World Health Organisation, WHO). It was the global and widespread nature of the disease which led US president Richard Nixon to announce the 'War on Cancer' in 1971, a simplistic and divisive metaphor but one which did convey the weight of this monumental challenge [1] [2]. Ultimately, is not a 'war' subject to the binary clarity of victory and defeat but one measured in terms of incidence rates, mortality rates and the burden on the lives of patients.

Recent studies regarding cancer mortality have indicated favourable, declining trends in both Europe and the United States of America (USA, Figure 1.1) [3] [4]. Mortality rates have dropped by 27% between 1991 and 2016 in the USA while Carioli et al estimate that over 5million cancer related deaths have been avoided in Europe during a similar period. This reduction can be attributed to advances in screening, early detection and the development of targeted therapies and improved personalised cancer treatment [5] [6] [7] [8] [9] [10][11] [12] [13] [14] [15] [16]. However, the incidence of cancer is increasing (age-standardised rate, 12% in the UK between 1993 and 2017, Cancer Research UK), in part attributable to an aging population, to a lag between exposure to carcinogens and cancer onset and to improved diagnostic practice (Figure 1.1) [17][18] [8] [19]. The rising incidence of cancer is a global health problem that must be managed. Moreover, despite advances in cancer therapy, such as the replacement of radical surgeries with systemic therapies, many patient groups urgently require safer and higher efficacy therapies [20] [21] [22] [23] [24].

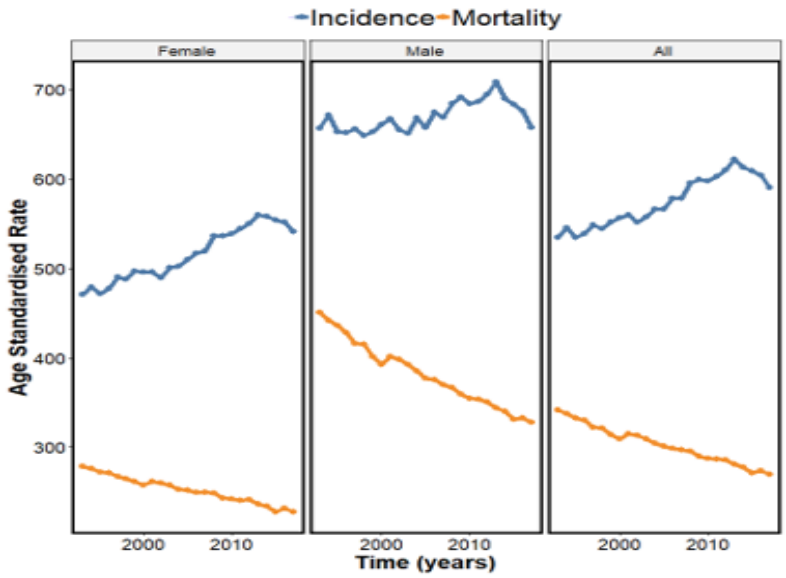


Figure 1.1: Cancer mortality and cancer incidence are showing opposite trends. Cancer mortality (orange) has been showing negative trends since the 1990s for both males and females but cancer incidence has been increasing during the same period. The rate of incidence has been higher among males throughout this period but the rate of increase has been higher in females. Data from Cancer Research UK.

1.2 Heterogeneity amongst cancer patients

Until the 1980s, the mainstay of cancer treatment was cytotoxic chemotherapy. This caused high toxicity burden: acute toxicities include bone marrow and gastro-intestinal tract damage, intermediate toxicities included neurological damage and alopecia and late toxicities (occurring many years after treatment) included infertility, cardiovascular complications and increased risk of other cancers [21] [25]. This was a particular problem for juvenile cancers including haematological malignancies, testicular cancer and CNS cancers [26]. Molecular targeted therapies differ from general cytotoxic chemotherapy in that they are designed to target specific molecules in order to inhibit the biological aberrations which drive the survival of cancer cells. The targeted molecules may harbor driver mutations or be involved in cell-fate decisions; for example, Ribociclib is an approved treatment for metastatic breast cancer which targets cyclin-dependent kinases [27]. Tamoxifen, targeting the oestrogen receptor in breast cancer patients, was the first example of a targeted therapy and is renowned for its excellent risk-benefit ratio [28] [29]. The astounding response rates achieved by Gleevic, targeting the BCR-ABL fusion protein in Chronic Myeloid Leukaemia (CML), furthered the case that targeted

therapies could supersede chemotherapy and provide effective target inhibition without the associated toxicities [12] [30] [27] [31]. However, these were met with their own challenges, particularly those of tumour heterogeneity (Figure 1.2). Inter-tumoral heterogeneity describes dissimilarities between cancers arising from different organs and tissues. Cells in different tissues behave differently, express different proteins and respond very differently to targeted therapies (Figure 1.2, Left panel). This means that regardless of the fact that tumours are underpinned by uncontrolled proliferation, most cancer-types are driven by different combinations of molecular signals and need to be targeted in different ways. Moreover, intra-tumoral heterogeneity is also pervasive within cancer types [32](Figure 1.2, Centre panel). First, molecular targeted therapies are less effective in tumors where the targeted molecule is not mutated or has low expression [12] [33] [34] [35]. Second, intra-tumoral heterogeneity relates to clonal molecular differences within a patients tumour and can underpin the inability to achieve a complete response to targeted therapies and/or the emergence of recurrent disease [32](Figure 1.2, Right panel). For example, while dominant clones harboring a driver kinase mutation could be successfully targeted by a specific RTK inhibitor, other clones which do not rely on the targeted kinase could persist and re-populate the tumour. In order to manage cancer in both small sub-populations and the broader population, we must address the issues of heterogeneity. One approach to this problem is N-of-one therapies whereby therapies are matched to the omics profile of individual patients [36]. Although small-scale studies have reported promising results, accurate and precise automation would be required for large-scale implementation [37][38].

1.3 Conventional Drug Discovery is Failing

Given the rising incidence of cancer and heterogeneous responses to therapy, new frameworks are required to better manage it in the broader population. The 'one mutation, one drug' paradigm, whereby a patient's cancer drivers direct oncologists to the most effective treatment regime, is currently unsuited to this task due to the huge pressures this would place on an already struggling drug discovery pipeline[39].

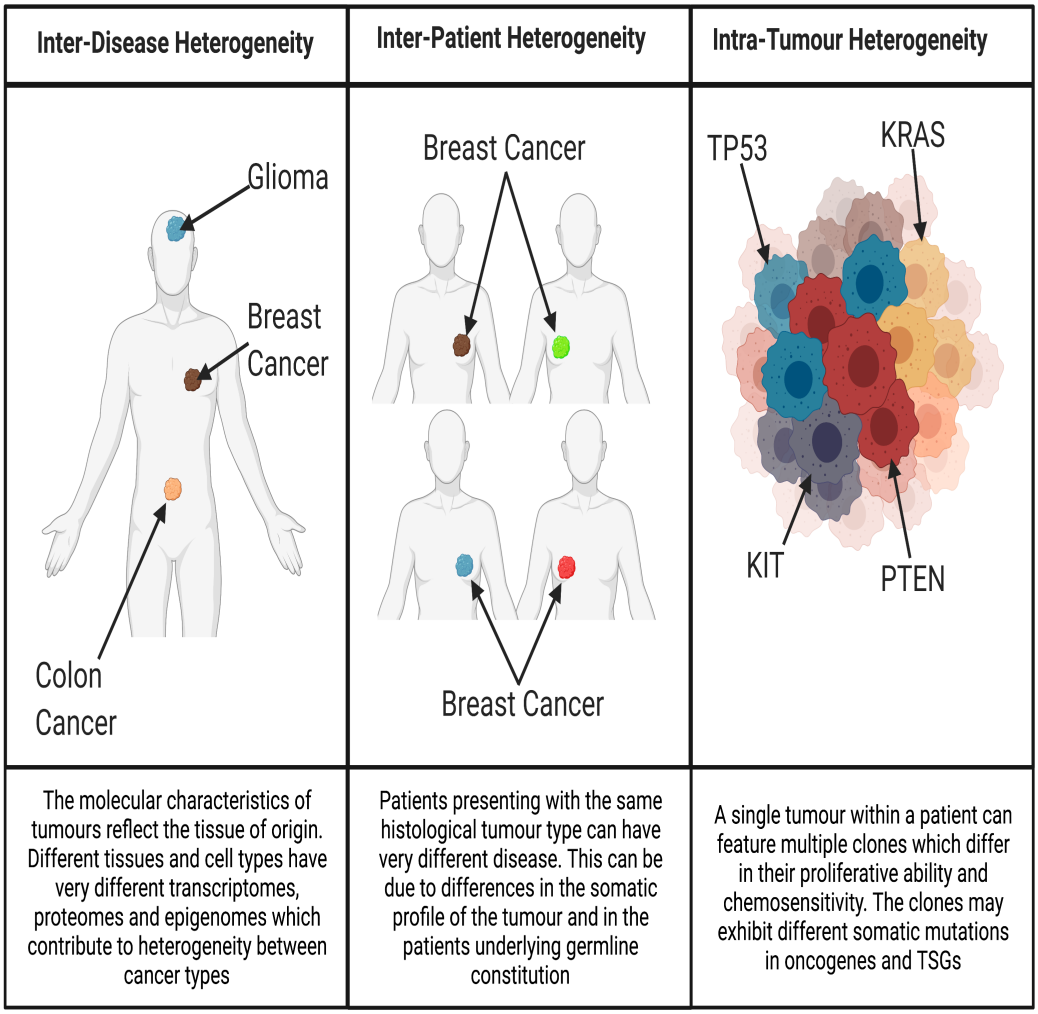


Figure 1.2: Heterogeneity in cancer is pervasive at multiple levels. (Inter-Disease Heterogeneity, left panel) Tumours derived from different tissues have very different molecular characteristics. These tumours behave and develop differently and are highly variable in terms of chemosensitivity. (Inter-Patient Heterogeneity, centre panel) Patients diagnosed with same histological malignancy can vary in the severity of their disease and their response to therapy. This can be due to different somatic mutations arising in their individual tumours and differences in their germline constitution. This variation between patients means different therapies may be most efficacious in different patients. (Intra-Tumour Heterogeneity, right panel) Within a cancer patient, heterogeneity can be present at two levels. Metastatic and primary lesions can behave differently (not shown) while variability between cancer cells within the same tumour mass can have important effects on outcome. Different clones of cancer cells may carry different potential driver mutations have different proliferative ability or 'fitness' in the tumour context. Treatment can change this context, killing the most populous clones but leaving infrequent resistant clones which then repopulate the tumour. This is the likely basis of partial responses and relapse.

High attrition rates mean that the cost of developing new drugs is unsustainable, estimated to be between 3.7 and 11.8 billion US$ per newly approved compound [40]. Indeed, the research and development efficiency of global pharmaceutical efforts has been declining steadily since the 1950s, so called Eroom's Law [41]. Many compounds fail due to lack of efficacy. This could be due to poor activity against the intended target, off target effects or lack of a biological basis linking the target to a trait. To address this, a strong proof of mechanism for any potential new treatment is required [42].

1.4 Germline Variants and the Management of Cancer

The identification and characterisation of key somatic driver mutations has improved personalised medicine. However, as previously discussed, cancer heterogeneity on multiple levels is limiting global progress in our 'War on Cancer' and conventional drug discovery pipelines are currently ill-equipped to tackle these issues and other approaches are sought. There is evidence to suggest that germline variants can inform the management of disease in the broader population [43][44][45]. The germline is defined as the hereditary genome. The germline is of particular importance in cancer where up to 33% of all cancer cases could have a heritable component [46] [47] [48]. The heritability of cancer refers to the proportion of variability in the risk of cancer in the population which can be explained by genetic factors; it is commonly estimated using quantitative genetic modeling of twin data. For cancer types with relatively high heritability, twins whose co-twin has been diagnosed with cancer have a higher cumulative risk and this effect is greater for mono-zygotic twins compared to di-zygotic twins [46] [47]. Germline variants can be distributed in terms of penetrance, the chance an individual will actually develop a disease given a particular genetic risk factor, and frequency, the proportion of people in a given population who carry a specific risk factor (Figure 1.3). In cancer cells, germline variants can mimic common somatic driver mutations. These variants are highly penetrant but are subject to strong negative selection due to the severity of their effects. For instance,

38% of mutations underpinning developmental disorders are in known cancer driver genes [49]. These rare variants are known as germline pathogenic variants [44]. For example, BRCA1 and BRCA2 mutations are associated with up to 60% lifetime risk of breast cancer and up to 40% risk of ovarian cancer but are only found in 0.06% to 0.2% of people [50] [51]. In total, germline pathogenic variants are estimated to underpin 5% of cancer cases, yet 33% appear to be explained by heritable factors [48][46]. The remaining unexplained heritability (28%) is known as the 'missing heritability' problem [52] [48] [53]. In this thesis, we focus on common germline variants, Single Nucleotide Polymorphisms (SNPs) which could underpin some of the missing heritability in cancer; for example SNPs have been found to explain 7.4% to 16.3% of heritability in colorectal cancer [52][54] [55]. By definition, SNPs are single base changes, are found at a frequency of 1% or greater in the population and have generally low penetrance. The most common version is known as the major or reference allele with other versions called the minor or alternative alleles. SNPs are associated with disease through Genome Wide Association Studies (GWAS).

1.5 Genome Wide Association Studies

A GWAS aims to identify variable regions (SNPs) in the genome whereby one allele is associated with a particular trait. A large population cohort, often comprised of tens of thousands of people, can be divided into those with a particular disease (cases) and those without (controls). Blood samples from this cohort can be used for whole genome sequencing (WGS) and statistical techniques are used to identify interesting genomic loci where one allele is over-represented in the cases compared to the controls. If statistically significant, this allele is described as being associated with increased risk of the disease. A genome-wide p-value threshold of 5x10-8 is most commonly used in multiple hypothesis testing [53]. The results of GWAS are then curated using the NHGRI-EBI GWAS catalogue with over 1,798 cancer associated SNPs to date [56]. More recently, lower-frequency variants (0.1-1%) with intermediate penetrance have been discovered; these variants do not demonstrate Mendelian segregation and could contribute substantially towards

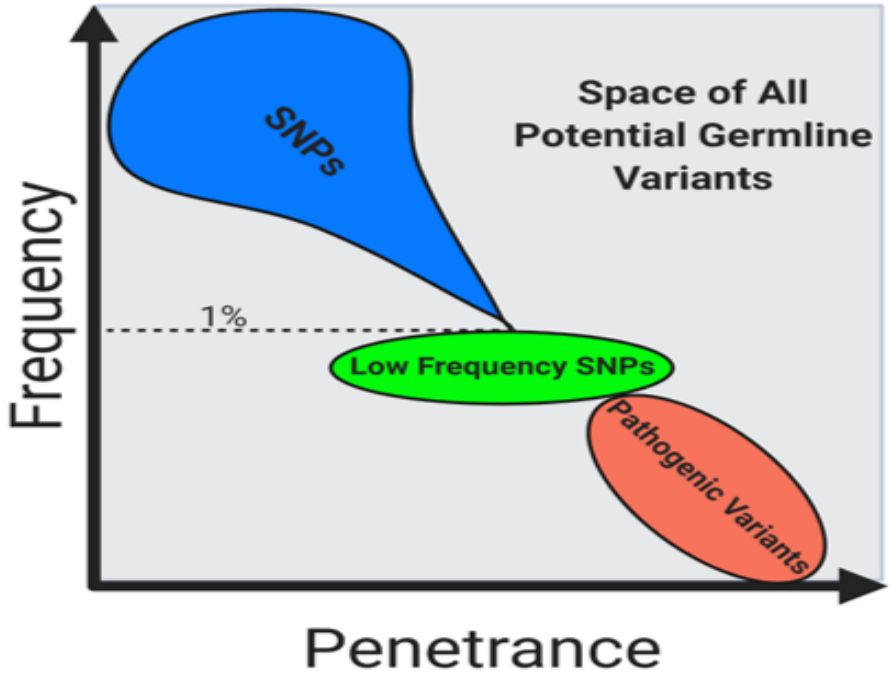


Figure 1.3: Germline variants can be thought of on a scale of Frequency in the general population and Penetrance, the degree of increased risk conferred by the variant over the general population. A variant could theoretically take any combination of values for Frequency and Penetrance but this is not the case in reality. Pathogenic variants are those variants which confer a very high risk for development of a disease such as BRCA mutations and breast cancer and TP53 mutations and Li-Fraumeni mutations. These variants are rare in the population with the higher the penetrance, the rarer the variant. This is likely due to negative selection against these deleterious variants. In contrast, single nucleotide polymorphisms (SNPs) are characterised by relatively high frequency (over 1%) and relatively low penetrance (average odds ratios < 1.5). Millions of SNPs with very low penetrance have been discovered. As sequencing depth has improved, some SNPs have been found with a frequency below 1% (0.1-1%). The impact of these SNPs on disease and their importance in the management of disease is an area of active research.

missing heritability[52]. However, these variants are difficult to identify due to their rarity and their impact on disease has not been fully resolved [57] (Figure 1.3). The use of SNPs in clinical contexts is not standard practice but they have the potential to allow more precise risk stratification, treatment selection and could guide therapeutic design (Figure 1.4).

1.5.1 Population Stratification

SNPs generally have low penetrance, with the majority conferring less than a 1.5-fold increase in risk, per allele, over the general population [53][58]. These small effects for individual SNPs do not preclude clinical utility as SNPs can be combined to generate polygenic risk scores (PRS, Figure 1.4). The models have been shown to achieve a high degree of risk discrimination for various cancers including colorectal cancer, prostate cancer and breast cancer [59] [60] [61]. PRS

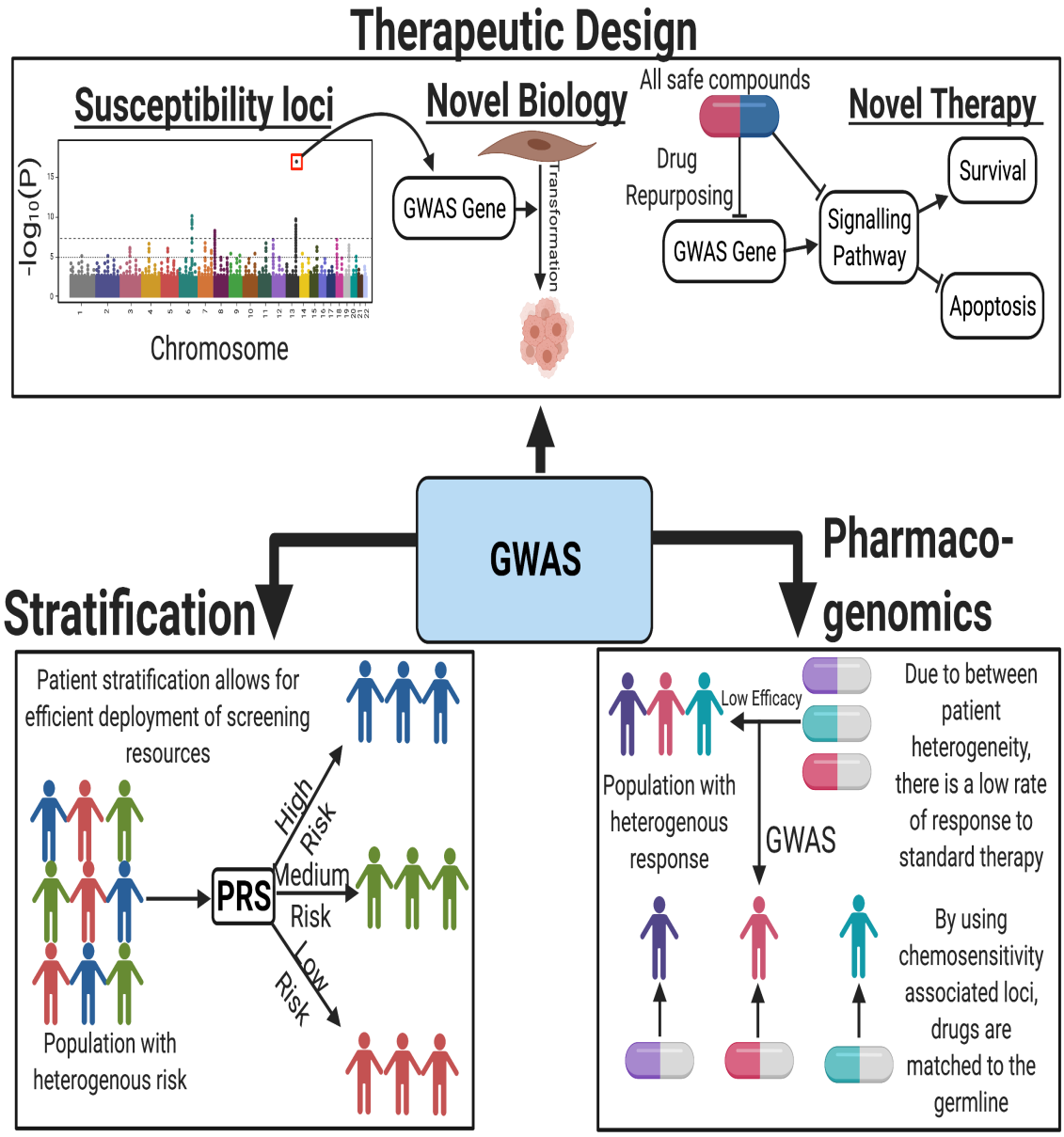


Figure 1.4: GWAS SNPs are not used in the clinic as of yet. This schematic displays some of the key potential clinical applications of cancer-susceptibility loci. (Stratification) Although the penetrance of individuals SNPs is relatively low, they can be incredibly powerful tools when disease relevant SNPs are combined. This is the basis for polygenic risk scores (PRS) which are able to discriminate high risk individuals from low risk with high accuracy and precision. Such stratification facilitates efficient usage of screening resources. (Pharmacogenomics) Some SNPs have been shown to have important effects on treatment response. A disease approved therapy may show highly variable response rates due to germline differences among patients. It will be interesting to see if groups of response-predicting SNPs could be used to match the germline profile of patients with suitable compounds. (Therapeutic Design) The potential for GWAS SNPs in therapy design is an under-explored area of research. Key susceptibility loci identified in GWAS are likely to be loci which are important for the development of the tumour and may indicate novel genes and pathways. If druggable, the novel biology discerned from cancer-susceptibility loci could manifest as novel therapies which have strong genetic support, a predictor of efficacy.

models may be useful for optimising screening programmes by ensuring resources are focused on those with the highest risk. However, some studies have questioned the rational of using SNPs to predict disease; for example, Patron et al studied 569 GWASes of 219 conditions and determined that most SNP-derived prediction models were not as good as clinical-based predictors[58]. Furthermore, PRS models exhibit ethnic disparity in that they are significantly more accurate for those of European descent compared to other ancestries due to an over-representation of Europeans in GWASes, raising the question of whether PRS models, in their current form, could further divide healthcare between ethnic groups [62].

1.5.2 Pharmacogenomics

SNPs have been shown to contribute to inter-patient variability in terms of progression, prognosis and response to treatment in multiple cancer types [63] [64] [65]. The results of these studies indicate that SNPs can inform treatment by predicting which patients might respond to a given therapy (Figure 1.4). For instance, variants of the CYP3A7 gene are known to confer resistance towards chemotherapies that require activation by this enzyme [65]. Moreover, SNPs have been shown to explain variation in toxicity related to anti-cancer therapies including cardiovascular complication from anthracyclines and damage to healthy tissues from radiotherapy [66] [67]. This is particularly relevant when comparing toxicities between populations; for example, after treatment of NSCLC patients with chemotherapy, severe haematological toxicity is significantly more common among Asian patients compared to white Europeans and could be explained by common genetic variants [68][69][70].

1.5.3 Therapeutic Design

Trait-associated SNPs represent a change in the molecular network of the cell and the association with a trait provides a layer of evidence that this part of the network might be important in the development of that trait. In this way, SNPs can provide a starting point for the discovery of novel biological mechanisms

(Figure 1.4). In the context of cancer, they can highlight regulatory regions, genes and pathways which could be involved in tumorigenesis. This is evidenced by how cancer-associated loci are often the site of somatic mutation in tumours [71]. Moreover, meta-analyses of GWASes and of 'big pharma' datasets have indicated that GWAS-associated loci should be considered as priority drug targets [72] [73]. Nelson *et al* and King *et al* demonstrated that drugs in development for a particular disease, were more likely to be successful if the drug target was associated with the same disease in GWAS. Indeed, multiple anti-cancer compounds with GWAS support have been developed including the BCL2 inhibitor, Venetoclax, for CLL [74] [75]. In addition to informing novel drug targets, SNPs can also be informative for the repurposing of already approved compounds [76] [77]. Drug repurposing involves either utilising a drug approved for one disease to treat a second disease or finding that a drug which was unsuccessful, for reasons other than safety, can be used to treat a previously non-indicated disease [78]. It is highly advantageous compared to traditional drug development due to being quicker, incurring lower costs and involves less risk to patients and to the industry [79]. Proof of principle for the use of GWAS loci in drug repurposing comes from the use of ustekinumab, an antibody targeting both IL-12 and IL-23 which have been identified in GWAS to be involved with psoriasis and inflammatory diseases respectively [80] [81] [82]. However, to date SNPs have not been used to repurpose drugs in the context of cancer. In this thesis, we explore how cancer associated SNPs can be informative for cancer therapy, with a focus on repurposing.

1.6 Challenges in Harnessing susceptibly loci for the management of cancer

Mining susceptibility loci identified in GWAS for drug targets is not a straightforward task [83]. The vast majority of SNPs are found in non-coding regions and have no clear causal mechanism [84]. Moreover, identifying likely causal SNPs is itself a challenging statistical problem. Linkage disequilibrium (LD) is one of the key factors which obstructs the clinical translation of SNPs [85]. LD refers to the biological

phenomenon that genetic material is inherited in haplotypes, a result of the fact that the rate of recombination during meiosis is not equal across chromosomes. Two variants are in high LD if they are frequently inherited together, essentially the status of variant A can be predicted with high confidence if the status of variant B is known. This poses a problem when determining the causal SNPs which underlie an association found in GWAS. Multiple SNPs in a genetic region may be found to associate with a trait but it is likely that only one is the causal SNP and the others are artefacts of high LD. A suite of fine-mapping technologies has been described which aim to delineate causal SNPs from variants which are simply correlated with the causal SNP [86]. Overlapping GWAS SNPs with genomic annotations can also help in identifying functional variants [86] (Figure 1.5). Over 80% of the human genome has been functionally annotated and indeed, SNPs have been found to be enriched for in regulatory elements [87] [88] [89]. SNPs which overlap with promoters, enhancers, silencers, miRNA binding sites and splice sites are more likely to be expression quantitative trait loci (eQTLs) meaning they can regulate the expression of a gene(s) [90] [91] [92] [93] [94] [95] [96] (Figure 1.5). Many cancer associated SNPs have been found to reside in eQTLs (eSNPs) but the translation of this information into cancer therapy has been limited to date [97]. In this thesis, we aim to explore the potential role of putatively causal SNPs, residing within regulatory elements, in guiding cancer management in the broader population.

1.7 The P53 Pathway is enriched for cancer-susceptibility loci

The aim of this thesis is to explore the role of cancer-susceptibility loci in guiding cancer management and to provide proof of principle that SNPs can be used to inform the development of novel therapeutics. To do so we focused on the genetics of the p53 tumour suppressor pathway. We chose to do so as the p53 pathway is enriched for cancer-susceptibility loci, is enriched for cancer-eSNPs, is commonly targeted for somatic inactivation in cancer and pathogenic germline variants are associated with Li-Fraumeni syndrome [97] [98] [99] [100].

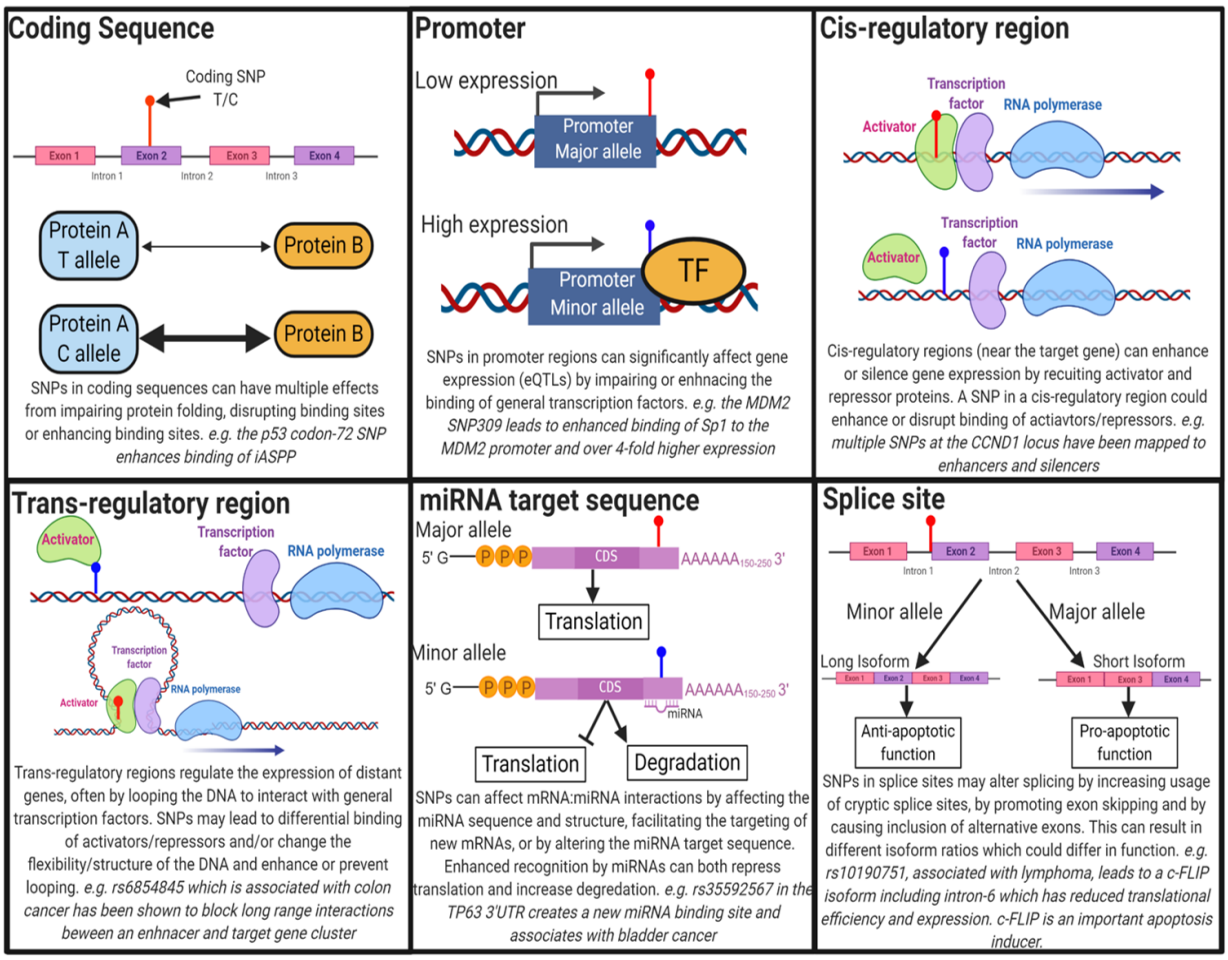


Figure 1.5: In order for SNPs to be clinical translated, it is vital to understand the molecular mechanism underpinning the SNP association. This involved identifying the causal SNP. A common method for this is fine-mapping the susceptibility loci and overlaying functional annotation. This panel displays some of the ways in which SNPs can alter functional genomic elements which might underpin SNP associations. SNPs might have a direct effect on coding sequences, however, the vast majority of SNPs are found in non-coding sequences. These SNPs are often in expression quantitative trait loci (eQTLs) meaning they effect expression of a gene. This could occur through changes to promoters, cis and trans regulatory regions and miRNA sequences (see the individual panels for details). Finally, SNPs could alter the balance of mRNA isoforms by altering splice sites.

1.7.1 TP53 encodes the p53 transcription factor

During research on tumour-related viruses in 1979, p53 was discovered as a 53kD protein bound to the simian virus 40 large T antigen (SV40) which we now know to exert its tumorigenic activity by inhibiting p53 [101] [102] [103]. However, it took a further decade before its primary role as a tumour suppressor was confirmed [104] [105].

TP53 (approximately 20kb) is located on the short arm of chromosome 17 (17p13.1). It encodes 14 exons; 10 constitute the canonical full-length coding

sequence, exon-1 is non-coding while three are alternative exons [106]. The full-length transcript is the major isoform but over 12 other isoforms derived from splicing events and alternative promoter usage have been described [107]. TTP53 mRNA expression levels can be cyclic, is tightly linked to the cell cycle with transcription regulated by RBP-Jk and C/EBPβ-2 [108].

P53 protein is 393 amino acids in length and has a modular structure (Figure 1.6). The main domains are the amino-terminal transactivation domain (TAD), the central DNA-binding domain (DBD), the oligomerisation domain (OD) and the carboxy-terminus regulatory domain [109]. P53 exerts much of its tumour suppressive function via its ability to regulate transcription of target-genes through the DBD. Cofactors bind to the TAD in order to regulate the transcriptional function of p53 [110]. The OD mediates aggregation of p53 monomers into a tetramer, allowing co-operative binding to specific sequences of duplex DNA [109][111]. These sequences, called p53 response elements (p53-RE), have been extensively mapped across the genome with hundreds of validated p53 target-genes described [112] [113] [114] [115].

1.7.2 p53 activity is negatively regulated by MDM2

At the centre of the p53 network is the p53-MDM2 negative feedback loop (Figure 1.7.A). MDM2 is induced by p53 and then inhibits p53 by three mechanisms; masking the p53 TAD, ubiquitination and promotion of degradation and by enhancing nuclear export of p53 [117][118]. MDM2-mediated p53 inhibition is a vital cytoprotective feature of normal, steady-state cells by dampening the p53 response after low-level stress; indeed, MDM2 deletion is embryonic lethal in mice [119][118]. MDM2 can be specifically inhibited by small-molcules called Nutlins which induce cell cycle arrest and apoptosis in numerous cancer cell-lines and models [120] [121]. Numerous MDM2 inhibitors are currently in clinical trials [122].

1.7.3 p53 integrates cellular stress signals

Upon cellular stress, including genotoxicity, hypoxia, ribosomal stress, over activation of oncogenes, telomere erosion and nutrient starvation, cells transduce a

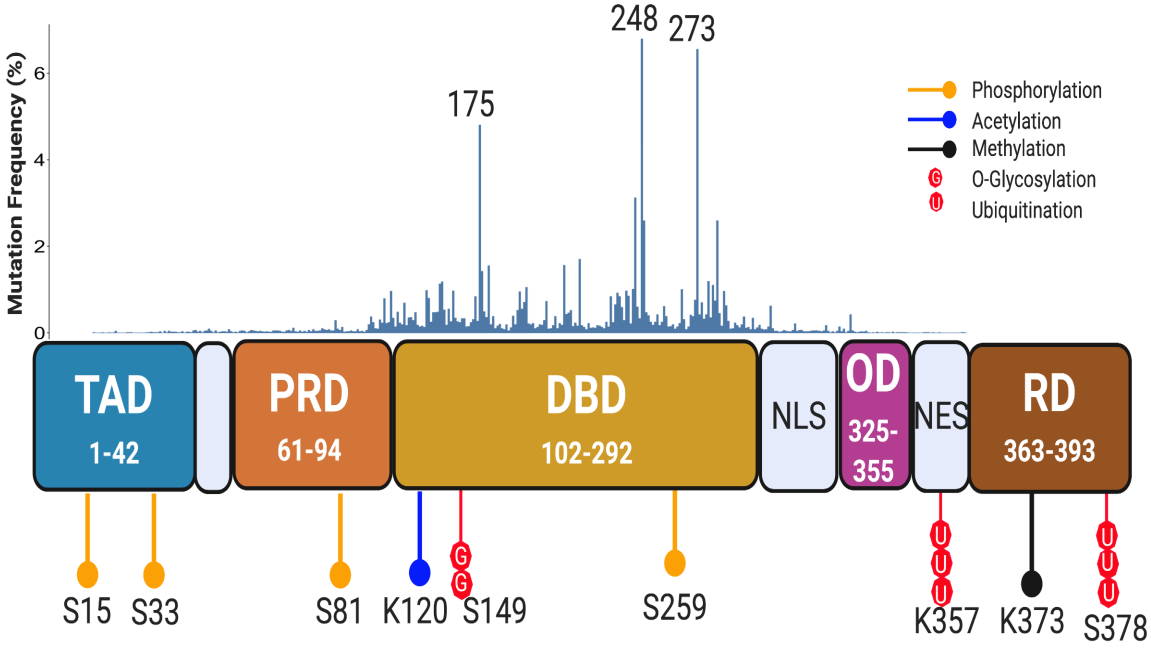


Figure 1.6: TP53 is a modular protein with multiple key domains. The transactivation domain (TAD) recruits cofactors for controlling the expression of target-genes. The proline rich domain (PRD) has been shown to be an important region of apoptosis. The DNA binding domain (DBD) is the core module and allows p53 to bind to specific DNA sequences. The nuclear localisation signal (NLS) mediates the import of p53 into the nucleus to carry its transcriptional program while the Nuclear export signal (NES) promotes translocation of p53 into the cytoplasm, a key method through which p53 is negatively regulated. The oligomerisation domain (OD) is involved in the aggregation of p53 into tetramers. The regulatory domain (RD) is targeted by multiple p53 modifying enzymes which confer an array of PTMs including ubiquitination, methylation, acetylation and phosphorylation. Some PTMs fully activate p53 while others inhibit p53. Some of p53 PTMs are indicated on the bottom of the p53 schematic [116]. TP53 is the most commonly mutated gene in cancer with over 80% of those falling in the DBD. The percentage frequency of each p53 mutation among all p53 mutations is indicated above the p53 schematic. Over 30% of DBD mutations are represented by six sites, the top 3 of which are labelled. The TP53 mutation frequency data was downloaded from the p53 IARC database.

stress signal and respond accordingly[123]. P53 is crucial to the cellular stress response by integrating signals from various upstream pathways and determining an output response (Figure 1.7.B). Many upstream regulators of p53 modulate the p53-MDM2 interaction to impair the negative regulation of p53 and lead to its stabilisation and activation [124](Figure 1.7.B). For example, after DNA damage, kinases such as ATM/ATR are activated which phosphorylate the p53-TAD domain and disrupt the binding of MDM2 [125]. Over 15% of p53 residues can be post-translationally modified (PTMs) including phosphorylation, acetylation, ubiquitination, SUMOylation, and methylation and crosstalk between them is evident [116](Figure 1.6).). PTM sites can be mutated in cancer although at a much

lower frequency compared to p53-DBD mutations; for example, Arg337, a methylated site, is often mutated in adrenocortical tumours [126] [127]. P53 PTMs differ between cell-types and stress, allowing fine-tuning of the p53-response [128] [129] [125].

1.7.4 The refined model of p53 activation

The refined model of p53 activation consists of three steps [130] [131](Figure 1.7.B). First, MDM2-mediated ubiquitination of p53 is inhibited, preventing degradation and allowing p53 protein stabilisation. Second, anti-repression involves specific p53 PTMs which prevent binding of other p53 repressors, leading to expression of genes involved in cell cycle arrest and DNA repair. Third, for full activation, specific cofactors interact with p53 at specific target-gene promoters[130] [131].

1.7.5 p53 promotes cell cycle arrest, apoptosis and cellular senescence

Upon activation, p53 induces a suite of target-genes which mediate one of several responses including cell cycle arrest to allow time for DNA repair (e.g. CDKN2A and GADD45G which inhibit CDKs) , senescence (PML and PAI1) and apoptosis after constitutive stress (e.g. BBC3, PMAIP1 and BAX) [132][115] [133] [134]. There is evidence to suggest that p53 PTMs, cofactors and p53RE sequence variation can control which response program is executed through differential binding of p53 to target-genes [123] [135][132]. For example, target-genes involved in apoptosis are known to have, on average, weaker p53 binding sites than target-genes which promote cell cycle arrest [136]. P53 can also induce apoptosis in a transcription-independent manner by interacting with pore proteins and BCL2 family proteins at the mitochondria [132] [137] [138]. More recently, p53 has been found to regulate other key cellular processes such as metabolism and autophagy [139] [140].

1.7.6 The p53 network is highly complex

p53 regulates key cell-fate decisions including cell-survival and cell-death; thus, its activity is tightly controlled by an extraordinarily complex network of interactions.

We previously discussed PTMs, but beyond these, a plethora of p53 interacting proteins have been described including negative and positive regulators. For example, iASPP is a negative regulator of p53 while the methyl transferases, CARM1 and PRMT1, interact with p53 and histone acetyltransferase p300 to facilitate its induction [141] [142]. Such a wide range of binding partners is afforded by the intrinsically disordered nature of the p53 core domain [143] [132]. miRNAs regulate gene expression by impeding translation and fostering deadenylation of mRNA [144]. P53 is known to regulate the expression of a suite of miRNAs but is also regulated by them. miR-125b and miR-504 have been shown to directly regulate p53 mRNA while others can indirectly modify p53 activity by acting on MDM2 [144]. Throughout this thesis we will refer to our own annotated list of p53 pathway genes comprising lists from KEGG, PANTHER, Biocarta and validated target-genes [115] (Supplementary Table C.1 and C.2).

1.7.7 The p53 network is widely inactivated in cancer

TP53 is mutated in approximately 50% of tumours but varies between cancer-types, <10% for hematopoietic malignancies to over 70% for head/neck [145] [146]. Over 500 unique TP53 mutations have been identified in human tumours, with the vast majority affecting the DBD [124](Figure 1.6). Some missense mutations lead to loss-of-function (LOF) while others promote a dominant-negative (DN) or gain-of-function (GOF) phenotype. GOF mutations confer oncogenicity through upregulation of new target-genes and new protein-protein interactions [147] [148]. DN mutations exert their oncogenic effect through binding and inhibiting wild-type p53, if retained [149]. Highly prevalent TP53 mutations are referred to as hot-spot mutations, accounting for approximately 30% of all mutations. R175, R248 and R273 are the three most common GOF mutations and associate with expression of pro-cell cycle genes, promote metastasis, alter cellular metabolism and induce chemoresistance (Figure 1.6) [150] [151] [152] [153] [154] [155] [156]. Beyond TP53 mutation, the complexity of the p53 network affords a multitudinous array of options for deregulation. For example, the p53 inhibitor, MDM2, is overexpressed

in sarcomas while the cell-cycle inhibitor, CDKN2A, which is upregulated by p53, is commonly deleted in brain tumours [157] [158]. As the fields understanding of the p53 network advances it is inevitable that novel mechanisms of p53 signalling inactivation will be unveiled.

1.7.8 Some cancer-susceptibility loci in the p53 pathway are mechanistically understood

P53 signalling is tightly regulated; thus, small disturbances can dramatically alter cell-fate, including the likelihood of tumorigenesis, a fact epitomised by the enrichment of cancer-SNPs in the p53 pathway compared to other pathways [99] [97]. The majority of cancer-SNPs are non-coding with unknown function, but several in the p53 pathway have been described mechanistically, providing motivation to continue studying this pathway [98]. The codon-72-SNP (rs1042522, C/G) associates with multiple cancer types; the risk allele binds the negative regulator iASPP more strongly, leading to impaired apoptosis induction [159] [160] [161] [162] [98] [163]. The MDM2-SNP309 is located in the first intron of the MDM2 gene. The G allele confers better binding of Sp1, higher MDM2 expression, reduced p53 activity and higher risk and earlier onset of multiple cancer-types [164][165].

Many other cancer-SNPs map to p53-pathway genes and associate with chemosensitivity and tumour-onset but are poorly understood mechanistically [166] [167]. The p53 pathway is intensely studied and therefore very well annotated, and should be prioritised for the study of causal SNPs which could be clinically and therapeutically informative. In this thesis, we will focus on two p53 pathway SNPs, the first is found in a p53 response element at the KITLG locus and the second in the p53 3'UTR.

1.8 Aims

In this thesis, we will explore the molecular mechanism(s) underpinning functional SNPs in the p53 pathway which are associated with cancer. We will determine how these SNPs might be used to inform therapy, in particular the design of novel therapies, and investigate how these SNPs interact with somatic mutations

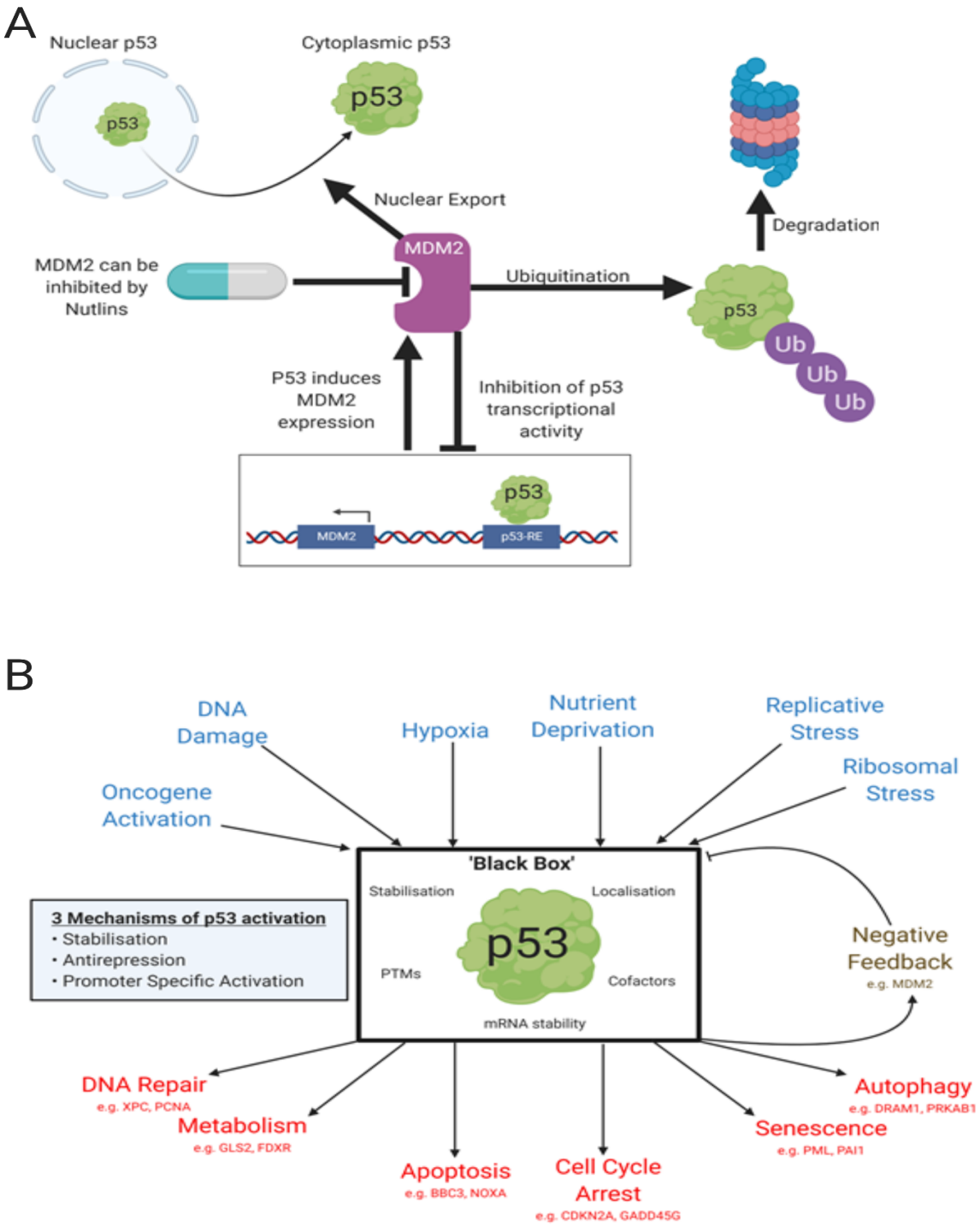


Figure 1.7: **A** - In untransformed cells, high levels of p53 activity can be toxic; therefore, a complex but elegant system of regulatory mechanisms have evolved to control p53. The most prominent of these is the p53-MDM2 interaction. MDM2 can ubiquitinate p53, promote its export from the nucleus and sterically block DNA-binding. Importantly, MDM2 is a target-gene of p53 and is induced even upon low level p53 activation. Multiple compounds have been developed which block the p53-MDM2 interaction, such as Nutlins. **B** - P53 is at the crux of the cell stress response. P53 integrates a multitude of signals from upstream pathways which detect cell stress. P53's integration of these signals is complex and can occur on multiple levels including inhibition of MDM2's enzymatic activity (Stabilisation), post-translational modification of p53 to prevent repression (Antirepression) and control of important cofactors (Promoter Specific Activation). Active p53 can direct the cell towards multiple fates.

within tumours. An understanding of these crucial concepts for cancer-susceptibility loci in the p53 pathway will pave the way for clinical translation of GWAS in the cancer setting.

2

The p53/KITLG/KIT axis promotes cell survival in TGCT and represents a therapeutic opportunity for a repurposed combination strategy

Contents

2.1 Abstract 22
2.2 Introduction 23
2.2.1 Single nucleotide polymorphisms in P53 response elements can influence cancer risk 23
2.2.2 KITLG is the ligand for the oncogenic c-KIT receptor which triggers pro-survival signalling 24
2.2.3 C-KIT is a pro-survival receptor tyrosine kinase 26
2.2.4 The KITLG-p53RE-SNP is associated with Testicular Germ Cell Tumours 27
2.2.5 KITLG/c-KIT signalling is important for normal development of the testes 29
2.2.6 Upregulation of KITLG expression could facilitate the early steps in TGCT development 29
2.2.7 P53 upregulates KITLG in an allelic-specific manner . . 31
2.3 Results 33
2.3.1 C-KIT promotes survival, proliferation and migration in two TGCT cell-lines 33
2.3.2 The p53/KITLG/KIT axis regulates cell survival, proliferation and migration and chemosensitivity in TGCT . 36
2.3.3 Pharmacological inhibition of the p53/KITLG/KIT axis and p53 activation have a synergistic effect on cell death 47

2.3.4 The combination of Dasatinib and Doxorubicin represents a novel, repurposing therapy for refractory TGCT . . . 57
2.4 Discussion 61
2.4.1 Summary 61
2.4.2 Platinum-Resistant TGCT is an increasingly urgent and unmet clinical need 61
2.4.3 Cancer-susceptibility loci may provide insights into chemoresistance 62
2.4.4 The emerging pro-survival role of p53 63
2.4.5 Polymorphic p53 response elements and disease 64
2.4.6 Estimating and predicting synergistic drug combinations 66

2.1 Abstract

Over 90% of functional SNPs are found in non-coding regions and may represent a change to a regulatory mechanism. Deciphering which SNPs are functional and could have clinical impact is a major challenge in the field of genomic medicine. In this Chapter, we investigate a cancer-susceptibility SNP found in a key base of a p53 response element (p53RE) at the KITLG locus, the ligand of c-KIT. The risk allele confers higher risk of testicular germ cell tumours (TGCT). Using TGCT cell-lines, we provide evidence that the KITLG-p53RE is crucial to the p53-dependent upregulation of KITLG, that the p53/KITLG/KIT axis promotes cell survival, proliferation and migration and that simultaneous inhibition of the p53/KITLG/KIT axis and p53 activation exerts a synergistic effect on cell death.

2.2 Introduction

2.2.1 Single nucleotide polymorphisms in P53 response elements can influence cancer risk

The p53 pathway is fundamental to tumour suppression, as evidenced by how approximately 50% of human cancers mutate p53 [168]. The majority of p53 mutations are found in the p53 DBD and when these mutations are found constitutionally in the germline, they give rise to Li-Fraumeni Syndrome (LFS), characterised by the increased risk of developing cancers across multiple sites in the body from an early age [169]. Recognition of p53RE's is crucial for gene transactivation upon activation of p53 due to cellular stress. Gene transactivation by p53 relies on the integrity of the DBD and the p53RE but although the effect of disrupting the p53-DBD has been clearly delineated, the molecular, cellular and clinical effects of changes to p53REs are less well established.

The canonical p53RE consists of two copies of the following half site sequence, RRRCWWGYYY, whereby R = purine, W = A or T and Y = pyrimidine (Figure 2.1.A). The half sites are separated by a spacer between 0-13bp [113][114]. P53 binds to DNA as a homodimer with each monomer contacting its own quarter site within each half site [170]. P53 homodimers can interact with each other to form homotetramers and in this way all four quarter sites within the two half sites are contacted by a p53 DBD (Figure 2.1.B). The key p53 residues and p53RE bases mediating the transactivation ability of p53 have been elucidated, 4, 7, 14 and 17 (Figure 2.1.A). These 4 bases are highly conserved among mammals and mutation severely reduces affinity for p53 [171][172][173][174].

Just as somatic and germline mutations in the p53 DBD can affect the ability of p53 to bind to DNA across the genome, inherited variants within p53RE's could modulate the ability of p53 to recognise and bind to specific regions of the DNA [173][174]. Indeed, multiple studies have demonstrated that SNPs in p53REs can affect p53-dependent gene regulation [175] [176]. SNPs which modulate the interaction between p53 and REs could lead to aberrant p53 target gene expression which is inappropriate for the cellular context. Although the direct effect size

might be small, multiple studies have explored the tight regulation of the p53 network and found that even small perturbations can have large knock-on effects on cell fate[130][168][177][178].

To determine whether cancer-associated SNPs modulate p53 bound REs, Zeron-Medina et al (2013) overlapped 892 cancer-risk SNPs and their proxies (LD >0.8, 62,567 SNPs in total) with p53 ChIP-seq experiments from 11 different combinations of cell lines and treatments (Figure 2.1.C)[176]. They found 86 SNPs to reside in genomic regions featuring a p53 peak in at least one study. To identify likely functional SNPs, they filtered for SNPs in a key base (4,7,14,17) of a p53RE predicted to strongly bind p53 (based on the Position Weight Matrix, PWM, score)[179]. Surprisingly, only one such SNP was found, rs4590952 G/A. The G allele gives a high PWM score of 15.6 for strong p53 binding while the A allele leads to a much lower PWM score of 11.1 (difference of 4.5) predicting reduced p53 binding. The SNP, rs4590952, maps to the KITLG locus on the long arm of chromosome 12 and resides in the key 17th base of the KITLG-p53RE (Figure 2.1.D). Importantly, this p53RE was found to be occupied by p53 in 10 of 11 ChIP-seq datasets tested, covering different cell types and conditions[176]. This genomic region is well conserved among primates with little change among the key bases indicating that the KITLG-p53RE could have important biological relevance (Supplementary Figure A.1). We will refer to this SNP as the KITLG-p53RE-SNP.

2.2.2 KITLG is the ligand for the oncogenic c-KIT receptor which triggers pro-survival signalling

KITLG (also known as Stem Cell Factor (SCF)) encodes a 45kDa glycoprotein capable of acting as a potent growth factor through activation of the c-KIT receptor, a receptor tyrosine kinase (RTK)[180]. KITLG can be membrane-bound or soluble depending on whether exon-6 is skipped or retained[181]. Both isoforms activate-KIT. Zeron-medina et al (2013) demonstrated that p53 could upregulate KITLG expression; in addition, the transcription factors SP1, HIF-1alpha and POU3F2 have been suggested to control KITLG expression[182][183][184][176].

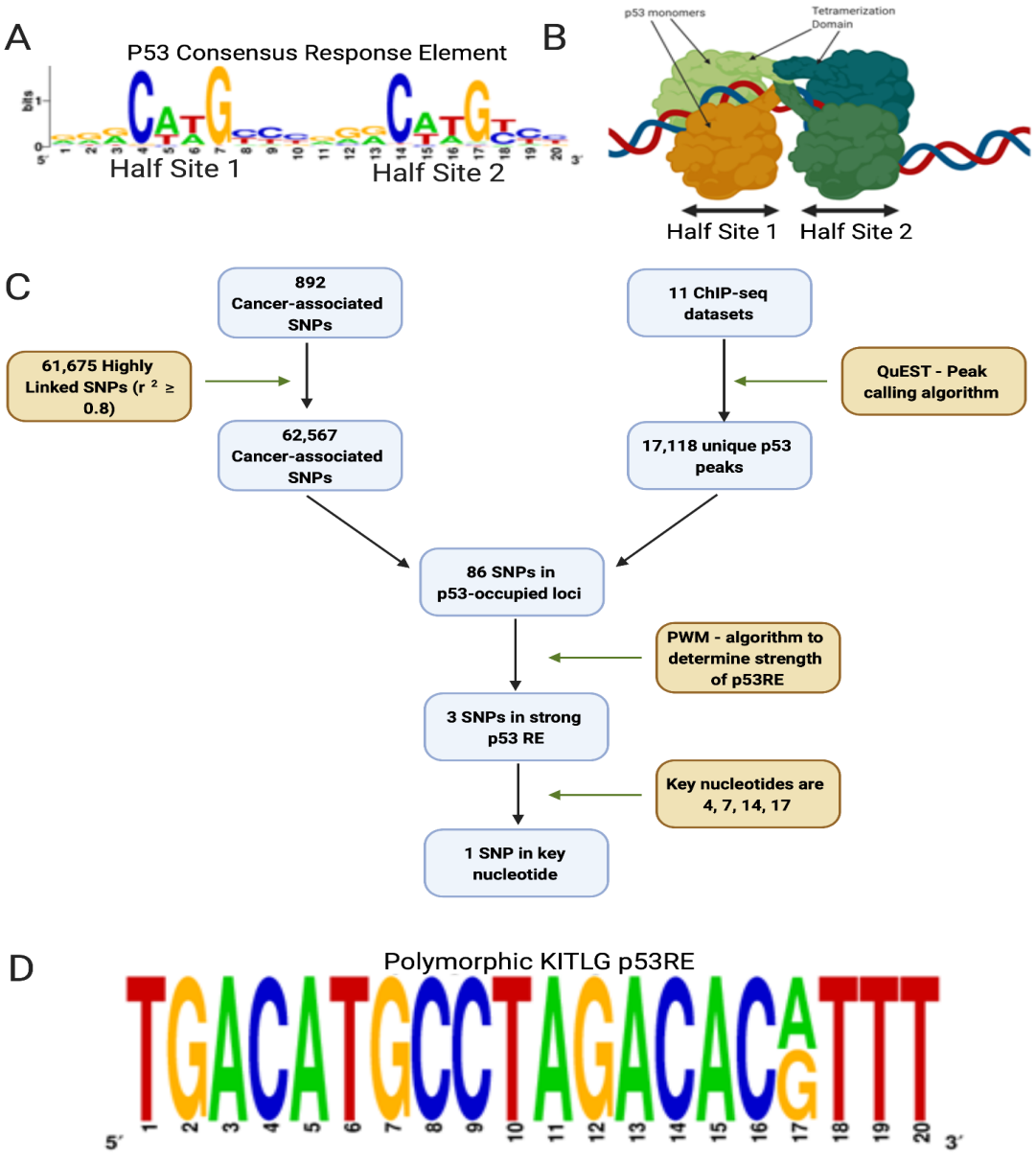


Figure 2.1: **A**) The p53RE consensus sequence consists of two copies of the RRRCWWGYYY sequence. Four bases are highly conserved, (4, 7, 14, 17). These key bases are involved in p53 binding. The key bases can be seen as C and G in each half site. This logo was computed using the p53RE sequences for validated p53 target genes from Tebaldi et al (2017) using WebLogo. **B**) p53 binds to DNA as a tetramer. P53 monomers are connected through the oligomerisation domain. **C**) Zeron-Medina et al (2013) identified the KITLG-p53RE-SNP by overlapping peaks from 11 p53 ChIP-seq datasets with 892 cancer susceptibility SNPs and their 61,675 highly linked proxies. This analysis found 86 SNPs in p53 occupied loci, of which only one, the KITLG-p53RE-SNP was found in a key base of a strong p53RE. **D**) The KITLG-p53RE-SNP is found at position 17, a key base.

2.2.3 C-KIT is a pro-survival receptor tyrosine kinase

C-KIT is a type III RTK and is similar in structure to the platelet derived growth factor receptors (PDGFRs). The c-KIT receptor features three functional regions: the extracellular domain features five Ig-like domains that recognise KITLG; a hydrophobic membrane-spanning region for anchoring the receptor at the cell membrane and an intracellular domain featuring two kinase domains separated by an 80 amino acid kinase insert region and the COOH terminal tail domain (Figure2.2.A). The core c-KIT protein is around 110kDA but N-linked glycosylation leads to a mature protein of between 145 and 160 kDa[185].

C-KIT activation requires dimerization, driven by the homodimer structure of KITLG with Ig-like domains 1-3 binding tightly to KITLG (Figure2.2.B)[186]. It is a rapid process and can be detected within minutes of KITLG treatment[187]. The c-KIT homodimer is stabilised by interactions between extracellular Ig-like domains 4 and 5; this brings the tyrosine kinase domains of proximal receptors close enough together to facilitate transphosphorylation of the juxtamembrane domains which relives autoinhibition, facilitating autophosphorylation and recruitment of downstream signalling molecules [188] [189]. Active c-KIT facilitates cell proliferation, migration and survival[185]. C-KIT is an oncogene and is frequently activated in tumours by mutation. For example, gastrointestinal stromal tumours (GIST), which arise from ICCs, are driven by c-KIT mutations in 80-85% of cases[190]. It was in this context that one of the first molecular targeted therapies was developed. Imatinib, an RTK inhibitor which potently inhibits c-KIT, is indicated for unresectable and metastatic GIST; however, many patients will develop resistance and progressive disease due to acquired secondary mutations[191][192][193]. For these patients, second-generation RTK inhibitors can be used, such as Sunitinib and Nilotinib[192][194]. More recently, c-KIT has been described as a dependence receptor whereby in the absence of KITLG, c-KIT can be cleaved at D816, activate caspase-9 and promote apoptosis[195]. In this model, the true oncogenic factor in KITLG/c-KIT signalling is KITLG itself.

Apart from the ability of p53 to upregulate KITLG expression, little has been uncovered about the crosstalk between p53 and KITLG/KIT. One study

of CRC cells has noted that p53 can upregulate miR-34 which suppresses c-KIT expression but the mechanisms by which KITLG/KIT signalling could regulate p53 signalling are unclear[196].

2.2.4 The KITLG-p53RE-SNP is associated with Testicular Germ Cell Tumours

In this chapter, we focus on the KITLG-p53RE-SNP which is associated with a significant increased risk to testicular germ cell tumours (TGCT). The KITLG-p53RE-SNP is in strong linkage disequilibrium with three SNPs which have been shown to associate with TGCT risk with a per allele odds ratio of up to 3.07 (Figure 2.3.A) (Table 2.1), making this cluster of SNPs one of the strongest cancer associated GWAS signals identified to date[197][198][199][200][201][202][203][204]. Interestingly, the risk allele, G, is also the major allele, found in 80% of Caucasians but in only 30% of Africans (Figure 2.3.B). The prevalence of testicular cancer also appears to correlate with the frequency of the minor allele; testicular cancer is 4-5-fold more prevalent in Caucasian populations compared to Africans[205].

TGCT can be broadly divided into three categories, Type I (Dermoid cyst, Epidermoid cyst and paediatric TGCT); Type II (tumours from IGCNU with 12p gain) and Type III (Spermatocytic seminoma). Type II tumours make up over 90% of TGCT cases and are the focus of this chapter. Type II TGCT can be divided into seminomas (55% of cases) which resemble PGCs and non-seminomatous (NSGCT, 45%). NSGCT can be of multiple different subtypes which reflect the differentiation state of the cells. NSGCT can be undifferentiated, embryonal carcinoma, or differentiated (teratoma, yolk sac tumour, choriocarcinoma)[206].

TGCT are generally highly sensitive to DNA damaging chemotherapeutics and most patients can be treated and cured in this manner[207]. The treatment regime depends upon the histology and staging of the tumour. Patients with stage one seminoma are treated with Carboplatin while those with stage one non-seminoma are treated with one or two cycles of Cisplatin, Etoposide and Bleomycin (BEP). Patients with advanced disease are often given more cycles of BEP or similar regimes

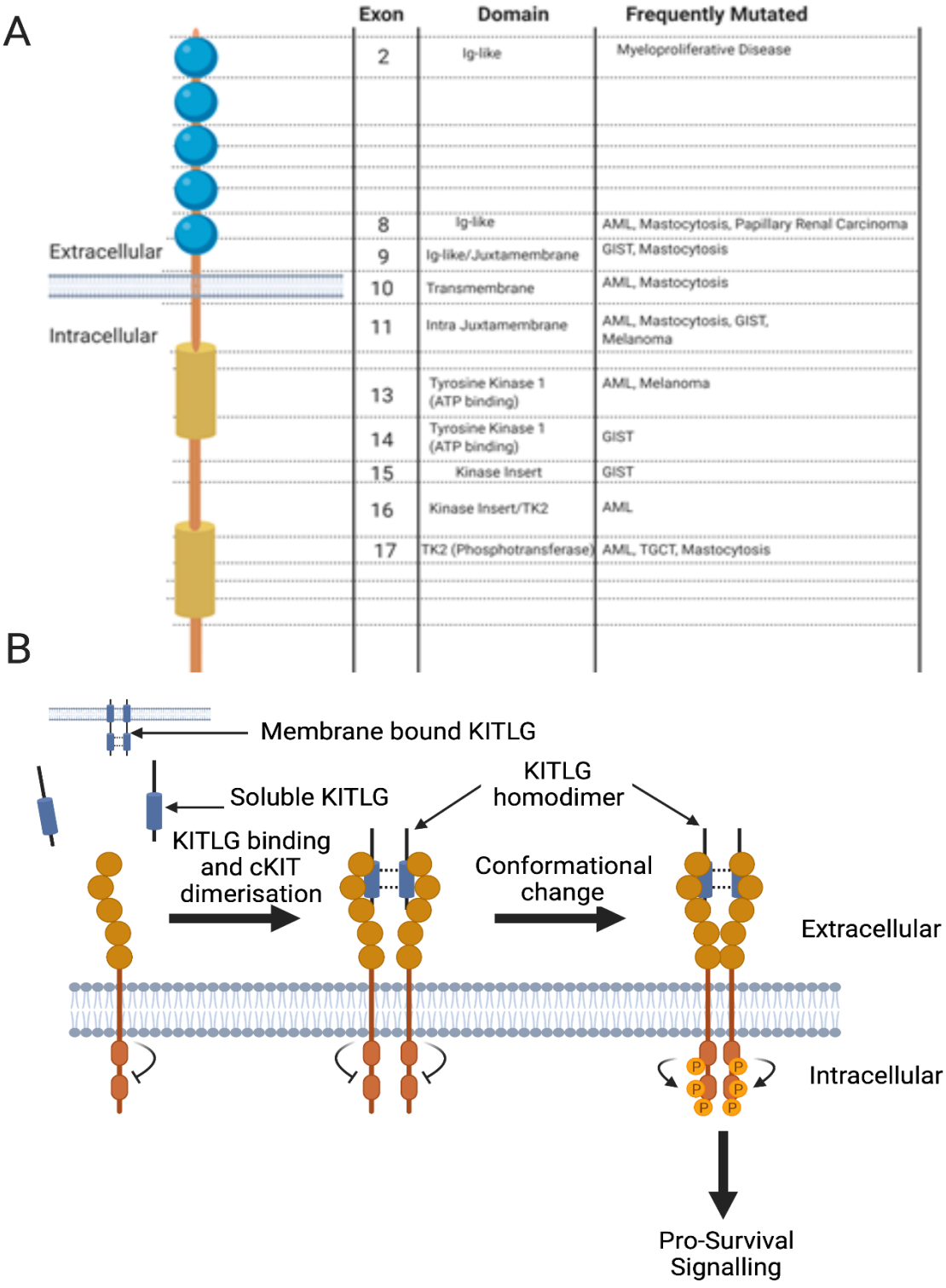


Figure 2.2: **A**) C-KIT is a large protein consisting of five extracellular Ig-like domains, a transmembrane domain, juxtamembrane domains two tyrosinse kinase domains, a kinase insert domain and a C-terminal tail domain. Multiple exons are frequently mutated in cancer with some mutations indicating cancer specificity while others are found in multiple cancers. **B**) KITLG can either be soluble or membrane bound. A homodimer of either can bind two c-KIT molecules and cause dimerization. Additionally, binding of the KITLG homodimer induces conformational changes which facilitate auto-phosphorylation of the intracellular tyrosine kinase domains.

such as VIP (Cisplatin, Etoposide, Ifosfamide, Mesna)[208]. Approximately 5% of patients either undergo relapse or disease-progression during first-line chemotherapy. These patients undergo salvage therapy, consisting of high-dose chemotherapy followed by surgery to remove residual tumour masses[208]. Although TGCT is often considered a paradigm for the successful treatment of solid cancers, further therapeutic developments are required in order to improve the prognosis for the subset of patients who are insensitive to platinum-based compounds and to alleviate the short and long-term treatment-related toxicities in survivors.

2.2.5 KITLG/c-KIT signalling is important for normal development of the testes

TGCT has a strong heritable component; from twin studies and GWAS it is estimated that 40% of cases can be attributed to genetic causes[209][46]. TGCT is thought to arise from aberrant embryonical development of the testes; indeed, developmental disorders such as cryptorchidism and hypospadias are important risk factors for TGCT[209]. KITLG/c-KIT signalling is known to be an important factor during testicular development[210][211][212]. Pluripotent primordial germ cells (PGCs) migrate to the genital ridge under the control of KITLG/c-KIT signalling where they are termed gonocytes (Figure 2.3.C). At this point, the gonocytes become erased (removal of DNA methylation patterns). Then, in the seminiferous tubules, stromal Sertoli cells trigger differentiation of the gonocytes to pre-spermatogonium which is marked by downregulation of pluripotency factors such as Oct4 and c-KIT. Following this, meiosis can occur which produces paternally imprinted germ cells[213]. P53 is crucial for quality control during spermatogenesis; p53 -/- mice show high levels of abnormal spermatozoa while p53 over-expressing mice have low spermatozoa counts[214][215].

2.2.6 Upregulation of KITLG expression could facilitate the early steps in TGCT development

The crucial point towards Type II TGCT development is thought to be downregulation of c-KIT signalling in the erased gonocytes. It has been postulated that stress

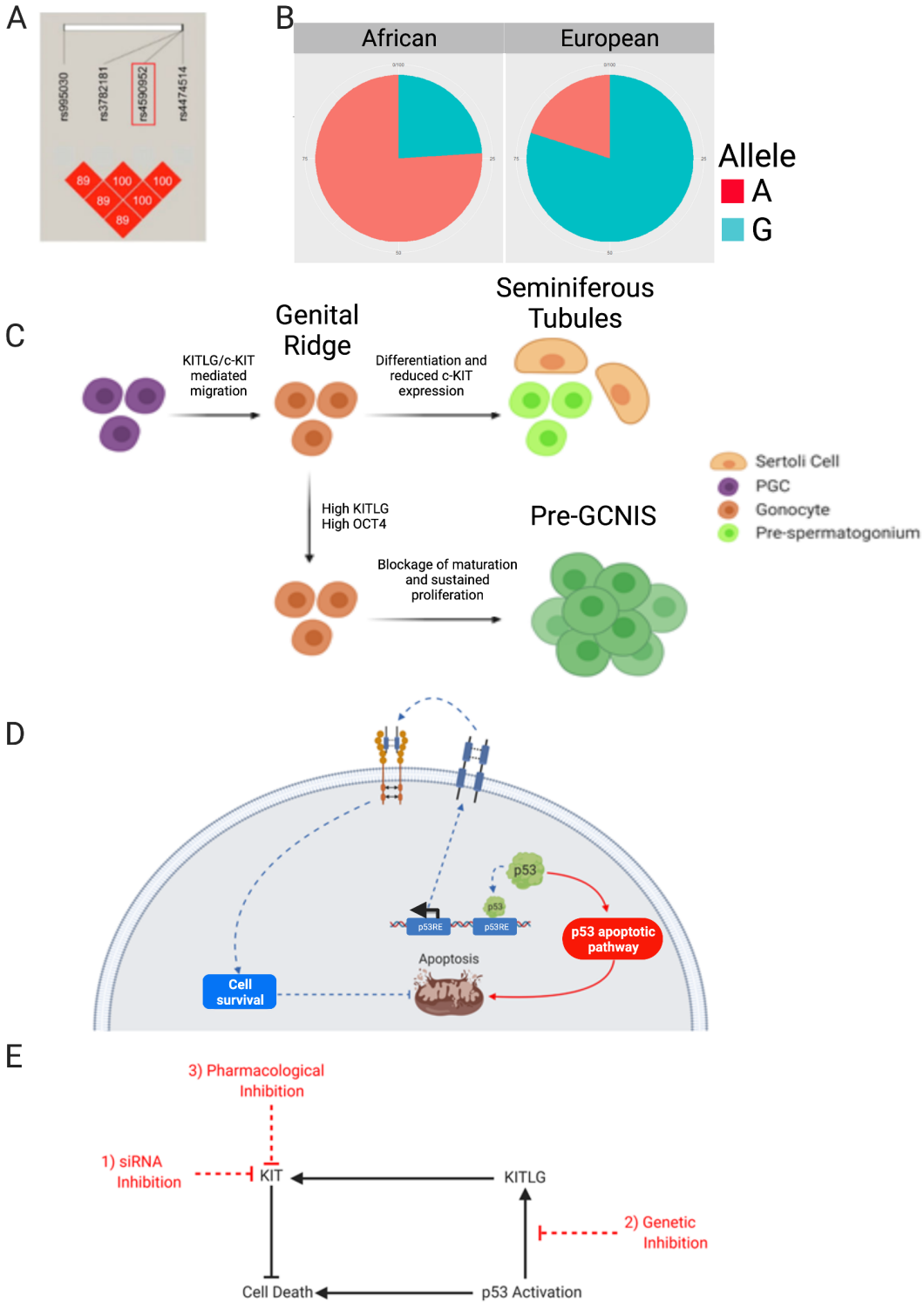


Figure 2.3: **A**) The KITLG-p53RE-SNP is in high linkage disequilibrium with three SNP which have been strongly associated with TGCT in GWAS. **B**) The risk allele is the major allele amongst Europeans (80%) and is the minor allele among Africans (30%). **C**) During testes development, KITLG/KIT signalling mediates migration of PGCs to the genital ridge (gonocytes). Normally they differentiate into pre-spermatogonia but high KITLG and OCT4 expression can maintain a totipotent state and block maturation and promote proliferation. These cells accumulate to a pre-GCNIS which can predispose to TGCT malignancies. **D**) P53 protein could promote a negative feedback loop to block its own apoptotic signalling pathway by upregulating KITLG expression. Solid red lines indicate pro-apoptotic signalling and blue dashed lines indicate pro-survival signalling. **E**) Three methods are used to inhibit p53/KITLG/C-KIT signalling, c-KIT siRNA, CRISPR-Cas9 editing to delete the KITLG p53RE and pharmacological inhibition of c-KIT.

Table 2.1: Table of GWAS associations of three SNPs, highly linked with KITLG-p53RE-SNP, with TGCT risk. Reported odds ratios are per alele.

	Study		
	Kanetsky et al., 2009	**Rapley et al., 2009**	**Turnbull et al., 2010**
Most Significant SNP	rs4474514	rs995030	rs3782181
Pvalue_Discovery	7.34 x 10-9	1.9 x 10-18	1.81 x 10-26
OR_Discovery	2.45	2.29	2.22
Pvalue_Replication	5.88 x 10-15	1.2 x 10-19	NA
OR_Replication	3.07	2.55	NA
Cancer_Type	TGCT	TGCT	TGCT
Population	White, non-hispanic, US	White, European	UK
r2 to rs4590952 (CEU)	1	0.89	1

(such as high levels of oestrogen) or genetic variations can facilitate higher levels of KITLG expression which in turn keeps c-KIT signalling active and Oct4 expression is retained[209]. Oct4 can trigger activity of the AKT promoter and results in expression of TSPY and cell survival. In this context, the normal maturation step towards pre-spermatogonium is blocked and a pre-germ cell neoplasia in situ (GCNIS) is formed (Figure 2.3.C). Polyploidization facilitates development of full GCNIS with amplification of the short arm of chromosome 12 (12p) a recurrent aberration which converts GCNIS to invasive TGCT[209]. TGCTs very rarely mutate p53; the KITLG-p53RE-SNP could drive high KITLG expression in erased gonocytes and predispose to TGCT[216].

2.2.7 P53 upregulates KITLG in an allelic-specific manner

It has been previously shown that KITLG expression is indeed activated by p53 and that there are allelic specific differences in p53 binding and KITLG expression[217][218][219][220][112][176].

Given the data from Zeron-Medina et al (2013) and the plethora of publications supporting the anti-survival and pro-survival effects of the p53 and KITLG/KIT pathways respectively, we hypothesised that p53-dependent upregulation of KITLG

stimulates a pro-survival signalling pathway which inhibits p53-dependent cell death (Figure 2.3.D)[176]. The first focus of this chapter will be to explore the role of the p53/KITLG/KIT axis in balancing cell death and survival in TGCT and determine if it constitutes a therapeutic opportunity. We will inhibit the axis in three ways, 1) siRNA silencing of c-KIT, 2) genetic inhibition of p53/KITLG through CRISPR-Cas9 genome-editing and 3) Pharmacological inhibition of c-KIT (Figure 2.3.E).

2.3 Results

2.3.1 C-KIT promotes survival, proliferation and migration in two TGCT cell-lines

rs4590952 was the only cancer-SNP to overlap with a p53RE, significantly affect the binding of p53 and to confer an allelic specific expression profile of the target gene, KITLG[176]. We hypothesised that the association with TGCT risk could be derived from attenuation of p53 signalling through negative feedback from the p53/KITLG/KIT axis (Figure 2.3.D). To explore the impact of the KITLG-p53RE-SNP on cell survival we selected two commonly used non-seminomatous testicular cancer cell line models, TERA1 and TERA2[221]. Both cell lines have wild-type p53 and are homozygous for the KITLG-p53RE-SNP risk alleles (p53-REs +/+).

C-KIT knockdown inhibits cell survival, proliferation and migration in two TGCT cell-lines

C-KIT has been shown to promote pro-survival signalling[185]. We hypothesised that knockdown of c-KIT by siRNA would reduce cell viability. TERA1 and TERA2 cells were transfected with two siRNAs targeted against c-KIT mRNA for 48hrs and indeed, both cell lines showed reduced c-KIT expression and cell viability ($p<0.05$, Figure 2.4.A,B). In line with this, increased levels of apoptosis were detected after c-KIT knockdown as indicated by higher levels of cleaved-caspase3 (15kDa, Figure 2.4.B).

C-KIT signalling can induce proliferation and cell migration[222][223]. To test this in TGCT cells, TERA1 and TERA2 cells were transfected with c-KIT siRNA and the rates of proliferation and migration were quantitatively measured in real-time using the Xcelligence system (in collaboration with Ping Zhang, Figure 2.4.C,D). Compared to scramble siRNA controls, c-KIT knockdown reduced proliferation 6.1-fold ($p<0.01$) and 3.6-fold ($p <0.0001$) in TERA1 and TERA2 cells respectively and reduced migration 13.7-fold ($p <0.005$) and 7-fold ($p<0.05$) in TERA1 and TERA2 cells respectively

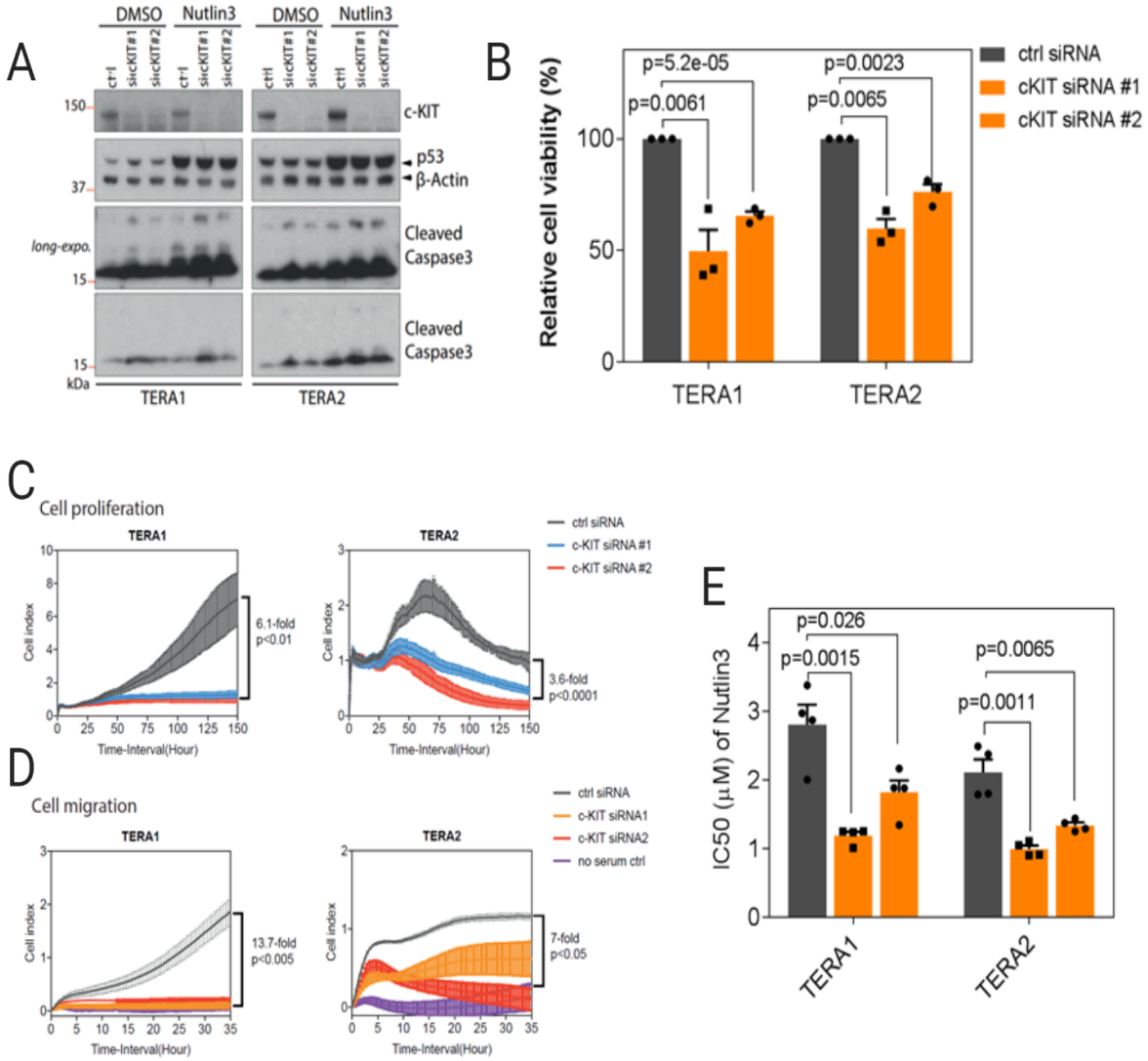


Figure 2.4: **A**) TERA1 and TERA2 cells were transfected with one of two c-KIT siRNAs or control siRNA for 24hrs followed by DMSO or Nutlin-3a (10uM) treatment for 6hrs. The protein fraction was isolated and the levels of c-KIT, p53 and cleaved caspase-3 were detected by immunoblotting. **B**) TERA1 and TERA2 cells were transfected with ctrl siRNA or one of two c-KIT siRNAs. After 48hrs, cell viability was assessed by MTT. Three biological replicates were carried out. Statistical significance was determined by one sample T-test with mu set to 100%. **C**) TERA1 and TERA2 cells were transfected with c-KIT siRNA or control siRNA and proliferation was measured using the Xcelligence system. **D**) TERA1 and TERA2 cells were transfected with c-KIT siRNA or control siRNA and migration was measured using the Xcelligence system. **E**) TERA1 and TERA2 cells were transfected with ctrl or one of two c-KIT targeting siRNA (orange bars). After incubation for 24hrs, cells were incubated with a range of concentrations of Nutlin-3a for a further 48hrs and cell viability was assessed by MTT. The absorbency values were used to calculate IC50 values. Four biological replicates were carried out for each cell line. Statistical significance determined by two-sample T-test.

C-KIT knockdown enhances sensitivity to p53 activation

Given our above findings, we tested how c-KIT knockdown affected sensitivity to p53 activation using the specific p53 activator Nutlin-3a, which inhibits MDM2. TERA1 and TERA2 cells were transfected with the c-KIT siRNA for 24hrs and then treated with a 2-fold serial dilution of Nutlin-3a (0.3125uM to 20uM) for 48hrs. The viability values for the different concentrations were used to calculate IC50 values: the concentration at which there is a 50% reduction in the cell viability (Materials and Methods). For two different c-KIT siRNAs in both TERA1 and TERA2 cells, c-KIT knockdown resulted in significantly lower Nutlin-3a IC50's ($p < 0.05$) indicating higher sensitivity to p53 activation (Figure 2.4.E). Furthermore, cells pre-treated with c-KIT siRNA exhibited greater cleavage of caspase-3 after Nutlin-3a treatment compared to control siRNA, indicating higher levels of apoptosis (Ping Zhang, Figure 2.4.A). Of note, p53 protein levels were strongly induced by Nutlin-3a treatment but were not further increased by c-KIT knockdown.

2.3.2 The p53/KITLG/KIT axis regulates cell survival, proliferation and migration and chemosensitivity in TGCT

Deletion of the KITLG-p53RE prevents p53-dependent upregulation of KITLG

C-KIT promotes survival, proliferation and migration in TGCT cells. We next sought to investigate if the KITLG-p53RE could mediate such phenotypes. We generated clones of TERA1 and TERA2 in which the 1KB region featuring the KITLG-p53REs was deleted by CRISPR-CAS9 (in collaboration with Ping Zhang). Briefly, cells were transfected with the Cas9 expression vector and sgRNAs and after 24hrs were incubated with puromycin for a further 48hrs. Cells were diluted to a single cell suspension, allowing monoclonal colonies to be picked up and tested for successful deletion of the KITLG-p53RE by PCR (Figure 2.5.A,B). Unedited clones would produce a PCR product of 1,278bp after amplification with primer F and primer R while knockouts would produce a smaller band. In addition, the second set of primers (F/sur-R) produced an 883bp product for wild-type clones while no amplification product was produced in knockouts as sur-R targeted a sequence within the deleted region. Two successful KITLG-p53RE knockouts were generated for TERA1 (TERA1 p53-REs -/-) and three were generated for TERA2 (TERA2 p53REs -/-). Three heterozygote knockouts were also generated for each cell line (p53-RE +/-).

Genetic inhibition of the p53/KITLG axis should reduce KITLG expression. To test this, we analysed the KITLG mRNA expression levels in TERA1 and TERA2 p53-RE +/+, p53-RE +/- and p53-RE -/- cells by qRT-PCR (Figure 2.5.C). In both TERA1 and TERA2 cells, heterozygote (+/-; TERA1, 1.6-fold, p = 7.3e-05; TERA2, 1.3-fold, p = 0.03) and homozygote (-/-; TERA1, 3.8-fold, 1.7e-09; TERA2, 4.1-fold, p = 1.2e-07) knockout cells showed significantly reduced basal levels of KITLG mRNA. To ascertain that KITLG expression was p53-dependent, we treated TERA1 and TERA2 p53-RE +/+ and p53-RE -/- cells with Nutlin-3a and measured KITLG mRNA levels after 6hrs (Figure 2.5.D). TERA1 p53-RE +/+

cells showed a 3.5-fold increase in KITLG levels while p53-RE -/- cells showed no increase in KITLG expression (p = 3.00e-6). A similar effect was found for TERA2 p53-RE +/+ and p53-RE -/- cells (p = 3.38e-4). These data indicate that the 1KB region featuring the polymorphic KITLG-p53REs is crucial for p53-dependent upregulation of KITLG expression, both basally and upon p53 activation.

We next examined whether the KITLG-p53RE exerted allelic differences in KITLG expression. We utilised two TGCT cell lines found to be heterozygous at this locus, SusaCR and GH. GH is from a primary non-seminomatous tumour while SusaCR is a cisplatin resistant clone derived from the cell line Susa which was established from a human teratoma[224][225][226]. As for the TERA1 and TERA2 cells, CRISPR-Cas9 was used to delete the 1kb region. In this experiment we looked for clones which had been edited on only one allele, providing us with cells featuring either the major (G, p53RE -/risk) or minor (A, p53RE -/non-risk) allele (Supplementary Figure A.2). To characterise the p53/KITLG/KIT axis of the heterozygote knockouts, cells were treated with either DMSO or Nutlin-3a and RNA was extracted (Figure 2.5.E). For both SusaCR and GH, upon DMSO, we found the p53RE -/non-risk cells to show significantly less KITLG expression compared to the +/+ cells (SusaCR p = 0.022; GH p = 0.018). Upon Nutlin-3a treatment, for both SusaCR and GH, the p53RE -/non-risk (SusaCR p = <1e-4; GH p = <1e-4) and p53RE -/risk cells (SusaCR p = <1e-4; GH p = 0.017) showed reduced induction of KITLG compared to +/+ while -/non-risk cells expressed significantly less KITLG compared to -/risk cells (SusaCR p = 0.0048; GH p = 5e-4).

Genetic inhibition of the p53/KITLG/KIT axis reduces cell proliferation and migration

Treatment with c-KIT siRNA reduced proliferation and migration. Genetic inhibition of the p53/KITLG/KIT axis should have similar effects compared to KITLG-p53RE +/+ cells. Indeed, TERA1 KITLG-p53-RE -/- cells (2 clones) showed a 1.9-fold reduction in proliferation (p<0.005) and 5.8-fold reduction in migration (p<0.005) while TERA2 KITLG-p53-RE -/- cells (3 clones) proliferated 1.9-fold less (p<0.001) and migrated 2.15-fold less (p<0.001) (in collaboration with Ping

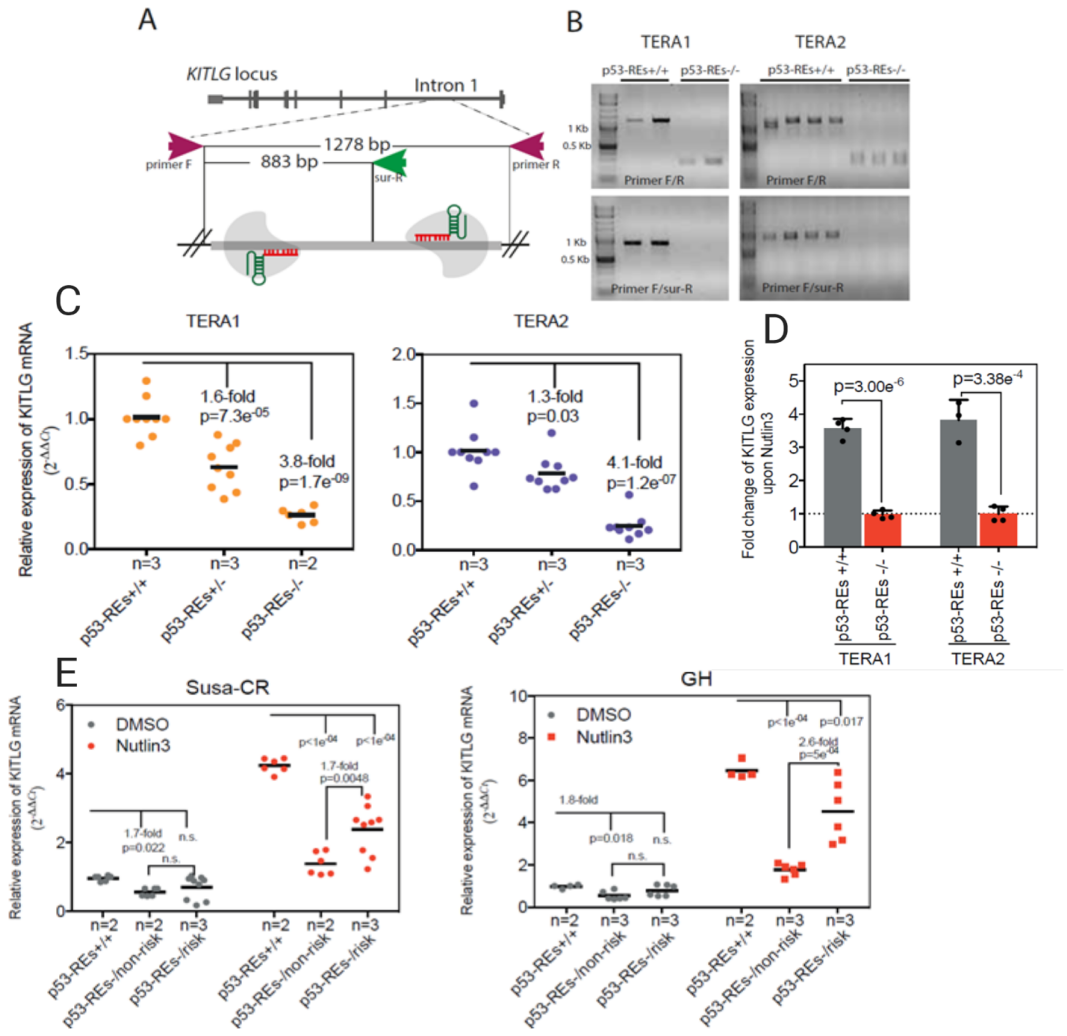


Figure 2.5: **A**) Schematic of method used to knockout the 1kb region containing the KITLG p53REs by CRISPR-Cas9. The deleted region localises to intron one of the KITLG gene. Wild-type cells produce a 1278bp PCR product for the F/R primer pair and an 883bp product for the F/sur-R primer pair. **B**) Clones were checked for successful deletion by PCR. True KITLG p53RE -/- clones show a smaller band for primer F/R and no band for primer F/sur-R. **C**) KITLG mRNA expression of multiple edited and unedited clones was determined by qRT-PCR. At least two biological replicates were carried out for each clone. The number of clones is indicated by the 'n' number. Statistical significance was determined by two sample T test. **D**) TERA1 and TERA2 KITLG p53RE +/+ and -/- cells were treated with Nutlin-3a (10uM, 6hrs) and the fold induction of KITLG mRNA was measured by qRT-PCR. Statistical significance was determined by two sample T test. **E**) The relative expression of KITLG mRNA in multiple clones of KITLG p53RE +/+, -/RISK and -/NONRISK cells of GH and SUSA-CR was measured, both basally and after Nutlin-3a (10uM) treatment, by qRT-PCR. At least two biological replicates were carried out for each clone. The number of clones is indicated by the 'n' number. Statistical significance was determined by two sample T test. Significance was determined by Two-sample T-test.

Zhang, Figure 2.6.A,B). These results indicate that the p53/KITLG/KIT axis is an important mediator of survival, proliferation and migration in testicular cancer cells.

Genetic inhibition of the p53/KITLG/KIT axis enhances sensitivity to p53 activation

c-KIT knockdown sensitised TERA1 and TERA2 cells to p53 activation; we speculated that the KITLG-p53-RE -/- cells, expressing lower levels of KITLG, might show the same effect. TERA1 and TERA2 KITLG-p53-RE +/+ and KITLG-p53-RE -/- cells were treated with Nutlin-3a for 48hrs and we calculated the respective IC50s. TERA1 and TERA2 KITLG-p53-RE -/- clones had a reduced IC50 for Nutlin-3a compared to KITLG-p53-RE +/+ cells (TERA1: 2.5-fold, $p = 0.022$; TERA2: 1.7-fold, $p = 0.04$, Figure 2.6.C). In line with this, after 6hrs of Nutlin-3a treatment, higher levels of cleaved-caspase-3 and cleaved-PARP were found for KITLG-p53RE-RE -/- cells compared to +/+ (Figure-6D). Even under basal conditions (DMSO treatment) higher levels of caspase-3 cleavage could be detected in TERA1 KITLG-p53-RE -/- cells (Figure 2.6.D). This indicates that the p53/KITLG/KIT axis inhibits apoptosis following p53 activation in TGCT cells.

To confirm the p53-dependency of the above described effects, we knocked-down p53 by siRNA. For KITLG-p53-RE +/+ and KITLG-p53-RE -/- cells treated with control siRNA, KITLG-p53-RE -/- cells were 2-fold more sensitive. However, p53 siRNA greatly increased the IC50s for Nutlin-3a (>10uM) and no difference was noted between the dose-response curves (Figure 2.6.E). Furthermore, no increases in caspase-3 cleavage could be detected after Nutlin-3a treatment for the cells subjected to p53 knockdown (Figure 2.6.F). Although, some caspase-3 cleavage could still be detected in p53-RE-/- cells after p53 knockdown, this was less than the basal level of caspase-3 cleavage after control siRNA and was not enhanced by Nutlin-3a treatment. These data indicate that deletion of the KITLG-p53RE sensitises to p53-dependent apoptosis.

Nutlin-3a is a specific activator of p53 which inhibits MDM2; however, p53 is normally stabilised and activated due to stress signalling within the cell. To clarify that the differential sensitivity to p53 activation demonstrated by p53-RE

+/+ and p53-RE -/- cells is not specific to Nutlin-3a, we determined the IC50s of TERA1 p53-RE +/+ and p53-RE -/- cells to three other compounds which have demonstrated activity in TGCT and activate p53. Etoposide is an inhibitor of Topoisomerase II, results in double-strand DNA breaks which activate p53 and is indicated for treatment of higher stage TGCT[227][228][229][26]. For Etoposide, p53-RE -/- cells were 4.5-fold more sensitive ($p < 0.0001$, Figure 2.6.G). Cisplatin and oxaliplatin are both platinum-based compounds. Cisplatin reacts with the N7 position of purines in the DNA to form platinum-DNA-adducts, activates p53 and is approved for treatment of lower stage TGCT and for higher stage as part of BEP cycles[230][231][232][233][26]. For Cisplatin, a 4-fold increase in sensitivity was found for p53-RE -/- cells ($p = 0.0012$, Figure 2.6.G). Oxaliplatin reacts with DNA to forms inter- and intra-crosslinks which block DNA synthesis, can activate p53 and has shown efficacy in TGCT models[234][235][236][237][238][239]. For Oxaliplatin, p53-RE -/- cells were 2.4-fold more sensitive ($p = 0.0032$, Figure 2.6.G). These data indicate that deletion of the KITLG-p53RE sensitises cells to multiple p53 activating compounds including approved TGCT chemotherapies.

Knocking-in the KITLG-p53REs restores the p53/KITLG/KIT axis and the wild-type response to p53 activation

Our previous experiments indicated that the KITLG-p53RE is necessary for pro-survival signalling from the p53/KITLG/KIT axis, to show it is sufficient we reinserted the previously deleted 1KB region into p53-RE -/- cells using CRISPR-Cas9 and a homology-directed repair (HDR) template (KITLG-p53RE -/KI) (Ping Zhang, Figure 2.7.A,B). We used PCR to determine which clones had integrated the template into the correct genomic region. For TERA1, two homozygous knock-ins were found (p53-RE -/KI) and for TERA2, one p53-RE -/KI was found and one homozygous knock-in (p53-RE KI/KI). Importantly, knocking-in of the KITLG-p53RE to -/- cells was able to rescue the expression of KITLG, both basally and after Nutlin-3a treatment, in both TERA1 and TERA2 cells (Figure 2.7.C). These data indicate that the KITLG-p53RE is sufficient and necessary for p53-dependent KITLG upregulation.

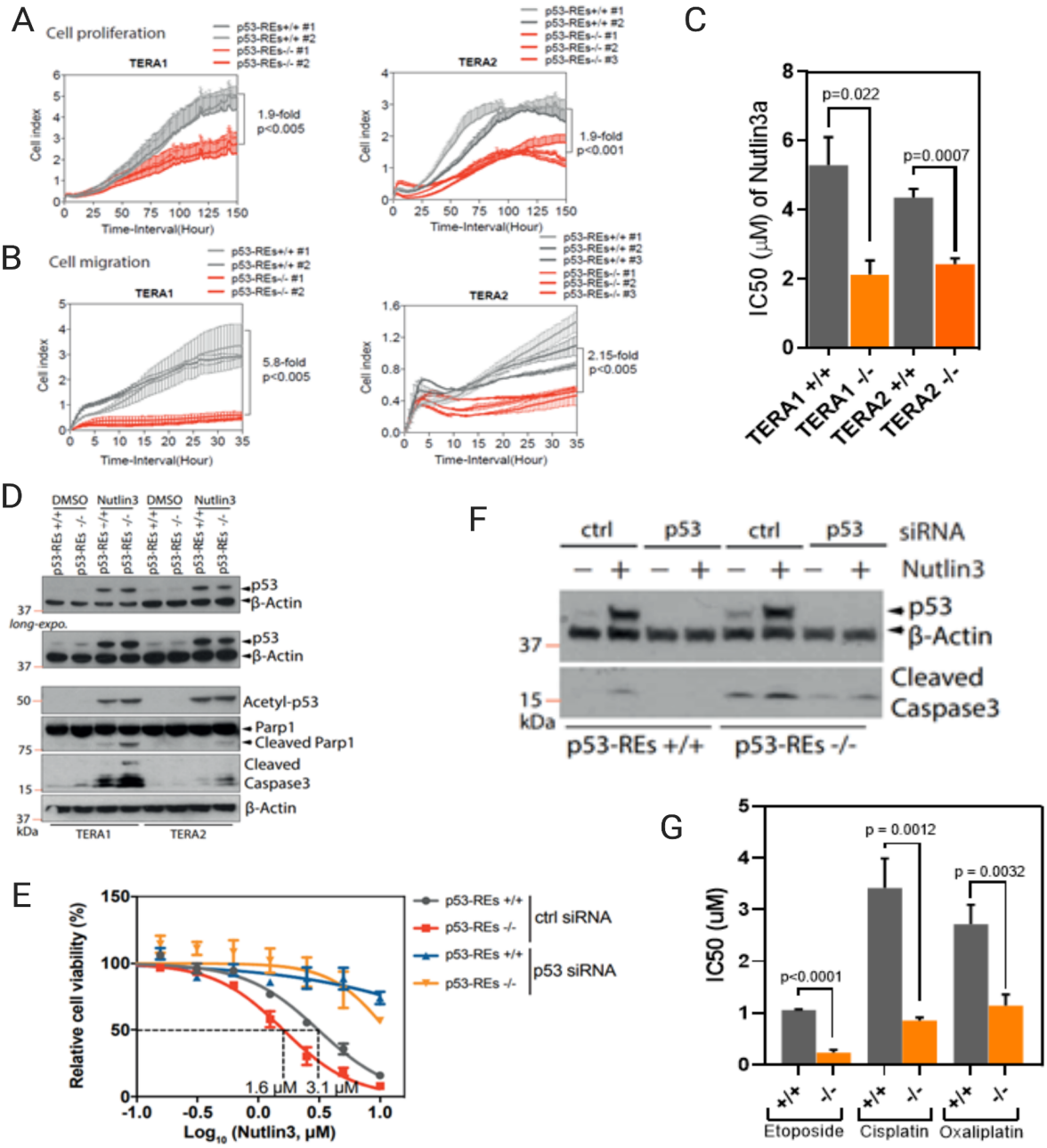


Figure 2.6: **A**) The proliferative ability of TERA1 and TERA2 KITLG p53RE +/+ and -/- cells was measured by the Xcelligence system. **B**) The migratory ability of TERA1 and TERA2 KITLG p53RE +/+ and -/- cells was measured by the Xcelligence system. **C**) TERA1 and TERA2 KITLG p53RE +/+ and -/- cells were treated with Nutlin-3a for 48hrs after which cell viability was measured by MTT. These values were used to calculate IC50s, a measure of sensitivity. Significance was determined by two-sample T-test. **D**) TERA1 and TERA2 KITLG p53RE +/+ and -/- cells were treated with Nutlin-3a (10uM) for 6hrs after which the level of apoptotic markers was analysed by immunoblotting. Actin was used as a loading control. **E**) TERA1 KITLG p53RE +/+ and -/- cells were incubated with p53 targeting or control siRNA and incubated for 24hrs. Cells were then treated with Nutlin-3a for 48hrs and cell viability was assessed by MTT. **F**) TERA1 KITLG p53RE +/+ and -/- cells were incubated with p53 targeting or control siRNA and incubated for 24hrs. Cells were then treated with Nutlin-3a (10uM) for 6hrs and the level of cleaved-caspase-3 was analysed by immunoblotting. Actin used a loading control. **G**) TERA1 KITLG p53RE +/+ and -/- cells were treated with three p53 activating compounds – Etoposide, Cisplatin and Oxaliplatin - for 48hrs after which cell viability was measured by MTT and IC50s were calculated. Significance was determined by Two-sample T-test.

To assess whether the presence of the KITLG-p53RE is sufficient to provide resistance against p53 dependent cell death, p53-RE -/KI and p53-RE KI/KI cells were treated with Nutlin-3a to determine the relative IC50s compared to p53-RE +/+ and p53-RE -/- cells. For TERA1, a 3-fold increase in sensitivity was found for p53-RE -/- cells compared to p53-RE +/+ (p=0.021) and this was rescued by the p53-RE -/KI cells (p = 0.035 compared to -/-, Figure 2.7.D). Similarly, for TERA2, p53-RE -/- cells showed over 2-fold greater sensitivity to Nutlin-3a (p=0.00071) and this was rescued by the p53-RE KI/KI cells (p = 0.033 compared to -/-, Figure 2.7.D).

To determine if KITLG-p53RE -/KI cells mirrored +/+ cells in terms of expression of apoptotic markers, TERA1 +/+, -/- and -/KI cells were treated with Nutlin-3a for 6hrs and then immunoblotted for p53, cleaved PARP and cleaved caspase-3 (Figure 2.7.E). Nutlin-3a induced higher levels of p53 but these were similar across the three genotypes. Caspase-3 and PARP cleavage was induced in all three genotypes but to a much higher degree and at lower concentrations for -/- cells. The levels of apoptotic markers were similar for +/+ and -/KI cells. This data indicates that the KITLG-p53RE is sufficient to induce p53 dependent negative feedback on apoptosis after p53 activation.

The role of the KITLG-p53RE in an intrinsically platinum resistant TGCT model

90% of TGCT patients are successfully treated with platinum-based therapies. The patients who do not respond to platinum-based chemotherapies often relapse and may develop refractory disease for which there is no standardised effective therapy[238]. To understand the role of the KITLG-p53RE in mediating the effect of p53 activating compounds in the context of platinum-resistance, we utilised the intrinsically platinum-resistant cell line 2102EP, derived from a primary testicular teratocarcinoma[240].

2102EP p53-RE -/- cells were generated using the same CRISPR-Cas9 constructs and protocol as for the TERA1 and TERA2 p53-RE -/- cells. After expanding monoclonal colonies, we tested for successful deletion of the KITLG-p53RE by PCR. Three clones were found to produce the p53-RE -/- band for the 3F/3R

primer combination and did not produce a PCR band using the 3F/SurR primer combination indicating deletion of the KITLG-p53RE 1KB region (Supplemental Figure A.3). Firstly, we checked the basal expression of KITLG in the 2102EP p53-RE +/+ and p53-RE -/- cells by qRT-PCR. -/- cells were found to express significantly less KITLG compared to +/+ cells (1.5-fold, $p = 0.044$). After Nutlin-3a treatment to active p53, significant KITLG mRNA induction was found for 2102EP p53-RE +/+ cells (5.2-fold) and this was significantly reduced in -/- cells ($p = 0.012$, Figure 2.7.F). These data indicate that the KITLG-p53RE is crucial for upregulation of KITLG after p53 activation in platinum-resistant TGCT cells. To establish if the reduced KITLG induction translated into differential response to p53 activating compounds, +/+ and -/- cells were treated for 48hrs with Nutlin-3a and Etoposide and IC50s were determined (Figure 2.7.G). For Nutlin-3a, -/- cells were 2-fold more sensitive (n=2) and for Etoposide a 3.5-fold increase in sensitivity was found (n=1). These preliminary data suggest that deletion of the p53-REs at the KITLG locus could sensitise platinum-resistant TGCT cell lines to p53 activating compounds.

TERA1 and TERA2 KITLG-p53RE -/- cells have heightened sensitivity to Topoisomerase Inhibitors

KITLG-p53RE -/- cells are more sensitive to p53 activation by the direct p53 activator, Nutlin-3a and to indirect activators, Cisplatin, Oxaliplatin and Etoposide. However, we hypothesised that we should be able to see heightened sensitivity in the KITLG-p53RE -/- cells for other anti-cancer agents which signal through p53[241]. To test this, KITLG-p53RE +/+ and -/- clones of both TERA1 and TERA2 were screened with 317 anticancer agents at four concentrations, 10nM, 100nM, 1uM and 10uM. Cell viability was assessed by imaging the plates and determining the number of viable cells (Figure 2.8.A, Materials and Methods, Supplementary Table C.3). In total, 198 and 112 drugs were found to kill significantly more KITLG-p53RE -/- cells at lower concentrations compared to KITLG-p53RE +/+ for TERA1 and TERA2 respectively. Of these compounds, 100 were overlapping between TERA1 and TERA2 (1.7-fold more overlap than expected by chance: p=1.06e-21, hypergeometric test, Figure 2.8.B) suggesting a shared mechanism

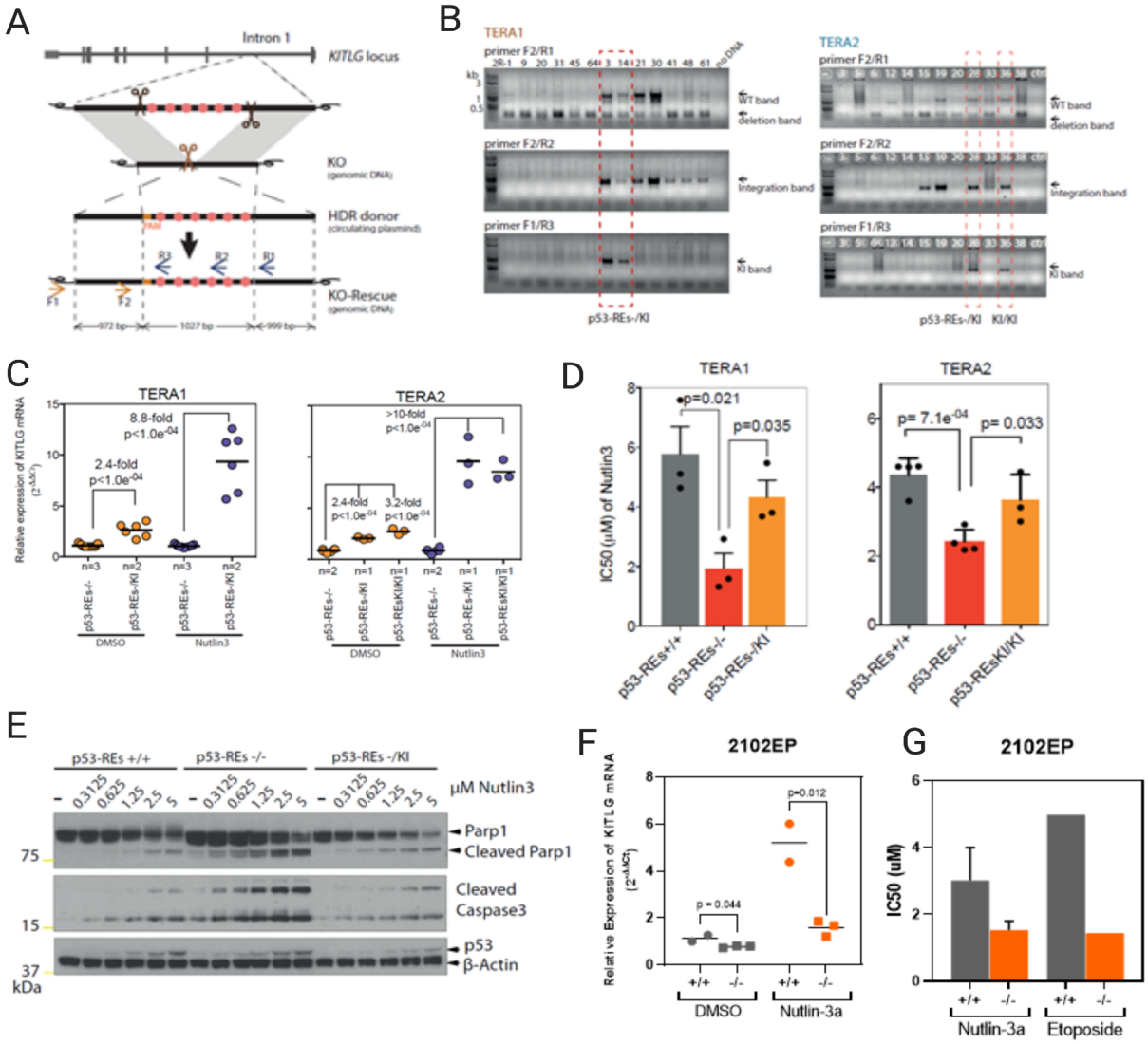


Figure 2.7: **A**) We generated KITLG p53 -/KI clones from KITLG p53 -/- clones using a HDR template with homology arms complementary to the sequences either side of the deleted 1KB region. **B**) TERA1 and TERA2 KITLG p53RE -/KI clones were identified by PCR. Primers F2/R1 indicate whether the WT or Deletion band is present. Primers F2/R2 indicate whether the HDR template has been integrated and primers F1/R3 indicate whether the HDR template has been integrated into the correct genomic location as F1 is outside of the homology arm. **C**) We measured the expression of KITLG mRNA of multiple +/+, -/- and -/KI clones for TERA1 and TERA2 cells, both basally and after Nutlin-3a (10uM, 6hrs) treatment, by qRT-PCR. At least two biological replicates were carried out for each clone. The number of clones is indicated by the 'n' number. Statistical significance was determined by two sample T test. **D**) We measured the Nutlin-3a sensitivity of multiple +/+, -/- and -/KI clones for TERA1 and TERA2 cells. Cells were treated with Nutlin-3a for 48hrs and cell viability was measured by MTT. Significance was determined by Two-sample T-test. **E**) TERA1 +/+, -/- and -/KI cells were treated with Nutlin-3a (10uM) for 6hrs and then immunoblotted for p53, cleaved PARP and cleaved caspase-3. Actin was used as a loading control. **F**) The relative expression of KITLG mRNA in multiple clones of 2102EP KITLG p53RE +/+ and -/- cells was measured, both basally and after Nutlin-3a (10uM, 6hrs) treatment, by qRT-PCR. One biological replicate was carried out for each clone. Significance was determined by Two-sample T-test. **G**) KITLG p53RE +/+ and -/- 2102EP clones were treated with Nutlin-3a, or Etoposide for 48hrs after which cell viability was assessed by MTT assay. The absorbency values were used to determine IC50s.

for the increase in sensitivity upon deletion of the KITLG-p53RE in TERA1 and TERA2 cells. Importantly, among these 100 compounds were both MDM2 inhibitors included within the screen, Nutlin-3a and Serdemetan (Figure 2.8.C). For TERA1, the KITLG-p53RE -/- cells were significantly more sensitive to 198 compounds and this list was found to be significantly enriched for Topoisomerase inhibitors which activate p53 by inducing DNA damage[242] (Figure-Figure 2.8.D). For TERA2, the KITLG-p53RE-/- cells were more sensitive to 112 drugs and this list was significantly enriched for inhibitors for PI3K/AKT/mTOR signalling; RTKs and Topoisomerases (Figure 2.8.D). Therefore, from the drug screen we were able to find a significant and consistent heightened sensitivity for Topoisomerase inhibitors upon deletion of the KITLG-p53RE with 14/14 (100%) compounds hitting for TERA1 and 10/14 (71%) for TERA2.

To validate the heightened sensitivity of -/- cells to Topoisomerase inhibitors, we tested the IC50 for two Topoisomerase-I inhibitors, Camptothecin and its clinically approved analogue Topotecan, and one further Topoisomerase-II inhibitor, Doxorubicin. Multiple clones of TERA1 were treated for 48hrs and cell viability assessed by MTT (Figure 2.8.E). KITLG-p53RE -/- cells were found to have significantly lower IC50s for all three Topoisomerase inhibitors: Topotecan ($p = 0.012$); Doxorubicin ($p = 0.014$); CPT ($p = 0.029$). Furthermore, the KITLG-p53RE +/+ response could be rescued by the knock-in clones: Topotecan ($p = 0.049$); Doxorubicin ($p = 0.045$); CPT ($p = 0.007$) (Figure 2.8.E). Topoisomerase enzymes regulate DNA topology and are important for maintaining the integrity of DNA during replication and transcription[242]. Topotecan, CPT and Doxorubicin induce DNA damage and activate p53[243][244][245][229]. Moreover, expression of wild-type p53 protein has been shown to be important for response to topoisomerase inhibitors in both cell lines and patients, including TGCT [246][247].

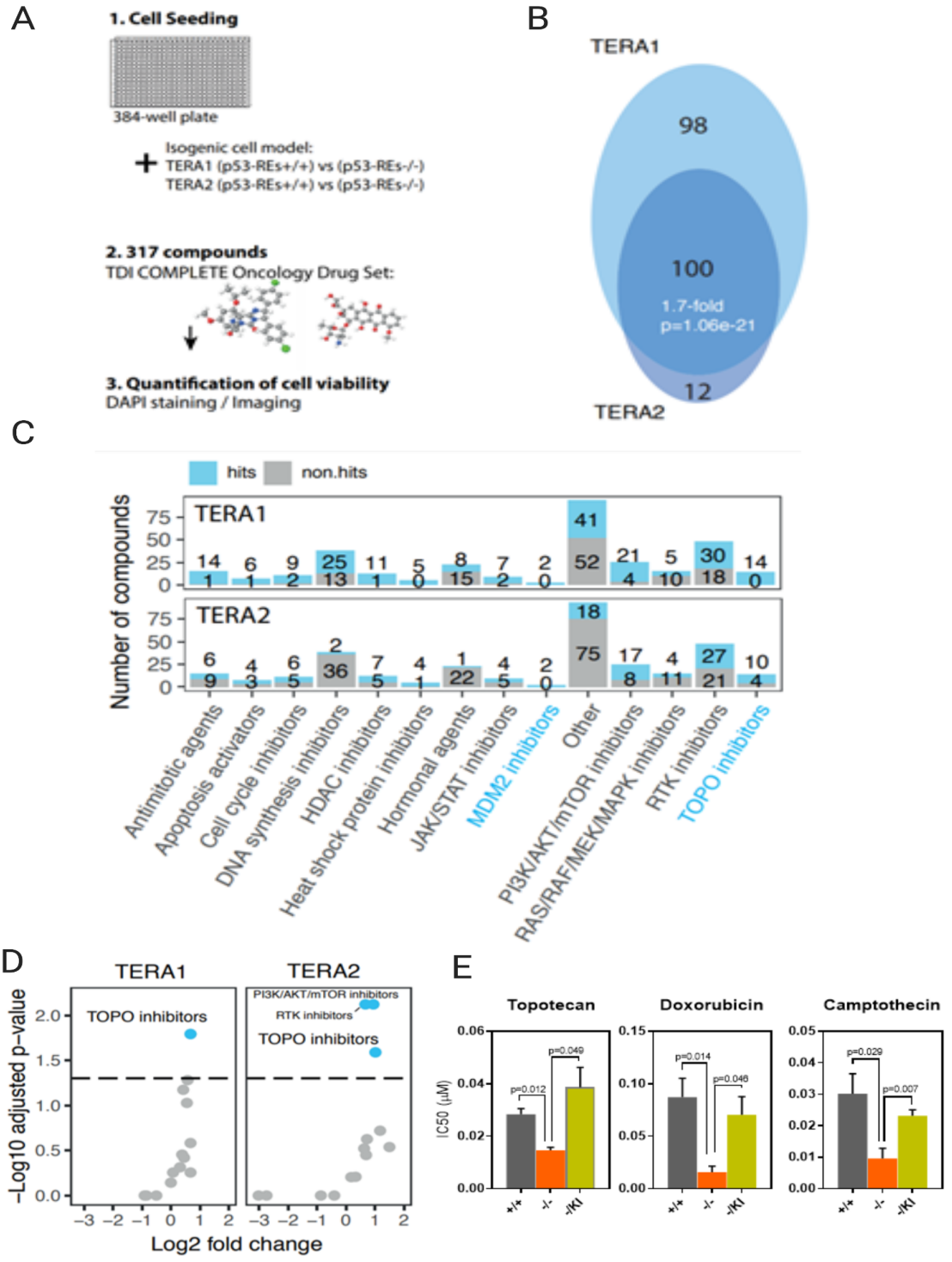


Figure 2.8: **A**) We performed a high-throughput screen to determine the sensitivity of TERA1 and TERA2 KITLG p53RE -/- cells compared to +/+ for 317 Oncology compounds. 4 concentrations were used for each compound and cell viability was assessed by DAPI staining and imaging. **B**) 100 compounds overlapped between significant hits for TERA1 and TERA2. Hits were determined as drugs which KITLG p53RE -/- cells were over 1.5-fold more sensitive to at at least one of the 4 concentrations tested. The significance of the overlap was determined by hypergeometric test. **C**) The 317 oncology compounds were assigned to 14 drug classes. The number of hit compounds for each drug class is indicated in blue and non-hits in grey. **D**) We determined which drug classes were enriched for hits in TERA1 and TERA2 cells. Enrichment was tested by two sided Fisher-test. **E**) TERA1 KITLG p53RE +/+, -/- and -/KI clones were treated with Topotecan, Doxorubicin or Camptothecin for 48hrs and IC50s were calculated. Statistical significant differences determined by Two-sample Student t-test.

2.3.3 Pharmacological inhibition of the p53/KITLG/KIT axis and p53 activation have a synergistic effect on cell death

The data provided so far suggest that deletion of the KITLG-p53RE uncouples the p53 and KITLG/KIT pathways, thereby preventing p53-dependent upregulation of a pro-survival pathway which we hypothesise to inhibit p53-dependent apoptosis. Given this data, we can hypothesise that a pharmacological recapitulation of the genetic knockout should also result in increased cell death. Treatment with a p53 activator whilst also inhibiting c-KIT should prevent the stimulation of pro-survival signalling via the p53/KITLG/c-KIT axis and lead to greater cell death upon p53 activation; in essence, p53 activators should synergise with c-KIT inhibitors to kill cells (Figure 2.9.A).

TGCT cells are highly sensitive to the c-KIT inhibitor, Dasatinib, in a way which is mediated by the KITLG-p53RE

To begin to test this hypothesis, we first determined the best c-KIT inhibitor for TGCT cells. Of the 100 drugs to which both TERA1 and TERA2 KITLG-p53RE -/- cells are more sensitive to compared to KITLG-p53RE +/+ cells, 12 are known to target c-KIT, out of a total of 20 c-KIT targeting compounds, this represents a significant enrichment of c-KIT inhibiting compounds compared to non-KIT targeting compounds (3.55-fold, $p = 0.011$, Figure 2.9.B,C). 4 of these were chosen, namely, Nilotinib (AMN107), Sunitinib (Suntent), Pazopanib (Votrient) and Dasatinib (Sprycel). Imatinib (Gleevac) was also chosen to use as a negative control as TERA1 and TERA2 KITLG-p53RE -/- cells did not show enhanced sensitivity. All five RTKs have been shown to inhibit c-KIT and are clinically approved for cancer treatment[248][249][185][250][251][252]. TERA1 and TERA2 KITLG-p53RE +/+ cells were treated with a 2-fold dilution series of each drug for 48hrs and IC50s were determined. Pazopanib was found to have the highest IC50 for both TERA1 (30uM) and TERA2 (40uM) cells while Dasatinib had the lowest IC50 in both TERA1 (1uM) and TERA2 (0.8uM) cells (Figure 2.9.D). Dasatinib is a second generation RTK inhibitor and has already been shown to

be successful in combination with chemotherapeutics including Oxaliplatin[253], Doxorubicin[254], Nutlin-3a[255], Topotecan[256] and Cisplatin[257]. Given the high potency of Dasatinib in TERA1 and TERA2 cells and the previous data suggesting it can be successfully combined with chemotherapeutics, we decided to focus on Dasatinib as our c-KIT inhibitor for future experiments.

Dasatinib is not a specific inhibitor of c-KIT, however, we reasoned that if the sensitivity of TERA1 and TERA2 cells to Dasatinib is due to inhibition of KIT signalling then KITLG-p53RE -/- cells should be more sensitive as KITLG/KIT signalling is already reduced in these cells. Indeed, when TERA1 KITLG-p53RE +/+ and -/- cells were treated with Dasatinib for 48hrs we found that KITLG-p53RE -/- cells were 10.4-fold more sensitive ($p = 0.0012$, Figure 2.9.E) while Sunitinib and Nilotinib showed non-significant trends towards higher sensitivity in the p53RE -/- cells (Figure 2.9.E). Deletion of the KITLG-p53RE in platinum resistant cells had a similar effect on Dasatinib sensitivity; Susa-CR KITLG-p53RE -/- showed 14.3-fold higher sensitivity compared to KITLG-p53RE +/+ cells ($p = 0.0032$). In addition, a nonsignificant trend was noted whereby Susa-CR KITLG-p53RE -/risk cells showed 2-fold increased IC50 for Dasatinib compared to Susa-CR KITLG-p53RE -/nonrisk cells ($p=0.11$, Figure 2.9.F). For GH, both the KITLG-p53RE -/risk and -/nonrisk clones showed significantly higher sensitivity to Dasatinib compared to KITLG-p53RE +/+ cells (-/risk, 4.8-fold, $p < 0.0001$; -/nonrisk, 6.8-fold, $p < 0.0001$) and a nonsignificant trend was noted towards higher Dasatinib IC50 in KITLG-p53RE -/risk clones compared to -/nonrisk (1.42-fold, $p = 0.085$, Figure 2.9.F). These data suggest that the KITLG-p53RE and potentially the SNP can affect sensitivity to Dasatinib. This is consistent with our model whereby KITLG-p53RE -/- and -/nonrisk cells have a suppressed p53/KITLG/KIT axis.

Pharmacological inhibition of c-KIT shows strong synergy with p53 activation

We reasoned that we could pharmacologically recapitulate the effect of deleting the KITLG-p53RE by combining a p53 activator with a c-KIT inhibitor. To test for synergy, we used the Combination Index (CI) method whereby the IC50s

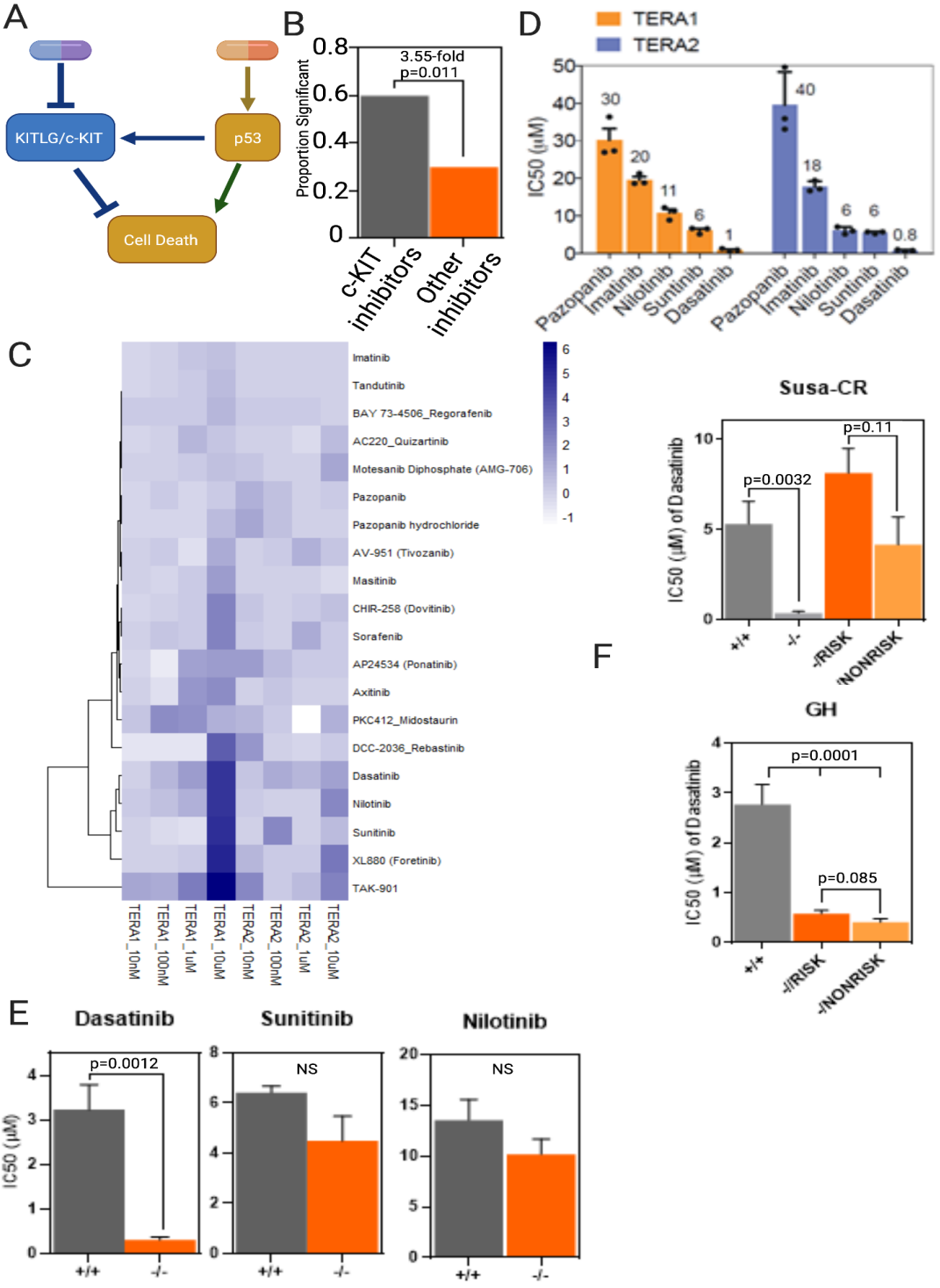


Figure 2.9: **A**) A model to indicate how co-stimulation of p53 and inhibition of KITLG/c-KIT signalling might impact synergistically on cell death. **B**) The bar chart indicates the proportion of RTK inhibitors which were found to be hits (-/- cells more sensitive than +/+ cells) in the drug screen compared to all drugs tested. Statistical significance of the enrichment was determined by Two-sided Fisher Test. **C**) A heatmap displaying the sensitivity of KITLG p5RE -/- cells to c-KIT targeting RTKs compared to +/+ TERA1 and TERA2 cells at 4 concentrations. Dark blue indicates the largest increase in sensitivity in -/- cells. **D**) KITLG p53RE +/+ TERA1 and TERA2 cells were treated with Dasatinib, Pazopanib, Imatinib, Sunitinib or Nilotinib for 48hrs treatment and IC50s were calculated. IC50 values are shown above each bar. **E**) TERA1 KITLG p53RE +/+ and -/- cells were treated with Dasatinib, Sunitinib or Nilotinib for 48hs and IC50s were calculated. Statistical significance determined by Two-sample student T-test. **E**) Susa-CR and GH +/+, -/-, -/RISK and -/NONRISK cells were treated with Dasatinib for 48hrs and IC50s were calculated. Statistical significance determined by Two-sample student T-test.

are found for each drug when used in isolation and in combination and used to generate CI values by Equation 2.1.

$$CI = \frac{(D_1)}{(D_50)_1} + \frac{(D_2)}{(D_50)_2} \tag{2.1}$$

where $(D)_1$ is the concentration of drug A required to kill 50% of cells in combination with drug B, $(D)_2$ is the concentration of drug B required to kill 50% of cells in combination with drug A; $(D_50)_1$ is the concentration of drug A required to kill 50% of cells in isolation and $(D_50)_2$ is the concentration of drug B required to kill 50% of cells in isolation.

This allows for computation of a CI value whereby CI = 1 indicates an additive effect, CI $<$ 1 indicates synergy and CI $>$ 1 indicates antagonism[258]. Briefly, cells were seeded in a 96well plate in an 8x8 matrix and treated the following day with an increasing concentration gradient of p53 activator across the plate and increasing concentration of c-KIT inhibitor down the plate. Treating in this fashion allows IC50s for the drugs in isolation to be calculated from the edges of the plate and the IC50s in combination to be calculated from the diagonal. After 48hrs of treatment, the MTT assay was used to assess cell viability (Figure 2.10.A). The fraction of cells killed for the different concentrations of the drugs used in isolation and combination were entered into CompuSyn for analysis[259]. An example matrix for TERA1 KITLG-p53RE +/+ cells treated with Dasatinib and Nutlin-3a is shown in Figure 2.10.B; the top row represents the cells treated with only Nutlin-3a while the first column represents cells treated with only Dasatinib. The diagonal from 0,0 represents the values where the two drugs increase in constant ratio to each other and is used to compute the IC50 values of each drug in combination. Following treatment with the combination of Dasatinib and Nutlin-3A in TERA1 and TERA2 KITLG-p53RE +/+ cells, CI values of less than 1 were calculated indicating significant synergy between p53 activation and c-KIT inhibition (TERA1: CI = 0.49; TERA2: CI = 0.63; Figure 2.10.C,J,K). From a biological perspective, it is important to understand if the synergistic relationship between two drugs is limited to a particular effect size window. Two drugs may show synergy at

the IC25 level (25% cells affected) but may be antagonistic at IC75 (75% of cells affected) in which case the drug combination would not be biologically interesting. We found that for effect sizes greater than 20%, Dasatinib and Nutlin-3a act synergistically (Figure 2.10.C). Importantly, strong synergy (CI = 0.24) was found for the very high effect sizes (FA = 0.90).

The synergy between pharmacological c-KIT inhibition and p53 activation enables profound dose reductions

Synergistic interactions can allow for dose reduction. It is important to understand such potential reductions in dosage when considering compounds which can have hazardous side effects in patients. The Dose Reduction Index (DRI) indicates the fold reduction in drug concentration afforded by using two drugs in combination compared to in isolation, for a given effect size. The combination of Dasatinib and Nutlin-3a affords significant reductions in concentration for both drugs across a wide range of effect sizes, including up to FA = 0.9 (Figure 2.10.D). For example, to achieve IC50, using Dasatinib and Nutlin-3a in combination allows for a 9.62-fold and 12.15-fold reductions in Dasatinib and Nutlin-3a concentrations respectively. To examine whether the synergy between Dasatinib and Nutlin-3a occurs at biologically meaningful concentrations, the isobologram method was used. The concentrations required to affect 50%, 75% or 90% of cells for Dasatinib and Nutlin-3a in isolation is marked on the axis of the plot and the combination concentration is indicated in red (Figure 2.10.E-G). If the combination point lies below the isobole then the drugs work synergistically. For example, for FA=0.5, the combination of Dasatinib and Nutlin-3a allows both drugs to be used in the high nanomolar range (710nM, 95% CL = 560nM - 860Nm). To determine if the synergy between Dasatinib and p53 activation was due to enhanced apoptosis, we treated cells with Nutlin-3a only, Dasatinib only or the combination of Dasatinib and Nutlin-3a for 6hrs and then immunoblotted for Caspase-3 cleavage. We found greater levels of Caspase-3 cleavage upon co-treatment (4.5-fold, Figure 2.10.H,I).

Testicular germ cell tumours are renowned for their sensitivity to platinum-based therapies[260]. The mechanisms of these therapies are thought to involve activation

of p53 by triggering the DNA damage response. We hypothesised that Dasatinib should also show synergy with Cisplatin, a commonly utilised platinum-based therapy in oncology[261]. TERA1 KITLG-p53RE +/+ cells were treated with Dasatinib and Cisplatin in isolation or in combination and cell viability was assessed after 48hrs. As for the combination of Dasatinib and Nutlin-3a, significant synergy was found (CI = 0.40, p = 0.0094, One-Sample T-test, Figure 2.10.J). The synergy between Dasatinib and Cisplatin afforded significant reductions in concentration for the IC50 effect level; a 4.2-fold reduction was afforded for Dasatinib (p =0.0051) and 5.8-fold for Nutlin-3a (p = 0.001). In combination, 780nM Dasatinib and 560nM Cisplatin was required to affect 50% of cells. This demonstrates that c-KIT inhibition by Dasatinib not only synergises with the direct p53 activator, Nutlin-3a, but can also synergise with Cisplatin which indirectly activates p53 by triggering upstream DNA damage signalling, suggesting that c-KIT inhibition could sensitise cells to general chemotherapeutics.

C-KIT inhibition synergises with p53 activation in a KITLG-p53RE dependent manner

Our model suggests that dual c-KIT inhibition and p53 activation should synergise due to the ability of p53 to both activate pro-apoptotic signalling and upregulate KITLG expression which has the knock-on effect of inhibiting apoptosis. Therefore for -/- cells (genetically inhibited p53/KITLG/KIT axis), the synergy should be largely reduced compared to +/+ cells. Indeed, the synergy was no longer detectable in the KITLG-p53RE -/- cells for both TERA1 (CI = 1.06, 2.16-fold higher compared to TERA1 +/+, p = 7.2E-4) and TERA2 (CI = 1.35, 2.14-fold higher compared to Tera2 +/+, p = 0.031; Figure 2.10.K). Moreover, the synergy could be rescued by knocking-in the p53RE for both TERA1 (p = 0.018) and TERA2 +/- (p = 0.038) cells (Figure-10K). These data indicate that the KITLG-p53RE is necessary and sufficient for synergy between c-KIT inhibition and p53 activation.

C-KIT inhibition synergises with p53 activation in platinum-resistant TGCT cell-lines

Significant synergy was measured between the c-KIT inhibitor, Dasatinib, and both the direct p53 activator, Nutlin-3a, and the indirect p53 activator, Cisplatin, in

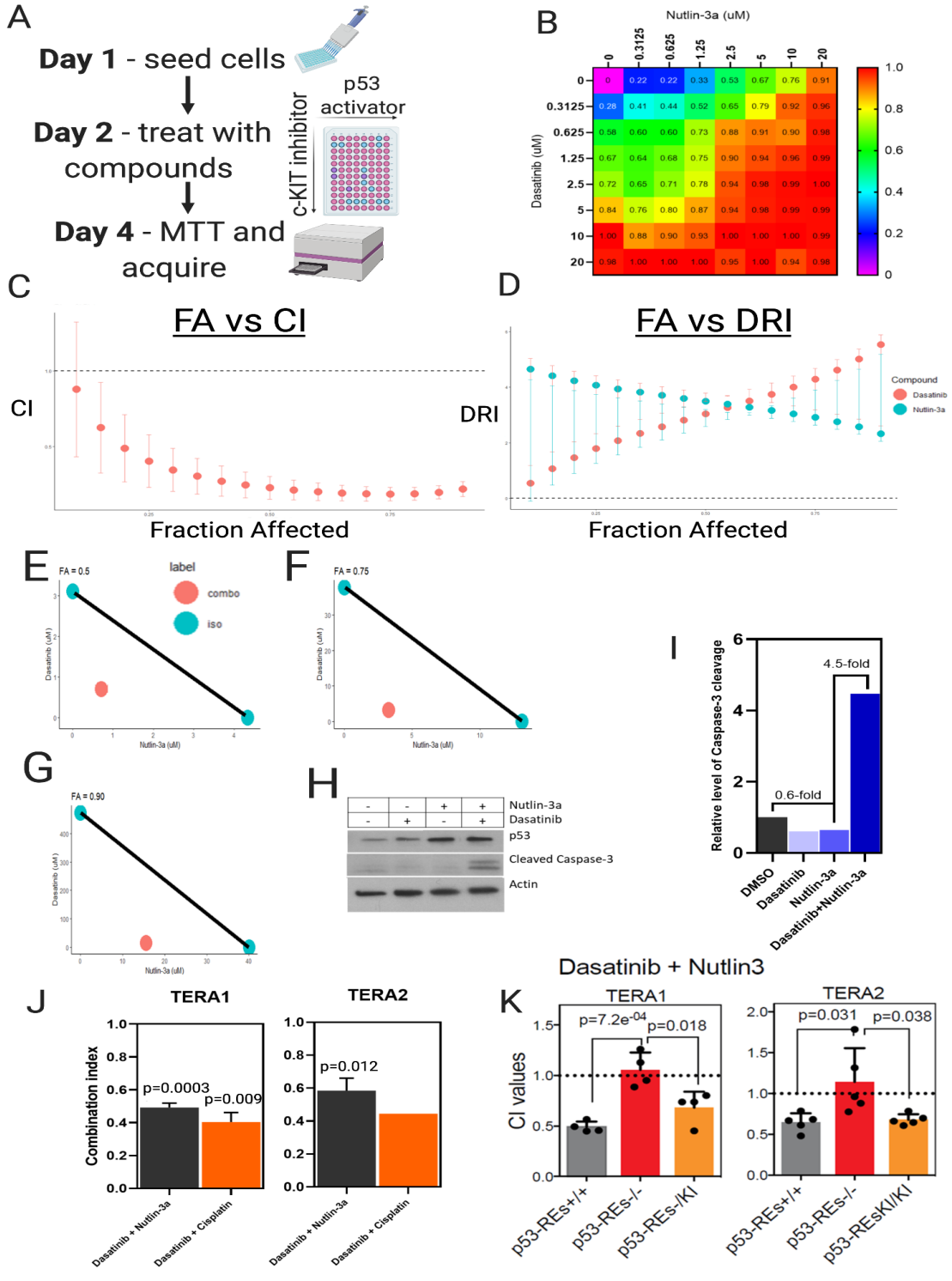


Figure 2.10

Figure 2.10: **A**) Cells were seeded in a 96well plate (4000-8000 per well, depending on the cell line) and were treated the following day. After 48hrs, cell viability was measured by MTT. **B**) A representative example of an 8x8 drug matrix to analyse the effects of Nutlin-3a and Dasatinib on the viability of TERA1 KITLG p53RE +/+ cells. The values indicate the fraction of cells affected after normalisation to the control wells.**C**) CI values for each level of effect were modeled using Compusyn. Error bars indicate the standard error of the mean across > 3 biological replicates in multiple clones. The dashed horizontal line indicates the additivity threshold (CI =1). **D**) DRI values for each level of effect were modelled using Compusyn. Error bars indicate the standard error of the mean across > 3 biological replicates in multiple clones. The dashed horizontal line indicates the additivity threshold (log2(DRI) = 0). **E-G**) Isobologram analyses for three different effect levels (FA = 0.5, 0.75 and 0.9). The two green points in each diagram indicate the concentration of each drug required to reach the respective effect level in isolation and are connected by the linear isobole; this isobole indicates the additive space within the graph. The area below the isobole indicates the synergistic space (CI < 1) and the area above indicate the antagonistic space (CI > 1). The red point indicates the concentrations of the two drugs required to reach the respective effect level in combination. The distance between the combination point and isolation points is representative of the DRI values. **H**) TERA1 KITLG p53RE +/+ cells were treated with DMSO, Nutlin-3a, Dasatinib or the Combo for 6hrs and caspase-3 cleavage was measured by immunoblotting. **I**) Quantification of the western blot in 10h using ImageJ. **J**) CI values for the combinations of Dasatinib and Nutlin-3a and Dasatinib and Cisplatin in multiple clones of TERA1 and TERA2 KITLG P53re +/+ cells. Statistical significance determined by One sample t-test (mu=1). **K**) CI values for Dasatinib and Nutlin-3a in TERA1 and TERA2 KITLG p53RE +/+, -/- and -/KI cells. The dashed horizontal line indicates CI=1. Statistical significance determined by Two sample Student T-test.

KITLG-p53RE +/+ TERA1 and TERA2 cells. A key factor in the heterogeneity in response to treatment for TGCT is the development of platinum-resistant disease. We reasoned that c-KIT inhibitors and p53 activators may still synergise in the refractory context and may even re-sensitise these cells to p53 activation. To test this, we utilised platinum-resistant TGCT cell lines. Two platinum sensitive embryonal carcinoma cell lines, GCT27 and Susa, were tested alongside their platinum-resistant clones, GCT27-CR and Susa-CR[262][263][264]. Firstly, we tested the sensitivity of the clones to p53 activation. GCT27, GCT27-CR, Susa and Susa-CR cells were treated with Nutlin-3a or Cisplatin for 48hrs. For Nutlin-3a, GCT27-CR cells were 2.8-fold more resistant ($p = 0.03$). For Cisplatin, GCT27-CR were 4.1-fold more resistant ($p = 0.0005$, Figure 2.11.A). Susa-CR cells were 2.8-fold more resistant to Nutlin-3a ($p = 0.039$) and 4.4-fold more resistant to Cisplatin ($p = 0.028$, Figure 2.11.B). We next explored whether combining the p53 activator with Dasatinib could overcome the resistance mechanisms evolved by the resistant cells (Figure 2.11.C). For the combination of Dasatinib and Nutlin-3a, synergy was found for all the cell lines (GCT27, CI = 0.67, $p = 0.0013$; GCT27-CR, CI = 0.40; Susa, CI = 0.56; Susa-CR, CI = 0.45, $p = <0.0001$). For the combination of Dasatinib and Cisplatin, synergy was found for both GCT27 and GCT27-CR (GCT27, CI = 0.11, $p <0.0001$; GCT27-CR, CI = 0.50, $p = 0.012$) while synergy was also found for Susa-CR (CI = 0.24, $p = 0.018$). Furthermore, the combinations of Dasatinib and Nutlin-3a

and Dasatinib and Cisplatin were tested in the intrinsically platinum-resistant cell line 2102EP. Synergy was found for both combinations (Dasatinib + Nutlin-3a, CI = 0.33, p = 0.0033; Dasatinib + Cisplatin, CI = 0.38, p = 0.023). These data indicate that c-KIT inhibition and p53 activators clearly synergise in platinum resistant TGCT cell line and suggest that c-KIT inhibitors might re-sensitise cells to p53 activators, including platinum-based therapies.

C-KIT inhibition and p53 activation synergises in the seminomatous cell-line TCAM2

This chapter has focused on elucidating the role of the KITLG-p53RE in response to p53 activating therapies in non-seminomatous TGCT cell lines. Non-seminomatous tumours make up 45% of Type II TGCT cases. To explore whether seminomatous tumours might also show synergy, we utilised the only seminomatous cell line established to date, TCAM-2. Firstly, the sensitivity of the TCAM-2 cell line to Nutlin-3a and Dasatinib was determined; although it is thought that seminomatous and non-seminomatous tumours are equally sensitive to chemotherapy, TCAM-2 was found to have higher IC50s for Nutlin-3a and Dasatinib compared to the non-seminomatous cell lines (Nutlin-3a, IC50 = 16.7uM; Dasatinib, IC50 = 27.8uM). For TCAM-2, a concentration range of 0.766uM to 50uM was used. Next, we investigated whether the KITLG-p53RE is functional in TCAM-2. TCAM-2 cells were treated with 10uM Nutlin-3a for 6hrs, lysed and the RNA fraction was extracted. qRT-PCR was used to determine the relative expression of KITLG, P21 and PMAIP1 in DMSO and Nutlin-3a treated cells. All three p53 target genes were induced by Nutlin-3a treatment, indicating that the KITLG-p53RE is functional in TCAM-2 (Figure 2.11.D).

We next explored whether Dasatinib could synergise with Nutlin-3a in this cell line. TCAM-2 cells were treated Dasatinib and Nutlin-3a for 48hrs. Significant synergy was found between the two compounds (CI = 0.50, p = 0.036, Figure 2.11.E). In addition, the synergy afforded a 4-5-fold reduction in concentration required to reach IC50 with DRI values of 4.9 and 4.1 bringing the concentrations required for IC50 to 4.45uM and 1.78uM for Dasatinib and Nutlin-3a respectively.

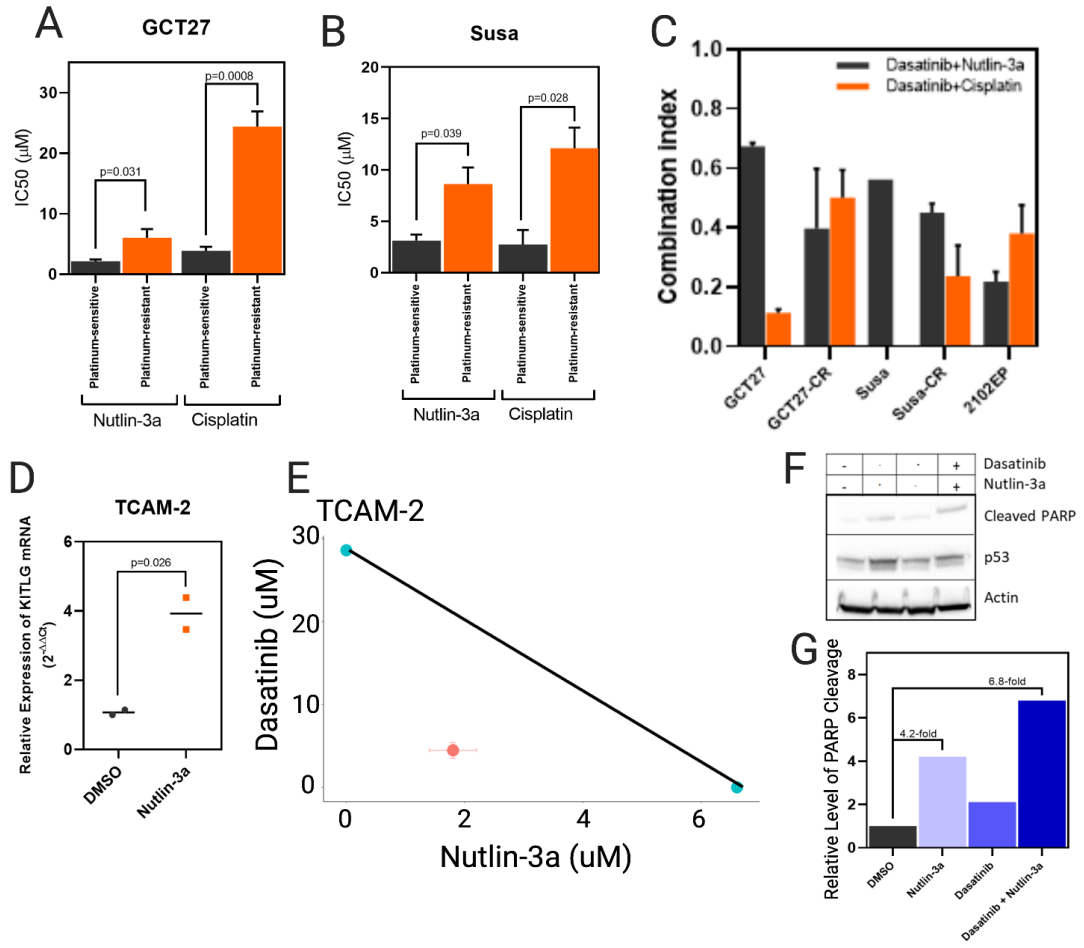


Figure 2.11: **A-B**) Platinum sensitive and resistant clones of GCT27 and Susa were treated with Nutlin-3a or Cisplatin (0.3125uM to 20uM) for 48hrs and IC50s were determined. Statistical significance determined by Two sample Student T-test. **C**) We determined the CI values for the combinations of Dasatinib+Nutlin-3a and Dasatinib+Doxorubicin for five TGCT cell lines including three platinum resistant cell lines (GCT27-CR, Susa-CR and 2102EP). Cells were treated for 48hrs after which cell viability was assessed by MTT assay. **D**) We determined the expression of KITLG mRNA after Nutlin-3a treatment (10uM, 6hrs) in TCAM-2 cells. Statistical significance determined by Two-sample student T test. **E**) Isobologram (described in 10E-G) for the combination of Dasatinib and Nutlin-3a in TCAM-2 cells. **F-G**) TCAM-2 cell treated with 10uM of Dasatinib and/or Nutlin-3a for 6hrs and PARP cleavage was analysed by immunoblotting. Actin was used as a loading control. The result of quantification of cleaved PARP by ImageJ is indicated in (G).

Finally, we checked to see if combining Nutlin-3a and Dasatinib in TCAM-2 cells resulted in greater apoptotic signalling. By western blot analysis, a greater degree of PARP cleavage could be determined in the combination treatment cells compared to Nutlin-3a and Dasatinib alone (1.6-fold compared to Nutlin-3a alone, Figure 2.11.F,G). These data demonstrate that coupling c-KIT inhibition and p53 activation could be leveraged for both Type II TGCT subtypes.

2.3.4 The combination of Dasatinib and Doxorubicin represents a novel, repurposing therapy for refractory TGCT

Dasatinib synergises with Topoisomerase inhibitors in a KITLG-p53RE dependent manner

In previous sections, we have established that KIT inhibition synergises with p53 activation in TGCT. We next focused on finding a suitable, already approved p53 activator. Multiple MDM2 inhibitors are in phase one clinical trials but none are clinically approved (Zhao, et al., 2015) (Azizi, et al., 2011) (Siu, et al., 2014). TGCT patients are routinely prescribed platinum-based therapies at high dosage so we aimed to repurpose a different p53 activator. We previously established that KITLG-p53RE -/- cells were more sensitive to topoisomerase inhibitors compared to KITLG-p53RE +/+ and -/KI cells. In order to fit within our framework of drug repurposing, we aimed to determine whether KIT inhibition synergised with 3 approved topoisomerase inhibitors, Doxorubicin (Topoisomerase II), Campthothecin and its derivative Topotecan (Topoisomerase I, Figure 2.12.A).

To test this, we utilised the CI method as described previously to determine the IC50s for the compounds in isolation and in combination. Strong synergy was found for both TERA1 and TERA2 KITLG-p53RE +/+ cells with CI < 1 for Dasatinib plus Topotecan (TERA1: CI = 0.27; TERA2: CI = 0.72), Doxorubicin (TERA1: CI = 0.50; TERA2: CI = 0.43) and Camptothecin (TERA1: CI = 0.28; TERA2: CI = 0.70) (Figure 2.12.B). Importantly, the synergy between Dasatinib and the Topoisomerase inhibitors was dependent on the p53/KITLG axis as reduced synergy was detected in KITLG-p53RE -/- cells for Topotecan (TERA1: CI = 1.65; TERA2: CI = 1.03), Doxorubicin (TERA1: CI = 3.29; TERA2: CI =) and Camptothecin (TERA1: CI = 0.97; TERA2: CI = 2.78) (Figure-12B). As for the combination of Dasatinib and Nutlin-3a, the synergy between Dasatinib and Doxorubicin could be rescued by the knock-in TERA1 (compared to -/-, p = 0.027) and TERA2 (compared to -/-, p = 0.032) cells (Figure 2.12.C). These data indicate

that the c-KIT inhibitor, Dasatinib, interacts synergistically with Topoisomerase inhibitors, in a way that is dependent on the p53/KITLG axis.

Dasatinib synergises with Doxorubicin in platinum-resistant TGCT cell lines

For future experiments we decided to focus on Doxorubicin as our p53 activating compound as the toxicity of combining Dasatinib with Doxorubicin in humans has already been profiled; Dasatinib was tested in combination with hyper-CVAD (hyperfractionated cyclophosphamide, Adriamycin (Doxorubicin), Vincristine and dexamethasone) in Philadelphia Chromosome positive Acute Lymphoblastic Leukaemia (Ph +ve ALL) (Ravandi, et al., 2010) (Benjamini, et al., 2014). We tested the combination of Dasatinib + Doxorubicin in a panel of TGCT cell lines including cisplatin-sensitive cells lines (GCT27 and GH) and cisplatin-resistant cell lines (SusaCR, GCT27CR and 2102EP). Importantly, we found synergy for the combination of Dasatinib and Doxorubicin in both cisplatin-sensitive cell lines (GH: CI = 0.46; GCT27: CI = 0.58) and cisplatin resistant cell lines (2102EP: CI = 0.15; SusaCR: CI = 0.17; GCT27CR: CI = 0.54) (Figure 2.12.D). Moreover, the combination of Dasatinib and Doxorubicin was also synergistic in the seminomatous cell line TCAM2 (Figure 2.12.D).

The combination of Dasatinib and Doxorubicin exerts a strong anti-tumour response in a murine xenograft model of refractory TGCT

The combination of Dasatinib and Doxorubicin confers greater anti-tumour efficacy compared to either compound alone. Having found evidence of synergy between Dasatinib and Doxorubicin in cisplatin-sensitive and resistant cell lines, we next tested this combination a murine xenograft model of cisplatin- resistant disease. 2102EP cells were injected subcutaneously and allowed to develop tumours, approximately 130mm3. Mice were separated into four groups; vehicle, Dasatinib only, Doxorubicin only and Dasatinib + Doxorubicin. They mice were treated over 12 days with tumour volume measured daily. Consistent with the observations made in cell culture, treatment of mice engrafted with 2102EP cells revealed stronger

anti-tumoral effects with the Dasatinib + Doxorubicin combination relative to single drug treatments ($p = 0.0077$ versus the Dasatinib group, $p=0.018$ versus the Doxorubicin group; Figure 2.12.E). Importantly, the regime was well tolerated by the mice with no bodyweight loss over the experiment.

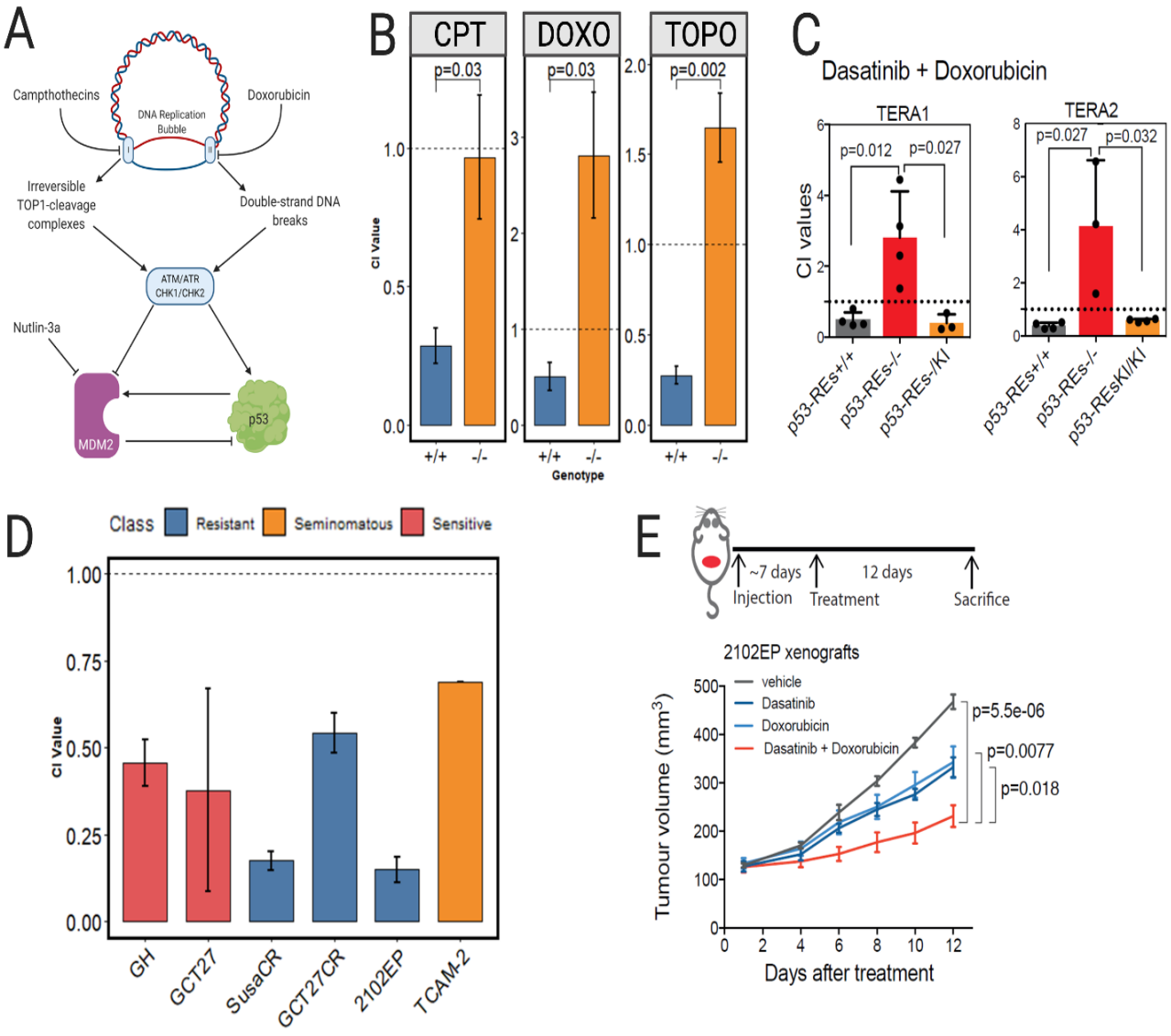


Figure 2.12: **A**) Schematic highlighting how p53 can activated by DNA damage induced by inhibition of Topoisomerases I and II. Topo I relieves DNA torsion by nicking the DNA and forming a complex with the free strand (TOP1-cleavage complex). The nicking allows release of torsion and supercoiling before the nicked strand is re-ligated. Inhibition of Topo I by campthothecins involves stabilising the TOP1-cleavage complex and preventing re-annealing of the nicked DNA strand. Topo II releases supercoiling by generating double strand breaks and unwinding the DNA by an ATP dependent mechanism. Inhibition of Topo II by compounds including Doxorubicin and etoposide leads to unrepaired double strand breaks. Both types of DNA damage lead to activation of ATM/ATR and CHK1/2 which in turn can activate p53 directly by phosphorylation and indirectly by inhibiting MDM2. **B**) CI values were determined for the combinations of Dasatinib (0.325uM to 20uM) with either CPT, Topotecan or Doxorubicin (0.03125uM to 2uM) in TERA1 KITLG P53re +/+ and -/- cells. Statistical significance determined by Two sample Student T-test. **C**) TERA1 and TERA2 cells KITLG-P53re +/+, -/- and -/KI cells were treated with Dasatinib, Doxorubicin or the combination of the two for 48hrs and CI values were calculate. Statistical significance determined by Two sample Student T-test. **D**) CI values were calculated for Dasatinib and Doxorubicin in other TGCT cell lines including platinum resistant cell lines and the seminomatous cell line TCAM-2. **E**) We examined the efficacy of Dasatinib+Doxorubicin in a murine xenograft model of cisplatin-resistant TGCT. 2102EP cells were injected sub-cutaneously and allowed to grow into tumours of roughly $130mm^2$. Mice were treated with either the vehicle, Dasatinib (25mg/kg), Doxorubicin (4mg/kg) or Dasatinib+Doxorubicin and tumour volume was measured over 12days.

2.4 Discussion

2.4.1 Summary

In this chapter, we have discussed the work undertaken to provide a proof of principle study to show that cancer susceptibility loci can inform novel cancer therapeutics. We hypothesised that the KITLG-p53RE genetically links the tumour suppressive, anti-survival p53 pathway to the tumour promoting, pro survival c-KIT signalling pathway (Figure 2.3.D). We have provided three separate methods of inhibiting the p53/KITLG/KIT axis which heighten sensitivity to p53 activation, c-KIT knockdown by siRNA, deletion of the KITLG-p53RE by CRISPR-Cas9 and pharmacological inhibition of c-KIT. These data have led to the development of a novel therapeutic strategy to take advantage of the synergy between inhibition of the p53/KITLG/KIT axis and p53 activation. We showed that the combination of Dasatinib and Doxorubicin is synergistic in cisplatin-sensitive and resistant TGCT cell lines, in non-seminomatous and seminomatous cell lines and in a murine xenograft model of cisplatin-resistant TGCT. This therapeutic opportunity could be useful for managing platinum-resistant TGCT patients.

2.4.2 Platinum-Resistant TGCT is an increasingly urgent and unmet clinical need

The epidemiology of TGCT is quite distinct compared to other malignancies. With the exception of paediatric cancers and inherited cancer syndromes, most cancers tend to develop later in life[265]. However, the mean age of incidence for TGCT is only 36yrs[266][267] (Figure 2.13). Indeed, TGCT is the most common cancer among young men between the ages of 15 and 45 [268]. Moreover, the incidence of TGCT is rising, approximately doubling in Western European countries in the last 40 years cumulating in over 18,000 new cases a year in Europe[269][270].

Over 80% of TGCT patients can be cured with chemotherapy, leading TGCT to be considered a paradigm for curative cancer. However, these therapies are also associated with metabolic syndromes, male infertility, psychological issues and secondary cancers[271][272][273] [274]. Furthermore, those patients who develop

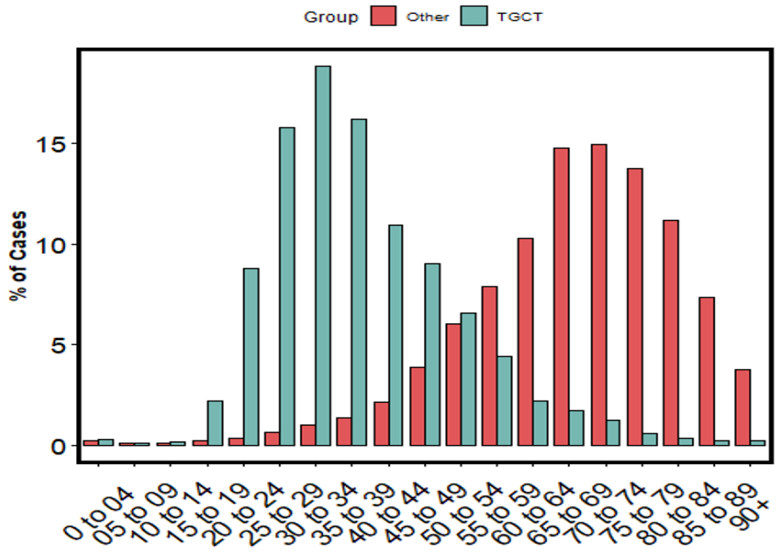


Figure 2.13: TGCT is an early onset cancer. The bar chart indicates the % of total cases belonging to each age group bin for TGCT in grey and other cancers in red. The histograms show very different profiles with TGCT peaking in the early to mid 30s and other cancers in the late 60s and 70s.

treatment-resistant, refractory disease have a much poorer outlook with only 10-15% of these patients surviving beyond 5yrs[275]. The alternative option is radical surgery and where this is not possible, patients are unlikely to be cured[276][277]. Despite intensive research into the mechanisms underpinning resistance and relapse, new therapies have not been forthcoming. It is imperative that new therapies are developed to both treat refractory patients and to mitigate adverse effects of current treatments among survivors.. This is particularly crucial given the increasing incidence of TGCT. In this Chapter we explored the therapeutic potential of targeting the p53/KITLG axis. Three methods of inhibiting the p53/KITLG/KIT axis enhanced sensitivity with p53 activation. These data suggest that cotreatment of refractory TGCT tumours with a KIT inhibitor such as Dasatinib and a p53 activating therapy may be a promising therapeutic avenue.

2.4.3 Cancer-susceptibility loci may provide insights into chemoresistance

TGCT is also a well-studied model for chemoresistance[275]. Several mechanisms have been postulated to explain chemoresistance in TGCT: mismatch repair (MMR) defects; cellular differentiation and reduced Oct4 expression; indirect mitigation

of p53 signalling, aberrant methylation patterns and activation of the PI3K/AKT signalling pathway[206][216]. The fact that TGCTs very rarely mutate p53 means the induction of KITLG expression in TGCT cells would be retained, possibly providing a mechanism behind the activation of PI3K/AKT signalling (which can be activated by c-KIT) previously reported in refractory TGCT. This is in line with our findings that inhibition of the p53/KITLG/KIT axis boosts sensitivity to p53 activation. Chemoresistance is one of the key reasons behind treatment failure across a broad range of cancers other than TGCT and is a major obstacle that current cancer research must overcome. The data presented in this chapter suggests that GWAS susceptibility loci could inform novel molecular mechanisms of chemoresistance in tumours. Indeed, cancer-associated genes (CAGs) have been shown to regulate drug response across tumours and cell lines[278][279][280]. For example, a SNP at the DDFB locus, encoding a subunit of the DDF complex which fragments DNA during apoptosis, was found to associate with response to cytotoxic therapy in breast cancer patients[280].

2.4.4 The emerging pro-survival role of p53

The p53 protein was first discovered in 1979, first cloned in 1983 and first thought of as a tumour suppressor in 1989; and yet, despite four decades of research, groups around the globe are still discovering novel and surprising attributes of p53[281]. The pro-survival function of p53 is emerging as a promising opportunity to boost p53-dependent cell death. Upon activation, p53 induces expression of a raft of target genes which arrest the cell cycle and promote DNA repair but do not stimulate cell death. In fact, some of these target genes, such as SFN, Rap2b and CDKN1A, can actively repress apoptosis[282][283][284]. However, our data highlights that the p53/KITLG/KIT axis represents a clearer pro-survival signal which promotes cell cycle progression and cell survival in TGCT. P53 is thought to be important in maintaining germ cell quality during spermatogenesis with very high levels of wild-type p53 in transgenic mice leading to small numbers of spermatozoa[215]. However, our data suggests that the p53/KITLG/KIT axis could deregulate this quality

control mechanism and protect aberrant germ cells from apoptosis. Interestingly, testicular cancers very rarely mutate p53; perhaps the p53/KITLG link reduces the selection pressure for testicular cancer cells to mutate the p53 gene, a possible example of where the inherited genetics can shape the somatic development of the tumour[285][286]. It will be interesting to explore whether the p53/KITLG/KIT axis could be targetable in other cancer types. Moreover, it raises the question of what other p53 target genes could exert negative feedback on p53 signalling and be druggable, like the p53/KITLG/KIT axis.

2.4.5 Polymorphic p53 response elements and disease

In this chapter, we demonstrated that the KITLG-p53RE-SNP can directly affect KITLG expression levels and that changes in KITLG expression manifested as differences in chemosensitivity. The identification of the KITLG-p53RE-SNP by Zeron-Medina et al (2013) was one of the first indications that polymorphic p53 response elements might contribute significantly to disease[176]. In the years since that publication, a handful of other polymorphic response elements have been reported. Wang et al (2014) analysed expression quantitate trait loci (eQTLs) at p53 response elements from bronchial epithelial cells from cigarette smokers[287]. They identified rs10993994 at the MSMB gene to associate with prostate cancer risk; a later study found that deleting one copy of the locus in LNCaP cells, heterozygous for the SNP, significantly affected MSMB expression and modestly affected expression of 3 other nearby genes[288]. The KITLG-p53RE-SNP has linked the p53 and c-KIT pathways in our work; likewise, a previous study utilised polymorphic response elements to link p53 and the VEGF pathways[289]. They found allelic differences in expression of the FLT1 gene (encoding a VEGF receptor) after p53 activation and later showed that control of FLT1 expression was dependent on both p53 and estrogen receptor[290][291]. This interaction between p53 and FLT1 may be important for angiogenesis-associated diseases and cancer; although, in contrast to our work, the FLT1 p53RE SNP is not associated with disease in GWAS.

SIRT1 is a well-established p53 target gene which is important in sensing nutrient deprivation. Naqvi et al (2010) identified a polymorphic p53 response element at the SIRT1 gene whereby the C allele of the SNP reduces p53 binding compared to the T allele[175]. They show that the C allele for worse p53 binding associates with reduced expression of SIRT1 target genes such as AMPKa2 indicating that the effect of p53RE SNPs is not limited to nearby genes but indeed can be propagated through the complex biological network. More recently, the same SNP, rs3758391, has been linked to risk of diffuse large B cell lymphoma in the Chinese Han population[292][293].

Shao et al (2019) explored a SNP affecting the complex interaction between p53 and TNFRSF19 in response to pulmonary carcinogens[294]. The risk alleles reduced chromatin looping and reduced p53-dependent upregulation of TNFRSF19, suggesting a tumour suppressive function for TNFRSF19 in lung cancer cells. This is a very good example of cancer susceptibility loci facilitating the discovery of new biologically relevant links and tumorigenic mechanisms.

The concept of immunotherapy has become of great interest in oncology. A recent publication has potentially linked polymorphic p53RE's and immunotherapy. Menendez et al (2019) identified a polymorphic p53RE at the TLR8 gene whereby highly linked SNPs associate with several infectious diseases[295]. They demonstrate allelic differences in TLR8 expression in response to p53 activation and that the TLR8 response is amplified by p53 activation. TLR8 activation can promote the activity of immune effector cells such as natural killer cells and they therefore postulate that combining p53 activation with TLR8 agonists may add another tool to the expanding immunotherapy arsenal.

Together with our work, these studies provide evidence that germline variants in p53RE's can contribute to disease; however, our work is unique in that the KITLG-p53RE-SNP has identified a novel and druggable therapeutic opportunity in cancer.

2.4.6 Estimating and predicting synergistic drug combinations

In this chapter, we determined that inhibition of the p53/KITLG/KIT axis synergised with p53 activation in TGCT cells. Here, we use the term synergistic in its strict sense whereby the interaction between two drugs is synergistic if the combined effect is greater than the additive effect when both drugs are used in isolation[258]. The Combination Index (CI) method of Chou-Talalay was used to determine synergistic interactions[296]. Multiple different models have been published to model the synergy between compounds. Early models included Bliss Independence[297], Loewe[298]) and the Highest single agent (HSA) while more recently, the Equivalent Dose Model[299]; the Partial Differential Equation -Hill model[300]; the Zero Interaction Potency model (ZIP)[301]; the Bivariate Response to Additive Interacting Doses (BRAID)[302] and multi-dimensional synergy of combinations (MuSyC)[303]. The foundations of all the models relies on one of two principles; the Dose Equivalence Principle (DEP) and the Multiplicative Survival Principle (MSP). The DEP was proposed by Loewe and asserts that two drugs are additive if the effect of reducing the concentration of one drug can be compensated by combining a second drug. Departure from this indicates synergy or antagonism. The MSP was suggested by Bliss and assumes the probability of being unaffected by the two drugs individually is independent. Therefore, by the MSP, the probability of being unaffected by the combination is the product of the two individual probabilities. Deviation from this proportion indicates synergy or antagonism. DEP models are dose-effect based strategies and quantify synergistic potency while MSP models are effect-based and quantify synergistic efficacy. Many studies have noted that these two principles are difficult to reconcile and often contradictory[304][305][306][307]. Most of the aforementioned models do not distinguish between potency and efficacy. The CI method can model efficacy and potency to some degree by the CI and DRI values, respectively. However, these values are linked and are not modelled separately. MuSyc is the most recently developed model and decouples synergistic efficacy and synergistic potency and show that some drug combinations can affect

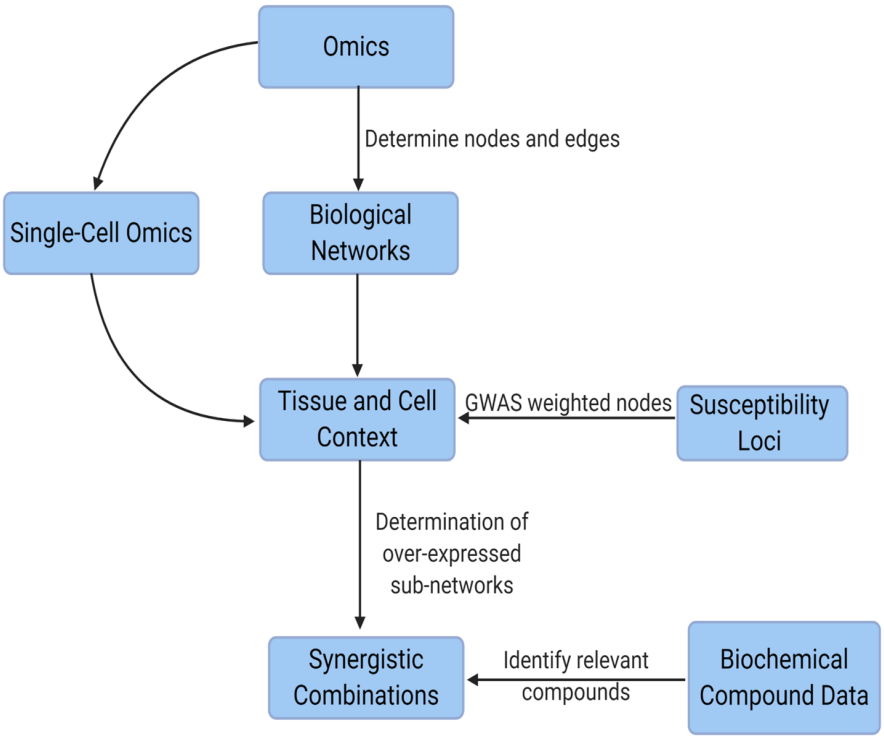


Figure 2.14: A model for how context specific synergistic drug combinations might be predicted using biological networks developed from relevant omics datasets and disease susceptibility loci from GWAS studies. Deep omics datasets can be used to build biological networks whereby nodes are genes/proteins and edges are interactions between them. It is important to understand the differences in the network between cell types; single cell omics can address such questions. Biological networks can be used to predict synergistic combinations by identifying over expressed sub-networks. It is possible that germline susceptibility loci could be used to weight nodes in order to make more accurate predictions of functional and important sub-networks. Once targetable pathways have been identified, one can screen against available compound databases to identify candidate inhibitors.

one and not the other. It will be interesting to see how this model is applied over the next few years and if it becomes a cornerstone of developing new combination therapies. However, at this time, the Chou-Talalay CI method remains the gold standard for determining synergistic interactions between compounds and is widely accepted in the field, particularly for mechanistic and clinical research whereby well supported dose-response curves can be generated as is the case for the data presented in this chapter[308].

Identifying compounds which interact synergistically is imperative for modern oncology, both to improve efficacy and to resolve therapy-associated toxicities. Such combinations can be identified empirically by high-throughput screens either of compounds or by dual CRISPR-Knockout screens. However, these large-scale experiments are costly, time consuming and generate a huge amount of negative

data. For example, a CRISPR Dual Knock out library generated by Han et al (2017) screened 21,321 drug target pairs[309]. From this, they discerned only 6 synergistic interactions (0.03%). The vast majority of dual knockouts did not produce a synergistic effect, likely to do the fact that the majority of the gene pairs are largely separated in the gene network. Indeed, multiple studies have noted that synergy is enriched in drug combinations whereby the drug targets are neighbours in the underlying biological networks[310][311]. In silico screens may be primed to uncover such combinations and effectively predict which compounds might synergistically interact[312][313][314][315]. For example, c-KIT and p53 are linked in the biological network by the KITLG-p53RE and so inhibitors of c-KIT and activators of p53 might be predicted to synergise. However, this approach relies upon well supported edges between nodes in the network; some drugs may synergise, but links have not yet been drawn between the two drug targets. Furthermore, synergy between two compounds may be tissue or cell-type specific. Some cancers do not express c-KIT and thus combining c-KIT inhibitors and p53 activators in these cases would likely prove futile. Transcriptomic data may be one way to bypass such issues; indeed multiple computational methods and machine learning algorithms have been employed to predict drug synergy from expression data after treatment[316][317]. One such algorithm, DeepSynergy, utilised deep learning and can predict synergy between known compounds in cell lines based solely on transcriptomic data and chemical information about the compounds, thus removing the complexity of interpreting drug response curves[318]. Interestingly, Dasatinib was predicted to synergise with carboplatin (platinum-based compound) and SN-38 (Topoisomerase I inhibitor), both of which activate p53[319][318][320].

There is evidence to suggest that cancer-susceptibility loci may be useful for predicting synergy. Firstly, genes associated with disease in GWAS are enriched for druggable genes while druggable and GWAS genes are also closer together in the biological network compared to randomised genes[321][322]. Causal SNPs may identify genes and/or pathways which are important for disease aetiology and may therefore indicate in which cells and tissues two drugs might synergise. In the case

of the KITLG-p53RE-SNP it directly links p53 activity to KITLG expression and c-KIT signalling, adding a new edge to the biological network, and indicates that this link may be important for the development of TGCT. It would be interesting to examine the benefits of combining information about cancer-susceptibility loci with transcriptomics for the purpose of predicting synergistic combinations; it is possible that weighting some nodes of the transcriptomic network based on inherited genetic data might improve the ability of algorithms to distil complex expression data into key druggable pathways to which the cancer may be 'addicted' to (Figure 2.14). The data presented in this chapter serves as proof-of-principle that cancer-susceptibly locus can inform a novel synergistic drug combination by identifying contextually important genes and pathways which are closely connected in the biological network. Future high-throughput computational studies aiming to predict synergistic combinations should take germline variants into account.

3

Investigating the mechanism of the synergy between inhibition of p53-mediated KITLG/KIT signalling and p53 activation in TGCT

Contents

3.1 Abstract 71
3.2 Introduction 72
3.2.1 Proof-of-mechanism is important for improving the approval rate of novel therapies 72
3.2.2 Downstream signalling from KITLG/KIT is complex and can vary between tissues 72
3.2.3 P53 can mediate both extrinsic and intrinsic apoptosis pathways 76
3.2.4 Hypothetical integration points between KITLG/KIT and p53 signaling 77
3.2.5 Multi-omics data for uncovering novel cancer biology . . 78
3.3 Results 80
3.3.1 The synergy between Dasatinib and Nutlin-3a is dependent on p53 80
3.3.2 Investigating the role of p53 activity in the synergy between KIT inhibition and p53 activation 82
3.3.3 Investigating the mechanism of signal transduction from KITLG/KIT in TGCT 98
3.3.4 Clinically relevant gene modules in TGCT are enriched for PI3K/AKT/mTOR genes 106

3.3.5 PI3K/AKT/mTOR is a potential therapeutic target in TGCT 114
3.3.6 BCL2 family factors integrate signals from pro-survival KITLG/KIT and apoptotic p53 signalling 120
3.4 Discussion 129
3.4.1 KITLG/KIT does not regulate p53 expression levels or transcriptional activity 130
3.4.2 Signalling from p53 and KITLG/KIT could integrate through control of mitochondrial apoptosis 131
3.4.3 PI3K/AKT/mTOR signalling is key to pro-survival signalling from KITLG/KIT in TGCT 134
3.4.4 AKT inhibitors as promising anti-cancer therapies . . . 136

3.1 Abstract

In Chapter 2, we identified a novel negative feedback loop involving p53 and KITLG/KIT signalling in TGCT cells. We demonstrated that this loop could be a novel therapeutic opportunity for platinum-resistant TGCT through inhibition of the pro-survival KITLG/KIT signalling and activation of canonical, anti-survival p53 signalling. A key predictor of efficacy and approval of new therapies is proof-of-mechanism. In this Chapter, we utilise multi-omics datasets to identify the underlying mechanisms of the synergy between KITLG/KIT inhibition and p53 activation. We demonstrate that p53 expression and transcriptional activity does not explain the synergy. However, we find evidence that the PI3K/AKT/mTOR pathway acts downstream of the KITLG/KIT and that this signal transduction axis could integrate with pro-apoptotic p53 signalling at the level of BCL2 family factors, key mediators of mitochondrial apoptosis.

3.2 Introduction

3.2.1 Proof-of-mechanism is important for improving the approval rate of novel therapies

Targeted or precision chemotherapeutics have become more frequent and are associated with high objective response rates (ORR) in particular patient groups[323][324]. For example, larotrectinib which inhibits tropomyosin kinase receptors (TRKs), was found to have an ORR of 75% in cancer patients with TRK fusions[325]. Individualised, N-of-one treatment strategies have also indicated promising results[37][36]. The WITHERS trial recommended treatment based on DNA sequencing and RNA expression for 107 patients with an ORR of 26%[38]. Personalised therapies require identifying novel targets and developing novel compounds. A major hurdle is the negative trend in the approval rates of new drugs per year in recent times, driven by high rates of attrition of compounds in the drug discovery pipeline[326][327][42]. Lack of efficacy and drug related toxicity underpin attrition and could be improved by proof-of-mechanism; mechanistic insights could enable prediction of toxicity, identification of biomarkers and highlight potential combinatorial therapies[42][328][329][330][331][332][333][334]. In this Chapter, we aim to unravel the molecular mechanism(s) underpinning the synergy between inhibition of KITLG/KIT and p53 activation in TGCT cells.

3.2.2 Downstream signalling from KITLG/KIT is complex and can vary between tissues

C-KIT is activated by binding of KITLG and can promote various signalling pathways (Figure 3.1)[335]. The Src family of Tyrosine Kinases (SFKs) are important in mediating downstream c-KIT signalling and includes eight cytoplasmic kinases, three of which are ubiquitously expressed (Src, Yes and Fyn). The SFK SH2 domain is recruited to the intracellular juxtamembrane domain of the c-KIT, leading to displacement of the inhibitory COOH domain[336]. SFKs have been implicated in protection from apoptosis and promoting cell migration and proliferation[336][337][338]. Some of these effects may come from the ability of

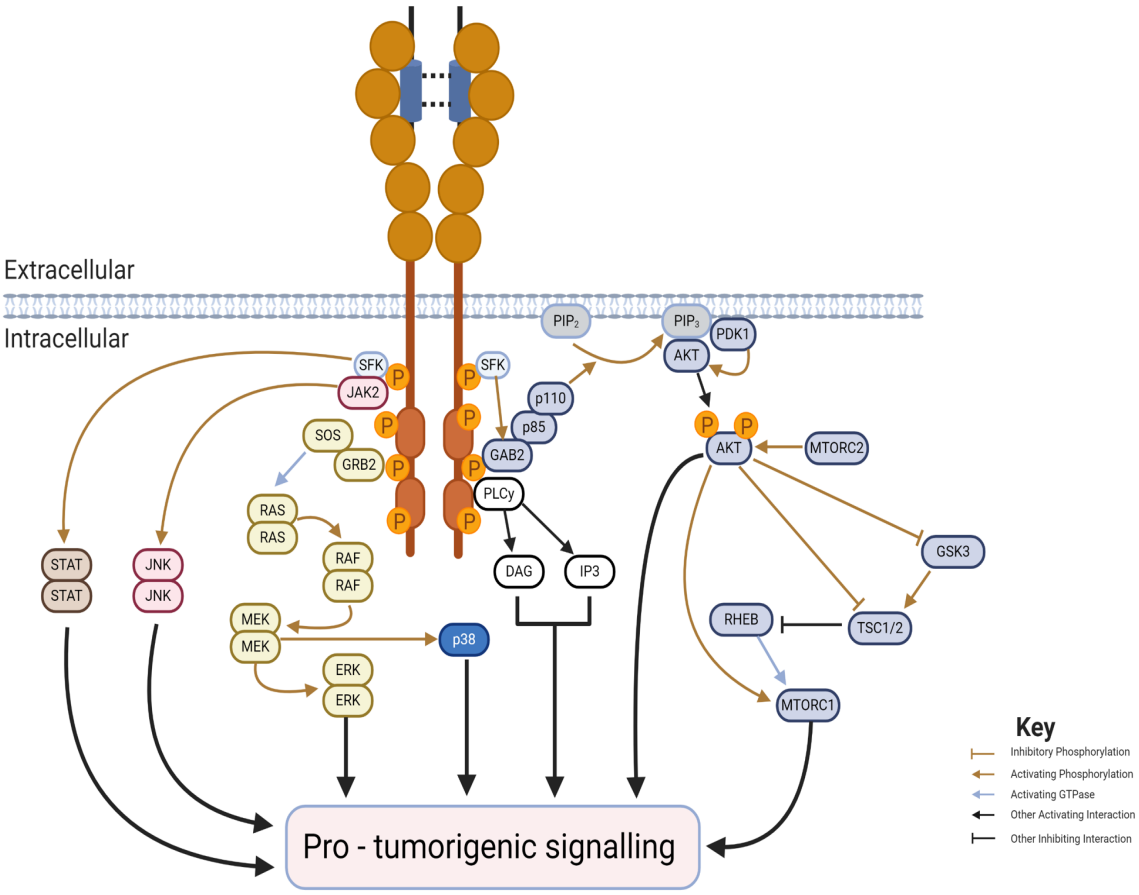


Figure 3.1: Downstream signalling from c-KIT is diverse and complex. Binding of KITLG to two c-KIT monomers causes conformational changes which bring the intracellular domains of c-KIT closer together and promotes autophosphorylation. This opens up binding sites for signal transduction molecules including SFKs which can trigger signal transduction through downstream pathways. SFKs and GAB2 bind activated c-KIT and promote activity of PI3K kinases. These kinases generate PIP3 from PIP2 on the cellular membrane, leading to recruitment of PDK1 and AKT. PDK1 phosphorylates AKT which can then phosphorylate target proteins such as GSK3 and TSC1/2, leading to mTORC1 activation. This is the basis of the PI3K/AKT/mTOR pathway which is coloured in light blue. GRB2 and SOS are important adaptor proteins which activate RAS/ERK signalling after c-KIT activation. They activate RAS proteins which dimerise and activate RAF proteins. RAF proteins activate MEK which in turn activates ERK. ERK dimers can trigger expression of genes to promote cell survival and proliferation. The RAS/ERK pathway is coloured yellow. The RAS/ERK pathway can also activate p38 (dark blue) which in some contexts acts to promote pro-tumour signalling but can also be important in triggering apoptosis in other contexts. JAK2 can bind active c-KIT and promotes activation of JNK (pink). SFKs are important in transducing signalling from c-KIT to various STAT family proteins (brown). Finally, c-KIT can bind PLC? which in turn releases DAG and IP3 (white). This figure has been adapted from Babaei *et al* 2016[341].

SFKs to activate signalling through other well documented pro-survival pathways such as PI3K/AKT/mTOR and RAS/ERK[336][339][340].

PI3K/AKT/mTOR

PI3K/AKT/mTOR is a key signalling pathway in cells, which inhibits apoptotic signalling and promotes survival and proliferation[342]. Unsurprisingly, this pathway

is frequently altered in cancer by activating mutations, overexpression of oncogenes, inactivating mutations or deletion of tumour suppressors[343]. When c-KIT is activated by KITLG, PI3K is recruited by binding of the SH2 domain of the p85 subunit to phosphorylated Tyr-721 in the kinase insert domain[344]. Activated PI3K can convert phosphatidylinositol 4,5-bisphosphate (PIP2) to phosphatidylinositol 3,4,5-trisphosphate (PIP3) which acts as a secondary messenger to recruit AKT and PDK1 via their pleckstrin homology (PH) domains[345]. PDK1 activates AKT by Thr-308 phosphorylation in the activation loop; AKT T308 can then be further activated by phosphorylation of Ser-473 by mTORC2 in the regulatory COOH domain[346][347]. Activated AKT phosphorylates many downstream targets to either inhibit their anti-survival function or promote their pro-survival function[335]. One such target is mTORC1; a complex composed of mTOR, Raptor, mLST8, PRAS40 and Deptor. mTORC1 is activated by the GTPase Rheb which is in turn negatively regulated by the TSC1/TSC2 complex. AKT can promote mTORC1 activity by phosphorylating three different targets: TSC1, GSK3 (an activator of TSC1) and PRAS40[348]. Active mTORC1 regulates autophagy and protein synthesis[348]. KITLG/KIT signalling has been shown by multiple studies to activate AKT and mTOR[349][350][351][352]. AKT can also regulate p53 levels and activity by modulating MDM2 activity. AKT has been shown to phosphorylate Ser183 of MDM2 which stabilises nuclear MDM2 and reduces p53 protein levels [353][354]. However, other studies have provided evidence showing constitutive AKT activation to inhibit MDM2 activity and promote p53-dependent senescence through regulation of the NPM/ARF MDM2-inhibitory complex [355][356].

RAS/ERK

The RAS/ERK pathway is a MAPK signalling cascade which is important for promoting cell proliferation and is frequently over-activated in cancer[357]. Three layers of kinase interactions transduce the signal from the plasma membrane to the nucleus. Upon c-KIT activation by KITLG, GRB2 is recruited with the Guanine Exchange Factor (GEF), Sos. Sos promotes exchange of GDP to GTP for the

Ras family GTPases (NRAS, HRAS and KRAS). The GTP-bound RAS proteins activate the downstream RAF effectors (CRAF, BRAF and ARAF)[358]. Active RAF dimers target MEK proteins by forming MEK:RAF:RAF:MEK tetramers and phosphorylating serine residues[359]. MEK activates ERK1/ERK2 dimers which translocate to the nucleus and modulate transcription factor activity[360]. KITLG/KIT signalling has been well established to promote phosphorylation of ERK1/ERK2[361][336][362].

JAK/STAT

The JAK/STAT pathway can be triggered by dimerization of cytokine JAK receptors but cytoplasmic STATs can also be activated by SFKs. There are seven mammalian STATs and all are transcription factors. Upon phosphorylation, they dimerize and translocate into the nucleus whereby they can modulate the expression of target-genes[363]. KITLG/KIT promotes dimerization of JAK2 but can be tissue specific[364][365].

Other

KITLG/c-KIT signalling has also been linked with two further MAPK cascades, p38 signalling and JNK signalling, and phospholipase C-γ (PLCγ)[366][367]. JNK dimers are activated by upstream kinases and can then migrate to the nucleus where they regulate multiple transcription factors including c-jun. p38 MAPK can be triggered by RTKs including c-KIT and once active can target many proteins to regulate pro- and anti-survival signalling[368][369]. Some studies have shown stimulation of PLCγ after KITLG stimulation and found this interaction can protect against apoptosis[370][371].

The dominant signalling pathway downstream of KITLG/KIT can vary depending on the cell type. For example, in myeloid progenitor cells, KITLG/KIT signalling has been shown to promote cell survival via PI3K/AKT but not by the RAS/ERK pathway[372]. In contrast, both PI3K/AKT and RAS/ERK are triggered by KITLG/KIT in cortical neurons while Hong et al (2004) highlighted

SFKs to be the key downstream factors in two haematopoietic cell lines[361][349] . In this Chapter, we aim to discern the key downstream pathway(s) in TGCT.

3.2.3 P53 can mediate both extrinsic and intrinsic apoptosis pathways

In Chapter Two, we identified that c-KIT inhibition and p53 activation have a synergistic effect on cell death which was associated with higher levels of cleaved caspase-3, indicating apoptosis. Apoptosis can be extrinsic, via activation of death receptors such as Fas and DR5, or intrinsic which involves depolarisation of the mitochondria and release of cytochrome C (Figure 3.2).

The extrinsic apoptosis pathway involves stimulation of death receptors on the plasma membrane; for example, the Fas receptor is stimulated by FasL and DR5 by TRAIL. Upon ligand binding, the Fas-associated death domain (FADD) is recruited along with caspase-8. Activation of caspase-3 triggers a caspase cascade and apoptosis[373]. P53 can mediate extrinsic apoptosis by inducing expression of death receptors including Fas and DR5. In addition, p53 can increase the expression of Fas by promoting trafficking from the Golgi[374].

The intrinsic apoptosis pathway involves stimulation of cell death through internal signals such as genotoxic stress and like the extrinsic pathway, results in a caspase-cascade. The key trigger for intrinsic apoptosis is mitochondrial outer membrane permeabilization (MOMP). If MOMP occurs, then mediators of apoptosis such as Cytochrome C and Diablo are released from the mitochondria and into the cytoplasm where they can trigger caspase activation. BCL2 family factors are key mediators of MOMP; Bax and Bak are multidomain (BH123) proteins which can oligomerise on the mitochondrial outer membrane and from pores. The oligomerisation of Bax and Bak is controlled by pro- and anti-apoptotic BCL2 family factors[375]. P53 can be directly and indirectly involved in MOMP by promoting expression of pro-apoptotic BCL2 family factors and by physical interactions with Bax and Bak at the mitochondria[373][374][376].

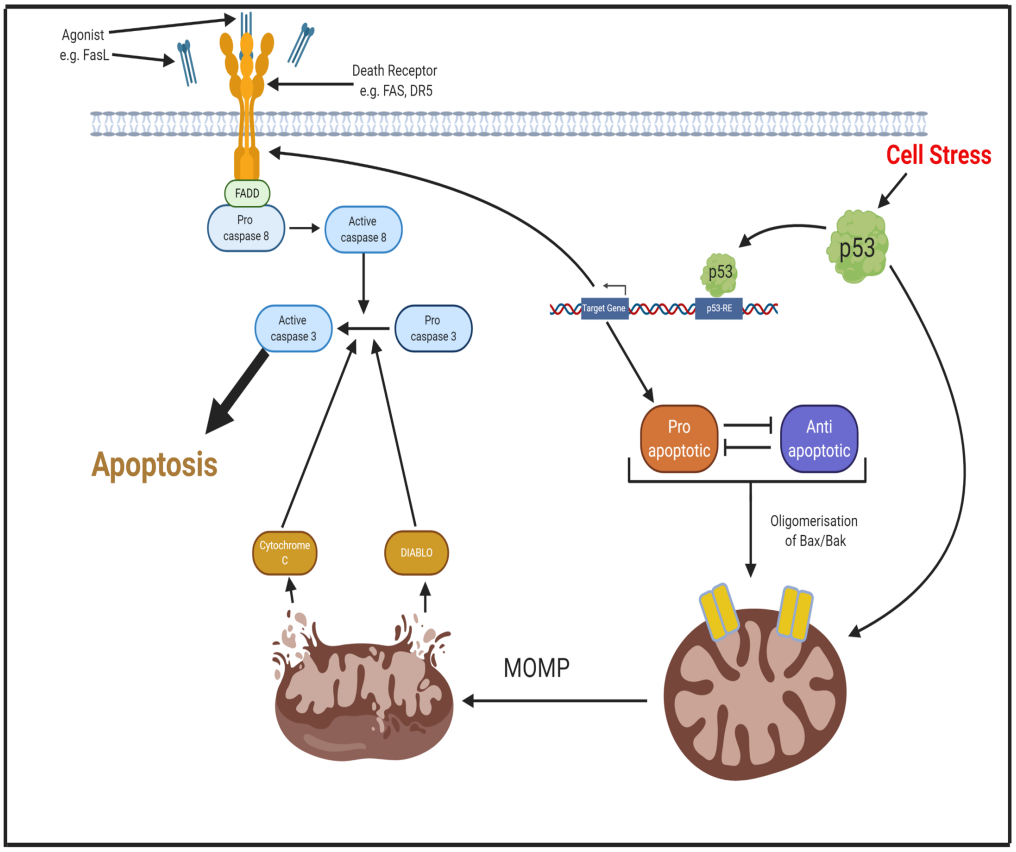


Figure 3.2: A schematic indicating how p53 functions in the intrinsic and extrinsic apoptotic pathways. Activated p53 can induce expression of death receptors such as FAS which can be activating by ligands such as FasL and induce apoptosis via a caspase cascade. P53 can also induce apoptosis directly by inducing expression of pro-apoptotic factors such as Puma which promote mitochondrial depolarisation of the mitochondria through the oligomerisation of Bax/Bak. Mitochondrial Outer Membrane Permeabilization (MOMP) releases cell death factors such as Cytochrome C which trigger a caspase cascade. P53 can also localise to the mitochondria in order to directly promote oligomerisation of Bax/Bak channels and promote apoptosis.

3.2.4 Hypothetical integration points between KITLG/KIT and p53 signaling

In Chapter Two, we found strong experimental evidence for a novel oncogenic, p53 dependent axis in TGCT cell-lines whereby active wildtype p53 could trigger upregulation of KITLG expression and inhibit p53-dependent apoptosis. We identified that inhibition of KITLG/KIT resulted in a synergistic effect on cell death. The focus of this chapter is to unravel the detailed molecular mechanism underpinning the synergy and how heightened KITLG expression negatively regulates the p53 pathway in TGCT cells. We reasoned that there are multiple levels at which feedback

could be exerted: 1) TP53 mRNA expression levels; 2) P53 protein levels; 3) the MDM2-p53 interaction; 4) Post translational modification of p53; 5) Induction of p53 target-genes; 6) Transcriptional independent functions of p53 and 7) Signalling further downstream of p53 (Figure 3.3). To explore these different possibilities, we make use of high throughput omics to profile TGCT cells with heightened sensitivity to p53 activation (KITLG-p53RE -/- clones) and in cells treated with Dasatinib and Nutlin-3a in combination or isolation.

3.2.5 Multi-omics data for uncovering novel cancer biology

Over the last couple of decades, huge amounts of data have been generated by high-throughput genomic technologies including whole-genome sequencing, RNA-seq and mass spectrometry for proteomics. These technologies have already transformed the diagnosis and treatment of some cancers, by identifying actionable driver mutations, but much of the data generated to date has not yet added years to the lives of patients[377]. However, the data generated by omics technologies has the power to uncover novel, targetable tumorigenic mechanisms and to match molecular and genomic characteristics with the most appropriate therapeutic[378][36]. For example, sequencing of tumours can indicate the mutational burden of the tumour which is an important predictor of response to immunotherapy[379]. In this chapter we take advantage of these technologies in order to better understand the molecular mechanisms underpinning the synergy between inhibition of KITLG/KIT and p53 activation in TGCT. We generate deep transcriptomic and proteomic datasets using our previously engineered isogenic TGCT cell-lines. In addition to our own datasets, we mine data repositories employing deep omics methods to characterise tumours and cell-lines in genomic space. These datasets can provide insight into the multitude of molecular mechanisms which can drive cancer and divide patient groups accordingly into molecular subtypes[380][381]. The datasets generated by these programs are rich resources for testing biological hypothesises and de novo discovery. The Cancer Genome Atlas (TCGA) is one such resource for patient data which incorporates gene and protein expression, mutational and copy-number

profiling and clinical data[382]. Similarly, the Genomics of Drug Sensitivity in Cancer (GDSC) dataset comprises hundreds of cancer cell-lines which have been characterised in terms of mutations, copy number alterations, drug sensitivity and mRNA expression[383]. This resource was developed in order to understand how somatic genetic variants impact the response of cancer cells to various inhibitors, the basis of pharmacogenetics. Two datasets are available, GDSC1 and GDSC2, which use different methods to measure cell viability. Between the two datasets, 446,146 unique IC50s have been generated with 11% of these tested in both datasets.

In Chapter Two we found that combining p53 activation with inhibition of KITLG/KIT in TGCT cells had a synergistic effect on cell death and reasoned that this could provide a novel therapeutic opportunity for TGCT patients. In this chapter, we firstly identify molecular mechanisms underpinning the synergy, by investigating the transcriptomic and proteomic changes induced by genetic and pharmacological inhibition of KITLG/KIT. We then further evidence our findings by exploring how the genes and pathways identified in the first analysis, associate with clinical factors, such as disease progression, and with drug sensitivity, by mining patient and cell-line databases.

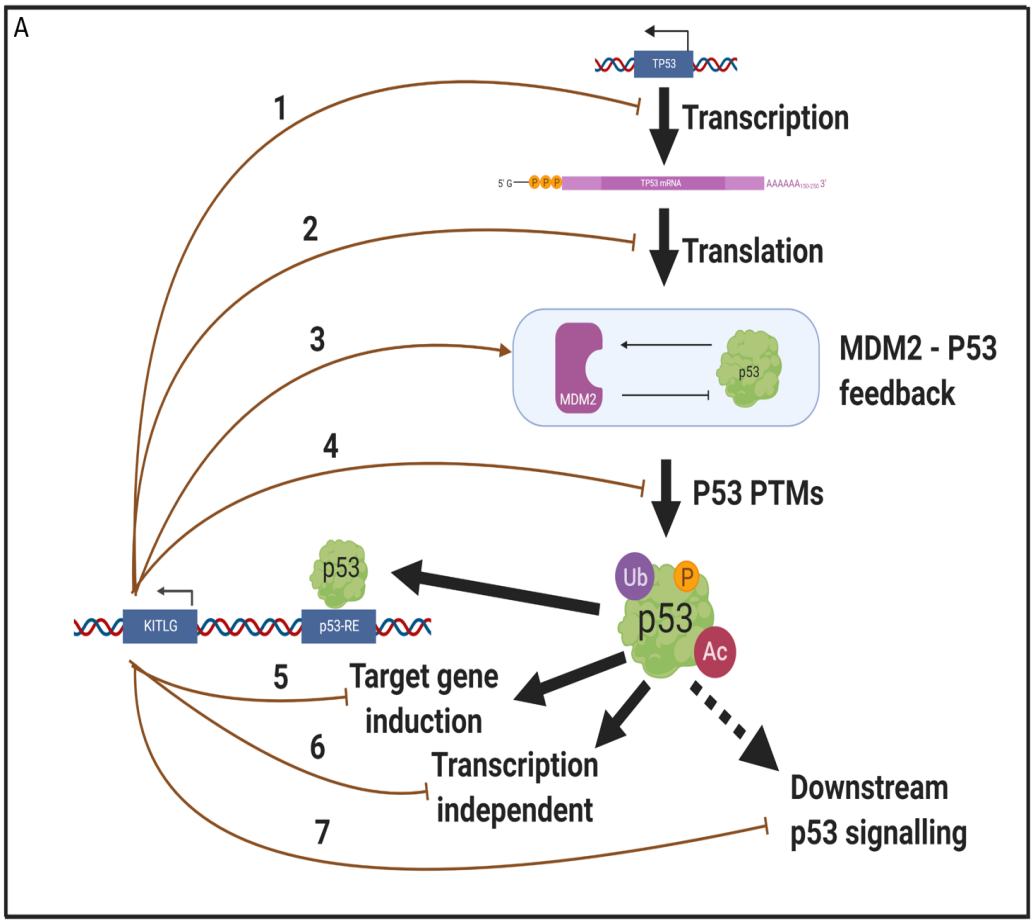


Figure 3.3: KITLG/KIT signalling could have a negative impact on p53 signalling at multiple different points in thep53 pathway. KITLG/KIT signalling could regulate p53 expression (Transcription, Translation, MDM2-p53). KITLG/KIT could regulate p53 activity (PTMS, target-gene induction, Transcription independent). KITLG/KIT signalling could be integrated with p53 signalling downstream of p53 activity.

3.3 Results

3.3.1 The synergy between Dasatinib and Nutlin-3a is dependent on p53

In Chapter Two, we noted that the heightened sensitivity of TERA1 KITLG-p53RE -/- cells to Nutlin-3a was dependent on p53. To confirm the role of p53 in the synergistic interaction between c-KIT inhibition and p53 activation in TGCT, TERA1 KITLG-p53RE +/+ cells were pre-treated with siRNA targeting p53 or a control siRNA for 24hrs and then treated with either Nutlin-3a alone or in combination with Dasatinib for 48hrs. A concentration range of 0.3125 to 20uM was used for both Nutlin-3a and Dasatinib. We analysed the normalised cell viability for

each concentration of Nutlin-3a in isolation and of Nutlin-3a in combination with Dasatinib for cells with and without p53 siRNA knockdown (Figure 3.4.A). For the control siRNA cells, at concentrations of 1.25uM and above, significant reductions in viability were found between Nutlin-3a + Dasatinib treated cells compared to Nutlin-3a alone (FDR < 0.05). For the p53 knock-down cells, no significant differences were found (FDR > 0.05) although there was a trend towards reduced viability in the combination treated cells, particularly at higher concentrations, perhaps due to p53-independent effects of Dasatinib and/or Nutlin-3a or residual p53. Importantly, for all concentrations, for both Nutlin-3a and for Nutlin-3a + Dasatinib, higher cell viability was found for p53 siRNA treated cells and this trend was significant for concentrations 2.5uM and higher ($p < 0.05$). These data suggest that the synergistic interaction between Dasatinib and Nutlin-3a in TGCT cells is dependent on p53.

3.3.2 Investigating the role of p53 activity in the synergy between KIT inhibition and p53 activation

The synergy between inhibition of KITLG/KIT and Nutlin-3a is dependent on p53. P53 is a transcription factor and important regulator of the molecular network controlling cell fate. To understand the role of p53 in the synergy, we studied the transcriptomic and proteomic effects of inhibiting KITLG/KIT in TERA1 cells. We performed 3' RNA-sequencing of TERA1 KITLG-p53RE +/+, -/- and -/KI cells treated with either DMSO, Nutlin-3a, Dasatinib or Dasatinib+Nutlin-3a (Combo) for 6hrs (Material and Methods). The KITLG-p53RE -/- cells represent a genetic inhibition of KITLG/KIT while Dasatinib, a c-KIT inhibitor, represents pharmacological inhibition of the same axis. Therefore, we have two distinct methods of inhibiting p53-mediated KITLG/KIT which we hypothesise should have overlapping mechanisms. A standard bioinformatics pipeline was used to analyse the transcriptomic data (Materials and Methods). Briefly, HISAT2 was used for read-mapping and featureCounts for generating the counts file. edgeR was used to determine significantly differential genes. In total, 15,995 genes were included in the analysis. By multidimensional scaling, the genotype (+/+, -/-, -/KI) and treatment (DMSO, Dasatinib, Nutlin-3a, Combo) replicates can be clearly separated by the expression profiles suggesting that transcriptomic changes could provide insight into the synergy between KITLG/KIT inhibition and p53 activation (Figure 3.4.B).

Transcriptomics does not account for post-transcriptional regulation which can have a profound effect on the molecular characteristics of a cell[384]. With this in mind, we also performed mass spectrometry on TERA1 KITLG-p53RE +/+ and -/- cells using the SILAC method. +/+ and -/- cells were cultured in light and heavy chain media respectively and submitted for analysis. Peptide identification, quantification and mapping was performed by MaxQuant with limma used for differential protein analysis (Materials and Methods, Figure 3.4.C).

P53 dependent induction of KITLG is blocked by genetic inhibition of the p53/KITLG axis

To establish the reliability of the transcriptomic dataset, the expression of KITLG was compared between the three genotypes after either DMSO or Nutlin-3a treatment (Figure 3.4.D). Consistent with our qRT-PCR data (Chapter Two), KITLG levels were 5-fold lower in KITLG-p53RE -/- cells compared to +/+ (FDR = 1.36e-08). Importantly, the -/KI cells also showed 3.3-fold higher KITLG expression compared to -/- (FDR = 1.64e-05) while no difference was found between +/+ and -/KI cells (FDR = 0.053). Furthermore, Nutlin-3a treatment induced KITLG expression 4.1-fold in +/+ cells compared to DMSO (FDR = 4e-09) and in -/KI cells (3.5-fold, FDR = 2e-07) but not in -/- cells (FDR = 0.90). Regulatory elements can have effects on neighbouring genes with some studies finding that enhancers up to 1MB away from a gene can still regulate its expression[385]. We assessed if deletion of the KITLG-p53RE could impact the expression of nearby genes (Figure 3.4.E). No significant differences were found for CEP290 and DUSP6 (FDR $>$ 0.05) while significant differences between KITLG-p53RE +/+ and -/- cells were found for C12orf29, TMTC3, POC1B and ATP2B1 (FDR $<$ 0.05). However, the effect sizes were low, between 1.4 and 1.8-fold compared to 5-fold for KITLG. Moreover, KITLG was the only one of these genes to be significantly upregulated by p53 activation in +/+ cells. These data show that genetic inhibition of KITLG/KIT primarily affects KITLG expression.

P53 expression is not affected by genetic or pharmacological inhibition of KITLG/KIT

In Figure-3A, we identified a number of different ways in which KITLG/KIT signalling might negatively regulate p53 signalling. We first tested the effect of inhibition of KITLG/KIT on p53 expression. We analysed the expression of TP53 mRNA in KITLG-p53RE +/+, -/- and -/KI cells after DMSO or Nutlin-3a treatment (Figure 3.4.F), TP53 mRNA expression was constant across all three genotypes and was not affected by Nutlin-3a treatment (FDR $>$ 0.05). Moreover, p53 mRNA

expression was not differentially regulated by Dasatinib treatment (FDR > 0.05), indicating that the KITLG/KIT is unlikely to regulate transcription from TP53.

The activity of many genes is regulated post-transcriptionally by miRNAs, splicing, mRNA localisation and m6a methylation while the expression of p53 protein is controlled by MDM2[386][387][388]. If KITLG/KIT signalling negatively impacted p53 activity via post-transcriptional mechanisms or by modulating the MDM2-p53 interaction then this would be evident at the p53 protein level in our proteomics data. However, no significant differences were found in p53 protein level between TERA1 KITLG-p53RE +/+ and -/- cells (FDR > 0.05). This is in keeping with our immunoblots whereby we found p53 levels to be consistent between +/+, -/- and -/KI cells and that the combination treatment did not enhance p53 protein expression over and above that of Nutlin-3a (Figures 2.6, 2.7). These data indicate that p53 expression levels do not underpin the synergy between inhibition of KITLG/KIT and p53 activation.

72% of p53 target-genes are induced by the direct p53 activator, Nutlin-3a, compared to DMSO in TERA1 cells

The study of p53 transcriptional targets has gathered pace in the last decade and over 300 validated target-genes are known[115]. KITLG/c-KIT signalling could modulate either the general ability of p53 to regulate transcription of target-genes, for example through cytoplasmic sequestration of p53, or specific target-genes only, perhaps by regulating p53 PTMs, the activity of transcriptional cofactors or chromatin accessibility[389][390] (Hypothesis 5, target-gene Induction Figure 3.3). To test this, we analysed our transcriptomic dataset comprising TERA1 KITLG-p53RE +/+, -/- and -/KI cells treated with either DMSO, Nutlin-3a, Dasatinib or Dasatinib+Nutlin-3a (Combo) (Materials and Methods). If the KITLG/KIT axis can regulate p53 activity more generally, we hypothesised that we would see large scale induction of p53 target-genes after inhibition of the KITLG/KIT axis and that differentially expressed genes (DEGs) would be enriched for p53 target-genes. However, if the KITLG/KIT axis regulates the ability of p53 to target a

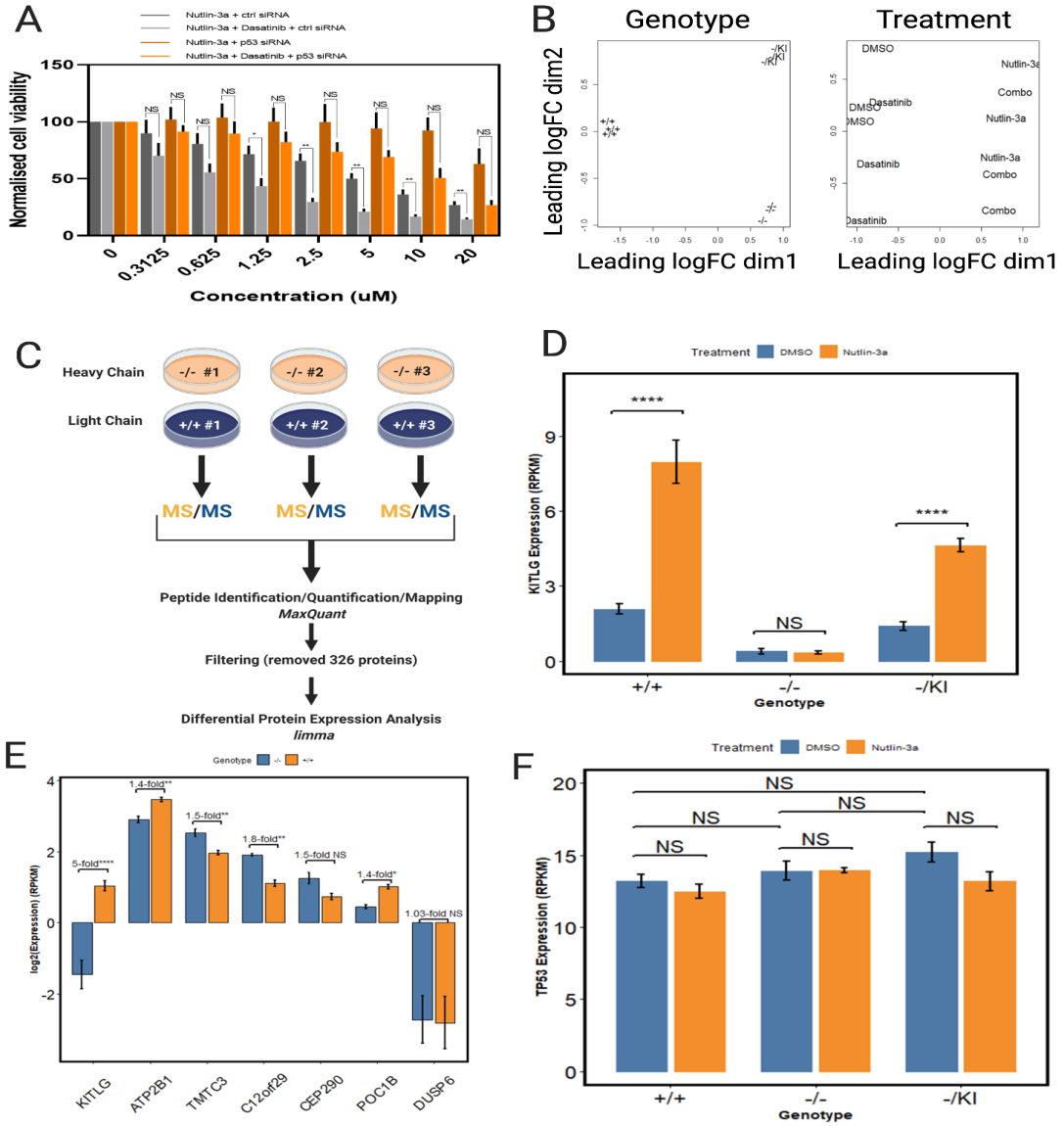


Figure 3.4: **A**) TERA1 KITLG p53RE +/+ cells were treated with ctrl or p53-siRNA for 24hrs. After 24hrs the media was replaced with fresh media containing either Nutlin-3a alone or in combination with Dasatinib at between 0.3125uM and 20uM. After a further 48hrs, cell viability was assessed by MTT assay. The absorbance values were normalised to the untreated control. Significance was tested by Student T-Test. **B**) Multi-dimensional scaling (MDS) plots are useful for visualising high dimensional datasets. In the first MDS plot, the DMSO treated samples are clustered based on their expression profiles. In the second MDS plot, the differently treated +/+ samples are clustered based on their expression profiles. **C**) We performed mass spectrometry of our TERA1 KITLG p53RE +/+ and -/- cells using the SILAC method. The process is shown in this schematic. +/+ and -/- cells were incubated in light and heavy chain media respectively. The raw spectra data were quantified and mapped to peptides and proteins by MaxQuant. 326 proteins were removed during data cleaning. Limma was then used to estimate differentially expressed proteins. **D**) Barplot indicating KITLG mRNA expression from the transcriptomics dataset where +/+, -/- and -/KI cells were treated with Nutlin-3a (10uM) for 6hrs. Three biological replicates were analysed. Significance indicates the FDR-q values derived from edgeR and the error bars indicate SEM. **E**) Bar plots indicating the differences in mRNA expression (log2 transformed RPKM) in the transcriptomics dataset for genes within 1MB of KITLG between +/+ (orange) and -/- (blue) cells. Significance reflects the FDR-q values from edgeR and error bars indicate SEM over the 3 biological replicates. **F**) Barplot indicating the mRNA expression of p53 in +/+, -/- and -/KI cells in the transcriptomic dataset. Cells were treated with DMSO or 10uM Nutlin-3a for 6hrs. Significance reflects FDR-q values from edgeR. FDR-q <0.05 was considered significant. Error bars indicate the SEM over three biological replicates.

specific subset of genes, we hypothesised these could be identified by finding target-genes inhibited by both genetic and pharmacological inhibition of KITLG/KIT signalling (Figure 3.5.A). P53-dependent induction of p53 target-genes can vary between tissue and cell types. To determine which p53 target-genes were induced by p53 activation in TGCT cells, we compared the transcriptomes of DMSO and Nutlin-3a treated TERA1 KITLG-p53RE +/+ cells. A total of 2,102 genes were found to be differentially expressed after Nutlin-3a treatment with 613 of these exhibiting a greater than 2-fold change in either direction. 214 p53 target-genes were differentially expressed with 139 showing over 2-fold change. 212 of these 214 p53 target-genes were upregulated (68% of expressed p53 target-genes, Figure 3.5.B-D). Importantly, significantly upregulated genes after Nutlin-3a treatment (FDR <0.05) were enriched for p53 target-genes compared to non-differentially expressed genes (212/1083 compared to 102/14810, OR=35.3, p=1.7e-175, Figure 3.5.E) while significantly downregulated genes were depleted for p53 target-genes (2/1019 compared to 312/14664, OR=0.09, p=4.8e-07). Similar results were found for -/- and -/KI cells after Nutlin-3a treatment indicating that p53 can induce target-gene expression regardless of KITLG/KIT (Figure 3.5.B-E). Across the three genotypes, 227 of 314 p53 target-genes (72%) were found to be induced by Nutlin-3a in at least one genotype. For the next analyses we focused only on the 227 p53 target-genes found to be inducible by p53 activation in TGCT (Supplementary Table C.4).

Genetic inhibition of KITLG/KIT does not regulate general p53 transcriptional activity

Genetic inhibition of KITLG/KIT heightens sensitivity to p53 activation. In order to determine if the heightened sensitivity of KITLG-p53RE -/- cells to p53 activation was due to differential expression of p53 target-genes, we analysed the expression of the 227 p53 inducible target-genes between KITLG-p53RE +/+ and -/- cells. Compared to +/+ cells, 2,388 and 2,204 genes were downregulated and upregulated in -/- cells respectively (Figure 3.6.A, left plot). 861 and 909 genes were found to be downregulated and upregulated with greater than 2-fold change respectively (Figure 3.6.A, Orange points). 38 p53 target-genes were downregulated in -/- cells compared

to +/+ and 49 were upregulated. Next, we determined which of these target-genes could be rescued or partially rescued by knocking-back in the KITLG-p53RE. To

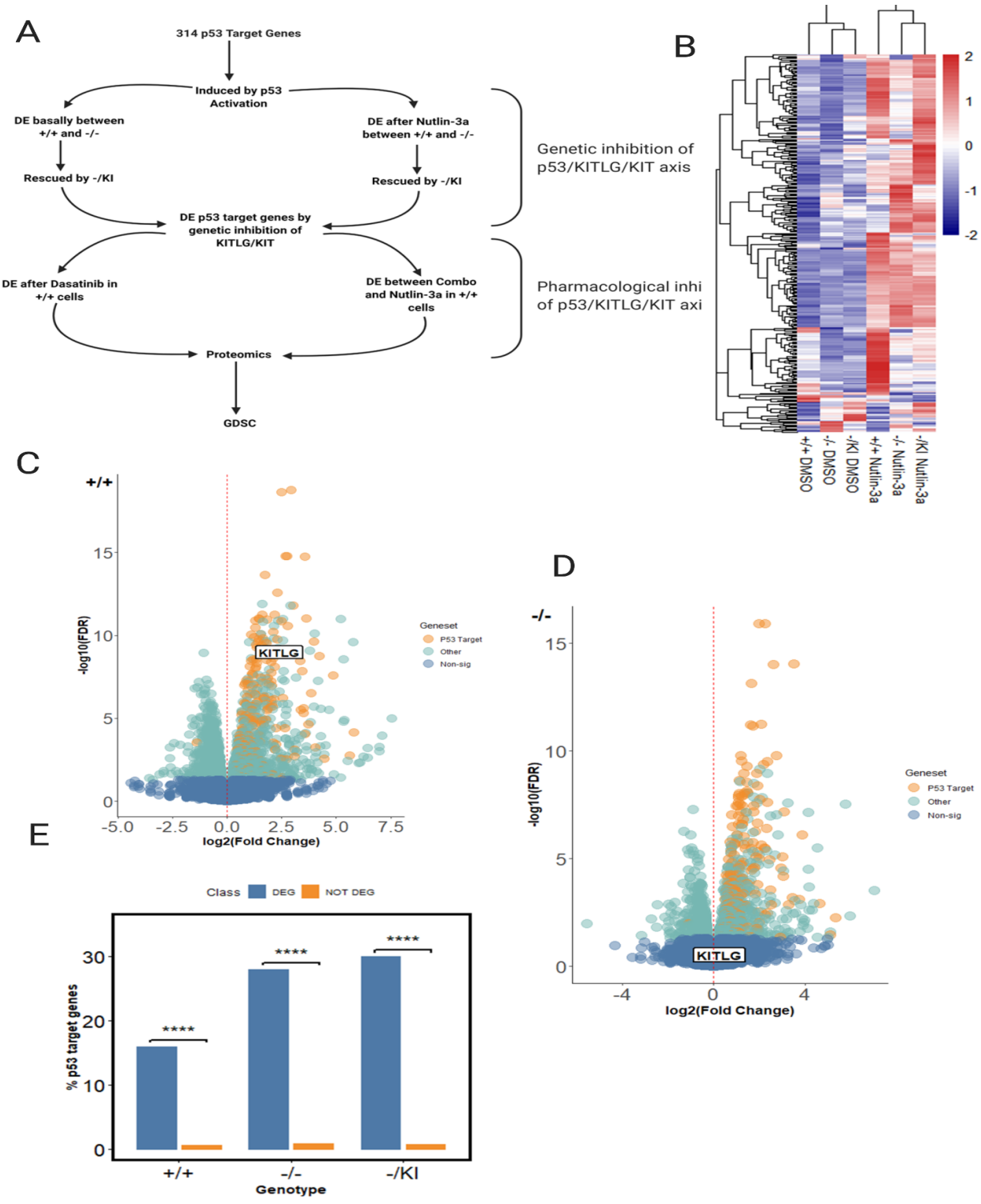


Figure 3.5

Figure 3.5: A) A flow chart indicating the process for identifying p53 target-genes which might be regulated by KITLG/KIT. We firstly focused on p53 target-genes which could be induced by p53 in our TGCT cell lines. We then identified target-genes which were differentially expressed by genetic inhibition of KITLG/KIT, either basally or after Nutlin-3a treatment, and could be rescued by knock-in of the KITLG p53RE (-/KI cells). For genes passing this threshold, we overlapped with target-genes which were differentially expressed after Dasatinib alone or by the combination treatment compared to Nutlin-3a treated cells. Genes passing this threshold too are genes which are regulated by both genetic and pharmacological inhibition of KITLG/KIT. We then validated these genes in the proteomics dataset and determined if they associates with Nutlin-3a sensitivity in the GDSC dataset. **B**) A heatmap showing the relative expression of 314 p53 target-genes (from Fischer *et al* 2017) across the +/+, -/- and -/KI cells treated with either DMSO or Nutlin-3a for 6hrs. The samples are clustered by hierarchical clustering using default pheatmap method. **C, D**) Volcano plots for the contrast between DMSO and Nutlin-3a (6hrs) treated +/+ cells (Left) and DMSO and Nutlin-3a (6hrs) treated -/- cells (right). Nonsignificant genes are marked in blue, significant genes in light green and significant p53 target-genes in orange. KITLG is labelled. Log2 transformed fold change in displayed on the X axis and -log10 transformed FDR on the Y. **E**) Barplots indicating the % of genes in the differentially and non-differentially expressed gene lists for +/+, -/- and -/KI cells which are annotated p53 target-genes or not. Enrichment for p53 target-genes was determined by a 2-tailed Exact Fisher Test.

do so, we assessed which p53 target-genes were up or downregulated between -/- and -/KI cells (Figure 3.6.A, right plot). 11 of the 38 p53 target-genes found to be downregulated between -/- and +/+ cells were upregulated in -/KI cells compared to -/- (Figure 3.6.B). Importantly, one of these 11 genes was KITLG. A total of 645 genes were found to be downregulated in -/- cells compared to +/+ cells and at least partially rescued in the -/KI cells. No enrichment for p53 target-genes was found amongst these 645 genes compared to non-p53 target-genes (11/645 compared to 216/15134, OR=1.22, p=0.50). Of the 49 upregulated genes between -/- and +/+ cells, 7 were upregulated in -/KI cells compared to -/- cells (Figure 3.6.B). A total of 393 genes were found to be upregulated in -/- cells compared to +/+ cells and at least partially rescued in the -/KI cells. No enrichment for p53 target-genes was found amongst these 393 genes compared to non-p53 target-genes (7/393 compared to 220/15382, OR=1.27, p=0.51). These data suggest that KITLG/KIT does not inhibit the general transcriptional activity of p53.

We next leveraged our proteomics data to determine if KITLG/KIT signalling could regulate expression of p53 target-genes post-transcriptionally. Of 227 p53 target-genes, 116 were identified in our proteomics analysis. Of these 116, 7 were found to be significantly downregulated which was not a significant enrichment compared to non-p53 target-genes, in line with our transcriptomic data (OR = 1.52, p = 0.24, Figure 3.6.C).

Although p53 target-genes were not significantly differentially regulated by the p53/KITLG axis at the basal level, we reasoned that KITLG/KIT signalling could

regulate the ability of p53 to induce target-genes after activation. To detect this, we compared the effects of Nutlin-3a on +/+ cells with the effect of Nutlin-3a on -/- cells. Surprisingly, the only differentially induced p53 target-gene was KITLG itself. Indeed, significant correlation was found between the fold change in expression of p53 target-genes by Nutlin-3a treatment in KITLG-p53RE +/+ and -/- cells (R2 = 0.77, p = 5.8e-45, Pearson, Figure 3.6.D). Similar correlation was found between KITLG-p53RE +/+ and -/KI cells (R2 = 0.81, p = 3e-54, Pearson). These analyses indicate that the vast majority of p53 inducible target-genes (93%) are not regulated by the p53/KITLG axis and suggests that KITLG/KIT signalling does not control the ability of p53 to induce target-gene expression in general.

Pharmacological inhibition of KITLG/KIT does not regulate general p53 transcriptional activity

The heightened sensitivity of -/- cells could be recaptured by pharmacologically inhibiting KITLG/KIT using the c-KIT inhibitor, Dasatinib. Pharmacological and genetic inhibition of KITLG/KIT should have similar effects on cells (Figure 3.5.A). Therefore, we analysed the transcriptomes of DMSO and Dasatinib treated +/+ cells. 74 genes were significantly upregulated and 63 downregulated after Dasatinib treatment (FDR <0.05, Figure 3.7.A). Of the 74 upregulated genes, 2 were found to be p53 target-genes which was not a significant enrichment compared to non-p53 target-genes (OR=2.1, p=0.26, Figure-7B). Of the 63 downregulated genes, 7 were found to be p53 inducible target-genes which did constitute a significant enrichment compared to non-p53 target-genes (OR=9.6, p=2e-05, Figure 3.7.B). One of the genes downregulated by Dasatinib overlapped with the list of downregulated inducible p53 target-genes between -/- and +/+ cells, SFN. This analysis indicates that pharmacological inhibition of KITLG/KIT does not regulate the expression of p53 target-genes generally, in line with the data from the genetic inhibition of the p53/KITLG axis. However, both genetic and pharmacological inhibition of KITLG/KIT were found to repress SFN expression.

Next, we determined if pharmacological inhibition of KITLG/KIT could regulate p53 dependent induction of p53 target-genes after Nutlin-3a treatment. To do

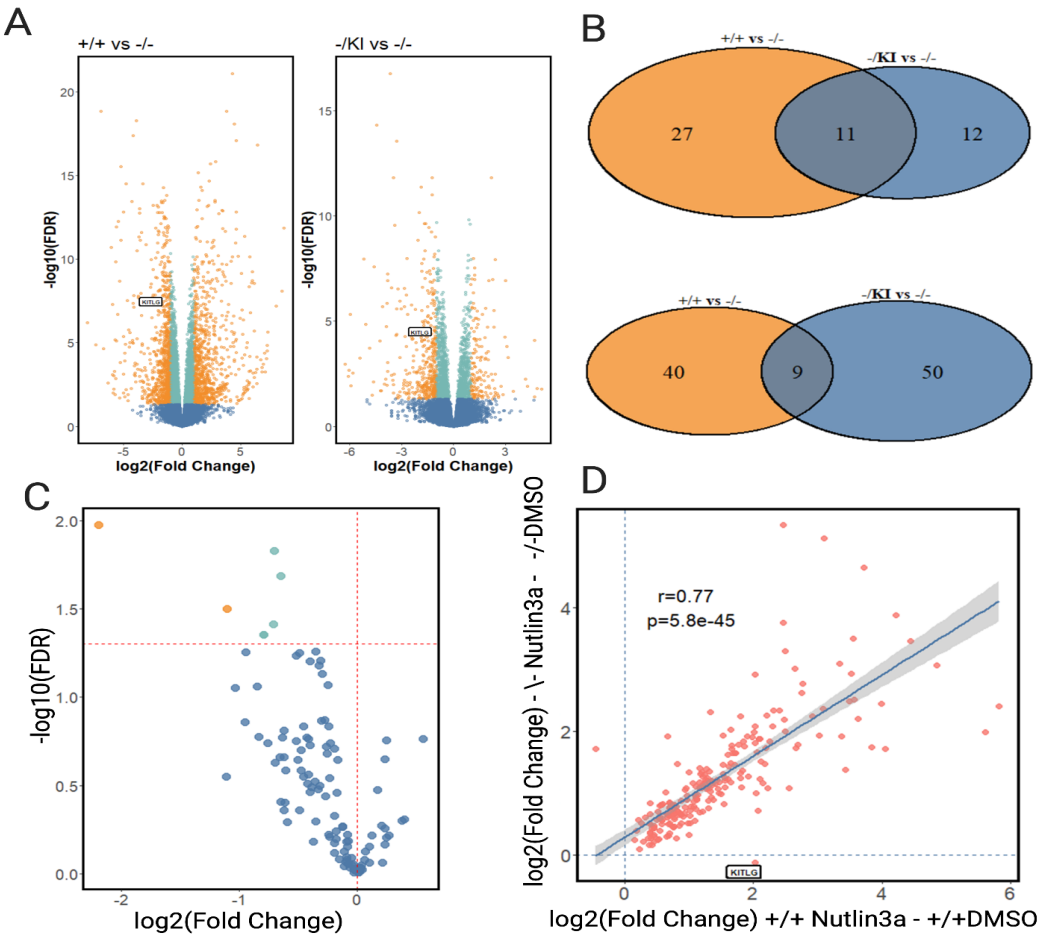


Figure 3.6: **A**) Volcano plots for the contrast between +/+ and -/- cells (Left) and -/KI and -/- cells (right). Nonsignificant genes are marked in blue, significant genes with log2 fold change < 1 in light green and significant genes with log2 fold change > 1 in orange. KITLG is labelled. Log2 transformed fold change in displayed on the X axis and -log10 transformed FDR on the Y. **B**) The top Venn diagram depicts the p53 target-genes found to be downregulated in DMSO treated -/- cells compared to both DMSO treated +/+ and -/KI cells. The bottom venn diagram indicates the crossover of p53 target-genes found to be upregulated in DMSO treated -/- cells compared to DMSO treated +/+ or -/KI cells. The overlapping genes represent high confidence genes. **C**) Volcano plot of inducible p53 target-genes for the contrast between the proteomes of +/+ and -/- cells. Nonsignificant genes are marked in blue, significant genes with log2 fold change < 1 in light green and significant genes with log2 fold change > 1 in orange. Log2 transformed fold change in displayed on the X axis and -log10 transformed FDR on the Y. **D**) The scatter plot indicates the correlation between the log2(Fold Change) of p53 target genes in Nutlin-3a treated +/+ and -/- cells. Each target-gene is shown in red and the regression line in blue. KITLG is labelled. Correlation was determined by Pearsons Correlation.

so, we compared the transcriptomes of Combo and Nutlin-3a only treated +/+ cells. In total, 63 genes were found to be downregulated in the Combo treated cells compared to Nutlin-3a which included six inducible p53 target-genes (Figure 3.7.C). This represented a significant enrichment for inducible p53 target-genes compared to non-p53 target-genes (OR=8.0, p=0.0002, Figure 3.7.D). Interestingly, all 6 inducible target-genes overlapped with those found to be downregulated by Dasatinib alone, including SFN.

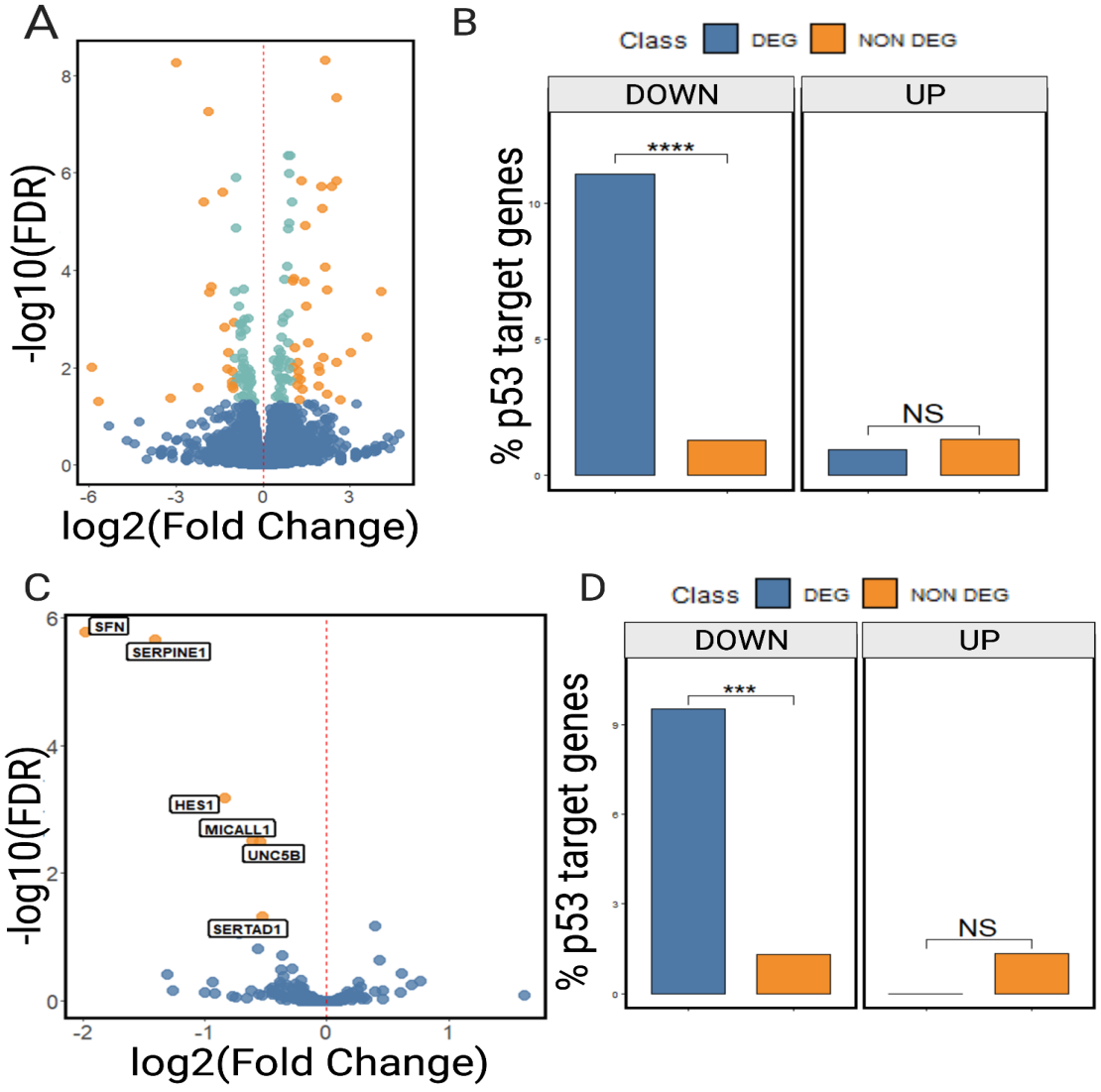


Figure 3.7: **A**) Volcano plots for the contrast between the transcriptomes of DMSO and Dasatinib (6hrs) treated +/+ cells. Nonsignificant genes are marked in blue, significant genes with log2 fold change < 1 in light green and significant genes with log2 fold change > 1 in orange. Log2 transformed fold change is displayed on the X axis and -log10 transformed FDR on the Y. **B**) The significantly upregulated and downregulated genes after 6hrs Dasatinib treatment (2uM) were tested for enrichment of p53 target genes by Exact Fisher Test. The bar plots indicate the % of p53 target-genes found amongst upregulated and downregulated genes. **C**) The transcriptomes of Combo treated +/+ cells (6hrs of 1-uM Nutlin-3a and 2uM Dasatinib) and Nutlin-3a (6hrs, 10uM) treated cells were compared to determine p53 target-genes differentially expressed by the combination treatment compared to Nutlin-3a alone. Significant p53 target-genes are coloured orange and labelled. **D**) The significantly upegulated and downregulated genes after 6hrs Combo treatment (10uM Nutlin-3a and 2uM Dasatinib) compared to 6hrs of Nutlin-3a (10uM) only were tested for enrichment of p53 target genes by Exact Fisher Test. The bar plots indicate the % of p53 target-genes found amongst upregulated and downregulated genes.

14-3-3sigma is downregulated after genetic inhibition of KITLG/KIT

Through transcriptomics we identified SFN to be repressed by both genetic and pharmacological inhibition of KITLG/KIT (Figure 3.8.A). SFN expression was found to correlate with the copy-number of the KITLG-p53RE, +/+ cells exhibited highest expression and -/- the lowest. The fold induction of SFN by Nutlin-3a was consistent across genotypes and Dasatinib prevented p53-dependent induction of SFN. SFN encodes the 14-3-3sigma protein. The 14-3-3 family of proteins bind specific phosphorylation sites and sequester the target protein. 14-3-3sigma has been shown to inhibit apoptosis by sequestering Bax after it has been phosphorylated by AKT[282]. We next checked whether 14-3-3sigma was downregulated in -/- in our proteomics data and found this to be the case (p=0.03, Figure 3.8.B). The transcriptomic and proteomic data suggests that KITLG/KIT may act to promote p53-dependent expression of the SFN gene. We validated this by qRT-PCR in TERA1 KITLG-p53RE +/+ cells. SFN expression was found to be increased after Nutlin-3a treatment and reduced after Dasatinib treatment. After Combo treatment, a smaller induction than Nutlin-3a was found (Figure 3.8.C).

SFN expression associates with reduced sensitivity to Nutlin-3a in cell-lines

Induction of SFN by p53 could inhibit p53-depedent apoptosis. To provide support for this, we extracted expression data for SFN and sensitivity data for Nutlin-3a, in the form of IC50s, from the GDSC dataset. We restricted to 291 TP53 WT cell-lines and determined if SFN expression associated with Nutlin-3a sensitivity by linear regression. Indeed, high SFN expression was found to significantly associate with higher Nutlin-3a IC50, indicating reduced sensitivity to p53 activation (2.0-fold, p=8e-06, Figure 3.8.D). A significant trend was also found for 648 TP53 mutant cell-lines but to a lesser degree (1.2-fold, p=0.002, a 1.7-fold reduction in effect size compared to TP53 WT).

Changes in the expression of p53 cofactors do not explain the synergy between KIT inhibition and p53 activation

Inhibition of KITLG/KIT reduces SFN expression. KITLG/KIT could regulate the promoter specific activity of p53 by modifying the expression of transcriptional cofactors. Multiple p53 cofactors have been identified which can direct p53 to specific target-genes[391][392]. We identified p53 cofactors via a literature search and determined if they were differentially expressed after deletion of the KITLG-p53RE or after Dasatinib treatment (Table 3.1). Of the 19 cofactors we identified, six cofactors were differentially regulated after genetic inhibition of KITLG/KIT and four after pharmacological inhibition. However, none overlapped between the two conditions and were in the same direction. This analysis suggests that inhibition of KITLG/KIT does not modulate the expression of known p53 cofactors.

KITLG/KIT signalling could modulate p53 post-translational modifications

Post-translational modifications of p53 can also confer selectivity of target-genes. Phosphorylation of S46 and acetylation of K120 are known to promote expression of pro-apoptotic target-genes[391]. Our cell-line work in Chapter Two suggested that acetylation of p53 was not different between KITLG-p53RE +/+ and -/- cells. To investigate whether KITLG/KIT could regulate SFN expression through p53 phosphorylation levels, we determined the levels of phosphorylation of three p53 phosphorylation sites using a phospho-kinase array featuring S15, S46 and S392 (Materials and Methods). Expression of S392 and S46 were found to be upregulated in -/- cells compared to +/+ while S15 was unchanged (S392, 3.3-fold; S46, 2.3-fold, Figure 3.8.E). We analysed the expression of S392 and S46 after Nutlin-3a and Combo treatment in KITLG-p53RE +/+ cells. As expected, stabilisation of p53 after Nutlin-3a treatment increased expression of both phosphorylation sites and Combo treatment increased expression further with a profound effect for S392 (1.8-fold higher after Combo compared to Nutlin-3a, Figure 3.8.F). The kinase(s) which phosphorylate p53 s392 are disputed. One of the kinases thought to be responsible is p38[393]. Interestingly, we found expression of a direct upstream regulator of

p38, MAP2K6, to be upregulated after 6hrs of Dasatinib treatment (2uM) in our transcriptomics dataset which was also validated by QRT-PCR in TERA2 cells (Figure 3.8.G). P53 S392 is thought to promote mitochondrial translocation of p53, offering a transcriptional independent mechanism for p53s role in the synergy between p53/KITLG/KIT inhibition and p53 activation[393].

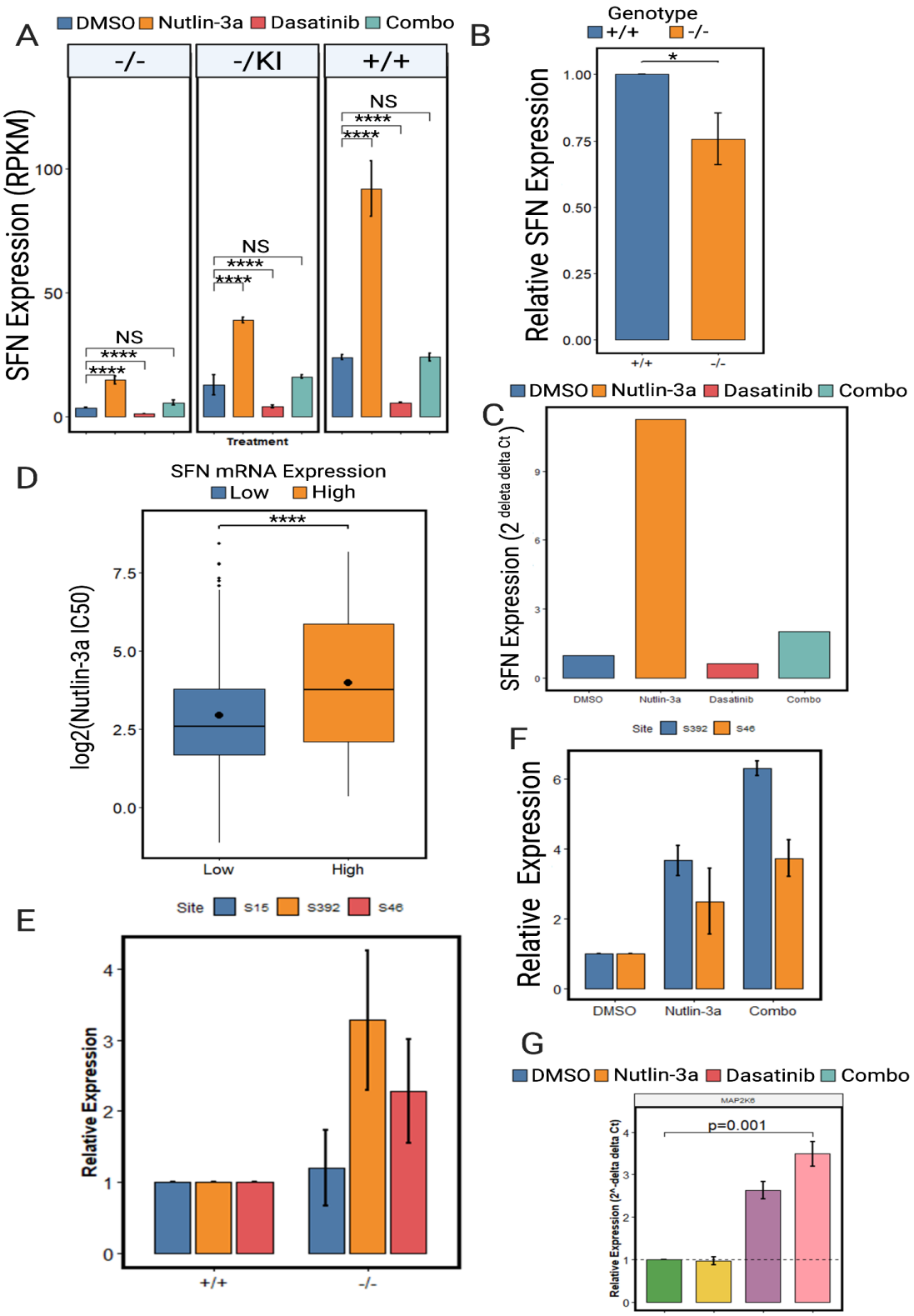

A
DMSO Nutlin-3a Dasatinib Combo
-/-
-/KI
+/+
SFN Expression (RPKM)
Treatment
NS
****
B
Genotype
+/+ -/-
Relative SFN Expression
*
C
DMSO Nutlin-3a Dasatinib Combo
SFN Expression (2^deleta delta Ct)
D
SFN mRNA Expression
Low High
log2(Nutlin-3a IC50)
E
Site S15 S392 S46
Relative Expression
F
Site S392 S46
Relative Expression
G
DMSO Nutlin-3a Dasatinib Combo
MAP2K6
p=0.001
Relative Expression (2^-delta delta Ct)

Figure 3.8

Figure 3.8: **A**) The faceted barplot indicates the expression of SFN mRNA (RPKM) for each treatment group in -/- (left), -/KI (middle) and +/+ (right) cells in the transcriptomic dataset. The indicated significance levels are representative of the FDR-q values from edgeR. Error bars indicate the SEM over three biological replicates. **B**) Barplot indicating the expression of SFN in the SILAC proteomics dataset for +/+ and -/- cells. The significance value indicates the FDR-q value from limma. The error bars indicate the SEM over three biological replicates. **C**) SFN mRNA expression was determined by qRT-PCR in TERA1 KITLG p53RE +/+ cells. The bar chart represents one independent experiment. **D**) TP53 WT cell lines from the GDSC dataset were split into high and low with regard to SFN expression using the surv cutpoint function. The Nutlin-3a IC50s of SFN high cell lines were compared to SFN low cell lines. Significance was determined by linear regression. **E**) The expression of p53 S392, S46 and S15 between +/+ and -/- cells was measured a by phospho-kinase array. Two biological replicates were performed with two technical replicates in each. Error bars indicate SEM. **F** The expression of p53 S392, S46 and S15 between cells treated with either DMSO, Nutlin-3a or the Combo treatment by phospho-kinase array. Two biological replicates were performed with two technical replicates in each. Error bars indicate SEM. **G**) The barplot indicates the expression of MAP2K6 mRNA in TERA2 cells treated with DMSO, 10uM Nutlin-3a, 2uM Dasatinib or the Combo for 6hrs. Error bars indicate the SEM over three biological replicates.

Table 3.1: A table of p53 transcriptional cofactors derived from a literature search.

Gene	**Protein**	**Function**	**Direction Genetic/ Pharma**
PPP1R13B	ASPP1	Promote apoptosis induction by p53	NS / NS
TP53BP2	ASPP2	Promote apoptosis induction by p53	NS / DOWN
PPP1R13L	iASPP	Inhibit apoptosis induction by p53	NS /NS
HIPK1	HIPK2	Phosphorylates S46 to promote apoptosis	NS /NS
KAT5	TIP60	Acetylates p53 to promote apoptosis	NS / NS
POU4F2	BRN3B	Enhances induction of pro-apoptotic genes	NS / NS
POU4F1	BRN3A	Represses induction of apoptotic genes	UP / NS
ZNF385A	Hzf	Promotes induction of cell-cycle arrest genes	NS / UP
EP300	p300	Acetylates and stabilises p53	UP/ DOWN
CREBBP	CBP	Acetylates and stabilises p53	DOWN / NS
KAT2A	GCN5	Mediates p53 dependent gene transactivation as part of the STAGA complex	NS / NS
TAF6	TAF6	General TF	NS / NS

Table 3.1 continued from previous page

Gene	**Protein**	**Function**	**Direction Genetic/ Pharma**
TAF9	TAF9	General TF	UP / NS
TBP	TBP	General TF	NS / NS
MED17	TRAP80	Part of the Mediator compelx which links p53 to core transcriptional machinery	NS / NS
ERCC3	TFIIH	General TF	NS / NS
SUB1	PC4	Promotes binding of p53 to pro-apoptotic genes	NS / NS
PML	PML	Promotes p53 dependent apoptosis	DOWN / UP
PIN1	PIN1	Promotes mitochondrial function of p53	DOWN / NS

3.3.3 Investigating the mechanism of signal transduction from KITLG/KIT in TGCT

Our analyses so far indicate that KITLG/KIT does not affect p53 expression or expression of the vast majority of target-genes. We next aimed to outline the mechanism of the pro-survival signal constituted by KITLG/KIT (Figure **??**.A). To do so, we utilised the multi-omics data from our own isogenic TGCT cell-lines, TGCT tumour data from the TCGA cohort, pharmacogenomic cell-line data and we further tested our findings using wet lab experiments (Figure **??**.B).

Genes regulated by genetic inhibition of KITLG/KIT are enriched for genes related to PI3K/AKT/mTOR signalling and cell cycle progression

We first focused on the transcriptomic and proteomic changes associated with genetic inhibition of KITLG/KIT. Pathways enriched for genes differentially regulated in both datasets could be important to the pro-survival signal. Through our transcriptomic analysis, we had previously found that a total of 654 genes were downregulated in TERA1 KITLG-p53RE -/- cells compared to +/+ and could be rescued by knock-in of the p53RE. We analysed these genes more closely and found enrichment for Hallmark genes related to PI3K/AKT/mTOR signalling (including MYC and mTORC1 target-genes and EMT genes) and cell cycle progression compared to all genes (Figure **??**.C). These enrichments suggested that PI3K/AKT/mTOR signalling could mediate the pro-survival signal from KITLG/KIT in TGCT. With regard to the proteomic data, we identified 19 upregulated proteins and 320 downregulated proteins in -/- cells compared to +/+ (Figure **??**.D). We assessed whether the differentially expressed proteins were enriched for Hallmark Gene sets relevant to PI3K/AKT/mTOR activity (PI3K/AKT/mTOR, EMT and target-genes of MYC, MTORC1, NFKB). Indeed, the downregulated genes were enriched for EMT, MYC targets and mTOR targets (FDR < 0.10, Figure **??**.E). Specifically, four known oncogenes which facilitate signal transduction from RTKs through these pathways were found to be downregulated in -/- cells (ICAM1, LYN, PIK3C3 and NFKB1)(Figure **??**.F)[394][395][396] [397][398][399]. 72 genes overlapped between

our list of downregulated transcripts and downregulated proteins, representing a greater overlap than expected by chance (OR=2.1, p=7.3e-07, Figure **??**.G). These 72 genes were also found to be enriched for EMT genes and MYC target-genes (FDR <0.05). Both the transcriptomic and proteomic differences associated with genetic inhibition of KITLG/KIT suggest a role for PI3K/AKT/mTOR signalling. For example, we found the upstream regulator, Lyn, to be downregulated at the protein level (2.45-fold, FDR =0.046) while downstream components such as RPS6KA3 (3.05-fold, FDR=3.6e-08) and PRPS2 (1.75-fold, FDR=1.73e-04) were found to have reduced mRNA expression[400][401].

Differentially Expressed PTMs are enriched for PI3K/AKT/mTOR signalling

To further support our model that PI3K/AKT/mTOR signalling transduces the survival signal from KITLG/KIT, we compared the expression of PTMs between +/+ and -/- cells. Using limma, we identified 7,930 peptide PTMs which were significantly different across 2,485 genes (Figure 3.10.A). For each PTM class (such as phosphorylation, methylation and acetylation), differential sites were determined, and Hallmark enrichments were calculated by the hypergeometric test (Figure 3.10.B). Here we focus on the methylation and phosphorylation PTMs.

Protein Methylation The vast majority of significant PTM changes involved methylation (70%, Figure 3.10.A). Methylation of DNA has been extensively studied. Conversely, the role of protein methylation on a protein by protein and site by site basis is poorly understood. Protein methylation is known to be important for protein-protein interactions and can influence signal transduction, transcription and DNA repair[402][403][404]. For example, methylation of AKT is known to promote its oncogenic kinase activity[405]. We found 2,014 proteins to exhibit a significant reduction in methylation (FDR <0.05) and these were enriched for PI3K/AKT/mTOR (OR=6.33, FDR=1.4e-11) and MYC (OR=24.8, FDR=1.05e-88) and MTORC1 (OR=11.98, FDR=1.29e-46) targets (Figure 3.10.B). Some of the proteins exhibiting reduced methylation were also reduced at the protein

level; for example, p62 (encoded by SQSTM1) which has been shown to activate NFKB, mTOR and MDM2[406].

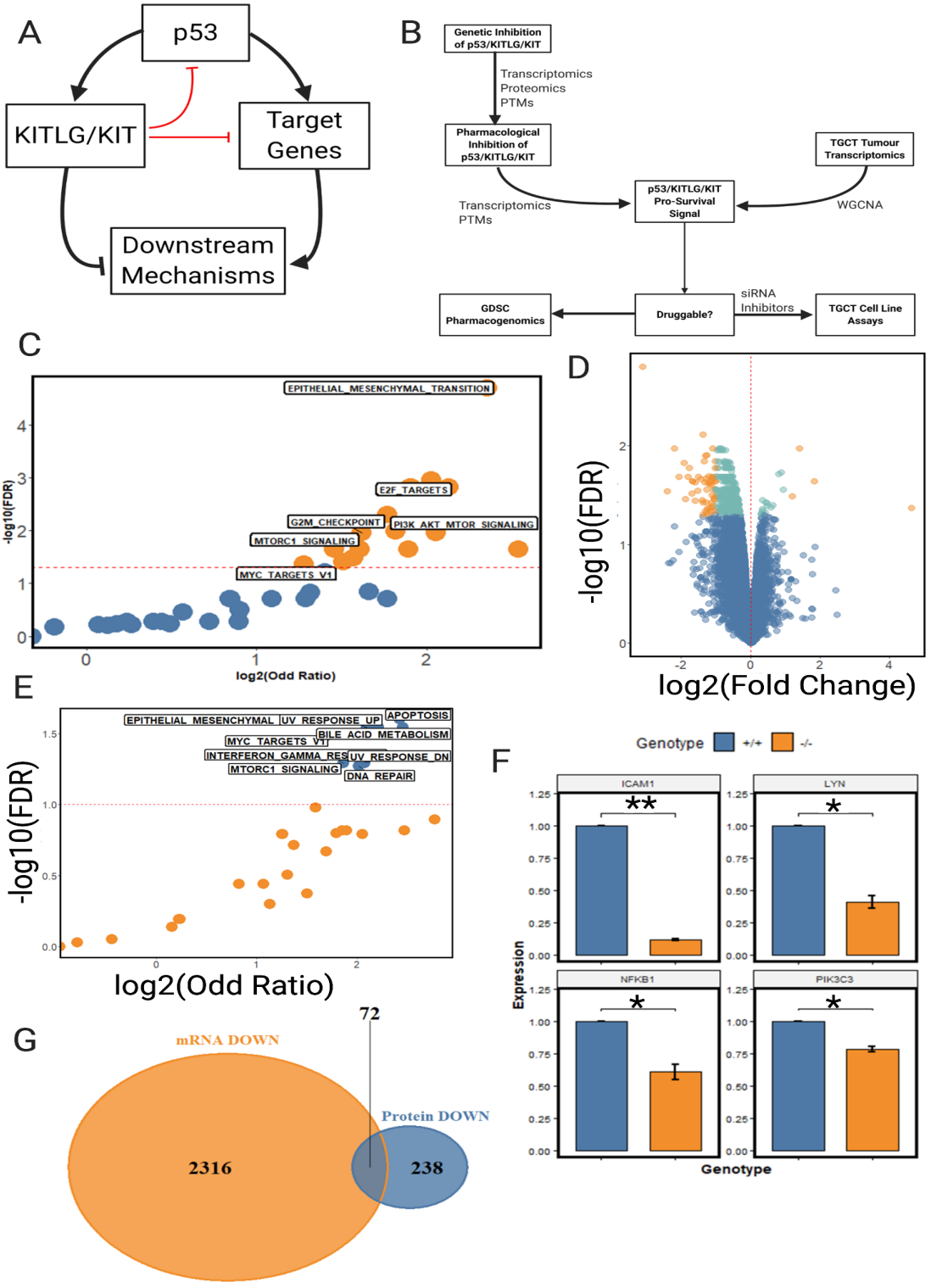


Figure 3.9

Figure 3.9: **A**) Simple schematic indicating the multiple levels at which KITLG/KIT signalling could impact p53 activity. Firstly, we previously reasoned that KITLG/KIT could impact p53 expression but we found this not to be the case (red line for disproved). Secondly, we reasoned KITLG/KIT could regulate the ability of p53 to induce p53 target-gene expression. Again we did not find evidence of this other than for SFN (red line). The third hypothesis, which we focus on in this section, is that KITLG/KIT could integrate with downstream mechanisms of p53 target-genes (black line). **B**) We used multiple methods and datasets to determine the cellular mechanisms responsible for transducing the pro-survival signal from KITLG/KIT. We began with the multi-omics datasets generated from our own isogenic cell lines and explored the differentially expressed transcripts, proteins and PTMs after genetic inhibition for KITLG/KIT. We then looked for evidence of the same pathways amongst the differentially regulated transcripts and PTMs after pharmacological inhibition of KITLG/KIT. In parallel, we performed an unsupervised analysis of transcriptomic data from TGCTs from the TCGA cohort. We applied WGCNA (Weighted Gene Correlation Network Analysis) to find clinically relevant modules and determined if these modules were enriched for similar pathways to those found in our multi-omics TGCT cell line data. We considered the overlapping pathways as candidate pathways for the pro-survival signal. Given these hits, we aimed to determine if they represented druggable targets. To do so, we tested how inhibition of these pathways affected sensitivity to p53 activation in TGCT cell line assays. Secondly, we utilised the GDSC pharmacogenomic resource to determine if KITLG expression associated with sensitivity to inhibitors of the pathway in TP53 WT and TP53 Mutant cell lines.**C**) 654 genes were significantly differentially expressed in -/- cells compared to +/+ cells in the transcriptomic dataset and were at least partially rescued by the -/KI. Functional enrichment of these genes was performed using the hypergeometric test and Hallmark gene sets. Significant Hallmarks are coloured orange (FDR <0.05). **D**) Volcano plots for the contrast between the proteomes of +/+ and -/- cells. Nonsignificant genes are marked in blue, significant genes with log2 fold change < 1 in light green and significant genes with log2 fold change > 1 in orange. Log2 transformed fold change in displayed on the X axis and -log10 transformed FDR on the Y. **E**) The differentially expressed proteins between +/+ and -/- cells were used as input for gene set enrichment analysis using the hypergeometric test. The X axis indicates the odd ratio of the enrichment and the Y axis indicates the -log10 transformed FDR-q value. Significant overlaps (FDR-q < 0.10) are coloured blue and labelled. **F**) Relative protein expression of ICAM1, LYN, NFKB1 and PIK3C3 in -/- cells compared to +/+. The significance level indicated in each facet reflects the FDR-q value determined for these genes by limma.**G**) A Venn diagram indicating the overlap between downregulated genes from the transcriptomic and proteomic analyses. This overlap was determined to be significant by Exact Fisher Test.

Protein Phosphorylation Protein phosphorylation is well studied and the effect of phosphorylation at specific sites for many proteins has been experimentally examined. Phosphorylation is key in signal transduction from extracellular signals and RTK activation[335]. 290 phospho-sites of 181 proteins were identified to be reduced in KITLG-p53RE -/- cells while 14 were upregulated across 12 proteins (Figure 3.10.A). Phosphorylation sites can be both activating and inhibitory. The differential phosphorylation sites were enriched for processes downstream of PI3K/AKT/mTOR (MYC Targets; OR=21.54, FDR = 5.64e-15; MTORC1 Targets; OR=6.72, FDR=5.92e-04; Figure 3.10.B). Three kinases which are part of the PI3K/AKT/mTOR pathway were found to show reduced phosphorylation status including SRC Ser17, PRKCI Thr564 (functions downstream of PI3Ks and SRC and inhibits BAD) and PAK4 Ser181[407][408][409]. Of particular note, we identified that phosphorylation of Raptor protein (a component of mTORC1 and encoded by RPTOR) at Ser722 was significantly increased in KITLG-p53RE -/- cells (Figure 3.10.C). Phosphorylation of this site forms a binding region for 14-3-3 proteins which can then bind and lead to mTOR inhibition[410]. AMPK is

one kinase known to phosphorylate Ser722 while PI3K/AKT and MAPK activity reduces phosphorylation of this site, suggesting that Raptor can integrate pro- and anti-proliferative upstream signals[410][411]. This result corroborates our previous findings, through transcriptomics and proteomics, that mTOR target-genes are downregulated and suggests a potential integration point between the canonical p53 apoptotic program and the pro-survival p53/KITLG axis.

Combination Specific Transcripts (CSTs) are enriched for genes targeted by the PI3K/AKT/mTOR pathway

Through transcriptomic and proteomic analyses, we found evidence to suggest genetic inhibition of KITLG/KIT reduced activity through the PI3K/AKT/mTOR signal transduction pathway. Next, we determined whether pharmacological inhibition of KITLG/KIT could recapture this result using our transcriptomic dataset. We hypothesised that those transcripts differentially expressed between Combo treated cells and both Nutlin-3a and Dasatinib treated cells would be enriched for genes relevant to the mechanism(s) underpinning the synergy between KITLG/KIT inhibition and p53 activation. The contrast between Combo and Nutlin-3a treated cells indicated 116 differentially regulated genes (FDR < 0.05) of which 40 showed greater than a 2-fold change in either direction (Figure 3.11.A, Left). As expected, many more genes were differentially expressed when contrasting Combo and Dasatinib treated cells. 1,758 genes were significant (FDR < 0.05) and 541 were found to have a fold change greater than 2-fold in either direction (Figure 3.11.A, Right). Among the 116 genes and 1,758 genes differentially expressed between Combo and Nutlin-3a and Combo and Dasatinib respectively, 43 were found to overlap (Figure 3.11.B). This overlap was a greater overlap than expected by chance (OR=4.9, p=1.4e-13). We termed these 43 genes the Combination Specific Transcripts (CSTs, Supplementary Table C.5). The 43 CSTs were found to be enriched for 10 Hallmark gene sets including genes targeted by NFKB, the PI3K/AKT/mTOR pathway and EMT genes (Figure 3.11.C). Six of the PI3K/AKT/mTOR-related CSTs overlapped with genes differentially expressed after genetic inhibition of KITLG/KIT. For example, MCL1 and SLC2A1 (encoding

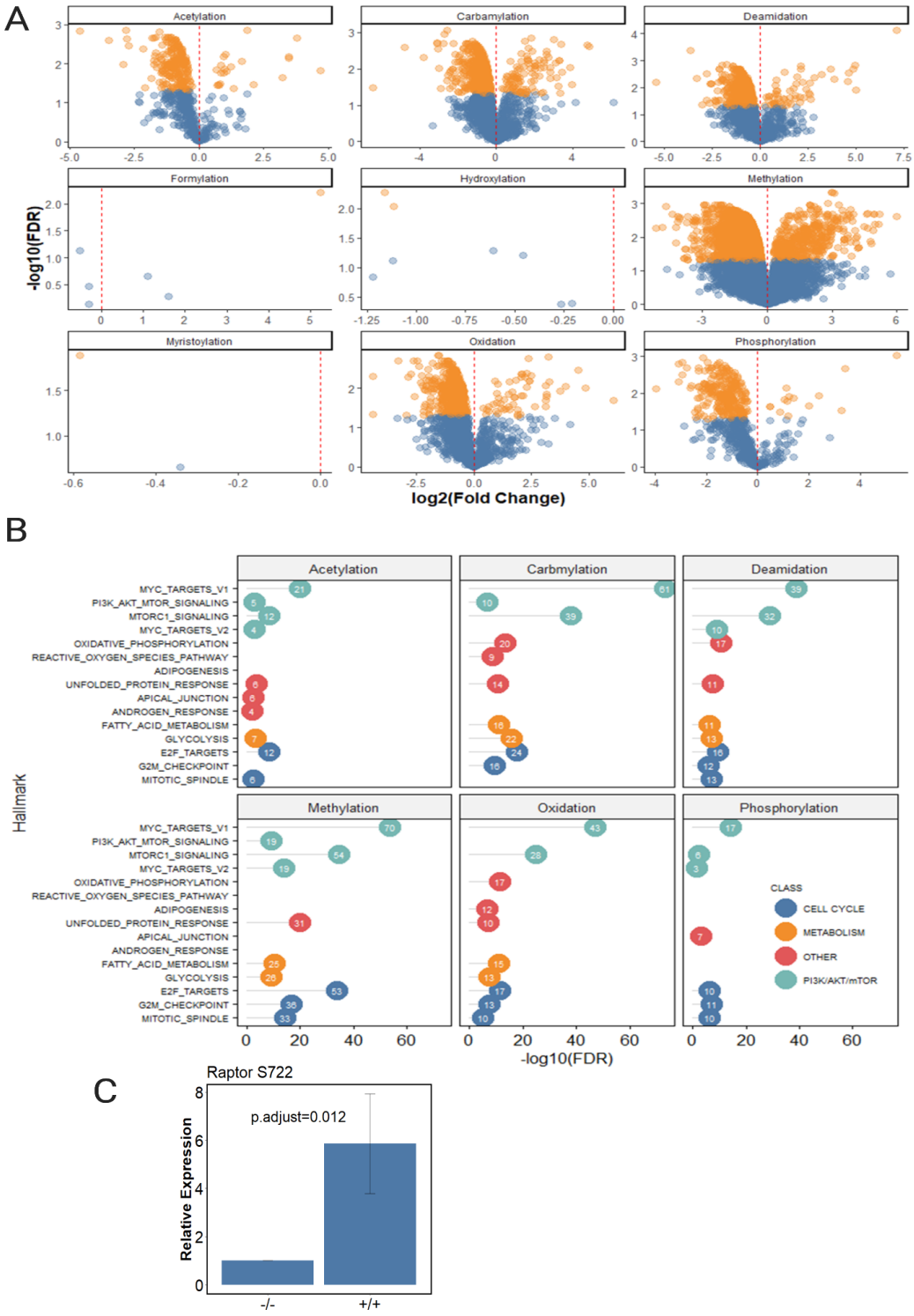


Figure 3.10: **A**) As part of our proteomics analysis, we analysed the differential expression of PTMs. 7,930 PTMs across 2,485 genes were significant. Volcano plots are shown for each PTM class. Significant PTMs are coloured orange. FDR < 0.05 was considered significant. **B**) A dot plot is shown for each PTM type whereby enough PTMs were differentially expressed to carry out functional enrichment analysis. Enrichment was tested by hypergeometric test using Hallmark gene sets. FDR-q < 0.05 was considered significant. **C**) Barplot indicating the relative expression of Raptor S722 in -/- and +/+ cells from the proteomics dataset. The significance value indicates the FDR-q value from limma. Error bars indicate SEM over three biological replicates.

GLUT1) were found to be downregulated by both genetic and pharmacological inhibition of KITLG/KIT, are upregulated by PI3K/AKT/mTOR signalling and inhibit apoptosis[412][413][414][415][416][417].

Multiplexed immunoblotting of phospho-kinases identifies PI3K/AKT/mTOR signalling to be downregulated

Our transcriptomic and proteomic analysis suggests that PI3K/AKT/mTOR signalling may be the dominant signal transduction pathway activated by the p53/KITLG/c-KIT axis in TGCT cells. In order to further support this model, we utilised a phospho-kinase array to simultaneously measure the levels of key phospho-sites across PI3K/AKT/mTOR, JAK/STAT and RAS/ERK signal transduction pathways (Materials and Methods). The 43 antibodies for the 43 phosphorylation sites are fixed onto a membrane in a dot like pattern and incubated with protein lysate. After exposure, the pixel density of the dots is directly related to the level of phosphorylation. We categorised the 43 epitopes as being part of the PI3K/AKT/mTOR pathway (n=9), the RAS/ERK pathway (n=4), the JAK/STAT pathway (n=7) or other (n=23). We determined which phosphorylation sites were differentially expressed after genetic (KITLG-p53RE +/+ vs KITLG-p53RE -/-) and pharmacological (+/+ DMSO vs +/+ Dasatinib 2uM 6hrs) inhibition of KITLG/KIT using our isogenic TERA1 cell-models. The phospho-kinase array identified consistent downregulation of three components of the PI3K/AKT/mTOR pathway (AKT, mTOR, CREB) which is consistent with our transcriptomic and proteomic data whereby we found reduced expression of genes upregulated by activated AKT and mTOR (Figure 3.11.D). However, no consistent downregulation of RAS/ERK or JAK/STAT components was found. Together, our transcriptomic, proteomic and PTM data indicate that PI3K/AKT/mTOR signalling is likely to mediate the pro-survival data from KITLG/KIT in TGCT cells.

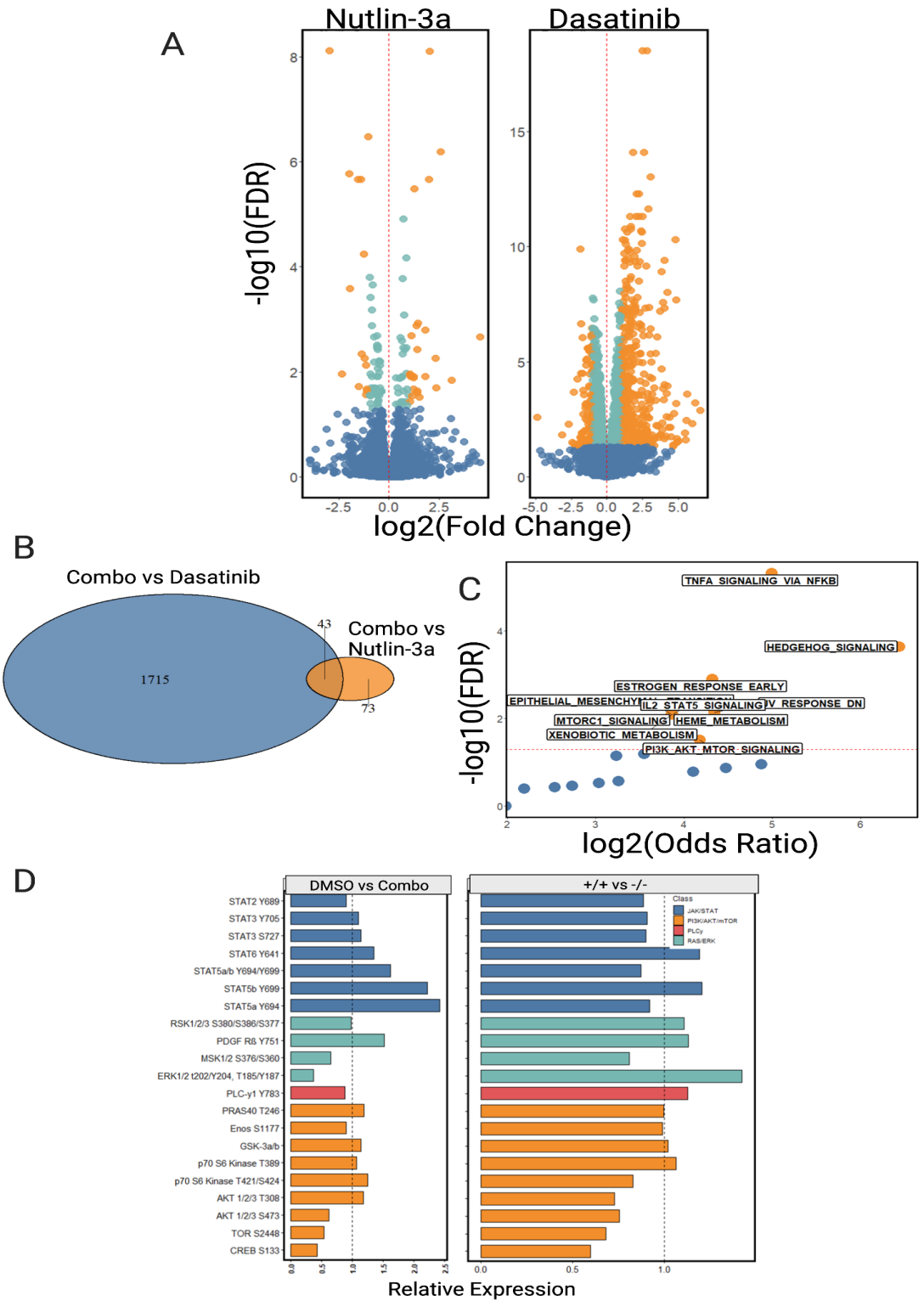

A
Nutlin-3a
Dasatinib
-log10(FDR)
log2(Fold Change)
B
Combo vs Dasatinib
1715
43
73
Combo vs Nutlin-3a
C
TNFA_SIGNALING_VIA_NFKB
HEDGEHOG_SIGNALING
ESTROGEN_RESPONSE_EARLY
IL2_STAT5_SIGNALING
MTORC1_SIGNALING
HEME_METABOLISM
XENOBIOTIC_METABOLISM
PI3K_AKT_MTOR_SIGNALING
-log10(FDR)
log2(Odds Ratio)
D
DMSO vs Combo
+/+ vs -/-
Class
JAK/STAT
PI3K/AKT/mTOR
PLCγ
RAS/ERK
STAT2 Y689
STAT3 Y705
STAT3 S727
STAT6 Y641
STAT5a/b Y694/Y699
STAT5b Y699
STAT5a Y694
RSK1/2/3 S380/S386/S377
PDGF Rß Y751
MSK1/2 S376/S360
ERK1/2 t202/Y204, T185/Y187
PLC-γ1 Y783
PRAS40 T246
Enos S1177
GSK-3a/b
p70 S6 Kinase T389
p70 S6 Kinase T421/S424
AKT 1/2/3 T308
AKT 1/2/3 S473
TOR S2448
CREB S133
Relative Expression

Figure 3.11

Figure 3.11: **A**) Volcano plots for the contrast between the transcriptomes of Combo and Nutlin-3a treated +/+ cells (Left) and Combo and Dasatinib treated +/+ (right). Nonsignificant genes are marked in blue, significant genes with log2 fold change < 1 in light green and significant genes with log2 fold change > 1 in orange. Log2 transformed fold change in displayed on the X axis and -log10 transformed FDR on the Y. **B**) The Venn diagram indicates the overlap of the DEGs from the comparison of Combo vs Nutlin-3a and Combo vs Dasatinib. The significance of the overlap was determined by the Exact Fisher Test. **C**) Functional enrichments were performed on the 43 Combination Specific Transcripts (CSTs) using Hallmarks gene sets. The log2 transformed odd ratio is shown on the X and -log10 transformed FDR on the Y axis. Enrichments were performed using hypergeometric test. Significant enrichments (FDR < 0.05) are coloured orange and labelled. **D**) The barplots indicate the results of a phospho-kinase array to measure the expression of 21 phosphorylation sures across PI3K/AKT/mTOR, RAS/ERK, JAK/STAT and PLCy signal transduction pathways. Bars indicate the mean of two independent biological replicates, each consisting of two technical replicates. The expression is normalised to the DMSO treated +/+ (dotted line) in both charts.

3.3.4 Clinically relevant gene modules in TGCT are enriched for PI3K/AKT/mTOR genes

Introduction to WGCNA

By analysing multi-omics datasets derived from our isogenic TGCT cell-lines, we found evidence that the PI3K/AKT/mTOR signal could be the predominant pro-survival signal transduction pathway downstream of c-KIT. Cell-lines are not always truly representative of patient tumours[418]. To address this, we performed an unsupervised analysis of TGCT patient transcriptomes to determine gene modules relevant to disease progression, high disease stage and early age of diagnosis. If the PI3K/AKT/mTOR pathway is truly important in TGCT tumours, it should be enriched for in such modules compared to other gene sets (Figure 3.12.A). To do this, we applied Weighted Gene Co-expression Network Analysis (WGCNA, Figure 3.12.A) to the TCGA cohort of TGCT samples. Briefly, this method detects correlation patterns amongst genes (features) and groups genes into modules of highly correlated genes by hierarchical clustering. Each module can be represented by an eigengene which can then be correlated with traits (Figure 3.12.B, see Materials and Methods for detailed information).

The Blue and Green modules associate with higher disease stage, earlier age of diagnosis and progression

We first determined the best soft threshold power value to use for network building (beta, see Materials and Methods) by finding the lowest value beta which afforded a scale free topology fit of above 0.9 and minimised the mean connectivity to below

< 100. In this case, we selected a value of 12 for beta as this provided values of 0.92 and 6.26 for the fit and connectivity respectively (Figure 3.12.C). After clustering into modules; 5,076 genes were not assigned to a module (grey). Twelve modules were formed ranging from 43 to 2,217 genes (See Materials and Methods for details on network building). The eigengene for each module was calculated and correlated with each trait of interest (Figure 3.13.A). From the heatmap, it is clear that the Blue (n= 1,582 genes) and Green (n= 782 genes) modules associate with earlier age of diagnosis (Blue; R=-0.17,p=0.03; Green; R=-0.21,p=0.01), higher disease stage (Blue; R=0.3,p=2e-04; Green; R=0.31,p=1e-04) and disease progression (Blue; R=0.2,p=0.01; Green; R=0.17,p=0.04). The Green module also associates with the incidence of lymph node metastases and the Blue module with poor prognostic score (igcccg stage). The Blue and Green modules also show strong positive correlation with KITLG and TP53 expression. The Turquoise module negatively correlates with KITLG and TP53 expression and shows the inverse trend for the clinical traits. We focused on the Blue and Green modules for further analysis.

The Blue and Green modules are enriched for PI3K/AKT/mTOR genes

For a given trait, each gene can be considered using two values, the Gene significance (GS) value and the Module Membership (MM). GS relates to the absolute correlation of the gene with a trait and MM to strength of the membership to its assigned module. Supplementary Figure A.4 show scatterplots of GS for Tumour Stage against MM for the Blue, Green and Turquoise modules. It is clear from these plots that the genes showing the highest correlation with Tumour Stage are also the core genes (highest MM) for the modules which correlate with Tumour stage. The fourth panel plots the Tumour Stage GS against MM for the Black module which does not associate with Tumour Stage. It is clear from this plot that GS and MM are not positively correlated. The adjacency between each eigengene and with Tumour Stage is shown in Supplemental Figure A.5. The green and blue modules show the highest adjacency with tumour stage suggesting that genes within these modules could contribute to advanced disease.

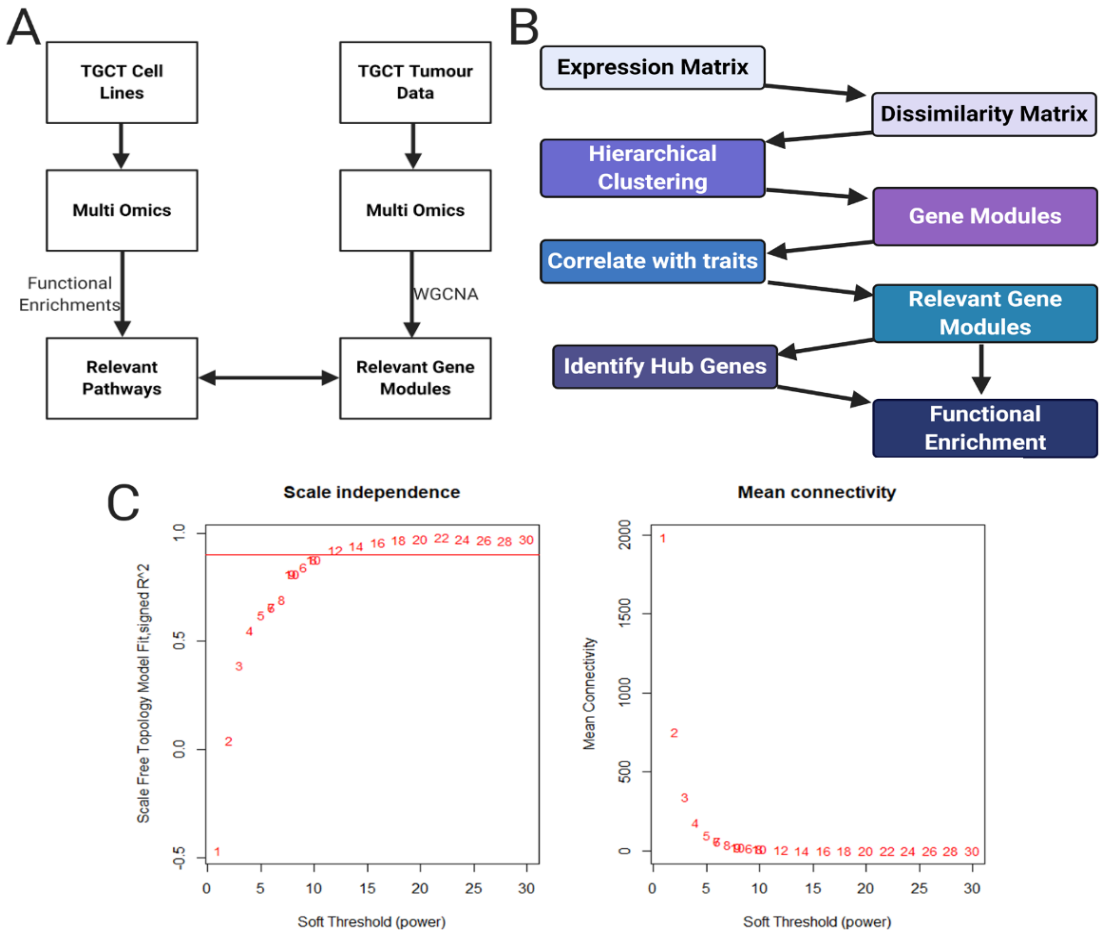


Figure 3.12: **A**) Schematic indicating the two approaches to identifying gene modules and pathways relevant to TGCT. In the previous sections, we utilised mutli-omics datasets derived from our isogenic TGCT cell lines. In this section we focus on the TGCT tumour data from the TCGA portal and apply WGCNA to identify relevant gene modules. We reasoned that overlapping pathways between our two approaches could be promising therapeutic opportunities for TGCT. **B**) We applied WGCNA to the TGCT transcriptomes of the TCGA cohort. The workflow is shown in this schematic. Using the expression matrix (samples and genes), a dissimilarity matrix is constructed which represents the correlation of each gene with all other genes. Hierarchical clustering is applied to this matrix to assign genes to gene modules. The module is decomposed to a modular eigengene which gives a single representative value of expression of that module in each sample. Eigengenes are correlated with traits of interest such as progression and age of diagnosis to identify relevant modules. Then functional enrichment of the modules can be determined while highly connected hub genes can be identified as these may represent the key genes and pathways which could be targeted. **C**) The soft thresholding power (β) is constant which is used to calculate the adjacency of two genes from their correlation. The absolute correlation estimate is raised to the power of beta. Beta therefore controls how much weight is given to small correlations in the network, higher betas mean smaller correlations are given less weight and connectivity is reduced. Scatter plots indicating how a suitable beta (Soft thresholding power) value was selected for network construction. The left hand plot (Scale independence) plots the Scale Free Topology (SFT) against values of beta from 1 to 30. The lowest beta value to fulfil SFT > 0.9 is optimal. The right hand figure plots the beta against the Mean Connectivity. In this case, lower Mean Connectivity values are better with a value below 100 required for reliable network building. A value of 12 was chosen for network building.

Next, we analysed the genes making up the Blue and Green modules. The Blue module consists of 1,582 genes with a mean Tumour Stage GS of 0.20 and mean MM of 0.71. The Green modules consists of 782 genes with a mean Tumour Stage GS of 0.22 and mean MM of 0.68. The GS scores for all modules with respect to Tumour Stage are indicated in Figure 3.13.D. To determine which annotated gene sets and pathways were encompassed within these modules, we tested for enrichment of Hallmark gene sets (Hypergeometric Test, Figure 3.14.A). The Blue module was found to be strongly enriched for Hallmarks associated with the interaction between cells and their microenvironment. For example, 94 genes within the EMT hallmark were found in this module; these genes are associated with shift of tumour cells to migratory and invasive phenotypes and can be induced by PI3K/AKT/mTOR signalling[419][420][421]. Moreover, the Blue module was found to be enriched for genes upregulated by KRAS and NFKB activity. KRAS is a key oncogene in TGCT and commonly features activating mutations while we found NFKB target-genes to be enriched in our transcriptomic and proteomic analyses of TERA1 cells[422]. The Green module was enriched for genes targeted by MYC, NFKB and PI3K/AKT/mTOR signalling. Interestingly, we found a significant overlap between the Blue and Green module genes and genes regulated by KITLG/KIT in TERA1 cells (1.6-fold, p=2e-05, Figure 3.14.B). Specifically, 136 genes which were downregulated after deletion of the KITLG-p53RE and rescued by the knock-in were found and these were enriched for EMT (14.1-fold, FDR=2.2e-06) and MYC targets (7.5-fold, FDR=6.3e-03) and included KITLG itself.

Blue hub genes are enriched for PI3K/AKT/mTOR genes

Hub genes are the most highly connected genes in the module and may be enriched for master regulatory pathways of the module. We utilised two approaches to identify hub genes, the absolute gene expression correlations and protein-protein interactions (PPI) mined from STRING.v12 (Materials and Methods). To calculate the 'degree' of each gene with relation to expression, a correlation matrix was computed and the sum of correlations for each gene was found. The top quartile

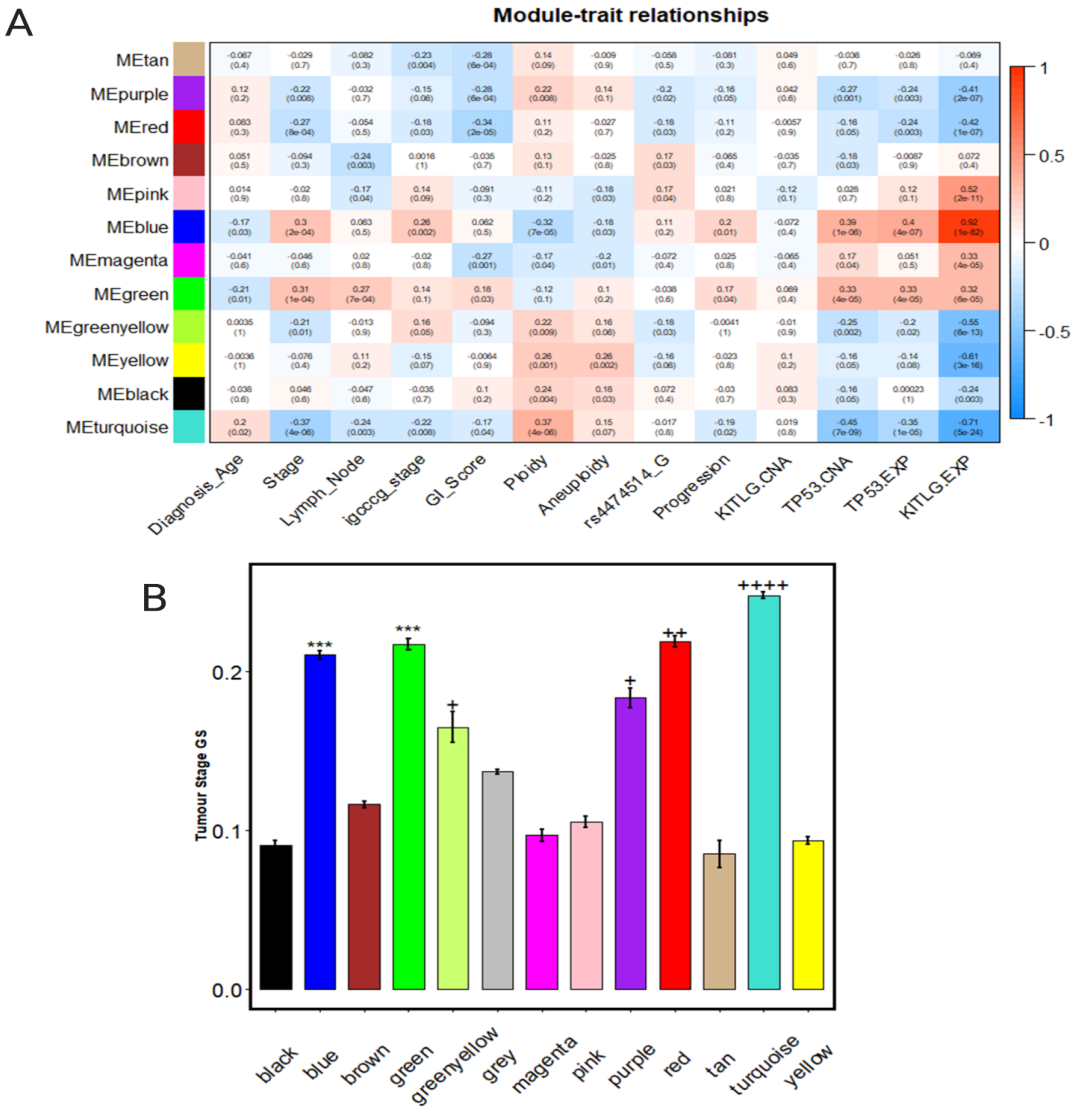


Figure 3.13: **A**) Heatmap indicating the correlation between each module eigengene and clinical and genomic traits. Colouring of each element reflects the direction and strength of correlation (red for positive and blue for negative). The exact correlation values and p values are noted in each element. **B**) The gene significance measures for each module can indicate which modules are most interesting for a given trait. This barplot indicates the gene significance scores for genes within each module with respect to Tumour Stage. Error bars indicates the standard error of the mean. Gene significance scores are the absolute measures of correlation (0-1). Significant positive associations are signified by the Asterix *. Significant negative associations are indicated by the addition sign +.

(25%) of genes with the highest degree were considered as hub genes (Supplemental Figure A.6, Upper row). Similarly, for PPI, the scores of the interactions between proteins were summed for each protein with the top quartile again considered as hub gene candidates (Supplemental Figure A.6, Lower row). The overlapping genes were considered as hub genes (Supplementary Table C.6). For the Blue module, 2,415 PPIs were found with high confidence (STRING Confidence > 700) and after calculating the degree for each gene 153 genes were found to constitute the top quartile. Of these, 64 overlapped with the top quartile of genes from the expression list, a significantly greater overlap than expected by chance (Fisher Exact Test, OR = 2.24, p=9.9e-06). By pathway analysis in STRING.v12, these 64 genes are enriched for PI3K/AKT signalling genes and genes involved with focal adhesion and ECM-receptor signalling (Figure 3.14.C). For the Green module, 2,884 PPIs were found, and 114 genes were found to contribute to the top quartile of PPI interactions. Of these, 34 overlapped with the top quartile of the expression list which did not constitute a significant overlap. These 34 genes formed three distinct clusters; one consisting of spliceosome factors, one of ribosome components and a third composed of cell cycle promoting and proteasome genes (Figure 3.14.D). These analyses found that the Blue and Green gene modules were positively correlated with Tumour stage, prognosis, disease progression and earlier age of diagnosis. We also highlighted that core genes within these two modules are enriched for genes regulated by PI3K/AKT/mTOR signalling such as IGFBP5 and RRM2 which are established mTORC1 target-genes[423][424].

Blue and Green MEs Associate with Progression in TGCT

The Blue and Green modules correlate with key clinical parameters such as disease stage. The modules can be represented by the eigengene values. We investigated whether the values of these eigengenes associate with progression in TGCT patients by the Kaplain-Meier method (Materials and Methods). Importantly, high expression of the Blue and Green module eigengenes was found to significantly associate with faster progression (p.blue = 0.004, p.green = 0.02, Figure 3.14.E)

while high expression of the Turquoise eigengene was found to associate with reduced progression (p=0.023, Figure 3.14.E). Of the Blue and Green modules, 256 genes (11%) are assigned to PI3K/AKT/mTOR-related Hallmarks (PI3K/AKT/mTOR; MYC targets; MTORC1 targets; EMT, NFKB targets). For 80 of these genes (31%), high expression significantly associated with faster progression in a univariate analysis (FDR < 0.05) with only one gene showing the opposite trend. Of the remaining 2,108 genes assigned to the Blue and Green modules, only 13 genes (0.6%) significantly associated with survival, constituting a 73-fold enrichment for PI3K/AKT/mTOR-related genes amongst significantly prognostic genes from the Blue and Green modules compared to unrelated genes (p=2e-68). The WGCNA analysis provides further evidence that KITLG/KIT promotes PI3K/AKT/mTOR signalling and that this pathway contributes to disease progression.

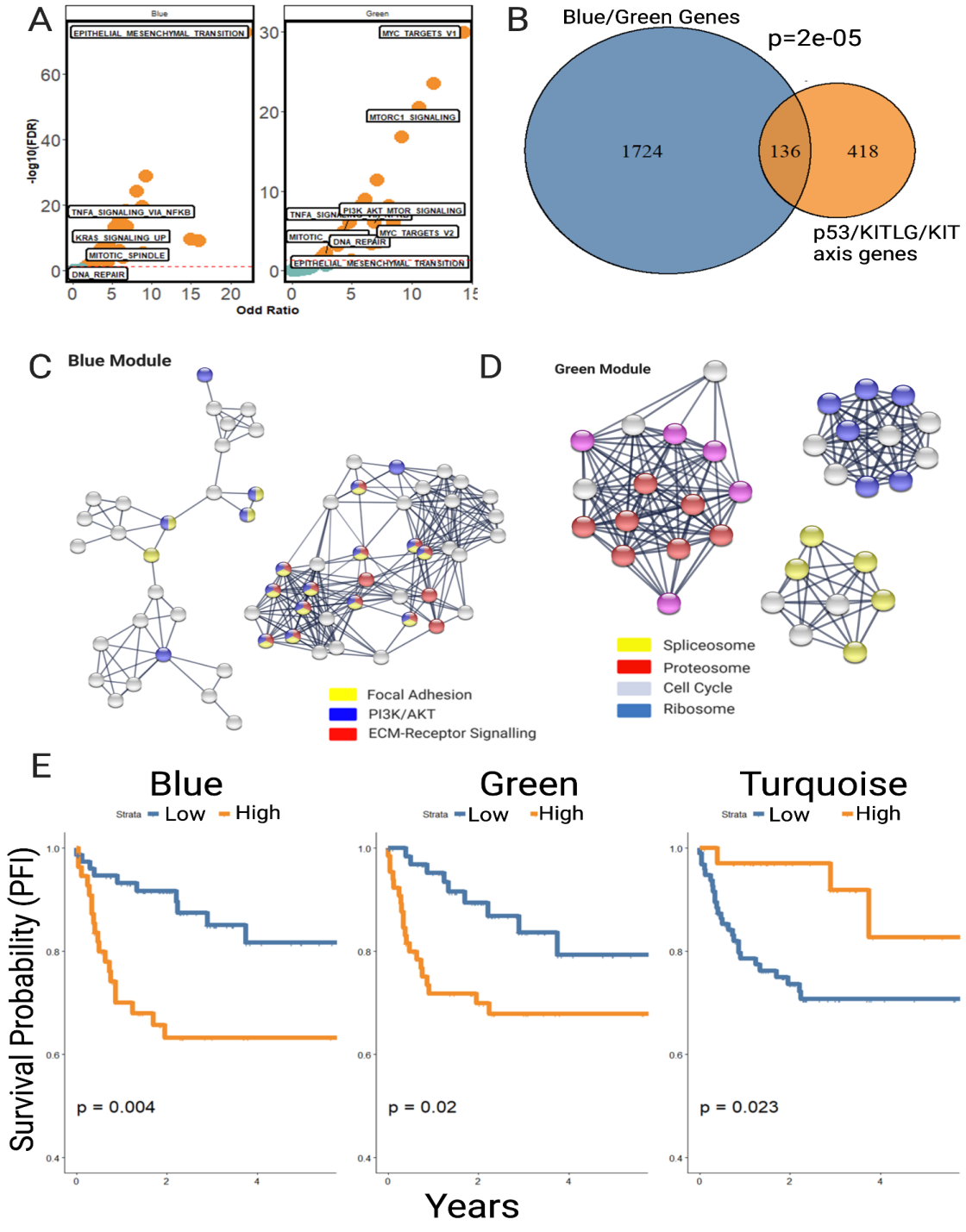


Figure 3.14: **A**) The genes comprising the Blue and Green modules were used as input for gene set enrichment using the hypergeometric test. The p-values were corrected by FDR and the -log10 transform of the FDR-q value is shown on the Y axis. The odd ratio of the enrichment is shown on the X. **B**) Venn diagram indicating the overlap between the genes making up the green and blue modules and genes regulated by the KITLG p53RE (genes downregulated in -/- cells and rescued by the -/KI). The significance of the overlap was determined by a two-tailed Exact Fisher Test. **C**) STRING.v12 network for the hub genes of the Blue module. Nodes are coloured based on their role in Focal Adhesion (Yellow), PI3K/AKT signalling (Blue) and ECM/Receptor signalling (Red). **D**) STRINGv.12 network for hub genes of the Green module. Nodes are coloured based on roles in the Spliceosome (yellow), Proteosome (red), cell cycle promotion (light blue) and the ribosome (dark blue). **E**) The expression of the Blue, Green and Turquoise eigengenes were found for the TGCT patients in the TCGA cohort. The cases were separated into high and low groups using the surv_cutpoint function. The association with progression was determined using the survfit function which uses the Kaplain-Meier method.

3.3.5 PI3K/AKT/mTOR is a potential therapeutic target in TGCT

Through multi-omics analysis of our own isogenic cell TGCT cell-lines and WGCNA of TGCT tumour samples, we have provided evidence that KITLG/KIT promotes PI3K/AKT/mTOR signalling and that this pathway associates with progression, higher disease stage and earlier age of diagnosis. This is in line with previously published evidence which suggests PI3K/AKT/mTOR signalling could be active in TGCT and mediate chemosensitivity[422][425][426][427][428][429]. We therefore investigated whether inhibition of the PI3K/AKT/mTOR axis could be a viable alternative to c-KIT inhibition by exploring the effect of PI3K/AKT/mTOR inhibition on sensitivity to p53 activation in our isogenic cell-lines and determining whether KITLG expression (a measure of signalling through KITLG/KIT) associates with sensitivity to PI3K/AKT/mTOR inhibitors (Figure **??**.A).

KITLG-p53RE -/- cells are more sensitive to AKT inhibitors compared to +/+ cells

Previously, we found that KITLG-p53RE -/- cells were more sensitive to the KIT inhibitor, Dasatinib, compared to KITLG-p53RE +/+ cells. Dasatinib is known to target multiple RTKs[430]. If PI3K/AKT/mTOR signalling does transduce the pro-survival signal from KITLG/KIT in TGCT, we should be able to recapitulate the effects we found for Dasatinib with specific inhibitors of AKT. We began by re-examining our drug screen data whereby TERA1 and TERA2 KITLG-p53RE +/+ and -/- cells were treated with 317 anti-cancer compounds. 20 of these are known to inhibit PI3K/AKT/mTOR signalling and for 16 of these, -/- cells were found to be more sensitive (greater than 2-fold change, Figure **??**.B). This constituted a significant enrichment for PI3K/AKT/mTOR inhibitors amongst significant compounds (3.8-fold, p=0.03). Only three of eleven inhibitors of the MEK/ERK pathway were significant, a significant depletion (OR=0.23, p=0.03). For JAK/STAT inhibitors, no significant effect was found (p=0.49). We selected three PI3K/AKT/mTOR inhibitors for testing by the MTT assay.

Ipatasertib and AZD5363 (Capivasertib) are competitive ATP inhibitors, prevent the phosphorylation of AKT targets and are currently in clinical trials for cancer treatment[431][432][433][434]. The third inhibitor, MK-2206, is an allosteric inhibitor of AKT which we chose as a negative control due to its mechanism of action. MK-2206 prevents phosphorylation and activation of AKT and its activity should therefore be independent of upstream signalling from KITLG/KIT[435]. TERA1 KITLG-p53RE -/- and +/+ cells were treated with a concentration range of each inhibitor for 48hrs and cell viability was determined by MTT. For Ipatasertib (22-fold, p=0.00052) and AZD5363 (11.6-fold, p=0.027), -/- cells were found to be significantly more sensitive while no difference was determined for MK-2206 (p=0.84; Figure **??**.C).

AKT knockdown and AKT inhibition enhance sensitivity to p53 activation

We next aimed to demonstrate that impairment of AKT activity could sensitise cells to p53 activation. We used two methods of AKT inhibition: 1) AKT knockdown by siRNA and 2) pharmacological inhibition of AKT using the three inhibitors. Firstly, for the knockdown of AKT, TERA1 KITLG-p53RE +/+ cells were pre-treated with AKT1 siRNA for 24hrs and then treated with Nutlin-3a for a further 24hrs. We calculated the dose response curve for the control and AKT targeted siRNAs and found AKT1 knock-down cells to be significantly more sensitive (p=0.03; Figure **??**.D). Secondly, as for the synergy experiments described in detail in Chapter Two, we treated TERA1 KITLG-p53RE +/+ and -/- cells with each AKT inhibitor and Nutlin-3a. Importantly, synergy was found in all cases for KITLG-p53RE +/+ cells (CI <1) and intriguingly, the synergy between Ipatasertib and AZD5363 with p53 activation was significantly reduced in -/- cells (Ipatasertib; 1.6-fold, p=0.037; AZD5363, 1.9-fold, p=0.049; Figure **??**.E). As we hypothesised, the synergy between MK-2206 and p53 activation was not dependent on the p53-KITLG axis (p=0.64). To demonstrate that the synergy between AKT inhibitors and p53 activation is not specific to Nutlin-3a, we investigated the synergy between AZD5363 and Ipatasertib with Doxorubicin. Importantly, synergy was found in in

both cases for KITLG-p53RE +/+ cells and was significantly reduced after deletion of the KITLG-p53RE (Ipatasertib; 1.7-fold, p=0.03; AZD5363, 2.2-fold, p=0.016; Figure **??**.F). These experiments in our isogenic cell-lines provide further support that KITLG/KIT confers signalling through the PI3K/AKT/mTOR pathway, and that inhibition of this pathway relinquishes p53 signalling from the negative feedback exerted by KITLG/KIT.

High KITLG Expression Associates with Lower Sensitivity to PI3K/AKT/mTOR Inhibitors

Our experiments with isogenic TCGT cell-lines indicates that the cells with high KITLG expression (+/+) are less sensitive to PI3K/AKT/mTOR inhibitors. We hypothesised that high KITLG expression could associate with reduced sensitivity to PI3K/AKT/mTOR inhibitors in other cell-lines and we tested this using the GDSC cell-line database. 33 drugs targeting the PI3K/AKT/mTOR pathway were found in GDSC1 and 21 in GDSC2 for a total of 44 unique inhibitors. For each compound we tested the effect of KITLG expression on the IC50 for cell-lines without TP53 mutation or deletion (Linear Regression, Supplemental Table C.7). For GDSC1, for 25 of 33 inhibitors (76%), high KITLG expression was found to associate with reduced sensitivity and for 6 of these (24%), including Capivasertib (AZD5363), the effect was dependent on TP53 WT (Figure 3.16.A). For GDSC2, 15 of 22 inhibitors (68%) were found to show higher IC50 with higher KITLG expression and 6 (40%) were p53 dependent, including Ipatasertib (Figure-16A). Importantly, in no cases did high KITLG expression associate with lower IC50 (higher sensitivity). RAS/ERK signalling can be activated downstream of c-KIT. To determine if KITLG expression also promotes insensitivity to RAS/ERK inhibitors, we repeated the analysis for this class of compounds. 16 and 11 RAS/ERK inhibitors were found in GDSC1 and GDSC2 respectively for 21 unique compounds. For GDSC1, 5 of 16 (31%) inhibitors were found to show a positive association with KITLG expression (higher KITLG, lower sensitivity) but none of these were dependent on wild-type TP53 (Figure-16B). Furthermore, four inhibitors (25%) indicated the opposite relationship whereby higher KITLG expression associated with higher sensitivity.

For GDSC2, only 2 of 11 (18%) were found to show a positive association with KITLG expression and neither were wild-type TP53 dependent (Figure 3.16.B). We

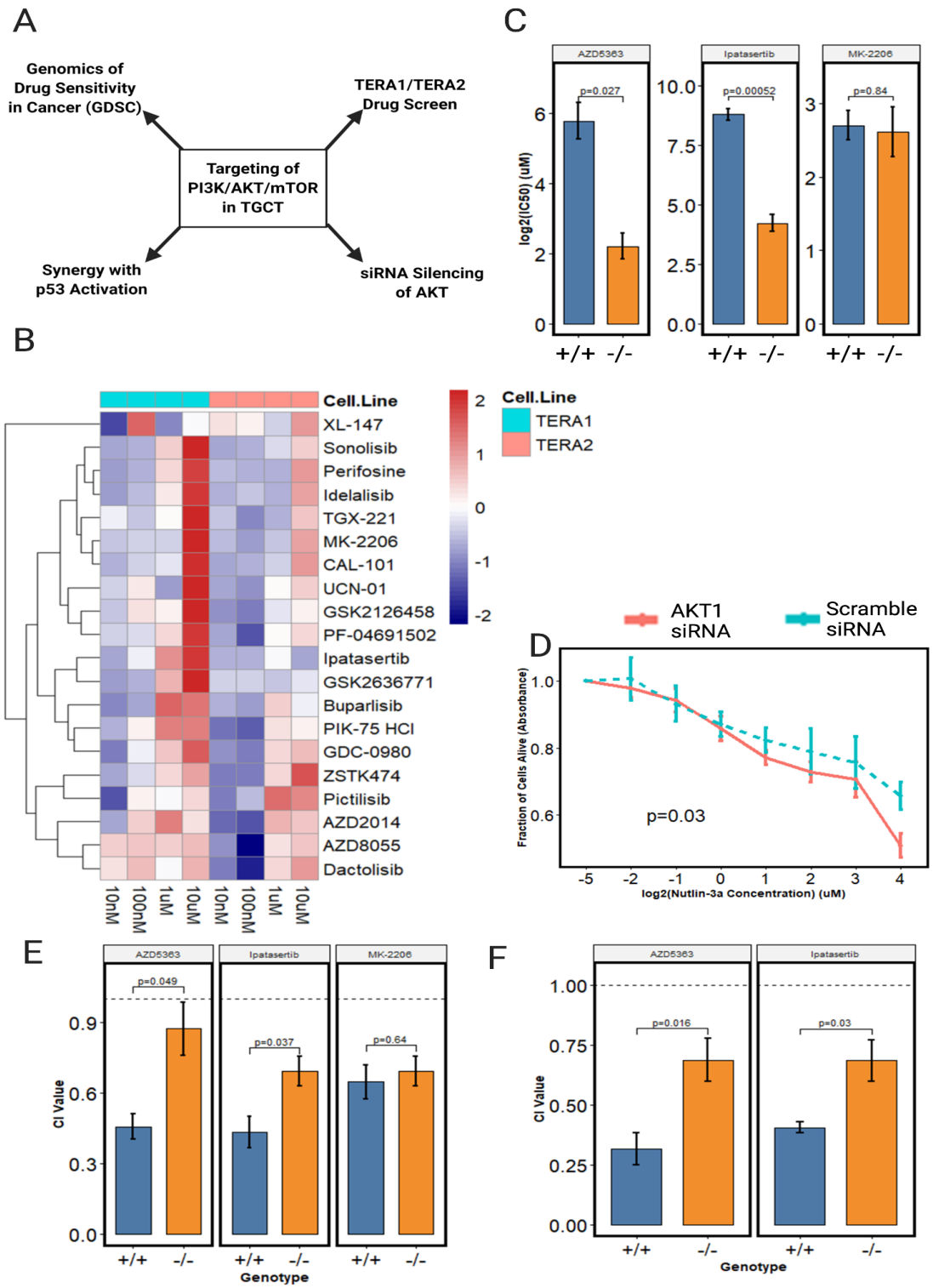


Figure 3.15

Figure 3.15: **A**) Schematic indicating the four lines of evidence indicating that PI3K/AKT/mTOR inhibition combined with p53 activation could be a therapeutic opportunity for TGCT. **B**) The heatmap indicates the sensitivity of TERA1 -/- cells PI3K/AKT inhibitors compared to TERA1 +/+ cells in the drug screen dataset which was introduced in Chapter Two. The higher the red colouration, the more sensitive KITLG p53RE -/- cells are to PI3K/AKT inhibitors. **C**) We validated by MTT assay the heightened sensitivity of -/- cells to AKT inhibitors compared to +/+ cells. Cells were seeded in a 96well plate, incubated for 24hrs and then treated for 48hrs with AZD5363, Ipatasertib or MK-2206 (0.3625uM to 20uM) at which point cell viability was measured. IC50s were calculated from the absorbance data. The error bars indicate the SEM over three biological replicates. **D**) We validated the survival effect of AKT on the sensitivity of TGCT cells to p53 activation by Nutlin-3a by silencing AKT by siRNA. Cells were pre-treated with AKT or ctrl siRNA for 24hrs before a further 24hrs of treatment with Nutlin3a. Cell viability was then measured by MTT. **E**) TERA1 +/+ and -/- cells were treated with one of AZD5363, Ipatasertib or MK2206 and Nutlin-3a (0.3625uM to 20uM). Viability was determined by the MTT method and synergy was calculated by the CI method. Error bars indicate the SEM over three biological replicates. **F** TERA1 +/+ and -/- cells were treated with AZD5363 or Ipatasertib (0.3625uM to 20uM) and Doxorubicin (0.03625uM to 2uM). Viability was determined by the MTT method and synergy was calculated by the CI method. Error bars indicate the SEM over three biological replicates

combined GDSC1 and GDSC2 to find the number of compounds significant in at least one of the datasets (Figure 3.16.C). 37 of the 44 (84%) unique PI3K/AKT/mTOR inhibitors associated with KITLG expression in at least one dataset with 12 unique inhibitors significant and p53 dependent (27%). In contrast, only 7 RAS/ERK inhibitors were significant across the datasets (33%), a 2.6-fold reduction compared to PI3K/AKT/mTOR. Moreover, none of the RAS/ERK inhibitors were significant in a way which was TP53 WT dependent. These data support our model that higher KITLG expression reduces sensitivity to PI3K/AKT/mTOR inhibition. Together with our previous data, we provide comprehensive evidence, from multiple sources, that the PI3K/AKT/mTOR pathway is key to the pro-survival function of KITLG/KIT in TGCT and constitutes a therapeutic opportunity (Figure 3.16.D).

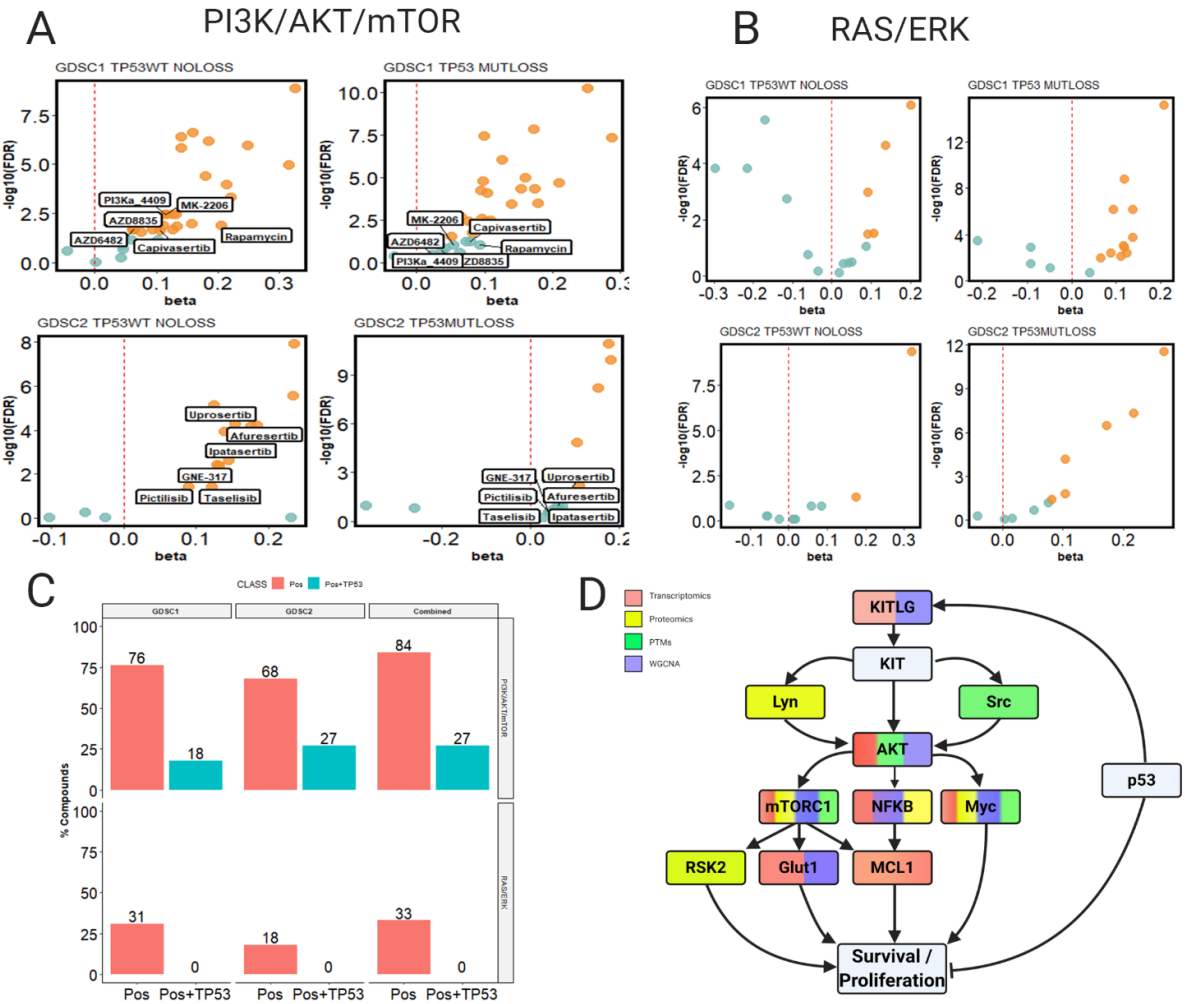


Figure 3.16: **A**) Using the Genomics of Drug Sensitivity (GDSC) dataset, for each PI3K/AKT/mTOR inhibitor in GDSC1 and GDSC2, we performed linear regression between KITLG expression and the log2 transformed IC50 of the compound in TP53 WT NOLOSS and TP53 MUTLOSS cell lines. Significant associations are coloured orange and TP53 Wild type dependent associations are labelled. **B**) As a control analysis, we determined the effect of KITLG expression on sensitivity to RAS/ERK inhibitors using the GDSC dataset. For each RAS/ERK inhibitor in GDSC1 and GDSC2, we performed linear regression between KITLG expression and the log2 transformed IC50 of the compound in TP53 WT NOLOSS and TP53 MUTLOSS cell lines. Significant positive associations are coloured orange and TP53 Wild type dependent associations are labelled. **C**) Summary barplots of the data in 16A and 16B. This plot indicates the percentage of compounds found to significantly associate with KITLG expression and to significantly associate with KITLG in a wild type TP53 dependent manner for PI3K/AKT/mTOR and RAS/ERK inhibitors in GDSC1, GDSC2 and the combined dataset. **D**) We identified multiple components and genes of the PI3K/AKT/mTOR pathway in the analyses of the transcriptomic, proteomic, PTM and TCGA datasets. Factors found by transcriptomics are coloured RED (KITLG, AKT, mTORC1, NFKB, Myc, Glut1, MCL1). Factors found by proteomics are shown in yellow (Lyn, mTORC1, NFKB, Myc and RSK2). Factors found by PTMs are indicated in green (SRC, AKT, mTORC1, Myc). Factors identified by WGCNA of the TCGA data are coloured blue (KITLG, AKT, mTORC1, NFKB, Myc, Glut1).

3.3.6 BCL2 family factors integrate signals from pro-survival KITLG/KIT and apoptotic p53 signalling

In this chapter, we have comprehensively shown that the general transcriptional function of p53 does not underlie the synergy between KITLG/KIT inhibition and p53 activation, yet the synergy is p53-dependent (Figures 3.6, 3.7). As part of the phospho-kinase array, we also found that expression of p53 S392 could be higher after inhibition of KITLG/KIT (Figure 3.8). This phosphorylation site promotes translocation of p53 to the mitochondria where p53 interacts with BCL2 family factors[393]. We found several other lines of evidence to suggest that modulation of BCL2 family factors could underlie the synergy between KITLG/KIT inhibition and p53 activation. Firstly, the single p53 target-gene which we found to be regulated by KITLG/KIT, SFN, encodes 14-3-3sigma which inhibits apoptosis by sequestering the pro-apoptotic BCL2 family factor, Bax (Figure 3.8)[282]. Secondly, we found MCL1, an anti-apoptotic BCL2 family factor, to be regulated by both genetic and pharmacological inhibition of KITLG/KIT (Figure 3.11). Thirdly, our results so far have indicated a role for the PI3K/AKT/mTOR axis which is known to upregulate anti-apoptotic BCL2 factors and repress pro-apoptotic factors [436] [437]. Fourthly, p53 is known to upregulate expression of pro-apoptotic BCL2 factors and we found BBC3 (Puma) and PMAIP1 (Noxa) to be induced by p53 activation in TGCT cells[438]. Given these data, we hypothesised that KITLG/KIT and p53 signalling might both modulate BCL2 factors to control mitochondrial apoptosis. We explored this possibility using our transcriptomic dataset.

Multiple BCL2 family factors are differentially expressed after modulation of p53 and/or c-KIT signalling

Mitochondrial apoptosis is controlled by the activity of BCL2 family factors. 22 BCL2 family factors have been described and 19 were expressed in our samples[439][436] (Table 3.2). Bax and Bak can oligomerise to form pores in the outer mitochondrial membrane which facilitates depolarisation and eventual rupture of the mitochondria. Other BCL2 family factors either promote or inhibit pore

formation; indeed, subtle changes in expression of BCL2 family factors can severely affect the probability of apoptosis[440]. To explore if BCL2 family factors could underpin the synergy between KITLG/KIT inhibition and p53 activation we analysed the expression of known BCL2 factors after p53 activation and after genetic or pharmacological inhibition of KITLG/KIT (Figure 3.17.A). After p53 activation through Nutlin-3a treatment, we found four BCL2 family factors to be differentially expressed. BBC3, PMAIP1 and BCL2L1 were upregulated while MCL1 was downregulated (FDR<0.05, Figure 3.17.B). Borderline upregulations were found for BIK and BAX (FDR=0.052). After pharmacological inhibition of KITLG/KIT (Dasatinib), six BCL2 factors were differentially expressed. HRK, BMF, BCL2L14 and BCL2L11 were upregulated and MCL1 and BCL2L1 were downregulated (Figure 3.17.B).

After the combined treatment, BBC3, PMAIP1, BCL2L14, BCL2L11 and BIK were significantly upregulated and trends towards upregulation were found for BAX, BMF and HRK. MCL1 was significantly downregulated and BCL2L1 was unchanged (Figure 3.17.B). BCL2L1 encodes the anti-apoptotic factor Bcl-X; interestingly, we found Dasatinib to prevent Nutlin-3a dependent induction of BCL2L1. These data indicate that after combination treatment, a greater number of pro-apoptotic BCL2 factors are upregulated compared to either drug alone. After genetic inhibition of KITLG/KIT, four pro-apoptotic BCL2 family factors were found to be higher in KITLG-p53RE -/- cells compared to +/+ cells (BID, HRK, BIK and BMF) while MCL1 was found to downregulated (Figure 3.17.C). Three of the five BCL2 factors affected by genetic inhibition of KITLG/KIT were also regulated, in the same direction, by pharmacological inhibition, suggesting a common mechanism. We did not utilise our proteomics dataset to examine the BCL2 factors as only four of the 10 differentially expressed genes were detected in our mass spectrometry analysis although MCL1 did show a trend towards reduced expression in -/- cells.

The ratio of the expression of anti-apoptotic and pro-apoptotic BCL2 factors is modulated by Dasatinib and Nutlin-3a treatment and by deletion of the KITLG-p53RE

The network of pro- and anti-apoptotic BCL2 family factors is heavily interconnected and the ratios in expression and activity of the numerous factors is thought to determine whether the threshold for mitochondrial depolarisation is reached[441][442][443]. To assess whether the ratio of anti- and pro-apoptotic factors acts as a rheostat in TGCT cells, we extracted the RPKM values for the 5 anti-apoptotic factors and 14 pro-apoptotic factors expressed in our samples and calculated the ratio of average expression of anti- versus pro-apoptotic factors; a lower ratio would indicate greater probability of apoptosis. In DMSO treated KITLG-p53RE +/+ cells, the ratio of anti- to pro-apoptotic BCL2 family factors was found to be 10; 3-fold and 1.3-fold reductions in the ratio were afforded by treatment with Nutlin-3a and Dasatinib respectively. Treatment with the combination of Dasatinib+Nutlin-3a led to a larger fold reduction in ratio compared to both individual treatment (3.5-fold). Under the rheostat model, simultaneous activation of p53 and inhibition of c-KIT appears to push the TGCT cells further towards apoptosis by reducing the anti- to pro-apoptotic ratio by a further 15% compared to Nutlin-3a alone. Interestingly, KITLG-p53RE -/- cells also show a smaller ratio compared to +/+ cells (1.4-fold reduction), similar to the difference achieved by pharmacological inhibition of KITLG/KIT. To determine which of the differentially regulated BCL2 family factors contribute most to the change in ratio, we calculated the ratios between the two anti-apoptotic factors (MCL1 and BCL2L1) and the six pro-apoptotic factors which were found to be differentially regulated after Nutlin-3a or Dasatinib treatment and are known to interact with either BCL2L1 or MCL1 [436]. Five of the six pro-apoptotic factors showed a significant reduction in the ratio with MCL1 and/or BCL2L1 after Nutlin-3a and/or Dasatinib treatment in isolation and 4 of these also showed a significant reduction in ratio with MCL1 and/or BCL2L1 after combo treatment ($p < 0.05$, BCL2L11, BBC3, PMAIP1 and BMF, Figure 3.17.D). Importantly, three of these four also showed significantly reduced ratio

with MCL1 and/or BCL2L1 in Combo treated cells compared to the individual treatments ($p < 0.05$, BCL2L11, BBC3, PMAIP1). This analysis highlights MCL1 and BCL2L1 as the key anti-apoptotic factors and BCL2L11, BBC3 and PMAIP1 as the key pro-apoptotic factors which could mediate the synergy between p53 activation and c-KIT inhibition (Figure 3.17.E).

Knockdown of MCL1 reduces cell viability and increases sensitivity to Nutlin-3a

In our high-throughput transcriptomics analysis we identified that both genetic uncoupling of the p53-KITLG axis and simultaneous inhibition of KIT with p53 activation modulated multiple BCL2 family factors which might contribute to the greater propensity towards apoptosis. We validated MCL1, PMAIP1 and HRK by qRT-PCR in both TERA1 and TERA2 cell-lines. The same conditions were used as for the RNA-seq samples (Materials and Methods). For TERA2 cells, we found that Nutlin-3a treatment increased expression of PMAIP1 while Dasatinib induced HRK (Figure 3.18.A). Moreover, both Nutlin-3a and Dasatinib led to reductions in MCL1 expression. For TERA1, we found similar results as for TERA2, although only two replicates were completed.

Next, we reasoned that if these genes are key factors in controlling apoptosis of TGCT cells then knocking-down their expression with siRNAs should affect cell viability. To do we pre-treated TERA1 +/+ cells with siRNAs targeted towards MCL1. As our model would suggest, we found that knockdown of MCL1 reduced viability (1.5-fold, p=0.019, Figure 3.18.B). Finally, we pre-treated TERA1 KITLG-p53RE +/+ cells with siRNA targeting MCL1 for 24hrs and then treated with Nutlin-3a for 24hrs. Knockdown cells were found to be significantly more sensitive to p53 activation compared to control cells (2.6-fold, p=0.036, Figure 3.18.C). Our cell-line work indicates that MCL1 is important for preventing apoptosis of TGCT cells both basally and after p53 activation.

Table 3.2: Summary of the 19 BCL2 family factors which were expressed in TERA1 cells.

Gene	**Synonyms**	**Apoptosis Anti/Pro**	**Detailed Function**
MCL1		Anti	Binds and inhibits BAX, Noxa , Puma, BIM, Bid
BCL2L1	BCL-X	Anti	Spliced into XL and XS variants, XL promotes survival by binding BAX and BAK
BCL2		Anti	Binds to BAX via BH1 and BH2 domains
BCL2L12		Anti	Can inhibit post-MOMP apoptosis
BCL2L2	BCL-W	Anti	Binds and inhibits BAX, BAK, BAD, BID, BIM, Puma, BMF and BIK
BBC3	Puma	Pro	Relives BAX/BAK of inhibiory action of anti-apoptotic factors
PMAIP1	Noxa	Pro	Binds MCL1 and BCL2A1
BIK	BLK	Pro	Binds BCL2, MCL1 and BCL2L1
BCL2L14	BCL-G	Potential Pro	Produces three isoforms and can bind BCL2L1
BECN1		Pro	Promotes crosstalk between apoptosis and autophagy
BID		Pro	Directactivator of BAX
HRK	DP5	Pro	Blocks BCL2 and BCL2L1 and deregulated in GBM
BAD		Pro	When dephosphorylated, inactivates BCL2 and BCL2L1
HUWE1	Mule	Pro	E3 ligase known to regulate MYC, p53 and MCL1
BMF		Pro	Cell damage releases BMF from the cytoskeleton and allows it to inhibit BCL2
BCL2L13	BCL-Rambo	Potential Pro	May induce apoptosis independently of classical mitochondrial pathways
BCL2L11	BIM	Pro	Inactivates BCL2 and BCL2L1

Table 3.2 continued from previous page

Gene	Synonyms	Apoptosis Anti/Pro	Detailed Function
BAX		Pro	Forms pores on the outer mitochondrial membrane to allow MOMP
BOK		Pro	Forms pores on the outer mitochondrial membrane to allow MOMP

The ratios of anti-apoptotic to pro-apoptotic BCL2 factors are significantly associated with TP53 and KITLG expression in cell-lines and associate with response to p53 activators

Our results so far indicate that p53 activation by Nutlin-3a and inhibition of the KITLG/KIT axis may synergise by modulating different fractions of the BCL2

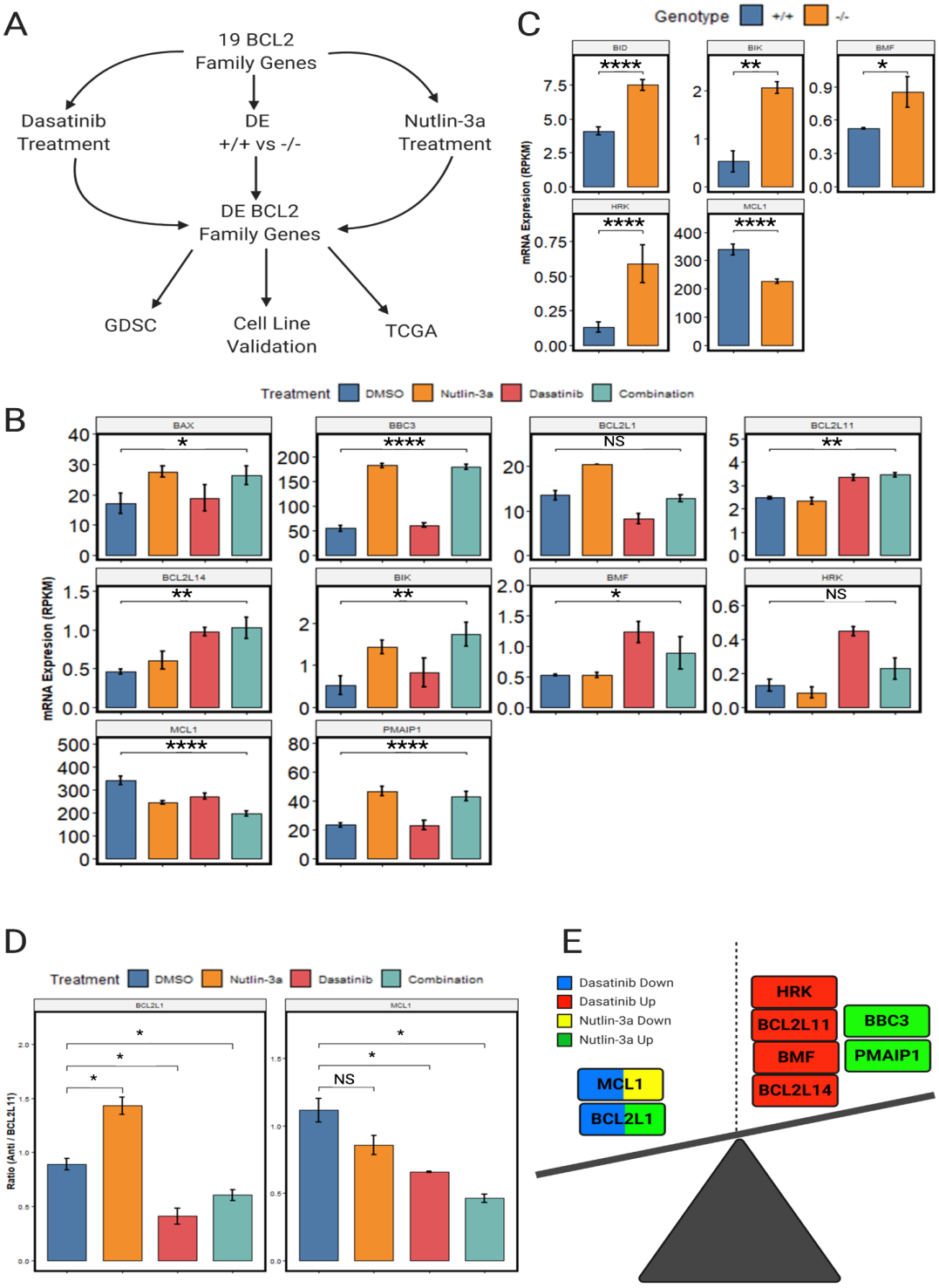


Figure 3.17

Figure 3.17: **A**) Schematic to indicate how we analysed the expression of BCL2 family factors in response to p53 activation and inhibition of KITLG/KIT. We identified BCL2 factors which were regulated by either genetic or pharmacological inhibition of KITLG/KIT or by p53 activation. We then explored the roles of the differentially regulated BCL2 family factors in our isogenic cell lines and their role in chemosensitivity in cell lines (GDSC) and in mediating progression in TGCT patients (TCGA).**B**) The barplots indicate the mRNA expression of 10 BCL2 family factors which are significantly differentially expressed after either Nutlin-3a or Dasatinib in TERA1 +/+ cells in the transcriptomics dataset. For each facet, the expression is shown for DMSO, Nutlin-3a, Dasatinib and combo treatment. The error bars indicate the SEM over three biological replicates and the signficance represents the FDR-q value from edgeR. **C**) Expression of the 5 BCL2 factors also found to be differentially expressed between TERA1 +/+ and -/- cells. Significance levels reflect the FDR-q values from edgeR for +/+ versus -/-. **D**) Barplots indicating the change in ratio of the anti-apoptotic factors BCL2L1 and MCL1 with BCL2L11 after Nutlin-3a, Dasatinib or Combination treatment from the transcriptomic data. Significance was tested by Student T-test. The higher the ratio, the lower the apoptotic potential of the cells. **E**) Schematic of how Dasatinib and Nutlin-3a may synergise in TGCT cells. Dasatinib induced expression of four pro-apoptotic factors (red) and reduced expression of two anti-apoptotic factors (blue). Nutlin-3a upregulated expression of two pro-apoptotic factors and one anti-apoptotic factor (green) and reduced expression of one antiapoptotic factor (yellow).

family rheostat which controls intrinsic apoptosis. We demonstrated in TERA1 cells that MCL1 expression associated with sensitivity to p53 activation. To test this more widely for the BCL2 factors, we utilised transcriptomic data for 304 TP53WT cell-lines (GDSC). For each cell-line, the ratio of MCL1 or BCL2L1 expression to each of BBC3, PMAIP1 and BCL2L11 was calculated and correlated with KITLG and TP53 expression. TP53 expression was found to significantly negatively correlate with MCL1/BBC3 (beta = -0.30, p = 1.6e-16, Figure 3.18.D) and BCL2L1/BBC3 (beta = 0.18, p = 5.2e-06). KITLG was found to have the opposite effect with higher expression associating with a higher ratio for BCL2L1 with all three pro-apoptotic factors (beta >0, p <0.05, Figure 3.18.D).

We next examined whether the anti/pro ratios significantly associated with response to five known p53 activating compounds (Nutlin-3a, Cisplatin, Doxorubicin, Etoposide and 5-Fluorouracil). 4/6 of the of the possible ratios positively associated with the IC50 of at least one p53 activating compound (beta >0, p<0.05). Specifically, MCL1/BBC3 was found to associate with Nutlin-3a IC50 (beta = 0.24, p = 1.2e-06), BCL2L1/BBC3 with 5/5 drugs, BCL2L1/PMAIP1 with 4/5 drugs and BCL2L1/BCL2L11 with 3/5 drugs (Figure 3.18.E). This analysis supports the model that p53 and KITLG/KIT can regulate expression of BCL2 family factors to control sensitivity to p53 activation.

The anti-/pro- ratio is significantly associated with TP53 and KITLG expression in tumours and associates with progression

Next, we hypothesised that the pro/anti ratios could be important in TGCT tumours. To test this, we calculated the ratios between MCL1 and BCL1L1 and each of PMAIP1, BBC3 and BCL2L11 for TP53 wild-type TGCT samples from the TCGA cohort and regressed these ratios against TP53 and KITLG expression. TP53 expression was found to associate with a reduced MCL1:BBC3 (beta = -0.40, p = 0.0069, Figure 3.18.F while non-significant negative trends were also found for MCL1:PMAIP1 and MCL1:BCL2L11. Surprisingly, TP53 expression also showed a positive association with BCL2L1:BCL2L11 (beta = 0.38, p = 0.0022), in line with our transcriptomics data. In contrast, KITLG expression was found to associate with significantly higher ratios for BCL2L1 and all 3 pro-apoptotic genes ($p < 0.05$, Figure 3.18.F) and for MCL1:PMAIP1 (beta = 0.08, p = 0.029), suggesting that p53 and KITLG/KIT could regulate the expression of BCL2 family factors in TGCT tumours. To determine if this translated into differential progression in TGCT patients, we employed a Cox regression model to analyse the effects of the ratios between MCL1:PMAIP1, BCL2L1:BBC3, BCL2L1:PMAIP1 and BCL2L1:BCL2L11 on the Progression Free Interval of 131 TP53WT TGCT patients. The ratio between BCL2L1:BCL2L11 was found to significantly associate with PFI whereby a higher ratio (lower apoptotic potential) associated with faster progression (p = 0.0023, Figure 3.18.G).

3.4 Discussion

In this chapter, we have explored the mechanism(s) through which inhibition of KITLG/KIT signalling might synergise with p53 activation. We utilised multi-omics datasets developed by ourselves and others in order to build a mechanistic model of the synergy. Synergy between two compounds suggests a common point

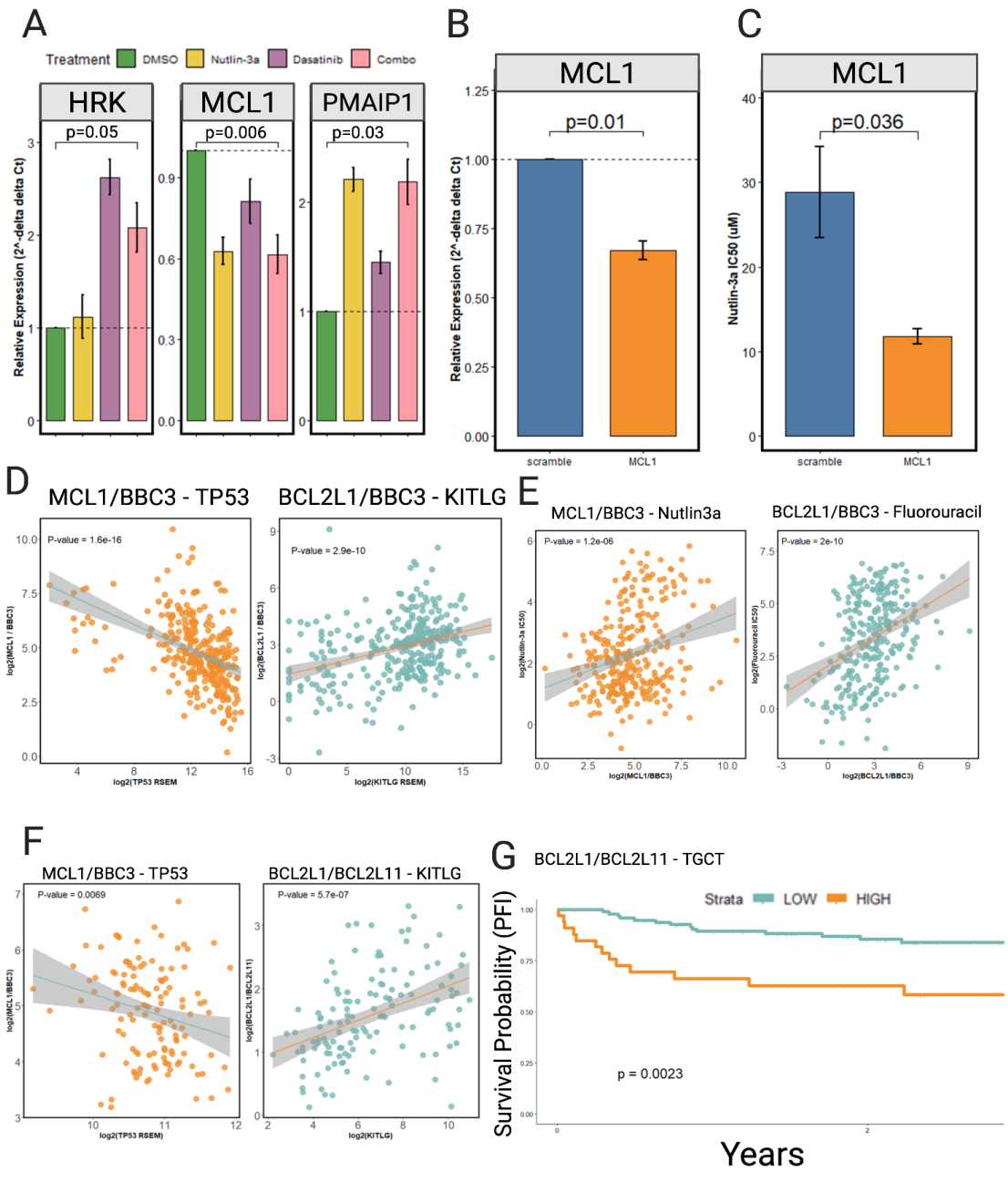


Figure 3.18

Figure 3.18: **A**) Boxplots indicating the change in expression of MCL1, PMAIP1 and HRK after Nutlin-3a (10uM), Dasatinib (2uM) or combination treatment for 6hrs in +/+ cells as determined by qRT-PCR. Significance determined by Student T-test. **B**) Bar plot indicating the effect of MCL1 siRNA knockdown on the viability of TERA1 KITLG p53RE +/+ cells. Cells were treated with control siRNA or MCL1 siRNA for 48hrs after which cell viability was assessedby MTT. Significance determined by Student T-test.**C**) Bar plots indicating the effect of MCL1 siRNA knockdown on the sensitivity of TERA1 KITLG p53RE +/+ cells to p53 activation by Nutlin-3a. Cells were treated with siRNA for 24hrs followed by Nutlin-3a (10uM) for 24hrs. Significance determined by Student T-test. **D**) To support our findings that KITLG/KIT signalling and p53 signalling could regulate BCL2 family factor expression, we explored the GDSC cell line data to see if this was also the case in a broader set of TP53 WT cell lines. For each cell line, the MCL1 and BCL2L1 ratios with each pro-apoptotic factor were found and the correlation with TP53and KITLG expression was calculated by Pearsons. The correlation between MCL1/BBC3 and TP53 is shown on the left and the correlation between BCL21/BBC3 and KITLG on the right. **E**) Using TP53 WT cell lines from the GDSC dataset, the MCL1 and BCL2L1 ratios with pro-apoptotic factors were correlated with sensitivity to p53 activating compounds including Fluorouracil and Nutlin-3a. The Statistical significance determined by Pearsons. The correlation between MCL1/BBC3 and Nutlin-3a is shown on the left and BCL21/BBC3 and Fluorouracil on the right. **F**) To support our findings that KITLG/KIT signalling and p53 signalling could regulate BCL2 family factor expression in TGCT, we explored the relationships between KITLG and p53 expression with BCL2 factor ratios in the TGCT tumour data from the TCGA. For each TGCT case, the BCL2 anti/pro ratio was determined. The correlation between MCL1/BBC3 and TP53 expression in TGCT tumours is shown on the left and the correlation between BCL2L1/BCL2L11 and KITLG in TGCT tumours on the right. Statistical significance determined by Pearsons. **G**) The anti/pro ratios were determined for each TGCT case and split into high and low ratio groups. The association with progression free survival was tested using the Kaplain-Meier method.

of integration between the two targeted pathways, in this case that KITLG/KIT promotes negative feedback on p53-dependent apoptosis. We reasoned there were at least six possible levels of integration which we could test (Figure 3.3).

3.4.1 KITLG/KIT does not regulate p53 expression levels or transcriptional activity

We found no evidence that KITLG/KIT could regulate p53 mRNA or protein levels (Figure 3.4). However, KITLG/KIT signalling has been found to regulate MDM2 activity in AML[444]. Dos Santos et al proposed a mechanism whereby c-KIT could inhibit p53 activity by promoting the phosphorylation of MDM2 by AKT. They found inhibition of c-KIT led to increase p53 protein levels and expression of BBC3, BAX and PAMIP1. Our data indicates that AKT is important but not by modulating MDM2 and p53. Moreover, we found no evidence for p53-mediated KITLG/KIT signalling in controlling general p53 dependent transcription (Figures 3.6, 3.7). This again highlights how our mechanism must be different to that published by[444]. We did find evidence that KITLG/KIT could regulate expression of the p53 target-gene, SFN, which has pro-survival function (Figure 3.8). Further experiments would be needed to decipher how KITLG/KIT might regulate the p53/SFN interaction.

3.4.2 Signalling from p53 and KITLG/KIT could integrate through control of mitochondrial apoptosis

We found preliminary evidence that KITLG/KIT signalling could negatively regulate phosphorylation of p53 S392 (Figure 3.8). Multiple earlier studies demonstrated that mutation of this site did not affect the transcriptional activity of p53[445][446][447]. This is in keeping with our omics data whereby we found very few p53 target-genes to be differentially expressed after KITLG/KIT inhibition. More recently, it has become clear that Ser392 phosphorylation promotes mitochondrial localisation of p53 which is important for apoptosis (Figure 3.19)[393][448]. How p53 Ser392 is regulated is controversial. CK2, p38, CDK9, PKR and IKKbeta have all been implicated and disproved by different studies[449][450][451][452][393][453][454][455][456]. One potential caveat to these studies is that dephosphorylation of p53 at S392 is thought to be a slow process meaning levels of phosphorylation could be detected after silencing of the responsible kinase and misinterpreted as a lack of effect[451]. Together with the fact that Dasatinib is a known inhibitor of CK2, can activate p38 and that we found a direct activator of p38 to be the top upregulated gene after Dasatinib treatment (MAP2K6), we reason that of previously noted kinases, p38 is most likely to mediate the link between KITLG/KIT signalling and p53 S392 in TGCT and warrants further exploration[457].

To provide further support for a role of mitochondrial p53 we began optimising immunofluorescence (IF) and cell fractionation protocols to study the subcellular localisation of p53 after inhibition of KITLG/KIT. In addition, we also planned to carry out immuno-precipitation experiments to determine if KITLG/KIT inhibited cells exhibited greater protein-protein interactions between p53 and BCL2 family factors. Our data provides motivation for future studies of mitochondrial p53 in TGCT. Moreover, future work should explore how KITLG/KIT regulates p53 S392. We found evidence that KITLG/KIT signalling might repress expression of MAP2K6, a direct activator of p38, one of the suggested kinases responsible for S392. It would be intriguing to further explore this link and determine whether MAP2K6/p38 are required for S392 in TGCT cells. To do so, TGCT cells could

be treated with p38 inhibitors or siRNA targeting MAP2K6 to determine if this prevented the heightened S392 phosphorylation after combination treatment and if so, does pre-treatment with MAP2K6/p38 inhibitors block the synergy between KIT inhibition and p53 activation.

In addition to the expression of p53 S392, we found multiple other lines of evidence to suggest that p53 signalling and KITLG/KIT could be integrated by regulating BCL2 family factors (Figures 3.17, 3.18). Firstly, Nutlin-3a and Dasatinib were found to upregulate different pro-apoptotic factors. Secondly, both Nutlin-3a and Dasatinib were found to reduce expression of the key anti-apoptotic factor, MCL1, and the combined effect was greater than either compound alone. MCL1 has been found to be highly expressed in multiple TGCT subtypes while a high MCL1/PMAIP1(Noxa) ratio has been shown to contribute to reduced sensitivity to p53 activation in embryonal carcinoma cells[458][459]. Thirdly, we found a second anti-apoptotic factor to be regulated by both Nutlin-3a and Dasatinib, BCL2L1. However, unlike MCL1, Dasatinib inhibits p53-dependent induction of BCL2L1. This is in line with other studies highlighting reduced BCL2L1 expression after Dasatinib treatment[460][461]. Our data indicates that inhibition of KITLG/KIT promotes mitochondrial priming whereby they are closer to the apoptotic threshold. Then, upon pro-apoptotic signalling by activated p53, these primed cells quickly undergo apoptosis at low drug concentrations. Mitochondrial priming has been shown to be controlled by the BCL2 family factors and is an important mediator of chemosensitivity in many contexts[462][463][464]. A similar mechanism has been eluded to before; in Blast Crisis CML (BC-CML) where Nutlin-3a was found to synergise with the c-KIT/BCR-Abl inhibitor Nilotinib[465][466]. By treating patient derived cells with Nutlin-3a and Nilotinib they were able to find that both compounds reduced the expression of MCL1 and BCL-x while Nutlin-3a also induced BAX and Puma. This supports our model for integration of KITLG/KIT and p53 signalling at the mitochondria through regulation of BCL2 family factors and provides a simple yet elegant model for the heightened sensitivity to p53 activation in KIT inhibited or KITLG-p53RE -/- TGCT cells.

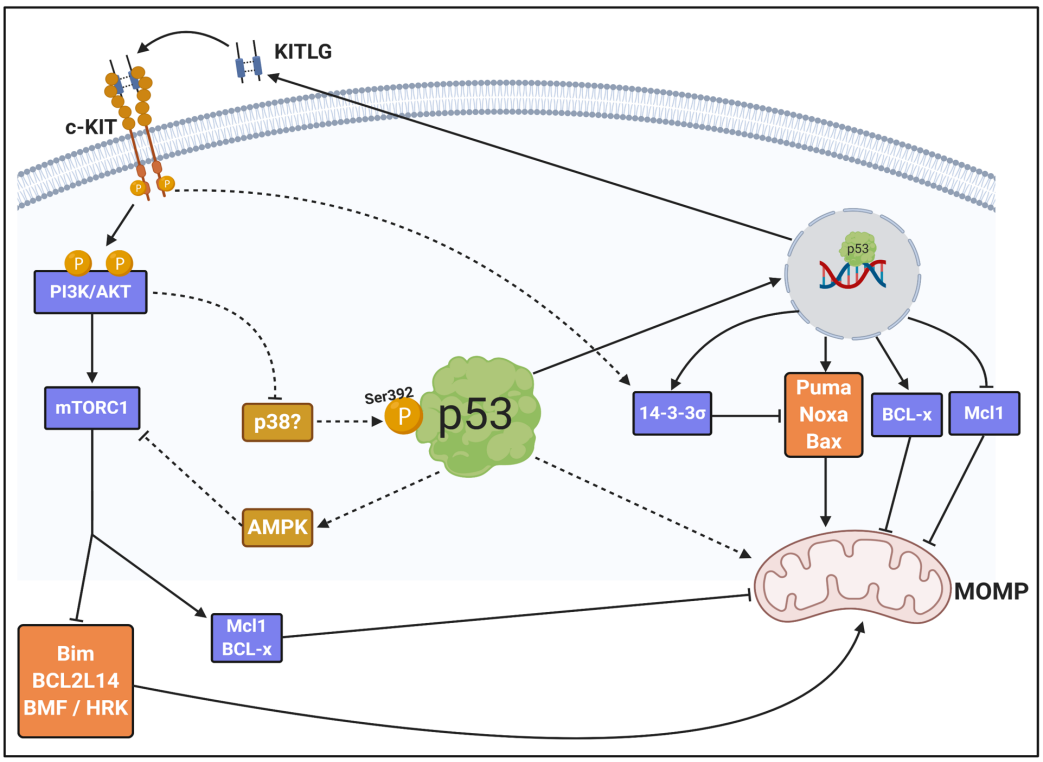


Figure 3.19: In this chapter we have provided preliminary evidence that the p53/KITLG axis and downstream signalling could integrate with p53 apoptotic signalling at multiple points. Firstly, we found phosphorylation of p53 S392 to be higher in KITLG P53re -/- cells and after the combination treatment suggesting that the pro-survival signal from c-KIT could repress phosphorylation of this site. We found evidence that an activator of p38, a kinase thought to phosphorylate S392, was upregulated after inhibition of c-KIT signalling. This phospho-site can promote p53 localisation to the mitochondria where it contributes to apoptosis. Secondly, we found an inhibitory phosphorylation site of Raptor to be increased in -/- cells. This site is phosphorylated by AMPK, a downstream signalling target of p53, and is dephosphorylated in an AKT dependent manner. S722 phosphorylated Raptor inhibits mTORC1. Thirdly, we found that both p53 signalling and c-KIT signalling modulated the expression of multiple pro- and anti-apoptotic BCL2 family factors which in turn control mitochondrial apoptosis. We also found evidence that KITLG/KIT could promote SFN expression after p53 activation. SFN encodes 14-3-3sigma which can sequester Bax and inhibit the apoptotic response. Putative interactions are indicated by dashed arrows. Factors with a pro-apoptotic function are indicated in orange while anti-apoptotic factors are coloured blue. MOMP – mitochondrial Outer Membrane Permeabilsation

The gold standard experiment for proving this model is BH3 profiling [462][467][468]. In this experiment, mitochondrial depolarisation is measured in cells subjected to different concentrations of pro- and anti-apoptotic BCL2 factor peptides. By monitoring the status of the mitochondria, the particular BCL2 factors which the cancer cells are addicted to for survival can be established. Given our preliminary data, we would hypothesise that TGCT are reliant on MCL1 for survival.

3.4.3 PI3K/AKT/mTOR signalling is key to pro-survival signalling from KITLG/KIT in TGCT

In this chapter, we aimed to delineate the mechanism(s) by which genetic and pharmacological inhibition of KITLG/KIT confer heightened sensitivity to p53 activation. One of the key steps in realising this mechanism was to determine which signalling pathway(s) transduce the survival signal from KITLG/KIT. Multiple well annotated pathways can transduce the signal, including PI3K/AKT/mTOR, RAS/ERK and JAK/STAT, but different pathways can be prevalent in different cell types[469][470][471][372]. Our analyses in this chapter provide multiple lines of evidence that PI3K/AKT/mTOR is the prevalent pathway in TGCT cells. First, we found that genes downregulated by genetic inhibition of KITLG/KIT and rescued by the knock-in were enriched for PI3K/AKT/mTOR (Figure **??**). Second, we found three components of the PI3K/AKT/mTOR/NFKB pathway to be downregulated at the protein level in KITLG-p53RE -/- cells (LYN, PIK3C3 and NFKB1, Figure **??**). Third, we found significant changes in PTMs of proteins involved in PI3K/AKT/mTOR signalling between KITLG-p53RE +/+ and -/- cells including higher phosphorylation of Raptor (proteomics) and reduced AKT phosphorylation (phospho-kinase array) in -/- cells (Figure 3.10). Fourth, we found CSTs to be enriched for genes upregulated by NFKB, mTORC1 and signalling through PI3K/AKT/mTOR (Figure 3.11). Fifth, by WGCNA of TCGA TGCT patient samples, we found the Green and Blue modules to associate with disease progression, higher clinical stage and higher TP53 and KITLG expression and to be enriched for PI3K/AKT/mTOR components (Figures 3.13, 3.14). Sixth, we found synergy between AKT inhibitors and p53 activation in TERA1 cells which was dependent on KITLG/KIT (Figure **??**). Seventh, in TP53 WT cell-lines from the GDSC data, we found high KITLG expression to associate with reduced sensitivity to AKT inhibitors in a wild-type TP53 dependent manner(Figure 3.16).

This is in keeping with previous findings that the PI3K/AKT/mTOR pathway is active in TGCT. Somatic mutations of PIK3CA and AKT have been found in cisplatin-resistant TGCT while some TGCT susceptibility loci identified in GWAS,

such as SPRY4, GAB2 and TDRG1 have been found to promote tumorigenesis via PI3K/AKT/mTOR[472][425][426][473]. Understanding the mechanisms of cisplatin-resistance in TGCT and targeting those mechanisms will be crucial for developing effective therapies for this patient group. We provide evidence that uncoupling the p53 pathway from the KITLG/KIT/AKT pathway could re-sensitise cisplatin-resistant TGCT. Together with previous publications which indicate the PI3K/AKT/mTOR pathway in cisplatin-resistance, these data suggest that targeting either c-KIT or AKT in combination with p53 activation could be a promising therapeutic avenue for refractory TGCT patients[474][475][476].

As part of the above analyses, we found preliminary evidence that p53 and KITLG/KIT could regulate an inhibitory phosphorylation site of Raptor (S722, Figure 3.10). Raptor is an mTORC1 component and can promote or inhibit mTOR activity depending on its phosphorylation status. Crosstalk between p53 and mTORC1 is complex but it is clear that they act antagonistically[477]. TSC2 is a p53 target-gene which converts Rheb-GTP to the inactive Rheb-GDP but we did not find evidence for a role for TSC2 in our analyses. Indeed, we did not find TSC2 to be upregulated by Nutlin-3a treatment in TERA1 KITLG-p53RE +/+ cells (FDR > 0.05). However, we did find the expression of two other p53 target-genes which are implicated in crosstalk with mTORC1, SESN1 and SESN2, to be strongly upregulated by Nutlin-3a treatment in TERA1 cells (SESN1, 2.9-fold, FDR=8.3e-11; SESN2, 3.5-fold, FDR=3.1e-09)[478][479]. SESN1 and SESN2 have been shown to activate AMPK in numerous contexts and that this interaction is important for sensitivity to ionising radiation in breast cancer cells[478][480][481][482]. Moreover, AMPK has been shown to phosphorylate Raptor at Ser722 and inhibit mTORC1 activity[410]. Interestingly, SESN1 has been found to be induced by cisplatin in TGCT cells[483]. It is possible that the combined effect of AMPK activation through p53 dependent induction of SESN1 and SESN2 and reduced signalling through the PI3K/AKT pathway act to keep mTOR activity low (Figure 3.19).

Multiple steps in this loop would need to be verified in TGCT cells. Firstly, the p53 dependent activation of AMPK would need to be established by immunoblotting

for AMPK phosphorylation after Nutlin-3a treatment. A role for SESN1 and SESN2 could be determined by siRNA targeting these two genes. Next, the phosphorylation status of Raptor at Ser722 would need to be validated. In our analyses we determined high phosphorylation on TERA1 KITLG-p53RE -/- cells compared to +/+ but we did not examine this after combination treatment. It would be intriguing to explore whether such a mechanism via AMPK could mediate the mTORC1 dependent expression of anti-apoptotic BCL2 family factors such as MCL1.

3.4.4 AKT inhibitors as promising anti-cancer therapies

In Chapter Two, we found that inhibition of c-KIT, through both genetic and pharmacological means, enhanced sensitivity to p53 activation. We utilised Dasatinib for c-KIT inhibition, an approved RTK inhibitor. In this Chapter, we have distilled the downstream signalling for c-KIT to the PI3K/AKT/mTOR pathway. Targeting this downstream pathway to block the effects of p53-dependent upregulation of KITLG could prove a better strategy than the use of Dasatinib which has the potential for more off target effects. Indeed, we found synergy between AKT inhibitors and p53 activators which was dependent on the p53/KITLG axis (Figure **??**). Although AKT has been considered an attractive anti-cancer target for many years, AKT inhibitors are yet to be approved for cancer treatment. However multiple AKT inhibitors are in clinical trials. Our cell-line work noted synergy between AZD5363 and Ipatasertib with both Nutlin-3a and Doxorubicin. Both of these compounds are ATP-competitive pan-AKT inhibitors which have been tested in humans. AZD5363 has shown effectiveness against breast and renal cancers in murine models and a basket trial for multiple solid tumour types indicated effectiveness against heavily pre-treated patients harbouring $AKT1^{E17K}$ mutations [484] [485]. Ipatasertib has indicated effectiveness against prostate cancer and ovarian cancer in mouse models and was found to be well tolerated in human patients with solid tumours[486] [485]. Our work adds more evidence to the potential benefits of AKT inhibitors as anti-cancer therapies. Firstly, we provide further molecular evidence to motivate the testing of AKT inhibitors in TGCT whilst we also demonstrate

effectiveness in TGCT cells. Secondly, we provide evidence that by combining AKT inhibitors with p53 activating therapies, we can leverage the p53/KITLG axis to boost tumour cell killing.

In some pre-clinical studies, it has been noted that inhibition of AKT could lead to compensatory changes in cellular signalling such as overexpression of upstream and downstream components[485]. Similar compensatory mechanisms have been found for single-compound treatments against PI3K and mTOR. For example, NVP-BEZ235 is dual inhibitor of PI3K and mTOR and was found to effectively inhibit AKT phosphorylation 1hr after treatment; however, 24hrs post treatment, AKT was again hyperphosphorylated[487]. To mitigate the compensatory effects, NVP-BEZ235 was combined with an AKT inhibitor and this both prolonged AKT inhibition and led to a significantly higher reduction in tumour volume in mice[487]. Triple targeting of PI3K/AKT/mTOR signalling may provide an effective approach for prolonged inhibition with high efficacy. Future studies exploring the potential for AKT inhibition in TGCT should explore combining triple targeting of PI3K/AKT/mTOR signalling with p53 activating therapies.

4

Identifying novel, druggable inhibitors of the p53-apoptotic response in the p53 network

Contents

4.1 Abstract 139
4.2 Introduction 140
4.2.1 The activity of wild-type p53 in cancer is clinically relevant 140
4.2.2 KITLG/c-KIT signalling is key in the development of multiple tissues 140
4.2.3 Tissue specificity of TP53 target-genes 141
4.3 Results 144
4.3.1 The p53 pathway in human cancer 144
4.3.2 KITLG/KIT alterations in human cancer 151
4.3.3 P53 target-gene expression accurately predicts the tissue of origin of tumours 169
4.3.4 Identifying p53 inhibitors using pharmacogenomics . . . 175
4.3.5 Exploring the role of pro-survival p53-target genes in human tumours 179
4.4 Discussion 186
4.4.1 Co-modulation of KITLG/KIT and p53 signalling could have therapeutic benefit in Skin Cutaneous Melanoma . 186
4.4.2 KITLG/KIT signalling could inhibit the p53-apoptotic response in TP53 wild-type Colon Adenocarcinoma . . . 189
4.4.3 CPE and PARD6G could represent cancer-type specific, druggable inhibitors of p53-mediated tumour-suppression 191
4.4.4 The importance of context 194

4.1 Abstract

We have identified a negative-feedback loop, involving KITLG, PI3K/AKT/mTOR signalling and BCL2 family factors, which negatively regulates p53-dependent apoptosis. TGCT very rarely mutates TP53; indeed, around 50% of all tumours retain wild-type p53 and yet are heterogeneous in their response to p53 activating therapies. In this Chapter, we couple patient and cell-line omics data with prognosis and drug sensitivity respectively, to identify novel inhibitors of p53-mediated apoptosis which have also previously been shown to be induced by p53. We find that the KITLG/KIT pathway could be targetable amongst TP53-wild-type melanoma and colon cancer patients while we identify two other druggable p53 pathway genes which associate with reduced sensitivity to p53 activation and with poorer prognosis in cancer.

4.2 Introduction

4.2.1 The activity of wild-type p53 in cancer is clinically relevant

TP53 mutation is common and clinically relevant; germline mutations define Li-Fraumeni syndrome (LFS) while somatic TP53 mutations can affect response to therapy and prognosis [488][489] [490][491]. Indeed, there is a substantial research effort to develop inhibitors of mutant p53 and regain wild-type function. Some compounds, such as APR-246, are in clinical trials [492]. 50% of tumours do not mutate TP53; these tumours likely inhibit p53 directly or downstream signalling[168][493][494]. For example, upregulation of negative regulators, such as MDM2/MDM4, and loss of downstream signalling components, such as p21, is common in human tumours and increase tumour burden in murine models[495][496][497][498][158][499][164]. In addition to MDM2/MDMX, other autoregulatory loops have been described which mediate chemoresistance (Figure 4.1)[500][501][502]. For instance, inhibition of the p53-induced phosphatase, WIP1, enhances p53 activation and sensitivity to Doxorubicin and Etoposide[503]. Despite early excitement regarding the re-activation of wild-type p53, therapeutic targeting of p53 regulators has so far proved futile due to unfavourable levels of specificity, toxicity and bioavailability[504][499]. We previously studied the KITLG-p53RE-SNP and established KITLG/KIT signalling as a targetable inhibitor of the p53-apoptotic response in TGCT. In this Chapter, we combine deep omics characterisation of human tumours and cancer cell-lines with clinical and drug sensitivity data respectively, to uncover other novel, inhibitors in the p53 pathway which could aid efforts to reactivate wild-type p53 in cancer.

4.2.2 KITLG/c-KIT signalling is key in the development of multiple tissues

KITLG/KIT signalling is important for normal development of testes, is hijacked during tumorigenesis and is a therapeutic target in TGCT[505][506]. A similar mechanism could underpin tumorigenesis in other tissues whereby, like TGCT, KITLG/KIT signalling is key to normal development (Figure 4.2.A).

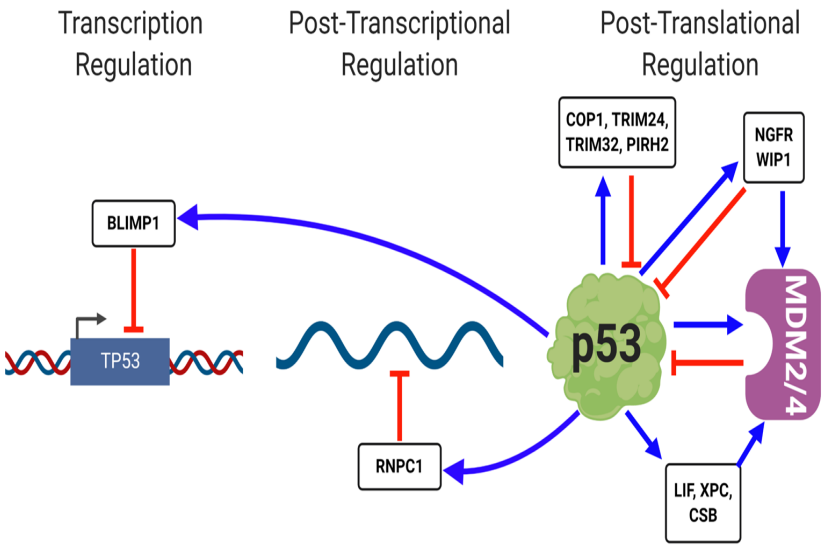


Figure 4.1: Autoregulatory loops involving p53. p53 upregulates multiple factors which negatively regulate p53 expression and activity. BLIMP1 inhibits transcription from TP53. RNPC1 binds to the 5' end of p53 mRNA and prevents cap-binding by eIF4E. Multiple factors are known to directly regulate p53 protein and/or the activity of the key negative regulators of p53, MDM2/MDM4. Like MDM2, PIRH2 and COP1 are E3 ubiquitin ligases which can target p53 for degradation. TRIM24 and TIM32 also promote p53 degradation. WIP1 is a phosphatase which reduces p53 transcriptional activity by dephosphorylating p53 Ser15. Moreover, WIP1 dephosphorylates p38, an activator of p53, and MDM2, leading to higher MDM2 activity towards p53. NGFR can bind to the p53 DBD to prevent gene transactivation while it also promotes MDM2 activity towards p53. LIF, XPC and CSB all promote MDM2 activity.

KIT signalling is key to haematopoiesis; expression levels are high in haematopoietic stem cells but expression is lost during differentiation [185]. KIT signalling is important for MITF activation and pigmentation [507]. KITLG/KIT signalling maintains the interstitial cells of Cajal and KIT loss impairs gut function and can cause constipation [508][509][510]. KITLG/KIT signalling regulates stem-cell populations and plays a role in the response of some tissues to injury, including the brain and lungs [511][512][513][514].

4.2.3 Tissue specificity of TP53 target-genes

Multiple feedback loops regulate p53 signalling[500]. Our work adds p53-mediated KITLG/KIT signalling to this network, but other negative-feedback loops could be hijacked by other cancer-types. Indeed, due to cell-type differences in DNA methylation and chromatin-accessibility, p53 induces expression of different target-genes in different tissues [515][516][517][518]. A meta-analysis of p53 target-genes found striking differences in reported p53 target-genes between studies. Of 3,661

reported p53 target-genes, only 343 (10%) were found in more than three datasets and of the 16 high-throughput studies, only two genes were found in all (CDKN1A and RRM2B)[115]. Moreover, a recent systematic survey of p53 DNA-binding in cell-lines from different cancer-types identified nearly 500 peaks (5% of peaks) which were highly variable between cell-lines [519]. The two studies described above suggest that a core suite of target-genes may be regulated by p53 in most tissues but that tissue-specific target-genes are likely to exist. We reason that tissue-specific p53 target-genes could be leveraged to better understand pro- and anti-tumour functions of p53 in different cancer-types. Therefore, in this Chapter we integrate omics and pharmacological data from cancer cell-lines to identify novel inhibitors of the p53-apoptotic response in the p53 network (Figure 4.2.B). We then utilise omics data from 33 cancer-types to highlight patient groups whereby these genes could inform the management of cancer.

Studies of p53 target-genes have also provided evidence that the ability of p53 to induce KITLG expression is not restricted to testicular cancer cells. Fischer et al noted that 8 of 16 high-throughput studies found p53 to be a regulator of KITLG expression, covering osteosarcoma, colorectal and breast cancer and human foreskin keratinocytes while Zeron-Medina et al demonstrated p53 to induce KITLG expression in cell-lines derived from testicular, breast and colorectal tumours[115][176]. Given the ability of p53 to regulate KITLG across multiple tissue-types and the pleiotropic nature of KITLG/KIT signalling (see above section), we hypothesised that cancer-types other than TGCT may also inhibit tumour suppression by wild-type p53 though KITLG/KIT signalling and therefore might represent a repurposing opportunity for combined KIT inhibition and p53 activation.

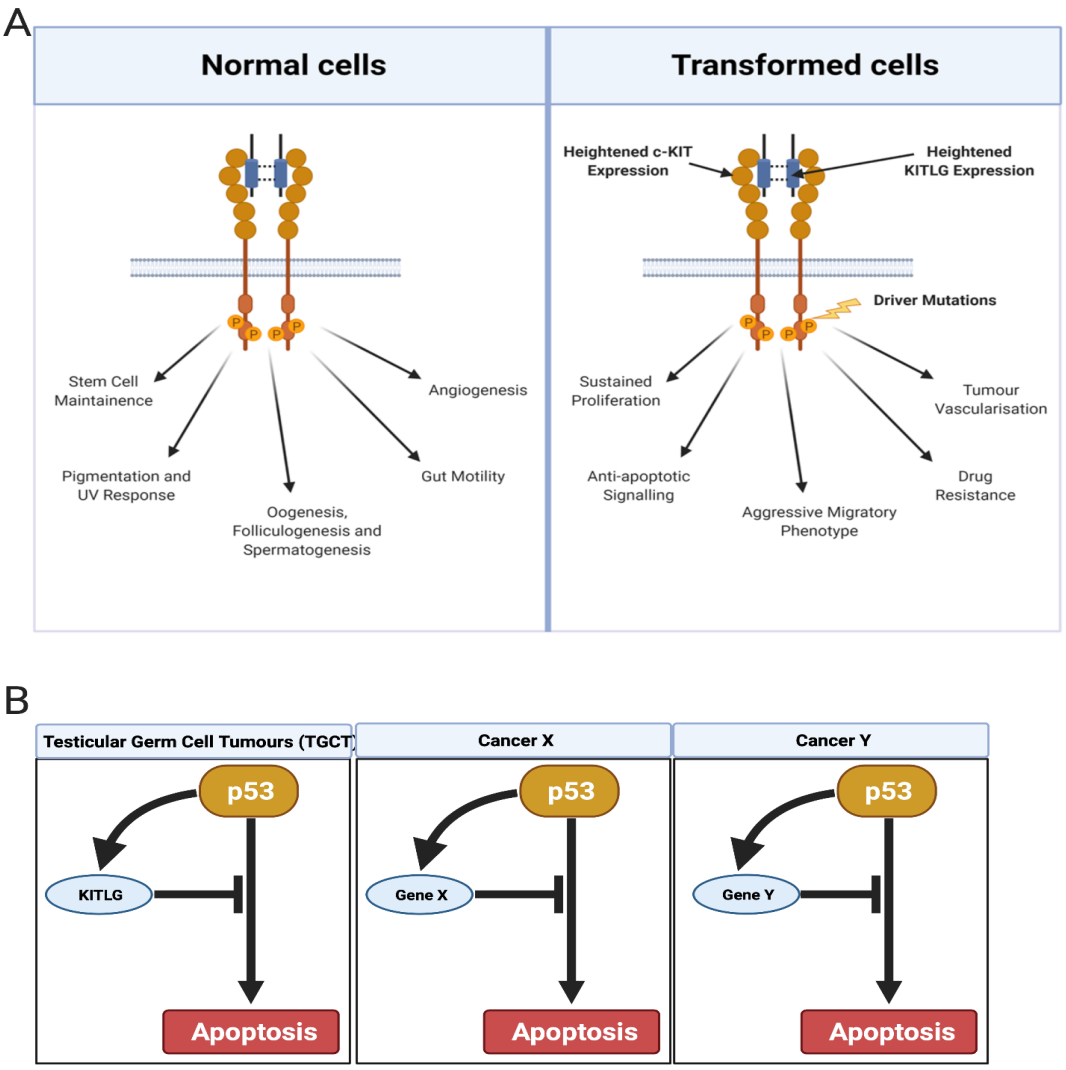


Figure 4.2: A) The KITLG/KIT signalling pathway is not restricted to the testes but is important in numerous tissues such as the gut and skin. The pathway is also key for maintaining stem cell populations in tissues such as the brain. Deregulation of KITLG/KIT signalling in these tissues can promote tumorigenesis by inducing proliferation, migration, invasion, angiogenesis and drug resistance. **B)** A schematic illustrating how different p53 target-genes could be responsible for negatively regulating p53 dependent apoptosis in different tissues. In TGCT, a negative-feedback loop exists between p53 and KITLG. In cancer X, a negative-feedback loop might involve gene A while in cancer Y, gene B might be responsible.

4.3 Results

4.3.1 The p53 pathway in human cancer

In this thesis, we address how SNPs can inform the management of cancer. By studying the KITLG-p53RE-SNP in testicular cancer, we indicated that germline variants modifying the interaction between p53 and specific p53REs can modulate the p53-apoptotic response, leading us to propose a novel therapy for refractory TGCT, activating p53 whilst inhibiting pro-survival signalling. In this Chapter, we expand this therapeutic strategy by identifying repurposing opportunities for p53 activation and KITLG/KIT inhibition in other cancers and provide evidence for other novel mechanisms which inhibit the p53-apoptotic response in tumours. We hypothesised that p53-inhibitors would be functional in tumours without TP53 mutation or deletion. Therefore we first analysed the known genomic lesions which impair the p53-apoptotic response in tumours to both identify biomarkers of p53 inactivation and define a cohort of patients who present with tumours with neither TP53 mutation nor deletion, who we reason could benefit the most from inhibition of factors which repress p53-dependent apoptosis.

TP53 is mutated or deleted in over 50% of tumours

Tumour-suppression by p53 can be inhibited through mutation and deletion of TP53 [105]. We analysed the genetic lesions which inhibit p53 function in The Cancer Genome Atlas (TCGA) cohort, introduced in Chapter Three. 10,631 cases in this cohort have been profiled for TP53 mutations and copy-number (GISTIC scores). 36% of tumours, across all cancer-types, feature at least one TP53 mutation while 38% of tumours indicate TP53 deletion (GISTIC <0, Figure 4.3.A-B). For cancers which mutate TP53, the wild-type allele may still produce functional, tumour suppressive p53 protein. For these cancers, there is a pressure to lose the wild-type copy, loss of heterozygosity (LOH). Indeed, 59% of TP53-MUTANT tumours exhibit LOH (TP53 MUTLOSS, Figure 4.3.C). Of those samples with mutant TP53, 368 (10%) have more than one (MULTI-MUTANT). Interestingly, TP53-LOSS is strongly enriched for in the tumours with only one TP53 mutation compared to

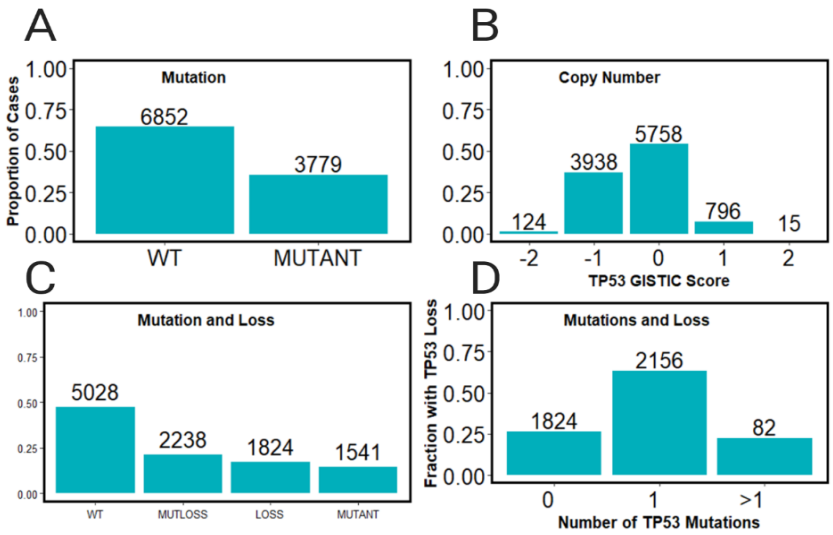


Figure 4.3: Barplots indicating the frequency of TP53 alteration by direct genetic lesions, mutation and copy number loss, in the pancancer TCGA cohort (10,631 cases). **A)** The proportion of TCGA tumours which feature a TP53 mutation, bars are labelled with the number of samples. **B)** The proportion of TCGA tumours with each TP53 GISTIC score. GISTIC < 0 indicates loss while GISTIC > 0 indicates gain, bars are labelled with the number of samples. **C)** The proportion of tumours which are wild-type (WT), have both copy number loss and TP53 mutation (MUTLOSS), only TP53 loss (LOSS) and only TP53 mutation (MUTANT), bars are labelled with the number of samples. **D)** The proportion of TCGA tumours with copy-number loss for differing numbers of TP53 mutations, bars are labelled with the number of samples.

MULTI-MUTANT suggesting that multiple mutations reduce the pressure for loss (Fisher Exact-Test, 5.91-fold, p=6.7e-51, Figure 4.3.D). 66% of TP53-MUTANT samples show either TP53 MUTLOSS or TP53 MULTI-MUTANT, these are the samples where both copies of TP53 are impaired (TP53-NF). In total, 53% of tumours exhibit TP53 mutation, loss or both, leaving 47% as TP53WT-NOLOSS.

TP53 mutation and deletion reduce the expression of p53 target-genes

Much of the tumour-suppressive function of p53 is mediated by its target-genes. We hypothesised that TP53 mutation and/or deletion should reduce the expression of p53 target-genes. Using the curated list of well supported p53 target-genes from Fischer (2017), we performed a pancancer analysis whereby tumours were separated into TP53 wild-type and TP53-MUTANT and used linear regression to test for differences in expression of each target-gene, adjusting for cancer-type [115]. The expression of 51% of the 340 target-genes was significantly reduced in TP53-MUTANT tumours compared to TP53 wild-type (beta > 0, FDR < 0.05, Figure 4.4.A, D). 35% of target-genes were found to show lower expression with

TP53-LOSS relative to TP53 wild-type without loss (Figure 4.4.B, D). For 91 target-genes, expression was significantly reduced by both TP53 mutation and TP53 copy-number loss, a significantly greater overlap than expected by chance (5.2-fold, p=1.2e-11, Fisher Exact-Test), indicating that mutation and copy-number loss reduce the ability of p53 to regulate a core set of target-genes. Comparing TP53 wild-type to TP53-NF, 49% of target-genes exhibited significantly lower expression in TP53-NF (Figure 4.4.C, D). When we compared the expression of p53 target-genes between tumours with biallelic TP53 inactivation (TP53-NF) with tumours with either one mutation or just copy-number loss, 39% of genes were expressed to a lower degree in TP53-NF tumours. This is in keeping with Knudson's Two-Hit Hypothesis that inactivation of both alleles of tumour-suppressor genes, such as TP53, has greater phenotypic effect.

TP53 mutation and deletion increase genomic instability

Tumours with somatic TP53 lesions have reduced expression of p53 target-genes. Many of p53's cellular functions are carried out by target-genes, including maintaining genomic stability. Genomic instability is a key cancer hallmark and it has been shown in many models systems and human tumours that mutant p53 can promote genomic instability [520][521][522]. We compared the different somatic TP53 lesions in our cohort and their potential associations with genomic instability using three measures: the genomic instability (GI) score, ploidy score and aneuploidy score (Materials and Methods)[523]. GI score and Ploidy score were found to be significantly higher in TP53-LOSS, TP53-MUTANT and TP53-NF groups compared to TP53WT-NOLOSS (p<5e-32,Linear Regression adjusted for cancer-type, Figures 4.4.E-F). Moreover, TP53-NF tumours exhibit significantly higher GI score compared to TP53-LOSS (beta=0.08, p=9.9e-28) and higher ploidy score compared to both TP53-LOSS and TP53-MUTANT (LOSS: beta=0.04, p=8.9e-04; MUTANT: beta=0.04, p=7.3e-03).The aneuploidy score represents count data; therefore, a Poisson regression model was used with all three groups showing significantly greater aneuploidy compared to TP53WT-NOLOSS (p 0,

Poisson Regression adjusted for cancer-type, Figure 4.4.G). Compared to both TP53-LOSS and TP53-MUTANT, TP53-NF exhibited a greater aneuploidy score (LOSS: beta=0.13, p=1e-47; MUTANT:beta=0.12,p=2.3e31). Together, these data provide evidence that somatic TP53 lesions significantly inhibit canonical p53 function to induce expression of target-genes and maintain genomic stability, whereby TP53-NF tumours exhibit the strongest signal of inhibited p53-pathway signalling.

Tumours with biallelic TP53 inactivation are less likely to respond to chemotherapy and radiation

Activation of p53 is a crucial for many DNA damage-inducing chemotherapies. TP53 mutations are generally considered to antagonise such treatments; although some studies on breast cancer have associated wild-type p53 with a senescence response to DNA damage and reduced tumour shrinkage compared to p53 mutant tumours [524][525][281][526][527]. However, how TP53-loss affects therapy response of both TP53WT and TP53Mutant tumours is unclear. To explore this in our cohort, patients were binned into responders and non-responders based on radiotherapy and first-line chemotherapy (Materials and Methods). In total, response data was compiled for 6,344 patients, 5,141 responders and 1,203 non-responders. Using logistic regression adjusted for cancer-type, TP53-NF status associated with non-responders (beta= -0.36, p=4.8e-04). When comparing TP53WT-NOLOSS and TP53WT-LOSS, a borderline effect was found whereby loss associated with non-responders (beta=-0.23, p=0.053) while no effect was noted for TP53MUTANT-NOLOSS compared to TP53WT-NOLOSS (beta=-0.03, p=0.78). In line with our above results that TP53-NF associated with greater effects on p53 target-gene expression and genomic instability, TP53-NF associated with non-responders compared to tumours with either TP53 mutation or deletion (beta=-0.23, p=0.039).

Patients with TP53 mutation and/or deletion have poorer prognosis

TP53 mutations have been linked with poorer prognosis in multiple cancer-types while TP53 loss associates with shorter survival in CLL [528][529]. Given our above data, we reasoned that TP53-MUTANT, TP53-LOSS and TP53-NF groups

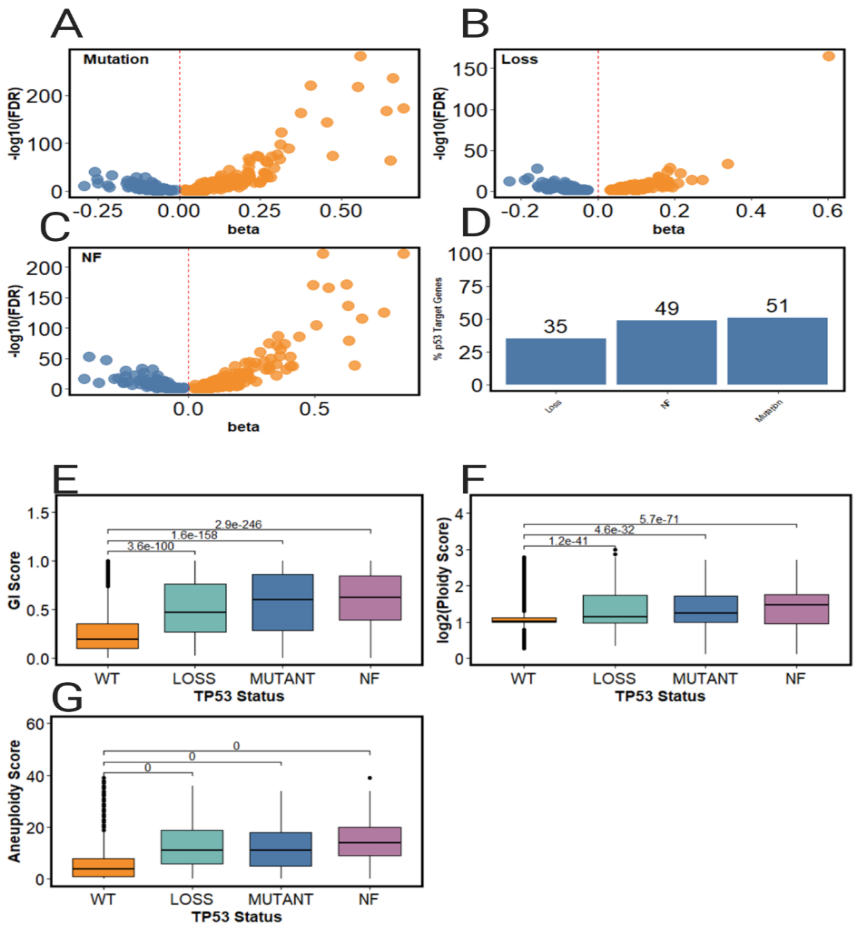


Figure 4.4: TCGA samples with altered TP53 status through mutation and/or loss express TP53 target genes to a lower degree. **A)** Scatter plot indicating the change in expression of each of 340 reproducible p53 target genes between TP53 Mutant and TP53 WT samples in the TCGA cohort, adjusted for cancer type. The effect magnitude is indicated by the beta whereby beta > 0 indicates higher expression in TP53 WT. The significance of the effect is indicated by the –log10 transformed FDR value. **B)** Scatter plot indicating the change in expression of each of 340 reproducible p53 target genes between TP53 wild-type Loss and TP53 WT NOLOSS samples in the TCGA cohort, adjusted for cancer type. **C)** Scatter plot indicating the change in expression of each of 340 reproducible p53 target genes between TP53 NF and TP53 WT samples in the TCGA cohort, adjusted for cancer type. **D)** Bar plot specifying the percentage of target genes found to be significantly reduced in expression in samples with TP53 WT Loss (LOSS), TP53 mutation (MUTANT) and TP53 mutation and loss or more than one TP53 mutation (NF), compared to TP53 WT NOLOSS. **E)** Boxplots indicating the distribution of Genomic Instability (GI) score amongst samples in the TCGA cohort with different mechanisms of TP53 alteration. Significant differences were tested by a linear regression model accounting for differences between cancer types. **F)** Boxplots indicating the distribution of ploidy score amongst samples in the TCGA cohort with different mechanisms of TP53 alteration. Significant differences were tested by a linear regression model accounting for differences between cancer types. **G)** Boxplots indicating the distribution of Aneuploidy count amongst samples in the TCGA cohort with different mechanisms of TP53 alteration. Significant differences were tested by a generalised linear regression model using the Poisson distribution accounting for differences between cancer types.

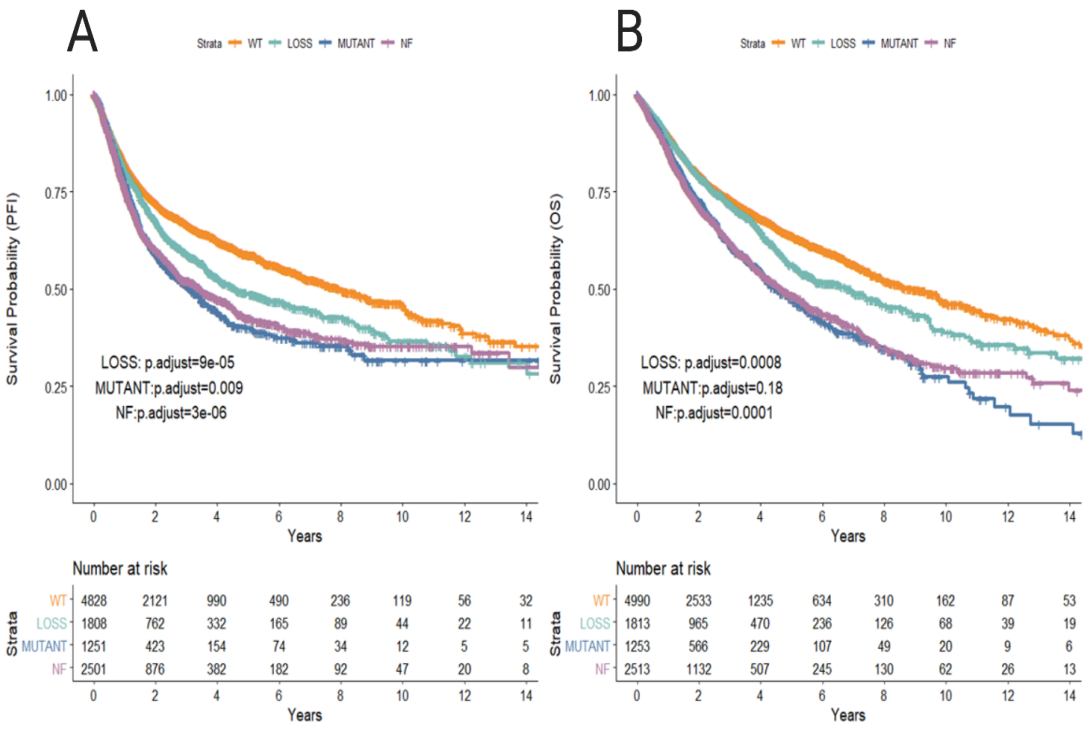


Figure 4.5: Pancancer Kaplain-Meier Survival curves indicating the effect of TP53 alteration through mutation and/or loss on Progression Free Interval (PFI, **A)**) and Overall Survival (OS, **B)**). P values are derived from the Cox regression model with cancer type as a covariate.

should show differences in terms of survival outcomes compared to TP53WT-NOLOSS in pan-cancer analyses. By Cox regression, adjusted for cancer-type, we found all three TP53-altered groups to associate with significantly faster progression compared to TP53WT-NOLOSS (Loss: HR=1.21, p=8.8e-05; Mutant: HR=1.15, p=0.009; NF: HR=1.25, p=2.5e-06) while TP53-LOSS and TP53-NF also demonstrated significantly shorter overall survival (Loss: HR=1.20, p=0.00078; Mutant:HR=1.08, p=0.18; NF:HR=1.21, p=0.0001, Figures 4.5.A-B). As with the above analyses, we compared TP53-NF tumours with those with just mutation or loss; patients who developed TP53-NF tumours had significantly shorter PFI and OS (PFI:HR=1.11,p=0.014; OS:HR=1.12, p=7.5e-05) but, unlike for the other phenotypes, these effects were not independent of cancer-type (p>0.05, Cox Regression adjusted for cancer-type).

The above analyses confirm that TP53 is frequently inhibited by mutation and/or deletion and that tumours with such lesions are distinct from TP53WT

tumours without loss in terms of p53 target-gene expression, genomic instability levels, response to therapy and survival (Figures 4.3, 4.4 and 4.5). Moreover, we found evidence that for at least three of the four phenotypes (p53 target-gene expression, genomic instability and therapy response) that tumours with biallelic TP53 inactivation are distinct from those with just one mutation or just deletion. In this chapter, we will explore how p53 signalling may be inhibited in the TP53WT-NOLOSS group with the TP53-NF group serving as a control group.

4.3.2 KITLG/KIT alterations in human cancer

In the previous analysis, we identified tumours which retained two copies of wild-type TP53 and therefore may show reliance on targetable inhibitors of the p53-apoptotic response, such as KITLG/KIT signalling in TGCT. To determine if KITLG/KIT inhibition could be a therapeutic strategy for TP53WT tumours of other cancer-types, we examined the TCGA cohort for KITLG/KIT alterations which promote downstream KIT signalling: KITLG and KIT copy-number gain, KIT activating mutations and the KITLG-p53RE-SNP risk-allele [530][531][532].

The KITLG-p53RE-SNP is specific to TGCT

The KITLG-p53RE-SNP associates with TGCT risk. For the TCGA-TGCT cohort, we imputed the genotype of the KITLG-p53RE-SNP using the linked SNP, rs4474514. In total, 94 TP53WT TGCT patients were found to be homozygous for the risk-allele and 22 heterozygous. Among higher stage TGCT tumours, RISK/RISK patients progressed significantly faster than NONRISK/RISK (log-rank test, p=0.016, Figure 4.6.A). This result indicates that the KITLG-p53RE-SNP not only mediates risk of TGCT, but can also associate with differences in tumor behavior after the initial development of the tumor.

The KITLG-p53RE-SNP has only been associated with risk of TGCT in GWAS; however, we found that the SNP could also associate with progression. To investigate whether similar associations might occur in other cancer-types, we imputed the KITLG-p53RE-SNP genotypes for 7,073 patients with available germline data (Supplementary Table C.8). The risk-allele frequency amongst these patients was found to be 0.81, in keeping with previously published data[176]. Next, taking all samples, irrespective of TP53 status, we calculated the risk-allele frequency for each cancer-type and determined whether any cancers were enriched for the risk-allele compared to other cancer-types. Importantly, TGCT was found to be enriched (2.4-fold, FDR=0.0005, Fisher Exact-Test, Figure 4.6.B) with a risk-allele frequency of 0.91. However, no other cancer-types were enriched, even after restricting to TP53 wild-type samples (Figure 4.6.C). Moreover, no cancer-types

were found to show an enrichment for the risk-allele in TP53WT tumours compared to TP53-NF (Figure 4.6.D). As expected, when we examined whether the risk-allele associated with progression of any cancer-types other than TGCT, none were found (FDR <0.05, Cox Regression). These data suggest that the effects of the KITLG-p53RE-SNP is likely specific to TGCT.

KITLG/KIT alterations associate with TP53WT Status

Our model of KITLG/KIT and p53 signalling suggests that other somatic alterations, which increase KITLG/KIT signalling, could also attenuate p53-dependent cell-killing. If true, the KIT activating alterations (KIT mutation, KIT amplification and KITLG amplification) could help identify cancer-types that could benefit from dual p53 activation and KIT inhibition. Oncogenic KIT mutations can confer constitutive activation or prime KIT for KITLG-dependent activation [533][534]. A high prevalence of these mutations suggests a reliance on KITLG/KIT signalling for cancer cell survival. Amongst the whole TCGA cohort, we found 258 (2.4%) tumours to have KIT mutations, of which 47 (18%) were known oncogenic driver mutations. KITLG copy-number gain could result in higher KITLG expression. We found 1,830 samples with KITLG gain (17%, GISTIC >0). Importantly, higher GISTIC scores associated with higher KITLG expression in TP53WT-NOLOSS samples (linear regression, beta=0.32, p=1.7e-12). Specifically, GISTIC>0 was found to associate with 1.7-fold higher KITLG expression compared to GISTIC=0 (p=6.2e-22, Figure 4.7.A). We found 1,165 cases to show KIT gain (11%, GISTIC>0). Importantly, higher KIT GISTIC scores associated with higher KIT expression (linear regression, beta=0.30, p=7.6e-06) with GISTIC>0 associating with 1.4-fold higher expression compared to GISTIC=0 (p=0.001, Figure 4.7.B). If these alterations inhibit p53-mediated cell killing in a similar manner to the TGCT KITLG risk locus, we reasoned that these alterations should be enriched in TP53WT-NOLOSS tumours relative to tumours where p53 is somatically mutated. We tested for enrichment in TP53WT-NOLOSS tumours relative to TP53-NF tumours by the Fisher Exact-Test and determined if this was independent of cancer-type and aneuploidy by

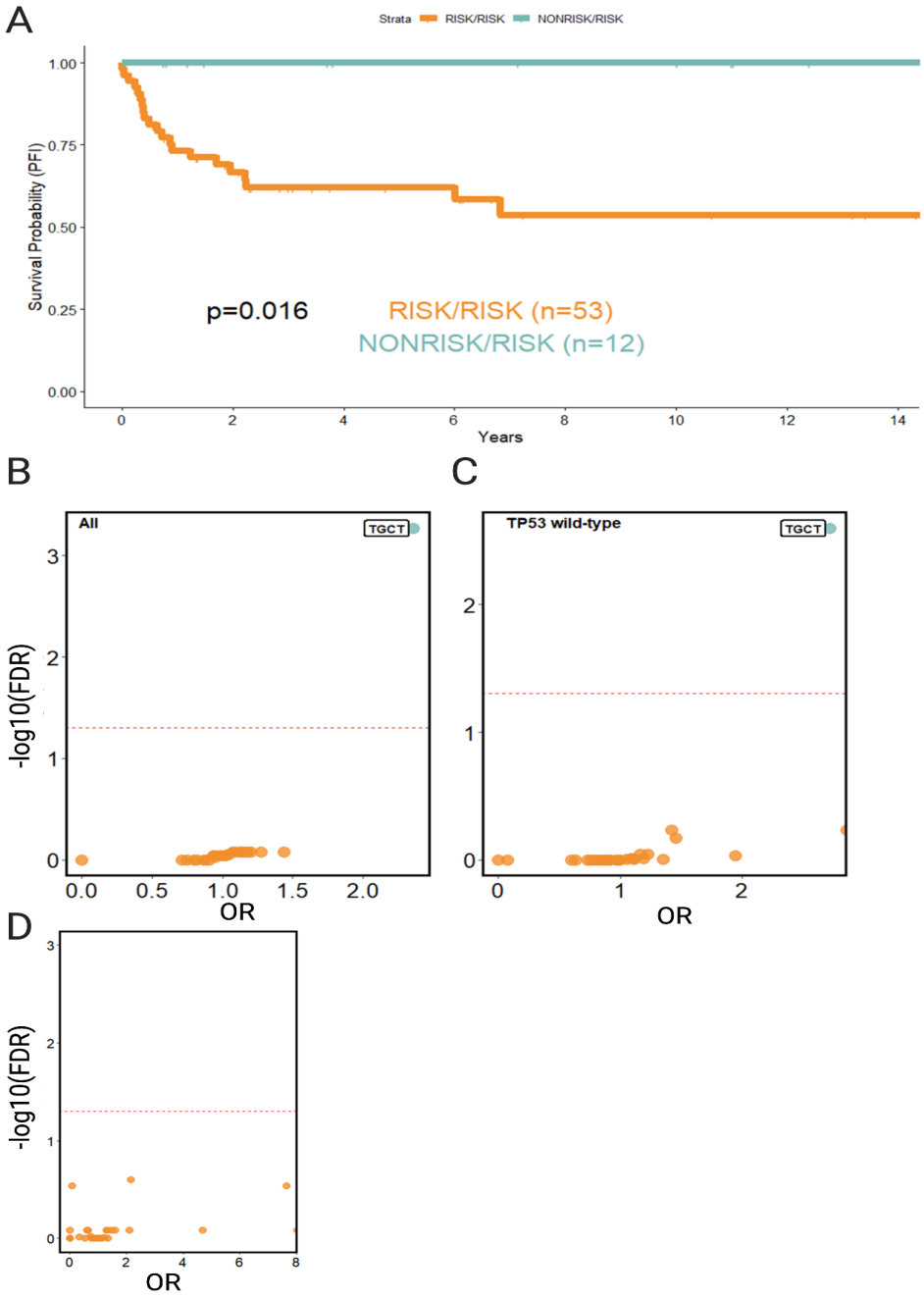


Figure 4.6: **A)** Kaplain-Meier survival curve indicating the association of the KITLG p53RE genotype with progression in the TCGA cohort of TP53 WT TGCT patients who have progressed to a higher stage tumour grade. The p value is calculated from the log-rank test. **B)** For each TCGA tumour type, without stratification by TP53 status, the enrichment for the risk allele of the KITLG-p53RE-SNP compared to other cancer types was determined by Fisher Exact-Test. **C)** For each TCGA tumour type, considering only TP53WT cases, the enrichment for the risk allele of the KITLG-p53RE-SNP compared to other cancer types was determined by Fisher Exact-Test. **D)** The risk allele frequency was compared between TP53WT-NOLOSS and TP53-NF tumours of each cancer-type. A two-tailed Fisher Exact-Test was used to determine enrichment for the risk allele in TP53WT-NOLOSS tumours. The -log10 transformed FDR q value is shown on the Y axis and the odd ratio on the X.

logistic regression. KITLG gain was enriched for in TP53WT-NOLOSS compared to TP53-NF (Fisher Exact-Test, 4.6-fold,p=3.53e-58) and significantly associated with TP53WT-NOLOSS status (Logistic regression, beta=0.67,p=1e-27). KIT gain was not enriched for in TP53WT-NOLOSS by Fisher Exact-Test (p=0.41) but a significant association was found by logistic regression (beta=0.20,p=4.8e-04). For KIT mutations, we considered the 47 oncogenic mutations only and due to the low number we separated the samples into TP53WT and TP53-MUTANT without consideration for TP53 copy-number change. 36 oncogenic KIT mutations were found in TP53WT and 11 in TP53-MUTANT, representing a significant enrichment of KIT mutations in TP53WT samples (2-fold, p=0.031). Oncogenic KIT mutations were not associated with TP53 status in a logistic regression model, suggesting they could be restricted to a small number of cancer-types (p>0.05). All three alterations associated with TP53WT status in at least one test suggesting that TP53WT tumours could utilise these alterations to harness the negative regulation exerted on p53-dependent apoptosis by KITLG/KIT signalling.

Some tumours may utilise multiple genetic lesions to promote KITLG/KIT signalling

KITLG/KIT alterations which act to enhance KIT signalling, associate with TP53WT status. These alterations could represent mutually exclusive methods to promote KIT signalling and act as biomarkers for different subgroups, or could be co-operative, in which case the different potential biomarkers might identify the same subgroup of tumours. To determine whether we should investigate KIT mutation, KIT gain and KITLG gain together or independently, we determined how many tumours harboured more than one type of KITLG/KIT alteration. Interestingly, of 1,457 TP53WT tumours exhibiting KITLG or KIT gain, 180 (12%) harboured both, a greater overlap than expected by chance (Fisher Exact-Test, OR=3.03, p=3.2e-26). Of the 36 TP53WT tumours with oncogenic KIT mutations, 10 (28%) also had KIT gain and 11 (31%) had KITLG gain, both greater overlaps than expected by chance (KIT: OR=5.57, p=0.00004; KITLG: OR=2.55,p=0.012, Fisher Exact-Test, Figure 4.7.C).

Although the overlaps described above were significant, the tumours with more than one KITLG/KIT alteration accounted for only 14% of TP53WT tumours with at least one KITLG/KIT alteration, suggesting that independent investigation of each biomarker may identify different patient subgroups. To identify the cancer-types most likely to be targetable by inhibiting the p53/KITLG/KIT axis, we determined which cancers were enriched for each alteration in TP53WT-NOLOSS tumours. TGCT and SKCM were enriched for oncogenic KIT mutations compared to other cancers, accounting for 70% of all mutations (Figure 4.7.D). For KITLG and KIT gain, we looked for cancers with a high gain to loss ratio compared to other cancers. Five cancer-types were found to be significantly enriched for KITLG gain, including TGCT, and four cancer-types for KIT gain, including SKCM (Figure 4.7.E-F). These enrichments will be explored further in the following sections.

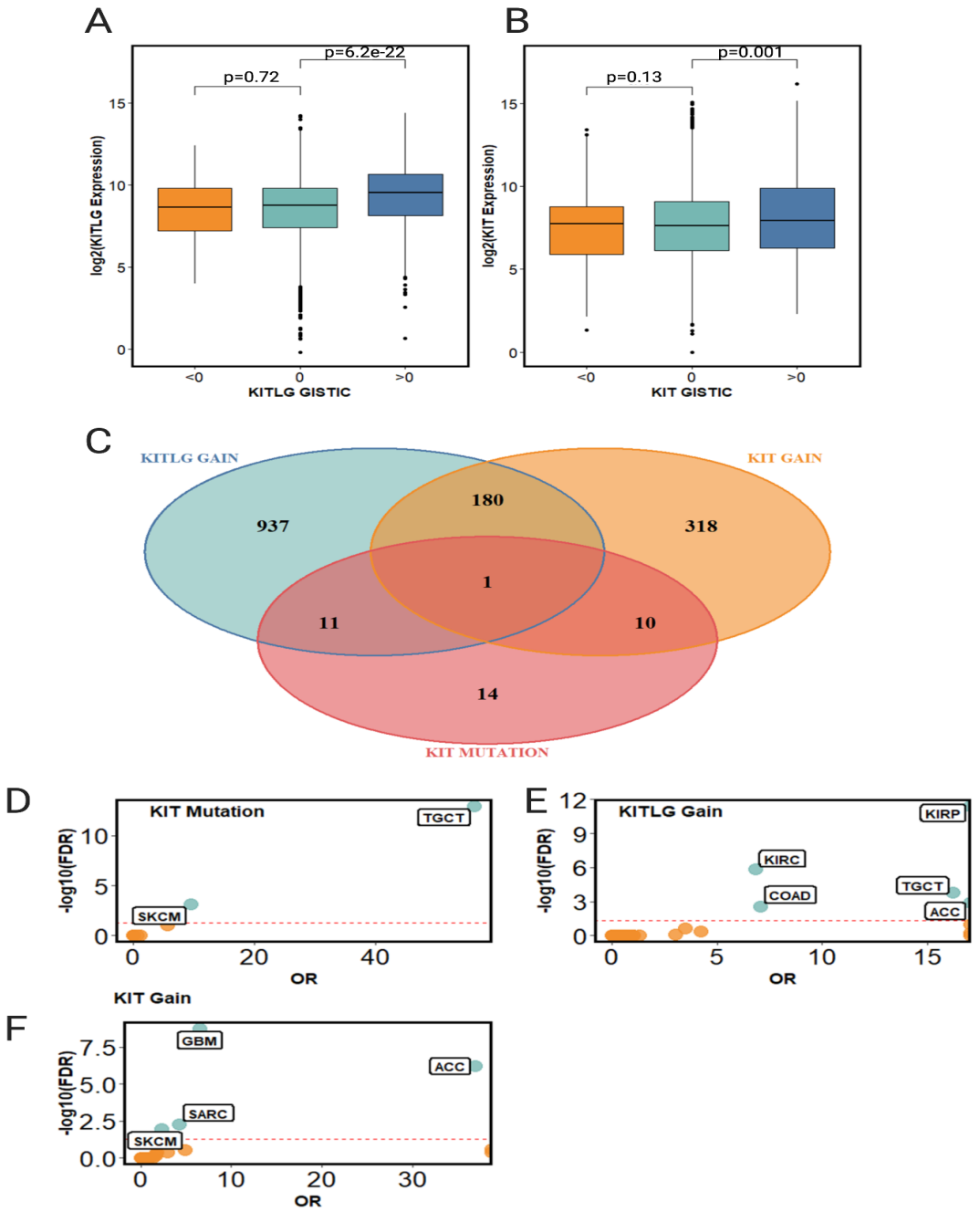


Figure 4.7: A) The boxplots indicate the log2 transformed KITLG expression for tumours with KITLG GISTIC scores of below 0 (loss), 0 (diploid) and greater than 0 (gain). Significant differences between groups were tested for by linear regression with log2 transformed mRNA expression as the dependent variable and GISTIC class and cancer type as independent variables. **B)** The boxplots indicate the log2 transformed KIT expression for tumours with KIT GISTIC scores of below 0 (loss), 0 (diploid) and greater than 0 (gain). Significant differences between groups were tested for by linear regression with log2 transformed mRNA expression as the dependent variable and GISTIC class and cancer type as independent variables **C)** The Venn diagram indicates the overlap between the tumours which have KITLG gain and KIT gain, KIT mutation and KITLG gain and KIT mutation and KIT gain. Scatter plots indicating the results of cancer enrichment analyses for KIT mutation **D)**, KITLG gain **E)** and KIT gain **F)** in TP53 WT tumours. The odds ratio was estimated by constructing a 2x2 contingency table and applying One Tailed Exact Fisher Test. Raw p values were corrected for MHT by FDR for 33 cancer types.

Melanoma is enriched for oncogenic KIT mutations

Oncogenic KIT mutations associate with poorer survival TGCT and SKCM, are enriched for oncogenic KIT mutations in TP53WT-NOLOSS tumours compared to other cancer-types. Importantly, no cancer-types were enriched when considering only TP53-NF samples, suggesting that KIT mutation affords a higher survival advantage to cancer-cells which retain wild-type TP53 compared to those which do not. KIT mutations lead to greater downstream, pro-survival signalling by conferring constitutive activation of KIT or by priming KIT for KITLG-dependent activation, suggesting that both high KITLG and KIT expression could also promote pro-survival signalling in melanoma [341][533]. In this section, we determine the prognostic value of KIT mutations and high KIT and KITLG expression (biomarkers of pro-survival signalling through KITLG/KIT) and investigate whether the KITLG/KIT pathway is targetable in conjunction with p53 activation.

14 of 369 TP53WT melanomas (4%) were found to have oncogenic KIT mutations. If these mutations promote pro-survival signalling and inhibition of p53 then, like the KITLG-p53RE-SNP risk-allele for TGCT, these mutations should associate with faster progression and/or shorter overall survival. Indeed, we found TP53WT KIT mutants to have significantly shorter overall survival compared to tumours with wild-type TP53 and KIT (log rank test, p=0.00027, Figure 4.8.A-B). Furthermore, the KIT mutations significantly co-occur with KIT gain (Fisher Exact-Test, OR=11.1, p=0.0009) and with higher KIT expression (linear regression, beta=5.3, p=9.1e-11, Figure 4.8.C) which is consistent with previous publications [535]. We examined the oncogenic KIT mutations in more detail to determine if they could be responsive to KITLG. The predominant mutation is K642E in tyrosine-kinase domain 1 (6/14 mutations). K642E is thought to have relatively weak oncogenicity and primes KIT for KITLG-dependent activation[536][534]. We separated the K642E mutants and found they were associated with significantly worse overall survival compared to SKCM KIT wild-type samples and SKCM samples with other KIT mutations (log-rank test, p<0.0001, Figure 4.8.B) and were still associated with high KIT expression (linear regression, beta=5.1, p=3.3e-05).

High KITLG and KIT expression associate with poorer survival in melanoma TP53WT SKCM is enriched for KIT mutations which prime KIT for KITLG-dependent activation and these mutations associate with KIT gain, higher KIT expression and shorter overall survival. These associations suggest that high KITLG and high KIT expression could also be markers of poor prognosis due to possible inhibition of p53. To test this, TP53WT tumours were split into high and low KITLG or KIT expressing groups. In a univariate analysis, high expression of both KITLG and KIT expression associated with worse overall survival (KITLG: HR=1.54, p=0.039 ; KIT: HR=2.23, p=4.2e-07). Furthermore, in a multivariate model, high KITLG, high KIT and K642E mutations were found to independently associate with poor overall survival (Appendix Figure A.7). Importantly, neither high KIT nor high KITLG expression was found to associate with overall survival in the 64 patients with TP53 mutations, suggesting that the worse survival associated with heightened KIT and KITLG is due to inhibition of wild-type p53 in melanoma.

We next examined whether the biomarkers of KITLG/KIT signalling associated with overall survival in a multivariate model with clinical parameters. Indeed, high KITLG expression, high KIT expression and KIT K642E mutations remained significant after accounting for sex, tumour stage, age at diagnosis and Clarks level (Appendix Figure A.8). Furthermore, addition of these biomarkers significantly improved upon the model with only the clinical parameters (ANOVA of log-likelihoods, p=7.7e-05). Finally, we validated this result using a second method, a time-dependent area under the curve (AUC) analysis. The AUC value was extracted at 1 year intervals for 10 years to examine the ability of each model to predict events at different time points (Table 4.1). We found the model with KITLG/KIT biomarkers to perform better at predicting events over a range of time intervals (Paired T-test, p=0.00012). These data indicate that KITLG/KIT signalling is oncogenic in SKCM and that markers of over-activation of this pathway associate with worse survival in TP53WT patients.

Table 4.1: Output from the tdAUC for SKCM. Two model were compared, the clinical only model and the full model featuring clinical factors plus KITLG expression, KIT expression and KIT mutation status. AUC generated every 12months

Time(Days)	**AUC_full_model**	**AUC_clinical_only**
365	0.63	0.58
730	0.71	0.67
1095	0.69	0.68
1460	0.67	0.65
1825	0.63	0.59
2190	0.63	0.61
2555	0.64	0.61
2920	0.65	0.62
3285	0.63	0.62
3650	0.65	0.60
Paired T-TEST (two tailed)	0.000116	

KITLG/KIT may be targetable in both primary and metastatic SKCM

The SKCM cohort is a mixture of primary and metastatic samples. Primary and metastatic melanomas can be molecularly, and clinically, different diseases[537][538]. Specifically, of the 306 TP53WT samples used in the above survival analysis, 59 are primary and 247 are metastatic. In line with previous publications, the metastatic samples have significantly lower KIT expression (3.3-fold, p=9.97e-07, Figure 4.8.D)[539]. Metastatic samples also have significantly lower TP53 expression (1.2-fold, p=0.015, Figure 4.8.E) but no difference in KITLG expression was found (p>0.05, Figure 4.8.F). Given these data we reasoned that the effect of KITLG/KIT signalling on survival may be more pronounced in primary samples compared to metastatic. We split the cohort into whether the tumour was a primary and metastatic tumour and performed a multivariate Cox regression for each subset. Intriguingly, KITLG expression was only found to associate with survival in primary samples (HR=17.2, p=0.0014) while KIT expression and K642E mutations only associated with survival in metastatic samples (KITexp:HR=2.1, p=0.0006; K642E:HR=4.2,p=0.05; Appendix Figures A.9 and A.10). These data suggest that there may be significant interplay between KITLG/KIT signalling and the metastatic potential of melanomas and that the pathway may be targetable in both contexts.

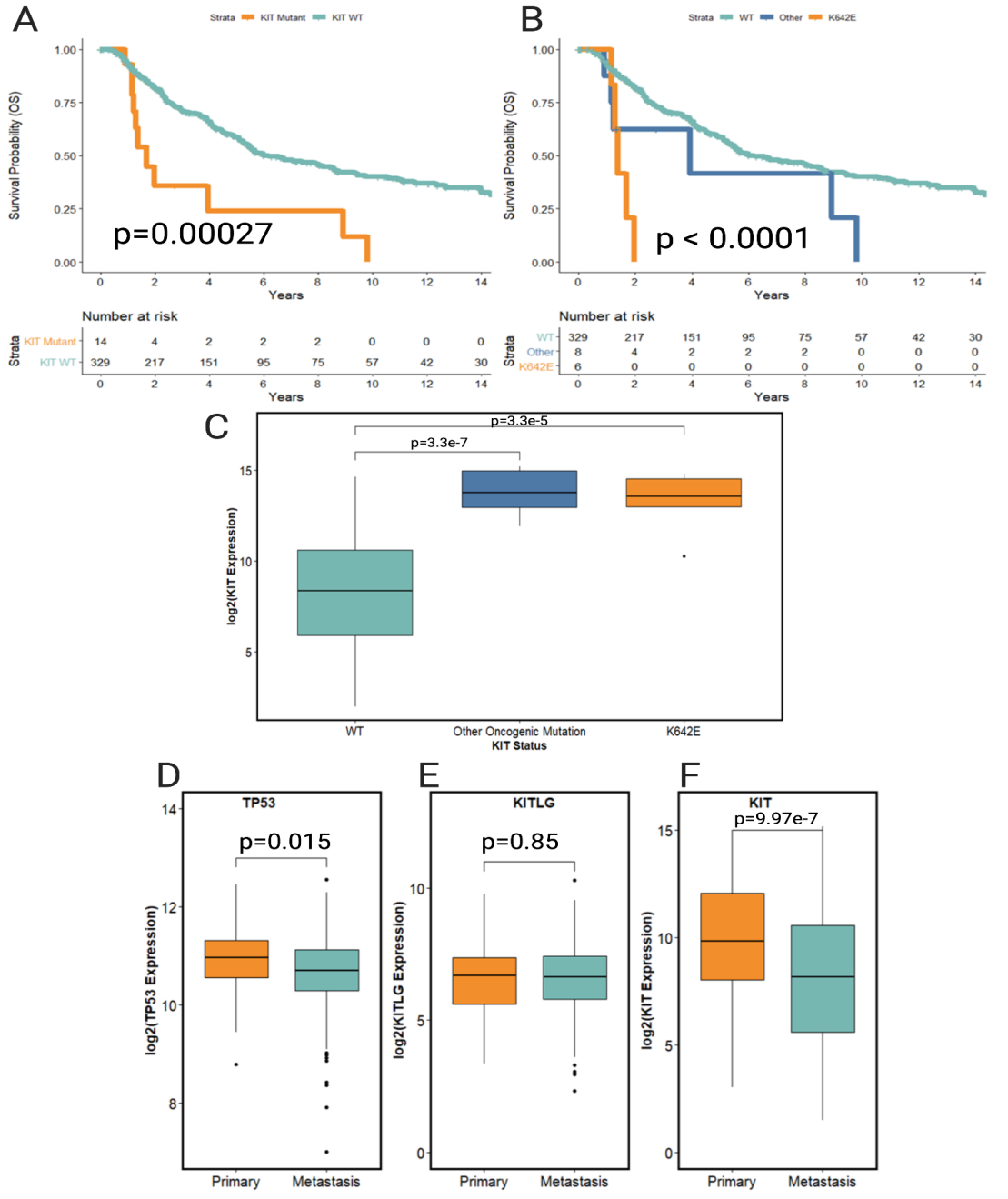


Figure 4.8: Kaplain-Mieier survival curves indicating the effect of oncogenic KIT mutations on overall survival in TP53WT SKCM. Log rank test was used to determine significance for all oncogenic KIT mutations **A)** and for oncogenic KIT mutations separated into K642E and Other **B)**. **C)** Boxplots indicating differences in KIT expression between KIT mutant TP53 WT SKCM and KIT WT TP53 WT SKCM. Significance was determined by linear regression. Boxplots indicating the expression of TP53 **D)**, KITLG **E)** and KIT **F)** in primary and metastatic SKCM samples. Significance determined by linear regression.

KIT inhibition synergises with p53 activation in melanoma Our analyses into melanoma thus far have suggested that elevated KIT-dependent inhibition of the p53-apoptotic response is pro-tumour and associates with poorer prognosis. Given these data, we reasoned that combined inhibition of KITLG/KIT signalling and p53 activation could synergise in melanoma cells in the way we found for TGCT. We therefore tested the combinations of Dasatinib + Nutlin-3a and Dasatinib + Doxorubicin in the TP53 and KIT wild-type cell-line SKMEL-5 (n=3). For both combinations, CI values below 1 were calculated, indicating synergy (Dasatinib+Nutlin-3a, CI= 0.75; Dasatinib+Doxorubicin; CI=0.55; Figure-9A).

Nutlin-3a induces KITLG, in a p53 dependent manner, in melanoma Dasatinib synergises with Nutlin-3a and Doxorubicin in a TP53 and KIT wild-type melanoma cell-line (Figure 4.9.A), suggesting that inhibiting KITLG releases the pro-apoptotic ability of p53. Our previous analyses into p53 and KITLG/KIT signalling in TGCT determined that KITLG/KIT signalling not only inhibits downstream signalling downstream of p53 but is also induced by p53 through the polymorphic KITLG-p53RE. The synergy between KIT inhibition and p53 activation could be due to the downstream and/or upstream interactions between KITLG/KIT signalling and the p53 pathway. To determine whether the upstream interaction (induction of KITLG by p53) occurs in melanoma, we downloaded microarray data for A375 cells treated with either DMSO or Nutlin-3a and with a control siRNA targeting GL2 or p53 targeting siRNA (GEO Accession: GSE39091, Materials and Methods). We performed differential gene expression analysis between the DMSO and Nutlin-3a treated control siRNA samples and found increased KITLG expression using three probes after p53 activation (207029_at : logFC=0.91, FDR=0.0009; 211124_s_at : logFC=2.63, FDR=0.048; 226534_at: beta=1.60, FDR=1.1e-08, Figures 4.9.B-C). Importantly, no increases in expression were found for the samples treated with p53 siRNA indicating that the upregulation of KITLG after Nutlin-3a treatment is p53-dependent (207029_at : logFC= -0.16, p=0.67; 211124_s_at : logFC= -2.22, p=0.24; 226534_at: logFC=-0.14, p=0.54, Figure 4.9.B-C).

Given the above cell-line data, indicating that p53 can induce KITLG expression in melanoma cells, we reasoned that high p53 expression may associate with poorer outcome in TP53WT melanoma patients, due to its ability to drive pro-survival signalling through the KITLG/KIT axis. Indeed, when we separated the 369 TP53WT melanoma tumours into high and low p53 mRNA expression, we found high expression to associate with shorter OS in both a univariate model (p=0.0079, log-rank, Figure 4.9.D) and in a multivariate model including all the covariates indicated in Appendix Figure A.8(HR=1.42, p=0.049, Cox regression). Importantly, high KITLG, high KIT and K642E mutations still associated with shorter OS. Together, these data suggest that p53-mediated induction of KITLG/KIT signalling could impair the p53-apoptotic response in melanoma, similar to what we found in TGCT. Specifically, we have shown that p53 can induce KITLG and that biomarkers of heightened signalling through the KITLG/KIT pathway associate with poorer prognosis. Moreover, KITLG/KIT inhibition synergised with p53 activation in a melanoma cell-line. However, unlike for TGCT, the KITLG-p53RE-SNP does not associate with melanoma risk. Additionally, our analyses of the TCGA SKCM cohort did not show the risk-allele homozygotes (GG) to significantly associate with higher KITLG expression compared to heterozygotes (GA) and minor-allele homozygotes (AA). However, the 3 TP53WT minor-allele carriers were found to show a non-significant trend towards reduced KITLG expression compared those with two copies of the risk-allele (Linear regression, 2.5-fold, p=0.12, Appendix Figure A.11). It is therefore possible that studies of larger cohorts or experimental studies of melanoma cell-lines could uncover a role for the KITLG-p53RE-SNP in mediating p53-induced KITLG expression.

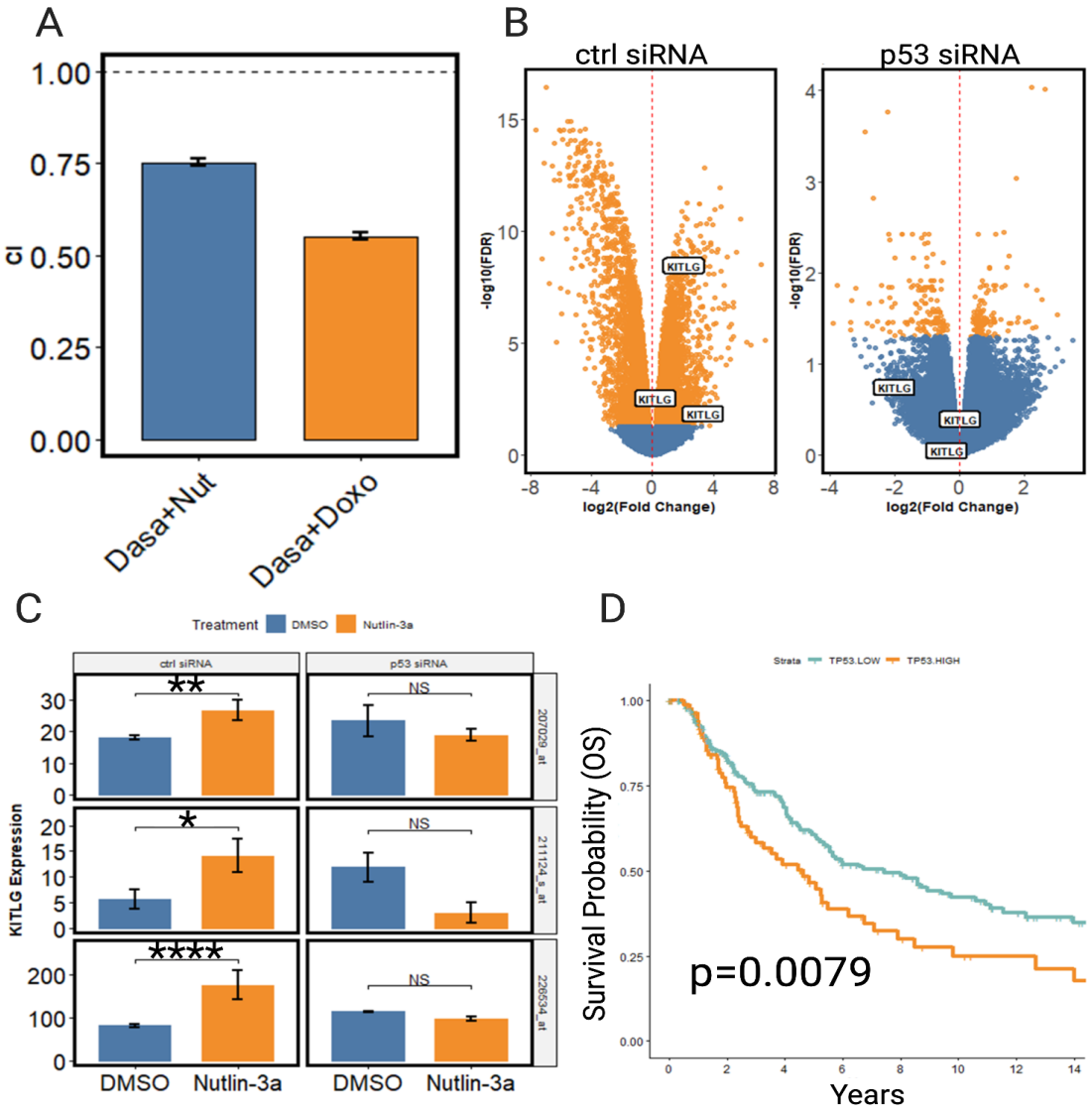


Figure 4.9: **A)** TP53 and KIT wild-type melanoma SK-MEL-5 cells were treated with serial dilutions of Dasatinib+Nutlin-3a, Dasatinib+Doxorubicin, Dasatinib, Nutlin-3a or Doxorubicin for 48hrs and cell viability was determined by MTT. The level of synergy was determined by the Combination Index. **B)** Microarray data for A375 melanoma cells pretreated with either control or p53 siRNA followed by treatment with Nutlin was accessed from GSE39091. Limma was used for differential gene analysis. Significant probes are indicated in orange and the 3 probes for KITLG are labelled. **C)** Barplots for KITLG expression as measured by three different probes from GSE39091. Indicated significance reflects the FDR q-values from limma. **D)** TP53 mRNA expression and survival data was downloaded for TP53WT patients of the TCGA-SKCM dataset. The log-rank test was used to determine the association of high p53 mRNA expression with Overall Survival (OS).

Colon cancer is enriched for KITLG copy-number gain

KITLG expression is significantly higher in TP53WT-NOLOSS colon cancer compared to TP53-NF We previously established that five cancer-types, including TGCT, were enriched for KITLG gain in TP53WT-NOLOSS tumours. If the increases in KITLG copy-number have a meaningful pro-tumour effect then they should associate with higher KITLG expression, should be enriched for in TP53WT-NOLOSS tumours compared to TP53-NF and therefore, KITLG expression should be higher in TP53WT-NOLOSS tumours compared to TP53-NF. Of KIRP, KIRC, COAD and ACC, only COAD fit these three criteria. Among the 435 colon adenocarcinomas in our cohort, 84 (19%) were found to have KITLG gain and KITLG expression was significantly higher for these tumours compared to those without gain (beta=0.44, p=0.0014, linear regression, Figure 4.10.A). We then compared KITLG gain between TP53WT-NOLOSS and TP53-NF COAD; 45 of 147 (31%) TP53WT-NOLOSS tumours exhibited KITLG gain compared to 21 of 174 (12%) TP53-NF tumours, representing a significant enrichment for KITLG gain in TP53WT-NOLOSS tumours (OR=3.2, p=5e-05, Fisher Exact-Test, Figure 4.10.B). Moreover, TP53-NF status was found to negatively associate with the probability of KITLG gain, accounting for aneuploidy (beta=-2.6, p=2.3e-08, logistic regression with aneuploidy). Finally, we found that the TP53WT-NOLOSS tumours showed significantly higher KITLG expression compared to TP53-NF tumours (linear regression, beta=0.79, p=3.5e-09, Figure 4.10.C). Given these data, we focused on COAD for further analyses.

BRAF mutations and KITLG/KIT signalling are probably mutually exclusive Colon cancer has a complex mutational landscape with mutations in tens of putative driver genes reported, multiple of which are involved in pro-survival signalling downstream of KIT, such as KRAS, NRAS and BRAF [540]. Mutations of these driver genes can constitutively activate downstream signalling and render the upstream KITLG/KIT axis unimportant [541][542]. We first aimed to identify such mutations which also associate with TP53 status so we could account for

them in our analyses. To do so we utilised the list of recurrently mutated genes in colorectal cancer (CRC) [540]. Of the 31 genes found to be recurrently mutated in CRC, 15 demonstrated enrichment of mutations in TP53WT-NOLOSS and one showed enrichment in TP53-NF (APC, Supplementary Table C.9). BRAF was the top hit for the TP53WT-NOLOSS enriched driver genes (Fisher Exact-Test, OR=5.65,FDR=8e-06, Figure 4.10.D). Interestingly, BRAF mutation and KITLG/KIT signalling have been shown to act antagonistically, whereby activation of KIT can suppress the oncogenic activity of constitutively-active mutant BRAF, perhaps by stimulating wild-type BRAF to dimerise with, and reduce the oncogenic ability of, mutant BRAF [543]. Indeed, BRAF mutant tumours appear to show reduced expression of KIT in TP53WT-NOLOSS but not TP53-NF tumours (linear regression, beta =-0.74, p=0.001, Figure 4.10.E-F). We therefore hypothesised that KITLG/KIT-mediated attenuation of p53-signaling may be important in BRAF and TP53 wild-type colon cancer.

High KITLG and KIT expression associate with poorer prognosis in TP53 and BRAF wildtype colon cancer We next ascertained whether KITLG/KIT signalling can affect tumour progression and survival in COAD patients. KITLG gain associates with higher KITLG expression, but the oncogenic effect of higher KITLG expression is still dependent on the expression of KIT to which it binds. We reasoned that given the high levels of KITLG gain in TP53WT-NOLOSS COAD, high KITLG and high KIT expression may be prognostic factors in these tumours. Indeed, in univariate models, both high KITLG and high KIT expression associated with shorter overall survival in TP53WT-NOLOSS and BRAF wild-type COAD cases (KITLG: HR=4.1,p=0.002; KIT: HR=5.9, p=0.005). In our Cox regression models we also included expression of the direct p53 regulator, MDM2. The genes encoding KITLG and MDM2 are part of the same genomic neighbourhood on chromosome 12q and as a result are nearly always gained or lost together in COAD. Indeed, only 3% of COAD samples show a discrepancy between KITLG and MDM2 GISTIC scores. There is also strong positive correlation between KITLG and

MDM2 expression in COAD (Figure 4.10.G). A multivariate model including the expression of KITLG, KIT and MDM2 demonstrated that KITLG and KIT are predictors of poor overall survival independently of MDM2 in TP53WT-NOLOSS and BRAF wild-type COAD (Figure 4.10.H). Importantly, this was not found to be the case for TP53-MUTLOSS COAD tumours where expression of KITLG, KIT and MDM2 does not associate with overall survival (Appendix Figure A.12). These data suggest that heightened KITLG/KIT signalling is pro-tumour in TP53 and BRAF wild-type COAD and that this association is due to inhibition of wild-type p53.

We next asked whether these variables were independent of known clinical prognostic parameters such as age at diagnosis, tumour staging, CMS and MSI/MSS status. With the additional clinical parameters, high KITLG expression was still found to associate with poorer overall survival (HR=6.74,p=0.008, Cox Regression, Appendix Figure A.13). Importantly, MDM2 expression was not a significant covariate ($p>0.05$) and KITLG expression did not associate with survival in TP53-MUTLOSS COAD with the same clinical parameters ($p>0.05$). Analysis of the log-likelihoods of the clinical only model and the clinical+KITLG model by ANOVA indicates that the addition of KITLG expression as a covariate significantly improves the model ($p=0.0046$). The clinical+KITLG model also performed significantly better in the tdAUC (Paired T-test, p=3.1e-07, Table 4.2). These data provide evidence that KITLG/KIT signalling is an independent prognostic factor for colon cancer patients retaining wild type TP53 and BRAF.

The analyses in the above sections highlights that multiple biomarkers of KITLG/KIT signalling can indicate cancer-types which may rely on signalling through this pathway and might be sensitive to combined p53 activation and KIT inhibition. The KITLG-p53RE-SNP identified TGCT but appears to be specific to TGCT. We find that SKCM is enriched for KIT mutations and KIT copy-number gain and that expression of KITLG and KIT and KIT K642E mutations associate with poor survival in TP53WT SKCM patients. Furthermore, we find that COAD is enriched for KITLG copy-number gain and that expression of KITLG associates with survival independently of KIT, MDM2 and clinical prognostic factors. The KIT-gain

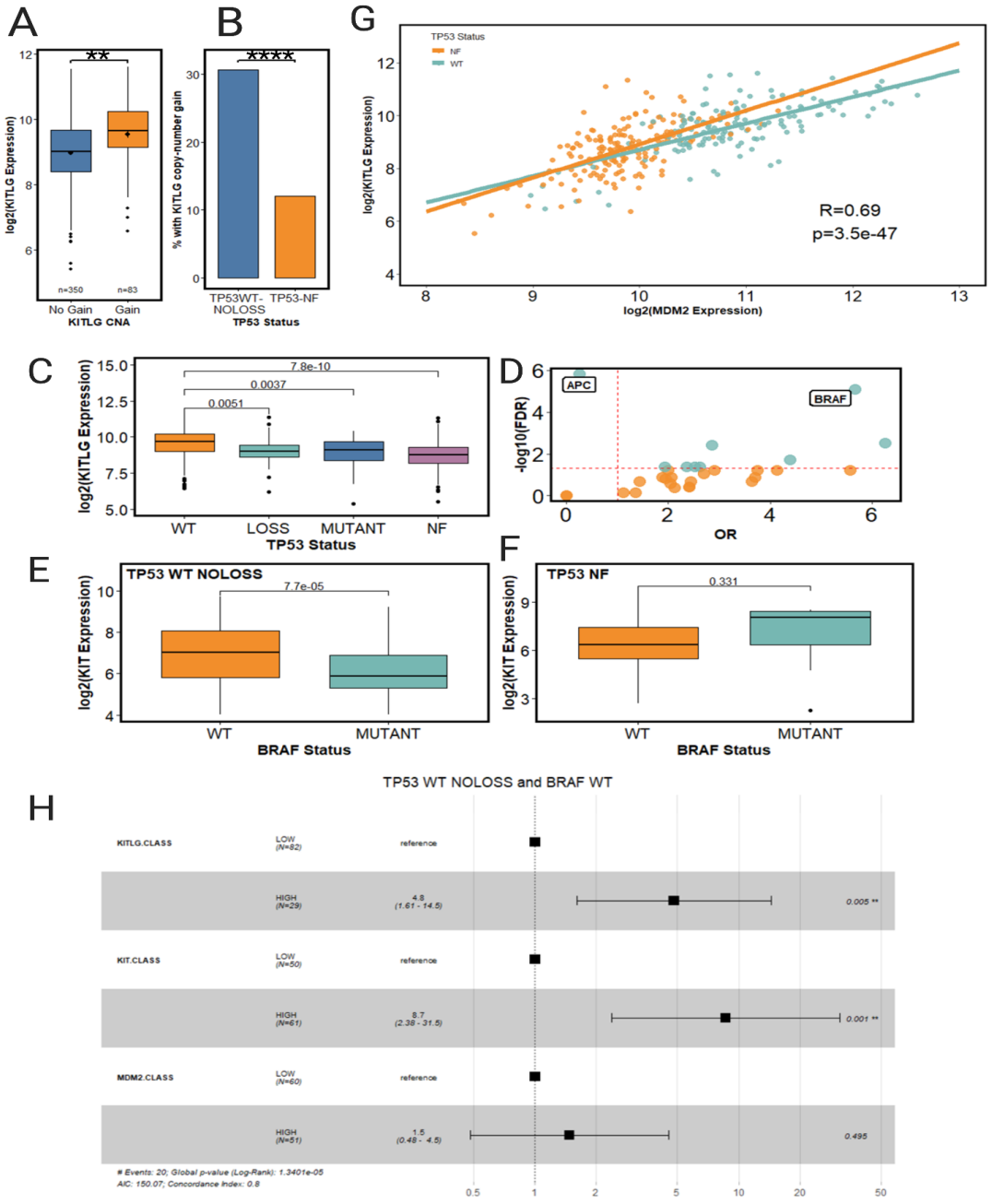


Figure 4.10: A) The barplot indicates the expression of KITLG mRNA in colon cancer tumours with KITLG copy number gain or no-gain. Significance was tested by linear regression. **B)** The barplot indicates the proportion of TP53WT-NOLOSS and TP53-NF colon tumours with KITLG copy-number gain. The significance of the enrichment was tested by Fisher Exact-Test. **C)** Boxplots indicating KITLG expression in colon tumours stratified by TP53 status. Significance was tested by linear regression. **D)** Scatter plot indicating the results of an enrichment analysis for COAD driver mutations in TP53 WT NOLOSS versus TP53 NF samples. The effect size was calculated by a two tailed Exact Fisher Test and raw pvalues were corrected for 30 tests by FDR. Grey dots indicate FDR <0.05. **E)** Boxplots indicating the relationship of BRAF mutation on KIT expression in TP53WT-NOLOSS colon tumours. **F)** Boxplots indicating the relationship of BRAF mutation on KIT expression in TP53-NF colon tumours. **G)** Scatter plot indicating the correlation between log2 transformed MDM2 and log2 transformed KITLG in TP53 WT NOLOSS (teal) and NF (orange) COAD. The R estimate of correlation and p value were estimated by Pearson's Correlation Test with NF and WT NOLOSS combined. **H)** Forest plot indicating the output of a Cox regression model in TP53WT NOLOSS BRAF WT COAD with Overall Survival as the dependent variable and KITLG, KIT and MDM2 expression as the independent variables. The expression values were split into high and low using surv_cutpoint.

Table 4.2: Output from the tdAUC for COAD. Two model were compared, the clinical only model and the full model featuring clinical factors plus KITLG expression. AUC generated every 3months.

Time(Days)	**AUC_full_model**	**AUC_clinical_only**
90	0.94	0.80
180	0.92	0.68
270	0.85	0.66
360	0.78	0.61
450	0.78	0.64
540	0.76	0.66
630	0.76	0.66
720	0.76	0.66
810	0.79	0.68
900	0.79	0.68
990	0.79	0.68
1080	0.79	0.68
1170	0.79	0.68
1260	0.77	0.75
1350	0.80	0.74
Paired T-TEST (two tailed)	3.08E-07	

cancers did not exhibit differences in KIT expression between TP53WT-NOLOSS and TP53-NF and were not further investigated. Together, our data suggests that co-modulation of the p53 pathway and KITLG/KIT signalling could be a therapeutic opportunity for TP53WT melanoma and colon cancer patients, indeed we provide evidence that KIT inhibition is synergistic with p53 activation in melanoma.

4.3.3 P53 target-gene expression accurately predicts the tissue of origin of tumours

So far in this thesis, we have studied the KITLG-p53RE-SNP and the interplay between p53 and KITLG/KIT signalling. In this Chapter, in a pan-cancer analysis we found biomarkers of over-active KITLG/KIT signalling to associate with TP53WT retention and then identified specific cancer-types enriched for these biomarkers (e.g. TGCT, SKCM and COAD), leading us to determine that simultaneous p53 activation and KITLG/KIT inhibition is synergistic in SKCM as well as TGCT. Given our success in targeting KITLG/KIT in TP53WT TGCT and SKCM and potentially COAD, we reasoned that other target-genes could have pro-survival function and be targetable in other cancer-types. In contrast to direct regulators of p53 which are generally core target-genes, pro-survival genes which inhibit p53-mediated apoptosis through downstream mechanisms (e.g. KITLG) could be more likely to be tissue-specific (Figure 4.11.A). Tissue-specific expression of p53 target-genes is evident from cell-line studies [544], but has not been fully described in the context of TP53WT human tumours. To explore this, we restricted to the 5,028 TP53WT-NOLOSS tumours in our cohort and computed a dissimilarity score between each pair of cancer-types, based on the mean mRNA expression of 340 p53 target-genes, and applied hierarchical clustering (5 clusters based on mclust package, Figures 4.11.B-C). Clear differences can be seen between cancer-types with those from similar tissues clustering together such as the three CNS cancers, PCPG, GBM and LGG.

The above dissimilarity scores consider all 340 p53 target genes; to determine if the differences between cancer-types included the most highly expressed target-genes, we ranked the target-genes by expression in each cancer-type and determined the top 10% most highly expressed target-genes in each cancer-type. 132 unique target-genes (39%) were found to be among the top 10% in at least one cancer-type. Surprisingly, only six target-genes (1.8%) were among the top 10% in all 33 cancer-types (GPX1, IGFBP7, MLF2, PCNA, PLXNB2 and RPS19) and 30 were among

the top 10% in at least half of the cancer-types, suggesting that the most highly expressed target-genes differ between cancer-types (Appendix Figure A.14).

Our analyses suggest that p53 target-gene expression exhibits tissue-specificity; however, we did not consider the variability in expression between tumours arising from the same tissue, nor whether tissue-specificity is restricted to TP53WT-NOLOSS tumours. To address these questions, we trained a machine-learning algorithm, random-forests (RF), to classify tumours into cancer-types based on p53 target-gene expression. Specifically, we used the seven cancer-types with at least 100 TP53WT-NOLOSS and TP53-NF tumours (14 classes, Table 4.3), and the target-genes which were found to be expressed to a significantly higher degree in TP53WT tumours compared to TP53Mutant tumours for at least one of the 7 cancer-types. This resulted in a total of 2,374 tumours, which we split into train and test sets (50% each), and 170 target-genes as predictors. Parameter optimisation was carried out by k-fold cross-validation using the training set (Materials and Methods, Appendix Figures A.15 and A.16). The RF algorithm was applied to the test set with an average balanced accuracy of 88% with 95% of the misclassifications occurring between TP53WT-NOLOSS and TP53-NF within a cancer-type (Table 4.3). This analysis suggests that, for both TP53WT-NOLOSS and TP53-NF tumours, the expression of p53 target-genes is largely determined by the tissue of origin, in line with a previous whole transcriptome analysis of the TCGA cohort and with cell-line studies [545][544]. Moreover, as expected from our initial comparisons of TP53WT-NOLOSS and TP53-NF tumours at the beginning of this chapter, we found that for most cancer-types TP53WT-NOLOSS and TP53-NF tumours could be correctly classified by their p53 target-gene expression profile.

In the above analyses, we have provided evidence that the tissue-of-origin is a powerful determinant of p53-target gene expression. Therefore, pro-survival target-genes which, like KITLG inhibit p53-mediated apoptosis downstream of p53 itself, could exhibit tissue-specific regulation by p53, perhaps derived from cellular mechanisms important for the normal function of healthy cells. In the following analyses we aim to identify other potentially pro-tumour target-genes

Table 4.3: Performance summary of the Random Forest model used to classify tumours into 14 classes based on the expression of 170 p53 target genes.

Class	Precision	Recall	F1	Prevalence	Balanced Accuracy
BLCA_MUTLOSS	0.708	0.780	0.742	0.049	0.881
BLCA_WT	0.780	0.661	0.716	0.049	0.826
BRCA_MUTLOSS	0.752	0.842	0.794	0.111	0.904
BRCA_WT	0.899	0.883	0.891	0.143	0.933
COAD_MUTLOSS	0.900	0.867	0.883	0.070	0.930
COAD_WT	0.763	0.795	0.779	0.061	0.889
LIHC_MUTLOSS	0.818	0.706	0.758	0.043	0.849
LIHC_WT	0.808	0.868	0.837	0.057	0.928
LUAD_MUTLOSS	0.780	0.753	0.766	0.071	0.868
LUAD_WT	0.805	0.838	0.821	0.062	0.912
STAD_MUTLOSS	0.814	0.625	0.707	0.047	0.809
STAD_WT	0.705	0.753	0.728	0.061	0.866
UCEC_MUTLOSS	0.926	0.472	0.625	0.044	0.735
UCEC_WT	0.830	0.968	0.893	0.131	0.969

and the cancer-types in which the pro-tumour effects might be exerted. As we did with KITLG, we begin with a pan-cancer analysis to identify p53 pathway genes which when highly expressed, associate with reduced sensitivity to p53 activating compounds. Then, we will identify which of these genes associate with TP53 status in tumours before identifying specific cancer-types which show positive correlation with p53 expression (evidence of regulation by p53) or frequent copy-number gain. We expect that high expression of the inhibitor gene could associate with poor prognosis in the matched patient group (Figure 4.11.D).

MDM2 inhibits the p53-apoptotic response, is highly expressed and amplified in TP53WT-NOLOSS tumours and high expression associates with poor prognosis

Before screening for other cancer-type specific p53 inhibitors within the p53 network, we first verified our approach using the best documented p53 inhibitor, MDM2. MDM2 is the E3 ubiquitin ligase responsible for driving proteolysis of p53 under steady state conditions and is over-expressed in several cancer-types [546][158]. We would expect MDM2 to be a hit in the approach outlined in Figure 4.11.D. To test the effect of MDM2 expression on sensitivity to p53 activation, we chose Cisplatin as MDM2 is the target of Nutlin-3a. As expected, high MDM2

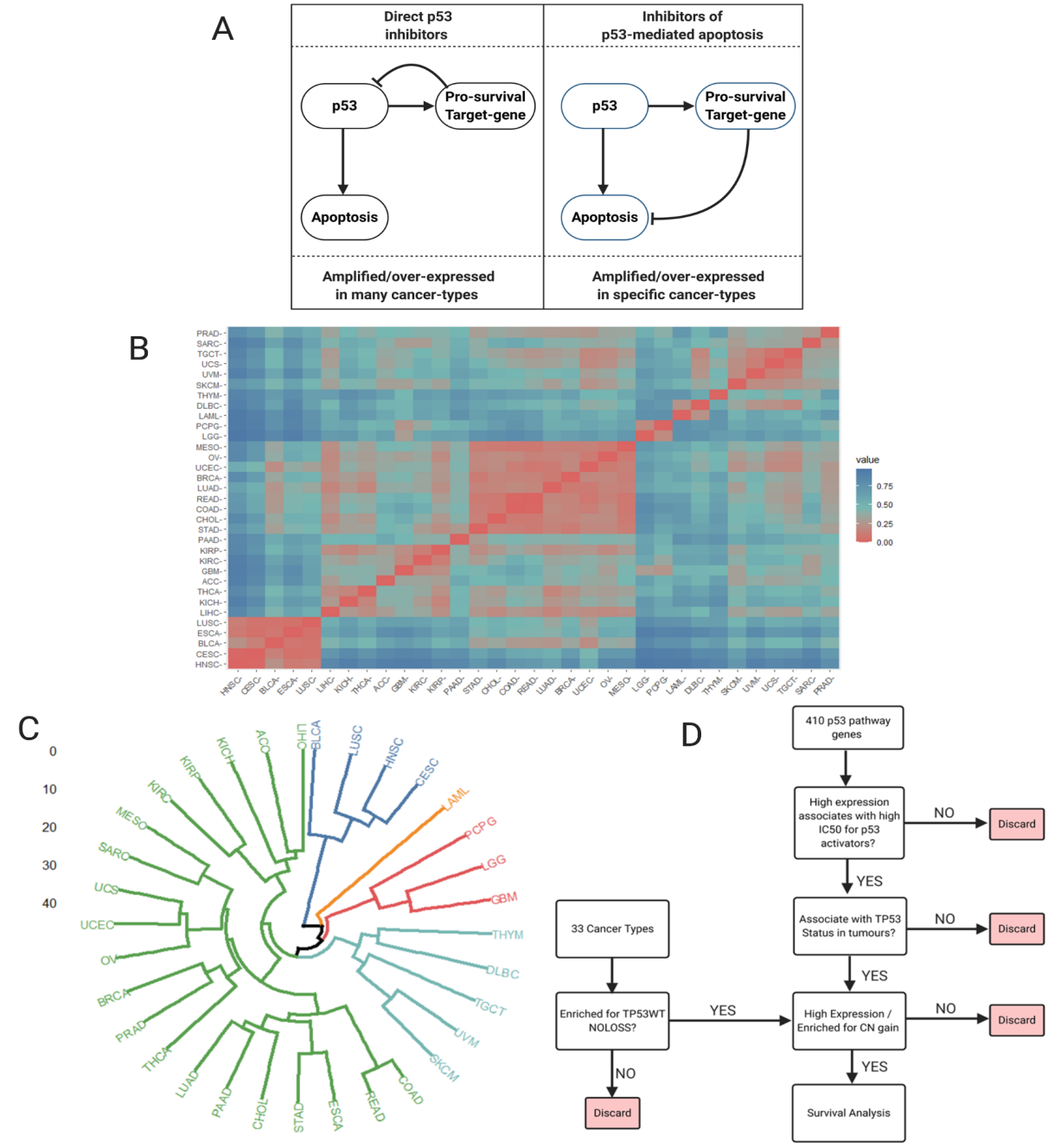


Figure 4.11: **A)** Pro-survival p53 target-genes can inhibit p53-mediated apoptosis in two ways, either by directly regulating p53 levels or activity (e.g. MDM2) or by inhibiting downstream pro-apoptotic signalling (e.g. KITLG/KIT signalling). Direct inhibitors of p53 are often core p53 target genes and are over-expressed in many TP53WT tumours across many cancer-types. In contrast, we reasoned indirect inhibitors of p53-mediated apoptosis may exhibit tissue specificity, if p53 target gene expression itself is tissue-specific. **B)** A dissimilarity matrix calculated using the log_2 expression profiles of 340 p53 target genes across each of the 33 cancer types. Only TP53 WT NOLOSS samples were used. The stronger the blue colouring, the greater the distance between the two cancer types. Pearsons's Correlation was used to calculate the distances. **C)** A circular dendrogram indicating the results of hierarchical clustering of the 33 cancer types based on the expression of 340 p53 target genes. The optimal number of clusters was determined *a priori* using the mclust package. **D)** The pipeline for identifying further inhibitors of p53-mediated apoptosis which could be targetable in cancer to reactivate wild-type p53. To do so, 410 p53 pathway genes were assessed for an association with sensitivity to p53 activating compounds. Of those genes whereby high expression associated with reduced sensitivity, those which were over-expressed in TP53WT tumours compared to TP53-NF were determined. To identify cancer-types of interest, those enriched for TP53WT-NOLOSS status were determined and then screened for enrichment for gain of one of the genes identified in the first analysis or positive correlation between p53 expression and expression of a putative inhibitor gene. Finally, given a list of potential interactions between pro-survival p53-target genes and cancer-types which infrequently mutate TP53, the prognostic value of the genes was determined.

expression associates with higher IC50 for Cisplatin (1.8-fold, p=0.004, Figure 4.12.A). Our analyses with KITLG suggest that pro-survival p53-target genes should be gained and/or overexpressed in TP53WT-NOLOSS tumours compared to TP53-NF. As expected, MDM2 gain is associated with TP53WT-NOLOSS status (logistic regression adjusted for cancer-type and aneuploidy, beta=0.80, p=8.1e-40) with an 8.15-fold ratio of gain to loss in TP53WT-NOLOSS tumours compared to 1.15-fold for TP53-NF (Figure 4.12.B). Moreover, as expected, MDM2 expression is strongly associated with TP53 status with significantly reduced expression amongst cancers with loss and/or mutation of TP53 (linear regression with cancer-type as a covariate, Figure 4.12.C). Looking into individual cancers, 13/33 (39%) show higher MDM2 GISTIC score to associate with TP53WT status (beta >0, FDR < 0.05) and 24/33 (73%) show higher expression in TP53WT-NOLOSS cases. 12/33 (36%) are significant in both tests, in keeping with our hypothesis that amplification and over-expression of direct p53 regulators among TP53WT tumours is a pan-cancer phenomenon. Of these 12 cancer-types, we found that high MDM2 expression associates with worse PFI and OS in a TP53WT dependent manner for LIHC and SARC (Figure 4.12.D). MDM2 has previously been shown to be amplified and over expressed in both LIHC and SARC, thus validating that our approach could be useful for identifying novel cancer specific p53 inhibitors [547][548].

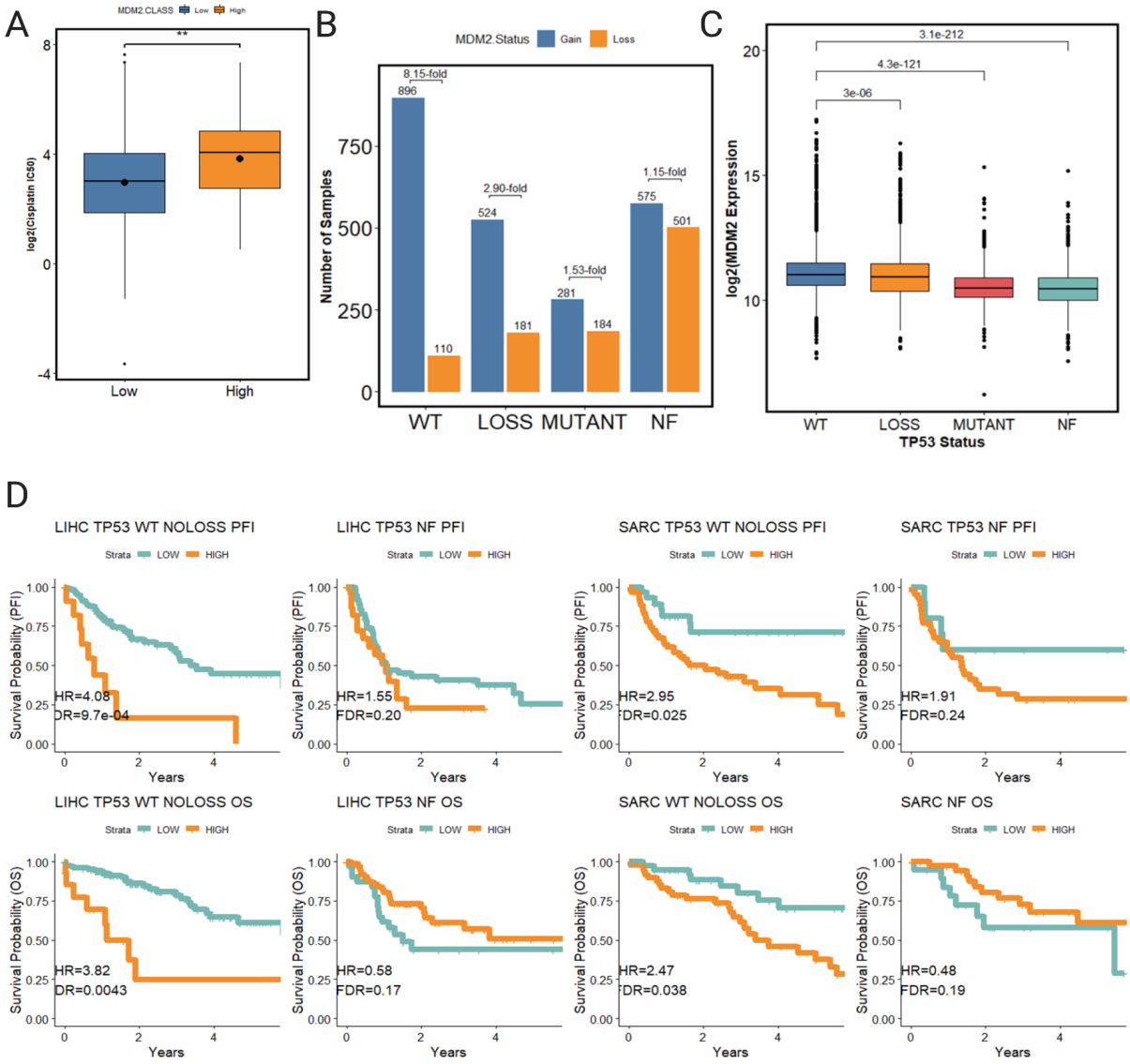


Figure 4.12: A) The boxplots indicate the log2 transformed Cisplatin IC50 for TP53WT cell lines in the GDSC dataset with high and low MDM2 mRNA expression. Significance was tested by linear regression. **B)** Barplot indicating the number of samples of each TP53 status group with either MDM2 gain (blue) or MDM2 loss (orange). The number of cases is shown above each bar and the gain/loss ratio is indicated for each TP53 status group. **C)** Boxplots indicating the relationship between log2 transformed MDM2 expression and TP53 status class. Magnitude and significance was tested by linear regression with cancer type as a covariate. **D)** Kaplain Meier survival curves indicating the effect of MDM2 expression on TP53 WT NOLOSS and TP53 NF LIHC and SARC for both Overall Survival and Progression Free Interval. Hazard Ratio and raw p values were estimated by Cox regression. Raw p values were corrected for the 12 cancer types tested. Samples were split into high and low MDM2 using the surv_cutpoint function.

4.3.4 Identifying p53 inhibitors using pharmacogenomics

In the above analyses, we have demonstrated that the expression of p53 pathway genes in TP53WT tumours can be cancer-type specific; providing motivation to identify genes which, like KITLG, could be novel targets for reactivating the p53 anti-tumour response. To do so we mined the GDSC1 (310,904 cell-line-drug IC50s) and GDSC2 (135,242 cell-line-drug IC50s) pharmacogenomic datasets (Materials and Methods). We isolated the 239 TP53WT-NOLOSS cell-lines from GDSC1 for our initial analyses. We considered hits to be those genes which firstly associated with reduced sensitivity to Nutlin-3a and then to at least 50% of the drugs which we define to be p53 dependent (Figure 4.13.A, see below). We then validate these genes using overlapping p53-dependent compounds in GDSC2. 808 of the 987 cell-lines in GDSC1 are in GDSC2 and 88 compounds overlap between the two datasets, an overlap of 48,617 cell-line-drug IC50s.

12% of p53 pathway genes associate with reduced Nutlin-3a sensitivity

First, we took the TP53WT-NOLOSS cell-lines and regressed the expression of each gene in our p53 pathway list (Materials and Methods) against the IC50 of Nutlin-3a (Supplementary Table C.10). 51 genes (12%) were found to show a positive correlation between expression and Nutlin-3a IC50 (FDR<0.05, Figure 4.13.B, orange dots). These 51 genes included known inhibitors such as KITLG and SFN. Importantly, none of these genes showed a significant effect in TP53 MUTLOSS cell-lines (Figure 4.13.C).

26 compounds indicate evidence of p53 dependency

Next, we aimed to validate these genes using other drugs which act through p53. In order to systematically identify these drugs, we utilised linear regression to determine significant differences between TP53WT-NOLOSS and TP53 MUTLOSS cell-lines for each compound in the database. In total, TP53WT-NOLOSS cell-lines were found to be more sensitive to 223 (61%) drugs and less sensitive to 0 drugs (0%, Figure 4.13.D). Of the 223 compounds, 30 showed greater than

a 2-fold change. TP53 copy-number loss reduces p53 expression and has been shown to associate with chemoresistance [549]. We reasoned that sensitivity to p53-dependent drugs may also correlate with p53 expression. 244 compounds demonstrated a negative correlation between TP53 expression and IC50, of which 153 show greater than 2-fold change (Figure 4.13.E). 26 compounds were significant and showed a greater than 2-fold change in both tests (Supplementary Table C.11). Of these 26, 12 have previously been shown to activate p53 including Nutlin-3a, Doxorubicin, Etoposide and 5-Fluorouracil.

31 p53 pathway genes consistently associate with reduced sensitivity to p53 activators

Having identified a list of p53 dependent compounds, we next used this list to validate the 51 genes found to associate with higher Nutlin-3a IC50. For the other 25 compounds found to be dependent on wild-type p53, we regressed the expression of each of the 51 genes with the IC50s of each compound in TP53WT-NOLOSS cell-lines. After MHT correction, we found 622 significant positive associations between expression and IC50 (Appendix Figure A.17). To select high confidence genes, we focused on those which exhibited a significant positive correlation with at least 12 of the 25 compounds, resulting in 31 genes (Appendix figure A.18). To further validate this list of potential pro-survival p53 pathway genes, we utilised the second GDSC dataset, GDSC2 (Materials and Methods). Of the 25 compounds we identified to be p53 dependent, 6 were also tested in GDSC2, including Nutlin-3a and 5-Fluorouracil. Linear regression was used to test how the expression of each of the 31 genes correlated with IC50 of the 6 drugs. In total, 167 of 186 tests (90%) exhibited significant positive associations with all 31 genes associating with at least 3 of the 6 drugs (Appendix figure A.19). Importantly, no negative associations, indicating high expression with high sensitivity, were found.

77% of the pro-survival p53-target genes are directly or indirectly druggable

Multiple negative regulators of the p53-apoptotic response have been established; although inhibitors targeting some of these are in human trials (e.g. MDM2 inhibitors), none are currently part of standard therapeutic protocols. To address this, we determined whether the pro-survival p53-target genes are druggable. Using the list of druggable genes from Finan et al (2017), we found 12 of the 31 genes (39%) to be druggable [550]. This represents a significant 5-fold enrichment over all genes in the genome (p=6.6e-05). Although 61% of the pro-survival p53-target genes we identified are not directly druggable, they could interact with druggable proteins, and thus be indirectly modulated pharmacologically. This is the basis of network pharmacology[551][552]. We applied this approach by identifying the known protein-protein interactions for each of the 31 pro-survival p53-target genes using STRING (confidence>700, Materials and Methods). This approach resulted in an interactome with 673 nodes and 843 edges. We characterised the druggable section of this interactome by removing nodes which did not form an edge with a druggable gene[550]. This resultant druggable interactome consisted of 294 genes with 631 edges, including 24 of the 31 pro-survival p53-target genes (77%). The number of interactors for these 24 pro-survival p53-target genes ranged from 0-134 with an average confidence score ranging from 822-981 out of 1000. For example, PARD6G, identified as a non-druggable inhibitor gene, was found to interact with 13 other proteins, five of which are druggable. These include PRKCZ and PRKCI which are targetable with aurothiomalate (an approved for treatment of rheumatoid arthritis), Cdc42 which has been shown to be targeted by small molecules CASIN and ML141, PDK1 for which numerous small molecules have shown pre-clinical promise, and F11R which can be inhibited in breast cancer cells by an antagonistic peptide, P4D (Figure 4.13.G)[553][550][554][555][556][557][558].

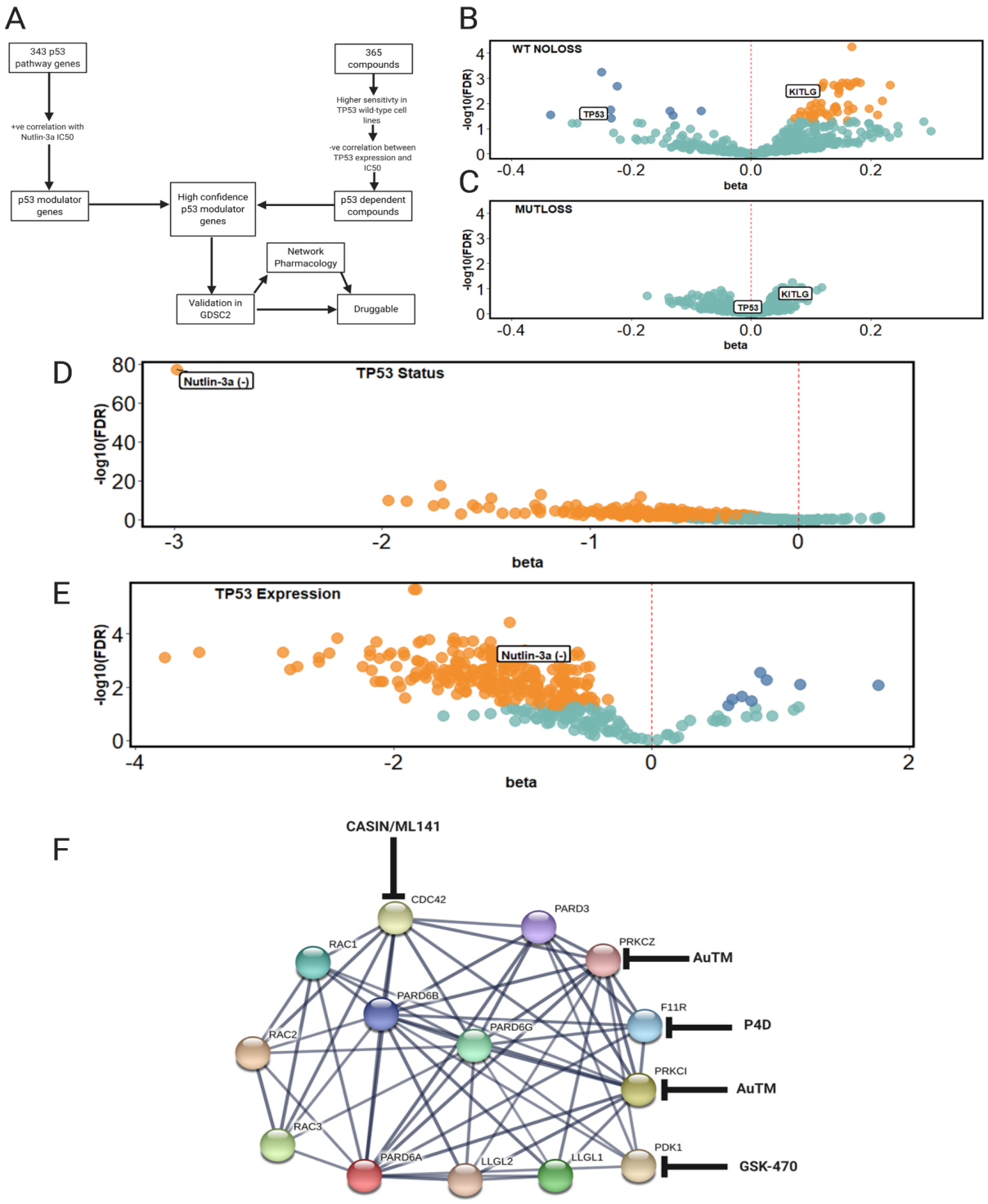

A
343 p53 pathway genes
+ve correlation with Nutlin-3a IC50
p53 modulator genes
365 compounds
Higher sensitivty in TP53 wild-type cell lines
-ve correlation between TP53 expression and IC50
p53 dependent compounds
High confidence p53 modulator genes
Network Pharmacology
Validation in GDSC2
Druggable
B
WT NOLOSS
-log10(FDR)
beta
TP53
KITLG
C
MUTLOSS
D
TP53 Status
Nutlin-3a (-)
E
TP53 Expression
F
CASIN/ML141
CDC42
PARD3
RAC1
PRKCZ
AuTM
PARD6B
F11R
P4D
RAC2
PARD6G
PRKCI
AuTM
RAC3
PARD6A
LLGL2
LLGL1
PDK1
GSK-470

Figure 4.13

Figure 4.13: A) We used the GDSC cell-line databases to identify p53 pathway genes which show negative correlation with sensitivity to p53 dependent compounds. We began by identifying p53 pathway genes which show positive correlation with Nutlin-3a IC50 (high expression associates with lower sensitivity). In parallel we identified p53 dependent compounds by finding those compounds which exhibit significantly higher sensitivity in TP53 WT cell lines and p53 expression negatively correlates with IC50s. We used these drugs to validate the genes from the Nutlin-3a screen by retaining only those genes which significantly associated with at least 50% of the p53 dependent drugs. We then used the GDSC2 dataset to validate these genes. Scatter plots indicating the results of a screen to identify which p53 pathway genes (n=410) show an association between expression and sensitivity to Nutlin-3a in TP53 WT NO LOSS **B)** and TP53 MUTLOSS **C)** cancer cell lines. Orange dots indicate genes whereby high expression associates with high IC50, reduced sensitivity, and blue dots indicate gene whereby high expression associates with lower IC50, higher sensitivity. Significance was determined by linear regression and raw p values were adjusted for 410 tests by FDR. Scatter plots indicating the results of a screen to identify p53 dependent compounds by TP53 status **D)** and TP53 expression **E)**. For TP53 status, we determined which compounds showed differential sensitivity between TP53 WT NOLOSS and TP53 MUTLOSS cell lines. For TP53 expression, we restricted to TP53 WT NOLOSS cell lines and used linear regression to determine the relationship between TP53 expression and IC50 of each compound. Orange dots indicate compounds whereby TP53 WT NOLOSS status (C) or high TP53 expression (D) associated with higher sensitivity. **F)** To determine the extent to which our list of pro-survival p53-target genes could be druggable, we employed network pharmacology to identify genes which are one node away from a druggable gene. PARD6G is shown as an example with druggable genes indicated by black arrows and their respective inhibitors are labelled. The edges between nodes indicate the degree of confidence (>700 for all edges, calculated without text mining).

4.3.5 Exploring the role of pro-survival p53-target genes in human tumours

In the above analyses, we combined transcriptomics and drug sensitivity data for a pan-cancer panel of cell-lines to identify 31 p53 pathway genes which consistently associated with reduced sensitivity to p53-dependent compounds. If these genes are truly hijacked in tumour cells to inhibit p53-dependent apoptosis then, like MDM2, they should be over-expressed and amplified in TP53WT-NOLOSS tumours compared to TP53-NF (Figure 4.14.A).

Five pro-survival p53-target genes associate with TP53 Status in tumours

We first analysed the mRNA expression of the 31 pro-survival p53-target genes in TP53WT-NOLOSS and TP53-NF tumours by linear regression (accounting for cancer-type). We found 12 to be expressed to a significantly lower degree in TP53-NF cells after correction by FDR (Figure 4.14.B, orange labelled points). For the second test, we analysed copy-number variation of each gene in TP53WT-NOLOSS and TP53-NF tumours by logistic regression (accounting for cancer-type and aneuploidy). We found 11 genes to be gained more frequently in TP53WT-NOLOSS after correction by FDR (Figure 4.14.C, labelled blue points). Five genes overlapped between the two tests which we considered to be tumour-relevant pro-survival p53-target genes (KITLG, CPE, MCC, FAM13C and PARD6G). Importantly,

KITLG (and its receptor KIT) and CPE are druggable genes. Moreover, PARD6G is indirectly druggable through direct protein-protein interactions with druggable genes such as PRKCZ and PRKCI which are targetable with aurothiomalate (approved for treatment of rheumatoid arthritis; Figure 4.13.G) [553][550].

High TP53 mRNA expression associates with poorer survival in cancers depleted of TP53 alterations

We have identified five p53 pathway genes which, when highly expressed, associate with reduced sensitivity to p53-dependent compounds and exhibit higher expression and more frequent copy-number gain in TP53WT-NOLOSS tumours compared to TP53-NF. We next aimed to match these genes to specific cancer-types whereby they may be relevant to tumour development. We reasoned that the cancer-types which most frequently retain TP53WT-NOLOSS status would be more likely to harbour negative-feedback loops involving p53 pathway genes (Figure 4.14.A). We identified 17 TCGA cancer-types to be enriched for TP53WT-NOLOSS status (Fisher Exact-Test, FDR < 0.05, Supplementary Table C.12) including THCA and UVM for which no TP53-NF patients were found (TP53WT Enriched Cancers, Figure 4.14.D-E). If p53 promotes signalling pathways which inhibit the p53-apoptotic response in this group of cancers, we would expect that higher p53 activity could associate with poorer outcome. We previously showed in TP53WT cell-lines that for 67% of anti-cancer compounds, low p53 mRNA expression associated with a higher IC50 (reduced sensitivity, Figure 4.13.E) while multiple studies have identified p53 mRNA as a point of regulation which can impact the activity of the p53-stress response [559][560][561]. Based on these findings, we used p53 mRNA expression as a surrogate for p53 pathway activity. Indeed, high TP53 mRNA expression among the TP53WT-NOLOSS Enriched Cancers associates with poorer survival and faster progression (OS: HR=1.54, p=0.00013; PFI: HR=1.40,p=0.00053; Cox regression with adjustment for cancer-types, Figure 4.14.F,H). This effect was not found in TP53WT-NOLOSS tumours of the Non-Enriched Cancers (Figure 4.14.G,I). One of the key canonical functions of p53 is to maintain genomic integrity. To determine if canonical p53 function was repressed in Enriched Cancers we tested for differences in

genomic instability between TP53WT-NOLOSS cases of Enriched and Non-Enriched Cancers. Intriguingly, we found the GI score to be lower in the Non-Enriched group (Linear regression with cancer-type as a covariate, beta=-0.42, p=0.0051) as well as aneuploidy score (Poisson regression with cancer-type as a covariate, beta=-1.14, p=3.3e-06). These analyses suggest that in a subset of cancers which frequently retain wild-type TP53 and normal TP53 copy-number, p53 may inadvertently promote disease progression, perhaps through pro-survival target-genes.

Identfying cancer-types wherein druggable pro-survival p53-target genes may be active

TP53WT-NOLOSS tumours of cancer-types with low TP53 mutation rates, show evidence for pro-cancer, wild-type p53 function. This effect could be explained by negative-feedback exerted on the p53-apoptotic response by p53 target-genes such as the five pro-survival p53-target genes we previously identified, including KITLG. To test this, we focused on the 2 novel, druggable p53 inhibitors, CPE and PARD6G. To identify cancer-types whereby these genes could be oncogenic and targetable, we determined which cancer-types, of those rarely mutating TP53, are enriched for copy-number gain of CPE or PARD6G compared to loss, or exhibit significant correlation between p53 and expression of one of the pro-survival p53-target genes (Figure 4.14.A). 4 and 5 cancers where enriched for copy-number gain over loss of CPE and PARD6G respectively relative to other TP53WT Enriched Cancer-types(Fisher Exact-Test, Figure 4.15.A). ACC was the top enriched cancer-type for CPE, with 14/15 (93%) tumours with CPE copy-number alteration (CNA) exhibiting gain, compared to 20% of other TP53WT-NOLOSS tumours (OR=56-fold, FDR=1.6e-07). For PARD6G, DLBC was the top enriched cancer-type with 11 of 14 (79%) tumours with CNA exhibiting gain, compared to 20% of other tumours (OR=14.5-fold, FDR=1.1e-04). For the correlation test, only KIRC was found to exhibit a positive correlation between p53 and CPE expression (beta=0.19, FDR=2.6e-04) while 5 cancers were found for PARD6G, the strongest being LGG (beta=0.44, FDR=2.3e-12, Figure 4.15.A). These analyses provide 14 unique cancer-gene pairings covering

11 cancer-types which either frequently gain CPE or PARD6G or show significant positive correlation between p53 expression and CPE or PARD6G expression.

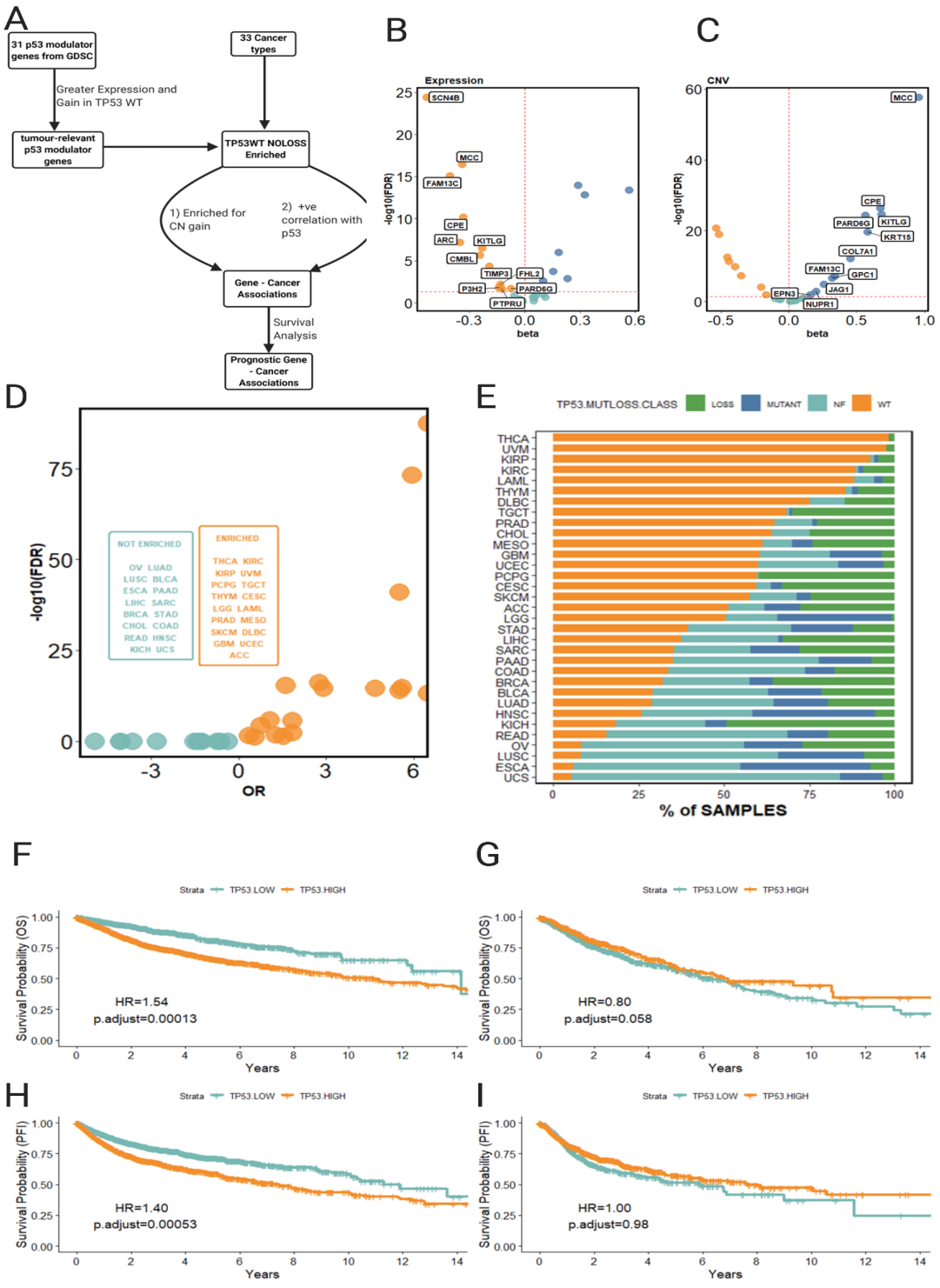


Figure 4.14

Figure 4.14: A) Schematic indicating how we identified tumours whereby the p53 modulating genes we previously identified could have prognostic value. We first reduced our list of modulator genes by finding the gene sto show higher expression and copy-number gain in TP53 WTNOLOSS tumours compared to TP53 NF. We then narrowed our search to cancer types enriched for TP53 WT NOLOSS status. To match modulator genes to tumours, we performed three tests. 1) tumour types enriched for copy number (CN) gain compared to other cancers. 2) Tumour types exhibiting a significant positive correlation between p53 expression and expression of the modulator gene. 3) Significantly higher expression compared to other cancer types. Having found these gene-cancer associations, we determined which were prognostic by survival analysis. Scatter plots indicating which pro-survival p53-target genes could be important in patient tumours. Linear regression (with cancer type as a covariate) was used to compare the expression of each of the 31 pro-survival p53-target genes between TP53 WT NOLOSS and TP53 NF samples **B)** Logistic regression was used to determine the relationship between CNV of each inhibitor gene with TP53 status (WT or NF) with cancer type and aneuploidy score as co-variates **C)**. For both tests, raw p values were adjusted for 31 tests by FDR. Orange dots indicate a significant negative beta and purple dots indicate a significant positive beta. For panel A, a significant negative beta indicates reduced expression in TP53 NF and a significant positive beta in B indicates higher GISTIC score associates with TP53 WT status. **D)** For each TCGA cancer type, enrichment for TP53-WTNOLOSS tumours compared to other cancer types was determined by Exact Fisher-Test. Significant cancer types (FDR-q below 0.05) are indicated in orange. **E)**. Stacked bar plot indicating the percentage of samples which are TP53 WT NOLOSS, MUTANT, LOSS or NF for each cancer type. TP53 WT NOLOSS is indicated by the orange bars. Kaplain-Meier survival curves indicating the association of TP53 mRNA expression with OS for TP53WT-NOLOSS Enriched cancers **F)** and non-enriched cancers **G)** and PFI for TP53WT-NOLOSS enriched cancers **H)** and non enriched **I)**. The indicated Hazard ratios and p values were calculated by Cox regression with cancer type as a covariate.

Expression of pro-survival p53-target genes associates with survival

If the cancer-gene associations found in the previous section are biologically relevant, we reasoned expression of the gene may associate with survival and/or progression in TP53WT-NOLOSS tumours (Figure 4.14.A). For each cancer-gene association, we separated the patients into high and low expression of either CPE or PARD6G (Materials and Methods) and determined the prognostic potential of expression using the Kaplan-Meier method. Importantly, both high CPE and PARD6G expression were found to be prognostic in at least one of the cancers we identified in the previous section (CPE: 1/5 cancers; PARD6G: 4/9 cancers). Specifically, for CPE, high expression associated with shorter OS and PFI for KIRC (OS:HR=1.78, p=0.009; PFI:HR=1.80,p=0.002, Figure 4.15.B) with both associations remaining significant after MHT. For PARD6G, high expression associated with shorter OS for SKCM and LGG and with shorter PFI for DLBC and UVM. However, only the association with DLBC remained significant after MHT (HR=7.64, p=0.01, Figure 4.15.B).

To confirm that CPE and PARD6G could be prognostic in KIRC and DLBC respectively, we determined whether the significant survival associations were independent of known clinical prognostic factors by Multivariate Cox Regression. For KIRC and CPE, high expression of CPE significantly associated with faster progression after adjustment for sex, age at diagnosis, tumour stage and serum

calcium levels (HR=2.07, p=0.0008, Appendix Figure A.20)[562]. Moreover, accounting for CPE expression significantly improved upon the clinical only model (p=0.0012, ANOVA). For DLBC and PARD6G, high expression of PARD6G significantly associated with faster progression after adjustment for sex, age at diagnosis and bone marrow involvement (HR=27.5, p=0.028; Appendix Figure A.21)[563]. Indeed, consideration of PARD6G expression significantly improved upon the clinical only model (p=0.029). These analyses highlight that CPE and PARD6G, potential druggable inhibitors of the p53-apoptotic response, could have prognostic effect in KIRC and DLBC respectively (Figure 4.15.C).

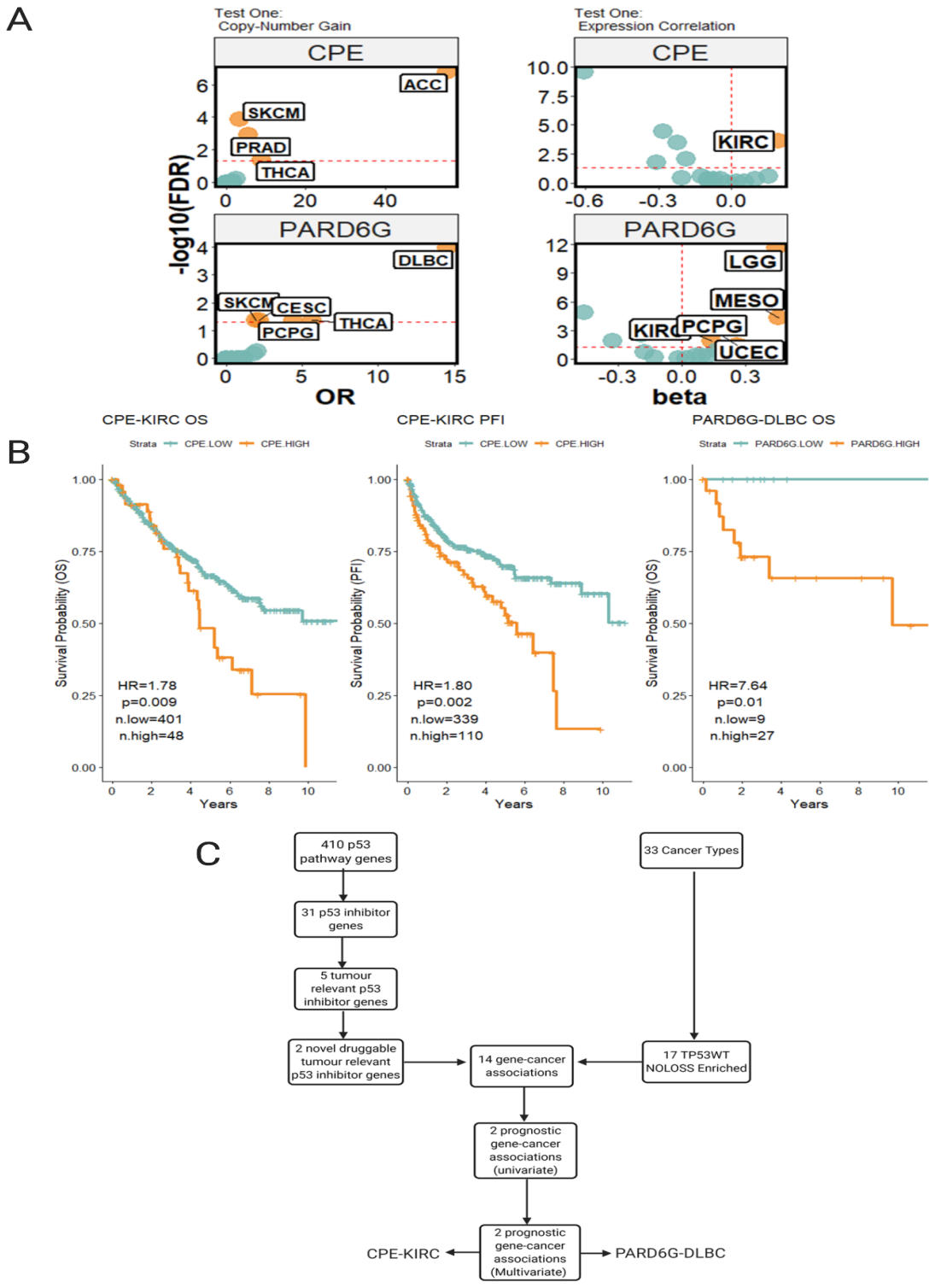


Figure 4.15: A) We focused on the two druggable p53 inhibitors, CPE and PARD6G and the TP53WT-NOLOSS enriched cancer-types. The four facets indicate the results of two tests for each gene: enrichment for CPE gain (top-left), enrichment for PARD6G gain (bottom-left), positive correlation with p53 expression for CPE (top right) and positive correlation with p53 expression for PARD6G (bottom right). Significance for enrichment test was determined by Exact Fisher-Test while linear regression was used for correlation with p53 expression. Significant cancer types, after correction for MHT with FDR, are coloured orange and labelled. **B)** The associations of CPE expression on KIRC OS (left) and KIRC PFI (middle) and of PARD6G with DLBC OS (right) were determined by Cox regression. The hazard ratio, p value and numbers in each group are shown for each test. **C)** Summary diagram of how we identified two druggable pro-survival p53-target genes, CPE and PARD6G, from 410 p53 pathway genes, and the TP53WT-NOLOSS cancer-types wherein they could have pro-tumour function, KIRC and DLBC.

4.4 Discussion

In this thesis, we focus on elucidating how SNPs could impact cancer management; our study of the KITLG-p53RE-SNP led us to firstly develop a combination treatment to harness p53 activation while inhibiting the pro-survival KITLG/KIT signalling and we provided evidence that this strategy could be fruitful for TP53WT melanoma and colon cancer patients. Secondly, our study of the interactions between p53 and KITLG/KIT signalling led us to consider the role of other p53 pathway genes in impairing the p53-apoptotic response in TP53WT tumours. We addressed this question by identifying two further druggable genes (CPE and PARD6G) which associate with reduced sensitivity to p53-dependent therapies, are amplified/overexpressed in TP53WT tumours and are prognostic in cancer-types where in the gene is clearly amplified or correlates with p53 expression. Together, our results suggest that p53 target-genes which can function to inhibit p53-mediated apoptosis could represent novel targets for p53 activation in multiple cancer-types.

4.4.1 Co-modulation of KITLG/KIT and p53 signalling could have therapeutic benefit in Skin Cutaneous Melanoma

Using multiple biomarkers of KITLG/KIT signalling we were able to identify Skin Cutaneous Melanoma (SKCM) as a potential repurposing opportunity for combination therapies which inhibit KITLG/KIT signalling and activate p53. The role of KIT signalling in the skin is well established with the pathway of crucial importance for the development of melanocytes[564]. In line with previous work, we found TP53 wild-type SKCM to be enriched for KIT mutations[565][566]. Furthermore, we found oncogenic KIT mutations (K642E in particular), high KIT expression and high KITLG expression to all associate independently with poorer overall survival in TP53WT SKCM patients. Our data provides molecular support for targeting of KITLG/KIT in melanoma. Indeed, multiple trials have tested KIT inhibitors in melanoma but study sizes have been small with average response rates[567][568][569][570]. Melanoma rarely mutates p53 and expresses high

levels of wild-type p53 protein, in line with the fact that we found SKCM to be enriched for TP53WT-NOLOSS[571]. Melanomas are hardwired to be resistant to p53 dependent apoptosis, perhaps because melanocytes are programmed to survive UV light[572]. Several mechanisms have been proposed for this inhibition of p53 triggered apoptosis, including the action of iASPP, deletion of the CDKN2A locus, aberrant phosphorylation of p53 and activation of MDM2 by downstream KIT signalling[573][572][574][575]. More recently, it has been shown that WNT5a signalling and wild-type p53 might co-operate in melanoma to drive cells into a slow cycling state which is therapy resistant [576]. It is possible that KITLG/KIT-mediated inhibition of the p53-apoptotic response adds a further mechanism through which wild-type p53 can be inhibited in melanoma without mutation, and opens up the possibility of harnessing the pro-apoptotic function of p53 by inhibiting the KITLG/KIT pathway. Indeed, we showed that the combination of Dasatinib and Nutlin-3a and Dasatinib and Doxorubicin are synergistic in a TP53 and KIT WT SKCM cell-line.

Metastatic and primary melanomas are known to be molecularly distinct and can be classified accurately using transcriptomic and methylation data[538]. In support of this, we found a prognostic effect for KITLG in primary samples and KIT expression and K642E mutations in metastatic samples. These differences may concern the KIT/MITF axis; KIT promotes MITF phosphorylation which can induce expression of pro-proliferation and pro-survival genes[577][578]. However, high MITF also reduces invasiveness, potentially explaining why metastatic samples have reduced KIT expression (Figure 4.16.A)[579][539]. Previous data also suggests that metastatic lesions with activating KIT mutations are susceptible to the KIT inhibitor Imatinib[580]. Likewise, our data suggests that metastases which retain higher levels of KIT may confer poorer prognosis. TP53 is rarely mutated in melanoma, including metastatic lesions, but is known to behave abnormally and not as a conventional tumour-suppressor. Indeed, expression of wild-type p53 has been shown to correlate with disease progression, in line with our finding that high p53 mRNA associates with poorer outcome, while knockdown of wild-type p53 has been

shown to reduce proliferation in metastatic melanoma cells. In addition to suggesting that KITLG/KIT signalling inhibits the p53-apoptotic response, our work supports the notion that wild-type p53 could have pro-tumour function in metastatic and primary melanoma. We showed that p53 activation can induce KITLG expression and that inhibition of KITLG/KIT signalling synergises with p53 activation.

In this chapter, we have highlighted that p53 can induce KITLG expression and that KITLG/KIT signalling could inhibit p53-dependent apoptosis in melanoma as well as TGCT. This is in keeping with the evolutionary theory behind why the risk-allele for the KITLG-p53RE-SNP is the major allele in Caucasians (80%) but the minor allele in Africans (30%)[176]. The p53/KITLG axis and the surrounding KITLG locus have been found to be subject to positive selection[581][176]. This raises the question of why the KITLG-p53RE-SNP risk-allele has been positively selected for despite the reduction in evolutionary fitness it confers. Genetic variants in other pigmentary genes have been found but these other variants confer impaired melanogenesis, possibly positively selected in Caucasians in order to enhance Vitamin-D absorption in northern latitudes[582][502]. In contrast, positive selection at the KITLG locus has led to variants which boost KITLG expression, perhaps to induce the UV protective tanning response and to maintain a high level of mitochondrial function and metabolism in cold climates[583][564][584][502] (Figure 4.16.B). This is in keeping with our data in TGCT and melanoma cells. P53 activation induces KITLG expression and through a negative-feedback loop impairs the p53 apoptotic pathway. This is important for both the melanogenesis and temperature hypotheses. The tanning response requires proliferation and migration of melanocytes while the BCL2 family factors (which we identified in Chapter Three) have been found to have key roles in controlling mitochondrial energetics[585]. For example, deletion of MCL1 causes reduced activity of various components of the electron transport chain and reduced oxygen consumption by mitochondria whilst it also inhibits autophagy[586][587]. Here then, lies an evolutionary reason why the risk-allele of the KITLG-p53RE-SNP could be selected for in Caucasians. Activated p53 could induce higher levels of KITLG, greater signalling through KIT and

downstream pathways and higher expression of anti-apoptotic factors such as MCL1. In the skin this would mediate UV protective melanogenesis whilst in brown adipose tissue (BAT) this would constitute higher mitochondrial function and metabolism, an advantageous trait in cold climates. However, due different roles of p53 and KITLG/KIT signalling in different tissues, these advantageous traits have come at the cost of increased risk of TGCT as the same signalling axis allows damaged germ cells to avoid apoptosis and predispose to cancer[588](Figure 4.16.B).

4.4.2 KITLG/KIT signalling could inhibit the p53-apoptotic response in TP53 wild-type Colon Adenocarcinoma

We identified COAD to be enriched for KITLG gain compared to other cancer-types and showed that these amplifications association with higher KITLG expression and are more frequent in TP53WT tumours compared to TP53Mutant tumours. Importantly, we found high KITLG and high KIT expression associated with worse survival in TP53 and BRAF WT tumours. This is in keeping with previous publications demonstrating that KITLG/KIT signalling promotes proliferation in colorectal cancer cells [589][590][471][591][592][593]. Inhibition of KITLG/KIT signalling in colorectal cancer cells and in murine models has elicited anti-tumour effects through a mechanism enhanced by the presence of wild-type p53[594]. Furthermore, the RTK inhibitor regorafenib, which targets KIT, has been approved for treatment of metastatic colorectal cancer[595][596]. The TP53 dependency of the associations we found for COAD suggests that KITLG/KIT signalling inhibits the anti-tumour function of wild-type p53. However, whether p53 can directly upregulate KITLG and KITLG/KIT signalling in colon cancers remains to be established; despite this, our analysis suggests a mechanistic relationship between the two pathways which could be upstream of KITLG/KIT (p53 induces KITLG/KIT) and/or downstream (KITLG/KIT negatively regulates p53 signalling). In either case, we would reason that KIT inhibition would synergise with p53 activation.

Mutation of TP53 is a well-established driver event in colon cancer, exhibited in around 60% of tumours, and associates with poorer prognosis[597][598][599].

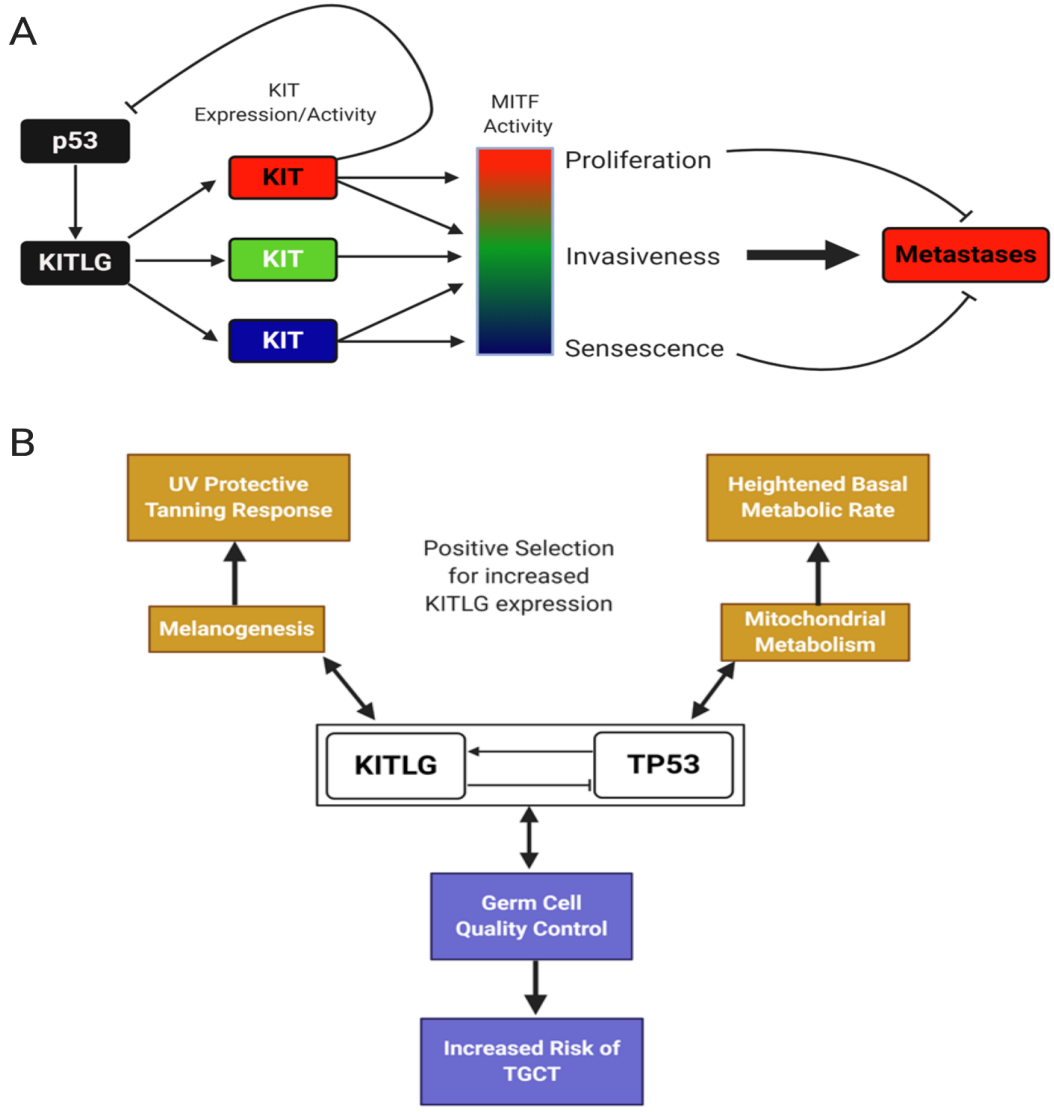


Figure 4.16: A) A schematic demonstrating how the p53/KITLG/KIT axis could control MITF activity to regulate metastasis in SKCM. In the wild-type TP53 context, p53 could trigger KITLG expression with the degree of KITLG/KIT signalling dependent upon the level of expression of KIT. High KIT expression/activity (red box) promotes high MITF activity and proliferative signalling. Low KIT expression (blue box) and activity could promote low MITF activity and allow senescence to occur. Both of these situations would reduce metastatic potential. Melanoma cells may reduce KIT expression in order to control MITF activity and promote invasive potential (green). Cancers which demonstrate the invasive phenotype while retaining higher levels of KIT expression may be more aggressive and have poorer prognosis. **B)** The risk allele for the KITLG p53RE SNP has a frequency of 80% in Caucasians with evidence of a positive selective sweep. This could be explained by the pleiotropic nature of KITLG/KIT signalling. Heightened KITLG/KIT signalling promotes melanogenesis in the skin. Upon p53 activation by UV light, the ability to upregulate KITLG to higher degrees could confer a better tanning response and protection from sun damage. Moreover, KITLG signalling has been shown to promote mitochondrial metabolism. Heightened mitochondrial energetics would increase the basal metabolic rate and heat production, a selective advantage for cold climates of the northern latitudes. However, these selective advantages come at a cost due to the role of KITLG/KIT signalling in germ cell quality control. KITLG/KIT signalling provides a survival signal for primordial germ cells which is required during testicular development. Heightened KITLG expression boosts this survival signal and can prevent damaged germ cells from undergoing cell death, increasing the likelihood of TGCT.

However, some subsets of colon cancer are relatively void of TP53 alterations, for example microsatellite instability high (MSI-H) have a low rate of p53 mutations, potentially due to hypermethylation of p14[600]. This is in keeping with the fact that colon cancer samples in the TCGA cohort which are classified as CMS1 (hypermutated, MSI-H) and CMS3 (Metabolic) are depleted for TP53 mutations (data not shown)[601]. In these subgroups with low rates of TP53 mutation, other mechanisms must negatively regulate the tumour-suppressive function of p53, such as KITLG/KIT signalling.

To verify that the p53 and KITLG/KIT pathways present a therapeutic opportunity for TP53WT SKCM and COAD, further wet-lab experiments would be required (Figure 4.17). We would need to clarify the ability of p53 to upregulate KITLG in cell-lines (1), explore the roles of components of the KITLG/KIT signalling pathway in controlling cell proliferation, migration and drug sensitivity (2) and determine whether KIT inhibition and p53 activation indeed synergises in colon cancer cells lines in a way which is dependent on wild-type p53 (3) and the TP53-KITLG axis (4). Finally, xenograft or transgenic mouse models would be required to show that the combination treatment effectively impairs tumour growth (5). In addition, for COAD it would be important to experimentally validate the dependency on wild-type BRAF status.

4.4.3 CPE and PARD6G could represent cancer-type specific, druggable inhibitors of p53-mediated tumour-suppression

In this Chapter, we integrated omics and pharmacological data from cancer cell-lines to identify inhibitors of the p53-apoptotic response in the p53 network. We then utilised omics data from 33 types of human cancer to highlight patient groups whereby these genes could be prognostic and/or druggable. We identified four pro-survival p53-target genes in addition to KITLG, two of which, CPE and PARD6G, are novel p53 inhibitors and directly or indirectly druggable.

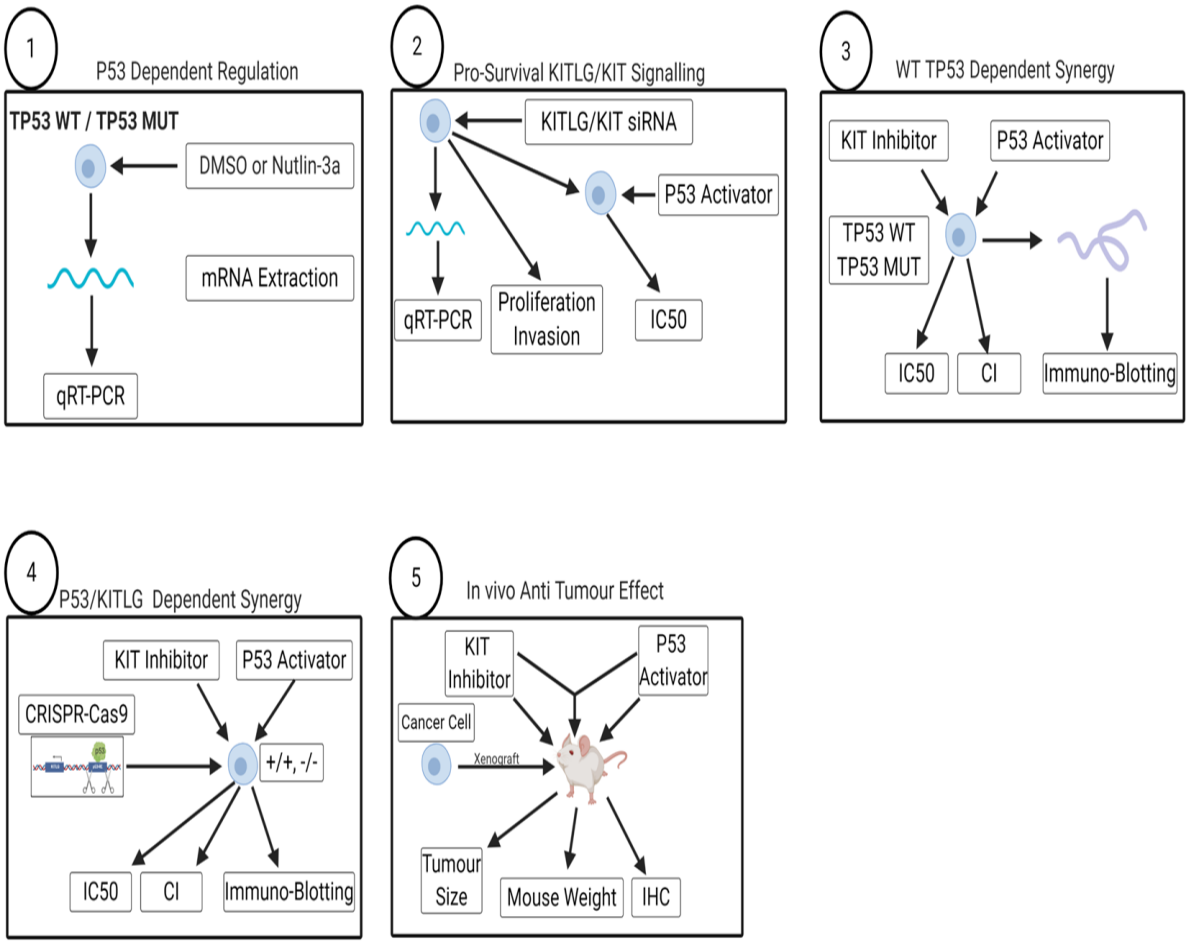


Figure 4.17: Schematic outlining some of the experiments which would be required to clarify the role of the p53/KITLG/KIT axis in SKCM and COAD. 1, Determine the role of p53 in the induction of KITLG mRNA expression 2, Highlight the pro-survival function of KITLG/KIT signalling by knockdown of KITLG/KIT components. 3, Determine the interaction between KIT inhibition and p53 activation and whether it is dependent on wild-type TP53 (and BRAF for COAD) and the p53/KITLG axis (4). 5, Determine whether the interaction between KIT inhibition and p53 activation facilitates a better anti-tumour response in a murine xenograft model.

Carboxypeptidase E (CPE)

Carboxypeptidase E is encoded by the CPE gene. CPE protein acts as a metalloexopeptidase which catalyses the cleavage of C-terminal amino acid residues, a key step in the biosynthesis and processing of peptide hormones[602][603][604]. CPE mutant or knockout mice exhibit obesity, diabetes, infertility and behavioural deficits[605][606][607]. Elevated CPE expression has been reported in cervical, colorectal, renal, bone and brain cancers[608]. CPE has been shown to promote proliferation, tumorigenicity and chemoresistance in cancer cell-lines through up-regulation of cell cycle genes and NFKB signalling[609][610][611][612][613][614].

These publications support a pro-tumour role for CPE. In our analyses we find that CPE expression strongly associates with reduced sensitivity to p53 dependent anti-cancer compounds, in line with Lui et al (2014) who showed CPE downregulation to enhance sensitivity to cisplatin.

High expression of CPE has previously been linked with pancreatic cancer and hepatocellular carcinoma; we found high expression to associate with poor prognosis in clear cell renal cancer (KIRC). Murthy et al (2010) noted elevated expression of CPE in renal cancers but our analysis is the first to associate CPE expression with survival[608]. Interestingly, high levels of some hormones which CPE plays a role in synthesising, such as gonadotropin, have previously been demonstrated to be abnormal in renal cancers[615][616]. Together with previous studies, our data suggests that CPE could a be a therapeutic target for renal cancer. Importantly, there is proof-of-principle CPE is druggable through a small-molecule, GEMSA, suggesting that compounds could be developed to target CPE[617][618][550]. Functional studies would be required to unpick the mechanism responsible for the proposed p53-mediated pro-tumour effect of CPE in KIRC.

Par-6 Family Cell Polarity Regulator Gamma/ Partitioning Defective 6 Homolog Gamma (PARD6G)

The PAR family of proteins were first identified as being key in controlling cell polarity and asymmetric cell division[619][620][621]. Cell polarity is key to a number of important cellular processes including directional migration[622][623]. PAR6 has been shown to be overexpressed in breast cancer, to promote proliferation by activation of MEK/ERK signalling, to be required for tight junction formation and to promote TGF-dependent EMT[624][625][626][627][628]. On this evidence, PAR6 could have pro-tumour function. In vertebrates the PAR6 gene has been multiplied to give three genes, PARD6A, PARD6B and PARD6G. These three genes are found on different chromosomes but show more than 70% sequence similarity. Many PAR6 studies do not distinguish between the three genes[629]. In one study of breast cancer cell-lines, they suggest that PARD6G is frequently lost in cancer while a pro-proliferation role for PARD6G has been noted in osteoblast

lineage cells[630][629]. The conflicting data concerning the PARD6 genes may reflect tissue specific differences in their roles. In our analysis, we found DLBC to be enriched for PARD6G gain and for high PARD6G expression to associate with faster progression in DLBC. This is the first analysis to link PARD6G to blood cancers. However, multiple loci which are thought to maintain cell polarity have previously been linked to DLBC including receptor tyrosine kinase-like orphan receptor (ROR) family proteins and EXOC2 while Par6 has been shown to be important for maintaining cell polarity in lymphocytes and proliferation of haemopoietic stem cells[631][632][633][634]. Importantly, we highlighted through network pharmacology, that PARD6G could be pharmacologically modulated by targeting druggable proteins with which it interacts (Figure 4.13.H). For example, PARD6G interacts with PRKCZ and PRKCI which are targetable by an approved compound for rheumatoid arthritis, Aurothiomalate[553]. It would be interesting to further investigate the role of PARD6G in DLBC and determine if it represents a repurposing opportunity for Aurothiomalate.

4.4.4 The importance of context

Categorisation is a cornerstone of oncology; as a field, we routinely classify tumours by their tissue of origin and genes by whether they are pro-tumour (proto-oncogenes) or anti-tumour (tumour suppressors). However, as the deep genomic approach to understanding cancer has developed, it has become clear that these categorisations are too imprecise and too inflexible. It is clear that genes involved in carcinogenesis can have very different effects depending on the cellular context, including but not restricted to, the cell-type, the genetic profile of the tumour and the tumour microenvironment[635][636][637]. For example, the transcription factor NFIB is under-expressed in NSCLC and low expression associates with shorter survival but is over-expressed and contributes to metastasis in SCLC, melanoma and breast cancer[638][639][640][641]. Indeed, the COSMIC Cancer Gene Census classifies 72 genes as having both oncogenic and tumour-suppressive function[642][643]. Our own work in this Chapter corroborates these findings; for example, our screen

for p53 pathway genes which inhibit the p53-apoptotic response to anti-cancer drugs, identified CPE as a potential pro-survival gene which we showed associates with poorer outcome in renal clear cell carcinoma (KIRC). However, CPE has also been linked with reduced migration of tumour cells in glioblastoma[644]. Even for p53, pro-cancer roles in specific cellular conditions are being defined. P53 GOF/DN mutants are well categorised to promote tumour progression but high expression of wild-type p53 has been shown to associate with poorer prognosis in melanoma (supported by our data) and renal cancer[645]. Therefore, it is becoming increasingly clear that classifications of genes as either tumour-suppressive or oncogenic must be contextualised.

Genes and genetic aberrations may have tissue-specific effects on tumorigenesis, but tissue-agnostic studies have highlighted that subgroups of patients from different cancer-types can share the same tumorigenic mechanisms and potentially be treated in the same way[36]. For example, gene fusions involving neurotrophic-tropomyosin receptor kinase (NTRK) genes have been found in small numbers of patients across multiple cancers including thyroid cancer, paediatric melanoma and paediatric glioma; importantly NTRK fusions are actionable and the FDA recently approved entrectinib for treatment of solid tumours with NTRK fusions[36][646][647]. In our work, we have identified subgroups of patients who exhibit signs of heightened KITLG/KIT signalling and inhibition of wild-type p53 anti-tumour function and could therefore benefit from simultaneous activation of p53 and inhibition of KITLG/KIT signalling (TP53WT TGCT, SKCM and COAD tumours). Identifying patients, across cancers, who harbour the same actionable cancer drivers is accelerating the arrival of the genomic era of medicine and is already motivating the switch from tumour-specific clinical trials to gene-specific basket trials. For example, a trial for pembrolizumab (PD-1 inhibitor), encompassing patients with microsatellite instability-high solid tumours from 15 cancer-types, achieved objective response rates of 40% leading to FDA approval[648]. With future multi-omic and whole-genome characterisation of human tumours, the tissue-specific role of p53

target-genes in cancer will be further unveiled and no doubt uncover novel pro-cancer mechanisms which are shared between subgroups of patients with tumours derived from distinct tissues.

5

A highly pleiotropic cancer-risk SNP in the p53 pathway could have clinical impact for multiple cancer types

Contents

5.1 Abstract 198
5.2 Introduction 199
5.2.1 Pleiotropic factors underpin multiple distinct traits . . . 199
5.2.2 SNP-level Pleiotropy has biological and clinical implications 200
5.2.3 Pleiotropy is prevalent in cancer 200
5.3 Results 203
5.3.1 Cancer-associated SNPs are enriched for pleiotropy compared to SNPs associated with other diseases 203
5.3.2 The p53 pathway is enriched for SNPs associated with multiple cancer-types 206
5.3.3 The TP53-PAS-SNP can have long-lasting associations in tumours 210
5.3.4 The TP53-PAS-SNP inhibits mutant p53 219
5.3.5 Insights into the mechanism of the TP53-PAS-SNP . . . 224
5.3.6 Modest reductions in p53 expression associate with reduced sensitivity to many anti-cancer compounds 229
5.4 Discussion 236
5.4.1 Summary 236
5.4.2 The mechanism of the TP53-PAS-SNP 236
5.4.3 Potential clinical impact of the TP53-PAS-SNP 239
5.4.4 Implications of the interplay between germline and somatic genetics 240

5.1 Abstract

Pleiotropy refers to how multiple traits can depend on a single factor such as a mutation or gene. When these traits represent different diseases, pleiotropy reveals shared aetiology and opportunities for drug repurposing[649][650][552]. In this Chapter, we focus on pleiotropic cancer-risk SNPs. We first explore GWAS summary data and highlight that cancer-risk SNPs are enriched for SNPs associated with multiple traits compared to SNPs associated with other diseases. Moreover, we find that of pleiotropic cancer-SNPs, a significantly higher proportion than expected map to p53 pathway genes. We focus on a highly pleiotropic SNP in the polyadenylation signal of TP53 which is associated with increased risk for multiple cancers. To explore the potential clinical utility of this SNP, we investigate whether this SNP continues to influence the course of the disease once the cancer has arisen in the patients. We explore its potential influence on the evolution of cancer genomes, disease progression, therapeutic responses and overall survival using a cohort of patients for which both germline and somatic mutation data was available, in addition to deep-omic characterisation and clinical data. Moreover, with this cohort and isogenic cell-line models, we provide evidence for a mechanistic model for the impact of this SNP on tumour p53 expression, p53 driver mutation accumulation and disease progression.

5.2 Introduction

5.2.1 Pleiotropic factors underpin multiple distinct traits

In this Chapter, we use the term 'trait' to refer to physical qualities which can be qualitatively or quantitively measured, such as height, hair colour or risk of a particular disease. Pleiotropy is defined as how multiple, distinct traits could appear correlated due to dependence on a single factor[651]. The literature refers to pleiotropy on multiple levels. Pleiotropy can be at the level of groups of genes such as signal transduction pathways; for example, NOTCH signalling has been shown to have multiple, cell-type specific, tumour-promoting and tumour-suppressive functions in haematological diseases[652]. Pleiotropy can be at the gene level through genes with multiple biochemical functions and genes with one function with multiple consequences (Figure 5.1). An example of the latter is phenylketonuria which is caused by defects in the phenylalanine hydroxylase enzymes encoded by PAH. Impaired PAH causes accumulation of phenylalanine and multiple symptoms including cognitive issues and eczema[653][654]. Single Nucleotide Polymorphisms (SNPs) can be pleiotropic if they are found to associate with multiple distinct traits in GWAS. SNP-level pleiotropy could stem from one SNP affecting expression of multiple genes, perhaps through a shared regulatory element, or through modulation of one gene/pathway which is important in multiple tissues (Figure 5.1)[655][656]. Gleason et al (2020) demonstrated the former; they identified 32 SNPs associated in GWAS with both height and BMI, 12 of which associated with expression of multiple genes[657]. SNP-level pleiotropy can also be defined as when two SNPs within the same locus are found to associate with different traits[552].

The extent of gene and SNP-level pleiotropy is unclear[651][655]. On one side, the Hypothesis of Universal Pleiotropy implies that all mutations affect all traits due to the highly connected network structure of cellular processes[658][659]. Empirical studies have provided evidence for a modular approach of gene-level pleiotropy whereby a gene can only affect similar traits[660][661]. SNP-level pleiotropy can be systematically detected by phenome-wide association studies

(PheWAS). PheWASes involve taking a small number of SNPs and testing for associations with many different traits[662][663]. Estimates of SNP-level pleiotropy vary from 5-32% [655][664][665].

5.2.2 SNP-level Pleiotropy has biological and clinical implications

SNP-level pleiotropy can be useful in a biological sense as it can indicate shared aetiology between previously unrelated traits. For example a SNP at the GALNT2 locus was known to be associated with high-density lipoprotein cholesterol levels and was found to also associate with hypertension and coronary heart disease in PheWAS[662]. Similarly, Pickrell et al (2016) identified a SNP within the ABO gene to associate with coronary artery disease and tonsillectomy[666]. Thus, pleiotropic SNPs can identify traits which could have shared molecular mechanisms; this suggests that these SNPs could also have a clinical utility in highlighting opportunities for drug repurposing (Figure 5.1)[552]. Indeed, SNPs at loci encoding oestrogen receptors have been linked to both osteoporosis and breast cancer; this has facilitated the repurposing of raloxifene, originally developed for osteoporosis, for breast cancer patients[667][668][552].

5.2.3 Pleiotropy is prevalent in cancer

Cancer is genetically complex and yet, significant correlations have been found between the heritable polygenic component of common cancers: e.g. up to 0.57 between lung and head/neck cancers[669][670]. Accordingly, some cancer-susceptibility loci have been found to be highly pleiotropic. For example, SNPs in TERT, encoding telomerase, have been linked with cancers of the breast, brain and lung, but has not been successfully targeted[649][671]. Identification of other pleiotropic SNPs and genes in cancer could open up new repurposing opportunities[650][552]. Indeed, a recent study performed GWASes for 18 cancer-types in two large cohorts and identified 100 SNPs associating with multiple cancers which were enriched for genes related to immune function, with drug resistance

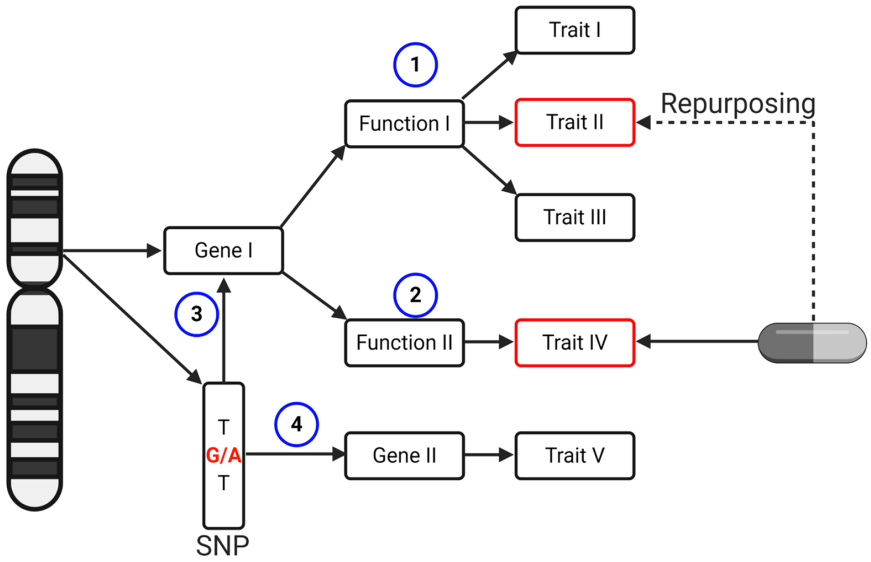


Figure 5.1: Pleiotropy refers to the phenomenon that multiple seemingly unrelated traits, across different tissues, can be mediated by one factor. This factor could be a gene or a single mutation including SNPs. 1) Gene-level pleiotropy could occur when a gene has a function which affects more than one trait. 2) Gene-level pleiotropy could also occur when a single gene has multiple separate biochemical functions which each affect different traits. 3) SNP-level pleiotropy can attributed to SNPs which regulate the expression of a single gene which affects multiple traits. 4) SNPs may modify a regulatory elements which affects multiple genes and thus the SNP may modulate expression of genes which affect different traits. Gene and SNP level pleiotropy can indicate drug repurposing opportunities. Traits which cause disease are indicated with red borders. A drug may already have been developed for Trait IV; in this case, the drug could be repurposed to treat Trait II which is associated with the same gene in GWAS.

and other hallmarks of cancer[672]. Further research of pleiotropic cancer-risk SNPs in key cancer pathways could inform drug design and drug repurposing for multiple cancer-types by identifying common targets.

An important step in linking pleiotropic SNPs with repurposing is unravelling the underpinning molecular mechanisms. An understanding of the genes and pathways involved can allow for combination of GWAS data with protein-protein interaction networks to identify druggable targets which are in the same pathway as the GWAS-associated gene[552]. This approach has recently been applied to a GWAS of BRCA-negative women with a family history of breast cancer; Climente-Gonzalez et al (2020) identify a gene module, enriched for breast cancer susceptibility genes, which could indicate novel mechanisms and therapeutic targets[673]. Furthermore, understanding the molecular mechanisms of pleiotropic SNPs is particularly crucial given how pleiotropy can be antagonistic. In these cases, the same SNP associates with increased risk of one disease but reduced risk for another. Rashkin et al (2020) identified 15 SNPs exhibiting antagonistic pleiotropy in cancer; rs62516012

(CASC8 gene) was found to associate with increased risk of prostate cancer but decreased risk of breast cancer[672].

Previously, we found evidence that genetic alterations of the p53/KITLG/KIT axis, such as oncogenic KIT mutations and KITLG copy-number gain, were enriched for in TP53 wild-type tumours of multiple cancer-types, suggesting that heightened signalling through this axis could have pleiotropic effects on multiple TP53 wild-type cancers. In this chapter, we focus on SNP-level pleiotropy in TP53 wild-type and mutant cancers. Somatic mutation of the p53 pathway is abundant in cancer genomes with TP53 frequently mutated in many cancer-types. Moreover, the p53 pathway is enriched for cancer-susceptibility SNPs[99]. Therefore, we hypothesised that the p53 pathway would be ideal to explore the use of pleiotropic SNPs for better management, both in terms of risk and treatment, of multiple cancer types. To test this hypothesis, we first identify pleiotropic cancer-susceptibility SNPs which map to p53 pathway genes and identify the most pleiotropic of these to be located in the canonical TP53 polyadenylation signal. We explore the association of this SNP with the evolution of cancer genomes, disease progression and therapeutic responses before investigating the molecular mechanism underpinning these associations. Finally, we provide evidence that this SNP associates with a reduction in p53 expression levels which is comparable to the reduction associated with TP53 copy-number loss and could therefore modify the response of tumour cells to p53-activating therapies.

5.3 Results

5.3.1 Cancer-associated SNPs are enriched for pleiotropy compared to SNPs associated with other diseases

We hypothesised that pleiotropic cancer-associated SNPs might provide insight into the management of multiple cancers in the broader population. We first aimed to determine the extent of pleiotropy amongst cancer-associated SNPs. To do so, we utilised the data recently publicised by Watanabe et al (2019)[664](Materials and Methods). Specifically, the authors collated data from GWASs of 551 traits (including 37 cancer-related traits covering 13 cancer types) and determined whether SNPs were associated with multiple traits across diseases. We define three measures of pleiotropy; the number of traits a cancer-SNP associates with, regardless of disease domain (Pan-Domain Pleiotropic SNPs, PDP-SNPs); the number of cancer-related traits associated with a cancer-SNP (Intra-Domain Pleiotropic SNPs, Intra-DP-SNPs) and the number of non-cancer traits associated with a cancer-SNP (Inter-DP-SNPs, Figure 5.2.A). In total, 60% of the 236,638 SNPs in the database were associated with more than one trait and 32% were associated with traits across multiple disease domains. We first asked whether SNPs associated with cancer (Neoplasm Domain) were enriched for PDP-SNPs. We found 740 of 965 cancer-associated SNPs to be PDP-SNPs (77%), representing a significant enrichment compared to SNPs not associated with cancer (OR=2.2, p=2e-27, Fisher Exact-Test,Figure 5.2.B). rs7030641, an intronic variant near the CDKN2B locus, associated with the most traits, 17 traits across 7 disease domains including malignant neoplasms of the skin and ischemic heart disease). We then examined the number of cancer-associated SNPs associating with more than one cancer-related trait (Intra-DP-SNPs). Although cancer-SNPs (Neoplasm-SNPs) were not enriched for Intra-DP-SNPs compared to other diseases, we did find Neoplasms to have the fourth highest proportion of Intra-DP-SNPs (521 of 965 SNPs), behind Immunological, Metabolic and Dermatological diseases. (Figure 5.2.C). Two SNPs at the CASP8 locus associated with the most cancer-related traits; five traits including basal cell carcinoma and number of self-reported cancers. Thirdly, we

examined how many cancer-associated SNPs were also associated with traits from other disease domains (Inter-DP-SNPs). 408 cancer-SNPs associated with non-cancer traits (42%) which represented a significant enrichment compared to SNPs not associated with cancer (OR=1.53, p=1.6e-10, Fisher Exact-Test Figure 5.2.D). Multiple SNPs at the FOXP1 locus associated with seven disease domains including schizophrenia (Psychiatric), skin cancer (Neoplasm) and vitiligo (Dermatological). These analyses highlight that cancer-SNPs exhibit relatively high levels of pleiotropy compared to other diseases.

Having determined that cancer-associated SNPs exhibit high levels of pleiotropy, both within cancer and with non-cancer traits, we hypothesised that cancer-associated PDP-, Intra-DP and Inter-DP-SNPs might map to genes in key signalling pathways for tumorigenesis, such as the p53 pathway. SNPs were assigned to genes using a 1kb window on each side (Cancer-associated genes, CAGs)[664]. Indeed, we found that for all three sets of SNPs, the genes which they are mapped to significantly overlap with our annotated list of 409 p53 pathway genes (Materials and Methods, PDP: 5 genes, OR=4.5,p=0.006; Intra-DP: 3 genes, OR=5.6, p=0.019; Inter-DP: 5 genes, OR=5.0, p=0.004, Fisher Exact-Test). To ascertain how significant this overlap is compared to other signalling pathways, we tested for enrichment of KEGG genesets (Fisher Exact-Test). PDP-SNP genes were found to be significantly enriched for two specific pathways, the p53 (OR=16.7, FDR=0.025) and TGF-beta (OR=13.1, FDR=0.039) pathways with the p53 pathway as the top pathway(Figure 5.2.E). Intra-DP-SNP genes were found to be significantly enriched for one specific pathway, the p53 pathway (OR=22.8, FDR=0.045, Figure 5.2.F). Inter-DP-SNP genes were found to be significantly enriched for two specific pathways, the p53 (OR=18.2, FDR=0.02) and TGF-beta (OR=14.3, FDR=0.03) pathways with the p53 pathway as the top pathway (Figure 5.2.G).

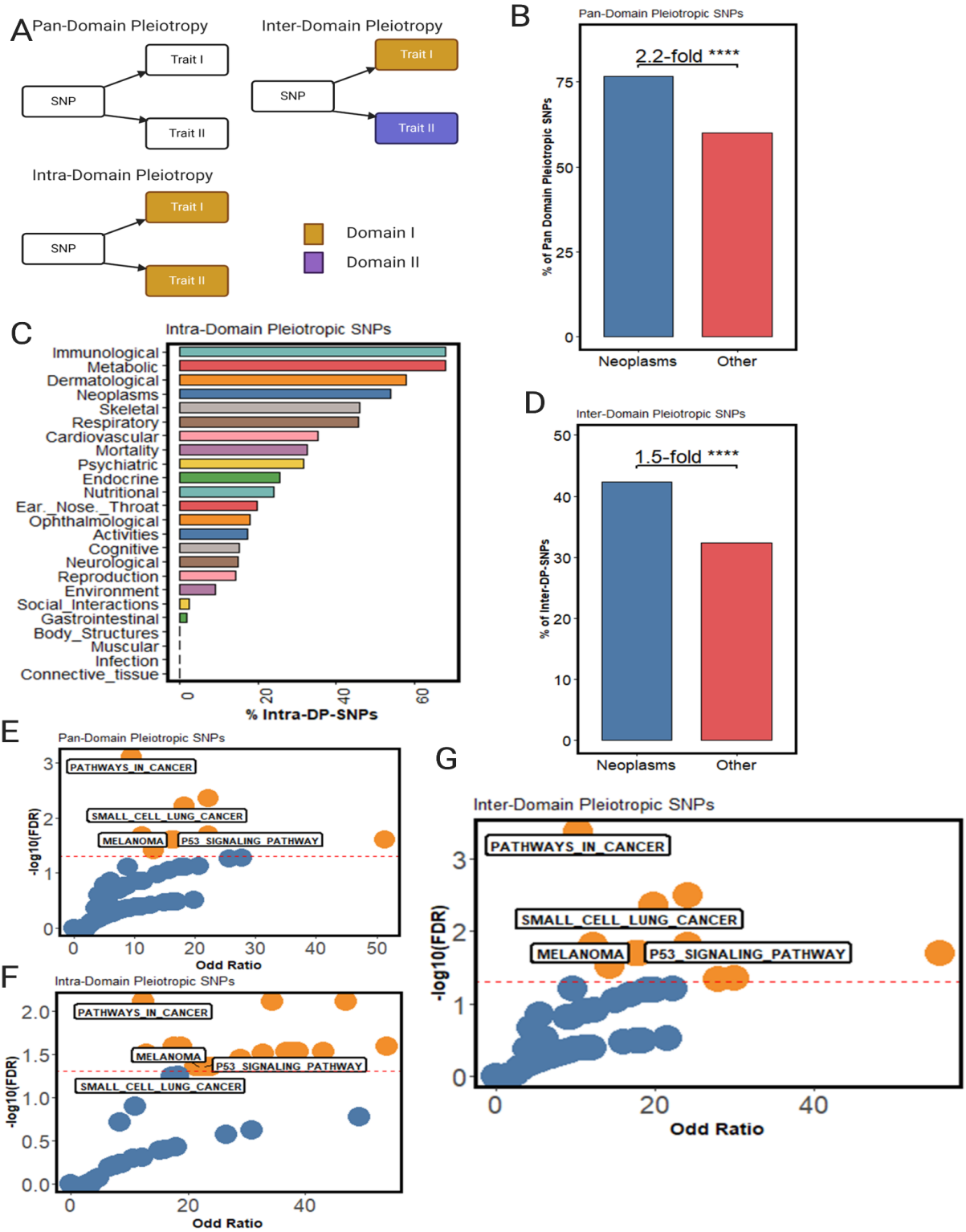

A
Pan-Domain Pleiotropy
Trait I
SNP
Trait II
Inter-Domain Pleiotropy
Trait I
SNP
Trait II
Intra-Domain Pleiotropy
Trait I
SNP
Trait II
Domain I
Domain II
B
Pan-Domain Pleiotropic SNPs
2.2-fold ****
% of Pan Domain Pleiotropic SNPs
Neoplasms
Other
C
Intra-Domain Pleiotropic SNPs
Immunological
Metabolic
Dermatological
Neoplasms
Skeletal
Respiratory
Cardiovascular
Mortality
Psychiatric
Endocrine
Nutritional
Ear._Nose._Throat
Ophthalmological
Activities
Cognitive
Neurological
Reproduction
Environment
Social_Interactions
Gastrointestinal
Body_Structures
Muscular
Infection
Connective_tissue
% Intra-DP-SNPs
D
Inter-Domain Pleiotropic SNPs
1.5-fold ****
% of Inter-DP-SNPs
Neoplasms
Other
E
Pan-Domain Pleiotropic SNPs
PATHWAYS_IN_CANCER
SMALL_CELL_LUNG_CANCER
MELANOMA
P53_SIGNALING_PATHWAY
-log10(FDR)
Odd Ratio
F
Intra-Domain Pleiotropic SNPs
PATHWAYS_IN_CANCER
MELANOMA
P53_SIGNALING_PATHWAY
SMALL_CELL_LUNG_CANCER
-log10(FDR)
Odd Ratio
G
Inter-Domain Pleiotropic SNPs
PATHWAYS_IN_CANCER
SMALL_CELL_LUNG_CANCER
MELANOMA
P53_SIGNALING_PATHWAY
-log10(FDR)
Odd Ratio

Figure 5.2

Figure 5.2: **A**) We define three measures of SNP level pleiotropy. Pan-Domain Pleiotropy refers to SNPs which associate with more than one trait, regardless of disease domain. Intra-domain Pleiotropy refers to SNPs which associate with multiple traits within a given disease domain, such as multiple cancer traits. Inter-Domain Pleiotropy refers to SNPs which associate with traits in different disease domains. **B**) The barplot indicates the proportion of cancer-associated SNPs and non-cancer associated SNPs which are Pan-Domain Pleiotropic SNPs. Significance determined by Two-tailed Exact Fisher Test. **C**) To assess Intra-DP-SNPs in cancer relative to other diseases, we found the percentage of SNPs associated with each disease domain to be Intra-DP-SNPs. The disease domains are ordered by the percentage of Intra-DP SNPs. **D**) The barplot indicates the proportion of cancer-associated SNPs and non-cancer associated SNPs which are Inter-Domain Pleiotropic SNPs. Significance determined by Two-tailed Exact Fisher Test. The genes to which the cancer associated PDP-SNPs **E**), Intra-DP-SNPs **F**) and Inter-DP-SNPs **G**) map to were used as input for functional enrichment. Gene set enrichment was performed by Fisher Exact-Test using KEGG gene sets. Raw p-values were corrected by FDR and an adjusted p-value of 0.05 was considered significant.

5.3.2 The p53 pathway is enriched for SNPs associated with multiple cancer-types

Using the data published by Watanabe *et al*, we showed that cancer-associated SNPs exhibit pleiotropy and that those pleiotropic SNPs are found in key cancer pathways. To investigate SNPs which could influence the management of multiple cancer-types, we aimed to identify those SNPs which associate with cancers from different tissues (Multi-Cancer SNPs). However, the analysis by Watanabe *et al* includes different traits which relate to the same cancer-type and ambiguous traits such as 'the number of self-reported cancers'. Therefore to specifically identify Multi-Cancer SNPs we accessed and curated the most recent version of the GWAS catalogue (Accessed May 2020)[56]. We filtered this list for traits relating to cancer (Materials and Methods) and extracted a total of 5,313 SNPs associated with 279 cancer-related traits (Figure 5.3.A). There are many overlapping traits in the GWAS catalog such as 'testicular cancer' and 'testis cancer'. We annotated the cancer-related traits by grouping closely related and overlapping terms to leave 33 unique cancer-types (Materials and Methods). SNPs associated with a trait which was not directly linked to a cancer-type or susceptibility were removed. After filtering out duplicated SNP-trait associations and SNPs not mapping to an identified gene, we found 3,091 SNPs associated with at least one of 33 cancers (3.2-fold more SNPs than used by Watanabe *et al*) which mapped to 2,036 unique genes (CAGs) (Figure 5.3.A). Of these cancer-associated SNPs, we found 135 (4.4%), mapping to 113 genes, to associate with more than one cancer (Multi-Cancer SNPs, Supplementary Table 24, Figure 5.3.B).20 of the 33 cancer types were represented amongst the Multi-Cancer

SNPs with the most SNPs associating with colorectal, breast, non-melanoma skin, lung and prostate cancer (>30 SNPs, Figure 5.3.C). A high proportion of shared pleiotropic SNPs could indicate common tumorigenic mechanisms. Taking each cancer-type in turn, we determined the proportion of pleiotropic SNPs shared with each other cancer-type (Figure 5.3.D). For example, for breast cancer, around 60% of Multi-Cancer SNPs were shared with ovarian, colorectal, prostate and lung. A high proportion of Multi-Cancer SNPs were found to be shared between the three haematological cancers (myeloma, lymphoma and CLL) while 81% of Gastic_Esophageal Multi-Cancer SNPs were shared with nonmelanoma skin cancers.

In our above analysis of the Watanabe *et al* data, we found p53 pathway genes to be over-represented among genes harbouring pleiotropic SNPs compared to all genes. To verify this, we overlaid our annotated list of 409 p53 pathway genes with the 2,036 CAGs (Materials and Methods). We found 91 cancer-SNPs which had been assigned to 52 p53 pathway genes. Eight of the 91 p53-pathway cancer-SNPs overlapped with the 135 Multi-Cancer SNPs and mapped to 7 p53 pathway genes (Table 5.1). This represented a significant enrichment for pleiotropic GWAS loci in the p53 pathway (OR=2.8, p=0.023, Fisher Exact-Test). Specifically, 7 of 52 (13.5%) CAGs in the p53 pathway were found to harbour Multi-Cancer SNPs compared to 106 of 1,984 (5.3%) CAGs of other pathways (Figure 5.4.A). Indeed, when we looked in detail at the enrichments of pleiotropic multi-cancer SNPs in all 186 KEGG annotated pathways, the p53 pathway demonstrated the largest and most significant enrichment compared to the other 6 significantly enriched pathways (Figure 5.4.B). The seven p53 pathway genes harbouring Multi-Cancer SNPs are ATM, CASP8, CHEK2, MDM4, KRT8, VCAN and TP53. One unique SNP was found for each gene except for the two unique SNPs found in CHEK2. The eight p53 pathway SNPs were found to associate with 11 cancers (Figure 5.4.C) and three of the SNPs associated with more than two cancers. rs17879961 (CHEK2) associated with increased risk of lung, breast and non-melanoma skin cancer while rs73110464 (KRT8) associated with lung, prostate, breast, ovarian and colorectal cancer. rs78378222 at the TP53 locus has been found to associate

strongly with differential risk of brain malignancies (GBM and non-GBM glioma), non-melanoma skin cancer, and a higher overall risk of any cancer over a lifetime.

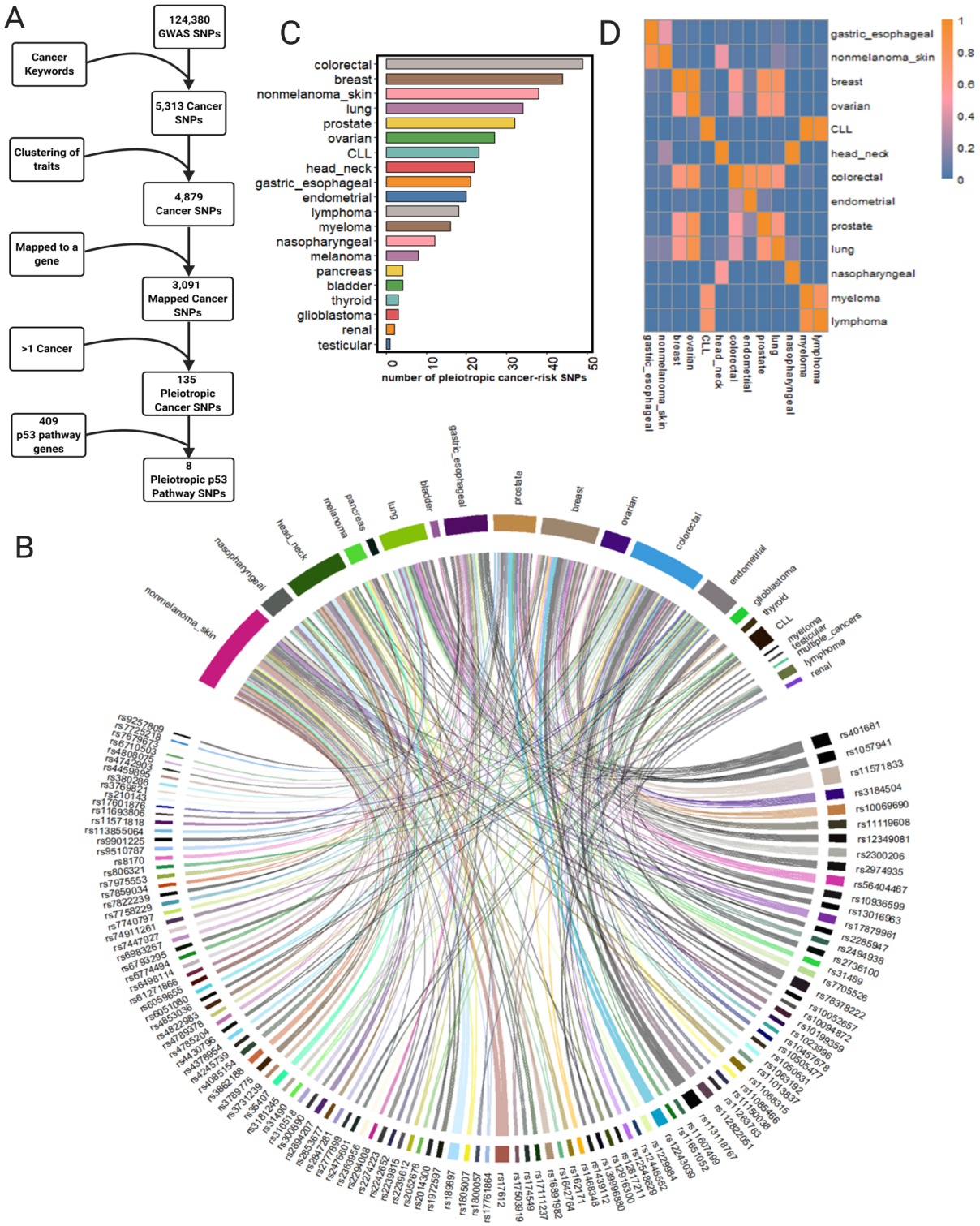


Figure 5.3

Figure 5.3: **A**) The GWAS catalog (as of May 2020) was precisely filtered to obtain cancer-SNPs mapped to genes. For the first filtering step we matched the mapped trait to a list of cancer keywords. We then used a second set of key words relating cancer types to group similar and overlapping traits into 33 cancer types. SNPs for traits which could not be clearly identified to a cancer type (or pancancer) were removed. After removing unmapped SNPs we identified those to associate with more than one cancer type and to map to p53 pathway genes. **B**) 135 Multi-Cancer SNPs were identified which associated with 20 cancer types. The bottom section of the chord diagram indicates different SNPs and the top section, the different cancer types. The SNPs are ordered by number of cancers with the most pleiotropic SNPs to the right of the plot. **C**) The barplot indicates the number of pleiotropic cancer-risk SNPs associated with each cancer-type. **D**) We compared the 20 cancer-types in a pairwise fashion and determined the proportion of pleiotropic SNPs to be shared between each pair of cancer-types. The cancer-type on the Y axis is used as the reference set of SNPs.

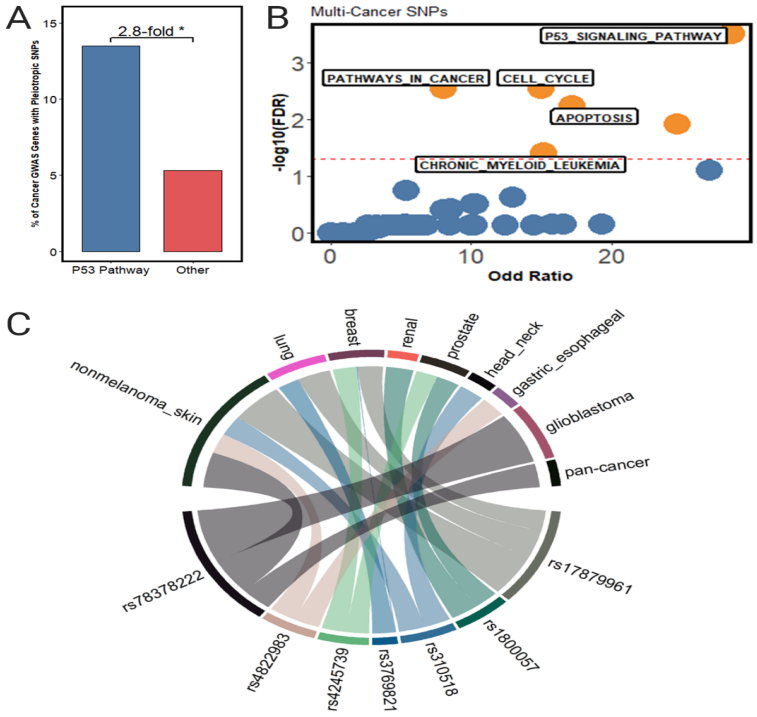


Figure 5.4: **A**) We determined the frequency of Multi-Cancer SNPs mapping to our list of p53 pathway genes and to other pathways. Statistical significance determined by Two sided Exact Fisher Test. **B**) We determined which other pathways the Multi-Cancer SNPs are enriched for. Enrichment was determined by Fisher Exact-Test using KEGG gene sets with raw p-values adjusted by FDR and an adjusted p-values < 0.05 considered significant. **C**) The Multi-Cancer SNPs in the p53 pathway are depicted in the chord diagram. The width of the chord indicates the size of the odd ratio. KRT8 was not included as no odds ratios were reported for the individual cancer types.

Moreover, it has recently been linked with risk of leiomyoma, soft-tissue sarcoma, malignant melanoma, breast cancer and lymphocytic leukemia (Supplementary Table C.13)[674][675][676][677][672]. Together, the results of these analyses demonstrate that the genes of the p53 pathway harbour the most multi-cancer risk SNPs relative to all well-annotated signalling pathways of the genome.

Table 5.1: The eight SNPs from the GWAS catalog which map to p53 pathway genes and associate with multiple cancer types.

SNPS	MAPPED_GENE	Grouped_trait	OR.or.BETA
rs17879961	CHEK2	nonmelanoma_skin	2.63
rs17879961	CHEK2	lung	1.67
rs17879961	CHEK2	breast	1.26
rs1800057	ATM	renal	1.38
rs1800057	ATM	prostate	1.16
rs310518	VCAN	nonmelanoma_skin	1.27
rs310518	VCAN	head_neck	1.27
rs3769821	CASP8	lung	1.08
rs3769821	CASP8	breast	0.06
rs4245739	MDM4	breast	1.19
rs4245739	MDM4	prostate	1.10
rs4822983	CHEK2	nonmelanoma_skin	1.27
rs4822983	CHEK2	gastric_esophageal	1.27
rs73110464	KRT8	lung	NA
rs73110464	KRT8	prostate	NA
rs73110464	KRT8	breast	NA
rs73110464	KRT8	ovarian	NA
rs73110464	KRT8	colorectal	NA
rs78378222	TP53	glioblastoma	3.26
rs78378222	TP53	nonmelanoma_skin	2.24
rs78378222	TP53	multiple_cancers	1.51

5.3.3 The TP53-PAS-SNP can have long-lasting associations in tumours

The aim of our studies is to determine if cancer-SNPs could help personalize cancer management and treatment strategies. If true, we reasoned that the SNPs in the p53 pathway should associate with other important cancer traits, not just susceptibility. For example, it is widely known that somatic mutation of TP53, resulting in attenuation of p53 signalling, can lead to greater metastatic potential of a tumour and a poorer response to DNA-damaging therapies[678]. These somatic alterations are also pleiotropic in the sense that they are found in many cancer types[529]. Multiple previous studies have provided evidence that the minor-allele of the above-mentioned TP53 SNP associates with reduced expression of p53 in normal tissues[679][680][674]. This is consistent with previous fine-mapping of this SNP; it is located within the polyadenylation signal (PAS) in the 3'UTR of TP53,

changing a canonical PAS to a weaker PAS. Taking the knowledge about these inherited and somatic p53 genetic variants together, we reasoned that the reduced levels of p53 expression associated with the minor-allele of the TP53-PAS-SNP could also associate tumour progression and patient outcome, if this cancer-risk associated locus can still mediate p53 expression even after the cancer has evolved to acquire the complex mutations required to transform a cell and create a tumour.

The TP53-PAS-SNP minor allele associates with reduced TP53 expression in tumours

As mentioned above, the minor-allele of the TP53-PAS-SNP has been found to associate with significantly reduced p53 RNA levels across multiple tissues[679] (GTEx Portal 07/10/2020, Appendix Figure A.22). For this SNP to be informative for cancer patients, we reasoned that such associations should also remain in tumours. To test this, we analysed data derived from 6,252 tumours, including germline, somatic mutation and transcriptomic data. Of these, 4,031 TP53WT cases were identified and 2,221 TP53Mutant cases. 153 patients were identified to be heterozygous for the TP53-PAS-SNP and one patient was homozygous for the minor-allele. The MAF was found to be 1.3%, in keeping with previous publications. To assess the association of the risk allele with expression, we excluded the cases with TP53 loss (GISTIC < 0). We found that the 153 heterozygous cases expressed significantly less p53 mRNA compared to those homozygous for the non-risk allele (linear regression, beta=-0.37, p=4.8e-05, Figure 5.5.A). Interestingly, we found that the risk allele of the TP53-PAS-SNP associates with reduced expression of both wild-type and mutant TP53 (Figure 5.5.B-C). Thus, the association of the minor-allele with lower p53 expression in normal tissues, clearly remains significant in tumours that have evolved in either the presence or absence of p53 driver mutations.

TP53-PAS-SNP minor allele carriers are more likely to develop TP53WT tumours

The TP53-PAS-SNP minor-allele associates with reduced expression of both WT and Mutant p53. In terms of tumour development and evolution, the minor-allele could

be oncogenic in TP53WT tumours by reducing the tumour-suppressive activity of p53. In contrast, the minor-allele could be tumour-suppressive in TP53Mutant tumours by reducing the oncogenic activity of TP53 dominant negative (DN) and/or gain of function (GOF) mutants. If true, we would expect minor-allele carriers to develop more TP53WT tumours relative to mutant tumours. Indeed, we found the 2,932 TP53WT NOLOSS tumours (MAF=1.3%) to be significantly enriched for minor-allele carriers compared to the 1,296 TP53MUTLOSS tumours (MAF=0.82%, Fisher Exact-Test, OR =1.66, p=0.023, Figure 5.5.D).

The TP53-PAS-SNP minor-allele associates with poorer prognosis and resistance to therapy

Loss of wild-type p53 function and some GOF mutants can facilitate metastasis which is a key factor in promoting disease progression, poor prognosis and cancer-related mortality[681][678][682][683][599]. In our previous analyses, we found that the minor-allele of the TP53-PAS-SNP associates with reduced p53 expression and therefore could, like somatic TP53 lesions, contribute towards reduced p53 activity and unfavourable outcome. To test this, we analysed the association of the minor-allele on overall survival (OS) and progression (PFI). Indeed, for the TP53WT-NOLOSS tumours, the 87 minor-allele carriers had significantly shorter OS and PFI compared to the 3,051 patients without the minor-allele (OS, HR=1.62, p=0.004; PFI, HR=1.61, p=0.009, Figure 5.5.E) with the association with PFI remaining significant after correction for cancer-type (HR=1.44, p=0.03, Cox Regression, Figure 5.5.F). Importantly, this association was not found for TP53MUTLOSS tumours; indeed, a nonsignificant trend towards longer PFI was noted for the 21 TP53MUTLOSS tumours with the minor-allele (HR=0.68, p=0.35).

The p53 apoptotic response is commonly activated by anti-cancer therapies and somatic lesions of TP53 can reduce the efficacy of treatments[684][685]. Similarly, our results so far would suggest that the minor-allele of the TP53-PAS-SNP could impair the p53-response to therapies in TP53WT tumours by reducing p53 expression. To test this, we identified 4,022 patients with germline and treatment response data including 1,656 TP53WTNOLOSS and 933 TP53MUTLOSS. When we stratified

based on TP53 status, we found an enrichment of the TP53-PAS-SNP minor-allele amongst non-responders in TP53WTNOLOSS patients compared to responders (Fisher Exact-Test, OR=3.5, p=0.0002, Figure 5.5.G) and no enrichment was found for TP53 MUTLOSS (p=1). Importantly, the association for TP53WT NOLOSS patients was still significant after correction for cancer type (Logistic Regression, beta=-0.90, p=0.019).

A subset of cancer-types with high MAF and low TP53 mutation frequency contribute most to the association of the minor-allele with reduced p53 expression, outcome and response to therapy

In our above, pan-cancer analyses, we found the TP53-PAS-SNP minor-allele to associate with reduced p53-mRNA expression, TP53 status, poorer outcome and resistance to therapy. We hypothesised that the association of the minor-allele with the aforementioned measures, may not be equal across cancer-types. To explore this, we first considered the relationship between the MAF and the frequency of TP53 inactivation. The frequency of somatic TP53 lesions varies between cancer-types, from 95% in Uterine Carcino-Sarcoma (UCS) to 0% in Thyroid Carcinoma (THCA) (Figure 4.14)[685]. If the minor-allele of the TP53-PAS-SNP has an inverse association in TP53WT (pro-cancer) and TP53Mutant (anti-cancer) tumours, then patients who develop generally TP53WT cancers (such as THCA) could have a higher MAF compared to patients who develop generally TP53Mutant cancers (such as UCS). As predicted, when we determined the minor-allele and TP53MUTLOSS frequency for each of the 30 cancer-types with at least one minor-allele carrier, a significant negative correlation was found between MAF and the TP53MUTLOSS frequency (beta= -0.40, p=0.03, Pearson's Correlation, Figure 5.6.A).

Given the negative correlation between MAF and MUTLOSS frequency, we reasoned that those cancer types with high MAF and low MUTLOSS frequency and low MAF and high MUTLOSS frequency could be driving the above enrichment for the minor-allele amongst TP53WT-NOLOSS tumours compared to those with mutation and loss. To test this, we identified and compared the 9 cancer-types with above average MAF and below average TP53MUTLOSS frequency ('H.MAF

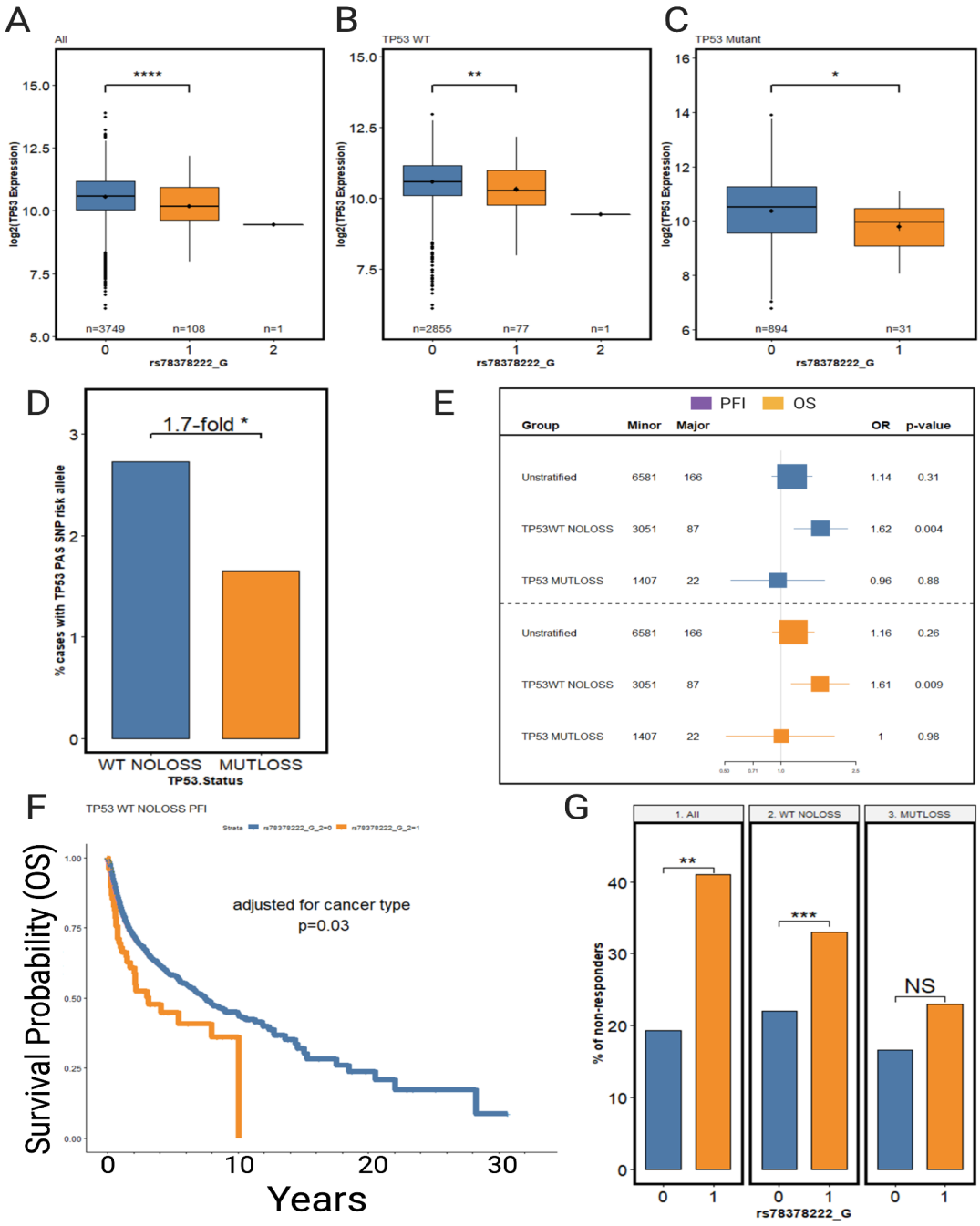


Figure 5.5: The boxplots indicate the expression of TP53 mRNA in tumours with or without the minor allele of the TP53-PAS-SNP, considering all tumours together **A**) and the TP53WT **B**) and TP53Mutant tumours separately **C**). Significance was determined by linear regression. **D**) The barplot indicates the proportion of TP53WT-NOLOSS and TP53-MUTLOSS tumours with the TP53-PAS-SNP minor allele. Significance was determined by Exact Fisher-Test. **E**) Forest plot indicating the association of heterozygosity at the TP53 PAS SNP locus on overall survival (OS) and progression free interval (PFI) for all TCGA patients, for TP53 WT NOLOSS only and for TP53 MUTLOSS only. Hazard ratios and significance determined by Cox regression. **F**) Kaplain-Meier plot indicating the association of heterozygosity at the TP53-PAS-SNP locus with progression free interval (PFI) of TP53 WT NOLOSS TCGA patients after adjustment for cancer type. The reported p value was derived from Cox regression with cancer type as a covariate. **G**) The % of non-responders to first line chemotherapy and radiotherapy in patients with or without the minor allele was determined for all tumours, for just TP53WT NOLOSS tumours and for just TP53MUTLOSS tumours. Significance determined by Exact Fisher Test.

L.MUT', top left quadrant of Figure 5.6.A) with the 9 cancer-types with below average MAF and above average TP53MUTLOSS frequency ('L.MAF H.MUT', bottom right quadrant of Figure 5.6.A) . As expected, the 9 'H.MAF L.MUT' cancer-types (MAF=2.2%) have significantly higher MAF compared to the 9 'L.MAF H.MUT' cancer-types (MAF=0.8%, 2.8-fold, p=2.8e-06, Student T-test, Figure 5.6.B). We examined the relationship between MAF and TP53 status when we removed the 'H.MAF L.MUT' and/or 'L.MAF H.MUT' cancer-types. After removing the 'H.MAF L.MUT' cancer-types, 40 of 1,894 (2.1%) TP53WT tumours were found to be minor-allele carries compared to 18 of 1,239 (1.5%) TP53MUTLOSS tumours which did not constitute a significant enrichment (p=0.22, Fisher Exact-Test, Figure 5.6.C). After removing the 'L.MAF H.MUT' cancer-types, 64 of 2,265 TP53WT (2.8%) tumours were found to be minor-allele carriers compared to 13 of 479 (2.7%) TP53MUTLOSS (p=1, Fisher Exact-Test, Figure 5.6.C). Moreover, when we restricted to 15 cancer-types not classed as 'H.MAF L.MUT' or L.MAF H.MUT, the minor-allele was not found to be enriched in the TP53WT tumours compared to TP53MUTLOSS (p=0.70, Figure 5.6.C). However, by restricting to the 18 cancer-types classed as 'H.MAF L.MUT' or L.MAF H.MUT, a significant enrichment for the minor-allele was found in TP53WT tumours (52/1551, 3.4%) compared to TP53MUTLOSS (11/832, 1.3%, OR=2.54, p=0.003, Figure 5.6.C). These analyses indicate that the 9 'H.MAF L.MUT' and 9 'L.MAF H.MUT' cancer-types drive the association of the minor-allele with TP53WT status.

Given the association of the minor-allele with TP53WT status appears to be driven by a subset of cancer-types with either high MAF and low MUTLOSS or vice versa, we reasoned that these cancer-types could also underpin the associations of the minor-allele with reduced p53 expression, shorter OS and resistance to survival. Indeed, the 59 'H.MAF L.MUT' tumours with the minor-allele had significantly lower p53 expression compared to 1,321 major-allele homozygotes (beta=-0.33,p=0.0001, Linear regression with cancer-type, Figure 5.6.D) and this association was marginally enhanced when we restricted to the TP53WT-NOLOSS tumours (beta=-0.36,p=7.1e-05, Figure-6E). For the 38 'L.MAF H.MUT' tumours with the minor-allele, p53

expression was not found to be significantly different compared to 2,360 major-allele homozygotes (p=0.73, Figure 5.6.D) and no association was found when restricting to TP53WT-NOLOSS tumours (p=0.55, Figure 5.6.E).

In our previous pan-cancer analyses, minor-allele carriers were found to associate with poorer outcome and faster disease progression. However, we also found the minor-allele to only associate with reduced p53 expression for the 9 cancer-types we identified as 'H.MAF L.MUT'. We reasoned that the minor-allele may associate with poorer outcome in this group but not the 'L.MAF H.MUT' group. Indeed, for 'H.MAF L.MUT' cancer-types, the 38 TP53WT-NOLOSS tumours with the minor-allele associate with significantly poorer outcome compared to 957 major-allele homozygotes (OS:HR=1.9,p=0.037; PFI:HR=1.8,p=0.045, Cox regression). After adjustment for cancer-type, neither test remained significant but trends towards poorer outcome were evident. For 'L.MAF H.MUT' cancer-types, no significant associations were found but for the 14 TP53WT-NOLOSS minor-allele tumours, a trend towards better outcome was evident compared to 584 major-allele homozygotes (HR=0.55,p=0.4).

In our pan-cancer analyses, the minor-allele associated with resistance to radiotherapy and chemotherapy. We reasoned that this association might also be restricted to TP53WT-NOLOSS tumours of 'H.MAF L.MUT' cancer-types. Indeed, for this group, 13 of 24 (54%) minor-allele carriers were non-responders compared to 132 of 559 (24%) major-allele homozygotes, representing a significant enrichment for non-responders amongst minor-allele carriers (OR=3.97,p=0.001, Fisher Exact-Test, Figure 5.6.F) which was independent of cancer-type (beta=-1.30, p=0.017, Logistic regression). As expected, for the 'L.MAF H.MUT' cancer-types, the minor-allele did not associate with non-responders for TP53WT-NOLOSS tumours (p=1, Fisher Exact-Test, Figure 5.6.F).

The aim of our studies is to determine if cancer-risk SNPs could help personalize cancer management and treatment strategies. The data presented so far regarding the TP53-PAS-SNP supports this hypothesis. We have shown that minor-allele carriers are more likely to develop TP53WT tumours and tumour-types which

rarely mutate TP53. We find evidence that the minor-allele associates with reduced expression of both wild-type and mutant p53 which could be oncogenic in the

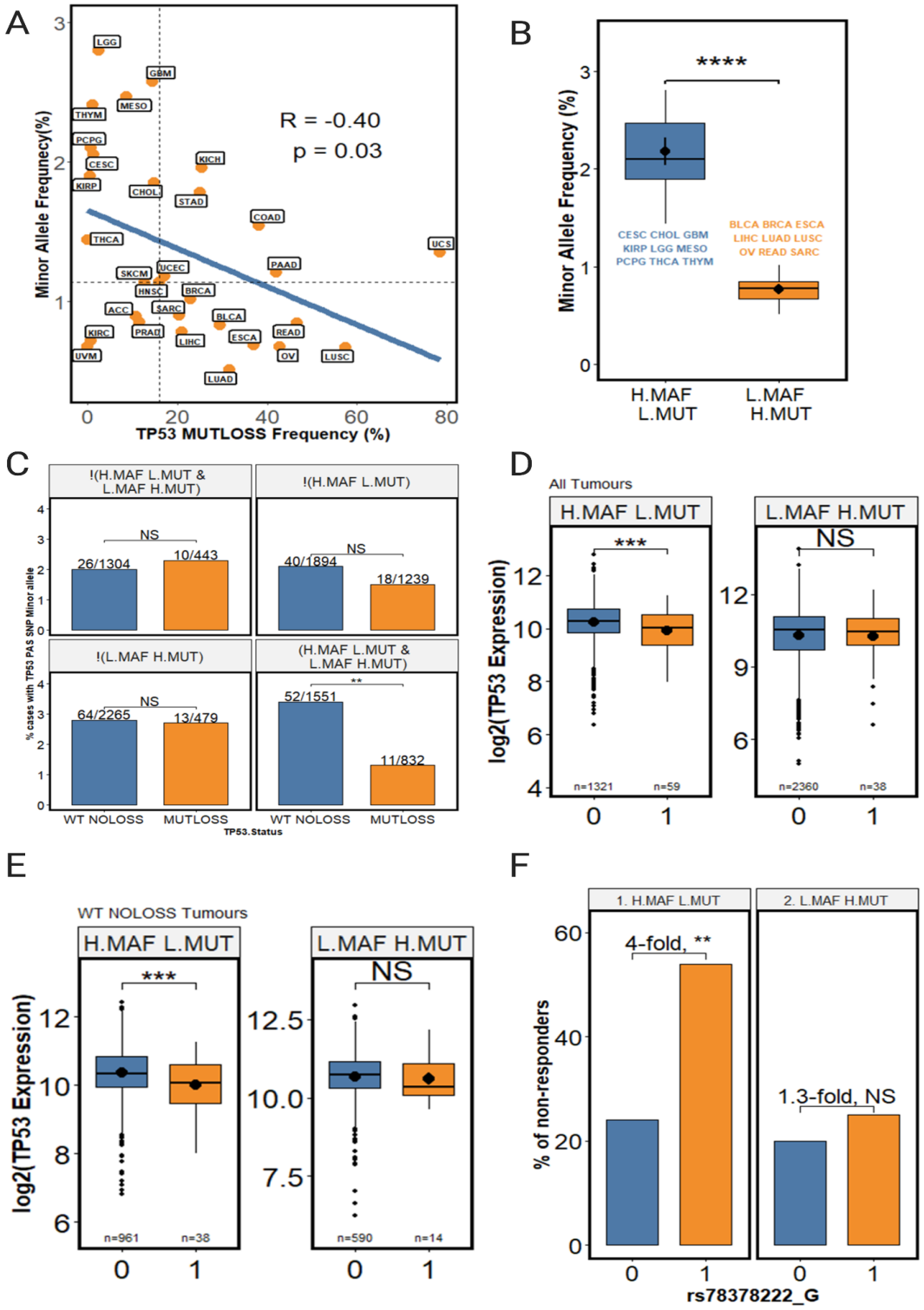


Figure 5.6

Figure 5.6: **A**) The 32 cancer-types with at least one minor allele carrier were plotted in terms of the TP53-PAS-SNP MAF and the frequency of TP53 MUTLOSS status. Pearson's Correlation was used to determine the relationship between TP53-PAS-SNP MAF and the frequency of TP53 MUTLOSS status. **B**) The boxplot indicates the minor allele frequnecy of the TP53-PAS-SNP for the tumour types with above average MAF and below average MUTLOSS frequency ('H.MAF L.MUT') and high MUTLOSS frequency and below average MAF ('L.MAF H.MUT'). The MAF was found to be significantly different between the two sets of cancer-types (Student T-test). **C**) The frequency of the TP53-PAS-SNP in TP53WT-NOLOSS and TP53-MUTLOSS tumours was repeated after removal of 'H.MAF L.MUT' and/or 'L.MAF H.MUT' cancer-types. The analysis was also repeated by restricting to just 'H.MAF L.MUT' and 'L.MAF H.MAF' cancer-types. The (!) mark is used to indicate exclusion. **E**) The association of the TP53-PAS-SNP minor allele with p53 mRNA expression was determined separately for 'H.MAF L.MUT' and 'L.MAF H.MUT' cancer-types (Linear regression). **F**) The association of the TP53-PAS-SNP minor allele with p53 mRNA expression was determined for TP53WT-NOLOSS tumours of 'H.MAF L.MUT' and 'L.MAF H.MUT' cancer-types (Linear regression). **G**) The percentage of non-responders to radiotherapy and first-line chemotherapy among minor-allele carriers and non-minor allele carriers was determined separately for 'H.MAF L.MUT' and 'L.MAF H.MUT' cancer-types.

wild-type setting but tumour-suppressive in the mutant context. Finally, we have indicated that cancer-types with high MAF and low TP53 mutation frequency (CESC, CHOL, GBM, KIRP, LGG, MESO, PCPG, THCA, THYM) contribute most to the associations of the minor-allele with reduced p53 expression, poorer outcome and resistance to therapy. These findings suggest that the TP53-PAS-SNP could help personalise cancer management for these cancer-types by identifying TP53WT patients with poorer prognosis and who may have reduced sensitivity to conventional therapies.

5.3.4 The TP53-PAS-SNP inhibits mutant p53

In our previous analyses, we highlighted that carriers of the TP53-PAS-SNP minor-allele exhibit reduced p53 expression regardless of TP53 mutational status. This raised the question of whether the minor-allele could have opposite effects on tumorigenesis in TP53WT and TP53Mutant tumours. Indeed, we were able to demonstrate that minor-allele carriers were more likely to develop p53wt tumours and less likely to develop p53mutant tumours. We reason that this supports a model, whereby the minor-allele attenuates the tumour suppressive activity of wtp53 and the oncogenic activities of mutant p53.

Isogenic Hap1 cell models for the TP53-PAS-SNP

To further define the TP53-PAS-SNP interaction with TP53 somatic mutational status, we engineered isogenic cellular models with the two different alleles of the TP53-PAS-SNP (A and C). In order to delineate allelic-specific effects, we used Hap1 cells, a fully haploid cell-line derived from the chronic myelogenous leukaemia (CML) cell-line KBM-7[686]. Using CRISPR-Cas9 mediated homology-directed repair (HDR), we developed two separate Hap1 clones with the minor-allele (AATACA). Hap1 cells feature a dominant-negative p53 missense mutation (p.S215G, COSV52675946, Figure 5.7.A) which has previously been found in multiple cancer types[687][688].

Minor-allele Hap1 cells express lower levels of p53

Using our isogenic Hap1 clones with either the A-allele (major) or C-allele (minor) of the TP53-PAS-SNP, we first explored how the SNP status affected p53 expression. Consistent with our findings in patient tumours and with previous publications, we found significantly reduced p53 mRNA expression in the C-allele clones compared to A-allele by qRT-PCR (2-fold, p = 6.8e-08 for clone #1 and 1.7-fold, p = 0.0038 for clone #2, 5.7.B). Furthermore, we also found significantly reduced p53 protein expression for the C-allele clones, specifically, 2.2-fold reductions in p53 protein levels were found for both clones (p=0.0069 for clone #1; p=0.0046 for clone #2,

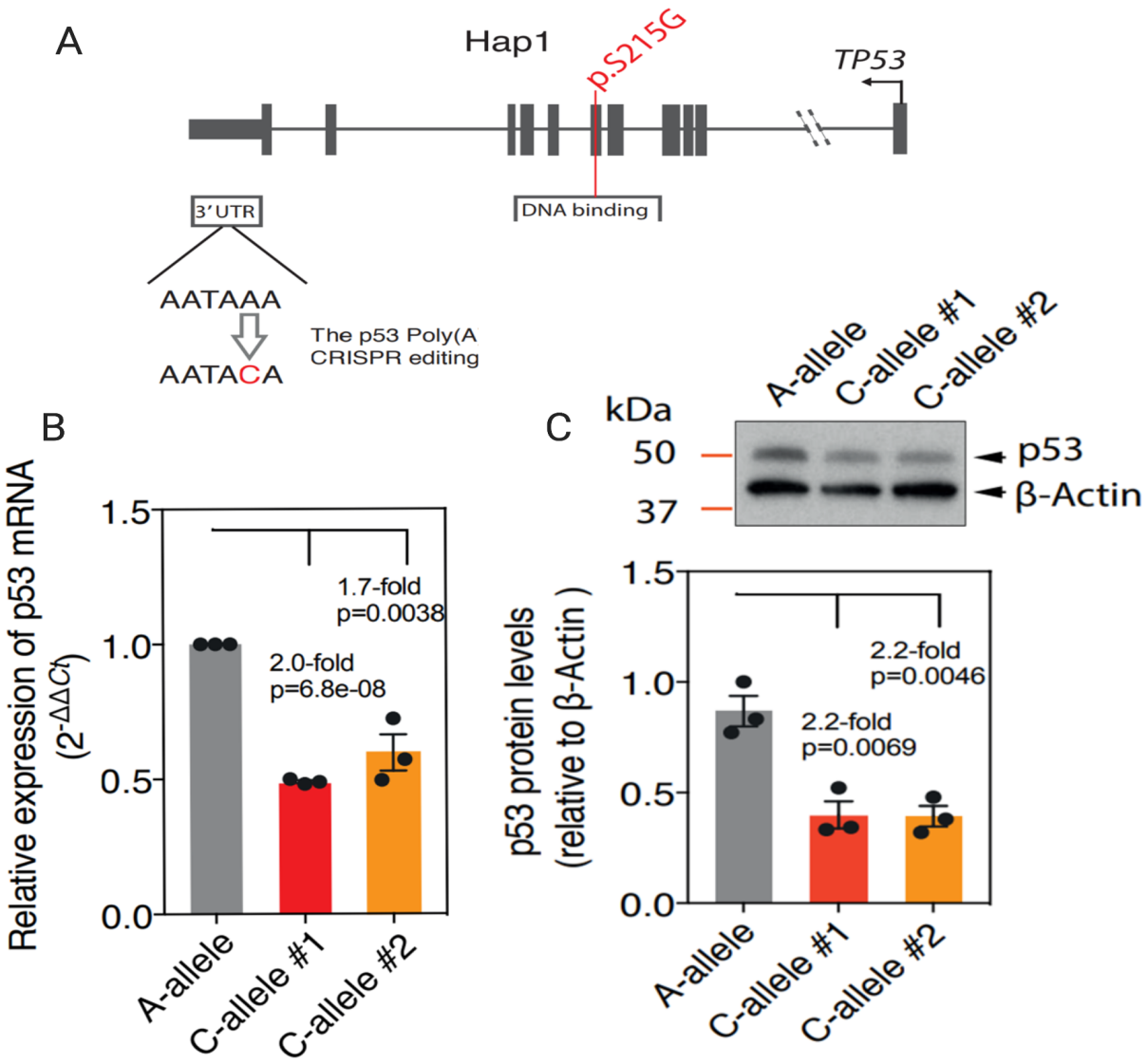


Figure 5.7: **A**) Schematic of TP53 in HAP1 cells, indicating the position of the coding mutation in the DNA binding domain and the SNP in the PAS of the 3'UTR. **B**) We measured the expression of TP53 mRNA in A-allele (major) and C-allele (Minor) Hap1 cells by qRT-PCR. Significance was tested by Student T test. **C**) We analysed TP53 protein expression in A and C allele Hap1 cells by immunoblotting. The western blot indicates a representative example with beta-actin used as a loading control. Blots from three independent experiments were quantified with the compiled data and indicated in the barplot. Significance tested by Student T-Test.

Student T-test ,5.7.C). Together, these data, acquired in a primarily isogenic system, indicate that the TP53-PAS-SNP directly reduces the expression of mutant p53 at both the transcript and protein level.

RNA-seq to explore the transcriptomic differences conferred by the TP53-PAS-SNP in the context of oncogenic, Mutant p53

There is growing evidence demonstrating that p53 proteins harbouring GOF mutations can still regulate gene expression but of different loci compared to wild-type p53[689][690]. For example, Scian et al (2005) showed that multiple p53 mutant proteins could regulate expression of 100 genes involved in cell growth and survival including components of the NF-kB pathway[691]. Using patient tumour data and isogenic cell-lines, we have indicated that the minor-allele of the TP53-PAS-SNP can reduce expression of mutant p53. Therefore, we reasoned that using our isogenic Hap1 cell-lines with either the A or C allele and expressing mutant p53, we should be able to detect differences in the p53 mutant transcriptome. To do so, we carried out 3'RNA-sequencing of the A-allele and C-allele Hap1 clones (Materials and Methods). By PCA analysis, we determined that the 3 clones are well separated indicating transcriptomic differences between the different clones (Figure 5.8.A).

The TP53-PAS-SNP C-allele associates with reduced expression of NFKB target genes Between the A-allele clone and C-allele #1, 129 genes were upregulated and 153 downregulated (FDR < 0.05). For C-allele #2, 169 were upregulated and 185 downregulated (Figure 5.8.B). To remove clonal specific effects, we considered only differentially expressed genes common to both C-allele clones. 83 genes were downregulated in both clones and 54 upregulated, both significant overlaps (Fisher Exact-Test, p<2e-16, Figure 5.8.C). Importantly, TP53 was significantly downregulated in both C-allele clones (Figure 5.8.D).

P53 proteins with GOF missense mutations are known to upregulate different target genes compared to wild-type p53 which can promote cell growth, survival, metastasis and chemoresistance[690] [156]. Given that the Hap1 C-allele clones express less mutant p53 protein, we reasoned that the differentially expressed genes between the A- and C-allele clones may indicate reduced oncogenic signalling. The 54 common upregulated genes were not found to be enriched for any particular hallmarks, but the downregulated genes were found to be enriched for genes regulated

by NFkB (OR=9.9, FDR=0.024, Figure 5.8.E). Interestingly, mutant p53 has previously been shown to promote NFkB activation, to associate with nuclear NFkB and to overlap NFKB binding sequences[692][693][694][689][695]. This is in keeping with our above enrichment for NFkB target genes among those downregulated in cells expressing 2-fold less mutant p53. For example, CD44, which has been shown to be specifically upregulated by mutant p53, to promote proliferation, to promote EMT, to suppress apoptosis and to activate AKT, was expressed 3.3-fold less in C-allele cells compared to A-allele (FDR=0.02, Figure 5.8.F)[696][697][698][699][700]. Together, these data support our hypothesis that the minor-allele of the TP53-PAS-SNP can interact with TP53 mutation status whereby in TP53WT tumours, it has an oncogenic effect but in tumours with DN/GOF mutations, it can be tumour suppressive by inhibiting the pro-tumour function of mutant p53 (Figure 5.8.G).

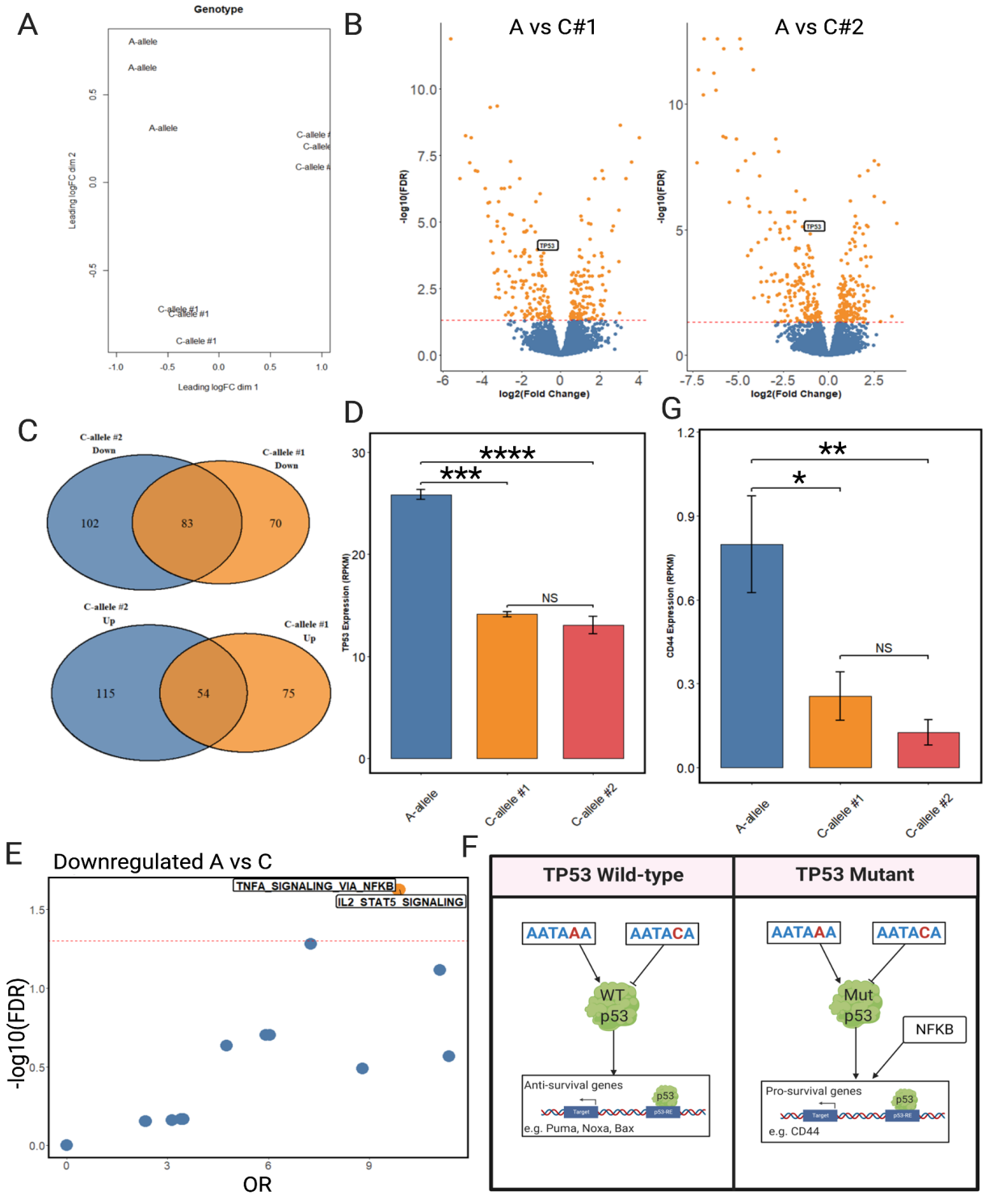

A
Genotype
A-allele
A-allele
A-allele
C-allele #1
C-allele #1
C-allele #1
Leading logFC dim 2
Leading logFC dim 1
B
A vs C#1
A vs C#2
-log10(FDR)
log2(Fold Change)
TP53
C
C-allele #2 Down
C-allele #1 Down
102
83
70
C-allele #2 Up
C-allele #1 Up
115
54
75
D
TP53 Expression (RPKM)
****
***
NS
A-allele
C-allele #1
C-allele #2
G
CD44 Expression (RPKM)
**
*
NS
E
Downregulated A vs C
TNFA_SIGNALING_VIA_NFKB
IL2_STAT5_SIGNALING
-log10(FDR)
OR
F
TP53 Wild-type
TP53 Mutant
AATAAA
AATACA
WT p53
Mut p53
NFKB
Anti-survival genes
e.g. Puma, Noxa, Bax
Pro-survival genes
e.g. CD44

Figure 5.8

Figure 5.8: **A**) MDS plot indicating the output of a PCA analysis for the TP53-PAS-SNP genotype of the samples (A, C#1, C#2). **B**) Volcano plots indicating differentially expressed genes for the contrasts of A-allele vs C-allele #1 and A-allele vs C-allele #2. Significant genes (FDR <0.05) are indicated in orange. **C**) We determined the genes which were consistently differentially expressed by the minor allele by finding the overlapping genes between the C-allele #1 and C-allele #2. **D**) Using the RNA-seq data, we examined TP53 expression in A-allele, C-allele #1 and C-allele #2. The indicated significance reflects the FDR-q value derived from edgeR. **E**) Scatter plot indicating which Hallmarks were found to be enriched for amongst the significantly downregulated genes common to both C-allele clones. Significant gene sets are coloured orange and labelled. Significant enrichment was determined by the hypergeometric test and raw pvalues corrected for the number of gene sets tested. **F**) Barplot indicating the expression of CD44 in A-allele, C-allele #1 and C-allele #2. The indicated significance reflects the FDR-q value derived from edgeR. **G**) TP53 mutational status and the TP53 PAS SNP might interact to regulate anti- and pro-survival genes with NFKB. In TP53 wild-type cells, p53 acts to upregulate genes with anti-survival function. In this context, the minor allele reduces p53 expression and reduces anti-survival signalling and promotes tumorigenesis. In TP53 Mutant cells, mutant p53 can co-operate with NFKB to promote expression of pro-survival genes. In this context, the minor allele can reduce expression of mutant p53, reduce pro-survival signalling and therefore be protective.

5.3.5 Insights into the mechanism of the TP53-PAS-SNP

Both our isogenic cell-line models and our analysis of patient tumours indicate that the minor-allele associates with reduced p53 expression. Moreover, we have provided evidence for a long-lasting effect of the minor-allele on tumours wherein the SNP clearly associates with allelic differences in somatic p53 mutational status, progression and responses to radiation treatment. However, the molecular mechanisms underpinning the reduced p53 expression levels are still a subject of intense research.

The minor-allele disrupts the canonical PAS site at the TP53 locus. The PAS is crucial for processing of nascent pre-mRNA transcripts; the Cleavage and Polyadenylation Specificity Factor (CPSF) complex is recruited to the PAS which in turn correctly positions CPSF-73 at the downstream cleavage site (Figure 5.9.A)[701][702]). Indeed, point mutations, including that conferred by the TP53-PAS-SNP, have long been known to reduce the efficiency of pre-mRNA processing[703]. This is in line with the observations by Stacey et al and Wang et al who noted elongated p53 mRNA transcripts among minor-allele carriers compared to individual's homozygous for the major allele. We reasoned we could leverage our cell-models with either the major or minor-allele to prove, in a more isogenic system, that the minor-allele impairs usage of the canonical PAS site. To do so, we first analysed our RNA-sequencing data to look for peaks beyond the normal termination site. Indeed, for the C-allele clones, clear peaks were evident beyond

the normal cleavage site which are not found for the A-allele clones (Figure 5.9.B). To validate this result, we performed qRT-PCR for TP53 in the Hap1 A and C-allele clones, using primer sequences beyond the normal mRNA cleavage site (Figure 5.9.C). The products of these primers represent the mRNA which is not cleaved at the canonical PAS site. Intriguingly, we found between 6.6 and 10.4-fold more uncleaved TP53 product from the C-allele clones compared to the A-allele Hap1 cells (Figure 5.9.C). Importantly, as part of our cDNA synthesis protocol, we used oligo(dT) primers to reverse transcribe only polyadenylated RNA suggesting that the elongated transcripts are still polyadenylated, perhaps through the use of an alternative polyadenylation (APA) sequence.

Alternative Polyadenylation is a common event at the TP53 locus in the brain

Our isogenic cell-line work suggests that the minor-allele of the TP53-PAS-SNP could promote an APA event and lead to an mRNA isoform with a longer 3'UTR. If this hypothesis is true, then an alternative PAS site should occur downstream of the TP53-PAS-SNP. To identify such as PAS site, we accessed a database of annotated PAS sites throughout the genome (PolyA_DB.v3.2, Materials and Methods). For TP53, we found 17 PAS sites (Figure 5.9.D, Supplementary Table C.14)[704]. The expression of TP53 from the canonical PAS site at 7,571,739 is the highest expressed isoform and was detected in 100% of samples (Figure 5.9.D). Interestingly, the final two PAS sites are found outside of the TP53 gene boundary, as defined by RefSeq, with their usage leading to an extended 3'UTR. These PAS sites are functional; indeed, the final PAS site (7,568,733) has the second highest expression, detected in 9.4% of samples.

We have found evidence that the minor-allele results in a longer p53 mRNA transcript, presumably with a longer 3'UTR due to usage of a downstream PAS site, and indeed, PAS sites downstream of the TP53 gene boundary exist and are functional. APA events can be highly tissue specific with several tissue-specific APA factors identified such as Nudt21 in the testes[705][706]. To determine which tissues exhibit the most usage of downstream PAS sites at the TP53 locus we accessed the

APAatlas (SAAP-RS algorithm) which details 435,797 APA events genome-wide, across 53 tissues[707]. The SAAP-RS algorithm computes the Relative Expression Difference (RED) score; a high positive RED score indicates high expression from downstream PAS sites (longer 3'UTR). For TP53, 27 of the 53 tissues were found to have a RED score significantly higher than 0 (FDR<0.05, Figure 5.9.E). Interestingly, the top 20% of tissues were all found to be brain tissues; indeed, the RED score was found to be significantly higher for brain-derived tissues compared to all other tissues (Linear regression, beta=-1.4, p=7.7e-92, Figure 5.9.F). Moreover, this correlates with reduced p53 expression in normal brain tissue compared to other tissues (p=3.2e-05, Linear Regression, Figure 5.9.G, GTEx). Intriguingly, the TP53-PAS-SNP has been found to show very strong associations with brain malignancies (Supplementary Table C.13).

Elongated 3'UTRs are subject to greater miRNA-mediated post-transcriptional regulation

The above data indicate that the minor-allele impairs termination of transcription from the TP53 locus and results in a longer, polyadenylated transcript. Longer mRNA transcripts can be subject to greater post-transcriptional repression[708]. Micro-RNAs (miRNA) play a key role in regulating expression post-transcriptionally; they are a class of small RNA regulators (approximately 21nt in length) which form a ribonucleoprotein complex with Argonaute family proteins and can hybridise with mRNA transcripts to control their stability and translation[709]. miRNAs can promote deadenylation of mRNA, block translation and lead to storage and degradation of mRNA at P-bodies[709]. Importantly, many miRNAs recognise sequences in the 3'UTR of mRNA[710][711].

Due to the elongation of the p53 mRNA 3'UTR amongst minor-allele carriers, the fact that p53 expression is reduced both at the protein and mRNA level and the known biology of miRNAs, we reasoned that the mechanism by which the minor-allele confers reduced p53 expression may involve miRNA-mediated degradation of the mRNA. Indeed, several papers have suggested that the minor-allele may generate novel miRNA binding sites (Supplementary Table C.15)[712][713][674]. To

investigate whether the elongated p53 mRNA may harbour additional miRNA seed sites, we assumed that the elongated 3'UTR could terminate at the downstream PAS site which we identified above. We extracted the genome sequence (Hg19) for the region between the canonical PAS site and the final downstream PAS site (ch17: 7568730 -7571756; 3,026bp) from the UCSC Genome Browser. Multiple biochemical features of mRNA 3'UTR and mRNA sequences can be used to predict miRNA target sites such as perfect-complementarity between the mRNA sequence and the 5' seed region of the miRNA and low GC content[714]. To predict what additional miRNAs might recognise the elongated p53 mRNA transcript we used the above p53 mRNA sequence as input for the prediction software, miRDB, which contains 2,656 miRNAs and 1,610,510 gene targets[715]. miRDB predicted that 88 unique human miRNAs could target the sequence covering the elongated region of the p53 3'UTR (score >50/100, Supplementary Table C.15, Figure 5.10.A).

If these miRNAs can repress p53 expression in a way which is dependent on usage of the downstream PAS site which is in turn promoted by the minor-allele, we reasoned that minor-allele carriers should exhibit a stronger negative correlation between expression of the miRNA and p53 mRNA expression. To test this, we downloaded expression data for 1,881 miRNAs from human tumours using the TCGAbiolinks R package. 82 of the 88 predicted miRNAs were measured in the TCGA cohort; we also included the 6 miRNAs which have previously been suggested to be dependent on the minor-allele (Supplementary Table C.15). 27 of the miRNAs were expressed in less than 10% of samples and were excluded. To determine which of the remaining 61 miRNAs exhibited negative correlation with p53 expression among minor-allele carriers regardless of cancer-type and TP53 mutation, we performed linear regression for each miRNA with cancer-type and TP53 mutational status as covariates. After FDR correction, three miRNAs exhibited a significant negative association with p53 expression among the 152 minor-allele carriers (FDR<0.05, Figure 5.10.B). Two of these remained significant when we split the tumours into high and low miRNA expression (Maxstats package,

Materials and Methods) and tested for differences between the two groups, hsa-miR-6788 and hsa-miR-6812 (6788: beta=0.38, p=0.047; 6812:beta=0.57,p=0.003, Linear Regression with cancer-type, Figure 5.10.C-D). Intriguingly, no significant association was found for these two miRNAs for the 6,274 individuals homozygous for the major allele. Moreover, both miRNAs were found to be expressed in all 33 cancer-types (Appendix Figure A.23). These data support a mechanistic model for the association of the minor-allele on p53 expression whereby the minor-allele promotes an APA event and expression of p53 with a longer 3'UTR which then subject to repression by miRNAs which cannot target the shorter 3'UTR.

5.3.6 Modest reductions in p53 expression associate with reduced sensitivity to many anti-cancer compounds

Our investigations into the TP53-PAS-SNP provide evidence that germline-mediated reductions in p53 expression levels can mediate increased risk of cancer, increased resistance to treatment and poorer prognosis. This resembles our analysis in Chapter Four that TP53WT tumours with TP53 copy-number loss exhibit reduced target gene expression, high genomic instability and poorer prognosis. We reasoned that if the minor-allele of the TP53-PAS-SNP and TP53 copy-number loss are phenocopies in terms of their respective effects on p53 expression, then we could estimate the impact of the TP53-PAS-SNP on chemosensitivity using TP53 copy-number loss as a surrogate. To do so, we first determined the association of TP53 copy-number loss with p53 mRNA expression in TP53WT tumours and cancer cell-lines. Using the patient tumour data, we found that the 1,171 TP53WT tumours with TP53 loss expressed 1.6-fold less p53 mRNA compared to 4,696 TP53WT tumours without loss (p=3.2e-185, Linear Regression, Figure 5.11.A). Using cell-line data, we found that 135 TP53WT cell-lines with loss expressed 2.3-fold less p53 mRNA compared to 239 TP53WT cell-lines without loss (p=6.1e-07, Figure 5.11.B). Both of these associations are comparable to what we found for the minor-allele in our HAP1 isogenic cell models (1.7 to 2-fold).

Next, to determine the impact of modest reductions in p53 expression on chemosensitivity, we accessed the previously described Genomics of Drug Sensitivity dataset (GDSC, Materials and Methods) and compared the sensitivity of TP53WT cell-lines with and without copy-number loss to 345 compounds in GDSC1 and 192 compounds in GDSC2. For GDSC1, we found 98 compounds (28%) to exhibit higher sensitivity and 0% to exhibit lower sensitivity in TP53WT cell-lines without loss compared to TP53WT cell-lines with loss (Figure 5.11.C). For GDSC2, we found 123 compounds (64%) to exhibit higher sensitivity and 0% to exhibit lower sensitivity in TP53WT cell-lines without loss compared to TP53WT cell-lines with loss (Figure 5.11.D). Across the two datasets, TP53WT cell-lines without loss were found to be significantly more sensitive to 204 of 449 compounds (45%) with 17

significant compounds overlapping both datasets. These 17 compounds included known p53 activators such as Nutlin-3a, Cisplatin and 5-Fluorouracil. We repeated the analysis for TP53Mutant cell-lines and found those cell-lines without loss to be more sensitive to 110 of 449 compounds (24%). This is line with Knudson's Two Hit hypothesis whereby TP53Mutant cancers lose the wild-type TP53 copy to further supress tumour suppressive signalling[716][529]. Interestingly, there was no significant overlap between the significant drugs for TP53WT and TP53Mutant cell-lines (p=0.13, Hypergeometric), suggesting the pharmacogenomic landscape of cells harbouring TP53 mutations could be different to that of TP53WT cells.

The above analyses suggest modest reductions in p53 expression could have significant impact on the response of cancer cells to therapies and that compounds capable of upregulating p53 expression, rather than stabilising p53 (e.g. MDM2 inhibitors), could be beneficial for cancer patients who retain wild-type p53 but exhibit reduced expression due to deletion of the minor-allele of the TP53-PAS-SNP.

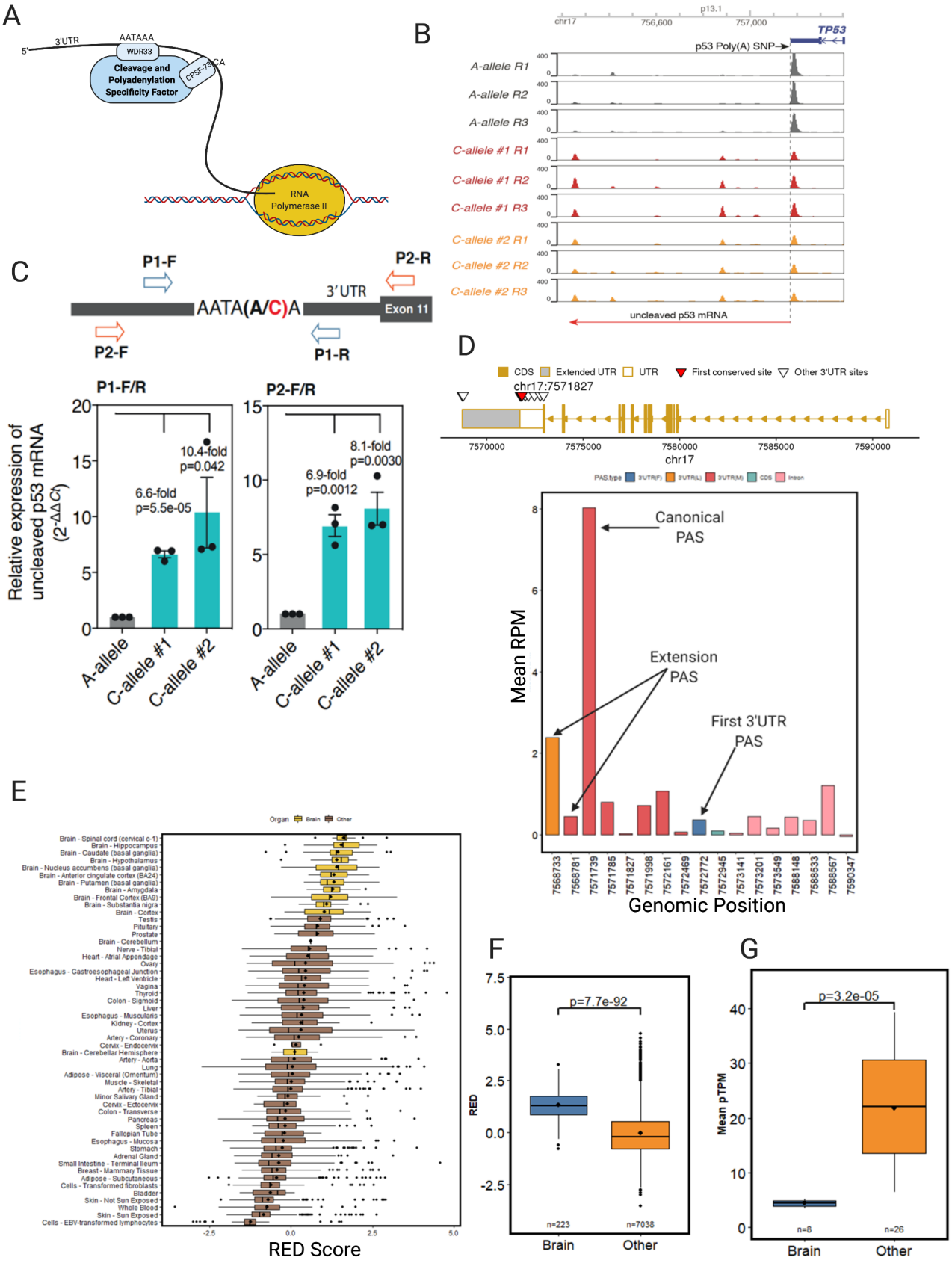

A
3'UTR
AATAAA
WDR33
Cleavage and Polyadenylation Specificity Factor
CPSF-73
CA
RNA Polymerase II
B
p13.1
chr17
756,600
757,000
TP53
p53 Poly(A) SNP
A-allele R1
A-allele R2
A-allele R3
C-allele #1 R1
C-allele #1 R2
C-allele #1 R3
C-allele #2 R1
C-allele #2 R2
C-allele #2 R3
uncleaved p53 mRNA
C
P1-F
P2-R
3'UTR
AATA(A/C)A
Exon 11
P2-F
P1-R
P1-F/R
P2-F/R
Relative expression of uncleaved p53 mRNA (2^-ΔΔCt)
10.4-fold p=0.042
6.6-fold p=5.5e-05
8.1-fold p=0.0030
6.9-fold p=0.0012
A-allele
C-allele #1
C-allele #2
D
CDS
Extended UTR
UTR
First conserved site
Other 3'UTR sites
chr17:7571827
7570000
7575000
7580000
7585000
7590000
chr17
Canonical PAS
Extension PAS
First 3'UTR PAS
Mean RPM
Genomic Position
E
Organ
Brain
Other
RED Score
F
p=7.7e-92
RED
n=223
n=7038
Brain
Other
G
p=3.2e-05
Mean pTPM
n=8
n=26
Brain
Other

Figure 5.9

Figure 5.9: **A**) Polyadenylation is coupled with termination of transcription. The cleavage and polyadenylation factor (CPSF) is key to this process. The WDR33 subunit of CPSF recognises and binds the PAS which in turn correctly positions the CPSF-73 subunit at the cleavage site, marked by a CA dinucleotide. **B**) We investigated the distribution of reads found in our RNAseq dataset which map to TP53 for the DMSO treated replicates. The coding TP53 sequence is indicated to the right of the plot. The position of the PAS SNP is indicated. The genomic region to the left of the main peak (location of the PAS SNP) is normally non-coding. The height of the peaks indicates the density of reads. **C**) We measured the expression of uncleaved TP53 mRNA in A-allele and C-allele Hap1 clones. The schematic (top) indicates the positions of the two primer pairs we used to amplify uncleaved, abnormally processed mRNA. The relative expression, as determined by qRT-PCR, is displayed in the barplots. Significance was determined by Student T Test. **D**) Schematic indicating the location of PAS sites across the TP53 gene (from APAatlas). PAS sites are indicated by triangles. The canonical PAS site, the first conserved site, is indicated by the red triangle. The grey box indicates the extended 3'UTR which is outside of the RefSeq/Ensembl annotations. We analysed the expression of TP53 from each putative TP53 PAS site from PolyA_DB.v3.2. The genomic positions of each PAS site on chromosome 17 are indicated on the X axis. The canonical PAS (red triangle in the above schematic), the PAS sites found beyond the annotated TP53 3'UTR and the first 3'UTR PAS site is indicated. **E**) Boxplots for RED score for TP53 in different normal tissues. The RED score indicates the ratio of expression from downstream PAS sites compared to upstream PAS sites. A positive RED score indicates the expression from downstream PAS sites is higher than upstream. Brain samples are coloured yellow. **F**) Brain tissues indicate significantly higher RED scores for TP53 compared to other tissues indicating increased usage of downstream PAS sites (APAatlas). Significance determined by linear regression. **G**) The boxplots indicate the expression of p53 mRNA in brain tissues compared to other GTEx tissues. The expression is shown in Transcripts Per Million (TPM). Significance determined by linear regression.

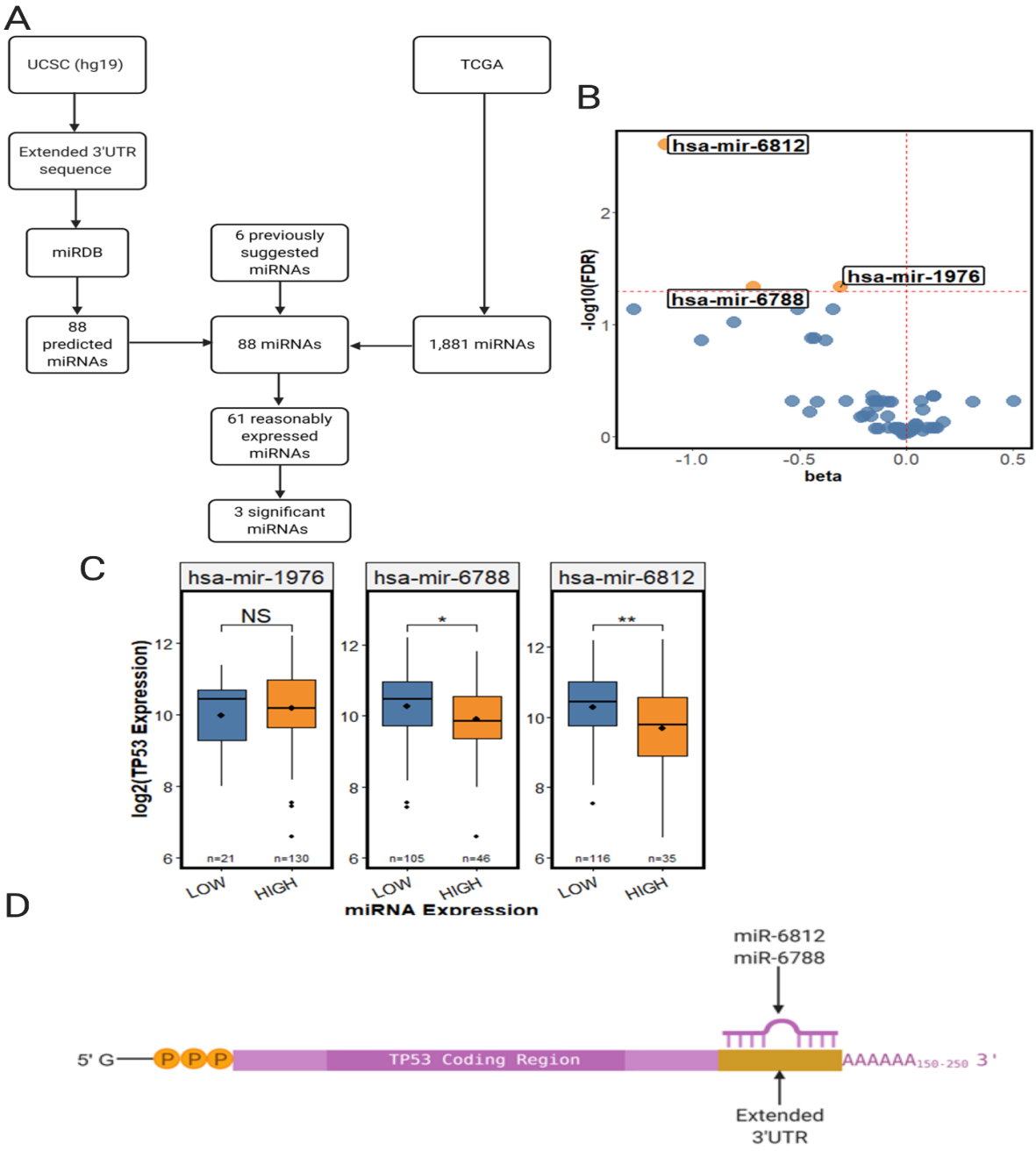

A
UCSC (hg19)
Extended 3'UTR sequence
miRDB
88 predicted miRNAs
6 previously suggested miRNAs
88 miRNAs
TCGA
1,881 miRNAs
61 reasonably expressed miRNAs
3 significant miRNAs
B
hsa-mir-6812
hsa-mir-1976
hsa-mir-6788
-log10(FDR)
beta
C
hsa-mir-1976
hsa-mir-6788
hsa-mir-6812
NS
*
**
log2(TP53 Expression)
n=21
n=130
n=105
n=46
n=116
n=35
LOW
HIGH
miRNA Expression
D
miR-6812
miR-6788
5' G
TP53 Coding Region
AAAAAA150-250 3'
Extended 3'UTR

Figure 5.10

Figure 5.10: **A**) Schematic indicating how we investigated whether the elongation of the 3'UTR, associated with the TP53-PAS-SNP minor allele, could enhance miRNA-mediated regulation of expression. We used the UCSC genome browser to extract the sequence for the elongated 3'UTR (between the canonical PAS and the last PAS identified with he APAatlas). We used an miRNA-target prediction tool, miRDB, to identify miRNAs which might target elongated p53 mRNA. Then we downloaded miRNA expression data from the TCGA human tumour cohort and overlapped the predicted miRNAs from miRDB with those measured in the TCGA cohort. We also included 6 miRNAs previously suggested in the literature. miRNAs with overall low expression were filtered out. Using just the tumours with the minor-allele, we used linear regression to determine the relationship between p53 mRNA expression and expression of each miRNA with adjustmnet for cancer-type and TP53 mutation status. **B**) For each miRNA, the correlation with p53 mRNA expression was determined. The effect size is shown on the X axis (beta) and the -log10 transformed FDR value on the Y axis. Significant miRNAs are coloured orange and labelled. **C**) For the three significant miRNAs, we split the minor allele carries into high and low expression (Maxstats package) and determined the difference in p53 expression between the two groups with adjustment for cancer-type and TP53 status. **D**) Schematic indicating that the extended 3'UTR of p53 mRNA as a result of the minor allele, could facilitate higher levels of regulation by two miRNAs, miR-6812 and miR-6788.

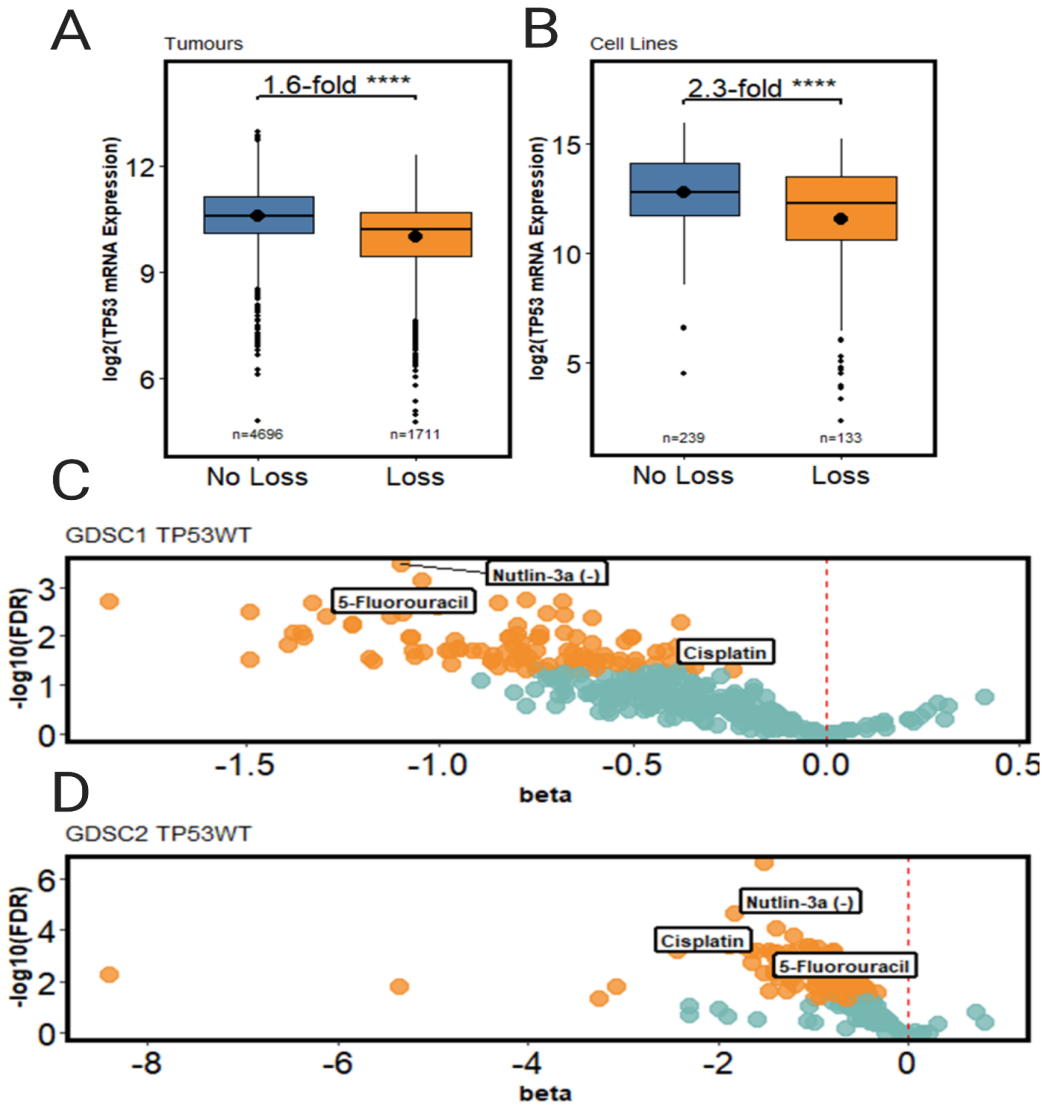


Figure 5.11: **A**) TP53WT tumour samples were separated into No Loss and Loss for TP53. We analysed the expression of p53 mRNA between these two groups with linear regression, adjusted for cancer type. TP53WT Loss tumours express significantly less p53 mRNA. **B**) TP53WT cell lines were separated into No Loss and Loss for TP53. We analysed the expression of p53 mRNA between these two groups with linear regression. **C**) We compared the sensitivity of TP53WT cell lines with and without TP53 loss to the 345 compounds used in GDSC1. Significant compounds after FDR correction are coloured orange. A negative beta indicates reduced IC50, higher sensitivity, in TP53WT cell lines without loss. **D**) We compared the sensitivity of TP53WT cell lines with and without TP53 loss to the 192 compounds used in GDSC2. Significant compounds after FDR correction are coloured orange. A negative beta indicates reduced IC50, higher sensitivity, in TP53WT cell lines without loss.

5.4 Discussion

5.4.1 Summary

In this chapter we explored the potential for pleiotropic SNPs in the management of cancer in the broader population. We found the p53 pathway to be enriched for pleiotropic cancer-SNPs compared to other pathways and focused on a pleiotropic SNP in the TP53 3'UTR which associates with heightened risk to multiple cancers including brain malignancies and melanoma, the TP53-PAS-SNP (Figures 5.2 to 5.4). By analysing human tumour data and generating isogenic cell models, we found the TP53-PAS-SNP to not only associate with cancer risk but also with reduced p53 expression, poorer prognosis, chemo-resistance, and TP53 somatic mutational status after tumour development (Figures 5.5 to 5.8). We then addressed the mechanism of how the minor-allele confers reduced p53 expression, we provided evidence that the minor-allele could promote usage of a downstream PAS site, resulting in a longer 3'UTR and increased susceptibility to miRNA-mediated repression (Figures 5.9 and 5.10). Finally, we demonstrated that TP53 copy-number loss exerts a similar reduction on p53 mRNA expression and that TP53WT cell-lines with loss are less sensitive to a wide range of anti-cancer compounds, suggesting that the TP53-PAS-SNP could also impact chemosensitivity (Figure 5.11).

5.4.2 The mechanism of the TP53-PAS-SNP

The aim of our studies is to determine if cancer-risk SNPs could help personalize cancer management and treatment strategies. A key step in realising this aim is discerning the biological mechanisms associated with the SNP both before and after a cancer develops. Through our study of the TP53-PAS-SNP, we have built upon the existing mechanistic knowledge regarding the SNP; specifically, our data supports a model whereby the minor-allele inhibits usage of the canonical PAS and promotes an APA event, leading to a longer 3'UTR which could then be subject to greater miRNA-mediated repression (Figure 5.12). This is in line with the previous studies by Stacey et al and Wang et al which highlighted that transcripts from the

minor-allele were elongated compared to the major allele. Other studies have also highlighted a role for SNPs in controlling APA for other genes[717]. For example, the alternative allele for rs10954213 at the IRF5 locus was found to lead to an APA event and expression of a shorter IRF5 isoform[718]. 3'UTR shortening has been shown to be common in cancer to allow heightened expression of oncogenic factors by escaping miRNA-mediated repression[719]. However, examples of our model, involving 3'UTR lengthening of a key tumour-suppressor gene in order to inhibit its expression, are few in the literature. 3'UTR lengthening of ZFR mRNA was shown to promote miRNA-mediated repression and reduce expression.

With regard to the specific miRNAs which could be responsible for repressing p53 expression in an allelic-dependent manner, several previous studies have reported that the minor-allele of the TP53-PAS-SNP could generate novel miRNA binding sites but we did not find evidence for these miRNAs in affecting p53 expression in our analyses[712][713][674]. This could be due to the fact that we predicted miRNA binding sites on the entire elongated 3'UTR rather than on the sequence immediately around the TP53-PAS-SNP. Secondly, we performed a pan-cancer analysis to detect which miRNAs associated with p53 expression in an genotype-specific manner; we did so in order to ensure samples sizes were sufficient for robust statistical testing and because the minor-allele is associated with heightened risk of cancer in general[720]. However, this could have led us to miss miRNA interactions specific to a small number of cancer-types. However, such associations would be difficult to pick up in our analysis due to the low incidence of the minor-allele (1%). To experimentally confirm a role for miR-6812 and miR-6788, we would inhibit the two miRNAs by treating our isogenic Hap1 cell-lines with perfectly complementary RNA molecules. This approach would sterically block the miRNAs and prevent targeting of p53 mRNA. If miR-6812 and miR-6788 mediate degradation of p53 mRNA in an allelic-specific manner, then we would expect their inhibition to rescue the expression of p53 in C-allele cells.

The TP53-PAS-SNP has been shown to strikingly associate with risk of brain malignancies with multiple studies reporting OR >3, but why this could be the case

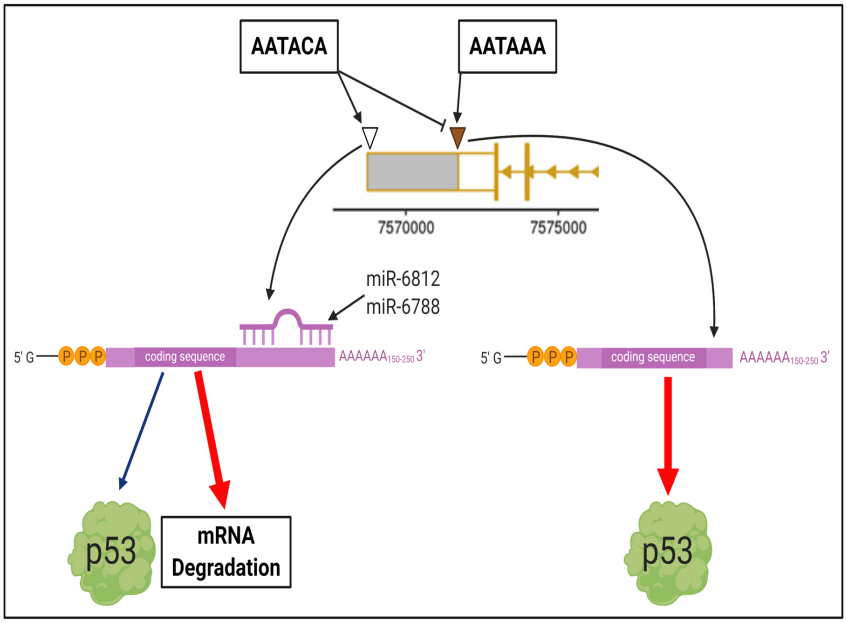


Figure 5.12: Schematic indicating how the TP53 PAS SNP might confer reduced TP53 expression by a combination of impaired 3' processing and increased miRNA targeting. In the case of individuals who are homozygous major (AA) for the TP53 PAS SNP, the majority of p53 transcripts will terminate at the canonical TP53 PAS site (red triangle). However, for carriers of the minor allele (AC or CC), the canonical PAS is no longer recognised and transcripts may terminate at an alternative PAS site (white triangle) further downstream, constituting an APA event. This elongates the 3'UTR of p53 mRNA (grey box) and incorporates new sequences which could be targetable by miRNAs. The miRNA activity leads to degradation of some p53 mRNA and the p53 protein pool is reduced compared to the AA case.

is unclear. Deng et al highlighted miR-392 to be highly expressed in the brain and to exert an allelic-specific association with p53 mRNA[674]. Although we cannot rule out this mechanism, our data suggests that the brain could be particularly susceptible to the minor-allele due to its intrinsic usage of downstream PAS sites and expression of mRNAs with longer 3'UTRs[721]. Indeed, we showed that the brain exhibits higher usage of downstream TP53 PAS sites compared to other tissues and that this correlates with lower p53 mRNA expression. Perhaps, in the brain, where cells are already conditioned to express longer transcripts and lower p53, the presence of the minor-allele may substantially increase the risk of tumorigenesis by further reducing p53 expression below a critical level.

5.4.3 Potential clinical impact of the TP53-PAS-SNP

In this chapter, we explored the potential for the TP53-PAS-SNP to inform the management of cancer. We reason that the TP53-PAS-SNP could have an impact in four different ways. Firstly, as genotyping becomes more readily available, the TP53-PAS-SNP could be useful in combination with other cancer risk SNPs for risk stratification and early detection of cancer by screening individuals with risk alleles more often. Secondly, our data and the general biology of the p53 pathway would suggest that the TP53-PAS-SNP could impact therapeutic decision-making and design. Our data suggests that minor-allele carries are less likely to respond to conventional chemotherapies, many of which stabilise p53 protein. However, the mechanism of the TP53-PAS-SNP opens up novel opportunities for intervention such as increasing transcription of wild-type TP53, inhibiting miRNAs or blocking APA; for example, Van Etten et al (2017) showed that blocking of an APA site at the AR locus in prostate cancer using morpholinos reduced expression of tumorigenic AR isoforms[722]. Enhancing transcription from the TP53 locus could be possible through modulation of the transcription factors which regulate p53 expression (Figure 5.13). Most notably, RBPJ, encoding a transcriptional repressor which is activated by NOTCH signalling, represses transcription from TP53 and its inhibition reduces tumour growth and enhances expression of the p53 target gene, p21[108][723][724][725]. Moreover, a small-molecule inhibitor of the NOTCH-RBPJ interaction (RIN1) has recently been developed which inhibits cancer-cell proliferation while a NOTCH inhibitor (LY3039478) has also shown efficacy in human trials[726][725]. It would be intriguing to investigate whether NOTCH/RBPJ inhibition could enhance p53 expression and mitigate the effects of the TP53-PAS-SNP minor allele and TP53 deletion.

Thirdly, the TP53-PAS-SNP could have an impact in the cancer prevention space. The risk attributed to the minor-allele is presumably due to reduced p53 expression and activity. Therefore, we reason that compounds capable of increasing p53 levels back to the normal level could alleviate the increased cancer risk. Finally, genetic pleiotropy has been applied in other disease contexts to drive drug discovery

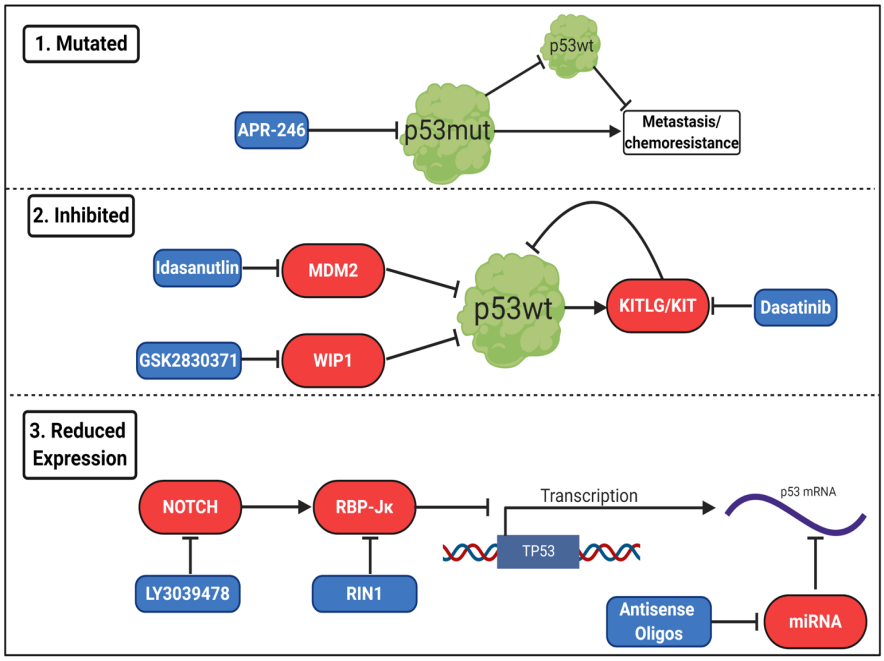


Figure 5.13: TP53 is mutated in over 50% of tumours and much research effort is dedicated to developing compounds capable of inactivating mutant p53 and rescuing wild-type p53 function. In this thesis we have explored mechansisms which might inhibit wild-type p53 and could be targetable. For example, KITLG/KIT signalling can, at least in some tissues, be induced by KITLG/KIT signalling which then inhibits p53-dependent apoptosis. We indicated that KITLG/KIT inhibition by Dasatinib synergised with the MDM2 inhibitor, Nutlin-3a. Nutlin derivitives, such as Idasanutlin, are currently in clinical trials. In this Chapter, we have explored mechanisms which could repress p53-mediated apoptosis by reducing p53 expression; specifically, the TP53-PAS-SNP minor allele and TP53 deletion. Methods to upregulate p53 mRNA expression, perhaps by inhibiting transcriptional repressors of the TP53 locus or miRNAs, could be beneficial for patients with reduced p53 expression. Pro-tumour factors are coloured in red. Anti-tumour compounds are coloured in blue.

and drug repurposing, for example in rheumatoid arthritis, and the TP53-PAS-SNP has the potential to have a similar impact in cancer[727][728][649]. As mentioned above, patients with the minor-allele may benefit from treatments which boost p53 expression; our data would suggest that such a therapy could be repurposed for the multiple cancer-types which rarely mutate TP53.

5.4.4 Implications of the interplay between germline and somatic genetics

The aim of our studies is to determine if cancer-risk SNPs could help personalize cancer management and treatment strategies. Our data indicates that one way the TP53-PAS-SNP could do so is by driving our understanding of the interplay between germline and somatic genetics in tumours. Specifically, we showed that the minor-allele of the TP53-PAS-SNP reduces expression of wild-type and mutant p53,

is enriched for among TP53WT tumours and cancer-types which rarely mutate TP53 and associates with poorer survival and resistance to therapy in a p53-dependent manner (Figures 5.5, 5.7 and 5.8). Moreover, our group also found that the minor-allele confers increased risk for breast and ovarian cancer subtypes with low TP53 mutation frequency but reduced risk for subtypes with high TP53 mutation frequency[97]. These data suggest that germline variants can continue to play a role in tumours after they have developed by determining the genetic evolution of the tumour. The genetic make-up of a tumour can be heavily influenced by treatment with many targeted therapies associated with development of mutations in specific genes, including TP53[729][730][731][732]. Given the germline-mediated suppression of p53 signalling in minor-allele carriers, it would be intriguing to investigate whether minor-allele carriers are less likely to mutate p53 in response to cytotoxic therapies.

The impact of other specific germline variants on specific somatic mutations in key oncogenes and tumour suppressors has not been fully explored. One study of human tumours identified several SNPs which associated with specific mutations, such as rs25673 and PTEN, while a recent high-throughput analysis of whole-genomes identified SNPs predictive of endogenous mutational processes[733] [382]. It is clear from these publications and from our own work that germline variants can impact the frequency and severity of somatic events during tumour development[97][734]. These somatic mutations are key sources of heterogeneity in treatment response amongst patient groups and of chemoresistance and relapse[735][736][737][738]. Anti-cancer therapies alter the tumour micro-environment and can lead to selection of previously low-frequency but resistant clones which are often characterised by these specific somatic mutations. Current sampling and sequencing techniques mean that this low-level intratumoral heterogeneity can be missed. With worldwide and genome-wide efforts such as that recently undertaken by Pan-Cancer Analysis of Whole Genomes (PCAWG), thorough mapping of the interactions between germline variants and somatic mutations could allow for prediction of these low-frequency somatic mutations and personalised treatment regimes which account for them (Figure 5.14).

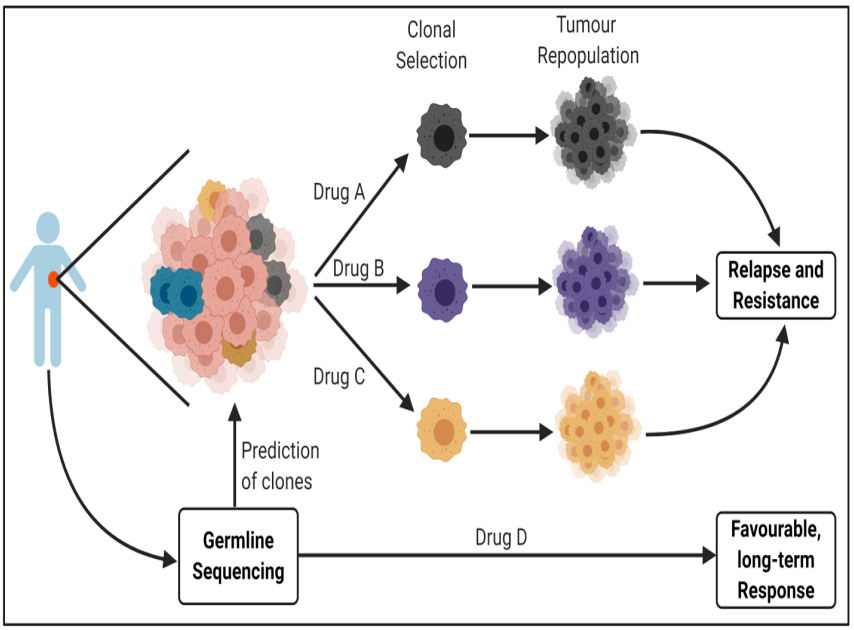


Figure 5.14: The interaction between germline and somatic mutations could be invaluable for determining the response of cancer patients to therapies. This figure pictorially indicates how low-frequency clones within a tumour, with specific somatic mutations, can be selected for when treatments alter the selection landscape of the tumour. The newly favoured clones can then repopulate the tumour. Then, despite initial good response to treatment, the patient eventually relapses. Many of these low frequency mutations can be difficult or even impossible to detect. However, with the huge amounts of somatic and germline data being made available, it may become possible to predict the likely low-frequency clones from the germline variants. For example, carriers of the minor allele of the TP53-PAS-SNP may be less likely to harbour clones with TP53 mutations. If these approaches are shown to be successful then the germline variants could be used to personalise treatments for patients in order to avoid selecting low-frequency clones.

6
Discussion

Contents

6.1 Summary 243
6.2 Novel approaches to therapeutically target the p53 pathway in cancer 245
6.3 High-throughput identification of functional cancer-SNPs is required for clinical translation 248
6.4 Practical and ethical challenges of the clinical translation of common germline variants 251
6.5 Conclusion 254

6.1 Summary

Genetic heterogeneity in cancer underpins the variability in response of patients to therapies and plays an important role in cancer re-occurrence and relapse. New frameworks for managing cancer heterogeneity are urgently required in order to meet the growing incidence of cancer and to maintain the downwards trajectory of cancer mortality rates. In this thesis, we have highlighted the potential for germline genetic variants in the p53 pathway to inform the management of cancer heterogeneity by studying two SNPs in particular, the KITLG-p53RE-SNP and the TP53-PAS-SNP. Importantly, we provide proof-of-principle that cancer susceptibility loci can uncover novel tumorigenic mechanisms, can direct therapy design, can direct

drug repurposing and provide evidence that they have the potential to influence cancer management in the broader population.

In Chapters Two and Three we experimentally modelled and investigated the mechanisms of a SNP within a p53RE at the KITLG locus whereby the risk-allele confers greater p53 binding, KITLG-p53RE-SNP. This SNP is strongly associated with risk of testicular germ cell tumours (TGCT) in GWAS studies (Table 2.1). Through genetic and pharmacological manipulations of p53 and KITLG/KIT signalling, we developed a mechanistic model for the KITLG-p53RE-SNP and designed a novel therapeutic strategy to leverage this mechanism using compounds approved for use in humans. Our results provide experimental evidence that cancer-susceptibility loci can inform novel biology, therapeutic design and repurposing opportunities[53][739][552]. These data could have important implications for the management of platinum-resistant TGCT patients (10% of all TGCT patients).

In Chapter Four, we extended our model, that KITLG/KIT signalling can inhibit p53-mediated apoptosis, to other cancer types. We demonstrated that melanoma (90% TP53WT) is enriched for oncogenic KIT mutations and KIT gain and that KITLG/KIT inhibition synergises with p53 activation in a melanoma cell-line. Importantly, KITLG/KIT signalling is known to be important for the normal biology of melanocytes[740][741]. Moreover, this analysis suggests that some p53 target genes (e.g. KITLG) can impair the p53-apoptotic response without directly regulating p53 expression levels. We reasoned that other p53 target-genes could inhibit p53-mediated apoptosis in a similar way to KITLG. We investigated the 340 validated p53 target-genes and other annotated p53 pathway genes (410 in total) and identified 31 genes whereby high expression associated with reduced sensitivity to multiple p53-dependent compounds. Five of these genes, including KITLG, were over-expressed and exhibited copy-number gain in TP53WT human tumours compared to those with biallelic TP53 inactivation. We focused on the two genes, CPE and PARD6G, which we found to be druggable. CPE is druggable by a small molecule, GEMSA, and we found high CPE expression to associate with poorer prognosis in KIRC wherein CPE is significantly positively correlated with

p53 expression[617][618][550]. PARD6G is druggable through multiple immediate protein-protein interactions including by Aurothiomalate, an approved compound for the treatment of rheumatoid arthritis[553]. We found high PARD6G expression to associate with poorer prognosis in DLBC which is significantly enriched for PARD6G copy-number gain.

In Chapter Five, we comprehensively analysed pleiotropic cancer-SNPs and found the p53 pathway to be the most enriched pathway for genes which harbour pleiotropic SNPs, indicating that further study of p53 pathway SNPs could inform the management of multiple cancer-types. We focused on a highly pleiotropic p53 pathway SNP which disrupts the canonical TP53 polyadenylation signal, the TP53-PAS-SNP. This SNP associates with risk of multiple cancer types, including pan-cancer risk, and has been linked to Li-Fraumeni Syndrome among patients without coding TP53 mutation (Supplementary Table C.13)[712]. By mining human tumour data and generating isogenic cell-line models, we found evidence that the minor-allele promotes an alternative-polyadenylation (APA) event, facilitates enhanced miRNA-mediated repression and reduces p53 expression. We suggest that this SNP could inform the management of cancer of a large number of people. World population stands at approximately 7.8 billion people meaning 78 million could carry the risk allele of the TP53-PAS-SNP. With further study of the mechanism which we propose, the TP53-PAS-SNP could have implication for prevention, stratification and therapy design (discussed below).

Overall, our research regarding the KITLG-p53RE-SNP and TP53-PAS-SNP highlight the importance of identifying and investigating functional cancer susceptibility loci. These germline variants have great potential to direct researchers to key tumorigenic mechanisms which in turn can reveal novel therapeutic opportunities.

6.2 Novel approaches to therapeutically target the p53 pathway in cancer

Our research on the germline genetics of the p53 pathway has added new complexity to the p53 network. P53 signalling is ubiquitously impaired in cancer through

mutation, deletion, over-expression of direct p53 regulators (e.g. MDM2) or inhibition of important downstream nodes (e.g. p21) and much research effort is devoted to therapeutically targeting such alterations[742][743]. In our study of p53 pathway germline variants, we provide evidence of two other tumorigenic and potentially targetable mechanisms: p53-induced pro-survival signalling which inhibits the downstream p53-apoptotic response (e.g. KITLG/KIT signalling) and modest reductions in p53 expression due to post-transcriptional regulation (e.g. TP53-PAS-SNP).

The canonical p53 negative-feedback loops involving MDM2 and its regulators have pro-tumour roles in multiple cancer-types[744][745][746]. For example, upon activation, p53 readily upregulates expression of cyclin G from the CCGN1 locus in a variety of cell types. Cyclin G complexes with PP2A phosphatase and together they can remove an inhibitory phosphate residue from MDM2 and facilitate MDM2-mediated p53 inhibition[747]. Multiple MDM2 inhibitors are in clinical trials but none are yet approved by the FDA[748][749]. Moreover, there are concerns that over-activation of p53 could lead to high levels of cell death in healthy tissues and unacceptable toxicity; for example, reactivation of p53 in MDM2-null mice led to tissue degeneration and death[750]. Our work in TGCT highlights a novel feedback loop which does not regulate p53 expression, whereby p53 upregulates KITLG expression which promotes signalling through KITLG/KIT/AKT to promote cell survival and inhibit downstream p53-dependent apoptosis. We show that inhibition of this pro-surival pathway synergises with p53 activating compounds such as Doxorubicin. In comparison to targeting the core regulatory feedback loops which involve MDM2 and regulate p53 expression and activity directly in most tissues, inhibition of p53-induced downstream signalling pathways which are over-activated in cancer and inhibit p53-mediated apoptosis , such as KITLG/KIT-mediated p53 inhibition, could be more tolerable. Targeting of direct p53 regulators, such as MDM2, would over-activate p53 and this could propagate throughout the whole p53 network. In contrast, targeting of a specific downstream signalling pathway,

such as KITLG/KIT, could be more specific to the cancerous cells which are addicted to this pathway for survival.

P53 can regulate the expression of at least 343 target genes and perhaps many more in a tissue- and cancer-type specific manner[115]. Given the plethora of p53 target genes and functions which they carry out, different target genes may become pro-tumour in different subgroups of different cancer-types. Indeed, we found preliminary evidence that CPE (bound and upregulated by p53 in 7 of 16 ChIP-seq studies) and PARD6G (bound and upregulated by p53 in 5 of 16 ChIP-seq studies) could be druggable, pro-survival p53 target-genes in renal clear cell carcinoma and diffuse large B-cell lymphoma respectively[115]. Future studies should focus on detailing the tissue-specific roles of p53 target genes in order to delineate novel pro-survival signalling axis which could be therapeutically targetable without incurring the toxicities associated with over-activation of p53.

Both the KITLG-p53RE-SNP and the TP53-PAS-SNP are expression quantitative trait loci (eQTLs) which associate with cancer susceptibility and could reduce the pressure to somatically mutate p53. The TP53-PAS-SNP is of particular interest as it regulates the expression of p53 itself, at both the mRNA and protein level. Most p53 studies focus on the activity levels of p53 protein as a determinant of the p53-apoptotic response, but our study of the TP53-PAS-SNP highlights that the expression levels of p53 mRNA can also be important. Not only does the reduced expression, directly caused by the minor allele, associate with heightened risk of multiple cancer-types, but we have demonstrated that the effects of the minor allele on p53 expression continue beyond tumour development and can confer resistance to therapy and poor prognosis. Moreover, the effect of the minor allele is comparable to copy-number loss of TP53 (approximately 2-fold reductions in p53 expression), which we have shown to be a frequent genetic effect in TP53WT tumours (27%) and can strongly determine sensitivity to anti-cancer compounds in cell-lines and outcome in human cancer-patients. Deletion of other tumour-suppressive genes both within and outside of the p53 pathway are known to be common in tumours, such as CDKN2A deletion in melanoma and APC deletion in

colon tumours[751][752]. Although we did not investigate it in this study, it could be interesting to determine the effects of such copy-number losses on chemosensitivity and patient outcome as we did for TP53.

By studying the TP53-PAS-SNP, we identified a pan-cancer subgroup with reduced p53 expression due to either TP53 deletion or the minor allele (approximately 28% of TP53WT tumours) which could benefit from therapeutic strategies to enhance p53 expression. In support of this model, that tumours can inhibit the p53-apoptotic response through mechanisms which reduce p53 expression, the recent PCAWG initiative identified somatic mutations at the 5' end of the TP53 locus, including the promoter region, to be frequent in cancer and to associate with reduced p53 mRNA expression[753]. However, the effect of these 5' mutations on chemosensitivity and patient outcome has not yet been studied. Given these data, we reason that pharmacological enhancement of transcription from the TP53 locus could alleviate the tumorigenic properties associated with TP53 deletion, the TP53-PAS-SNP minor allele and TP53 promoter mutations. We discussed possible strategies for this in Chapter Five. The minor allele of the TP53-PAS-SNP confers a longer 3'UTR and could enhance miRNA-mediate repression. Inhibitors of these miRNAs, such as miR-6788 and miR-6812, could boost p53 expression; indeed, multiple oligonucleotide inhibitors of miRNAs have been tested in humans with promising results[754][755]. Another approach could involve targeting RBP-J$\varkappa$, a transcriptional repressor which is activated by NOTCH signalling and binds to the TP53 locus[725]. Future studies should explore novel regulators of transcription from TP53 and determine the feasibility, efficacy and safety of pharmacologically increasing p53 mRNA levels to treat cancer.

6.3 High-throughput identification of functional cancer-SNPs is required for clinical translation

In this thesis, we have provided evidence that germline single nucleotide polymorphisms (SNPs) can uncover novel biological processes and inform therapeutic

design. The use of germline variants could improve our biological understanding of cancer, the success with which drugs are repurposed and the selection of the right treatments for the right patient groups[53]. However, a major barrier to doing so is the identification of functional cancer-susceptibility loci and the underpinning mechanisms. In this thesis, we focused on two SNPs in the p53 pathway and comprehensively investigated their molecular mechanisms. However, in order to drive clinical translation of GWAS data, high-throughput methods must be developed in order to systematically identify causal SNPs and the tissues wherein they could be clinically informative. Identification of functional coding SNPs is relatively straightforward with multiple tools available to estimate the effect of a mutation on a protein such as PolyPhen-2[756]. However, the vast majority of SNPs are non-coding and highly correlated, making identifying functional non-coding SNPs a difficult challenge[89][757]. A key approach to identifying functional SNPs is the use of genomic annotations, for example, transcription factor binding sites, measures of chromatin accessibility and epigenetic sites. Recent advances in the genetic annotation of the human genome has allowed development of increasingly complex machine learning algorithms to predict functional SNPs from such annotations[758][759]. With the increase in the number of features, has come improved accuracy. For instance, a recent algorithm with 258 features, applied to 39,038 SNPs including 2,529 known functional SNPs, was able to correctly classify SNPs as functional or non-functional 84% of the time[759]. Indeed, some of the error in the model may have been derived from undiscovered functional SNPs.

Approaches to identify functional SNPs should consider context. It is clear from large-scale projects, such as GTEx, that germline variants can have tissue-specific effects on gene expression with a recent study confirming that some SNPs have opposing effects in different tissues[760][761]. In this thesis, we demonstrated this concept for both the KITLG-p53RE-SNP (TGCT specific) and the TP53-PAS-SNP which associated with reduced p53 expression in those cancer-types with high MAF and low TP53 mutation rates but not in those cancer-types with low MAF and high TP53 mutation rates. Context can be critical in ways other than tissue-type.

For example, Fairfax et al (2014) detected functional SNPs in IFNy and LPS-stimulated monocytes which were not detected in untreated cells, indicating the importance of studying SNPs in appropriate pathophysiological environments[762]. The KITLG-p53RE-SNP could exhibit such pathophysiological dependencies; if p53 is inactivated then the effect of the SNP on KITLG expression would not be detectable. In addition, studies have discovered eQTLs dependent on other genetic factors (germline and somatic), sex and age[763][764][765]. Due to the complex interactome which governs when and where SNPs might be functional, it is likely that approaches which account for all of the aforementioned variables will be needed to fully understand the role of common genetic variants in complex diseases such as cancer. Tissue- and stimulus-specific SNPs could be detected through burgeoning single-cell technologies (e.g. scATAC-seq and scRNA-seq), large-scale meta-analyses may be needed to unpick age- and sex-specific variants while germline-germline and germline-somatic interactions will undoubtedly be uncovered through whole-genome and multi-omics approaches (e.g. TCGA, PCAWG) (Figure 6.1).

As described above, multiple contextual factors should be considered when developing high-throughput methods to detect functional SNPs. In our work, we have also studied the long-lasting effects of SNPs on tumours and show that the KITLG-p53RE-SNP associates with poorer outcome in TGCT patients (a predominantly TP53 wild-type cancer-type) and that the TP53-PAS-SNP associates with poorer outcome in a way which is dependent on retention of wild-type TP53. Indeed, we also found the minor allele of the TP53-PAS-SNP to be enriched for amongst patients with TP53WT tumours compared to those with TP53 mutations. Thus, our work suggests that somatic and germline variants interact; this interaction could work in both directions. First, SNPs could modify the somatic evolution of tumours, as suggested by the over-representation of the TP53-PAS-SNP minor allele among tumours retaining wild-type TP53. The study of germline-somatic interactions is incomplete. Although allelic specific imbalance (ASI), whereby the copy of a gene harbouring a risk allele of a GWAS SNP is preferentially

gained compared to the non-risk allele, is a well-established in cis, germline-somatic interaction, in trans interactions have not been extensively studied[734]. Carter et al (2017) observed that rs25673 (ch:19) could impact PTEN (ch:10) mutation rates in multiple cancer-types while rs132985 (ch:22) has been shown to influence BRAF mutations in melanoma[733][766]. Second, somatic mutations could dictate the functionality of SNPs in developed tumours; for example, BRAF mutations lead to constitutive activation and could therefore render meaningless the increased KITLG/KIT signalling induced by the risk-allele of the KITLG-p53RE-SNP. Currently, only a handful of well-supported germline-somatic interactions have been identified; future studies should comprehensively characterise the extent to which germline-somatic interactions could shape tumour evolution and how this could impact therapy response and patient outcome (Figure 5.14)[734].

6.4 Practical and ethical challenges of the clinical translation of common germline variants

Analysis of the germline could greatly improve the management of cancer and other diseases, both pre-diagnosis (e.g. risk stratification) and post-diagnosis (e.g. therapeutic decision-making). However, despite the scientific evidence for the potential impact of SNPs, several practical challenges must be overcome (Genomics in practice, 2019). For instance, healthcare systems are generally divided based on organs (e.g. cardiology) or specific diseases (e.g. oncology); yet germline variants could be useful across different specialities and at different times in an individual's lifetime. This raises three important questions. First, the timing of germline analysis must be considered; sequencing of symptomatic individuals could allow for focused testing on candidate variants linked to the diagnosis, saving resources in the short-term but perhaps becoming costly if individuals must be sequenced multiple times throughout their lifetime. Alternatively, pre-emptive new-born screening would ensure that germline data is available throughout an individual's lifetime but would require gene-agnostic approaches to cover all potential diagnoses. A pre-emptive approach would lead to the second question: how to

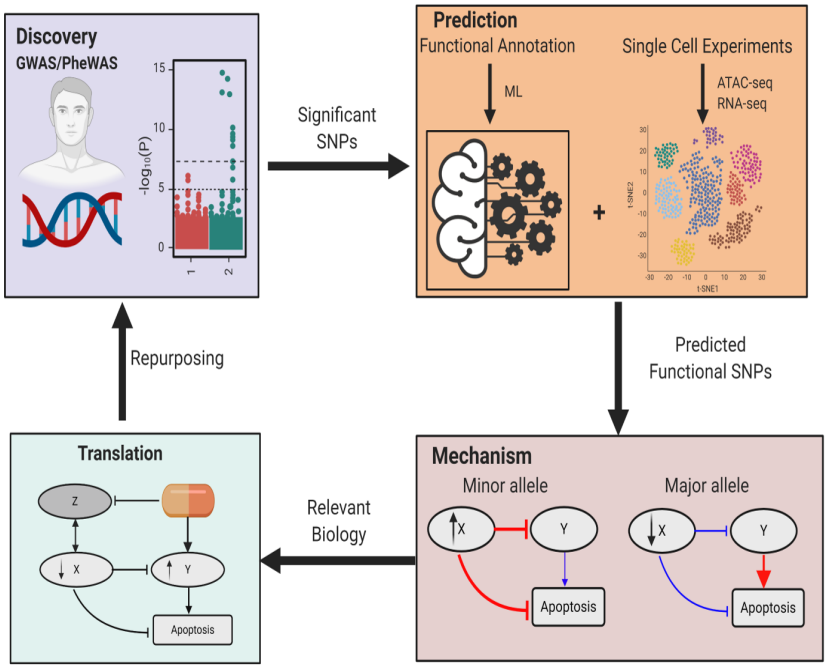


Figure 6.1: In this thesis, we have outlined evidence that germline cancer susceptibility in the form of SNPs can lead to novel biological mechanisms, inform therapeutic design and have the potential to improve management of cancer. In this schematic we outline key steps in automating this process to quickly identify and validate functional SNPs which could inform clinical practices. In the discovery phase, relevant SNPs are identified by GWAS studies. Of these significant SNPs, likely functional SNPs can be predicted using machine learning algorithms trained on data about already validated SNPs such as the genomic structure of the surrounding sequence and functional annotation such as transcription factor binding sites. Importantly, as we identify more functional SNPs, these algorithms will improve. As a second part of the prediction phase, it is important to identify the cell types where SNPs are functional. Single cell experiments will be key to unravelling the context specific role of SNPs. The prediction phase vastly reduces the number of possible functional SNPs and thus allows wet lab experiments in the Mechanism phase to be more direct and detailed. These experiments may include CRISPR-Cas9 models as we showed in this thesis and further evaluation by omics. As indicated in this thesis, these experiments can highlight novel pathways and mechanisms underpinning the SNP association. Novel relevant biology opens up novel druggable opportunities. In this basic example, a SNP regulates the expression of X which in turn inhibits Y and apoptosis. X may not be druggable but a regulator of X, such as Z could be. Inhibition of Z with activation of Y could be therapeutically interesting. The SNP which lead to such a therapeutic opportunity could be pleiotropic and the treatment already designed could therefore be repurposed. To identify repurposing opportunities, PheWAS studies can be employed to discover other traits which associates with the SNP.

store the data. Standard genome-wide SNP array arrays generate gigabytes of data; to be implemented on a population-wide scale, new approaches for data-management would be required. Third, once securely stored, cross-pathway systems would be needed to ensure medical professionals across different fields can access and interpret the data in real-time. This final challenge is particularly pertinent as most medical professionals are not geneticists and the rapid increase in the number of pharmaco-genes means it is infeasible to learn them. Novel methods of data summarisation and visualisation will be needed to ensure the wealth of

germline data is appropriately applied[767]. Providing the logistical challenges regarding clinical genomics are overcome, ethical problems concerning the usage and disclosure of germline data must also be addressed. Disclosure of genetic susceptibility to disease could have psychological impacts for the patients and families, although many surveys have reported that high proportions of responders would be willing to receive genetic information[768]. Such issues are readily becoming more pertinent due to companies, such as 23andMe, offering direct-to-customer genetic testing[769]. Frameworks are in place for the disclosure of rare, pathogenic Mendelian germline variants, such as those pre-disposing to cancer syndromes, which can be life-changing and potentially lifesaving. In contrast, some argue that the modest risk modifications indicated for most SNPs in GWASes are not sufficiently clinically actionable to nullify ethical quandaries such as the threat to privacy and confidentially[770][771]. However, the work presented in this thesis indicates that it would be unwise to judge the effects of germline variants in established tumours based on GWAS summary data. For both the KITLG-p53RE-SNP and TP53-PAS-SNP, we studied their associations with biological mechanisms in disease models and with disease endpoints and found significant long-lasting effects on tumours. It is imperative that more studies follow our example and, in the process, generate greater confidence in the biological and clinical relevance of SNPs for patient stratification, pharmacogenomics, personalised medicine and design of novel therapies. This will drive the tackling of the aforementioned logistical and ethical challenges of clinically implementing common germline variants towards necessity rather than possibility.

6.5 Conclusion

Over the last 80 years, the management of cancer has transitioned in line with the development of novel technologies, from surgery to chemotherapy to molecularly targeted therapies. Now, the field of medical oncology is arguably going though its biggest transition, into personalised genomic medicine. Although treatment can be tailored to a number of known somatic driver mutations, heterogeneity in response rates is still rife and a substantial number of patients do not present with clear, actionable mutations. In this thesis, we have provided evidence that functional cancer-associated SNPs in a key cancer pathway, the p53 pathway, can modify the biology of cancer cells and the evolution of tumours, inform the design of novel molecularly targeted therapies and affect patient outcome. Thus, with further study of functional cancer-SNPs, we predict that common germline variants will improve the management of cancer in the broader population both at the level of designing new, informed therapies and by matching patients to treatments which offer the highest chance of success.

7

Materials and Methods

Contents

7.1 P53 pathway gene set 256
7.2 Omics analyses 256
7.2.1 RNA-seq 256
7.2.2 Proteomics 258
7.2.3 Sample Preparation 258
7.2.4 Pathway Enrichment Analysis 258
7.3 Data Mining 260
7.3.1 The Cancer Genome Atlas (TCGA) 260
7.3.2 Weighted Gene Co-expression Network Analysis 262
7.3.3 Genomics of Drug Sensitivity in Cancer (GDSC) 263
7.3.4 Gene Expression Omnibus 264
7.3.5 GWAS Datasets 264
7.3.6 Druggable Genome 265
7.3.7 STRING Protein-Protein Interactions 265
7.4 Statistical Analyses 266
7.4.1 Machine Learning 266
7.5 Experimental Techniques 267
7.5.1 CRISPR-Cas9 Genome Editing 267
7.5.2 Cell culture and their treatments 268
7.5.3 Drug screening 268
7.5.4 IC50 and combination index CI analyses 268
7.5.5 In vivo study 269
7.5.6 SDS-PAGE and western blotting 269
7.5.7 RNA isolation, cDNA synthesis and qRT-PCR 270
7.5.8 MTT assay 270
7.5.9 Cell proliferation and migration 270
7.5.10 Phospho-kinase assay 271

7.1 P53 pathway gene set

Annotated p53 pathway genes from KEGG, PANTHER and Biocarta were compiled with 343 target-genes from Fischer *et al*, totalling 410 unique p53 pathway genes [772][773][774][115].

7.2 Omics analyses

7.2.1 RNA-seq

Sample Preparation

3' bulk RNA-sequencing was performed on three biological replicates of TERA1 KITLG-p53RE +/+, -/- and -/KI clones treated with either DMSO, Nutlin-3a (10uM), Dasatinib (2uM) or Dasatinib+Nutlin-3a for 6hrs and on logarithmically growing Hap1 cells (A, C#1, C#2). RNA was extracted using the Qiagen RNeasy Mini Kit (Cat. No.74104) by following the manufacturer's instructions. Cells were disrupted, homogenised by vortexing and centrifuged in RNeasy Mini columns. RNA was eluted in RNAse-free water and the $A_{260/280}$ ratios were checked by nanodrop to be within 1.9-2.1.

Sequencing and Pre-processing

3' RNA-seq library was prepared using a standardised protocol followed by sequencing using a HiSeq4000 platform (Illumina) at the Oxford Genomics Centre (Wellcome Trust Centre for Human Genetics, Oxford, UK). Sequencing reads were mapped to hg19 using the HISAT2 alignment algorithm (version 2.1.0) and counts were determined from the BAM file using featureCounts (version 1.6.2)[775][776].

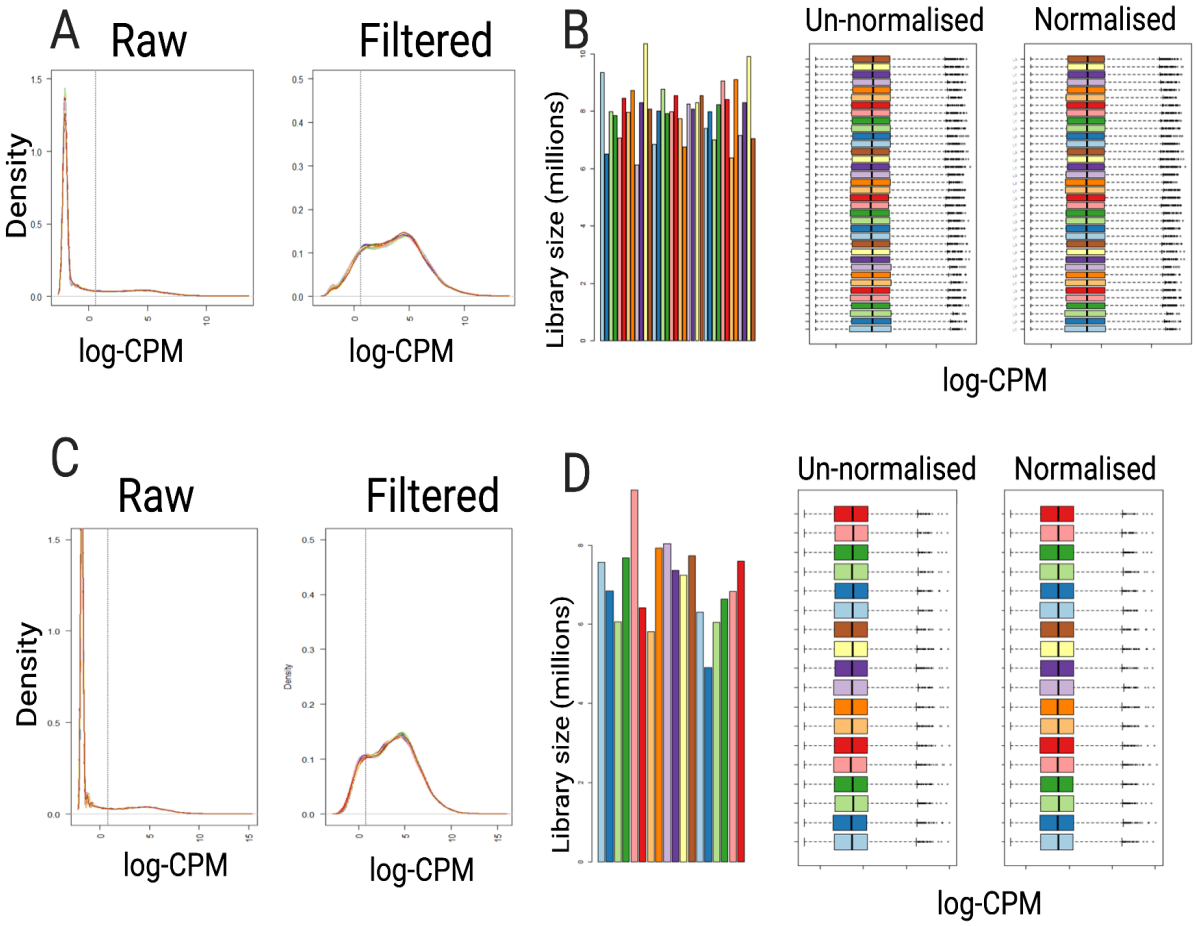


Figure 7.1: **A**) Density plots for the expression of genes prior to filtering (left) and after filtering (right) for the TERA1 RNA-seq dataset. **B**) Library sizes and composition bias normalisation for the TERA1 RNA-seq dataset. **C**) Density plots for the expression of genes prior to filtering (left) and after filtering (right) for the HAP1 RNA-seq dataset. **D**) Library sizes and composition bias normalisation for the HAP1 RNA-seq dataset.

Differential Gene Analysis

edgeR (version 3.30.3) was used in RStudio to determine differentially expressed genes (Additional Methods)[777]. Libraries were normalised for composition bias with factors between 0.92 and 1.06 found (Figures 7.1.A,B). The libraries were normalised to account for composition bias. Normalisation factors were found to be between 0.92 and 1.06 for both experiments indicating little composition bias (Figures 7.1.C,D). Nominal p-values were corrected for MHT by FDR and FDR q-values <0.05 were considered significant unless otherwise stated. RPKM was calculated by normalised for sequencing depth and gene length.

7.2.2 Proteomics

7.2.3 Sample Preparation

TERA2 KITLG-p53RE +/+ and -/- cells were incubated with R0K0 (light) or R10K8 (heavy) RPMI SILAC media, supplemented with dialysed FBS (Dundee Cell Products Ltd) for 9 doublings.

Mass Spectrometry and pre-processing

Mass Spectrometry was carried out as described in Davis et al [778]. MaxQuant software was used to identify peptides, map peptides to proteins and quantify the expression values[779]. 7,869 peptides were mapped to 7,915 proteins.

Differential Protein Expression Analysis

Contaminated peptides and those detected in only one biological replicates were discarded, leaving 7,589 peptides. Limma was used for differential protein analysis with nominal p-values corrected by FDR[780].

Differential protein Post Translational Modification (PTM) Analysis

Modified peptides were binned into 9 PTM classes: Methylation, Carbamylation, Oxidation, Deamidation, Phosphorylation, Acetylation, Hydroxylation, Formylation and Myristoylation. Peptides were discarded if they were detected in only one replicates, PEAKS -log10P <15 or were not assigned a UNIPROT ID, leaving 21,032 PTMs assigned to 3,936 proteins (Figures 7.2.A-B). Limma was used for differential PTM analysis with nominal p-values corrected by FDR [780].

7.2.4 Pathway Enrichment Analysis

Pathway enrichment was carried our using the hypergeometric test (Equation 7.1) and curated Hallmarks Collection or KEGG gene sets[781][772].

$$P(X = k) = \frac{\binom{K}{k}\binom{N-K}{n-k}}{\binom{N}{n}} \tag{7.1}$$

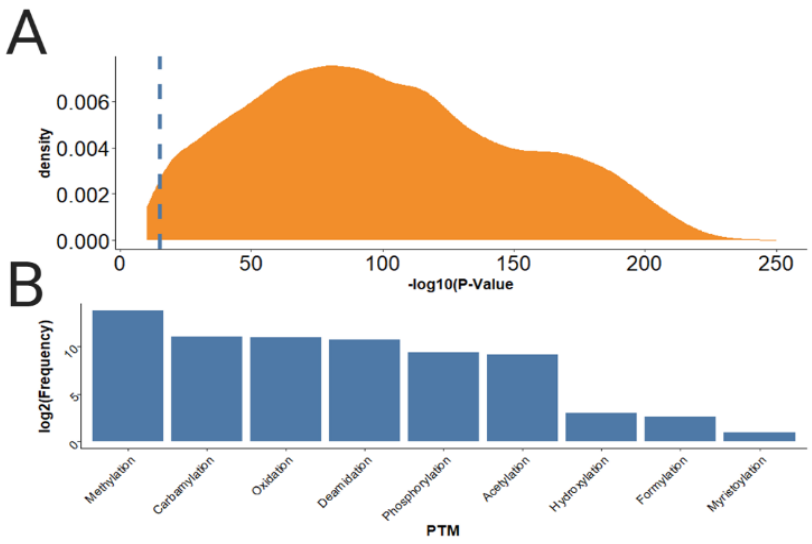


Figure 7.2: **A**) Density plot indicating the cutoff we applied for PTMs. We excluded PTMs with -log10P-value < 15. **B**) We binned PTMs into nine categories. The frequency of each category in the retained PTMs is indicated.

Where k=the number of overlapping genes, K=number of genes in the gene set, n=the number of input genes and N=number of background genes. Raw p-values were corrected by FDR with FDR-q value < 0.05 considered significant unless otherwise specified.

7.3 Data Mining

All datasets used in this thesis are listed in Supplementary Table C.16.

7.3.1 The Cancer Genome Atlas (TCGA)

Accessing the TCGA Data

TCGA data was accessed by the TCGAbiolinks package in RStudio using the GDCquery(), GDCdownload() and GDCprepare() functions[782]. We downloaded mutation data, copy number data in the form of GISTIC scores, mRNA expression data either as FPKM or RSEM, miRNA expression data and clinical data as a BCR Biotab[783]. Survival data was downloaded from the TCGA-CDR[784]. For instances where more than one sample was assigned to the same patient ID, we retained only the primary tumour sample.

TP53 Status Classification of TCGA Patients

We classified the TCGA patients based on the mutation status of TP53 and the GISTIC score of TP53 (Figure 7.3.A). Patients with any mutation within TP53 were classified as TP53-MUTANT. Samples with more than one TP53 mutation were classified as TP53-NF. TP53 mutant samples with TP53 GISTIC<0 were classified as TP53-NF. TP53-WT samples with GISTIC<0 were classified as TP53WT-LOSS. TP53-WT samples with GISTIC>=0, were classified as TP53WT-NOLOSS.

Therapy Response

Patients with complete or partial remission/response to radiotherapy or other first-line therapies were considered as responders and others were considered as non-responders.

Tumour Stage

Tumours with AJCC pathologic tumour stage of II or higher were considered as high stage with others as low stage.

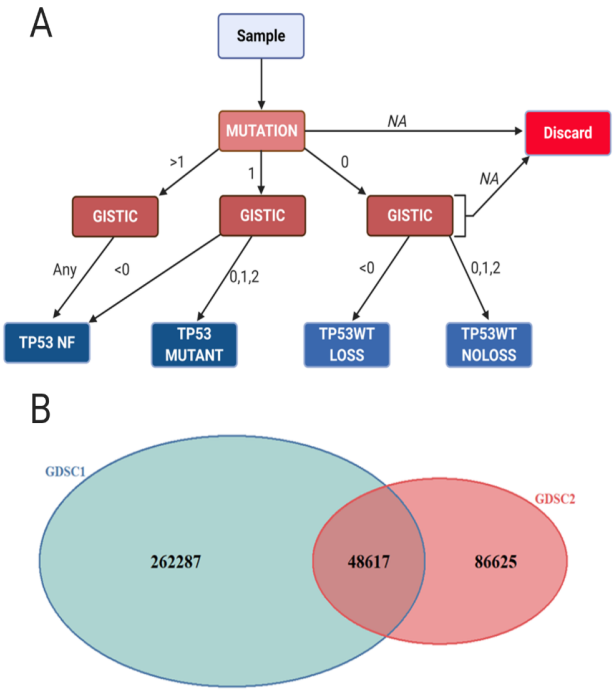


Figure 7.3: **A**) A flowchart to indicate how we binned TCGA samples based on TP53 status. **B**) We utilised both GDSC1 and GDSC2 in this thesis. This Venn diagram indicates the overlapping drug responses evaluated in each dataset.

Oncogenic mutations

KIT mutations were classified as oncogenic if identified to be likely pathogenic, predicted oncogenic or oncogenic by OncoKB. Mutations annotated as inconclusive or unknown were grouped as unknown and not considered in the analyses.

Genome Instability Measures

Aneuploidy and ploidy scores for TCGA samples were downloaded from[523]. Ploidy is the number of complete sets of chromosomes in a cell[785]. The aneuploidy score ranges from 0-39 and indicates the number of chromosome arm level events in the sample[523].

Genotype imputation for TCGA Patients

Genotype data was obtained and filtered as described in Carter et al (2017)[733]. Briefly, we obtained genotype calls from the Birdsuite-processed Affymetrix 6.0

SNP arrays for matched normal samples from the TCGA data portal (`https://gdc-portal.nci.nih.gov/`), set low confidence SNP calls to missing, filtered individuals and SNPs with < 95% call rate and SNPs with MAF < 1% and imputed untyped genotypes using the secure Michigan Imputation Server[786][787]. We used a PCA analysis over genotypes to remove samples that did not cluster tightly with Europeans from the HapMap III reference population. The genotype data of 7,021 TCGA patients were clustered tightly with Europeans.

7.3.2 Weighted Gene Co-expression Network Analysis

WGCNA aims to find clusters of highly correlated genes which can be summarised into a single eigengene (Additional Methods). The comprehensive WGCNA R package was used for this analysis (WGCNA_1.69 on RStudio running R version 4.0.2)[788][789].

For WGCNA, we downloaded mRNA expression (FPKM), mutation (muse, somaticsniper, varscan2 and mutect2), copy-number (GISTIC) and clinical data for the TCGA-TGCT cohort using the TCGAbiolinks package (2.16.1)[782]. Data was accessed on 17th July 2020. From a total of 156 samples, we removed secondary samples where the primary sample was available and excluded 2 samples with TP53 mutation, leaving 148 TP53WT samples. From a total of 56,493 genes, we included 14,002 genes with FPKM>1 (Figure 7.4.A). No samples were found to be outliers based on the expression data (Figure 7.4.B).

Networks were generated and analysed as outlined in the WGCNA R package tutorials, accessible at (`https://horvath.genetics.ucla.edu`)(Additional Methods).

Identifying Hub Genes

Hub genes were identified through expression correlation (Pearson's) and PPI (STRING.v.11 interaction scores). The degree of the gene ($D_{i=1}$) was defined as the sum of the correlation statistics or interaction scores (Equation 7.2)

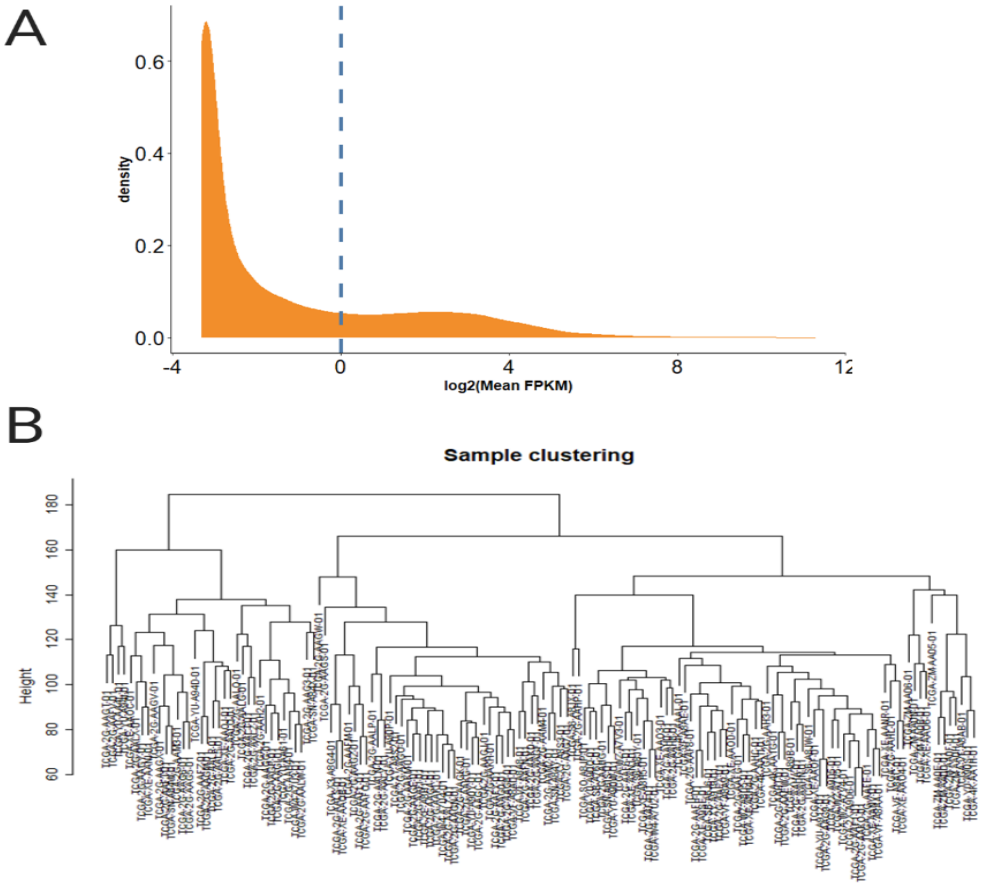


Figure 7.4: **A**) Density plot indicating the cutoff we applied for genes to use in the WGCNA analysis. We excluded genes with FPKM <1. **B**) We checked for sample outliers prior to WGCNA by applying hierarchical clustering based on the expression data for each samples. The dendrogram indicates no clear outliers.

$$D_{i=1} = \sum_{j=2}^{n} cor(x_{i=1}, x_{j=2}...n) \tag{7.2}$$

STRING scores >700/1000 with textmining disabled were considered [790]. Genes were ranked based on their degree calculated from Pearson's or interaction scores and those in the top quartile of both lists were designated hub genes.

7.3.3 Genomics of Drug Sensitivity in Cancer (GDSC)

Accessing GDSC Datasets

The Genomics of Drug Sensitivity in Cancer (GDSC) data was downloaded from `https://www.cancerrxgene.org/`[383]. Specifically, the following files were accessed. 'mutations_20191101', 'rnaseq_read_count_20191101' and

'cnv_gistic_20191101' detail the mutations, transcriptomic and copy number data respectively and were accessed 07/11/2019. 'GDSC1_fitted_dose_response_25Feb20' and 'GDSC2_fitted_dose_response_25Feb20' contain the cell line drug sensitivity data for the two separate experiments and were accessed 21/07/2020. GDSC1 utilised 987 cell lines, each treated with 367 compounds to measure a total of 310,904 IC50s. GDSC2 comprises 809 cell lines, treated with 198 compounds to give 135,242 IC50s. 48,617 IC50s overlap between the two datasets (Figure 7.3.B).

TP53 Status Classification of Cell Lines

Cell-lines were binned into four TP53 status groups based TP53 mutation and copy-number. Cell-lines with mutation and loss were classified as MUTLOSS. Cell-lines with only mutation as MUTANT, with only GISTIC<0 as LOSS and those with neither were classified as WT. Cell-lines without mutation or copy number data were discarded.

7.3.4 Gene Expression Omnibus

Microarray data for melanoma A375 cells treated with Nutlin-3a and p53 siRNA was downloaded from the Gene Expression Omnibus (GSE39091) using the getGEO() function from the GEOquery package. Cells were transfected with control or p53 siRNA, incubated for 48hrs and further incubated for 26hrs in the presence of 0.065% DMSO or 5uM Nutlin-3a.

7.3.5 GWAS Datasets

The data published by Watanabe *et al* comprises summary statistics from GWASes covering 551 traits with SNPs mapped to genes using a 1kb window either side [664].

Multi-cancer SNPs were identified using the GWAS catalog (Accessed August 2020). Cancer-SNPs were identfiied whereby the mapped trait featured at least one of the following keywords: cancer, carcinoma, glioma, melanoma, sarcoma, lymphoma, myeloma, neuroblastoma, germ cell, glioblastoma, meningioma, leukemia, tumour, tumor or adenoma. Similar and overlapping traits were grouped. SNPs in the GWAS catalog are mapped to genes using a 50kb window.

7.3.6 Druggable Genome

The list of druggable genes was downloaded from Finan et al (2017)[550].

7.3.7 STRING Protein-Protein Interactions

Protein-protein interactions (PPI) were accessed by downloading the '9606.protein.links.detailed.v11.0.txt.gz' file from STRING. The Combined Score was recalculated for each PPI without using textmining (Equation 7.3)[791].

$$CombinedScore = 1 - \Pi_i(1 - S_i) \tag{7.3}$$

7.4 Statistical Analyses

All statistical analyses were carried out in RStudio (R version 4.0.2) or GraphPad Prism (Version)[792]. All R packages are listed in Supplementary Table C.17. lm() was used for linear regression; glm() for logistic and poisson regressions; survfit() for Kaplain-Meier survival analyses, coxph() for Cox regression with cox.zph() used to check the proportional hazards assumption was met. Student T-Tests and Exact Fisher Tests were two-sided. For the time dependent area under the curve (tdAUC) analysis, a Cox regression model was fitted and used to predict events at different time points. The true positive rate and false positive rate were calculated for each time point and the AUC was determined. A paired T-test was used to determine significant differences between two models.

7.4.1 Machine Learning

We classified tumours into cancer-types based on the expression of p53 target genes using the Random Forests (RF) algorithm (Additional Methods). Cancer-types with at least 100 TP53WTNOLOSS and TP53MUTLOSS samples were used. Target genes which were expressed to a higher degree in TP53WTNOLOSS compared to TP53MUTLOSS tumours in at least one cancer-type were retained as predictors. K-fold cross validation was used to optimise the RF parameters.

7.5 Experimental Techniques

7.5.1 CRISPR-Cas9 Genome Editing

The Cas9 expression vector was obtained from Addgene (#62988). sgRNA oligos were designed and analysed using the CRISPR design tool (`http://crispr.mit.edu/`), and the ones with highest rating sores were selected. For the human U6 promoter-based transcription, a guanine (G) base was added to the 5? of the sgRNA when the 20bp guide sequence did not begin with G. The oligo sequences for the sgRNA synthesis are listed in Supplementary Table C.18. Annealed oligos were cloned into the BbsI restriction sites of the Cas9 expression vector. The donor construct pMK-RQ-HDR-donor for generating the p53-REs knock in clones was synthesized by GeneArt Gene Synthesis service and integrated into the G418 resistant vector pMK-RQ (ThermoFisher). The donor construct rs78378222-HDR-donor was generated for the homology directed repair (HDR) in Hap1 cells. For genomic deletions, $5x10^5$ cells were seeded in a 12-well plate and transfected with 0.5g of each sgRNA constructs. After 24 hours, cells were incubated in puromycin for 48 hours. A single-cell suspension was prepared and seeded in 96-well plate for 3-4 weeks. Individual colonies were selected, expanded for genotyped by PCR (Supplementary Table C.18). Edited clones were further confirmed by Sanger sequencing or TagMan genotyping, and the copy-number of the heterozygous knock-out cells was confirmed by TaqMan Copy Number Assays. For the knock-in, cells were transfected with a guide RNA (Supplementary Table C.18) together with a recombination donor flanked with 1-kb right and left homology arms where the PAM site was mutated to prevent donor DNA cleavage (a point mutation from CCA to GCA). Transfected cells were selected by treatment with puromycin and G418 for 48 hours. Edited clones were validated as for genomic deletion. For experiments utilising multiple clones (e.g. QRT-PCR), the number of separate clones used is indicated by the 'n' value in the figure and figure legend.

7.5.2 Cell culture and their treatments

The cell-lines and culture methods used in this study are detailed in Supplementary Table C.19. FuGENE 6 Transfection Reagent (Promega) and DharmaFECT 1 (Horizon Discovery Ltd) were used for DNA and siRNA transfection respectivley. Compounds used in this work are detailed in Supplementary Table C.20.

7.5.3 Drug screening

Cells were seeded in 384-well plates (black with flat, clear bottom, Greiner) at density of about 2,000 cells per well in 81ul with cell dispenser (FlexDrop, PerkinElmer) and liquid handling robotics (JANUS, PerkinElmer) and incubated overnight. Library compounds (Supplementary Table C.3) were added to a final concentration of 10uM, 1uM, 100nM or 10nM. Dasatinib (1uM) was added as positive control and DMSO (Vehicle, 0.1%) was added as negative control. After 72 hours, cells were fixed with 4% paraformaldehyde for 10 min, permeabilized with 0.5% Triton X-100 for 5 min, stained with 1:1000 dilution of 5mg/ml DAPI for 5 min, imaged using a high-content analysis system (Operetta, PerkinElmer) and analysed using appropriate software (Columbus, PerkinElmer). The cells with nuclear area>150 and nuclear intensity<700 were counted, and cell number was used as the viability readout. The screen was performed in duplicate. The Pearson Correlation Coefficient, a measurement for inter-assay variability, averaged 0.98 and an average Z-factor, a measure employed in high-throughput screens to measure effect size, of 0.69 for all plates was recorded, leading to high confidence in the primary screen positive hits.

7.5.4 IC50 and combination index CI analyses

To determine an IC50, 8 multiply diluted concentrations were used including a PBS control for 48hour treatment and then cell viability was assessed by MTT assay. The IC50 was calculated using Graphpad Prism software. For Doxorubicin, Topotecan, Etoposide and CPT, a concentration range of 0.03125uM to 2uM was used unless otherwise stated. For Pazopanib and Imatinib, a concentration range from 0.766uM to 50uM was used. For all other compounds a range from 0.3125uM to 20uM

was used unless otherwise stated. A constant ratio matrix approach was used to determine the combination index (CI) values[793]. Single drug data and combination data was entered into Compusyn software (`http://www.combosyn.com`) to compute CI (Equation 7.4) and dose-reduction index (DRI). The CI50 values quantitatively depict synergistic (CI<1), additive (CI=1), and antagonistic effects (CI>1). For each experiment, measurements were made in triplicate (three technical replicates). Each experiment was repeated for at least three biological replicates.

$$CI = \frac{(D_1)}{(D_{50})_1} + \frac{(D_2)}{(D_{50})_2} \tag{7.4}$$

7.5.5 In vivo study

All animal procedures were carried out under a Home Office licence (PPL30/3395), and mice were housed at Oxford University Biomedical Services, UK. 6-8 week-old female BALB/c nude mice (Charles River, UK) were injected subcutaneously with $5x10^6$ 2102EP cells in a 1:1 mixture of serum-free medium and Matrigel. When the average tumor volume reached approximately 130mm3, animals were divided into four groups (6 per group) and received the following treatments: 1. Vehicle group: p.o. vehicle A (2% DMSO/ 30% PEG300/ dH2O) on day 1-5 and day 8-12, once daily; i.p. vehicle B (saline) on day 1, 8 and 12, once daily; 2. Doxorubicin group: i.p. Doxorubicin 4mg/kg (Sigma) in vehicle B on day 1, 8 and 12, once daily; 3. Dasatinib group: p.o. Dasatinib 25mg/kg (Selleckchem) in vehicle A on day 1-5 and day 8-12, once daily; 4. Combination group: p.o. Dasatinib 25mg/kg on day 1-5 and day 8-12, once daily; i.p. Doxorubicin 4mg/ kg 1h after Dasatinib dosing on day 1, 8 and 12, once daily. Mouse weights and tumor volumes were measured 3 times per week. All mice were sacrificed on day 12, 2h after final treatments.

7.5.6 SDS-PAGE and western blotting

SDS-PAGE and western blotting was performed as described in[794]. The antibodies against p53 (DO-1), c-KIT (E-1), PARP1 (H-250), and ?-Actin (C4) were from Santa Cruz (Dallas, TX, USA). The antibodies against acetylated p53

(K382), phosphorylated p53 (S392) and cleaved Caspase 3 (Asp175) were from Cell Signalling (Danvers, MA, USA). HRP-coupled secondary antibodies were from Dako (Darmstadt, Germany).

7.5.7 RNA isolation, cDNA synthesis and qRT-PCR

Cells were lysed and total RNA was prepared using the RNeasy kit (Qiagen) according to the manufacturer's protocol. cDNA was synthesized using First Strand cDNA Synthesis Kit (Life Technologies, K1612) with oligo-dT primers (Life Technologies). Quantitative real-time reverse transcription PCR (qRT-PCR) was carried out in triplicate with Fast SYBR Green Master Mix (Life Technologies, 4385616) on an ABI StepOnePlus System (Applied Biosciences). The transcript levels were normalised against GAPDH.

7.5.8 MTT assay

MTT (3-(4,5-Dimethylthiazol-2-yl)-2,5-Diphenyltetrazolium Bromide) (ThermoFisher) was dissolved in PBS and added to the cells to a final concentration of 0.75 mg/ml for 4h. Thereafter, the medium was aspirated. The formazan salt was solubilised in isopropanol and measured at 570 nm using an ELISA reader.

7.5.9 Cell proliferation and migration

The proliferation and migration rates of the cells were determined by using the xCELLigence system[795]. For cell proliferation, 3,000 cells were seeded in the 16-well E-Plate incorporated with sensor electrode arrays, and the cell index, which is an impedance-based readout of cell numbers, was continuously monitored for 150 hours. For cell migration, 30,000 cells were seeded in the 16-well CIM-Plate with a lower chamber and upper chamber. The upper chamber contains a microporous membrane (8μm pore diameter) with electrode arrays on the bottom side. The real-time cell index readouts were monitored for 35 hours. Three biological replicates were carried out for each condition.

7.5.10 Phospho-kinase assay

The expression of 43 phosphorylation sites was determined using the Proteome Profiler Human Phospho-Kinase Array Kit (R&D Systems, ARY003B) by following the manufacturers instructions. Briefly, the antibody membranes were blocked for 1hr at RT (Array Buffer 1) and then incubated in lysate overnight at $2 - 8°C$ with rocking. Membranes were washed and incubated in Antibody Cocktail for 2hrs at RT with rocking. Membranes were washed and incubated in Streptavidin-HRP for 30min at RT with rocking. Membranes were washed, activated with the Chemi Reagent Mix and exposed to x-ray film. The pixel density of the dots was quantified using imageJ (1.52a)[796].

Appendices

A

Supplementary Figures

Contents

A.1 The p53/KITLG/KIT axis promotes cell survival in TGCT and represents a therapeutic opportunity for a repurposed combination strategy 274

A.2 Investigating the mechanism of the synergy between inhibition of the p53/KITLG/KIT axis and p53 activation in TGCT 276

A.3 Identifying novel, druggable negative-feedback loops in the p53 network 278

A.4 A highly pleiotropic cancer-risk SNP in the p53 pathway could have clinical impact for multiple cancer types 288

A.5 Materials and Methods 291

This section of the Appendix includes Figures which relate to the main text and are referred to in the main text.

A.1 The p53/KITLG/KIT axis promotes cell survival in TGCT and represents a therapeutic opportunity for a repurposed combination strategy

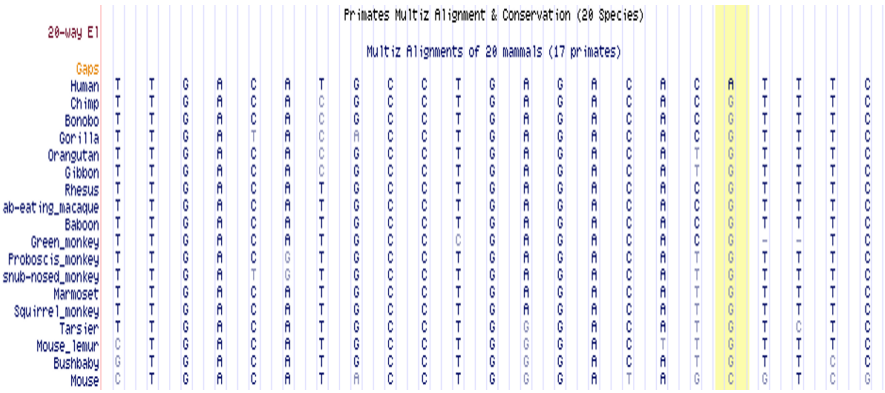


Figure A.1: Alignment of the KITLG p53RE sequence across 17 primates and mouse. The sequence is highly conserved among the primates but the mouse shows multiples substitutions at this locus. Sequences were aligned using the UCSC Genome Browser. The site of the SNP is highlighted in green.

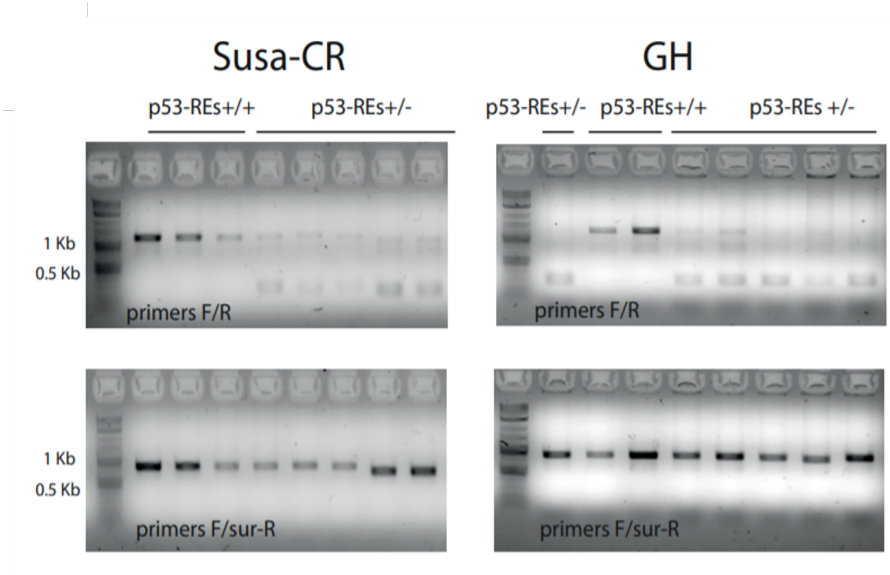


Figure A.2: CRISPR-Cas9 editing was used to delete the KITLG p53RE region in two cell lines heterozygous for the KITLG p53RE SNP, GH and Susa-CR. Heterozygous -/+ were identified by PCR using the same primer pairs as previously described. The F/R primers produce a band approximately 1KB for unedited +/+ cells. -/- cells produce only the small band for the F/R primers while heterozygous knock-outs (-/+) show both a small and 1KB band. The F/sur-R primers amplify a region within the 1KB region targeted by the CRISPR-Cas9 construct and so all cells which are +/+ or -/+ produce a band. The retained allele was determined by Sanger sequencing.

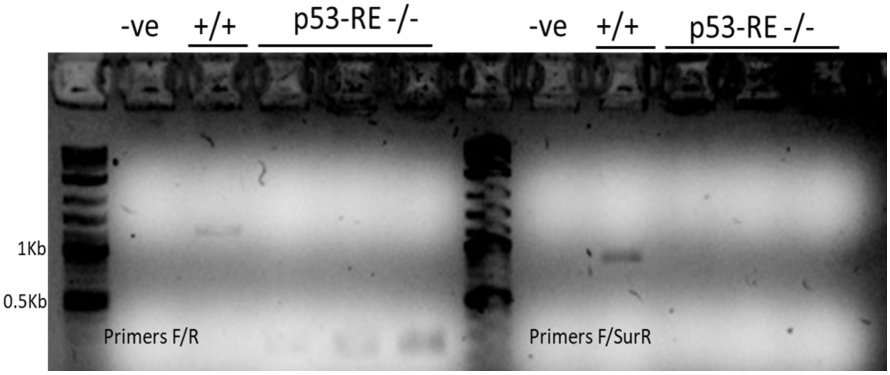


Figure A.3: CRISPR-Cas9 editing was used to delete the KITLG p53RE region in the intrinsically platinum-resistant cell-line, 2102EP. Homozygous knock-outs (-/-) were identified by PCR using the same primer pairs as previously described. The F/R primers produce a band approximately 1KB for unedited +/+ cells. -/- cells produce only the small band for the F/R primers. The F/sur-R primers amplify a region within the 1KB region targeted by the CRISPR-Cas9 construct and so all cells which are +/+ produce a band while -/- cells do not.

A.2 Investigating the mechanism of the synergy between inhibition of the p53/KITLG/KIT axis and p53 activation in TGCT

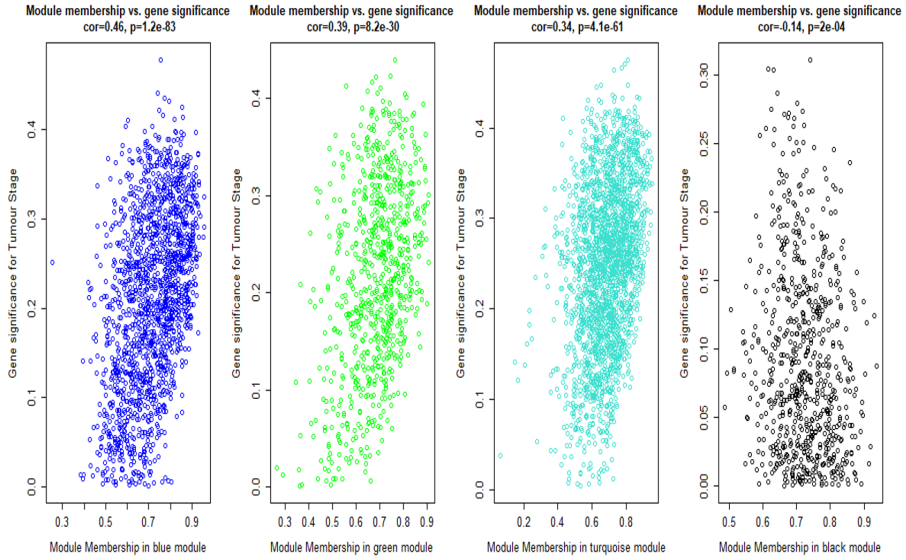


Figure A.4: Each gene is given a Gene Significance (GS) and Module Membership (MM) value. The GS indicates the correlation between a gene a trait of interest, in this case it is tumour stage. The MM indicates the correlation between the module eigengene and the real gene. It is expected that the genes with high MM for a module associated with a trait, should also have a high GS for that trait. This is clear from the scatter plots whereby GS and MM show strong correlation for Blue, Green and Turquoise but not for Black.

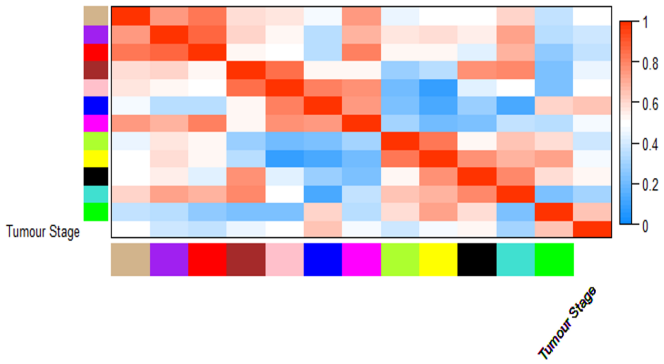


Figure A.5: Focusing on the tumour stage trait, this heatmap exhibits the adjacency measures between each gene module and with Tumour Stage. Adjacency is measured from 0-1 with values closer to 1 indicating high adjacency. The highest adjacency for Tumour stage is for Blue and Green.

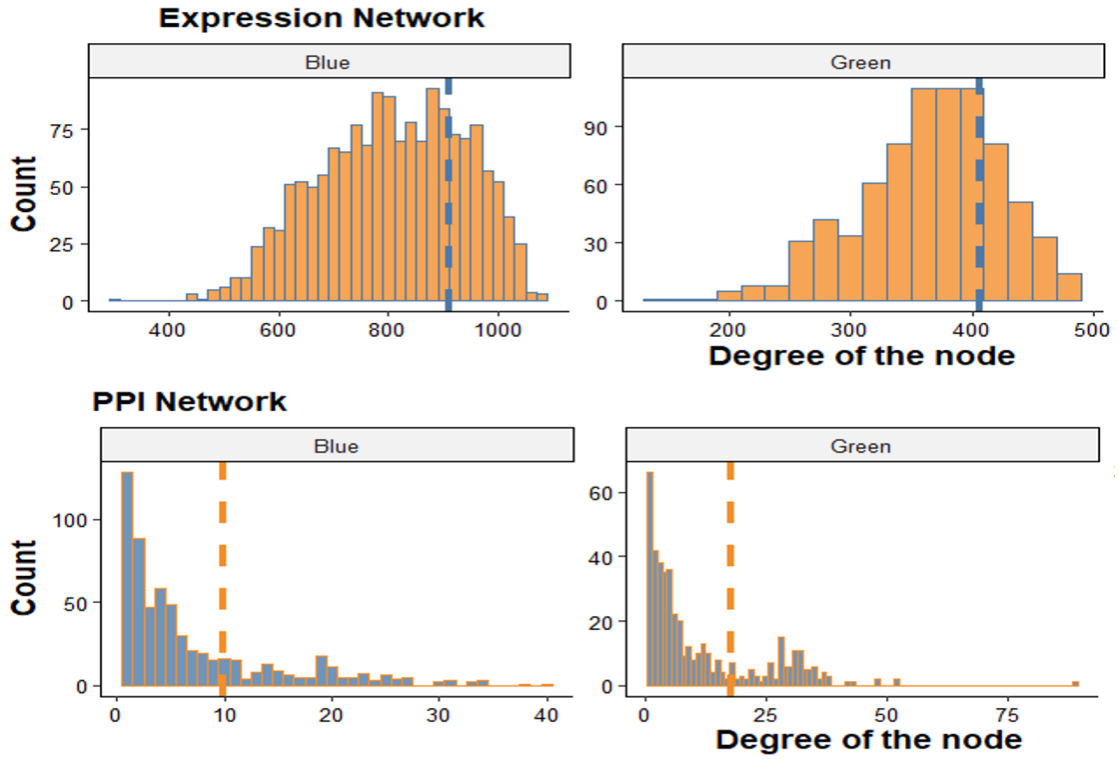


Figure A.6: We determined Hub genes for each module by two methods. Firstly, we determined hub genes by expression correlation. The degree of each gene was determined by summing the correlation statistic with all genes in the module (top row) and taking the top quartile. Secondly, we found the degree of each gene based on protein-protein interactions downloaded from STRING and overlapped the 25% with the genes from the expression analysis. Hub genes were defined as genes common to both lists.

A.3 Identifying novel, druggable negative-feedback loops in the p53 network

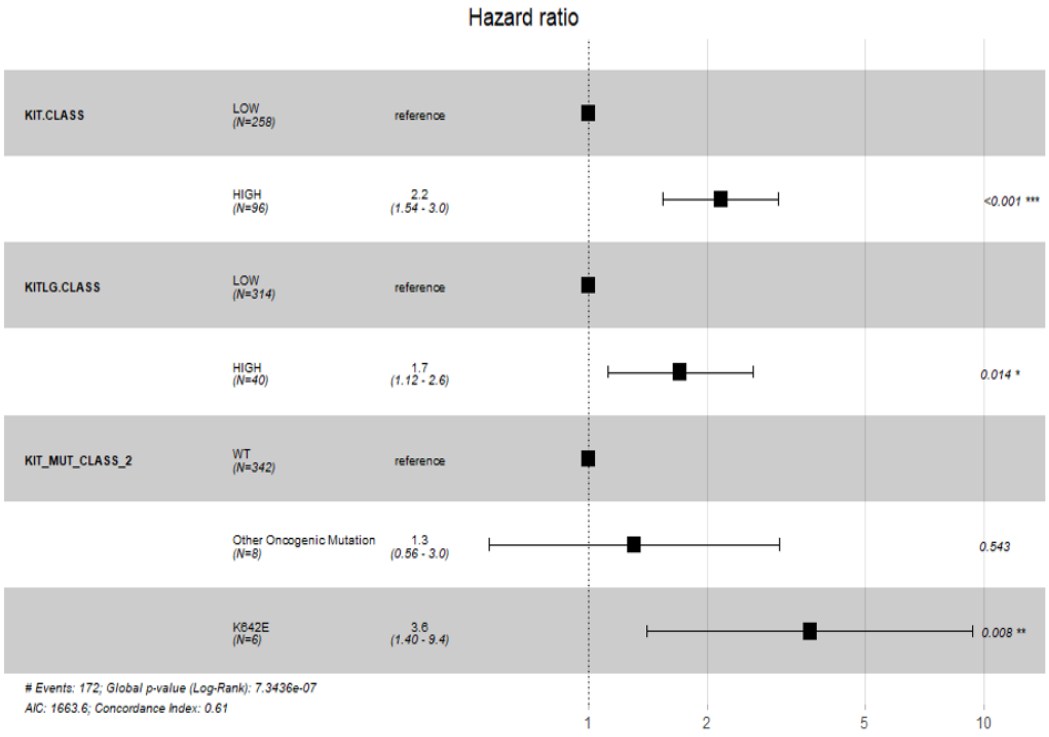


Figure A.7: Forest plot indicating the results of a multivariate Cox regression model estimating the effects of High KIT, high KITLG and KIT mutation on overall survival of TP53 WT SKCM. KIT and KITLG expression was separated into low and high using the surv_cutpoint function.

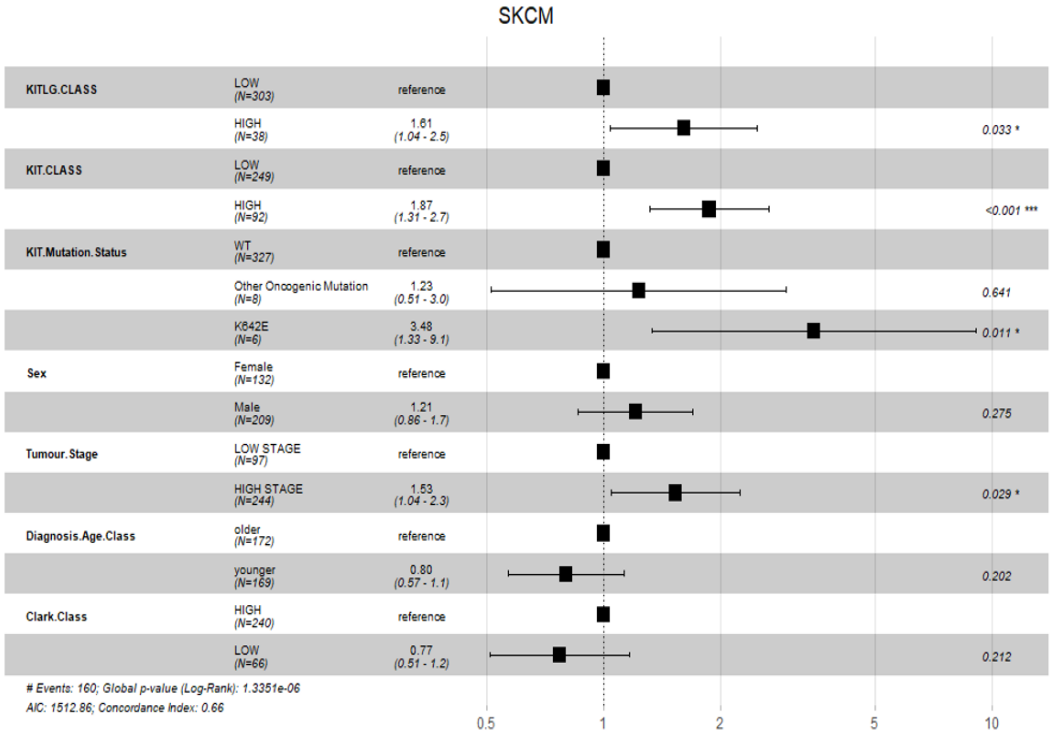


Figure A.8: Forest plot indicating the results of a multivariate Cox regression model estimating the effects of High KIT, high KITLG and KIT mutation on overall survival of TP53 WT SKCM with clinical prognostic factors included. Tumour stage, Diagnosis Age and Clark Level were binned into high and low classes (Materials and Methods).

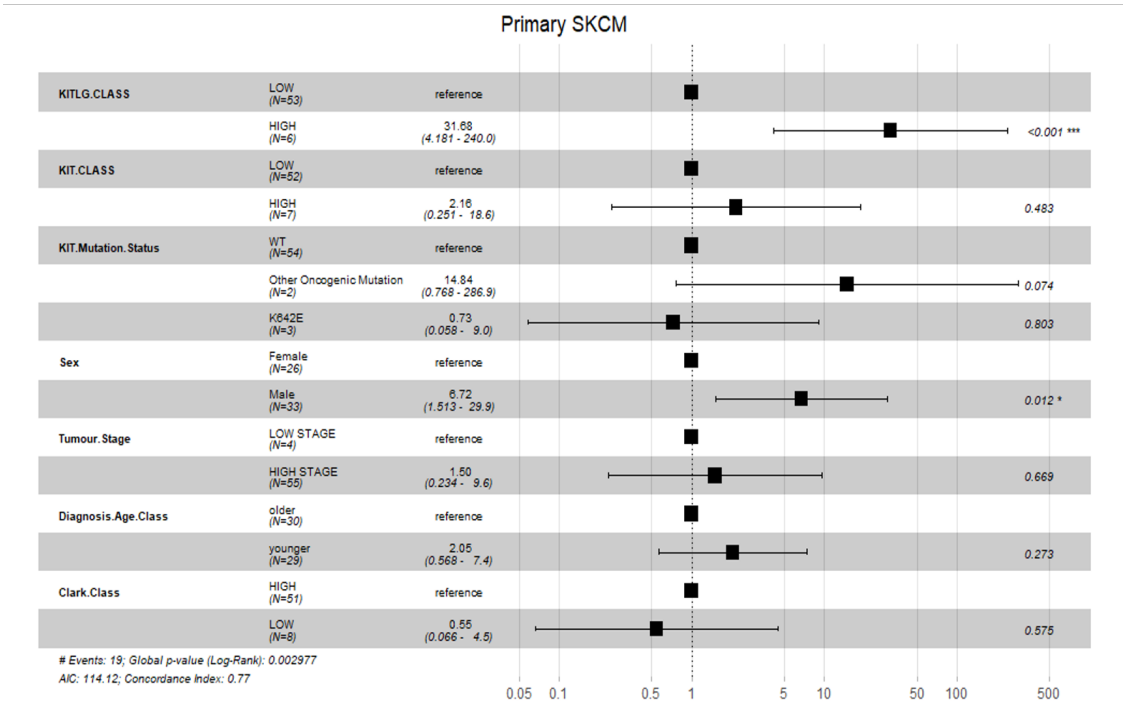


Figure A.9: Forest plot indicating the effect of KITLG expression, KIT expression and KIT mutation on Overall Survival in primary SKCM samples which are TP53WT. Expression of KITLG and KIT were split into high and low using the surv_cutpoint function. Tumour stage, Diagnosis Age and Clark Level were binned into high and low classes (Materials and Methods).

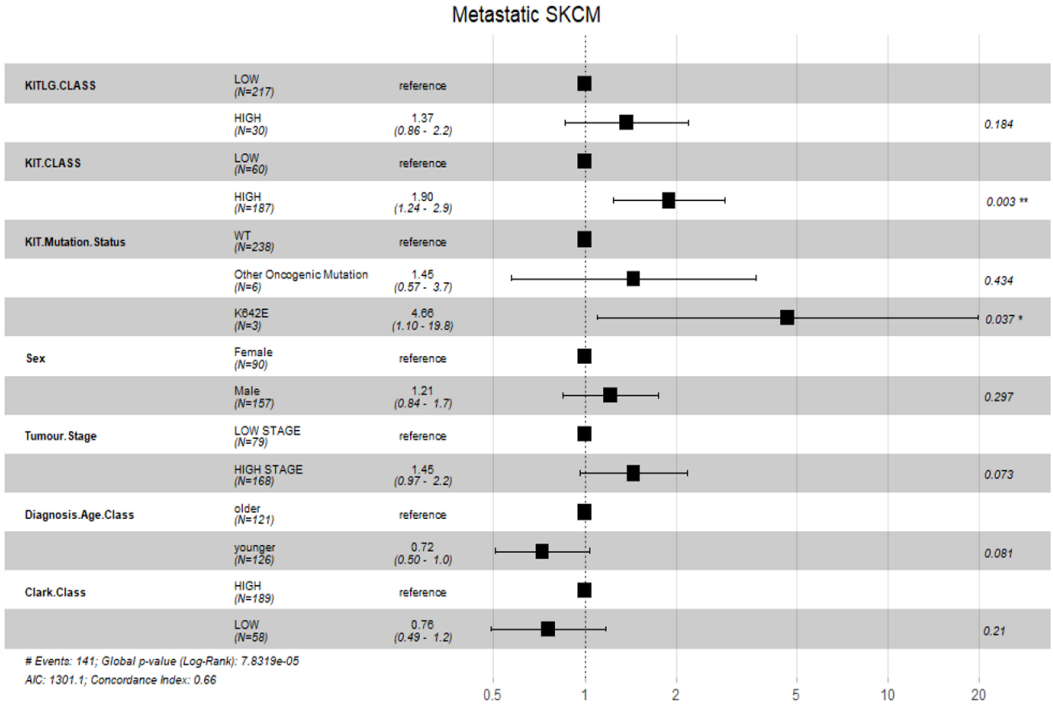


Figure A.10: Forest plot indicating the effect of KITLG expression, KIT expression and KIT mutation on Overall Survival in metastatic SKCM samples which are TP53WT. Expression of KITLG and KIT were split into high and low using the surv_cutpoint function. Tumour stage, Diagnosis Age and Clark Level were binned into high and low classes (Materials and Methods).

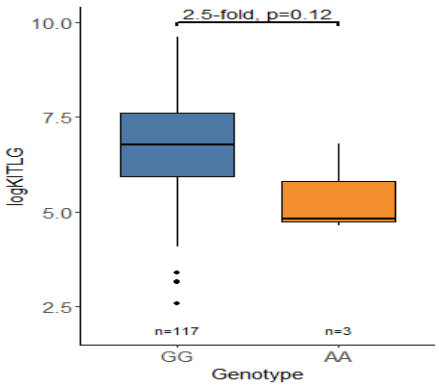


Figure A.11: Of the 179 TP53WT melanomas with germline data, we idnentified 3 tumours to be homozygous for the minor allele of the KITLG-p53RE-SNP (AA, reduced p53 binding) and 117 homozygous for the risk allele (GG, increased p53 binding). The 3 AA tumours exhibit a clear, but non-significant trend towards reduced KITLG expression (linear regression).

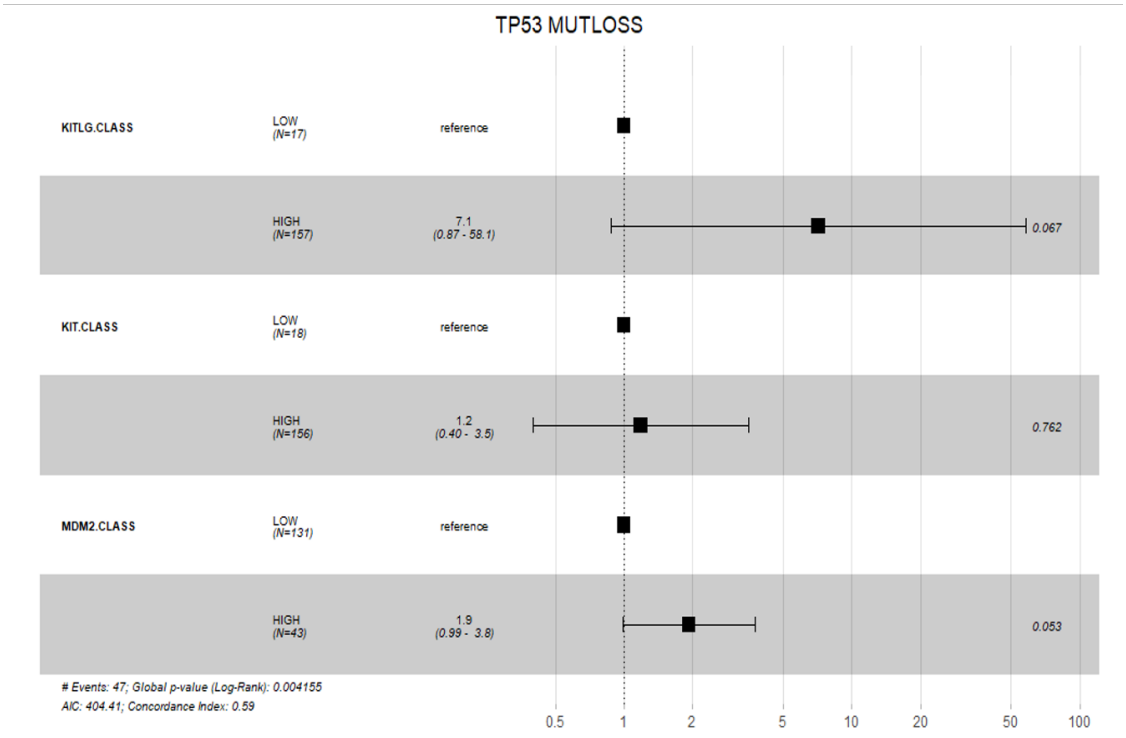


Figure A.12: Forest plot indicating the output of a Cox regression model in TP53 NF COAD with Overall Survival as the dependent variable and KITLG, KIT and MDM2 expression as the independent variables. The expression values were split into high and low using surv_cutpoint.

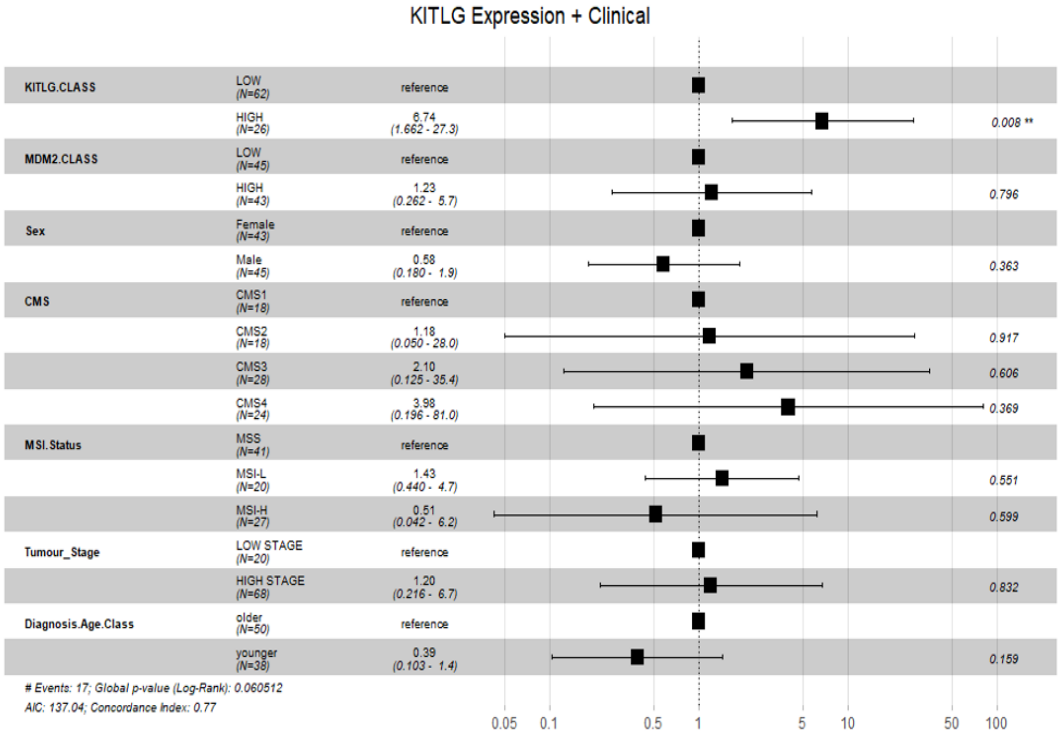


Figure A.13: Forest plot representing the output of a multivariate Cox regression model estimating the effect of KITLG expression on overall survival of TP53 WT NOLOSS and BRAF WT COAD patients while adjusting for MDM2 expression and clinical prognostic factors. The expression values were split into high and low using surv_cutpoint. Consensus Molecular Subtypes (CMS) were provided by a collaborator (Materials and Methods). MSI status was downloaded via TCGAbiolinks. Tumour stage and Diagnosis Age were binned into high and low classes.

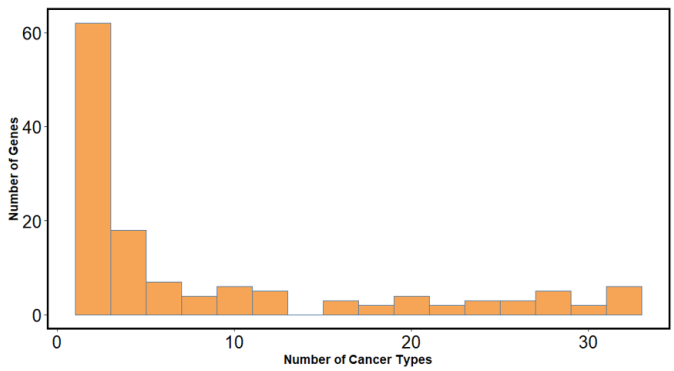


Figure A.14: The 340 p53 target genes were ranked in descending order by expression in each cancer type. The number of times each gene appeared in the top 10% of the list was found (max = 33). The bars of the histogram indicate the number of genes found for each number of cancer types. Bin width is 2.

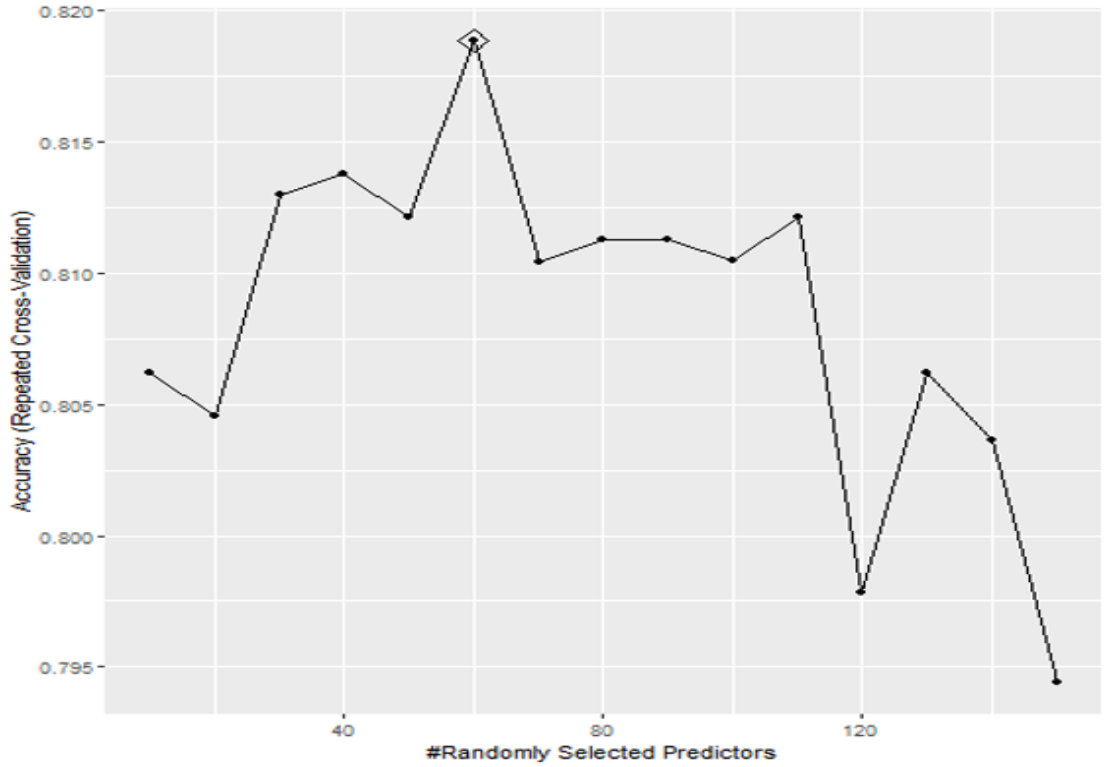


Figure A.15: The value of *mtry* indicates how many predictors should be considered at each split point in a decision tree. The optimal value of *mtry* was determined by repeated k-fold cross-validation with 2 repeats and 5 folds. Values of *mtry* from 10 to 150 were estimated with the optimal value found to be 60.

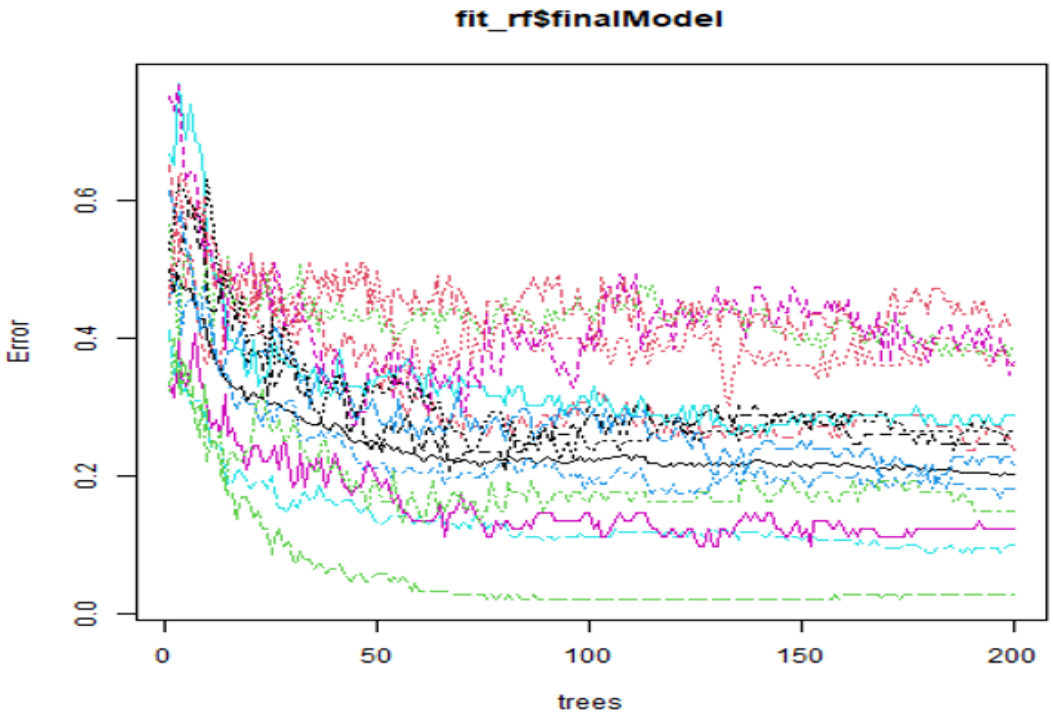


Figure A.16: The error for each class is plotted against tree number. The final model averages across all 200 trees.

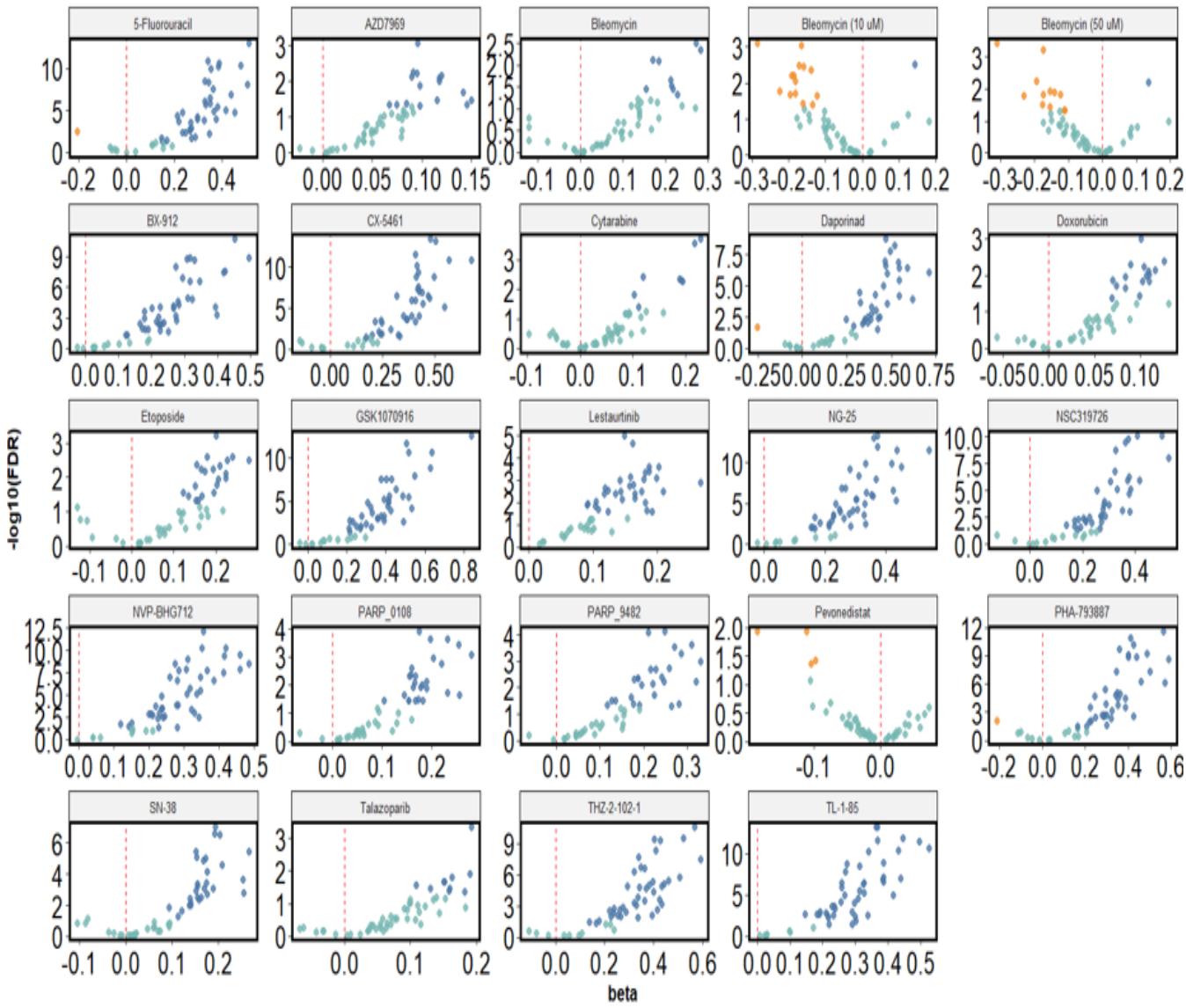


Figure A.17: Scatter plots for each of the 25 additional p53 dependent drugs in Table C.11. Each dot is one of the 51 Nutlin-3a inhibitor genes. Purple dots are those which are significant inhibitors of the indicated compound. Orange dots indicate significant activators. Significance was tested by linear regression and raw p values corrected for 1275 tests by FDR.

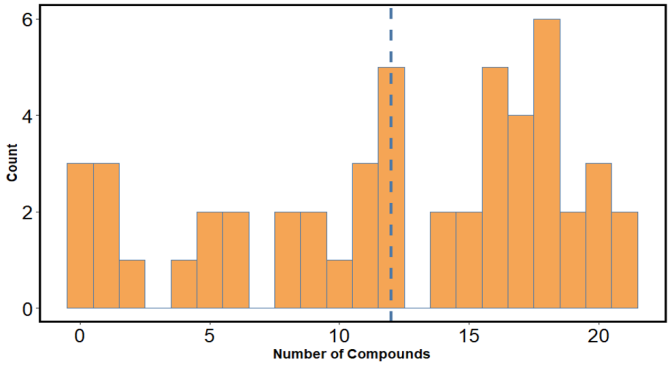


Figure A.18: A histogram indicating the number of Nutlin-3a inhibitor genes which are found to also be inhibitors of the given number of TP53 dependent compounds. Bin size = 1. The vertical dashed line indicates the 12th bin. We focused on the genes which were found to be inhibitors of at least 12 TP53 dependent compounds.

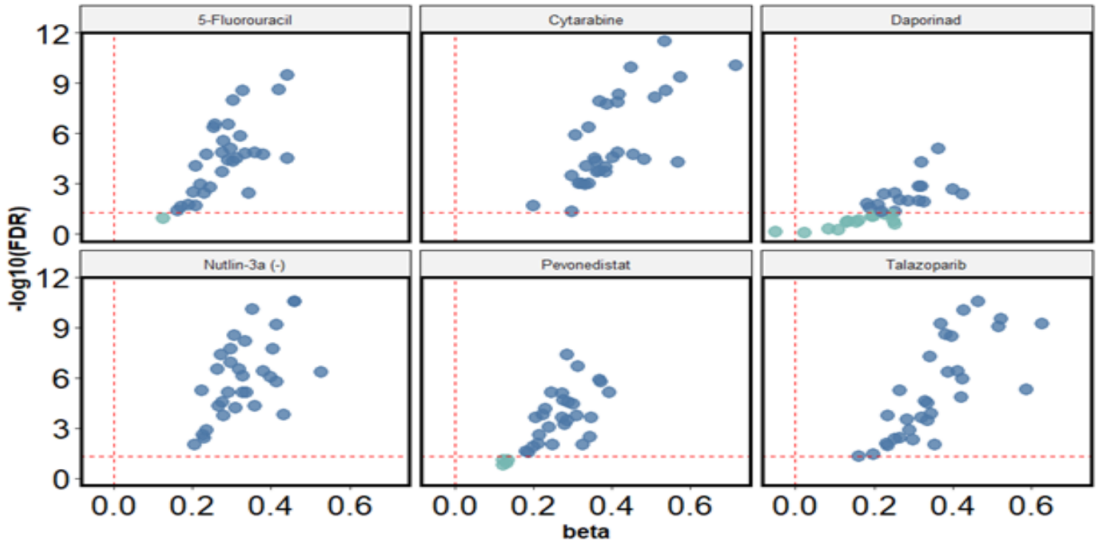


Figure A.19: 6 of the TP53 dependent compounds were also tested in GDSC2. Linear regression was used to determine the relationship between 34 inhibitor genes and the 6 compounds. Raw pvalues were corrected for 186 tests by FDR. Purple dots indicate significant inhibition..

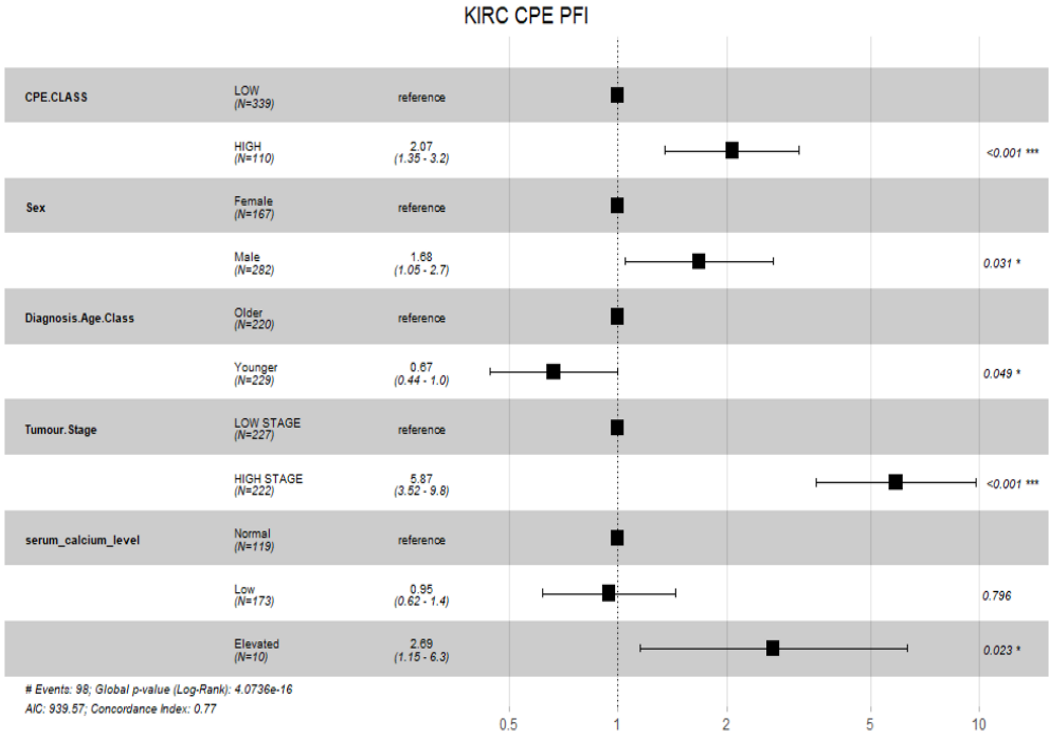


Figure A.20: Forest plot indicating that high CPE expression associates with shorter PFI in TP53WT-NOLOSS KIRC in a multivariate including clinical factors: Sex, age at diagnosis, tumour stage and serum calcium levels.

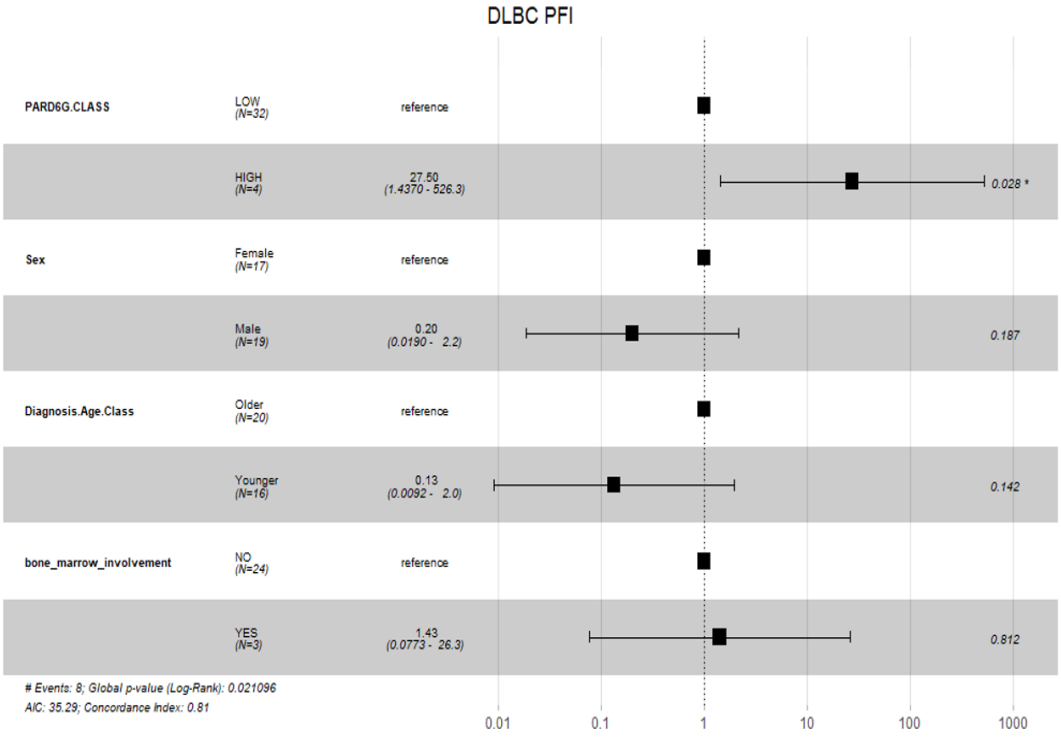


Figure A.21: Forest plot indicating that high PARD6G expression associates with shorter OS in TP53WT-NOLOSS DLBC in a multivariate including clinical factors: Sex, age at diagnosis and bone marrow involvement.

A.4 A highly pleiotropic cancer-risk SNP in the p53 pathway could have clinical impact for multiple cancer types

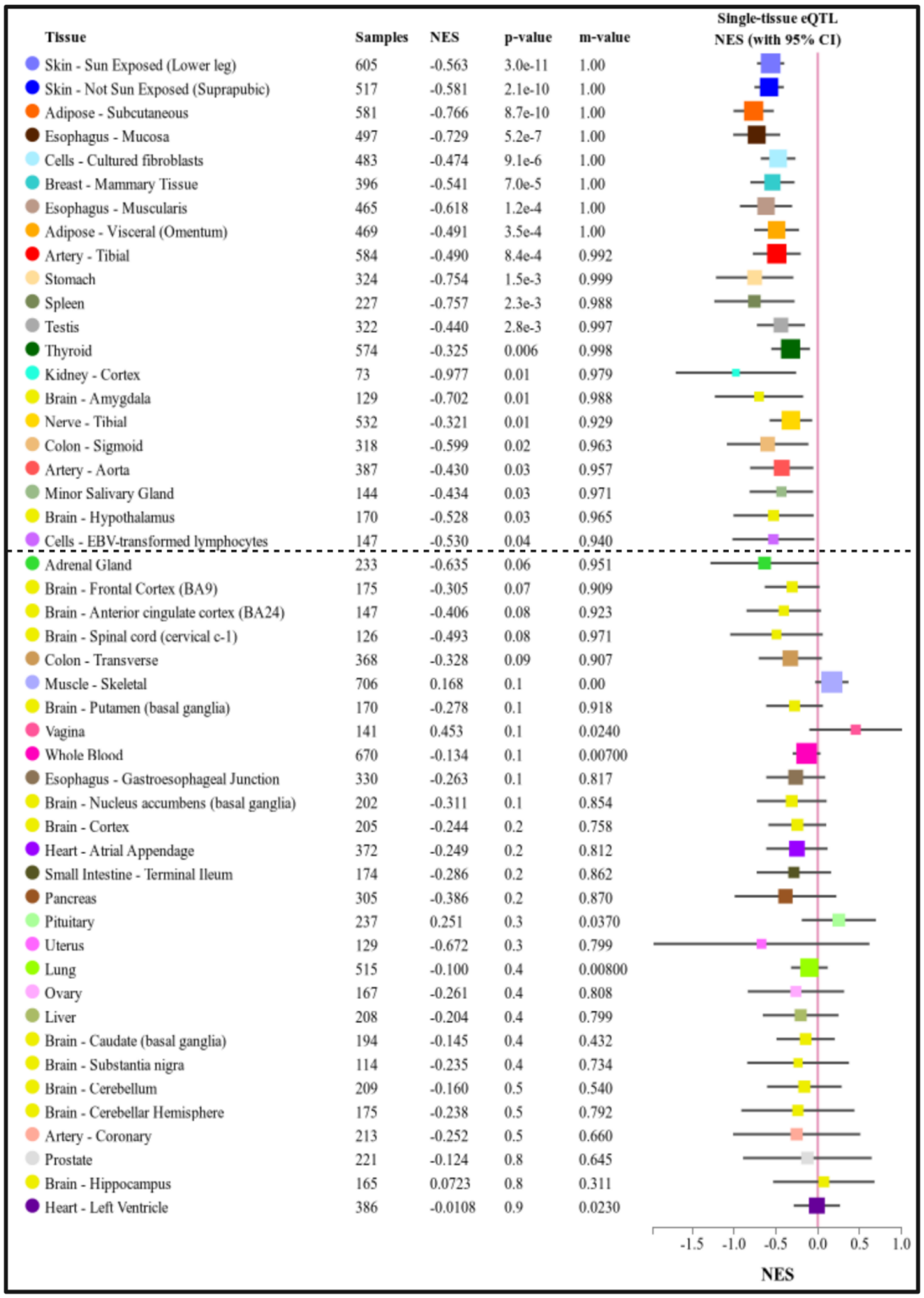


Figure A.22: The TP53-PAS-SNP has been shown to be an eQTL for p53 mRNA expression in multiple normal tissues. Data is obtained from GTEx. A negative normalised expression score (NES) indicates lower expression associated with the minor allele of the TP53-PAS-SNP.

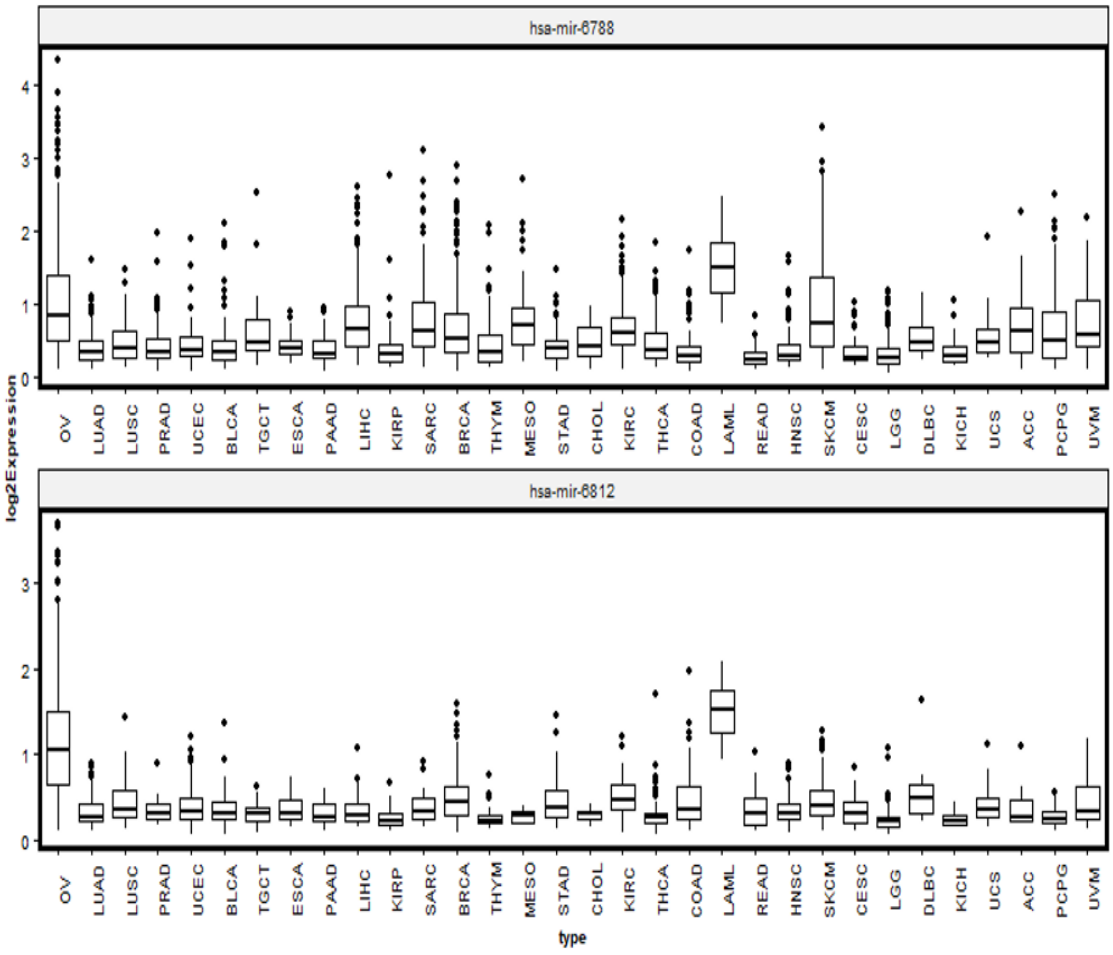


Figure A.23: The log2 transformed expression of miR-6788 and miR-6812 for each cancer type in the TCGA cohort. Both miRNAs were found to be expressed to some degree in all cancer-types.

A.5 Materials and Methods

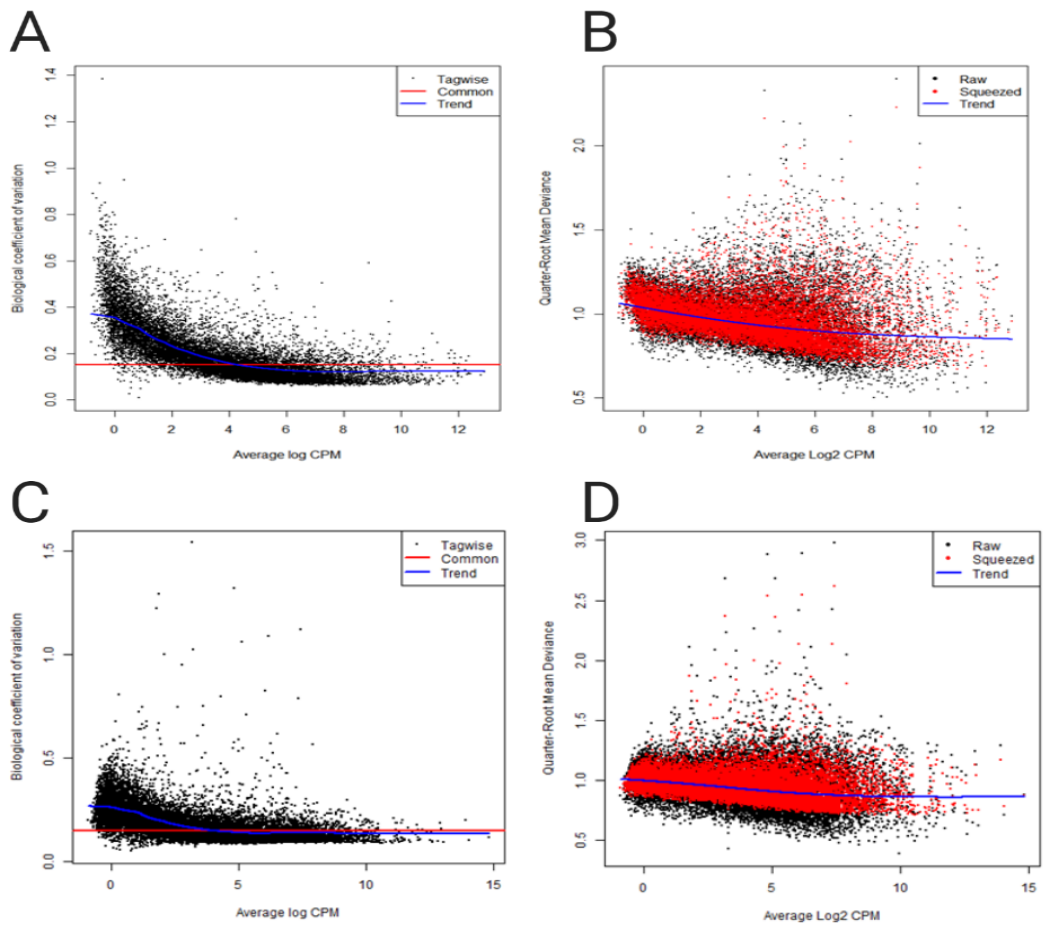


Figure A.24: **A**) BCV plot for the TERA1 RNA-seq dataset after fitting the negative binomial model. **B**) Estimates of the deviation for each gene of the TERA1 RNA-seq dataset after squeezing the estimates by applying the quasi-likelihood model. **C**) BCV plot for the HAP1 RNA-seq dataset after fitting the negative binomial model. **D**) Estimates of the deviation for each gene of the HAP1 RNA-seq dataset after squeezing the estimates by applying the quasi-likelihood model.

B

Supplementary Methods

B.1 RNA-sequencing

B.1.1 Overview of methodology

High-throughput transcriptomics is now a readily available technology which allows researchers to interrogate gene expression with an unbiased and hypothesis-free approach. We used 3' RNA-seq which is an alternative to whole transcript sequencing; this method is better able to detect shorter transcripts and is not biased towards transcript length but generally detects fewer differentially expressed genes[797]. In this method, cDNA is transcribed only from the 3' end of the mRNA with one cDNA molecule synthesised for each mRNA transcript. This is unlike other traditional methods whereby the entire mRNA transcript is fragmented, reverse transcribed, and then pieced back together. However, due to the high-throughput nature of the approach, tens of thousands of different transcripts can be detected, meaning the data is hugely multi-dimensional. This poses statistical challenges such as distinguishing between biological and technical variation and addressing the problem of multiple hypothesis testing (MHT). We used the purpose-built edgeR package to analyse the data while addressing this problems.

B.1.2 Additional details regarding differential gene analysis

Lowly expressed genes were removed using the filterByExpr function from the edgeR package. Lowly expressed transcripts are unlikely to be translated and be biologically important while it confers greater statistical power to downstream analyses by reducing the number of tests executed[798]. Following filtering, the libraries were normalised for composition bias by the Trimmed Mean of M values (TMM) method using the calcNormFactors function[799]. Low normalisation factors (below 1) indicate that a sample might contain some very highly upregulated genes which mean other genes are inferred to be more lowly expressed for the given library size. These normalisation factors are used to generate effective library sizes. A negative binomial distribution is used by edgeR to model the expression of each gene (g) in each sample (i) (Equation B.1)[777][800].

$$Y_{gi}\ NB(M_i p_{gj}, \phi_g \tag{B.1}$$

Here, NB refers to the negative binomial parametrisation, M_i is the library size of sample i, ϕ_g is the dispersion and p_{gj} is the relative abundance of gene g in sample i of treatment group j. The NB distribution improves upon the use of simple t-tests to discern differential expression as, unlike the t-distribution, it can more accurately model transcripts with low counts and can account for variation between biological replicates. The estimates of biological variation (BCV) from the NB approach, for both the TERA1 and Hap1 RNA-seq experiments are shown in Figures A.24.A,C. The NB approach can be further improved by quasi-likelihood (QL) methods which account for gene-specific variability between factors and between replicates (Equation B.3).

$$var(y_{gi}) = \sigma_g^2(\mu_{gi} + \mu_{gi}^2\phi) \tag{B.2}$$

Here, y_{gi} is the read count for gene g in sample i and μ_{gi} is the expected count given the sequencing depth and treatments. ϕ is the NB dispersion parameter and σ_g^2 is the QL dispersion. The NB part of this model estimates the overall biological

variation across all genes between samples while the QL estimates gene-specific effects over the overall level. To overcome the fact that most RNA-seq experiments have low numbers of replicates (3 in our case), an empirical Bayes approach is used to squeeze the QL dispersions towards a mean-dependent trend. The empirical Bayes moderated values are used for further analysis. This strategy reduces uncertainty and improves power. The squeezed QL values for our TERA1 and Hap1 data-sets were generated with the glmQLFit() function and are shown in Figures A.24.B,D [801]. Differential expressed genes were found by the glmQLFTest() function with the FDR used to account for multiple hypothesis testing.

For complex analyses involving multiple factors, we used the generalised linear model (GLM) approach which is available through edgeR (Equation B.3) [801].

$$log(\mu_{gi}) = x_{i1}\beta_{g1} + x_{i2}\beta_{g2} + ... + x_{in}\beta_{gn} + O_i \tag{B.3}$$

Here, there are n number coefficients (j) and β_{ij} indicates the effect of that factor (e.g. Nutlin-3a treatment) on expression of gene g. x_{ij} is the sample-specific predictor for coefficient j and O_i is the sample-specific offset.

B.2 WGCNA

B.2.1 Network Construction

The premise of WGCNA is to construct an adjacency matrix (a_{ij}) whereby each element represents the adjacency between two nodes (genes) in the network. The adjacency value lies between 0 and 1 whereby 0 represents unconnected nodes and 1 fully connected. The adjacency values are derived from the Pearson's correlation statistic between the two nodes, raised to the power of the soft-thresholding power (β, Equation B.4). The higher the value of β, the greater the degree to which small correlations are suppressed in the network.

$$a_{ij} = [cor(x_i, x_j)]^{\beta} \tag{B.4}$$

There are multiple options for considering correlation in biological networks. Unsigned networks are where correlation is considered as a connection between

two nodes, regardless of directionality. However, a signed network preserves the directionality of the correlation by only regarding positive correlations as connections between nodes. Under the signed network, strongly negatively correlated genes are considered to be unconnected. A third option is the signed-hybrid network. In this case, a hard threshold is set at the point of zero correlation meaning that only correlation values greater than 0 can give an adjacency value of greater than 0 (Equation B.5 and B.6).

$$a_{ij} = [cor(x_i, x_j)]^{\beta} \; forcor(x_i, x_j) > 0 \tag{B.5}$$

$$a_{ij} = 0 \; forcor(x_i, xj) \leq 0 \tag{B.6}$$

For our analysis, a signed-hybrid approach was used. To find the optimal value of β, the scale free topology fit R2 was calculated for values of beta ranging from 1-30. Ideally, the lowest value of β should be used which affords an R2 value of greater than 0.9 and a connectivity value below 100. In this case, β=12 was found to be appropriate which is in keeping with published β's from signed-hybrid networks (Figure 3.12).

B.2.2 Eigengene Calculation and Correlation with Traits

The adjacency matrix is transformed to a topological overlap matrix (TOM) which is used to assign genes to modules using hierarchical clustering. Each module is then summarised as a modular eigengene (ME) which is defined as the first principle component of the module (Equation B.7), where q represents the qth module.

$$ME_i^q = princomp(x_{ij}^q) \tag{B.7}$$

To identify biologically and clinically interesting modules, the ME is correlated with each trait. The core genes within a module can be identified by analysis of the Gene Significance (GS) and Module Membership (MM) scores. The GS score estimates the absolute correlation between the gene and the trait of interest

while MM is the correlation between the ME and the gene (Equation B.8). Core genes should contribute strongly to the ME (high MM) and correlate with the trait (high GS).

$$MM_i^q = cor(x_i, ME_I^q) \tag{B.8}$$

B.3 GISTIC scores

The GISTIC module assigns copy number changes in the genome a G-score based on the amplitude of change and the frequency with which it occurs. FDR q-values are determined for each aberration. If this q-value does not pass the low thresholds, then a '0' is given. If the aberration passes the lower amplification or deletion threshold than a '1' or –'1' is given respectively and if the upper thresholds are passed then a '2' or '-2' is given. The low-level thresholds are equal to the noise thresholds and are the same for all thresholds. The upper level thresholds are calculated sample by sample and are based on the median arm-level copy number changes within the sample.

B.4 Random Forest ML

RF uses decision trees to separate observations into partitions. Many individual trees are generated, each with a different set if predictors, and the final model averages these trees by a majority vote. Partitions are chosen based on the Gini Index (Equation B.9).

$$Gini(j) = \sum_{k=1}^{k} \hat{p}_j, k(1 - \hat{p}_j, k) \tag{B.9}$$

where $\hat{p}_j, k$ = the proportion of observations in partition j with class k.

We performed k-fold cross-validation (5-folds, B) on the training set to find the number of trees, the minimum nodesize and the number of predictors randomly selected for each tree split (mtry), which minimise the loss function. These parameters are represented by λ in Equation B.10

$$loss(\lambda) = \frac{1}{B}\sum_{(b=1)}^{B}\frac{1}{N}\sum_{(i=1}^{N})(\hat{y}_i^b(\lambda) - y_i^b)^2 \tag{B.10}$$

λ refers to the parameters being optimised. N is the number of observations in fold B, y is the true class of observation i and $\hat{y}$ is our estimate of the class of observation i. The number of trees was set to 200 and the minimum nodesize was set to 1. A value of 60 performed optimally for mtry.

C
Supplementary Tables

Table C.1: Table of p53 target genes validated by Fischer 2017. Each gene has been classified as pro-survival, anti-survival or Other based on the literature.

ENTREZID	symbol	ensembl.ID	Classification
182	JAG1	ENSG00000101384	pro-survival
220	ALDH1A3	ENSG00000184254	pro-survival
240	ALOX5	ENSG00000012779	pro-survival
389	RHOC	ENSG00000155366	pro-survival
598	BCL2L1	ENSG00000171552	pro-survival
639	PRDM1	ENSG00000057657	pro-survival
655	BMP7	ENSG00000101144	pro-survival
780	DDR1	ENSG00000204580	pro-survival
824	CAPN2	ENSG00000162909	pro-survival
857	CAV1	ENSG00000105974	pro-survival
1026	CDKN1A	ENSG00000124762	pro-survival
1435	CSF1	ENSG00000184371	pro-survival
1643	DDB2	ENSG00000134574	pro-survival
1647	GADD45A	ENSG00000116717	pro-survival
1907	EDN2	ENSG00000127129	pro-survival
2274	FHL2	ENSG00000115641	pro-survival
2810	SFN	ENSG00000175793	pro-survival
2817	GPC1	ENSG00000063660	pro-survival
2872	MKNK2	ENSG00000099875	pro-survival
2876	GPX1	ENSG00000233276	pro-survival
3783	KCNN4	ENSG00000104783	pro-survival
3976	LIF	ENSG00000128342	pro-survival
3985	LIMK2	ENSG00000182541	pro-survival
4035	LRP1	ENSG00000123384	pro-survival
4193	MDM2	ENSG00000135679	pro-survival

Table C.1 continued from previous page

4254	KITLG	ENSG00000049130	pro-survival
4814	NINJ1	ENSG00000131669	pro-survival
4851	NOTCH1	ENSG00000148400	pro-survival
5054	SERPINE1	ENSG00000106366	pro-survival
5111	PCNA	ENSG00000132646	pro-survival
5364	PLXNB1	ENSG00000164050	pro-survival
5429	POLH	ENSG00000170734	pro-survival
5453	POU3F1	ENSG00000185668	pro-survival
5564	PRKAB1	ENSG00000111725	pro-survival
5912	RAP2B	ENSG00000181467	pro-survival
6385	SDC4	ENSG00000124145	pro-survival
6774	STAT3	ENSG00000168610	pro-survival
7039	TGFA	ENSG00000163235	pro-survival
7803	PTP4A1	ENSG00000112245	pro-survival
7832	BTG2	ENSG00000159388	pro-survival
8061	FOSL1	ENSG00000175592	pro-survival
8444	DYRK3	ENSG00000143479	pro-survival
8493	PPM1D	ENSG00000170836	pro-survival
8793	TNFRSF10D	ENSG00000173530	pro-survival
8794	TNFRSF10C	ENSG00000173535	pro-survival
8812	CCNK	ENSG00000090061	pro-survival
8837	CFLAR	ENSG00000003402	pro-survival
9404	LPXN	ENSG00000110031	pro-survival
9518	GDF15	ENSG00000130513	pro-survival
9766	SUSD6	ENSG00000100647	pro-survival
9848	MFAP3L	ENSG00000198948	pro-survival
10076	PTPRU	ENSG00000060656	pro-survival
10769	PLK2	ENSG00000145632	pro-survival
10973	ASCC3	ENSG00000112249	pro-survival
10978	CLP1	ENSG00000172409	pro-survival
22837	COBLL1	ENSG00000082438	pro-survival
22954	TRIM32	ENSG00000119401	pro-survival
23479	ISCU	ENSG00000136003	pro-survival
23654	PLXNB2	ENSG00000196576	pro-survival
25816	TNFAIP8	ENSG00000145779	pro-survival
26154	ABCA12	ENSG00000144452	pro-survival
27165	GLS2	ENSG00000135423	pro-survival
50484	RRM2B	ENSG00000048392	pro-survival
50650	ARHGEF3	ENSG00000163947	pro-survival
51278	IER5	ENSG00000162783	pro-survival
51499	TRIAP1	ENSG00000170855	pro-survival
51513	ETV7	ENSG00000010030	pro-survival
51768	TM7SF3	ENSG00000064115	pro-survival
53354	PANK1	ENSG00000152782	pro-survival

Table C.1 continued from previous page

53836	GPR87	ENSG00000138271	pro-survival
55544	RBM38	ENSG00000132819	pro-survival
55733	HHAT	ENSG00000054392	pro-survival
55959	SULF2	ENSG00000196562	pro-survival
57103	TIGAR	ENSG00000078237	pro-survival
80315	CPEB4	ENSG00000113742	pro-survival
84280	BTBD10	ENSG00000148925	pro-survival
93129	ORAI3	ENSG00000175938	pro-survival
144455	E2F7	ENSG00000165891	pro-survival
257397	TAB3	ENSG00000157625	pro-survival
59	ACTA2	ENSG00000107796	other
98	ACYP2	ENSG00000170634	other
421	ARVCF	ENSG00000099889	other
1056	CEL	ENSG00000170835	other
1294	COL7A1	ENSG00000114270	other
1462	VCAN	ENSG00000038427	other
1947	EFNB1	ENSG00000090776	other
2632	GBE1	ENSG00000114480	other
3300	DNAJB2	ENSG00000135924	other
3866	KRT15	ENSG00000171346	other
4000	LMNA	ENSG00000160789	other
4043	LRPAP1	ENSG00000163956	other
4051	CYP4F3	ENSG00000186529	other
4808	NHLH2	ENSG00000177551	other
5268	SERPINB5	ENSG00000206075	other
5360	PLTP	ENSG00000100979	other
5565	PRKAB2	ENSG00000131791	other
5791	PTPRE	ENSG00000132334	other
6223	RPS19	ENSG00000105372	other
6273	S100A2	ENSG00000196754	other
6301	SARS	ENSG00000031698	other
6548	SLC9A1	ENSG00000090020	other
6560	SLC12A4	ENSG00000124067	other
7011	TEP1	ENSG00000129566	other
7098	TLR3	ENSG00000164342	other
7748	ZNF195	ENSG00000005801	other
7779	SLC30A1	ENSG00000170385	other
8079	MLF2	ENSG00000089693	other
8496	PPFIBP1	ENSG00000110841	other
8553	BHLHE40	ENSG00000134107	other
8601	RGS20	ENSG00000147509	other
8824	CES2	ENSG00000172831	other
9050	PSTPIP2	ENSG00000152229	other
9249	DHRS3	ENSG00000162496	other

Table C.1 continued from previous page

9873	FCHSD2	ENSG00000137478	other
10148	EBI3	ENSG00000105246	other
10346	TRIM22	ENSG00000132274	other
22824	HSPA4L	ENSG00000164070	other
22906	TRAK1	ENSG00000182606	other
23228	PLCL2	ENSG00000154822	other
23245	ASTN2	ENSG00000148219	other
25841	ABTB2	ENSG00000166016	other
25987	TSKU	ENSG00000182704	other
26152	ZNF337	ENSG00000130684	other
26263	FBXO22	ENSG00000167196	pro-survival
27244	SESN1	ENSG00000080546	other
29085	PHPT1	ENSG00000054148	other
50808	AK3	ENSG00000147853	other
51090	PLLP	ENSG00000102934	other
51222	ZNF219	ENSG00000165804	other
51313	FAM198B	ENSG00000164125	other
51321	AMZ2	ENSG00000196704	other
53944	CSNK1G1	ENSG00000169118	other
54626	HES2	ENSG00000069812	other
54858	PGPEP1	ENSG00000130517	other
55191	NADSYN1	ENSG00000172890	other
55240	STEAP3	ENSG00000115107	other
55245	UQCC1	ENSG00000101019	other
55362	TMEM63B	ENSG00000137216	other
55924	FAM212B	ENSG00000197852	other
57523	NYNRIN	ENSG00000205978	other
57763	ANKRA2	ENSG00000164331	other
57828	CATSPERG	ENSG00000099338	other
64787	EPS8L2	ENSG00000177106	other
79714	CCDC51	ENSG00000164051	other
79828	METTL8	ENSG00000123600	other
80055	PGAP1	ENSG00000197121	other
80705	TSGA10	ENSG00000135951	other
81553	FAM49A	ENSG00000197872	other
83667	SESN2	ENSG00000130766	other
84284	NTPCR	ENSG00000135778	other
85363	TRIM5	ENSG00000132256	other
85377	MICALL1	ENSG00000100139	other
93134	ZNF561	ENSG00000171469	other
94027	CGB7	ENSG00000196337	other
116151	FAM210B	ENSG00000124098	other
127544	RNF19B	ENSG00000116514	other
132671	SPATA18	ENSG00000163071	other

Table C.1 continued from previous page

132864	CPEB2	ENSG00000137449	other
134147	CMBL	ENSG00000164237	other
137695	TMEM68	ENSG00000167904	other
144811	LACC1	ENSG00000179630	other
147965	FAM98C	ENSG00000130244	other
164668	APOBEC3H	ENSG00000100298	other
196513	DCP1B	ENSG00000151065	other
204962	SLC44A5	ENSG00000137968	other
219699	UNC5B	ENSG00000107731	other
220001	VWCE	ENSG00000167992	other
220965	FAM13C	ENSG00000148541	other
257068	PLCXD2	ENSG00000240891	other
283130	SLC25A45	ENSG00000162241	other
285343	TCAIM	ENSG00000179152	other
333926	PPM1J	ENSG00000155367	other
343263	MYBPHL	ENSG00000221986	other
353135	LCE1E	ENSG00000186226	other
375449	MAST4	ENSG00000069020	other
441631	TSPAN11	ENSG00000110900	other
642938	FAM196A	ENSG00000188916	other
307	ANXA4	ENSG00000196975	pro-survival
583	BBS2	ENSG00000125124	other
604	BCL6	ENSG00000113916	pro-survival
694	BTG1	ENSG00000133639	anti-survival
740	MRPL49	ENSG00000149792	other
1006	CDH8	ENSG00000150394	pro-survival
1363	CPE	ENSG00000109472	other
1606	DGKA	ENSG00000065357	pro-survival
2770	GNAI1	ENSG00000127955	other
3140	MR1	ENSG00000153029	other
3265	HRAS	ENSG00000174775	other
3280	HES1	ENSG00000114315	anti-survival
3293	HSD17B3	ENSG00000130948	other
3553	IL1B	ENSG00000125538	anti-survival
3628	INPP1	ENSG00000151689	pro-survival
3675	ITGA3	ENSG00000005884	pro-survival
3856	KRT8	ENSG00000170421	pro-survival
4638	MYLK	ENSG00000065534	pro-survival
4646	MYO6	ENSG00000196586	pro-survival
4747	NEFL	ENSG00000277586	anti-survival
4792	NFKBIA	ENSG00000100906	pro-survival
5168	ENPP2	ENSG00000136960	pro-survival
5228	PGF	ENSG00000119630	pro-survival
5507	PPP1R3C	ENSG00000119938	other

Table C.1 continued from previous page

5613	PRKX	ENSG00000183943	pro-survival
5724	PTAFR	ENSG00000169403	other
5875	RABGGTA	ENSG00000100949	pro-survival
5889	RAD51C	ENSG00000108384	pro-survival
5900	RALGDS	ENSG00000160271	pro-survival
5980	REV3L	ENSG00000009413	pro-survival
6004	RGS16	ENSG00000143333	anti-survival
6326	SCN2A	ENSG00000136531	other
6643	SNX2	ENSG00000205302	pro-survival
7157	TP53	ENSG00000141510	anti-survival
7161	TP73	ENSG00000078900	anti-survival
7205	TRIP6	ENSG00000087077	pro-survival
7421	VDR	ENSG00000111424	other
7633	ZNF79	ENSG00000196152	anti-survival
8446	DUSP11	ENSG00000144048	anti-survival
8507	ENC1	ENSG00000171617	pro-survival
8844	KSR1	ENSG00000141068	pro-survival
9289	ADGRG1	ENSG00000205336	other
9538	EI24	ENSG00000149547	anti-survival
9635	CLCA2	ENSG00000137975	anti-survival
9648	GCC2	ENSG00000135968	other
10142	AKAP9	ENSG00000127914	other
10228	STX6	ENSG00000135823	pro-survival
10475	TRIM38	ENSG00000112343	other
10898	CPSF4	ENSG00000160917	pro-survival
10950	BTG3	ENSG00000154640	anti-survival
11072	DUSP14	ENSG00000276023	other
22861	NLRP1	ENSG00000091592	pro-survival
23041	MON2	ENSG00000061987	other
23179	RGL1	ENSG00000143344	other
23237	ARC	ENSG00000198576	other
23308	ICOSLG	ENSG00000160223	other
23513	SCRIB	ENSG00000180900	anti-survival
23768	FLRT2	ENSG00000185070	anti-survival
24139	EML2	ENSG00000125746	other
25946	ZNF385A	ENSG00000161642	pro-survival
26509	MYOF	ENSG00000138119	pro-survival
27350	APOBEC3C	ENSG00000244509	other
27445	PCLO	ENSG00000186472	other
29901	SAC3D1	ENSG00000168061	other
51477	ISYNA1	ENSG00000105655	anti-survival
54677	CROT	ENSG00000005469	other
54790	TET2	ENSG00000168769	other
54884	RETSAT	ENSG00000042445	other

Table C.1 continued from previous page

55040	EPN3	ENSG00000049283	anti-survival
55214	P3H2	ENSG00000090530	anti-survival
55671	PPP4R3A	ENSG00000100796	other
55800	SCN3B	ENSG00000166257	anti-survival
56963	RGMA	ENSG00000182175	anti-survival
56997	ADCK3	ENSG00000163050	anti-survival
57722	IGDCC4	ENSG00000103742	other
60492	CCDC90B	ENSG00000137500	other
63874	ABHD4	ENSG00000100439	anti-survival
80025	PANK2	ENSG00000125779	other
81607	PVRL4	ENSG00000143217	pro-survival
81704	DOCK8	ENSG00000107099	pro-survival
83719	YPEL3	ENSG00000090238	anti-survival
83959	SLC4A11	ENSG00000088836	pro-survival
84659	RNASE7	ENSG00000165799	other
84883	AIFM2	ENSG00000042286	anti-survival
84958	SYTL1	ENSG00000142765	other
85477	SCIN	ENSG00000006747	pro-survival
113189	CHST14	ENSG00000169105	other
114907	FBXO32	ENSG00000156804	anti-survival
115548	FCHO2	ENSG00000157107	other
118738	ZNF488	ENSG00000265763	other
119032	BORCS7	ENSG00000166275	other
122809	SOCS4	ENSG00000180008	anti-survival
126820	WDR63	ENSG00000162643	other
127707	KLHDC7A	ENSG00000179023	other
128414	NKAIN4	ENSG00000101198	other
154810	AMOTL1	ENSG00000166025	pro-survival
157638	FAM84B	ENSG00000168672	other
164091	PAQR7	ENSG00000182749	pro-survival
205860	TRIML2	ENSG00000179046	anti-survival
255488	RNF144B	ENSG00000137393	anti-survival
282991	BLOC1S2	ENSG00000196072	anti-survival
284184	C17orf89	ENSG00000224877	other
374618	TEX9	ENSG00000151575	other
388407	C17orf82	ENSG00000187013	other
494514	TYMSOS	ENSG00000176912	other
317	APAF1	ENSG00000120868	anti-survival
355	FAS	ENSG00000026103	anti-survival
390	RND3	ENSG00000115963	anti-survival
467	ATF3	ENSG00000162772	anti-survival
581	BAX	ENSG00000087088	anti-survival
839	CASP6	ENSG00000138794	anti-survival
900	CCNG1	ENSG00000113328	anti-survival

Table C.1 continued from previous page

1263	PLK3	ENSG00000173846	anti-survival
1612	DAPK1	ENSG00000196730	anti-survival
1847	DUSP5	ENSG00000138166	anti-survival
1849	DUSP7	ENSG00000164086	anti-survival
1969	EPHA2	ENSG00000142627	anti-survival
2232	FDXR	ENSG00000161513	anti-survival
2517	FUCA1	ENSG00000179163	anti-survival
3490	IGFBP7	ENSG00000163453	anti-survival
3732	CD82	ENSG00000085117	anti-survival
4088	SMAD3	ENSG00000166949	anti-survival
4163	MCC	ENSG00000171444	anti-survival
5143	PDE4C	ENSG00000105650	anti-survival
5366	PMAIP1	ENSG00000141682	anti-survival
5371	PML	ENSG00000140464	anti-survival
5625	PRODH	ENSG00000100033	anti-survival
6236	RRAD	ENSG00000166592	anti-survival
6330	SCN4B	ENSG00000177098	anti-survival
7508	XPC	ENSG00000154767	anti-survival
7805	LAPTM5	ENSG00000162511	anti-survival
7869	SEMA3B	ENSG00000012171	anti-survival
8436	SDPR	ENSG00000168497	anti-survival
8795	TNFRSF10B	ENSG00000120889	anti-survival
8797	TNFRSF10A	ENSG00000104689	anti-survival
9076	CLDN1	ENSG00000163347	anti-survival
9263	STK17A	ENSG00000164543	anti-survival
9537	TP53I11	ENSG00000175274	anti-survival
9540	TP53I3	ENSG00000115129	anti-survival
9618	TRAF4	ENSG00000076604	anti-survival
10904	BLCAP	ENSG00000166619	anti-survival
23569	PADI4	ENSG00000159339	anti-survival
23612	PHLDA3	ENSG00000174307	anti-survival
26471	NUPR1	ENSG00000176046	anti-survival
26999	CYFIP2	ENSG00000055163	anti-survival
27113	BBC3	ENSG00000105327	anti-survival
29950	SERTAD1	ENSG00000197019	anti-survival
29965	CDIP1	ENSG00000089486	anti-survival
51065	RPS27L	ENSG00000185088	anti-survival
51754	TMEM8B	ENSG00000137103	anti-survival
54541	DDIT4	ENSG00000168209	anti-survival
55294	FBXW7	ENSG00000109670	anti-survival
55332	DRAM1	ENSG00000136048	anti-survival
55367	PIDD1	ENSG00000177595	anti-survival
57060	PCBP4	ENSG00000090097	anti-survival
57822	GRHL3	ENSG00000158055	anti-survival

Table C.1 continued from previous page

60401	EDA2R	ENSG00000131080	anti-survival
64065	PERP	ENSG00000112378	anti-survival
64393	ZMAT3	ENSG00000172667	anti-survival
64782	AEN	ENSG00000181026	anti-survival
79156	PLEKHF1	ENSG00000166289	anti-survival
84552	PARD6G	ENSG00000178184	anti-survival
91012	CERS5	ENSG00000139624	anti-survival
94241	TP53INP1	ENSG00000164938	anti-survival
121457	IKBIP	ENSG00000166130	anti-survival
340485	ACER2	ENSG00000177076	anti-survival

Table C.2: Table of p53 pathway genes including p53 targets from C.1 and pathway genes annotated by KEGG, PANTHER and BIOCARTA.

SYMBOL	with.cancer.risk.loci	Classifiers
TP53	yes	KEGG Biocarta PANTHER Fischer
APOBEC3H	no	Fischer
CYFIP2	no	Fischer
KITLG	yes	Fischer
TRIM22	no	Fischer
BAX	no	KEGG Biocarta Fischer
SERPINB5	no	KEGG Fischer
APOBEC3C	no	Fischer
MDM2	no	KEGG Biocarta PANTHER Fischer
PERP	no	KEGG Fischer
CDKN2A	yes	KEGG PANTHER
EDA2R	no	Fischer
CPE	no	Fischer
BBC3	no	KEGG Fischer
CDK6	no	KEGG
KRT15	no	Fischer
LAPTM5	no	Fischer
TNFRSF10B	yes	KEGG Fischer
ZMAT3	no	KEGG Fischer
SDC4	no	Fischer
CLDN1	no	Fischer
GPC1	no	Fischer
VWCE	no	Fischer
ADGRG1	no	Fischer
ZNF488	no	Fischer
RRM2B	no	KEGG Fischer
EPS8L2	no	Fischer
SFN	no	KEGG PANTHER Fischer
AEN	no	Fischer
RPS27L	no	Fischer
ACTA2	yes	Fischer
DDB2	no	KEGG Fischer
FDXR	no	Fischer
TSKU	no	Fischer
EDN2	no	Fischer
LPXN	no	Fischer
TRIM5	yes	Fischer
RND3	no	Fischer
COBLL1	no	Fischer
DCP1B	no	Fischer
DHRS3	no	Fischer
KRT8	yes	Fischer

Table C.2 continued from previous page

RPS19	no	Fischer
TP53AIP1	no	KEGG
EBI3	no	Fischer
EPN3	no	Fischer
CDKN1A	yes	KEGG Biocarta PANTHER Fischer
GLS2	no	Fischer
XPC	no	Fischer
MYO6	yes	Fischer
PGPEP1	no	Fischer
CCNG1	no	KEGG Fischer
TMEM63B	no	Fischer
KSR1	no	Fischer
LMNA	no	Fischer
MCC	no	Fischer
PIDD1	yes	KEGG Fischer
PTPRU	no	Fischer
SCIN	no	Fischer
TP63	yes	PANTHER
ATM	yes	KEGG Biocarta PANTHER
FCHO2	no	Fischer
THBS1	no	KEGG
FAM84B	no	Fischer
CMBL	no	Fischer
RNF144B	no	Fischer
TEX9	yes	Fischer
TIGAR	no	Fischer
CD82	no	KEGG Fischer
CCNE2	no	KEGG
PTPRE	no	Fischer
E2F1	no	Biocarta
SESN1	yes	KEGG Fischer
TP53I11	no	Fischer
ARC	no	Fischer
CAPN2	no	Fischer
CASP6	no	Fischer
CGB7	no	Fischer
GNAI1	no	Fischer
BCL2	yes	Biocarta
TP53INP1	no	Fischer
HES1	no	Fischer
FAM210B	no	Fischer
NOTCH1	yes	Fischer
TRIM38	yes	Fischer
ZNF337	no	Fischer

Table C.2 continued from previous page

UNC5B	no	Fischer
DDR1	no	Fischer
ORAI3	no	Fischer
S100A2	no	Fischer
EPHA2	no	Fischer
POU3F1	no	Fischer
HRAS	no	Fischer
ITGA3	no	Fischer
VDR	no	Fischer
FBXO32	yes	Fischer
BLCAP	no	Fischer
ZNF195	no	Fischer
MDM4	yes	KEGG PANTHER
TIMP3	no	Biocarta
AIFM2	no	Fischer
GRHL3	no	Fischer
CASP3	no	KEGG
CCND2	yes	KEGG
FBXW7	no	Fischer
POLH	no	Fischer
RRM2	no	KEGG
GADD45G	no	KEGG PANTHER
PLXNB1	no	Fischer
IGF1	no	KEGG
C17orf82	no	Fischer
PPP1R3C	no	Fischer
PLK3	no	Fischer
NHLH2	no	Fischer
INPP1	no	Fischer
PLK2	no	Fischer
SESN2	no	KEGG Fischer
FAM13C	no	Fischer
PRKX	no	Fischer
FAS	yes	KEGG Fischer
NUPR1	no	Fischer
FHL2	no	Fischer
TRAF4	no	Fischer
VCAN	no	Fischer
EFNB1	no	Fischer
IGFBP3	no	KEGG
PLCL2	no	Fischer
SCN4B	no	Fischer
CCNB2	no	KEGG
DGKA	no	Fischer

Table C.2 continued from previous page

MAST4	no	Fischer
CERS5	yes	Fischer
DYRK3	no	Fischer
SEMA3B	no	Fischer
CCDC90B	no	Fischer
P3H2	no	Fischer
RPRM	no	KEGG
KCNN4	yes	Fischer
NADSYN1	no	Fischer
RNASE7	no	Fischer
ATF3	no	Fischer
BTG2	no	Fischer
PCLO	no	Fischer
TGFA	no	Fischer
PML	no	PANTHER Fischer
SLC9A1	no	Fischer
PPM1J	no	Fischer
WRN	no	PANTHER
CCNB1	no	KEGG PANTHER
RB1	no	Biocarta
PRDM1	no	Fischer
TNFRSF10C	no	Fischer
SLC25A45	no	Fischer
DAPK1	no	Fischer
PMAIP1	no	KEGG Fischer
GPX1	no	Fischer
JAG1	no	Fischer
PLLP	no	Fischer
ALDH1A3	no	Fischer
HSPA4L	no	Fischer
MKNK2	no	Fischer
MYOF	no	Fischer
RGS20	no	Fischer
TRIAP1	no	Fischer
ARVCF	no	Fischer
BORCS7	no	Fischer
ANKRA2	no	Fischer
FBXO22	no	Fischer
DRAM1	no	Fischer
SHISA5	no	KEGG
KLHDC7A	yes	Fischer
BTG3	no	Fischer
ICOSLG	no	Fischer
IGDCC4	no	Fischer

Table C.2 continued from previous page

DUSP5	no	Fischer
RBM38	no	Fischer
ABHD4	no	Fischer
COQ8A	no	Fischer
ISCU	no	Fischer
MRPL49	no	Fischer
PPM1D	no	KEGG Fischer
ENPP2	no	Fischer
IKBIP	no	Fischer
DOCK8	no	Fischer
PLCXD2	no	Fischer
CPEB4	no	Fischer
CLCA2	no	Fischer
GPR87	no	Fischer
PIK3CA	no	PANTHER
CDK2	no	KEGG Biocarta PANTHER
REV3L	no	Fischer
ETV7	no	Fischer
TEP1	no	Fischer
SIRT1	no	PANTHER
CCND3	no	KEGG
DNAJB2	no	Fischer
METTL8	no	Fischer
LACC1	no	Fischer
MYLK	no	Fischer
BCL2L1	no	Fischer
LIMK2	no	Fischer
PPP2CA	no	PANTHER
PRKAB2	no	Fischer
RCHY1	no	KEGG
KAT2B	no	PANTHER
EP300	no	PANTHER
PHLDA3	yes	Fischer
AMOTL1	no	Fischer
BTBD10	no	Fischer
CDK1	no	KEGG
CPSF4	no	Fischer
TAB3	no	Fischer
NLRP1	no	Fischer
RHOC	no	Fischer
PRODH	no	Fischer
CAVIN2	no	Fischer
APAF1	no	KEGG Biocarta Fischer
BLOC1S2	no	Fischer

Table C.2 continued from previous page

E2F7	no	Fischer
ADGRB1	no	KEGG
KAT6B	no	PANTHER
TP73	no	KEGG PANTHER Fischer
DUSP14	no	Fischer
CREBBP	no	PANTHER
NDUFAF8	no	Fischer
RGMA	no	Fischer
ENC1	no	Fischer
HES2	no	Fischer
PTAFR	no	Fischer
ZNF219	no	Fischer
GDF15	no	Fischer
CYP4F3	no	Fischer
BCL6	no	Fischer
SIAH1	no	KEGG
ABTB2	no	Fischer
PLEKHF1	no	Fischer
BTG1	no	Fischer
CFLAR	yes	Fischer
NKAIN4	no	Fischer
MYBPHL	no	Fischer
CAV1	no	Fischer
PAQR7	no	Fischer
SYTL1	no	Fischer
CASP8	yes	KEGG
CASP9	no	KEGG
SERTAD1	no	Fischer
EI24	no	KEGG Fischer
FAM196A	no	Fischer
PADI4	no	Fischer
CROT	no	Fischer
PLTP	no	Fischer
PSTPIP2	no	Fischer
PTEN	no	KEGG PANTHER
YPEL3	no	Fischer
ATR	no	KEGG PANTHER
GBE1	no	Fischer
RABGGTA	no	Fischer
STK17A	no	Fischer
FCHSD2	no	Fischer
RGL1	no	Fischer
PARD6G	no	Fischer
ASTN2	yes	Fischer

Table C.2 continued from previous page

PHPT1	no	Fischer
AKT2	no	PANTHER
STEAP3	no	KEGG Fischer
NTPCR	no	Fischer
PRKAB1	no	Fischer
CSF1	no	Fischer
HMGB1	no	PANTHER
RETSAT	no	Fischer
COL7A1	no	Fischer
MR1	no	Fischer
TYMSOS	no	Fischer
CSNK1G1	no	Fischer
TRIML2	no	Fischer
CDC25C	no	PANTHER
NECTIN4	no	Fischer
BHLHE40	no	Fischer
CES2	no	Fischer
NYNRIN	no	Fischer
PPP2CB	no	PANTHER
ZNF561	no	Fischer
CHEK1	no	KEGG
TSGA10	no	Fischer
ISYNA1	yes	Fischer
EML2	no	Fischer
SAC3D1	no	Fischer
RNF19B	no	Fischer
RGS16	no	Fischer
GCC2	no	Fischer
SESN3	no	KEGG
AK3	no	Fischer
CCNK	no	Fischer
BID	no	KEGG
PPFIBP1	no	Fischer
CEL	no	Fischer
SERPINE1	no	KEGG Fischer
TSC2	no	KEGG
AKT3	yes	PANTHER
CCNB3	no	KEGG
MICALL1	no	Fischer
CDH8	no	Fischer
STAT3	no	Fischer
TMEM68	no	Fischer
PGF	no	Fischer
TCAIM	no	Fischer

Table C.2 continued from previous page

CPEB2	no	Fischer
BBS2	no	Fischer
DDIT4	no	Fischer
PANK1	no	Fischer
SUMO1	no	PANTHER
TNFAIP8	no	Fischer
AMZ2	no	Fischer
TRIM32	yes	Fischer
FAM49A	no	Fischer
TET2	yes	Fischer
CLP1	no	Fischer
IL1B	no	Fischer
MFAP3L	no	Fischer
UQCC1	no	Fischer
TP53I3	no	KEGG Fischer
TNFRSF10A	no	Fischer
NINJ1	no	Fischer
PTP4A1	no	Fischer
CCND1	yes	KEGG Biocarta
DUSP11	no	Fischer
ABCA12	no	Fischer
CCNE1	yes	KEGG Biocarta PANTHER
CHEK2	yes	KEGG PANTHER
CHST14	no	Fischer
COP1	no	KEGG
FAM198B	no	Fischer
HSD17B3	no	Fischer
RAP2B	no	Fischer
TRAK1	yes	Fischer
SMAD3	yes	Fischer
FAM212B	no	Fischer
PGAP1	no	Fischer
SOCS4	no	Fischer
PCNA	no	Biocarta Fischer
DUSP7	no	Fischer
ASCC3	no	Fischer
PDE4C	no	Fischer
CATSPERG	no	Fischer
IGFBP7	no	Fischer
RRAD	no	Fischer
MLF2	no	Fischer
PLXNB2	no	Fischer
ANXA4	no	Fischer
CCNG2	no	KEGG

Table C.2 continued from previous page

FAM98C	no	Fischer
IER5	no	Fischer
PANK2	no	Fischer
RAD51C	yes	Fischer
SCN3B	no	Fischer
SLC4A11	no	Fischer
SUSD6	no	Fischer
TLR3	no	Fischer
TRIP6	no	Fischer
WDR63	no	Fischer
FUCA1	no	Fischer
SCRIB	no	Fischer
BMP7	no	Fischer
MON2	no	Fischer
SLC12A4	no	Fischer
TSPAN11	no	Fischer
NEFL	no	Fischer
GTSE1	no	KEGG PANTHER
CDK4	no	KEGG Biocarta
CDKN2D	no	PANTHER
PDPK1	no	PANTHER
SIN3A	no	PANTHER
CCDC51	no	Fischer
ALOX5	no	Fischer
ARHGEF3	no	Fischer
CYCS	no	KEGG
GADD45A	no	KEGG Biocarta PANTHER Fischer
HDAC1	no	PANTHER
LRPAP1	no	Fischer
SULF2	no	Fischer
ZNF79	no	Fischer
AKT1	yes	PANTHER
FLRT2	no	Fischer
LIF	no	Fischer
SLC44A5	no	Fischer
ACER2	no	Fischer
AKAP9	yes	Fischer
STX6	no	Fischer
NFKBIA	no	Fischer
CDIP1	no	Fischer
SCN2A	no	Fischer
MTA2	no	PANTHER
PPP4R3A	yes	Fischer
LRP1	no	Fischer

Table C.2 continued from previous page

RALGDS	no	Fischer
SARS	no	Fischer
TRAF2	no	PANTHER
HHAT	no	Fischer
PCBP4	no	Fischer
SLC30A1	no	Fischer
TMEM8B	no	Fischer
GADD45B	no	KEGG PANTHER
ZNF385A	no	Fischer
SPATA18	no	Fischer
ACYP2	no	Fischer
FOSL1	no	Fischer
SNX2	no	Fischer
TNFRSF10D	no	Fischer
TM7SF3	no	Fischer

Table C.3: The compounds used as part of the Oncology drug screen comparing KITLG p53RE +/+ and -/- TERA1 and TERA2 cells.

Compound	Target.Class
(5Z)-7-Oxozeaenol	RAS/RAF/MEK/MAPK inhibitors
(R)-Flurbiprofen (Tarenflurbil)	Other
1-methyl-D-tryptophan, 95%	Other
17-AAG (Tanespimycin, Geldanamycin)	Heat shock protein inhibitors
17-DMAG (Alvespimycin)	Heat shock protein inhibitors
2-methoxyestradiol (Panzem)	Other
4-hydroxytamoxifen	Hormonal agents
Abiraterone	Other
Abitrexate/Methotrexate	Other
ABT-199	Apoptosis activators
ABT-263 (Navitoclax)	Apoptosis activators
ABT-751	Antimitotic agents
ABT-869_Linifanib	RTK inhibitors
ABT-888 (Veliparib)	Other
AC220_Quizartinib	RTK inhibitors
AG-014699_Rucaparib	Other
Alectinib	RTK inhibitors
Allopurinol	Other
Altretamine	Other
Amifostine	Other
Aminoglutethimide	Hormonal agents
Aminolevulinic acid hydrochloride	Other
Amonafide	TOPO inhibitors
Anagrelide	Other
Anastrozole	Hormonal agents
AP24534 (Ponatinib)	RTK inhibitors
ARQ 197_Tivantinib	RTK inhibitors
ARRY-162_MEK-162	RAS/RAF/MEK/MAPK inhibitors
Arsenic(III) oxide	Other
AS703026_Pimasertib	RAS/RAF/MEK/MAPK inhibitors
Aspirin (Acetylsalicylic Acid)	Other
AT 101	Apoptosis activators
AT-406	Apoptosis activators
AT9283	Antimitotic agents
Atorvastatin Ca	Other
Auranofin	Other
AV-951 (Tivozanib)	RTK inhibitors
AVN944	Other
Axitinib	RTK inhibitors
AZ 3146	Cell cycle inhibitors
Azacitidine	Other
AZD 7762 hydrochloride	Cell cycle inhibitors

Table C.3 continued from previous page

Compound	Target.Class
AZD1152-HQPA	Antimitotic agents
AZD1480	JAK/STAT inhibitors
AZD2014	PI3K/AKT/mTOR inhibitors
AZD4547	RTK inhibitors
AZD6244 (Selumetinib)	RAS/RAF/MEK/MAPK inhibitors
AZD8055	PI3K/AKT/mTOR inhibitors
BAY 73-4506_Regorafenib	RTK inhibitors
Belinostat (PXD101)	HDAC inhibitors
Bendamustine hydrochloride	DNA synthesis inhibitors
Bexarotene	Other
BI 2536	Cell cycle inhibitors
BI 6727_Volasertib	Cell cycle inhibitors
BIBF 1120_Nintedanib	RTK inhibitors
BIBW2992 (Tovok)_Afatinib	RTK inhibitors
Bicalutamide	Hormonal agents
BIIB021	Heat shock protein inhibitors
Bimatoprost	Other
BIRB 796 (Doramapimod)	RAS/RAF/MEK/MAPK inhibitors
BKM-120_Buparlisib	PI3K/AKT/mTOR inhibitors
Bleomycin sulfate	Other
BMS-754807	RTK inhibitors
BMS-911543	JAK/STAT inhibitors
Bortezomib	Other
Bosutinib	Other
Brivanib	RTK inhibitors
Busulfan	Other
Cabazitaxel	Antimitotic agents
CAL-101	PI3K/AKT/mTOR inhibitors
Camptothecin	TOPO inhibitors
Canertinib	RTK inhibitors
Capecitabine	DNA synthesis inhibitors
Carboplatin	DNA synthesis inhibitors
Carfilzomib	Other
Carmustine	DNA synthesis inhibitors
Celecoxib	Other
Ceritinib	RTK inhibitors
CHIR-258 (Dovitinib)	RTK inhibitors
Chlorambucil	DNA synthesis inhibitors
Chloroquine diphosphate	Other
CHR 2797_Tosedostat	Other
CI-994_Tacedinaline	HDAC inhibitors
Cisplatin aq	DNA synthesis inhibitors
Cladribine	DNA synthesis inhibitors

Table C.3 continued from previous page

Compound	Target.Class
Clafen (Cyclophosphamide, Endoxan)	DNA synthesis inhibitors
Clofarabine	DNA synthesis inhibitors
Clomifene citrate	Hormonal agents
Cobimetinib	RAS/RAF/MEK/MAPK inhibitors
CPI-613	Other
Crenolanib	RTK inhibitors
Crizotinib	RTK inhibitors
CUDC-101	HDAC inhibitors
Cyclophosphamide	DNA synthesis inhibitors
CYT-387_Momelotinib	JAK/STAT inhibitors
Cytarabine hydrochloride	DNA synthesis inhibitors
Dabrafenib Mesylate	RAS/RAF/MEK/MAPK inhibitors
Dacarbazine	DNA synthesis inhibitors
Dacomitinib (monohydrate) (PF-00299804)	RTK inhibitors
Dactinomycin	TOPO inhibitors
Dasatinib	RTK inhibitors
Daunorubicin hydrochloride	TOPO inhibitors
DCC-2036_Rebastinib	RTK inhibitors
Decitabine (Dacogen)	Other
Deferoxamine mesylate	Other
Dexamethasone (Decadron)	Other
Dexrazoxane	Other
Dinaciclib (SCH727965)	Cell cycle inhibitors
Docetaxel	Antimitotic agents
Doxorubicin	TOPO inhibitors
EMD1214063	RTK inhibitors
EMPTY	Other
Entinostat	HDAC inhibitors
Enzalutamide	Hormonal agents
Enzastaurin	Other
Epirubicin hydrochloride	TOPO inhibitors
Epothilone B (Patupilone)	Antimitotic agents
Erismodegib	Other
Erlotinib hydrochloride	RTK inhibitors
Estramustine sodium phosphate	Hormonal agents
Etoposide	TOPO inhibitors
Everolimus	Other
Exemestane	Hormonal agents
FG-4592	Other
Finasteride	Other
FK 506_Tacrolimus	Other
FK-866 HCl_Daporinad	Other
Floxuridine	DNA synthesis inhibitors

Table C.3 continued from previous page

Compound	Target.Class
Fludarabine phosphate	DNA synthesis inhibitors
Fluorouracil	DNA synthesis inhibitors
Flutamide	Hormonal agents
Fulvestrant	Hormonal agents
Galiellalactone	JAK/STAT inhibitors
GDC-0068	PI3K/AKT/mTOR inhibitors
GDC-0941_Pictilisib	PI3K/AKT/mTOR inhibitors
GDC-0980	PI3K/AKT/mTOR inhibitors
Gefitinib	RTK inhibitors
Gemcitabine hydrochloride	DNA synthesis inhibitors
Goserelin acetate	Other
GSK 269962	Other
GSK 650394	Other
GSK1120212_Trametinib	RAS/RAF/MEK/MAPK inhibitors
GSK2126458	PI3K/AKT/mTOR inhibitors
GSK2636771	PI3K/AKT/mTOR inhibitors
HA-1077 (Fasudil)	Other
Homoharringtonine	Other
Hydroxyurea	DNA synthesis inhibitors
I-BET151 (GSK1210151A)	Other
Idarubicin HCl	TOPO inhibitors
Idelalisib	PI3K/AKT/mTOR inhibitors
Ifosfamide	DNA synthesis inhibitors
Imatinib	RTK inhibitors
Imiquimod	Other
INCB018424 (free base, Ruxolitinib)	JAK/STAT inhibitors
Indibulin	Antimitotic agents
Iniparib (BSI-201, IND-71677)	Other
INK128	PI3K/AKT/mTOR inhibitors
Irinotecan	TOPO inhibitors
Irinotecan hydrochloride	TOPO inhibitors
Ixabepilone	Antimitotic agents
Ixazomib citrate	Other
JNJ 26854165 (Serdemetan)	MDM2 inhibitors
JNJ-26481585_Quisinostat	HDAC inhibitors
KX2-391	Other
Lapatinib	RTK inhibitors
Lapatinib, di-p-toluenesulfonate salt	RTK inhibitors
Lasofoxifene	Hormonal agents
Lenalidomide	Other
Lenvatinib	RTK inhibitors
Lestaurtinib	JAK/STAT inhibitors
Letrozole	Hormonal agents

Table C.3 continued from previous page

Compound	Target.Class
Lomeguatrib	DNA synthesis inhibitors
Lomustine	DNA synthesis inhibitors
LY 333531 mesylate_Ruboxistaurin	Other
LY2157299	RTK inhibitors
LY2228820 (CP868569)	RAS/RAF/MEK/MAPK inhibitors
LY2603618_Rabusertib	Cell cycle inhibitors
LY2784544_Gandotinib	JAK/STAT inhibitors
Masitinib	RTK inhibitors
MDV3100_Enzaluamide	Hormonal agents
Mechlorethamine hydrochloride	DNA synthesis inhibitors
Megestrol acetate	Hormonal agents
Melphalan	DNA synthesis inhibitors
Melphalan hydrochloride	DNA synthesis inhibitors
Mercaptopurine	DNA synthesis inhibitors
Metformin hydrochloride aq	DNA synthesis inhibitors
Methotrexate	Other
Methoxsalen	Other
Methylprednisolone	Hormonal agents
MGCD-265	RTK inhibitors
MGCD0103_Mocetinostat	HDAC inhibitors
Mithramycin A	Other
Mitomycin	DNA synthesis inhibitors
Mitotane	Hormonal agents
Mitoxantrone	TOPO inhibitors
MK-0752	Other
MK-2206	PI3K/AKT/mTOR inhibitors
MK-4827, HCl salt	Other
MK1775	Cell cycle inhibitors
MLN4924	Other
MLN8237_Alisertib	Antimitotic agents
Motesanib Diphosphate (AMG-706)	RTK inhibitors
Nelarabine	DNA synthesis inhibitors
Nilotinib	RTK inhibitors
Nilutamide	Hormonal agents
Nutlin-3	MDM2 inhibitors
NVP-AUY922	Heat shock protein inhibitors
NVP-BEZ235_Dactolisib	PI3K/AKT/mTOR inhibitors
NVP-BGJ398	RTK inhibitors
NVP-LDE225 (Diphosphate salt)	Other
Obatoclax Mesylate (GX15-070)	Apoptosis activators
Olaparib	Other
Omacetaxine mepesuccinate	Other
OSI-027	PI3K/AKT/mTOR inhibitors

Table C.3 continued from previous page

Compound	Target.Class
OSI-906_Linsitinib	RTK inhibitors
Osimertinib	RTK inhibitors
Oxaliplatin	DNA synthesis inhibitors
PAC-1	Apoptosis activators
Paclitaxel	Antimitotic agents
Palbociclib	Cell cycle inhibitors
Panobinostat	HDAC inhibitors
Pazopanib	RTK inhibitors
Pazopanib hydrochloride	RTK inhibitors
PCI-32765_Ibrutinib	Other
PD-0332991	Cell cycle inhibitors
Pemetrexed	DNA synthesis inhibitors
Pemetrexed, Disodium salt, Heptahydrate	DNA synthesis inhibitors
Pentostatin	DNA synthesis inhibitors
Perifosine aq/PBS	PI3K/AKT/mTOR inhibitors
PF 431396	Other
PF 477736	Cell cycle inhibitors
PF-04691502	PI3K/AKT/mTOR inhibitors
PF-04708671	Other
PF-2341066 (Crizotinib)	RTK inhibitors
PF-3845	Other
PF4800567 hydrochloride	Other
PF670462	Other
PHA-739358 (Danusertib)	Antimitotic agents
PIK-75 HCl	PI3K/AKT/mTOR inhibitors
Pilocarpine	Other
Pipobroman	Other
PKC412_Midostaurin	RTK inhibitors
Plerixafor	Other
Plicamycin	Other
PLX4032_Vemurafenib	RAS/RAF/MEK/MAPK inhibitors
Pomalidomide	Other
Pralatrexate	Other
Pravastatin	Other
Prednisolone	Hormonal agents
Prednisone	Hormonal agents
Prima-1 Met	Other
Procarbazine hydrochloride	DNA synthesis inhibitors
PX-866_Sonolisib	PI3K/AKT/mTOR inhibitors
Quinacrine HCl	Other
R406_Tamatinib	Other
RAF265	RAS/RAF/MEK/MAPK inhibitors
Raloxifene	Hormonal agents

Table C.3 continued from previous page

Compound	Target.Class
Rapamycin (sirolimus)	PI3K/AKT/mTOR inhibitors
RD162	Hormonal agents
RDEA119_Refametinib	RAS/RAF/MEK/MAPK inhibitors
Ridaforolimus	PI3K/AKT/mTOR inhibitors
Rofecoxib (Vioxx)	Other
Romidepsin	HDAC inhibitors
Roscovitine_Selicilib	Cell cycle inhibitors
S-trityl-L-cysteine, 40 mM	Other
SB 743921	Antimitotic agents
Simvastatin	Other
Sorafenib	RTK inhibitors
Sotrastaurin	Other
SR1 HCl	Other
Stattic	JAK/STAT inhibitors
Streptozocin	DNA synthesis inhibitors
Sunitinib	RTK inhibitors
TAK-733	RAS/RAF/MEK/MAPK inhibitors
TAK-901	RTK inhibitors
Tamoxifen citrate	Hormonal agents
Tandutinib	RTK inhibitors
Tasocitinib_Tofacitinib	JAK/STAT inhibitors
Temozolomide	DNA synthesis inhibitors
Temsirolimus	PI3K/AKT/mTOR inhibitors
Teniposide	TOPO inhibitors
Tetramisole HCl	Other
TGX-221	PI3K/AKT/mTOR inhibitors
Thalidomide	Other
Thio-TEPA	DNA synthesis inhibitors
Thioguanine	DNA synthesis inhibitors
Tipifarnib (Zarnestra)	Other
Topotecan hydrochloride	TOPO inhibitors
Toremifene citrate	Hormonal agents
Tretinoin	Other
Triethylenemelamine	Other
Trifluridine	DNA synthesis inhibitors
Tubacin	HDAC inhibitors
Tubastatin A HCl	HDAC inhibitors
UCN-01	PI3K/AKT/mTOR inhibitors
Uracil mustard	DNA synthesis inhibitors
Uridine triacetate	Other
Valproic acid	HDAC inhibitors
Valrubicin	TOPO inhibitors
Vandetanib	RTK inhibitors

Table C.3 continued from previous page

Compound	**Target.Class**
Varespladib	Other
Vatalanib	RTK inhibitors
Vemurafenib	RAS/RAF/MEK/MAPK inhibitors
VER 155008	Heat shock protein inhibitors
Vinblastine sulfate	Antimitotic agents
Vincristine Sulfate (Oncovin)	Antimitotic agents
Vinorelbine tartrate	Antimitotic agents
Vismodegib	Other
Vorinostat	HDAC inhibitors
VX-11e	RAS/RAF/MEK/MAPK inhibitors
XAV-939	Other
XL-147	PI3K/AKT/mTOR inhibitors
XL184_Cabozantinib	RTK inhibitors
XL880 (Foretinib)	RTK inhibitors
YM155	Apoptosis activators
Zoledronic acid	Other
ZSTK474	PI3K/AKT/mTOR inhibitors

Table C.4: The 227 p53 target genes found to be inducible by Nutlin-3a in TERA1 cells.

Gene_Symbol	KITLG_p53RE +/+			KITLG_p53RE -/-			KITLG_p53RE -/KI		
	log2FC	Pvalue	FDR	log2FC	Pvalue	FDR	log2FC	Pvalue	FDR
ABCA12	4.05	1.93E-05	5.86E-04	1.72	3.79E-02	2.26E-01	3.04	2.80E-03	4.55E-02
ABHD4	1.25	2.61E-09	3.45E-07	1.30	5.68E-10	1.57E-07	1.21	3.67E-09	7.93E-07
ABTB2	0.45	4.36E-03	3.73E-02	0.47	3.66E-03	5.02E-02	0.57	7.57E-04	1.87E-02
ADCK3	1.60	4.15E-15	5.64E-12	1.63	2.64E-15	6.03E-12	1.44	9.65E-14	1.25E-10
AEN	0.52	2.00E-05	6.05E-04	0.24	2.80E-02	1.88E-01	0.35	1.95E-03	3.59E-02
AKAP9	0.68	7.12E-04	9.85E-03	0.32	9.31E-02	3.67E-01	0.19	2.98E-01	6.54E-01
ALDH1A3	1.64	4.08E-10	7.02E-08	2.02	3.84E-11	1.76E-08	2.31	2.01E-12	1.53E-09
AMOTL1	0.84	8.20E-08	6.46E-06	0.48	3.02E-04	8.54E-03	0.59	2.31E-05	1.33E-03
AMZ2	0.70	4.86E-08	4.05E-06	0.83	1.32E-09	3.35E-07	0.76	9.13E-09	1.78E-06
ANKRA2	1.98	2.27E-08	2.13E-06	1.91	2.90E-08	4.70E-06	1.92	3.38E-08	5.35E-06
ANXA4	0.98	5.84E-06	2.29E-04	0.90	1.95E-05	1.08E-03	0.79	1.00E-04	4.06E-03
APOBEC3C	1.86	1.95E-10	3.90E-08	1.75	9.26E-11	3.53E-08	1.76	1.27E-10	4.84E-08
APOBEC3H	2.03	4.99E-03	4.14E-02	2.92	3.18E-03	4.54E-02	2.63	8.81E-04	2.10E-02
ARC	2.46	1.40E-04	2.77E-03	5.33	1.74E-04	5.72E-03	4.00	2.14E-06	1.87E-04
ARHGEF3	0.40	7.13E-02	2.44E-01	0.50	3.56E-02	2.17E-01	0.98	1.14E-04	4.45E-03
ASCC3	0.77	3.93E-06	1.68E-04	0.67	4.58E-05	2.09E-03	0.60	1.75E-04	6.33E-03
ASTN2	1.28	4.00E-07	2.43E-05	1.11	3.20E-06	2.44E-04	1.00	1.31E-05	8.35E-04
ATF3	2.10	8.31E-12	2.42E-09	1.23	1.46E-07	1.87E-05	1.09	1.52E-06	1.39E-04
BBC3	1.82	1.20E-14	1.06E-11	1.36	1.96E-11	1.08E-08	1.25	1.44E-10	5.03E-08
BCL2L1	0.68	1.60E-03	1.81E-02	0.50	1.83E-02	1.43E-01	0.68	1.88E-03	3.48E-02
BCL6	1.33	3.60E-05	9.68E-04	2.31	1.65E-09	4.05E-07	2.18	5.12E-09	1.07E-06
BLCAP	0.50	1.12E-04	2.36E-03	0.57	2.64E-05	1.35E-03	0.52	7.42E-05	3.26E-03
BLOC1S2	1.29	1.60E-14	1.28E-11	1.20	1.03E-13	1.65E-10	1.25	3.43E-14	6.12E-11
BMP7	0.78	1.31E-03	1.54E-02	0.61	7.01E-03	7.65E-02	0.67	2.62E-03	4.36E-02
BTBD10	0.52	3.23E-03	3.02E-02	0.70	1.74E-04	5.72E-03	0.53	2.70E-03	4.45E-02

Table C.4 continued from previous page

Gene_Symbol	KITLG_p53RE +/+			KITLG_p53RE -/-			KITLG_p53RE -/KI		
	log2FC	Pvalue	FDR	log2FC	Pvalue	FDR	log2FC	Pvalue	FDR
BTG2	2.76	4.14E-19	1.66E-15	2.62	2.37E-18	9.49E-15	1.81	1.90E-14	5.06E-11
C17orf89	0.88	2.69E-10	5.06E-08	0.65	1.84E-07	2.27E-05	0.64	2.15E-07	2.79E-05
CCDC90B	0.81	1.28E-05	4.19E-04	0.78	2.01E-05	1.10E-03	0.82	9.69E-06	6.65E-04
CCNG1	0.66	3.69E-03	3.33E-02	0.30	1.51E-01	4.67E-01	0.50	1.93E-02	1.62E-01
CD82	3.44	6.35E-11	1.45E-08	1.38	2.90E-05	1.43E-03	1.60	2.24E-06	1.91E-04
CDH8	0.67	1.29E-02	7.91E-02	1.92	8.24E-10	2.23E-07	1.56	2.42E-08	3.99E-06
CDIP1	0.95	5.44E-10	8.74E-08	0.77	3.14E-08	5.03E-06	0.97	1.34E-10	4.93E-08
CDKN1A	2.92	1.04E-23	1.67E-19	2.25	1.34E-20	1.22E-16	1.89	1.62E-18	9.90E-15
CEL	1.60	2.01E-07	1.36E-05	1.23	5.06E-05	2.26E-03	1.31	2.43E-05	1.39E-03
CES2	0.86	5.17E-06	2.09E-04	0.68	2.57E-04	7.60E-03	0.69	1.67E-04	6.11E-03
CHST14	0.40	9.12E-03	6.27E-02	0.84	1.81E-06	1.54E-04	0.92	3.49E-07	4.07E-05
CLCA2	3.08	2.69E-05	7.65E-04	2.36	8.53E-05	3.30E-03	4.03	2.29E-06	1.95E-04
CLDN1	5.61	8.03E-05	1.81E-03	1.99	3.44E-04	9.40E-03	2.79	1.37E-06	1.27E-04
CLP1	0.32	3.08E-02	1.43E-01	0.62	1.25E-04	4.45E-03	0.57	3.25E-04	1.00E-02
CMBL	1.71	5.28E-13	2.22E-10	1.46	1.11E-11	7.38E-09	1.45	1.43E-11	9.50E-09
COL7A1	1.51	7.08E-06	2.62E-04	0.99	1.57E-03	2.74E-02	0.74	1.12E-02	1.15E-01
CPEB2	0.64	2.57E-02	1.26E-01	1.02	1.37E-03	2.52E-02	0.83	5.81E-03	7.52E-02
CPEB4	0.88	4.09E-03	3.57E-02	0.52	4.01E-02	2.34E-01	0.51	4.05E-02	2.44E-01
CPSF4	0.45	2.85E-03	2.77E-02	0.44	3.86E-03	5.22E-02	0.55	5.30E-04	1.45E-02
CROT	1.53	1.81E-04	3.41E-03	1.94	7.18E-05	2.91E-03	1.28	2.74E-03	4.48E-02
CSF1	2.77	4.07E-14	2.74E-11	2.76	9.53E-14	1.65E-10	2.80	1.18E-13	1.35E-10
CSNK1G1	1.21	2.55E-13	1.31E-10	1.13	2.86E-12	2.41E-09	1.27	1.02E-13	1.25E-10
CYFIP2	1.14	3.28E-08	2.90E-06	0.98	5.15E-07	5.38E-05	0.82	8.71E-06	6.14E-04
CYP4F3	2.47	5.69E-03	4.51E-02	3.75	1.32E-05	7.76E-04	4.16	8.46E-05	3.59E-03
DDB2	1.56	1.08E-12	3.82E-10	1.25	9.48E-11	3.53E-08	0.90	1.08E-07	1.54E-05
DDIT4	3.57	1.82E-06	8.91E-05	2.52	2.80E-05	1.41E-03	2.71	5.14E-06	3.95E-04

Table C.4 continued from previous page

Gene_Symbol	KITLG_p53RE +/+			KITLG_p53RE -/-			KITLG_p53RE -/KI		
	log2FC	Pvalue	FDR	log2FC	Pvalue	FDR	log2FC	Pvalue	FDR
DDR1	1.09	1.71E-13	9.14E-11	0.55	5.86E-07	5.97E-05	0.60	1.12E-07	1.58E-05
DGKA	2.25	6.62E-07	3.82E-05	1.83	6.81E-06	4.48E-04	1.54	8.87E-05	3.73E-03
DHRS3	0.81	6.99E-05	1.64E-03	0.27	1.37E-01	4.46E-01	0.40	3.24E-02	2.17E-01
DRAM1	2.02	7.93E-11	1.79E-08	1.81	2.21E-09	5.35E-07	1.58	1.39E-08	2.53E-06
DUSP14	1.34	1.78E-11	4.51E-09	1.20	1.88E-10	6.39E-08	1.05	4.01E-09	8.55E-07
E2F7	1.01	1.00E-03	1.27E-02	1.33	3.28E-05	1.59E-03	1.33	4.01E-05	2.04E-03
EBI3	1.68	3.24E-03	3.03E-02	1.65	2.81E-03	4.19E-02	1.97	3.38E-04	1.03E-02
EDA2R	1.37	1.09E-09	1.59E-07	1.14	2.57E-07	2.94E-05	0.92	7.00E-06	5.09E-04
EFNB1	0.73	7.34E-05	1.71E-03	0.81	3.13E-05	1.53E-03	0.53	2.86E-03	4.60E-02
EI24	0.77	6.40E-10	1.00E-07	0.80	3.14E-10	9.31E-08	0.79	4.38E-10	1.30E-07
EML2	1.77	1.66E-07	1.18E-05	1.78	2.17E-07	2.56E-05	1.74	3.23E-07	3.85E-05
EPS8L2	2.41	3.77E-12	1.16E-09	2.34	5.69E-11	2.46E-08	2.28	8.82E-11	3.72E-08
FAM198B	4.22	6.02E-12	1.82E-09	3.88	3.58E-09	7.95E-07	4.02	1.95E-10	6.49E-08
FAM210B	1.11	1.26E-11	3.34E-09	1.11	1.68E-11	9.61E-09	1.09	2.57E-11	1.52E-08
FAM212B	2.10	9.87E-14	6.07E-11	1.88	1.09E-12	1.08E-09	1.59	5.24E-11	2.39E-08
FAM84B	0.70	2.07E-05	6.17E-04	0.76	3.41E-06	2.57E-04	0.63	6.47E-05	2.94E-03
FAM98C	2.06	1.21E-08	1.32E-06	1.66	3.09E-07	3.43E-05	1.28	6.49E-06	4.78E-04
FAS	1.66	3.79E-07	2.34E-05	1.72	2.50E-07	2.88E-05	1.68	3.63E-07	4.18E-05
FBXO22	0.86	1.23E-08	1.32E-06	0.67	1.38E-06	1.24E-04	0.71	4.95E-07	5.38E-05
FBXW7	1.31	3.17E-11	7.80E-09	1.35	1.44E-11	9.02E-09	1.07	3.43E-09	7.72E-07
FCHSD2	0.45	1.54E-02	8.91E-02	0.44	2.07E-02	1.56E-01	0.78	1.21E-04	4.73E-03
FDXR	2.49	1.78E-14	1.35E-11	2.19	3.43E-13	4.22E-10	1.89	1.10E-11	8.01E-09
FLRT2	0.15	2.82E-01	5.46E-01	0.25	9.93E-02	3.79E-01	0.49	1.43E-03	2.89E-02
FOSL1	1.16	4.03E-07	2.44E-05	0.69	5.78E-04	1.38E-02	1.09	1.59E-06	1.44E-04
FUCA1	1.01	1.01E-04	2.17E-03	0.52	5.23E-02	2.69E-01	0.27	2.52E-01	6.10E-01
GADD45A	1.44	3.59E-13	1.69E-10	1.22	2.46E-11	1.27E-08	1.43	4.97E-13	4.68E-10

Table C.4 continued from previous page

Gene_Symbol	KITLG_p53RE +/+			KITLG_p53RE -/-			KITLG_p53RE -/KI		
	log2FC	Pvalue	FDR	log2FC	Pvalue	FDR	log2FC	Pvalue	FDR
GBE1	1.02	2.70E-09	3.50E-07	0.64	1.11E-05	6.75E-04	0.62	1.89E-05	1.11E-03
GDF15	3.55	5.50E-19	1.76E-15	3.50	1.74E-18	9.29E-15	3.52	1.86E-18	9.90E-15
GLS2	1.67	5.01E-09	6.03E-07	1.77	2.10E-10	6.87E-08	1.74	3.40E-09	7.72E-07
GPC1	1.31	1.23E-08	1.32E-06	0.76	2.77E-04	8.01E-03	0.66	4.14E-04	1.21E-02
GPR87	3.33	1.27E-11	3.34E-09	3.09	2.02E-10	6.72E-08	2.94	2.91E-10	8.94E-08
GPX1	0.67	6.19E-06	2.37E-04	0.61	2.29E-05	1.21E-03	0.48	4.39E-04	1.26E-02
GRHL3	3.51	5.79E-08	4.70E-06	2.93	2.32E-07	2.69E-05	2.53	1.05E-06	1.01E-04
HES1	1.21	5.73E-10	9.07E-08	0.71	8.70E-06	5.59E-04	0.45	1.69E-03	3.24E-02
HES2	3.50	2.70E-08	2.47E-06	2.48	3.89E-06	2.84E-04	1.52	2.04E-03	3.70E-02
HRAS	1.10	1.02E-05	3.52E-04	0.95	8.28E-05	3.23E-03	1.04	3.49E-05	1.85E-03
HSD17B3	1.20	1.79E-07	1.25E-05	1.09	1.71E-06	1.48E-04	1.34	2.95E-07	3.68E-05
HSPA4L	1.81	3.88E-08	3.32E-06	1.10	1.04E-05	6.39E-04	1.35	7.61E-07	7.85E-05
ICOSLG	1.18	6.92E-06	2.57E-04	1.31	6.36E-06	4.24E-04	1.65	6.98E-08	1.04E-05
IER5	0.70	8.61E-07	4.75E-05	0.78	1.18E-07	1.54E-05	0.79	9.22E-08	1.35E-05
IKBIP	1.20	1.04E-11	2.86E-09	1.34	1.15E-12	1.08E-09	1.46	6.54E-14	9.52E-11
INPP1	2.17	4.23E-15	5.64E-12	1.48	1.52E-11	9.02E-09	1.39	3.87E-11	1.93E-08
ISCU	1.35	1.08E-07	8.34E-06	1.20	9.99E-07	9.52E-05	1.40	5.58E-08	8.42E-06
ISYNA1	0.92	2.06E-05	6.15E-04	0.68	8.18E-04	1.76E-02	0.57	2.73E-03	4.48E-02
ITGA3	1.06	2.51E-03	2.52E-02	1.17	1.82E-03	3.05E-02	1.60	2.62E-05	1.47E-03
JAG1	0.21	1.86E-01	4.35E-01	0.57	8.70E-04	1.83E-02	0.29	6.82E-02	3.24E-01
KCNN4	3.72	3.69E-07	2.29E-05	4.64	2.27E-05	1.21E-03	1.76	7.22E-03	8.61E-02
KITLG	2.03	1.53E-11	3.94E-09	-0.11	7.20E-01	9.03E-01	1.81	7.07E-10	2.02E-07
KLHDC7A	2.15	5.92E-09	7.01E-07	1.17	8.31E-04	1.77E-02	0.89	1.25E-02	1.23E-01
LACC1	3.37	3.68E-08	3.17E-06	1.92	1.94E-06	1.62E-04	1.90	3.13E-06	2.54E-04
LAPTM5	2.23	1.07E-05	3.65E-04	1.08	8.92E-02	3.59E-01	4.85	1.00E-03	2.31E-02
LIF	2.09	2.35E-03	2.40E-02	1.88	8.27E-04	1.77E-02	1.41	7.56E-03	8.83E-02

Table C.4 continued from previous page

Gene_Symbol	KITLG_p53RE +/+			KITLG_p53RE -/-			KITLG_p53RE -/KI		
	log2FC	Pvalue	FDR	log2FC	Pvalue	FDR	log2FC	Pvalue	FDR
LIMK2	0.69	1.08E-06	5.80E-05	0.65	2.92E-06	2.26E-04	0.47	2.73E-04	8.71E-03
LMNA	0.72	5.78E-03	4.56E-02	0.71	7.94E-03	8.30E-02	0.66	1.16E-02	1.18E-01
LPXN	0.55	7.43E-02	2.50E-01	0.80	3.25E-02	2.05E-01	1.53	2.76E-05	1.53E-03
LRP1	0.59	1.53E-04	2.98E-03	0.83	8.09E-07	7.79E-05	0.58	1.87E-04	6.62E-03
LRPAP1	0.55	7.65E-06	2.79E-04	0.39	5.96E-04	1.42E-02	0.43	2.17E-04	7.34E-03
MAST4	1.36	9.35E-09	1.05E-06	1.17	1.54E-07	1.96E-05	0.87	2.06E-05	1.20E-03
MDM2	2.49	2.96E-23	2.37E-19	1.99	1.52E-20	1.22E-16	2.00	1.38E-20	2.21E-16
MICALL1	1.31	1.03E-12	3.74E-10	1.09	5.36E-11	2.38E-08	1.05	1.36E-10	4.93E-08
MLF2	0.36	1.20E-03	1.46E-02	0.27	1.15E-02	1.06E-01	0.24	2.30E-02	1.78E-01
MON2	0.43	2.16E-03	2.26E-02	0.44	1.23E-03	2.32E-02	0.35	9.76E-03	1.05E-01
MR1	4.44	1.35E-04	2.69E-03	3.46	1.08E-05	6.57E-04	4.86	2.46E-07	3.12E-05
MRPL49	0.81	6.28E-05	1.50E-03	0.71	2.08E-04	6.52E-03	0.68	3.64E-04	1.09E-02
MYBPHL	2.70	1.48E-04	2.90E-03	1.79	2.27E-02	1.64E-01	1.93	9.92E-03	1.06E-01
MYO6	1.47	1.06E-14	1.00E-11	1.00	1.02E-10	3.61E-08	1.21	1.02E-12	8.12E-10
NADSYN1	1.29	5.33E-14	3.41E-11	1.24	1.98E-13	2.88E-10	1.18	5.33E-13	4.74E-10
NEFL	2.03	7.10E-10	1.10E-07	1.00	5.11E-06	3.52E-04	1.24	1.62E-07	2.19E-05
NINJ1	1.28	2.00E-08	1.92E-06	1.39	1.89E-08	3.32E-06	1.16	1.33E-07	1.84E-05
NOTCH1	0.76	3.82E-05	1.01E-03	0.45	8.73E-03	8.88E-02	0.53	2.69E-03	4.45E-02
NTPCR	0.57	3.24E-06	1.42E-04	0.56	4.47E-06	3.15E-04	0.61	1.16E-06	1.10E-04
NUPR1	4.85	1.21E-10	2.54E-08	3.06	6.68E-07	6.68E-05	3.53	2.22E-07	2.84E-05
NYNRIN	1.90	5.67E-03	4.51E-02	1.92	1.21E-03	2.29E-02	1.29	8.36E-03	9.48E-02
ORAI3	1.81	1.26E-08	1.34E-06	2.24	1.97E-08	3.38E-06	1.47	6.99E-07	7.30E-05
PANK1	1.11	2.00E-07	1.35E-05	0.94	3.44E-06	2.57E-04	1.06	4.41E-07	4.90E-05
PAQR7	1.54	3.64E-07	2.26E-05	0.83	1.24E-03	2.33E-02	0.69	4.32E-03	6.15E-02
PARD6G	0.70	9.34E-06	3.28E-04	0.85	5.95E-07	6.03E-05	0.78	2.04E-06	1.79E-04
PCNA	0.39	1.70E-03	1.90E-02	0.51	9.60E-05	3.62E-03	0.57	2.09E-05	1.21E-03

Table C.4 continued from previous page

Gene_Symbol	KITLG_p53RE +/+			KITLG_p53RE -/-			KITLG_p53RE -/KI		
	log2FC	Pvalue	FDR	log2FC	Pvalue	FDR	log2FC	Pvalue	FDR
PDE4C	3.83	2.22E-09	3.03E-07	1.74	4.36E-03	5.68E-02	3.26	1.67E-07	2.24E-05
PERP	0.28	5.09E-03	4.20E-02	0.22	2.48E-02	1.74E-01	0.31	2.25E-03	3.93E-02
PGAP1	0.73	1.06E-05	3.63E-04	0.66	4.16E-05	1.94E-03	0.62	6.12E-05	2.85E-03
PHLDA3	1.26	1.34E-06	6.97E-05	1.07	1.98E-05	1.09E-03	1.22	2.56E-06	2.14E-04
PHPT1	0.75	2.50E-03	2.51E-02	0.46	4.89E-02	2.61E-01	0.34	1.43E-01	4.67E-01
PLCL2	1.31	4.19E-11	1.00E-08	0.88	4.72E-08	6.99E-06	0.57	5.12E-05	2.48E-03
PLK2	0.76	2.17E-07	1.46E-05	0.71	5.39E-07	5.56E-05	0.92	5.52E-09	1.12E-06
PLK3	1.13	3.68E-08	3.17E-06	0.89	4.15E-06	2.98E-04	0.68	1.77E-04	6.38E-03
PLTP	1.26	1.15E-04	2.38E-03	1.22	4.33E-05	2.01E-03	0.93	1.01E-03	2.32E-02
PLXNB1	0.69	6.58E-06	2.46E-04	0.35	1.10E-02	1.04E-01	0.22	9.36E-02	3.78E-01
PLXNB2	1.29	2.65E-09	3.47E-07	1.09	2.20E-07	2.57E-05	0.96	6.82E-07	7.18E-05
PMAIP1	1.07	1.78E-08	1.77E-06	0.87	1.40E-06	1.26E-04	1.10	2.03E-08	3.56E-06
PML	0.58	1.30E-04	2.61E-03	0.81	1.37E-06	1.24E-04	0.64	3.76E-05	1.95E-03
POLH	1.80	7.74E-13	2.88E-10	1.24	9.83E-10	2.58E-07	1.34	2.05E-10	6.57E-08
POU3F1	1.71	3.85E-09	4.77E-07	1.65	1.97E-08	3.38E-06	1.66	8.82E-09	1.74E-06
PPM1D	1.17	9.47E-11	2.09E-08	1.10	3.58E-10	1.03E-07	0.89	2.88E-08	4.61E-06
PRDM1	2.08	1.96E-08	1.90E-06	0.71	5.48E-02	2.77E-01	0.35	2.74E-01	6.29E-01
PRKAB1	0.96	3.34E-10	5.93E-08	1.08	3.00E-11	1.46E-08	0.96	2.00E-10	6.51E-08
PRKAB2	0.55	3.83E-06	1.65E-04	0.62	7.03E-07	6.94E-05	0.50	2.47E-05	1.40E-03
PRKX	0.92	4.03E-09	4.95E-07	0.63	6.83E-06	4.48E-04	0.76	2.08E-07	2.75E-05
PSTPIP2	1.66	4.96E-09	6.01E-07	1.18	7.88E-06	5.10E-04	1.42	2.00E-07	2.66E-05
PTAFR	2.55	5.13E-09	6.13E-07	1.08	1.41E-03	2.56E-02	1.14	5.10E-04	1.41E-02
PTP4A1	0.70	6.90E-07	3.96E-05	0.52	7.56E-05	3.02E-03	0.58	1.72E-05	1.04E-03
PTPRU	1.38	8.76E-09	9.94E-07	0.89	2.06E-05	1.11E-03	0.82	2.58E-05	1.45E-03
PVRL4	3.99	5.86E-13	2.34E-10	2.44	8.36E-08	1.16E-05	3.02	2.01E-08	3.56E-06
RABGGTA	0.88	9.62E-04	1.23E-02	0.89	9.08E-04	1.89E-02	0.87	1.01E-03	2.32E-02

Table C.4 continued from previous page

Gene_Symbol	KITLG_p53RE +/+			KITLG_p53RE -/-			KITLG_p53RE -/KI		
	log2FC	Pvalue	FDR	log2FC	Pvalue	FDR	log2FC	Pvalue	FDR
RAD51C	0.67	2.47E-04	4.41E-03	0.67	2.81E-04	8.09E-03	0.44	8.28E-03	9.40E-02
RALGDS	2.19	3.22E-11	7.81E-09	1.73	8.69E-09	1.76E-06	2.19	4.87E-11	2.29E-08
RAP2B	0.94	1.50E-09	2.10E-07	1.06	9.92E-11	3.60E-08	1.32	4.18E-13	4.18E-10
RBM38	0.97	4.72E-06	1.93E-04	0.90	1.16E-05	6.94E-04	0.95	5.26E-06	4.00E-04
RETSAT	1.72	8.71E-18	2.32E-14	1.65	2.31E-17	7.39E-14	1.49	3.32E-16	1.06E-12
RGL1	1.01	1.40E-07	1.03E-05	0.32	3.63E-02	2.20E-01	0.49	2.43E-03	4.13E-02
RGMA	1.35	1.58E-12	5.49E-10	0.93	9.58E-09	1.89E-06	0.68	2.60E-06	2.14E-04
RGS16	2.67	3.03E-19	1.61E-15	1.72	3.50E-15	7.00E-12	1.93	2.59E-16	1.03E-12
RGS20	1.11	3.82E-05	1.01E-03	0.75	2.27E-03	3.60E-02	0.84	5.67E-04	1.52E-02
RNF144B	1.85	2.96E-08	2.66E-06	1.84	5.73E-08	8.33E-06	1.73	9.36E-08	1.36E-05
RNF19B	0.97	2.28E-06	1.04E-04	0.96	4.31E-06	3.05E-04	0.96	3.00E-06	2.45E-04
RPS27L	0.83	4.58E-10	7.78E-08	0.72	8.26E-09	1.70E-06	0.78	1.43E-09	3.62E-07
RRAD	5.82	1.37E-06	7.06E-05	2.40	7.94E-03	8.30E-02	7.24	2.55E-06	2.14E-04
RRM2B	1.41	5.70E-13	2.34E-10	1.15	7.62E-11	2.98E-08	1.14	1.72E-10	5.85E-08
SARS	0.77	1.44E-04	2.85E-03	0.82	6.07E-05	2.58E-03	0.74	2.62E-04	8.44E-03
SCN2A	1.65	4.19E-04	6.51E-03	1.49	6.81E-04	1.56E-02	1.17	5.15E-03	6.90E-02
SCN3B	2.21	2.68E-05	7.65E-04	2.25	1.16E-04	4.19E-03	2.20	5.97E-05	2.82E-03
SCN4B	-0.44	7.44E-01	8.88E-01	1.71	2.78E-02	1.88E-01	2.36	6.91E-04	1.74E-02
SCRIB	0.77	3.04E-05	8.46E-04	0.46	5.06E-03	6.22E-02	0.64	3.40E-04	1.03E-02
SDC4	0.60	2.66E-03	2.62E-02	0.58	3.71E-03	5.06E-02	0.60	2.59E-03	4.32E-02
SDPR	3.09	9.58E-05	2.08E-03	5.12	2.15E-03	3.45E-02	2.95	2.25E-02	1.76E-01
SEMA3B	1.56	1.08E-03	1.34E-02	1.09	3.39E-02	2.12E-01	2.29	1.90E-04	6.68E-03
SERPINE1	1.53	1.68E-10	3.45E-08	1.31	4.56E-09	9.86E-07	1.34	3.27E-09	7.57E-07
SERTAD1	1.62	3.08E-13	1.50E-10	1.44	3.72E-12	2.83E-09	1.28	5.45E-11	2.42E-08
SESN1	1.53	1.45E-13	8.25E-11	1.46	4.48E-13	5.11E-10	1.61	3.40E-14	6.12E-11
SESN2	1.80	1.12E-11	3.05E-09	1.32	1.09E-08	2.12E-06	1.24	3.99E-08	6.25E-06

Table C.4 continued from previous page

Gene_Symbol	KITLG_p53RE +/+			KITLG_p53RE -/-			KITLG_p53RE -/KI		
	log2FC	Pvalue	FDR	log2FC	Pvalue	FDR	log2FC	Pvalue	FDR
SFN	2.03	3.26E-10	5.85E-08	2.09	1.22E-08	2.30E-06	1.66	5.35E-08	8.14E-06
SLC25A45	2.12	8.36E-06	3.01E-04	1.52	2.99E-03	4.35E-02	1.56	7.01E-04	1.76E-02
SLC30A1	0.54	9.53E-05	2.07E-03	0.26	3.98E-02	2.32E-01	0.40	2.55E-03	4.29E-02
SLC4A11	0.42	1.07E-03	1.33E-02	0.17	1.57E-01	4.74E-01	0.33	6.04E-03	7.69E-02
SMAD3	1.45	7.67E-15	9.43E-12	1.08	2.10E-11	1.12E-08	0.99	1.11E-10	4.46E-08
SNX2	0.39	4.58E-04	7.00E-03	0.37	7.89E-04	1.72E-02	0.36	1.03E-03	2.35E-02
SOCS4	0.46	3.79E-03	3.40E-02	0.22	1.39E-01	4.50E-01	0.48	2.06E-03	3.72E-02
SPATA18	1.24	6.84E-05	1.61E-03	1.17	1.09E-04	4.01E-03	1.09	2.60E-04	8.39E-03
STAT3	0.57	7.13E-03	5.31E-02	0.82	2.88E-04	8.20E-03	0.67	2.22E-03	3.91E-02
STK17A	0.39	1.32E-03	1.55E-02	0.17	1.28E-01	4.30E-01	0.29	1.27E-02	1.25E-01
STX6	0.66	7.72E-08	6.18E-06	0.66	7.73E-08	1.09E-05	0.52	4.92E-06	3.82E-04
SULF2	1.21	2.91E-07	1.88E-05	1.27	1.11E-07	1.48E-05	0.94	1.07E-05	7.19E-04
SYTL1	3.63	8.59E-15	9.82E-12	2.21	1.74E-08	3.16E-06	2.03	2.31E-08	3.89E-06
TAB3	0.18	2.91E-01	5.55E-01	0.40	5.31E-02	2.71E-01	0.66	7.20E-04	1.79E-02
TM7SF3	0.54	4.58E-06	1.88E-04	0.58	1.34E-06	1.23E-04	0.63	2.98E-07	3.70E-05
TMEM63B	1.01	1.17E-04	2.40E-03	0.71	5.80E-03	6.80E-02	0.79	2.27E-03	3.95E-02
TMEM68	0.69	2.54E-03	2.53E-02	0.63	4.69E-03	5.96E-02	0.86	2.08E-04	7.11E-03
TMEM8B	0.81	8.48E-04	1.12E-02	1.47	1.68E-06	1.47E-04	0.98	9.15E-05	3.80E-03
TNFAIP8	0.25	2.49E-02	1.24E-01	0.51	4.86E-05	2.19E-03	0.46	1.42E-04	5.42E-03
TNFRSF10A	1.16	2.59E-04	4.58E-03	1.18	2.61E-04	7.69E-03	1.20	2.22E-04	7.45E-03
TNFRSF10B	0.79	1.21E-07	9.16E-06	0.68	1.90E-06	1.60E-04	0.57	2.41E-05	1.38E-03
TNFRSF10D	0.85	1.08E-05	3.67E-04	0.65	3.12E-04	8.73E-03	0.62	5.78E-04	1.54E-02
TP53I3	2.31	3.91E-13	1.79E-10	2.34	2.27E-13	3.03E-10	2.21	8.42E-13	7.09E-10
TP53INP1	2.29	1.19E-16	2.71E-13	2.08	2.22E-15	5.91E-12	1.82	6.21E-14	9.52E-11
TRAF4	1.16	1.81E-08	1.79E-06	1.41	2.18E-10	6.98E-08	1.19	1.00E-08	1.91E-06
TRAK1	1.03	2.90E-11	7.26E-09	0.78	1.56E-08	2.90E-06	0.70	1.48E-07	2.02E-05

Table C.4 continued from previous page

Gene_Symbol	KITLG_p53RE +/+			KITLG_p53RE -/-			KITLG_p53RE -/KI		
	log2FC	Pvalue	FDR	log2FC	Pvalue	FDR	log2FC	Pvalue	FDR
TRIAP1	1.13	9.55E-11	2.09E-08	0.91	1.12E-08	2.16E-06	0.91	9.91E-09	1.91E-06
TRIM22	1.33	9.70E-12	2.72E-09	1.03	3.63E-09	7.95E-07	1.30	4.02E-11	1.95E-08
TRIM32	0.42	4.02E-04	6.35E-03	0.27	1.49E-02	1.25E-01	0.39	6.87E-04	1.74E-02
TRIML2	0.46	2.01E-03	2.14E-02	0.32	2.62E-02	1.81E-01	0.20	1.43E-01	4.67E-01
TRIP6	0.45	2.96E-05	8.28E-04	0.31	2.37E-03	3.72E-02	0.25	1.07E-02	1.12E-01
TSGA10	0.40	2.65E-01	5.28E-01	0.67	4.54E-02	2.50E-01	1.21	1.08E-03	2.41E-02
TSKU	0.24	6.33E-02	2.25E-01	0.10	4.10E-01	7.25E-01	0.44	1.46E-03	2.93E-02
TSPAN11	1.92	5.10E-10	8.41E-08	1.27	8.17E-07	7.82E-05	1.75	1.01E-09	2.78E-07
UNC5B	0.78	1.05E-08	1.16E-06	0.58	2.55E-06	2.02E-04	0.60	1.34E-06	1.25E-04
UQCC1	0.39	1.07E-03	1.33E-02	0.36	2.55E-03	3.89E-02	0.24	3.73E-02	2.34E-01
VWCE	3.03	9.58E-16	1.57E-12	1.93	6.13E-12	4.26E-09	1.81	3.15E-11	1.68E-08
WDR63	2.50	4.27E-03	3.68E-02	3.29	2.81E-05	1.41E-03	2.86	5.26E-05	2.53E-03
XPC	1.19	1.09E-10	2.35E-08	1.09	9.84E-10	2.58E-07	0.93	1.59E-08	2.86E-06
YPEL3	2.01	7.01E-09	8.25E-07	1.99	6.75E-08	9.72E-06	1.74	2.22E-07	2.84E-05
ZMAT3	1.56	2.83E-12	9.05E-10	1.21	1.00E-09	2.58E-07	1.44	1.96E-11	1.20E-08
ZNF195	0.57	2.15E-06	9.97E-05	0.51	1.30E-05	7.65E-04	0.31	4.14E-03	6.02E-02
ZNF385A	2.65	7.10E-07	4.03E-05	3.01	5.47E-08	8.03E-06	1.81	1.01E-05	6.91E-04
ZNF488	0.98	6.44E-04	9.10E-03	0.52	6.31E-02	3.00E-01	0.75	7.25E-03	8.63E-02
ZNF561	1.07	1.08E-07	8.34E-06	0.79	2.04E-05	1.11E-03	1.23	8.00E-09	1.60E-06
ZNF79	1.47	2.12E-06	9.91E-05	1.18	2.53E-05	1.32E-03	0.86	1.75E-03	3.32E-02

Table C.5: The overlapping significant genes between the Combo vs Nutlin-3a contrast and Combo vs Dasatinib (CSTs).

Gene_Symbol	Entrez_ID	log2FC	PValue	FDR	Contrast
SLC2A1	6513	-1.04	6.24E-11	3.33E-07	Nutlin-3a
SFN	2810	-1.97	5.29E-10	1.69E-06	Nutlin-3a
RHOB	388	-1.55	8.63E-10	2.18E-06	Nutlin-3a
SERPINE1	5054	-1.41	1.02E-09	2.18E-06	Nutlin-3a
MYO10	4651	0.72	7.75E-09	1.24E-05	Nutlin-3a
NANOG	79923	-1.26	3.95E-08	5.74E-05	Nutlin-3a
PSPH	5723	0.66	1.47E-07	1.67E-04	Nutlin-3a
HES1	3280	-0.84	7.51E-07	6.68E-04	Nutlin-3a
TBC1D16	125058	0.73	9.80E-07	8.25E-04	Nutlin-3a
SLC7A11	23657	1.37	1.83E-06	1.33E-03	Nutlin-3a
RPRM	56475	1.12	3.14E-06	2.06E-03	Nutlin-3a
ZFP36L2	678	-0.75	3.68E-06	2.18E-03	Nutlin-3a
CARS	833	0.57	3.92E-06	2.24E-03	Nutlin-3a
MICALL1	85377	-0.61	5.81E-06	3.10E-03	Nutlin-3a
UNC5B	219699	-0.55	6.26E-06	3.23E-03	Nutlin-3a
ETS2	2114	-0.59	7.17E-06	3.43E-03	Nutlin-3a
FAM174B	400451	-0.55	7.51E-06	3.43E-03	Nutlin-3a
PLK1S1	NA	1.39	9.02E-06	3.79E-03	Nutlin-3a
WNT9A	7483	-1.35	1.10E-05	4.50E-03	Nutlin-3a
PHLDA2	7262	-1.23	1.42E-05	5.45E-03	Nutlin-3a
TSC22D3	1831	-0.75	1.87E-05	6.51E-03	Nutlin-3a
GJA1	2697	-0.57	2.64E-05	8.61E-03	Nutlin-3a
SRGAP3	9901	0.85	3.41E-05	1.07E-02	Nutlin-3a
PTCH1	5727	1.05	3.96E-05	1.15E-02	Nutlin-3a
LPAR1	1902	1.22	4.33E-05	1.22E-02	Nutlin-3a
ETV1	2115	0.64	4.62E-05	1.22E-02	Nutlin-3a

TLE3	7090	0.63	5.02E-05	1.28E-02	Nutlin-3a
PICALM	8301	-0.44	9.26E-05	2.01E-02	Nutlin-3a
KCNA5	3741	2.36	9.36E-05	2.01E-02	Nutlin-3a
TNFRSF8	943	-0.71	9.40E-05	2.01E-02	Nutlin-3a
FAXDC2	10826	1.21	1.02E-04	2.11E-02	Nutlin-3a
NAPG	8774	-0.76	1.13E-04	2.26E-02	Nutlin-3a
ELK3	2004	-0.42	1.28E-04	2.38E-02	Nutlin-3a
MCL1	4170	-0.36	1.30E-04	2.38E-02	Nutlin-3a
CDV3	55573	-0.43	1.33E-04	2.41E-02	Nutlin-3a
TMEM158	25907	-0.54	1.45E-04	2.50E-02	Nutlin-3a
TP53BP1	7158	0.46	1.46E-04	2.50E-02	Nutlin-3a
RASL11B	65997	-0.62	1.59E-04	2.70E-02	Nutlin-3a
SLCO1A2	6579	0.96	1.65E-04	2.75E-02	Nutlin-3a
CBX2	84733	0.51	2.90E-04	4.14E-02	Nutlin-3a
TMEM35	NA	0.64	3.13E-04	4.39E-02	Nutlin-3a
SERTAD1	29950	-0.52	3.43E-04	4.78E-02	Nutlin-3a
RASGRF2	5924	-0.83	3.58E-04	4.93E-02	Nutlin-3a
SERTAD1	29950	2.06	3.46E-15	4.63E-12	Dasatinib
TMEM35	NA	2.47	3.48E-15	4.63E-12	Dasatinib
TNFRSF8	943	-1.84	1.98E-13	1.27E-10	Dasatinib
SRGAP3	9901	1.76	7.06E-11	2.02E-08	Dasatinib
MICALL1	85377	1.08	2.51E-10	5.36E-08	Dasatinib
SERPINE1	5054	1.51	3.16E-10	6.32E-08	Dasatinib
UNC5B	219699	0.90	8.11E-10	1.43E-07	Dasatinib
SFN	2810	2.11	1.98E-09	3.07E-07	Dasatinib
HES1	3280	1.18	2.07E-09	3.19E-07	Dasatinib
CBX2	84733	-0.99	2.33E-09	3.48E-07	Dasatinib
FAXDC2	10826	2.43	2.77E-09	3.99E-07	Dasatinib

ETS2	2114	-0.80	2.78E-08	2.87E-06	Dasatinib
TLE3	7090	-0.92	4.30E-08	4.05E-06	Dasatinib
LPAR1	1902	-1.46	1.06E-07	8.36E-06	Dasatinib
PSPH	5723	0.63	3.47E-07	2.35E-05	Dasatinib
RASL11B	65997	-0.91	5.37E-07	3.35E-05	Dasatinib
CDV3	55573	-0.60	8.33E-07	4.71E-05	Dasatinib
TBC1D16	125058	-0.63	7.34E-06	2.88E-04	Dasatinib
ZFP36L2	678	-0.72	7.58E-06	2.95E-04	Dasatinib
TMEM158	25907	-0.66	8.18E-06	3.11E-04	Dasatinib
MCL1	4170	-0.42	1.56E-05	5.34E-04	Dasatinib
NANOG	79923	-0.89	1.81E-05	6.03E-04	Dasatinib
ETV1	2115	-0.65	2.04E-05	6.64E-04	Dasatinib
WNT9A	7483	1.39	2.32E-05	7.37E-04	Dasatinib
RHOB	388	0.84	6.60E-05	1.77E-03	Dasatinib
FAM174B	400451	-0.46	1.03E-04	2.54E-03	Dasatinib
PHLDA2	7262	-1.06	1.08E-04	2.62E-03	Dasatinib
NAPG	8774	-0.68	4.17E-04	7.58E-03	Dasatinib
PLK1S1	NA	1.00	4.27E-04	7.72E-03	Dasatinib
KCNA5	3741	-1.37	4.66E-04	8.29E-03	Dasatinib
SLCO1A2	6579	0.86	5.25E-04	9.08E-03	Dasatinib
PTCH1	5727	-0.75	5.78E-04	9.80E-03	Dasatinib
TP53BP1	7158	-0.39	6.49E-04	1.07E-02	Dasatinib
ELK3	2004	-0.37	6.64E-04	1.09E-02	Dasatinib
RPRM	56475	-0.67	1.10E-03	1.59E-02	Dasatinib
GJA1	2697	-0.42	1.11E-03	1.60E-02	Dasatinib
MYO10	4651	0.33	1.23E-03	1.72E-02	Dasatinib
SLC2A1	6513	-0.37	1.73E-03	2.19E-02	Dasatinib
RASGRF2	5924	-0.68	2.54E-03	2.90E-02	Dasatinib

SLC7A11	23657	0.73	3.06E-03	3.33E-02	Dasatinib
TSC22D3	1831	0.47	3.46E-03	3.61E-02	Dasatinib
PICALM	8301	-0.30	4.58E-03	4.44E-02	Dasatinib
CARS	833	0.31	5.13E-03	4.77E-02	Dasatinib

Table C.6: Hub genes for the Blue and Green Modules identified by WGCNA.

Gene_Symbol	Degree_Correlation	Degree_PPI	Module
ACKR3	959.4682	14.485	Blue
ADCY5	1020.833	21.954	Blue
AGRN	998.3433	25.427	Blue
BMP1	1013.422	11.066	Blue
CCND1	956.7421	16.207	Blue
CKAP4	954.6536	26.181	Blue
COL16A1	1002.808	21.122	Blue
COL18A1	983.5569	21.838	Blue
COL1A1	998.7649	29.875	Blue
COL1A2	942.4109	31.485	Blue
COL3A1	1015.503	30.137	Blue
COL5A1	929.7831	25.173	Blue
COL5A2	1021.536	25.876	Blue
COL6A1	946.8461	24.116	Blue
COL6A2	995.0795	22.292	Blue
COL6A3	953.4679	22.99	Blue
COL9A2	920.0077	21.807	Blue
CX3CL1	988.0092	14.418	Blue
DCN	919.7101	24.856	Blue
EDN1	948.4704	14.592	Blue
EDNRA	980.5898	10.975	Blue
FAM20C	929.98	19.126	Blue
FN1	966.6544	40.174	Blue
FZD2	1051.608	10.02	Blue
FZD4	924.2471	16.294	Blue
GNG11	1007.471	27.307	Blue
GPC3	938.4842	34.242	Blue
GPC6	1047.825	14.545	Blue
GPSM1	1048.348	12.694	Blue
HEBP1	979.0179	14.401	Blue
HSPG2	911.5753	26.468	Blue
IGF2	925.8596	17.107	Blue
IGFBP3	963.3188	20.115	Blue
IGFBP4	932.6541	20.019	Blue
IGFBP5	973.8268	20.128	Blue
ITGA1	920.7034	34.224	Blue
ITGA5	943.1307	11.108	Blue
JUN	968.4852	24.484	Blue
KLHL22	1001.568	9.911	Blue
LAMB1	918.0703	38.343	Blue
LAMB2	1020.337	32.861	Blue
LAMB3	955.5324	12.815	Blue
LTBP1	1019.055	20.917	Blue

Table C.6 continued from previous page

Gene_Symbol	Degree_Correlation	Degree_PPI	Module
MAGED2	943.0993	11.693	Blue
MAML2	934.1538	12.897	Blue
MFAP2	968.684	10.084	Blue
MXRA8	1027.772	19.043	Blue
NGF	996.8668	13.552	Blue
NOTCH1	915.6104	19.314	Blue
NOTCH3	940.6592	11.11	Blue
NOTCH4	1007.55	10.12	Blue
PDGFRA	1016.536	10.7	Blue
PDGFRB	985.0919	10.856	Blue
RHOB	1008.73	27.412	Blue
RHOBTB1	1009.22	19.935	Blue
RHOD	943.5924	20.835	Blue
RHOJ	977.6977	19.128	Blue
RHOU	917.0692	20.023	Blue
SDC1	911.7568	26.213	Blue
SPARC	923.9927	16.077	Blue
STAT6	914.4649	10.836	Blue
SYNJ2	932.7012	9.953	Blue
THBS1	922.6018	25.211	Blue
VCAN	959.6182	32.562	Blue
AURKB	462.9995	36.641	Green
CDC20	479.451	43.038	Green
CDC6	434.6854	29.85	Green
FUS	430.5007	31.987	Green
HNRNPD	426.8546	32.488	Green
MAD2L1	445.8811	37.376	Green
MAGOH	465.2608	37.724	Green
MAGOHB	422.5412	36.366	Green
MRPL10	410.8058	27.859	Green
MRPL11	473.1559	34.769	Green
MRPL13	429.9103	33.622	Green
MRPL19	408.5685	31.074	Green
MRPL21	431.2157	34.077	Green
MRPL37	421.593	28.132	Green
MRPL45	420.1556	28.172	Green
MRPL48	424.9991	28.201	Green
MRPL51	448.0644	28.3	Green
MRPS34	458.912	27.701	Green
MRPS7	417.4466	42.446	Green
ORC1	419.4912	18.368	Green
PCBP2	443.2741	31.446	Green
PLK1	441.6995	37.358	Green

Table C.6 continued from previous page

Gene_Symbol	Degree_Correlation	Degree_PPI	Module
PPIH	432.2566	31.81	Green
PSMA5	460.4963	28.243	Green
PSMA7	453.8809	29	Green
PSMB2	481.0318	26.54	Green
PSMB5	416.7932	26.475	Green
PSMB6	462.9831	26.455	Green
PSMD10	413.0381	25.02	Green
PSMD11	445.9228	28.145	Green
PSMD3	458.0588	26.494	Green
RBM22	409.0664	31.649	Green
RRM2	417.9476	19.427	Green
SF3A3	408.4174	31.672	Green

Table C.7: Results of linear regressions between KITLG expression and IC50s for inhibitors of the PI3K/AKT/mTOR and ERK/MAPK pathways for TP53 WT and Mutant cell lines in the GDSC datasets.

drug.name	beta	Pvalue	FDR	TP53_Status	Dataset	Drug_Class
Rapamycin	0.21	7.23E-03	1.33E-02	WT	GDSC1	PI3K/AKT /mTOR
JW-7-52-1	0.04	5.62E-01	5.79E-01	WT	GDSC1	PI3K/AKT /mTOR
A-443654	0.10	5.75E-02	6.78E-02	WT	GDSC1	PI3K/AKT /mTOR
TGX221	-0.05	2.54E-01	2.71E-01	WT	GDSC1	PI3K/AKT /mTOR
AZD6482	0.06	1.48E-02	2.20E-02	WT	GDSC1	PI3K/AKT /mTOR
AKT inhibitor VIII	0.14	3.54E-08	3.90E-07	WT	GDSC1	PI3K/AKT /mTOR
ZSTK474	0.21	2.99E-05	1.10E-04	WT	GDSC1	PI3K/AKT /mTOR
AS605240	0.13	1.44E-02	2.20E-02	WT	GDSC1	PI3K/AKT /mTOR
IC-87114	0.16	1.49E-08	2.46E-07	WT	GDSC1	PI3K/AKT /mTOR
Idelalisib	0.18	9.26E-06	3.82E-05	WT	GDSC1	PI3K/AKT /mTOR
Omipalisib	0.22	1.50E-04	4.95E-04	WT	GDSC1	PI3K/AKT /mTOR
OSI-027	0.32	2.17E-06	1.02E-05	WT	GDSC1	PI3K/AKT /mTOR
PIK-93	0.32	3.93E-11	1.30E-09	WT	GDSC1	PI3K/AKT /mTOR

Table C.7 continued from previous page

drug.name	beta	Pvalue	FDR	TP53_Status	Dataset	Drug_Class
YM201636	0.19	7.70E-08	6.36E-07	WT	GDSC1	PI3K/AKT /mTOR
WYE-125132	0.16	4.91E-03	1.01E-02	WT	GDSC1	PI3K/AKT /mTOR
GSK690693	0.25	1.55E-07	1.02E-06	WT	GDSC1	PI3K/AKT /mTOR
AT7867	0.13	1.33E-03	3.63E-03	WT	GDSC1	PI3K/AKT /mTOR
Torin 2	0.13	8.58E-03	1.49E-02	WT	GDSC1	PI3K/AKT /mTOR
Pilaralisib	0.04	1.17E-01	1.33E-01	WT	GDSC1	PI3K/AKT /mTOR
GSK1059615	0.00	9.88E-01	9.88E-01	WT	GDSC1	PI3K/AKT /mTOR
Voxtalisib	0.06	1.53E-02	2.20E-02	WT	GDSC1	PI3K/AKT /mTOR
Apitolisib	0.11	6.57E-03	1.28E-02	WT	GDSC1	PI3K/AKT /mTOR
Temsirolimus	0.13	1.54E-03	3.63E-03	WT	GDSC1	PI3K/AKT /mTOR
MK-2206	0.12	1.50E-03	3.63E-03	WT	GDSC1	PI3K/AKT /mTOR
Dactolisib	0.06	5.62E-02	6.78E-02	WT	GDSC1	PI3K/AKT /mTOR
Pictilisib	0.08	4.09E-03	9.00E-03	WT	GDSC1	PI3K/AKT /mTOR

Table C.7 continued from previous page

drug.name	beta	Pvalue	FDR	TP53_Status	Dataset	Drug_Class
AZD8055	0.14	2.55E-07	1.40E-06	WT	GDSC1	PI3K/AKT /mTOR
PF-4708671	0.05	5.18E-02	6.57E-02	WT	GDSC1	PI3K/AKT /mTOR
Capivasertib	0.11	1.66E-02	2.28E-02	WT	GDSC1	PI3K/AKT /mTOR
AZD2014	0.08	2.09E-02	2.76E-02	WT	GDSC1	PI3K/AKT /mTOR
AZD8186	0.05	1.92E-01	2.11E-01	WT	GDSC1	PI3K/AKT /mTOR
AZD8835	0.09	1.30E-02	2.14E-02	WT	GDSC1	PI3K/AKT /mTOR
PI3Ka_4409	0.11	1.46E-03	3.63E-03	WT	GDSC1	PI3K/AKT /mTOR
Rapamycin	0.09	7.12E-02	9.15E-02	Mutant	GDSC1	PI3K/AKT /mTOR
JW-7-52-1	0.06	2.28E-01	2.59E-01	Mutant	GDSC1	PI3K/AKT /mTOR
A-443654	-0.03	3.83E-01	4.08E-01	Mutant	GDSC1	PI3K/AKT /mTOR
TGX221	0.00	9.62E-01	9.62E-01	Mutant	GDSC1	PI3K/AKT /mTOR
AZD6482	0.02	2.95E-01	3.25E-01	Mutant	GDSC1	PI3K/AKT /mTOR
AKT inhibitor VIII	0.06	9.61E-04	2.11E-03	Mutant	GDSC1	PI3K/AKT /mTOR

Table C.7 continued from previous page

drug.name	beta	Pvalue	FDR	TP53_Status	Dataset	Drug_Class
ZSTK474	0.16	1.87E-06	1.03E-05	Mutant	GDSC1	PI3K/AKT /mTOR
AS605240	0.08	1.21E-02	1.90E-02	Mutant	GDSC1	PI3K/AKT /mTOR
IC-87114	0.10	3.32E-09	3.65E-08	Mutant	GDSC1	PI3K/AKT /mTOR
Idelalisib	0.10	2.78E-05	7.64E-05	Mutant	GDSC1	PI3K/AKT /mTOR
Omipalisib	0.17	1.39E-05	4.58E-05	Mutant	GDSC1	PI3K/AKT /mTOR
OSI-027	0.29	5.13E-09	4.23E-08	Mutant	GDSC1	PI3K/AKT /mTOR
PIK-93	0.25	1.63E-12	5.37E-11	Mutant	GDSC1	PI3K/AKT /mTOR
YM201636	0.17	8.30E-10	1.37E-08	Mutant	GDSC1	PI3K/AKT /mTOR
WYE-125132	0.21	4.77E-06	1.97E-05	Mutant	GDSC1	PI3K/AKT /mTOR
GSK690693	0.14	1.58E-04	3.73E-04	Mutant	GDSC1	PI3K/AKT /mTOR
AT7867	0.11	1.69E-03	3.28E-03	Mutant	GDSC1	PI3K/AKT /mTOR
Torin 2	0.18	1.19E-04	3.02E-04	Mutant	GDSC1	PI3K/AKT /mTOR
Pilaralisib	0.08	1.92E-03	3.52E-03	Mutant	GDSC1	PI3K/AKT /mTOR

Table C.7 continued from previous page

drug.name	beta	Pvalue	FDR	TP53_Status	Dataset	Drug_Class
GSK1059615	0.07	4.36E-02	5.99E-02	Mutant	GDSC1	PI3K/AKT /mTOR
Voxtalisib	0.09	1.85E-05	5.56E-05	Mutant	GDSC1	PI3K/AKT /mTOR
Apitolisib	0.10	2.14E-03	3.72E-03	Mutant	GDSC1	PI3K/AKT /mTOR
Temsirolimus	0.15	1.19E-05	4.37E-05	Mutant	GDSC1	PI3K/AKT /mTOR
MK-2206	0.05	7.21E-02	9.15E-02	Mutant	GDSC1	PI3K/AKT /mTOR
Dactolisib	0.08	2.78E-03	4.59E-03	Mutant	GDSC1	PI3K/AKT /mTOR
Pictilisib	0.05	1.98E-02	2.96E-02	Mutant	GDSC1	PI3K/AKT /mTOR
AZD8055	0.12	1.28E-07	8.44E-07	Mutant	GDSC1	PI3K/AKT /mTOR
PF-4708671	0.10	3.52E-06	1.66E-05	Mutant	GDSC1	PI3K/AKT /mTOR
Capivasertib	0.08	4.13E-02	5.92E-02	Mutant	GDSC1	PI3K/AKT /mTOR
AZD2014	0.09	1.21E-03	2.50E-03	Mutant	GDSC1	PI3K/AKT /mTOR
AZD8186	0.04	1.13E-01	1.38E-01	Mutant	GDSC1	PI3K/AKT /mTOR
AZD8835	0.04	1.80E-01	2.13E-01	Mutant	GDSC1	PI3K/AKT /mTOR

Table C.7 continued from previous page

drug.name	beta	Pvalue	FDR	TP53_Status	Dataset	Drug_Class
PI3Ka_4409	0.00	9.21E-01	9.49E-01	Mutant	GDSC1	PI3K/AKT /mTOR
MK-2206	0.23	2.58E-07	2.71E-06	WT	GDSC2	PI3K/AKT /mTOR
Dactolisib	0.18	2.25E-05	6.76E-05	WT	GDSC2	PI3K/AKT /mTOR
Pictilisib	0.09	2.66E-02	3.84E-02	WT	GDSC2	PI3K/AKT /mTOR
AZD8055	0.23	8.44E-01	9.33E-01	WT	GDSC2	PI3K/AKT /mTOR
Rapamycin	0.18	3.02E-04	7.04E-04	WT	GDSC2	PI3K/AKT /mTOR
PF-4708671	-0.03	9.52E-01	9.52E-01	WT	GDSC2	PI3K/AKT /mTOR
AZD2014	0.08	5.23E-02	6.87E-02	WT	GDSC2	PI3K/AKT /mTOR
Uprosertib	0.15	1.23E-05	5.18E-05	WT	GDSC2	PI3K/AKT /mTOR
Alpelisib	0.13	1.96E-03	3.75E-03	WT	GDSC2	PI3K/AKT /mTOR
Taselisib	0.12	2.74E-02	3.84E-02	WT	GDSC2	PI3K/AKT /mTOR
OSI-027	-0.05	4.54E-01	5.29E-01	WT	GDSC2	PI3K/AKT /mTOR
CZC24832	0.14	3.69E-06	1.94E-05	WT	GDSC2	PI3K/AKT /mTOR

Table C.7 continued from previous page

drug.name	beta	Pvalue	FDR	TP53_Status	Dataset	Drug_Class
Buparlisib	0.12	9.73E-07	6.81E-06	WT	GDSC2	PI3K/AKT /mTOR
Afuresertib	0.18	1.79E-05	6.25E-05	WT	GDSC2	PI3K/AKT /mTOR
AZD8186	0.07	1.16E-01	1.44E-01	WT	GDSC2	PI3K/AKT /mTOR
Ipatasertib	0.14	1.11E-03	2.33E-03	WT	GDSC2	PI3K/AKT /mTOR
GNE-317	0.13	2.32E-03	4.07E-03	WT	GDSC2	PI3K/AKT /mTOR
AMG-319	0.24	5.35E-10	1.12E-08	WT	GDSC2	PI3K/AKT /mTOR
LJI308	0.14	4.30E-05	1.13E-04	WT	GDSC2	PI3K/AKT /mTOR
AZD6482	-0.10	9.29E-01	9.52E-01	WT	GDSC2	PI3K/AKT /mTOR
AT13148	0.13	7.90E-03	1.28E-02	WT	GDSC2	PI3K/AKT /mTOR
MK-2206	0.14	7.03E-04	1.85E-03	Mutant	GDSC2	PI3K/AKT /mTOR
Dactolisib	0.13	3.53E-04	1.24E-03	Mutant	GDSC2	PI3K/AKT /mTOR
Pictilisib	0.04	2.34E-01	2.75E-01	Mutant	GDSC2	PI3K/AKT /mTOR
AZD8055	-0.10	4.11E-01	4.54E-01	Mutant	GDSC2	PI3K/AKT /mTOR

Table C.7 continued from previous page

drug.name	beta	Pvalue	FDR	TP53_Status	Dataset	Drug_Class
Rapamycin	0.13	2.19E-04	9.21E-04	Mutant	GDSC2	PI3K/AKT /mTOR
PF-4708671	-0.26	1.07E-01	1.60E-01	Mutant	GDSC2	PI3K/AKT /mTOR
AZD2014	0.11	2.97E-03	6.93E-03	Mutant	GDSC2	PI3K/AKT /mTOR
Uprosertib	0.06	5.80E-02	1.11E-01	Mutant	GDSC2	PI3K/AKT /mTOR
Alpelisib	0.09	8.50E-03	1.79E-02	Mutant	GDSC2	PI3K/AKT /mTOR
Taselisib	0.03	5.32E-01	5.58E-01	Mutant	GDSC2	PI3K/AKT /mTOR
OSI-027	-0.04	6.11E-01	6.11E-01	Mutant	GDSC2	PI3K/AKT /mTOR
CZC24832	0.17	5.48E-13	1.15E-11	Mutant	GDSC2	PI3K/AKT /mTOR
Buparlisib	0.10	2.71E-06	1.42E-05	Mutant	GDSC2	PI3K/AKT /mTOR
Afuresertib	0.07	7.49E-02	1.21E-01	Mutant	GDSC2	PI3K/AKT /mTOR
AZD8186	0.05	1.19E-01	1.67E-01	Mutant	GDSC2	PI3K/AKT /mTOR
Ipatasertib	0.05	2.36E-01	2.75E-01	Mutant	GDSC2	PI3K/AKT /mTOR
GNE-317	0.04	2.27E-01	2.75E-01	Mutant	GDSC2	PI3K/AKT /mTOR

Table C.7 continued from previous page

drug.name	beta	Pvalue	FDR	TP53_Status	Dataset	Drug_Class
AMG-319	0.18	1.10E-11	1.15E-10	Mutant	GDSC2	PI3K/AKT /mTOR
LJI308	0.15	8.90E-10	6.23E-09	Mutant	GDSC2	PI3K/AKT /mTOR
AZD6482	-0.37	6.42E-02	1.12E-01	Mutant	GDSC2	PI3K/AKT /mTOR
AT13148	0.14	6.92E-04	1.85E-03	Mutant	GDSC2	PI3K/AKT /mTOR
AZ628	-0.04	6.18E-01	6.59E-01	WT	GDSC1	ERK/MAPK
HG6-64-1	0.09	5.55E-02	8.87E-02	WT	GDSC1	ERK/MAPK
VX-11e	0.05	2.42E-01	3.22E-01	WT	GDSC1	ERK/MAPK
FR-180204	0.09	3.93E-04	1.05E-03	WT	GDSC1	ERK/MAPK
BIX02189	0.20	5.12E-08	8.19E-07	WT	GDSC1	ERK/MAPK
KIN001-266	0.14	4.30E-06	2.29E-05	WT	GDSC1	ERK/MAPK
Refametinib	-0.17	3.47E-07	2.78E-06	WT	GDSC1	ERK/MAPK
CI-1040	-0.06	1.19E-01	1.73E-01	WT	GDSC1	ERK/MAPK
PLX-4720	0.03	3.19E-01	3.65E-01	WT	GDSC1	ERK/MAPK
PD0325901	-0.22	4.37E-05	1.49E-04	WT	GDSC1	ERK/MAPK
SB590885	0.09	1.76E-02	3.13E-02	WT	GDSC1	ERK/MAPK
Selumetinib	-0.12	7.91E-04	1.81E-03	WT	GDSC1	ERK/MAPK
XMD8-92	0.11	1.51E-02	3.01E-02	WT	GDSC1	ERK/MAPK
Trametinib	-0.30	4.65E-05	1.49E-04	WT	GDSC1	ERK/MAPK
Dabrafenib	0.02	7.81E-01	7.81E-01	WT	GDSC1	ERK/MAPK
RAF_9304	0.04	2.72E-01	3.34E-01	WT	GDSC1	ERK/MAPK
AZ628	0.12	2.74E-03	3.99E-03	Mutant	GDSC1	ERK/MAPK
HG6-64-1	0.11	5.19E-03	6.92E-03	Mutant	GDSC1	ERK/MAPK
VX-11e	0.12	3.79E-04	8.66E-04	Mutant	GDSC1	ERK/MAPK

Table C.7 continued from previous page

drug.name	beta	Pvalue	FDR	TP53_Status	Dataset	Drug_Class
FR-180204	0.12	2.12E-10	1.69E-09	Mutant	GDSC1	ERK/MAPK
BIX02189	0.21	4.06E-17	6.50E-16	Mutant	GDSC1	ERK/MAPK
KIN001-266	0.14	1.66E-07	6.62E-07	Mutant	GDSC1	ERK/MAPK
Refametinib	-0.09	6.37E-04	1.13E-03	Mutant	GDSC1	ERK/MAPK
CI-1040	0.04	1.98E-01	1.98E-01	Mutant	GDSC1	ERK/MAPK
PLX-4720	0.09	1.26E-07	6.62E-07	Mutant	GDSC1	ERK/MAPK
PD0325901	-0.09	2.77E-02	3.16E-02	Mutant	GDSC1	ERK/MAPK
SB590885	0.06	7.54E-03	9.28E-03	Mutant	GDSC1	ERK/MAPK
Selumetinib	-0.05	6.48E-02	6.92E-02	Mutant	GDSC1	ERK/MAPK
XMD8-92	0.12	5.94E-04	1.13E-03	Mutant	GDSC1	ERK/MAPK
Trametinib	-0.21	1.12E-04	2.98E-04	Mutant	GDSC1	ERK/MAPK
Dabrafenib	0.14	5.57E-05	1.78E-04	Mutant	GDSC1	ERK/MAPK
RAF_9304	0.09	2.61E-03	3.99E-03	Mutant	GDSC1	ERK/MAPK
PLX-4720	0.08	5.98E-02	1.44E-01	WT	GDSC2	ERK/MAPK
PD0325901	0.02	7.85E-01	8.52E-01	WT	GDSC2	ERK/MAPK
Trametinib	-0.16	3.60E-02	1.32E-01	WT	GDSC2	ERK/MAPK
Dabrafenib	0.17	8.70E-03	4.78E-02	WT	GDSC2	ERK/MAPK
SCH772984	-0.06	3.07E-01	5.62E-01	WT	GDSC2	ERK/MAPK
ERK_2440	-0.03	6.15E-01	8.46E-01	WT	GDSC2	ERK/MAPK
ERK_6604	0.01	8.52E-01	8.52E-01	WT	GDSC2	ERK/MAPK
Selumetinib	-0.06	3.58E-01	5.63E-01	WT	GDSC2	ERK/MAPK
KRAS (G12C) Inhibitor-12	0.32	3.70E-11	4.07E-10	WT	GDSC2	ERK/MAPK
Ulixertinib	0.06	6.56E-02	1.44E-01	WT	GDSC2	ERK/MAPK
VX-11e	0.02	7.28E-01	8.52E-01	WT	GDSC2	ERK/MAPK
PLX-4720	0.17	8.80E-08	3.23E-07	Mutant	GDSC2	ERK/MAPK
PD0325901	0.10	7.16E-03	1.58E-02	Mutant	GDSC2	ERK/MAPK

Table C.7 continued from previous page

drug.name	beta	Pvalue	FDR	TP53_Status	Dataset	Drug_Class
Trametinib	-0.04	4.37E-01	5.34E-01	Mutant	GDSC2	ERK/MAPK
Dabrafenib	0.27	2.41E-13	2.65E-12	Mutant	GDSC2	ERK/MAPK
SCH772984	0.00	9.39E-01	9.39E-01	Mutant	GDSC2	ERK/MAPK
ERK_2440	0.08	4.30E-02	6.76E-02	Mutant	GDSC2	ERK/MAPK
ERK_6604	0.05	1.48E-01	2.04E-01	Mutant	GDSC2	ERK/MAPK
Selumetinib	0.02	7.19E-01	7.91E-01	Mutant	GDSC2	ERK/MAPK
KRAS (G12C) Inhibitor-12	0.22	8.59E-09	4.72E-08	Mutant	GDSC2	ERK/MAPK
Ulixertinib	0.10	2.42E-05	6.64E-05	Mutant	GDSC2	ERK/MAPK
VX-11e	0.08	2.01E-02	3.68E-02	Mutant	GDSC2	ERK/MAPK

Table C.8: Risk allele frequencies for the KITLG-p53RE-SNP for each TCGA study where data genotyping data was available. Cases are also split into TP53 WT and TP53 Mutant.

type	RISK	NONRISK	RISK_ALLELE_FREQ	TP53_Status
GBM	519	119	81.34796	ALL
OV	726	172	80.84633	ALL
LUAD	626	170	78.64322	ALL
LUSC	632	130	82.93963	ALL
PRAD	481	111	81.25	ALL
UCEC	502	112	81.75896	ALL
BLCA	399	101	79.8	ALL
TGCT	214	22	90.67797	ALL
ESCA	123	31	79.87013	ALL
PAAD	198	66	75	ALL
KIRP	262	54	82.91139	ALL
LIHC	203	61	76.89394	ALL
CESC	246	60	80.39216	ALL
SARC	285	63	81.89655	ALL
BRCA	1122	294	79.23729	ALL
THYM	142	30	82.55814	ALL
MESO	135	27	83.33333	ALL
COAD	488	104	82.43243	ALL
STAD	377	119	76.00806	ALL
SKCM	622	146	80.98958	ALL
CHOL	43	11	79.62963	ALL
KIRC	553	151	78.55114	ALL
THCA	513	115	81.6879	ALL
HNSC	595	143	80.62331	ALL
LAML	0	0	NA	ALL
READ	196	42	82.35294	ALL
LGG	579	139	80.64067	ALL
DLBC	36	6	85.71429	ALL
KICH	79	23	77.45098	ALL
UCS	63	15	80.76923	ALL
ACC	111	27	80.43478	ALL
PCPG	222	42	84.09091	ALL
UVM	118	30	79.72973	ALL
GBM	340	86	79.81221	WT
OV	66	24	73.33333	WT
LUAD	198	50	79.83871	WT
LUSC	41	13	75.92593	WT
PRAD	321	75	81.06061	WT
UCEC	326	66	83.16327	WT
BLCA	106	30	77.94118	WT
TGCT	149	13	91.97531	WT
ESCA	14	0	100	WT

Table C.8 continued from previous page

type	RISK	NONRISK	RISK_ALLELE_FREQ	TP53_Status
PAAD	62	24	72.09302	WT
KIRP	241	51	82.53425	WT
LIHC	87	21	80.55556	WT
CESC	157	43	78.5	WT
SARC	101	29	77.69231	WT
BRCA	367	87	80.837	WT
THYM	124	26	82.66667	WT
MESO	92	18	83.63636	WT
COAD	175	29	85.78431	WT
STAD	161	49	76.66667	WT
SKCM	293	65	81.84358	WT
CHOL	27	7	79.41176	WT
KIRC	484	126	79.34426	WT
THCA	508	110	82.20065	WT
HNSC	173	33	83.98058	WT
LAML	0	0	NA	WT
READ	29	5	85.29412	WT
LGG	286	68	80.79096	WT
DLBC	25	3	89.28571	WT
KICH	17	5	77.27273	WT
UCS	1	3	25	WT
ACC	50	14	78.125	WT
PCPG	112	18	86.15385	WT
UVM	114	30	79.16667	WT
GBM	42	8	84	Mutant
OV	330	76	81.28079	Mutant
LUAD	192	62	75.59055	Mutant
LUSC	368	70	84.01826	Mutant
PRAD	54	14	79.41176	Mutant
UCEC	85	21	80.18868	Mutant
BLCA	123	33	78.84615	Mutant
TGCT	2	0	100	Mutant
ESCA	45	9	83.33333	Mutant
PAAD	86	24	78.18182	Mutant
KIRP	1	1	50	Mutant
LIHC	39	15	72.22222	Mutant
CESC	7	1	87.5	Mutant
SARC	60	14	81.08108	Mutant
BRCA	257	67	79.32099	Mutant
THYM	2	0	100	Mutant
MESO	12	2	85.71429	Mutant
COAD	182	40	81.98198	Mutant
STAD	97	29	76.98413	Mutant

Table C.8 continued from previous page

type	RISK	NONRISK	RISK_ALLELE_FREQ	TP53_Status
SKCM	65	21	75.5814	Mutant
CHOL	8	0	100	Mutant
KIRC	2	4	33.33333	Mutant
THCA	0	0	NA	Mutant
HNSC	88	36	70.96774	Mutant
LAML	0	0	NA	Mutant
READ	91	21	81.25	Mutant
LGG	12	6	66.66667	Mutant
DLBC	6	0	100	Mutant
KICH	20	6	76.92308	Mutant
UCS	48	10	82.75862	Mutant
ACC	11	1	91.66667	Mutant
PCPG	2	0	100	Mutant
UVM	0	0	NA	Mutant

Table C.9: Associations of known COAD driver gene mutations with TP53 status in COAD samples from TCGA.

driver_gene	N.MUT.p53wt	N.WT.p53wt	N.MUT.p53mut	N.WT.p53mut	OR	Pval	FDR
BRAF	38	111	10	166	5.65	5.3E-07	7.9E-06
APC	80	69	144	32	0.26	5.0E-08	1.5E-06
DMD	33	116	22	154	1.99	2.6E-02	6.0E-02
CASP8	10	139	6	170	2.03	2.0E-01	2.6E-01
MIER3	10	139	3	173	4.13	2.5E-02	6.0E-02
ATP6V0D2	6	143	3	173	2.41	3.1E-01	3.7E-01
SLC9A9	7	142	4	172	2.11	3.6E-01	4.1E-01
PTPN12	6	143	3	173	2.41	3.1E-01	3.7E-01
CDC27	6	143	2	174	3.64	1.5E-01	2.1E-01
MAP7	9	140	2	174	5.57	2.7E-02	6.0E-02
FZD3	9	140	3	173	3.69	7.2E-02	1.3E-01
MYO1B	12	137	4	172	3.75	2.0E-02	6.0E-02
TCERG1	17	132	5	171	4.39	3.2E-03	1.9E-02
PIK3CA	55	94	41	135	1.92	1.0E-02	4.0E-02
KRAS	64	85	71	105	1.11	6.5E-01	7.0E-01
FBXW7	40	109	20	156	2.85	5.0E-04	3.8E-03
SMAD4	25	124	17	159	1.88	6.8E-02	1.3E-01
TCF7L2	25	124	13	163	2.52	9.6E-03	4.0E-02
TTN	99	50	102	74	1.43	1.4E-01	2.0E-01
NRAS	9	140	8	168	1.35	6.2E-01	6.9E-01
CTNNB1	18	131	11	165	2.06	7.9E-02	1.3E-01
GRIK3	24	125	12	164	2.62	1.2E-02	4.0E-02
SMAD2	16	133	7	169	2.90	2.8E-02	6.0E-02
KIAA1804	0	149	0	176	0.00	1.0E+00	1.0E+00
ACVR1B	19	130	4	172	6.25	3.1E-04	3.1E-03
GPC6	8	141	4	172	2.43	1.5E-01	2.1E-01

Table C.9 continued from previous page

driver_gene	N.MUT.p53wt	N.WT.p53wt	N.MUT.p53mut	N.WT.p53mut	OR	Pval	FDR
EDNRB	15	134	7	169	2.69	4.4E-02	8.8E-02
SOX9	30	119	17	159	2.35	1.1E-02	4.0E-02
WBSCR17	20	129	13	163	1.94	9.6E-02	1.5E-01
FAM123B	0	149	0	176	0.00	1.0E+00	1.0E+00

Table C.10: Results of linear regressions between expression of each p53 pathway gene and Nutlin-3a IC50 for TP53 WT and TP53 MUTLOSS cell lines in GDSC1.

gene	beta	pval	FDR	TP53_Status
SERPINB5	0.17	1.4E-07	5.65E-05	WT
KRT15	0.18	1.0E-05	1.37E-03	WT
CPE	0.12	2.3E-05	1.47E-03	WT
EPN3	0.17	2.0E-05	1.47E-03	WT
PTPRU	0.18	1.6E-05	1.47E-03	WT
S100A2	0.15	2.5E-05	1.47E-03	WT
MCC	0.16	3.0E-05	1.51E-03	WT
RNASE7	0.23	4.6E-05	1.88E-03	WT
GPR87	0.14	4.4E-05	1.88E-03	WT
CLCA2	0.16	5.2E-05	1.93E-03	WT
KITLG	0.12	7.7E-05	2.09E-03	WT
ZNF488	0.15	7.3E-05	2.09E-03	WT
SCN4B	0.17	6.5E-05	2.09E-03	WT
GPC1	0.14	9.3E-05	2.25E-03	WT
SFN	0.12	9.2E-05	2.25E-03	WT
CDKN2A	0.10	1.1E-04	2.54E-03	WT
FHL2	0.15	1.3E-04	2.87E-03	WT
FAM13C	0.15	2.0E-04	4.03E-03	WT
RND3	0.11	2.1E-04	4.12E-03	WT
TP53AIP1	0.22	4.2E-04	7.86E-03	WT
SDC4	0.11	5.5E-04	9.37E-03	WT
DHRS3	0.12	5.5E-04	9.37E-03	WT
CGB7	0.16	6.9E-04	1.13E-02	WT
PERP	0.10	7.5E-04	1.17E-02	WT
GLS2	0.14	8.5E-04	1.29E-02	WT
CMBL	0.14	1.0E-03	1.45E-02	WT
DDR1	0.14	1.0E-03	1.45E-02	WT
HES1	0.12	1.1E-03	1.49E-02	WT
FAM210B	0.17	1.3E-03	1.63E-02	WT
UNC5B	0.10	1.3E-03	1.63E-02	WT
PARD6G	0.20	1.3E-03	1.63E-02	WT
EPHA2	0.10	1.9E-03	2.00E-02	WT
HES2	0.16	1.8E-03	2.00E-02	WT
P3H2	0.08	2.0E-03	2.06E-02	WT
ARC	0.12	2.1E-03	2.19E-02	WT
COL7A1	0.14	2.2E-03	2.22E-02	WT
LMNA	0.14	2.3E-03	2.22E-02	WT
JAG1	0.12	2.6E-03	2.46E-02	WT
NUPR1	0.11	2.7E-03	2.53E-02	WT
EDN2	0.11	3.0E-03	2.76E-02	WT
TEX9	0.21	3.2E-03	2.79E-02	WT
MYO6	0.13	3.6E-03	2.95E-02	WT

TP63	0.09	3.6E-03	2.95E-02	WT
TP73	0.10	3.6E-03	2.95E-02	WT
ADGRG1	0.10	3.7E-03	2.95E-02	WT
KRT8	0.08	3.8E-03	2.97E-02	WT
TIMP3	0.07	5.1E-03	3.82E-02	WT
EPS8L2	0.10	5.6E-03	4.10E-02	WT
NHLH2	0.13	6.4E-03	4.61E-02	WT
EFNB1	0.16	6.6E-03	4.64E-02	WT
BMP7	0.10	6.7E-03	4.64E-02	WT

Table C.11: The 26 compounds in GDSC1 for which TP53 wild-type cell lines are more sensitive compared to TP53 Mutants and for which high wild-type TP53 expression associates with high sensitivity.

DRUG_NAME	PUTATIVE_TARGET	PATHWAY_NAME	Previously linked to TP53	Reference
Doxorubicin	Anthracycline	DNA replication	YES	Fritsche et al, 1993
Etoposide	TOP2	DNA replication	YES	Grandela et al, 2008
5-Fluorouracil	Antimetabolite (DNA & RNA)	Other	YES	Sun et al, 2007
Bleomycin	dsDNA break induction	DNA replication	YES	Mishra et al, 1999
BX-912	PDK1 (PDPK1)	Metabolism	NO	
GSK1070916	AURKA, AURKC	Mitosis	NO	
NG-25	TAK1, MAP4K2	Other, kinases	NO	
TL-1-85	TAK	Other, kinases	NO	
NVP-BHG712	EPHB4	RTK signaling	NO	
CX-5461	RNA Polymerase 1	Other	YES	Calo et al, 2018
PHA-793887	CDK2, CDK7, CDK5	Cell cycle	NO	
THZ-2-102-1	CDK7	Cell cycle	NO	
NSC319726	P53 Mut specific	p53 pathway	YES	Yu et al, 2017
Cytarabine	Antimetabolite	Other	YES	Ng et al, 2011
Lestaurtinib	FLT3, JAK2, NTRK1, NTRK2, NTRK3	Other, kinases	NO	
Nutlin-3a (-)	MDM2	p53 pathway	YES	Vassilev et al, 2004
Daporinad	NAMPT	Metabolism	NO	
Talazoparib	PARP1, PARP2	Genome integrity	NO	
Bleomycin (50 uM)	dsDNA break induction	DNA replication	YES	Mishra et al, 1999

Table C.11 continued from previous page

DRUG_NAME	PUTATIVE_TARGET	PATHWAY_NAME	Previously linked to TP53	Reference
Bleomycin (10 uM)	dsDNA break induction	DNA replication	YES	Mishra et al, 1999
AZD7969	GSK3B	WNT signaling	NO	
RAF_9304	ARAF, BRAF, CRAF	ERK MAPK signaling	NO	
PARP_0108	PARP1, PARP2, PARP6	Genome integrity	NO	
PARP_9482	PARP1, PARP2, PARP5a	Genome integrity	NO	
SN-38	TOP1	DNA replication	YES	Lee et al, 2019
Pevonedistat	NAE	Other	YES	Ferris et al, 2020

Table C.12: Results of enrichment analysis to determine cancer types enriched for TP53WT NOLOSS status compared to NF status.

type	OR	p.val	FDR
GBM	1.77	1.2E-02	2.4E-02
OV	0.07	1.0E+00	1.0E+00
LUAD	0.36	1.0E+00	1.0E+00
LUSC	0.06	1.0E+00	1.0E+00
PRAD	2.79	4.7E-14	1.7E-13
UCEC	1.32	9.2E-03	2.0E-02
BLCA	0.43	1.0E+00	1.0E+00
TGCT	40.80	8.7E-14	2.9E-13
ESCA	0.07	1.0E+00	1.0E+00
PAAD	0.36	1.0E+00	1.0E+00
KIRP	40.79	2.3E-38	2.5E-37
LIHC	0.58	1.0E+00	1.0E+00
SARC	0.75	9.6E-01	1.0E+00
BRCA	0.53	1.0E+00	1.0E+00
THYM	22.91	2.7E-14	1.1E-13
MESO	3.16	9.7E-06	2.5E-05
STAD	0.59	1.0E+00	1.0E+00
SKCM	2.00	4.6E-06	1.3E-05
CHOL	2.54	5.2E-02	9.5E-02
KIRC	54.49	1.6E-67	2.6E-66
THCA	Inf	3.2E-81	1.1E-79
COAD	0.37	1.0E+00	1.0E+00
LAML	7.33	1.4E-14	6.8E-14
READ	0.13	1.0E+00	1.0E+00
HNSC	0.59	1.0E+00	1.0E+00
CESC	7.82	1.9E-17	1.3E-16
LGG	9.18	2.8E-27	2.3E-26
DLBC	3.18	5.4E-03	1.3E-02
KICH	0.31	1.0E+00	1.0E+00
UCS	0.03	1.0E+00	1.0E+00
ACC	2.15	2.7E-02	5.2E-02
PCPG	43.09	1.4E-14	6.8E-14
UVM	Inf	3.7E-13	1.1E-12

Table C.13: Summary of associations between the TP53-PAS-SNP and cancer in GWAS.

Cancer	Population	Odds Ratio (OR)	Significance (p,CI)	Reference
Basal Cell Carcinoma	Icelandic	2.25	5.4 x 10^{19}	Stacey et al, 2011
Basal Cell Carcinoma	Denmark	2.06	0.0057	Stacey et al, 2011
Prostate	Icelandic	1.44	2.4 x 10^{6}	Stacey et al, 2011
Prostate	United States	2.24	0.0026	Stacey et al, 2011
Prostate	Spain	2.52	0.037	Stacey et al, 2011
Glioma	Icelandic	2.35	1.0 x 10^{5}	Stacey et al, 2011
Glioma	USA UCSF	2.65	0.0063	Stacey et al, 2011
Glioma	USA Mayo Clinic	2.05	0.053	Stacey et al, 2011
Glioma	GliomaScan (meta-analysis)	3.14	6.48 x 10^{11}	Wang et al, 2015
Glioma	France	3.52	2.16 - 5.74	Enciso-Mora et al, 2013
Glioma	Germany	1.94	1.11 - 3.40	Enciso-Mora et al, 2013
Glioma	USA	5.14	3.32-7.96	Enciso-Mora et al, 2013
Glioma	UK	4.86	2.61-9.07	Enciso-Mora et al, 2013
Glioma	Overall	3.65	2.83x10^{9}	Enciso-Mora et al, 2013
GBM	France	10.06	4.04-25.01	Enciso-Mora et al, 2013
GBM	Germany	2.43	1.12-5.3	Enciso-Mora et al, 2013
GBM	USA	8.69	4.57-16.52	Enciso-Mora et al, 2013
GBM	UK	3.6	1.26-10.29	Enciso-Mora et al, 2013
GBM	Overall	5.36	2.32x10^{6}	Enciso-Mora et al, 2013
Glioma (non-GBM)	France	4.06	2.29-7.21	Enciso-Mora et al, 2013
Glioma (non-GBM)	USA	9.57	4.95-18.47	Enciso-Mora et al, 2013
Glioma (non-GBM)	UK	9.27	4.08-21.08	Enciso-Mora et al, 2013

Table C.13 continued from previous page

Cancer	Population	Odds Ratio (OR)	Significance (p,CI)	Reference
Glioma (non-GBM)	Overall	5.09	8.64x10-6	Enciso-Mora et al, 2013
Glioma grade II	France	11.8	4.57-30.44	Enciso-Mora et al, 2013
Glioma grade II	USA	32.85	9.12-118.33	Enciso-Mora et al, 2013
Glioma grade II	UK	6.03	1.61-22.65	Enciso-Mora et al, 2013
Glioma grade II	Overall	7.77	8.99x10-4	Enciso-Mora et al, 2013
Glioma grade III	France	11.38	4.08-31.75	Enciso-Mora et al, 2013
Glioma grade III	Germany	4.65	1.49-14.52	Enciso-Mora et al, 2013
Glioma grade III	USA	27.71	9.43-81.45	Enciso-Mora et al, 2013
Glioma grade III	UK	52.44	12.75-215.73	Enciso-Mora et al, 2013
Glioma grade III	Overall	15.88	2.75x10-8	Enciso-Mora et al, 2013
Glioma grade IV	France	10.06	4.04-25.01	Enciso-Mora et al, 2013
Glioma grade IV	Germany	2.43	1.12-5.3	Enciso-Mora et al, 2013
Glioma grade IV	USA	8.69	4.57-16.52	Enciso-Mora et al, 2013
Glioma grade IV	UK	3.6	1.26-10.29	Enciso-Mora et al, 2013
Glioma grade IV	Overall	5.36	2.32x10-6	Enciso-Mora et al, 2013
Glioma (All)	SE Usa	3.54	0.0001	Egen et al, 2012
Glioblastoma	SE Usa	3.51	0.0006	Egen et al, 2012
Astrocytic tumours	SE Usa	4.04	0.0016	Egen et al, 2012
Esophageal Squamous Cell Carcinoma	Chinese Han	3.22	$1.34x10^4$	Zhou et al, 2012
Neuroblastoma	Eurpean Ancestry	2	1.1x10-8	Diskin et al, 2014
Neuroblastoma	African Ancestry	5.1	4.2x10-5	Diskin et al, 2014
Neuroblastoma	Italian	4.6	4.2x10-2	Diskin et al, 2014
Colorectal Adenoma	Icelandic	1.39	1.6×10^4	Stacey et al, 2011
Colorectal Cancer	Spain	3.54	0.052	Stacey et al, 2011

Table C.13 continued from previous page

Cancer	Population	Odds Ratio (OR)	Significance (p,CI)	Reference
Melanoma	Netherlands	1.6	0.042	Stacey et al, 2011
SCCHN protective	US non-Hispanic whites	0.41	95% CI 0.21-0.79	Guan et al, 2013
LFS/LFL Patients without TP53 coding mutations	Brazil	NA	0.002	Macedo et al 2016
Overall Cancer	Meta-analysis	1.511	95% CI 1.285-1.777	Wang et al, 2016
leiomyoma	European, Meta-analysis	1.74	4.00E-37	Rafnar et al, 2018
Breast Cancer	Chinese Han	0.573	0.0078	Deng et al, 2019
Sarcoma	Chinese Han	3.29	0.0014	Deng et al, 2019
Soft Tissue Sarcoma	Chinese Han	4.55	3.30E-05	Deng et al, 2019
non-melanomatous skin cancer	UK BioBank	1.36	7.60E-63	Di Giovannantonio et al 2020
Brain malignancy	UK BioBank	3.12	1.40E-12	Di Giovannantonio et al 2020
ER +ve Breast Cancer	European	>1	1.00E-03	Zhang et al, 2020
ER -ve Breast Cancer	European	<1	2.30E-04	Zhang et al, 2020
High Grade Serous Ovarian Cancer	European	<1	3.70E-04	Zhang et al, 2020
Low Grade Serous Ovarian Cancer	European	>1	1.60E-02	Zhang et al, 2020
Melanoma	European	1.39	1.18E-08	Rashkin et al, 2020
Lymphocytic Leukemia	European	1.39	1.89E-09	Rashkin et al, 2020
Cutaneous Melanoma	Meta-analysis	0.044 (beta)	3.30E-10	Landi et al, 2020

Table C.13 continued from previous page

Cancer	Population	Odds Ratio (OR)	Significance (p,CI)	Reference
Triple Negative Breast Cancer	Meta-analysis	1.45	1.40E-08	Zhang et al, 2020 (2)

Table C.14: Details of the 17 putative TP53 PAS sites identified using PolyA_DB.v3.2.

PAS_ID	Chromosome	Position	Mean. RPM	Intron.exon. location	Extension	PAS.type	PSE	PAS.Signal
chr17:7568733:-	chr17	7568733	2.39	3' most exon	YES	3'UTR(L)	9.35%	AUUAAA
chr17:7568781:-	chr17	7568781	0.45	3' most exon	YES	3'UTR(M)	14.02%	AAUAAA
chr17:7571739:-	chr17	7571739	8.02	3' most exon	NO	3'UTR(M)	100.00%	AAUAAA
chr17:7571785:-	chr17	7571785	0.79	3' most exon	NO	3'UTR(M)	2.80%	NoPAS
chr17:7571827:-	chr17	7571827	0.02	3' most exon	NO	3'UTR(M)	1.87%	NoPAS
chr17:7571998:-	chr17	7571998	0.72	3' most exon	NO	3'UTR(M)	1.87%	NoPAS
chr17:7572161:-	chr17	7572161	1.06	3' most exon	NO	3'UTR(M)	1.87%	NoPAS
chr17:7572469:-	chr17	7572469	0.06	3' most exon	NO	3'UTR(M)	11.21%	NoPAS
chr17:7572772:-	chr17	7572772	0.35	3' most exon	NO	3'UTR(F)	2.80%	NoPAS
chr17:7572945:-	chr17	7572945	0.09	3' most exon	NO	CDS	33.64%	OtherPAS
chr17:7573141:-	chr17	7573141	0.04	Intron	NO	Intron	10.28%	OtherPAS
chr17:7573201:-	chr17	7573201	0.44	Intron	NO	Intron	4.67%	AAUAAA
chr17:7573549:-	chr17	7573549	0.16	Intron	NO	Intron	5.61%	NoPAS
chr17:7588148:-	chr17	7588148	0.43	Intron	NO	Intron	1.87%	NoPAS
chr17:7588533:-	chr17	7588533	0.35	Intron	NO	Intron	1.87%	NoPAS
chr17:7588567:-	chr17	7588567	1.20	Intron	NO	Intron	76.64%	AAUAAA
chr17:7590347:-	chr17	7590347	-0.05	Intron	NO	Intron	1.87%	AAUAAA

Table C.15: Summary of miRNAs which were predicted to bind the extended p53 3'UTR and of those which have previously been linked to p53 regulation in a way which may be impaired or enhanced by the TP53-PAS-SNP.

miRNA	Source	Target_ Rank	Target_ Score	Comment
hsa-mir-4775	miRDB	1	92	Nonsignificant
hsa-mir-9985	miRDB	2	90	Not Tested
hsa-mir-27b	miRDB	3	90	Nonsignificant
hsa-mir-27a	miRDB	4	90	Nonsignificant
hsa-mir-590	miRDB	5	89	Nonsignificant
hsa-mir-4282	miRDB	6	86	Not Expressed
hsa-mir-335	miRDB	7	83	Nonsignificant
hsa-mir-627	miRDB	8	82	Nonsignificant
hsa-mir-8073	miRDB	9	81	Not Expressed
hsa-mir-221	miRDB	10	81	Nonsignificant
hsa-mir-6778	miRDB	11	80	Not Expressed
hsa-mir-346	miRDB	12	79	Nonsignificant
hsa-mir-519d	miRDB	13	78	Nonsignificant
hsa-mir-5089	miRDB	14	78	Nonsignificant
hsa-mir-8485	miRDB	15	78	Not Expressed
hsa-mir-4279	miRDB	16	76	Not Expressed
hsa-mir-6785	miRDB	17	74	Nonsignificant
hsa-mir-4728	miRDB	18	74	Nonsignificant
hsa-mir-494	miRDB	19	72	Nonsignificant
hsa-mir-410	miRDB	20	72	Nonsignificant
hsa-mir-323b	miRDB	21	72	Nonsignificant
hsa-mir-6883	miRDB	22	71	Nonsignificant
hsa-mir-149	miRDB	23	71	Nonsignificant
hsa-mir-10524	miRDB	24	71	Not Tested
hsa-mir-6819	miRDB	25	69	Not Expressed

Table C.15 continued from previous page

miRNA	Source	Target_ Rank	Target_ Score	Comment
hsa-mir-4743	miRDB	26	68	Nonsignificant
hsa-mir-488	miRDB	27	68	Nonsignificant
hsa-mir-6875	miRDB	28	67	Nonsignificant
hsa-mir-766	miRDB	29	67	Nonsignificant
hsa-mir-6852	miRDB	30	65	Nonsignificant
hsa-mir-6783	miRDB	31	65	Nonsignificant
hsa-mir-4799	miRDB	32	64	Not Expressed
hsa-mir-6867	miRDB	33	64	Not Expressed
hsa-mir-6802	miRDB	34	63	Nonsignificant
hsa-mir-1343	miRDB	35	62	Nonsignificant
hsa-mir-4534	miRDB	36	62	Not Expressed
hsa-mir-6727	miRDB	37	61	Nonsignificant
hsa-mir-6504	miRDB	38	61	Not Expressed
hsa-mir-504	miRDB	39	60	Nonsignificant
hsa-mir-5690	miRDB	40	60	Nonsignificant
hsa-mir-5008	miRDB	41	60	Nonsignificant
hsa-mir-6788	miRDB	42	59	Minor Allele Specific
hsa-mir-30c-2	miRDB	43	59	Nonsignificant
hsa-mir-30c-1	miRDB	44	59	Nonsignificant
hsa-mir-6506	miRDB	45	59	Nonsignificant
hsa-mir-7151	miRDB	46	59	Nonsignificant
hsa-mir-5680	miRDB	47	58	Nonsignificant
hsa-mir-625	miRDB	48	58	Nonsignificant
hsa-mir-4695	miRDB	49	58	Not Expressed
hsa-mir-153	miRDB	50	58	Not Tested

Table C.15 continued from previous page

miRNA	Source	Target_ Rank	Target_ Score	Comment
hsa-mir-3915	miRDB	51	58	Not Expressed
hsa-mir-6812	miRDB	52	57	Minor Allele Specific
hsa-mir-6737	miRDB	53	57	Nonsignificant
hsa-mir-1273h	miRDB	54	57	Nonsignificant
hsa-mir-619	miRDB	55	57	Not Expressed
hsa-mir-6890	miRDB	56	57	Not Expressed
hsa-mir-10399	miRDB	57	57	Not Tested
hsa-mir-5699	miRDB	58	57	Nonsignificant
hsa-mir-8085	miRDB	59	57	Not Expressed
hsa-mir-6731	miRDB	60	57	Nonsignificant
hsa-mir-6747	miRDB	61	57	Nonsignificant
hsa-mir-1200	miRDB	62	56	Not Expressed
hsa-mir-4425	miRDB	63	55	Not Expressed
hsa-mir-4722	miRDB	64	55	Not Expressed
hsa-mir-651	miRDB	65	55	Nonsignificant
hsa-mir-7845	miRDB	66	55	Nonsignificant
hsa-mir-922	miRDB	67	54	Not Expressed
hsa-mir-1976	miRDB	68	54	Nonsignificant
hsa-mir-552	miRDB	69	54	Nonsignificant
hsa-mir-660	miRDB	70	54	Nonsignificant
hsa-mir-6748	miRDB	71	53	Nonsignificant
hsa-mir-4499	miRDB	72	53	Not Expressed
hsa-mir-519e	miRDB	73	53	Not Expressed
hsa-mir-515	miRDB	74	53	Not Tested
hsa-mir-3121	miRDB	75	53	Not Expressed

Table C.15 continued from previous page

miRNA	Source	Target_ Rank	Target_ Score	Comment
hsa-mir-92a-1	miRDB	76	52	Nonsignificant
hsa-mir-765	miRDB	77	52	Nonsignificant
hsa-mir-605	miRDB	78	52	Nonsignificant
hsa-mir-33a	miRDB	79	52	Nonsignificant
hsa-mir-596	miRDB	80	51	Not Expressed
hsa-mir-6893	miRDB	81	51	Not Expressed
hsa-mir-218-1	miRDB	82	51	Nonsignificant
hsa-mir-4768	miRDB	83	51	Nonsignificant
hsa-mir-4719	miRDB	84	51	Not Expressed
hsa-mir-11181	miRDB	85	51	Not Tested
hsa-mir-6887	miRDB	86	51	Nonsignificant
hsa-mir-6081	miRDB	87	51	Not Expressed
hsa-mir-146a	miRDB	88	50	Nonsignificant
hsa-mir-382	Deng et al 2019	NA	NA	Nonsignificant
hsa-mir-325	Deng et al 2019	NA	NA	Not Expressed
hsa-mir-545	Macedo et al 2016	NA	NA	Nonsignificant
hsa-mir-152a	Zhang et al 2009	NA	NA	Nonsignificant
hsa-mir-152b-1	Wu et al 2013	NA	NA	Nonsignificant
hsa-mir-152b-2	Wu et al 2013	NA	NA	Nonsignificant

Table C.16: Table of datasets generated within this thesis or used in this thesis.

Datasets	**Source**	**Accessed**	**Reference**
TERA1 RNA-seq	This thesis	NA	NA
TERA1 Proteomics	This thesis	NA	NA
Hap1 RNA-seq	This thesis	NA	NA
TERA1/TERA2 Drug Screen	This thesis	NA	NA
Hallmarks Collection	MSIGDB	31/08/2020	Liberzon et al, 2015
KEGG Collection	MSIGDB	31/08/2020	Kanehisa & Goto, 2000
Biocarta Collection	MSIGDB	31/08/2020	Nishimura, 2000
PANTHER Collection	http://www.pantherdb.org/	31/08/2020	Thomas et al, 2003
TCGA Transcriptomic data	Genomic Data Commons	18/07/2020	Hoadley et al 2018
TCGA Copy Number data	Genomic Data Commons	18/07/2020	Hoadley et al 2018
TCGA Mutation data	Genomic Data Commons	18/07/2020	Hoadley et al 2018
TCGA Clinical data	Genomic Data Commons	18/07/2020	Hoadley et al 2018
TCGA miRNA data	Genomic Data Commons	20/08/2020	Hoadley et al 2018
TCGA CDR	Genomic Data Commons	03/05/2020	Liu et al, 2018
GDSC1	https://www.cancerrxgene.org/	21/07/2020	Iorio et al, 2016
GDSC2	https://www.cancerrxgene.org/	21/07/2020	Iorio et al, 2016
GSE39091	Gene Expression Omnibus	12/08/2020	Blank et al, 2013
SNP Pleiotropy	Supplementary Data	24/08/2020	Watanabe et al, 2019
GWAS Catalog	NHGRI-EBI	20/08/2020	Buniello et al, 2019
APA RED Scores	APAatlas	25/08/2020	Hong et al, 2020
PolyA_DB.v3.2	PolyA DB	20/08/2020	Wang et al, 2018

Table C.17: Table of R packages used for data analysis in this thesis.

Package	Version
broom	0.5.6
caret	6.0-86
circlize	0.4.10
clusterProfiler	3.16.0
cowplot	1.0.0
data.table	1.12.8
dendsort	0.3.3
DEoptimR	1.0-8
desc	1.2.0
DescTools	0.99.37
DESeq2	1.28.1
devtools	2.3.0
DiagrammeR	1.0.6.1
dplyr	1.0.0
e1071	1.7-3
edgeR	3.30.3
EnvStats	2.3.1
factoextra	1.0.7
FactoMineR	2.3
forcats	0.5.0
GEOquery	2.56.0
ggplot2	3.3.2
ggplotify	0.0.5
ggpmisc	0.3.5
ggpubr	0.4.0
ggraph	2.0.3
ggrepel	0.8.2
ggridges	0.5.2
ggsci	2.9
ggsignif	0.6.0
ggthemes	4.2.0
glue	1.4.1
Gmisc	1.11.0
gridExtra	2.3
Hmisc	4.4-0
knitr	1.29
limma	3.44.3
lme4	1.1-23
lmtest	0.9-37
magick	2.4.0
magrittr	1.5
markdown	1.1
MASS	7.3-51.6

Table C.17 continued from previous page

Package	Version
MatrixModels	0.4-1
matrixStats	0.56.0
maxstat	0.7-25
mclust	5.4.6
memoise	1.1.0
NbClust	3
openxlsx	4.1.5
org.Hs.eg.db	3.11.4
PerformanceAnalytics	2.0.4
pheatmap	1.0.12
purrr	0.3.4
qusage	2.22.0
qvalue	2.20.0
RColorBrewer	1.1-2
rcompanion	2.3.25
reshape2	1.4.4
rstatix	0.6.0
stringr	1.4.0
SummarizedExperiment	1.18.1
survivalROC	1.0.3
survminer	0.4.7
survMisc	0.5.5
TCGAbiolinks	2.16.1
tibble	3.0.1
tidyr	1.1.0
tidyverse	1.3.0
vcd	1.4-7
VennDiagram	1.6.20
WGCNA	1.69
xgboost	1.1.1.1
base	4.0.2

Table C.18: Table of oligos used in this thesis.

CRISPR guide RNA	**Oligo sequence (5' to 3')**
KITLG.KO-guide RNA 1	CGTGACTGCAAGATCTGATA
KITLG.KO-guide RNA 2	TATAACTGTAGCATCAACTG
KITLG.KO.Rescue-guide RNA	ATCTTGCAGTCACGCCTAAT
rs78378222-guide RNA 1	CGTTCACCCCTCAGACACAC
rs78378222-guide RNA 2	TGCAGGCTACTGGGGTCAGC

Genotyping PCR primer	**Oligo sequence (5' to 3')**
KITLG-3F	TCATGGCTGGAAAGCTAAAAA
KITLG-3R	GGGAGGCAGAGGATAAATGAG
KITLG-sur-3R	GGATTACAACACGTGACAGCA
KITLG-out-3F	ATAAAAATCTGAGGAAGCAGCTC
KITLG-out-1R	GCCTGTCTTCTCGAGTATTTCC

qRT-PCR primer	**Oligo sequence (5' to 3')**
RT-KITLG-F	AGCAGTAATAGGAAGGCCAAA
RT-KITLG-R	CTTGGCTGTCTCTTCTTCCA
RT-p21-F	TGAGCCGCGACTGTGATG
RT-p21-R	GTCTCGGTGACAAAGTCGAAGTT
RT-GAPDH-F	AGCCACATCGCTCAGACAC
RT-GAPDH-R	GCCCAATACGACCAAATCC
RT-PUMA-F	GACCTCAACGCACAGTACGA
RT-PUMA-R	TGGGTAAGGGCAGGAGTC
RT-14-3-3σ-F	GTCTGATCCAGAAGGCCAAG
RT-14-3-3σ-R	CTCCTCGTTGCTTTTCTGCT
RT-FAS-F	AAGCTCTTTCACTTCGGAGG
RT-FAS-R	GGGCATTAACACTTTTGGACG
RT-BAX-F	AGTAACATGGAGCTGCAGAG
RT-BAX-R	AGTAGAAAAGGGCGACAACC

siRNA	**Oligo sequence (5' to 3')**
cKIT siRNA #1-Sense	AGACUAAACUACAGGAGAAUU
cKIT siRNA #1-Antisense	UUCUCCUGUAGUUUAGUCUUU
cKIT siRNA #2-Sense	GGAGAUAAAUGGAAACAAUUU

Table C.18 continued from previous page

CRISPR guide RNA	**Oligo sequence (5' to 3')**
cKIT siRNA #2-Antisense	AUUGUUUCCAUUUAUCUCCUU
Control siRNA	ON-TARGETplus Non-targeting Pool (D-001810-10-05)
p53 siRNA	ON-TARGETplus Human TP53 siRNA - SMARTpool (L-003329-00-0005)

Table C.19: Table of cell lines used in this thesis.

Cell Line Name	Cancer type	Histology	Media
TERA1	TGCT	embryonal carcinoma	RPMI, 10% FBS 1% P/S
TERA2	TGCT	embryonal carcinoma	RPMI, 10% FBS 1% P/S
GCT27	TGCT	Teratoma	DMEM, 10% FBS 1% P/S
GCT27-CR	TGCT	Cisplatin-resistant clone of GCT27	DMEM, 10% FBS 1% P/S
Susa	TGCT	Teratoma	RPMI, 20% FBS 1% P/S
Susa-CR	TGCT	Cisplatin-resistant clone of Susa	RPMI, 10% FBS 1% P/S
2102EP	TGCT	embryonal carcinoma	RPMI, 10% FBS 1% P/S
TCAM-2	TGCT	Seminoma	RPMI, 10% FBS 1% P/S
SK-MEL-5	Melanoma	Cutaneous	RPMI, 10% FBS 1% P/S
Hap1	Chronic Myeloid Leukemia	Haploid	IMDM, 10% FBS 1% P/S

Table C.20: Table of compounds used in this thesis.

Compound	**Provider**	**Catalogue No.**	**Solvent**
Nutlin-3a	Merck	N6287-5MG	DMSO
Cisplatin	Sigma-Aldrich	232120-50MG	dH2O
Oxaliplatin	Sigma-Aldrich	O9512-5MG	DMSO
Etoposide	Sigma-Aldrich	E1383-25MG	DMSO
Topotecan	Sigma-Aldrich	T2705-10MG	DMSO
Camptothecin	Sigma-Aldrich	C9911-100MG	DMSO
Doxorubicin	Sigma-Aldrich	44583-1MG	DMSO
Dasatinib	Cambridge Bioscience	1586-25	DMSO
Imatinib mesylate	Sigma-Aldrich	SML1027-100MG	DMSO
Nilotinib	Sigma-Aldrich	Y0002097	DMSO
Sunitinib malate	Sigma-Aldrich	PZ0012-25MG	DMSO
Pazopanib	Sigma-Aldrich	CDS023580-25MG	DMSO
MK-2206	Stratech Scientific	S1078-SEL-5mg	DMSO
Ipatasertib	Stratech Scientific	S2808-SEL-5mg	DMSO
AZD5363	Stratech Scientific	S8019-SEL-5mg	DMSO

Table C.21: Table of software used in this study.

Software	**Version**	**Reference**
Rstudio	4.0.2	R Core Team, 2020
GraphPad Prism	8.3.1 (549)	Motulsky and Christopoulos, 2004
ImageJ	1.52a	Schneider et al, 2012
HISAT2	2.1.0	Kim et al 2015
FeatureCounts	1.6.2	Liao et al 2014
MaxQuant		Tyanova et al, 2016
STRING	11	Szklarczyk et al, 2019
Compusyn		Chou 2006

References

[1] V. DeVita Jr. “The ’War on Cancer’ and its impact”. en. In: *Nature Clinical Practice Oncology* 1 (2004).

[2] M. Coleman. “War on cancer and the influence of the medical-industrial complex”. en. In: *Journal of Cancer Policy* 1 (2013), pp. 31–34.

[3] G. Carioli, P. Bertuccio, et al. “European cancer mortality predictions for the year 2020 with a focus on prostate cancer”. en. In: *Annals of Oncology* 31.5 (2020), pp. 650–658.

[4] R. Siegel, K. Miller, et al. “Cancer statistics, 2019”. io. In: *CA Cancer J Clin* 69.1 (2019), pp. 7–34.

[5] G. Tweedale. “Asbestos and its lethal legacy”. en. In: *Nature Reviews Cancer* 2 (2002), pp. 311–314.

[6] S. Steck and A. Murphy. “Dietary patterns and cancer risk”. en. In: *Nature Reviews Cancer* 20 (2020), pp. 125–138.

[7] N. Zandwijk, G. Reid, et al. “Asbestos-related cancers: the ‘Hidden Killer’ remains a global threat”. en. In: *Expert Review of Anticancer Therapy* 20.4 (2020).

[8] S. Hecht. “Tobacco carcinogens, their biomarkers and tobacco-induced cancer”. en. In: *Nature Reviews Cancer* 3 (2003), pp. 733–744.

[9] I. Issa and M. Noureddine. “Colorectal cancer screening: an updated review of the available options”. en. In: *World J Gastroenterol* 23 (2017), pp. 5086–5096.

[10] A. Chrysostomou, D. Stylianou, et al. “Cervical cancer screening programs in Europe: the transition towards HPV vaccination and population-based HPV testing”. en. In: *Viruses* 10 (2018).

[11] M. Malvezzi, G. Carioli, et al. “European cancer mortality predictions for the year 2019 with focus on breast cancer”. en. In: *Ann Oncol* 30 (2019).

[12] B. Druker, F. Guilhot, et al. “Five-Year Follow-up of Patients Receiving Imatinib for Chronic Myeloid Leukemia”. en. In: *N Engl J Med* 355 (2006).

[13] U. McDermott and J. Settleman. “Personalized cancer therapy with selective kinase inhibitors: an emerging paradigm in medical oncology”. en. In: *J Clin Oncol* 27.33 (2009).

[14] F. Stegmeier, M. Warmuth, et al. “Targeted Cancer Therapies in the Twenty-First Century: Lessons From Imatinib”. en. In: *Clinical Pharmacology & Therapeutics* 87.5 (2010).

[15] P. Chapman, A. Hauschild, et al. “Improved Survival with Vemurafenib in Melanoma with BRAF V600E Mutation”. en. In: *N Engl J Med* 364.26 (2011).

[16] B. Vogelstein, N. Papadopoulos, et al. “Cancer Genome Landscapes”. en. In: *Science* 339.6127 (2013), pp. 1546–1558.

[17] A. Ahmad, N. Ormiston-Smith, et al. “Trends in the lifetime risk of developing cancer in Great Britain: comparison of risk for those born from 1930 to 1960”. en. In: *Br J Cancer* 112.5 (2015), pp. 943–947.

[18] A. Renehan, M. Tyson, et al. “Body-mass index and incidence of cancer: a systematic review and meta-analysis of prospective observational studies”. en. In: *Lancet* 371.9612 (2008), pp. 569–578.

[19] J. Oke, J. O’Sullivan, et al. “The mapping of cancer incidence and mortality trends in the UK from 1980–2013 reveals a potential for overdiagnosis”. en. In: *Sci Rep* 8 (2018).

[20] K. Nurgali, R. Jagoe, et al. “Editorial: Adverse Effects of Cancer Chemotherapy: Anything New to Improve Tolerance and Reduce Sequelae?” en. In: *Front Pharmacol* 9.245 (2018).

[21] N. Gegechkori, L. Haines, et al. “Long Term and Latent Side Effects of Specific Cancer Types”. en. In: *Med Clin North Am* 101.6 (2017), pp. 1053–1073.

[22] M. Davis. “Glioblastoma: Overview of Disease and Treatment”. en. In: *Clin J oncol Nurs* 20.5 (2016), pp. 2–8.

[23] A. Mejean, A. Ravaud, et al. “Sunitinib Alone or after Nephrectomy in Metastatic Renal-Cell Carcinoma”. en. In: *N Engl J Med* 379 (2018), pp. 417–427.

[24] M. Markham, K. Wachetr, et al. “Clinical Cancer Advances 2020: Annual Report on Progress Against Cancer From the American Society of Clinical Oncology”. en. In: *ournal of Clinical Oncology* 38.10 (2020).

[25] V. Schirrmacher. “From chemotherapy to biological therapy: A review of novel concepts to reduce the side effects of systemic cancer treatment (Review”. en. In: *Int J Oncol* 54.2 (2019), pp. 407–419.

[26] T. Gil, S. Sideris, et al. “Testicular germ cell tumor: Short and long-term side effects of treatment among survivors”. en. In: *Molecular and Clinical Oncology* 5.3 (2016), pp. 258–264.

[27] Yeuan Ting Lee, Yi Jer Tan, et al. “Molecular targeted therapy: Treating cancer with specificity”. In: *European Journal of Pharmacology* 834 (2018), pp. 188–196. URL: `https://www.sciencedirect.com/science/article/pii/S0014299918304011`.

[28] V. Craig Jordan. “Tamoxifen: a most unlikely pioneering medicine”. In: *Nature Reviews Drug Discovery* 2.3 (Mar. 2003), pp. 205–213. URL: `https://doi.org/10.1038/nrd1031`.

[29] V. Craig Jordan. “Tamoxifen: catalyst for the change to targeted therapy.” eng. In: *European journal of cancer (Oxford, England : 1990)* 44.1 (Jan. 2008), pp. 30–38.

[30] X. Ke and L. Shen. “Molecular targeted therapy of cancer: The progress and future prospect”. en. In: *Frontiers in Laboratory Medicine* 1.2 (2017), pp. 69–75.

[31] P. Reichardt. “The Story of Imatinib in GIST – a Journey through the Development of a Targeted Therapy”. en. In: *Oncol Res Treat* 41 (2018), pp. 472–477.

[32] N. Saijo. “Present Status and Problems on Molecular Targeted Therapy of Cancer”. en. In: *CancerRes Treat* 44.1 (2012), pp. 1–10.

[33] M. Soda, Y. Choi, et al. “Identification of the transforming EML4-ALK fusion gene in non-small-cell lung cancer”. en. In: *Nature* 7153.561 (2007), pp. 561–566.

[34] K. Flaherty, I. Puzanov, et al. “Inhibition of mutated, activated BRAF in metastatic melanoma”. en. In: *N Engl J Med* 363.9 (2010), pp. 809–819.

[35] A. Marchetti, L. Felicioni, et al. “Clinical Features and Outcome of Patients With Non–Small-Cell Lung Cancer Harboring BRAF Mutations”. en. In: *Journal of Clinical Oncology* 29.26 (2011), pp. 3574–3579.

[36] Jacob J. Adashek, Vivek Subbiah, et al. “From Tissue-Agnostic to N-of-One Therapies: (R)Evolution of the Precision Paradigm”. In: *Trends in Cancer* (). Publisher: Elsevier. URL: https://doi.org/10.1016/j.trecan.2020.08.009 (visited on 10/03/2020).

[37] Jason K. Sicklick, Shumei Kato, et al. “Molecular profiling of cancer patients enables personalized combination therapy: the I-PREDICT study.” eng. In: *Nature medicine* 25.5 (May 2019), pp. 744–750.

[38] Jordi Rodon, Jean-Charles Soria, et al. “Genomic and transcriptomic profiling expands precision cancer medicine: the WINTHER trial.” eng. In: *Nature medicine* 25.5 (May 2019), pp. 751–758.

[39] M. Martins, A. Zhou, et al. “Linking Tumor Mutations to Drug Responses via a Quantitative Chemical–Genetic Interaction Map”. en. In: *Cancer Discovery* 5.2 (2015).

[40] O. Yildirim, M. Gottwald, et al. “Opportunities and Challenges for Drug Development: Public–Private Partnerships, Adaptive Designs and Big Data”. it. In: *Front Pharmacol* 7.461 (2016).

[41] B. Munos. “Lessons from 60 years of pharmaceutical innovation”. en. In: *Nature Reviews Drug Discovery* 8 (2009), pp. 959–968.

[42] I. Kola and J. Landis. “Can the pharmaceutical industry reduce attrition rates?” en. In: *Nature Reviews Drug Discovery* 3 (2004), pp. 711–716.

[43] Peng-Chan Lin, Yu-Min Yeh, et al. “Germline susceptibility variants impact clinical outcome and therapeutic strategies for stage III colorectal cancer”. In: *Scientific Reports* 9.1 (Mar. 2019), p. 3931. URL: https://doi.org/10.1038/s41598-019-40571-0.

[44] K. Huang, R. Mashl, et al. “Pathogenic germline variants in 10,389 adult cancers”. en. In: *Cell* 173.2 (2018), pp. 355–370.

[45] Ajay Chatrath, Roza Przanowska, et al. “The pan-cancer landscape of prognostic germline variants in 10,582 patients”. In: *Genome Medicine* 12.1 (Feb. 2020), p. 15. URL: https://doi.org/10.1186/s13073-020-0718-7.

[46] L. Mucci, J. Hjelmborg, et al. “Familial Risk and Heritability of Cancer Among Twins in Nordic Countries”. en. In: *JAMA* 315.1 (2016), pp. 68–76.

[47] P. Lichtenstein, N. Holm, et al. “Environmental and heritable factors in the causation of cancer–analyses of cohorts of twins from Sweden, Denmark, and Finland”. en. In: *N Engl J Med* 343.2 (2000), pp. 78–85.

[48] W. Bodmer and I. Tomlinson. "Rare genetic variants and the risk of cancer". en. In: *Curr Opin Genet Dev* 20.3 (2010), pp. 262–267.

[49] H. Qi. "Deep genetic connection between cancer and developmental disorders". en. In: *Hum Mutat* 37.10 (2016), pp. 1042–1050.

[50] A. Whittemore, G. Gong, et al. "Prevalence of BRCA1 mutation carriers among U.S. non-Hispanic Whites". da. In: *Cancer Epidemiol Biomarkers Prev* 13.12 (2004), pp. 2078–2083.

[51] D. Ford, D. Easton, et al. "Estimates of the gene frequency of BRCA1 and its contribution to breast and ovarian cancer incidence". en. In: *Am J Hum Genet* 57.6 (1995), pp. 1457–1462.

[52] T. Manolio, F. Collins, et al. "Finding the missing heritability of complex diseases". en. In: *Nature* 461.7265 (2009), pp. 747–753.

[53] A. Sud, B. Kinnersley, et al. "Genome-wide association studies of cancer: current insights and future perspectives". en. In: *Nature Reviews Cancer* 17 (2017), pp. 692–704.

[54] S. Jiao, U. Peters, et al. "Estimating the heritability of colorectal cancer". en. In: *Human Molecular Genetics* 23.14 (2014), pp. 3898–3905.

[55] J. Dai, W. Shen, et al. "Estimation of Heritability for Nine Common Cancers Using Data from Genome-Wide Association Studies in Chinese Population". en. In: *Int J Cancer* 140.2 (2017), pp. 329–336.

[56] A. Buniello, J. MacArthur, et al. "The NHGRI-EBI GWAS Catalog of published genome-wide association studies, targeted arrays and summary statistics 2019". en. In: *Nucleic Acids Research* 47 (2019).

[57] L. Bomba, K. Walter, et al. "The impact of rare and low-frequency genetic variants in common disease". en. In: *Genome Biology* 18 (2017).

[58] Jonas Patron, Arnau Serra-Cayuela, et al. "Assessing the performance of genome-wide association studies for predicting disease risk." eng. In: *PloS one* 14.12 (2019), e0220215.

[59] M. Frampton, P. Law, et al. "Implications of polygenic risk for personalised colorectal cancer screening". en. In: *Ann Oncol* 27.3 (2016), pp. 429–434.

[60] T. Tasa, M. Puustusmaa, et al. "Precision Prostate Cancer Screening with a Polygenic Risk Score". en. In: *medRxiv* (2020).

[61] J. Lecarpentier, V. Silvestri, et al. "Prediction of Breast and Prostate Cancer Risks in Male BRCA1 and BRCA2 Mutation Carriers Using Polygenic Risk Scores". en. In: *J Clin Oncol* 35.20 (2017), pp. 2240–2250.

[62] Alicia R Martin, Masahiro Kanai, et al. "Clinical use of current polygenic risk scores may exacerbate health disparities". eng. In: *Nature genetics* 51.4 (Apr. 2019), pp. 584–591. URL: `http://europepmc.org/abstract/MED/30926966`.

[63] V. Perez-Andreu, K. Roberts, et al. "Inherited GATA3 variants are associated with Ph-like childhood acute lymphoblastic leukemia and risk of relapse". en. In: *Nat Genet* 45.12 (2013), pp. 1494–1498.

[64] C. Wu, L. Dong, et al. “Genome-wide association study identifies common variants in SLC39A6 associated with length of survival in esophageal squamous-cell carcinoma”. en. In: *Nat Genet* 45.6 (2013), pp. 632–638.

[65] D. Johnson, N. Weinhold, et al. “Genome-wide association study identifies variation at 6q25.1 associated with survival in multiple myeloma”. en. In: *Nat Commun* 7 (2016).

[66] F. Aminkeng, A. Bhavsar, et al. “A coding variant in RARG confers susceptibility to anthracycline-induced cardiotoxicity in childhood cancer”. en. In: *Nat Genet* 47.9 (2015), pp. 1079–1084.

[67] L. Fachal, A. Gomez-Caamano, et al. “A three-stage genome-wide association study identifies a susceptibility locus for late radiotherapy toxicity at 2q24.1”. en. In: *Nat Genet* 46 (2014), pp. 891–894.

[68] Peter H. O’Donnell and M. Eileen Dolan. “Cancer pharmacoethnicity: ethnic differences in susceptibility to the effects of chemotherapy.” eng. In: *Clinical cancer research : an official journal of the American Association for Cancer Research* 15.15 (Aug. 2009), pp. 4806–4814.

[69] Yoshikazu Hasegawa, Tomoya Kawaguchi, et al. “Ethnic Difference in Hematological Toxicity in Patients with Non-small Cell Lung Cancer Treated with Chemotherapy: A Pooled Analysis on Asian versus Non-Asian in Phase II and III Clinical Trials”. In: *Journal of Thoracic Oncology* 6.11 (2011), pp. 1881 –1888. URL: `http://www.sciencedirect.com/science/article/pii/S1556086415322516`.

[70] Masaaki Komatsu, Heather E. Wheeler, et al. “Pharmacoethnicity in Paclitaxel-Induced Sensory Peripheral Neuropathy.” eng. In: *Clinical cancer research : an official journal of the American Association for Cancer Research* 21.19 (Oct. 2015), pp. 4337–4346.

[71] D. Glodzik, S. Morganella, et al. “A somatic-mutational process recurrently duplicates germline susceptibility loci and tissue-specific super-enhancers in breast cancers”. en. In: *Nat Genet* 49.3 (2017), pp. 341–348.

[72] M. Nelson, H. Tipney, et al. “The support of human genetic evidence for approved drug indications”. en. In: *Nat Genet* 47.8 (2015), pp. 856–860.

[73] E. King, J. Davis, et al. “Are drug targets with genetic support twice as likely to be approved?” en. In: *PLOS Genetics* (2020).

[74] L. Juarez-Salcedo, V. Desai, et al. “Venetoclax: evidence to date and clinical potential”. it. In: *Drugs Context* 8 (2019).

[75] S. Berndt, C. Skibola, et al. “Genome-wide Association Study Identifies Multiple Risk Loci for Chronic Lymphocytic Leukemia”. en. In: *Nat Genet* 45.8 (2013), pp. 868–876.

[76] P. Sanseau, P. Agarwal, et al. “Use of genome-wide association studies for drug repositioning”. en. In: *Nature Biotechnology* 30 (2012), pp. 317–320.

[77] J. Zhang, K. Jiang, et al. “Use of Genome-Wide Association Studies for Cancer Research and Drug Repositioning”. en. In: *PLoS ONE* 10.3 (2015).

[78] J. Hernandez, M. Pryszlak, et al. “Giving Drugs a Second Chance: Overcoming Regulatory and Financial Hurdles in Repurposing Approved Drugs As Cancer Therapeutics”. en. In: *Front Oncol* 7.273 (2017).

[79] H. Xue, J. Li, et al. “Review of Drug Repositioning Approaches and Resources”. en. In: *Int J Biol Sci* 14.10 (2018), pp. 1232–1244.

[80] C. Griffiths, B. Strober, et al. “Comparison of ustekinumab and etanercept for moderate-to-severe psoriasis”. en. In: *N Engl j Med* 362.2 (2010), pp. 118–128.

[81] R. Nair, K. Duffin, et al. “Genome-wide scan reveals association of psoriasis with IL-23 and NF-kappaB pathways”. en. In: *Nat Genet* 41.2 (2009), pp. 199–204.

[82] P. Di Meglio, A. Di Cesare, et al. “The IL23R R381Q gene variant protects against immune-mediated diseases by impairing IL-23-induced Th17 effector response in humans”. en. In: *PLoS ONE* 6.2 (2011).

[83] M. Yurgelun, G. Chenevix-Trench, et al. “Translating Germline Cancer Risk into Precision Prevention”. en. In: *Cel* 168.4 (2017), pp. 566–570.

[84] E. Cano-Gamez and G. Trynka. “From GWAS to Function: Using Functional Genomics to Identify the Mechanisms Underlying Complex Diseases”. en. In: *Front Genet* 11.424 (2020).

[85] M. Slatkin. “Linkage disequilibrium–understanding the evolutionary past and mapping the medical future”. en. In: *Nat Rev Genet* 9 (2008), pp. 477–485.

[86] D. Schaid, W. Chen, et al. “From genome-wide associations to candidate causal variants by statistical fine-mapping”. en. In: *Nature reviews Genetics* 19.8 (2018), pp. 491–504.

[87] E. Pennisi. “Genomics. ENCODE project writes eulogy for junk DNA”. fr. In: *Science* 337.6099 (2012).

[88] M. Ma, Y. Ru, et al. “Disease-associated variants in different categories of disease located in distinct regulatory elements”. en. In: *BMC Genomics* 16 (2015).

[89] M. Maurano, R. Humbert, et al. “Systematic localization of common disease-associated variation in regulatory DNA”. en. In: *Science* 337.6099 (2012), pp. 1190–1195.

[90] N. Ueffing, K. Singh, et al. “A single nucleotide polymorphism determines protein isoform production of the human c-FLIP protein”. en. In: *Blood* 114.3 (2009), pp. 572–579.

[91] J. French, M. Ghoussaini, et al. “Functional variants at the 11q13 risk locus for breast cancer regulate cyclin D1 expression through long-range enhancers”. en. In: *Am J Hum Genet* 92.4 (2013), pp. 489–503.

[92] M. Wang, M. Du, et al. “A functional variant in TP63 at 3q28 associated with bladder cancer risk by creating an miR-140-5p binding site”. en. In: *Int J Cancer* 139.1 (2016), pp. 65–74.

[93] A. Moszynska, M. Gebert, et al. “SNPs in microRNA target sites and their potential role in human disease”. en. In: *Open Biol* 7.4 (2017).

[94] Z. Cong, Q. Li, et al. “The SNP of rs6854845 suppresses transcription via the DNA looping structure alteration of super-enhancer in colon cells”. en. In: *Biochemical and Biophysical Research Communications* 514.3 (2019), pp. 734–741.

[95] J. Ni, B. Deng, et al. “Integration of GWAS and eQTL Analysis to Identify Risk Loci and Susceptibility Genes for Gastric Cancer”. en. In: *Front Genet* 11.679 (2020).

[96] E. Mucaki, B. Shirley, et al. “Expression Changes Confirm Genomic Variants Predicted to Result in Allele-Specific, Alternative mRNA Splicing”. en. In: *Front Genet* 11.109 (2020).

[97] P. Zhang, I. Kitchen-Smith, et al. “Germline and somatic genetic variants in the p53 pathway interact to affect cancer risk, progression and drug response”. en. In: *bioRxiv* (2020).

[98] L. Grochola, J. Zeron-Medina, et al. “Single-nucleotide Polymorphisms in the p53 Signaling Pathway”. en. In: *Cold Spring Harbor perspectives in biology* 2.5 (2010).

[99] G. Stracquadanio, X. Wang, et al. “The importance of p53 pathway genetics in inherited and somatic cancer genomes”. en. In: *Nat Rev Cancer* 16.4 (2016), pp. 251–265.

[100] D. Malkin. “Li-Fraumeni Syndrome”. en. In: *Genes Cancer* 2.4 (2011), pp. 475–484.

[101] D. Lane and L. Crawford. “T antigen is bound to a host protein in SV40-transformed cells”. no. In: *Nature* 15.278 (1979), pp. 261–263.

[102] D. Linzer and A. Levine. “Characterization of a 54K dalton cellular SV40 tumor antigen present in SV40-transformed cells and uninfected embryonal carcinoma cells”. it. In: *Cell* 17.1 (1979), pp. 43–52.

[103] D. Ahuja, M. Saenz-Robles, et al. “SV40 large T antigen targets multiple cellular pathways to elicit cellular transformation”. da. In: *Oncogene* 24 (2005), pp. 7729–7745.

[104] S. Baker, E. Fearon, et al. “Chromosome 17 deletions and p53 gene mutations in colorectal carcinomas”. fr. In: *Science* 244.4901 (1989), pp. 217–221.

[105] M. Hollstein, D. Sidransky, et al. “p53 mutations in human cancers”. fr. In: *Science* 253.5015 (1991), pp. 49–53.

[106] P. Hainaut and G. Pfeifer. “Somatic TP53 Mutations in the Era of Genome Sequencing”. en. In: *Cold Spring Harb Perspect Med* 6.11 (2016).

[107] V. Marcel, M. Dichtel-Danjoy, et al. “Biological functions of p53 isoforms through evolution: lessons from animal and cellular models”. en. In: *Cell Death Differ* 18.12 (2011), pp. 1815–1824.

[108] D. Reisman, P. Takahashi, et al. “Transcriptional Regulation of the p53 Tumor Suppressor Gene in S-Phase of the Cell-Cycle and the Cellular Response to DNA Damage”. en. In: *Biochemistry Research International* (2012).

[109] A. Joerger and A. Fersht. “The Tumor Suppressor p53: From Structures to Drug Discovery”. en. In: *Cold Spring Harbor perspectives in biology* (2010).

[110] N. Raj and L. Attardi. “The transactivation domains of the p53 protein”. en. In: *Cold Spring Harb Perspect Med* 7.1 (2017).

[111] R. Weinberg, D. Veprintsev, et al. “Cooperative binding of tetrameric p53 to DNA”. en. In: *J Mol Biol* 341.5 (2004), pp. 1145–1159.

[112] C. Wei, Q. Wu, et al. “A global map of p53 transcription-factor binding sites in the human genome”. en. In: *Cell* 124.1 (2006), pp. 207–219.

[113] B. Wang, Z. Xiao, et al. “Redefining the p53 response element”. et. In: *Proc Natl Acad Sci U S A* 106.34 (2009).

[114] T. Tebaldi, S. Zaccara, et al. “Whole-genome cartography of p53 response elements ranked on transactivation potential”. fr. In: *BMC Genomics* 16.1 (2015).

[115] M. Fischer. “Census and evaluation of p53 target genes”. da. In: *Oncogene* 36 (2017), pp. 3943–3956.

[116] Y. Liu, O. Tavana, et al. “p53 modifications: exquisite decorations of the powerful guardian”. en. In: *Journal of Molecular Cell Biology* 11.7 (2019), pp. 564–577.

[117] Y. Barak, T. Juven, et al. “mdm2 expression is induced by wild type p53 activity”. en. In: *EMBO J* 12.2 (1993), pp. 461–468.

[118] V. Pant, S. Xiong, et al. “The p53–Mdm2 feedback loop protects against DNA damage by inhibiting p53 activity but is dispensable for p53 stability, development, and longevity”. en. In: *Genes Dev* 27.17 (2013), pp. 1857–1867.

[119] S. Jones, A. Roe, et al. “Rescue of embryonic lethality in Mdm2-deficient mice by absence of p53”. es. In: *Nature* 378.6553 (1995), pp. 206–208.

[120] L. Vassilev, B. Vu, et al. “In vivo activation of the p53 pathway by small-molecule antagonists of MDM2”. en. In: *Science* 303.55659 (2004), pp. 844–848.

[121] C. Tovar, J. Rosinksi, et al. “Small-molecule MDM2 antagonists reveal aberrant p53 signaling in cancer: Implications for therapy”. en. In: *PNAS* 103.6 (2006), pp. 1888–1893.

[122] L. Jiang and J. Zawacka-Pankau. “The p53/MDM2/MDMX-targeted therapies—a clinical synopsis”. en. In: *Cell Death and Disease* 11 (2020).

[123] K. Vousden and D. Lane. “p53 in health and disease”. en. In: *Nature Reviews Molecular Cell Biology* 8 (2007), pp. 275–283.

[124] A. Levine. “The many faces of p53: something for everyone”. en. In: *Journal of Molecular Cell Biology* 11.7 (2019), pp. 524–530.

[125] E. Appella and C. Anderson. “Post-translational modifications and activation of p53 by genotoxic stresses”. en. In: *European Journal of Biochemistry* 268.10 (2001).

[126] A. Latronico, E. Pinto, et al. “An inherited mutation outside the highly conserved DNA-binding domain of the p53 tumor suppressor protein in children and adults with sporadic adrenocortical tumors”. en. In: *J Clin Endocrinol Metab* 86.10 (2001), pp. 4970–4973.

[127] T. Nguyen, D. Menendez, et al. “Mutant TP53 Posttranslational Modifications: Challenges and Opportunities”. en. In: *Hum Mutat* 35.6 (2014), pp. 738–755.

[128] A. Bode and Z. Dong. “Post-translational modification of p53 in tumorigenesis”. en. In: *Nature Reviews Cancer* 4 (2004), pp. 793–805.

[129] A. Hafner, M. Bulyk, et al. “The multiple mechanisms that regulate p53 activity and cell fate”. cs. In: *Nature Reviews Molecular Cell Biology* 20 (2019), pp. 199–210.

[130] J. Kruse and W. Gu. “Modes of p53 Regulation”. en. In: *Cell* 137.4 (2009), pp. 609–622.

[131] C. Brooks and W. Gu. “New insights into p53 activation”. en. In: *Cell Research* 20 (2010), pp. 614–621.

[132] J. Chen. “The Cell-Cycle Arrest and Apoptotic Functions of p53 in Tumor Initiation and Progression”. en. In: *Cold Spring Harb Perspect Med* 6.3 (2016).

[133] J. Purvis. “p53 dynamics control cell fate”. fr. In: *Science* 336 (2012), pp. 1440–1444.

[134] X. Chen, J. Chen, et al. “DNA damage strength modulates a bimodal switch of p53 dynamics for cell-fate control”. en. In: *BMC Biol* 11 (2013).

[135] M. Wu, H. Ye, et al. “p53 dynamics orchestrates with binding affinity to target genes for cell fate decision”. en. In: *Cell Death & Disease* 8 (2017).

[136] M. Horvath, X. Wang, et al. “Divergent evolution of human p53 binding sites: cell cycle versus apoptosis”. en. In: *PLoS Genet* 3.7 (2007).

[137] A. Vaseva, N. Marcgenko, et al. “p53 opens the mitochondrial permeability transition pore to trigger necrosis”. en. In: *Cell* 149.7 (2012), pp. 1536–1548.

[138] Y. Tomita, N. Marchenko, et al. “WT p53, but not tumor-derived mutants, bind to Bcl2 via the DNA binding domain and induce mitochondrial permeabilization”. en. In: *J Biol Chem* 281.13 (2006), pp. 8600–8606.

[139] K. Vousden and K. Ryan. “p53 and metabolism”. en. In: *Nature Reviews Cancer* 9 (2009), pp. 691–700.

[140] E. White. “Autophagy and p53”. en. In: *Cold Spring Harb Perspect Med* 6.4 (2016).

[141] D. Bergamaschi, Y. Samuels, et al. “iASPP preferentially binds p53 proline-rich region and modulates apoptotic function of codon 72-polymorphic p53”. en. In: *Nat Genet* 38.10 (2006).

[142] W. An, J. Kim, et al. “Ordered cooperative functions of PRMT1, p300, and CARM1 in transcriptional activation by p53”. en. In: *Cell* 117 (2004), pp. 735–748.

[143] A. Friedler, D. Veprintsev, et al. “205. Binding of Rad51 and other peptide sequences to a promiscuous, highly electrostatic binding site in p53”. en. In: *J Biol Chem* 280.9 ().

[144] Z. Feng, C. Zhang, et al. “Tumor suppressor p53 meets microRNAs”. it. In: *J Mol Cell Biol* 3.1 (2011), pp. 44–50.

[145] T. Soussi and G. Lozano. “p53 mutation heterogeneity in cancer”. en. In: *Biochem Biophys Res Com* 331 (2005), pp. 834–842.

[146] K. Suzuki and H. Matsubara. “Recent Advances in p53 Research and Cancer Treatment”. en. In: *BioMed Research International* 2011 (2011).

[147] A. Sigal and V. Rotter. “Oncogenic mutations of the p53 tumor suppressor: the demons of the guardian of the genome”. en. In: *Cancer Res* 60 (2000), pp. 6788–6793.

[148] E. Kim and W. Deppert. “Transcriptional activities of mutant p53: when mutations are more than a loss”. en. In: *J Cell Biochem* 93 (2004), pp. 878–886.

[149] A. Willis, E. Jung, et al. “Mutant p53 exerts a dominant negative effect by preventing wild-type p53 from binding to the promoter of its target genes”. en. In: *Oncogene* 23 (2004), pp. 2330–2338.

[150] Y. Cho, S. Gorina, et al. “Crystal structure of a p53 tumor suppressor-DNA complex: understanding tumorigenic mutations”. en. In: *Science* 265.5170 (1994), pp. 346–355.

[151] N. Rivlin, R. Brosh, et al. “Mutations in the p53 Tumor Suppressor Gene”. en. In: *Genes Cancer* 2.4 (2011), pp. 466–474.

[152] S. Di Agostino, S. Strano, et al. “Gain of function of mutant p53: the mutant p53/NF-Y protein complex reveals an aberrant transcriptional mechanism of cell cycle regulation”. en. In: *Cancer Cell* 10 (2006), pp. 191–202.

[153] P. Do, L. Varanasi, et al. “Mutant p53 cooperates with ETS2 to promote etoposide resistance”. en. In: *Genes Dev* 26 (2012), pp. 830–845.

[154] C. Zhang, J. Liu, et al. “Tumour-associated mutant p53 drives the Warburg effect”. en. In: *Nat Commun* 4 (2013).

[155] L. Ji, J. Xu, et al. “Mutant p53 promotes tumor cell malignancy by both positive and negative regulation of the transforming growth factor β (TGF-β) pathway”. en. In: *J Biol Chem* 290 (2015).

[156] X. Zhou, Q. Hao, et al. “Mutant p53 in cancer therapy—the barrier or the path”. en. In: *Journal of Molecular Cell Biology* 11.4 (2019), pp. 293–305.

[157] C. Hartmann, L. Kluwe, et al. “The rate of homozygous CDKN2A/p16 deletions in glioma cell lines and in primary tumors”. en. In: *Int J Oncol* 15.5 (1999), pp. 975–982.

[158] J. Oliner, A. Saiki, et al. “The Role of MDM2 Amplification and Overexpression in Tumorigenesis”. en. In: *Cold Spring Harb Perspect Med* 6.6 (2016).

[159] C. Kung, J. Leu, et al. “The P72R polymorphism of p53 predisposes to obesity and metabolic dysfunction”. en. In: *Cell Rep* 14.10 (2016), pp. 2413–2425.

[160] R. Gunaratna, A. Santos, et al. “Dynamic role of the codon 72 p53 single-nucleotide polymorphism in mammary tumorigenesis in a humanized mouse model”. da. In: *Oncogene* 38 (2019), pp. 3535–3550.

[161] N. Harris, E. Brill, et al. “Molecular basis for heterogeneity of the human p53 protein”. en. In: *Mol Cell Biol* 6 (1986), pp. 4650–4656.

[162] P. Dumont, J. Leu, et al. “The codon 72 polymorphic variants of p53 have markedly different apoptotic potential”. en. In: *Nat Gen* 33 (2003), pp. 357–365.

[163] D. Bergamaschi, M. Gasco, et al. “p53 polymorphism influences response in cancer chemotherapy via modulation of p73-dependent apoptosis”. en. In: *Cancer Cell* 3 (2003), pp. 387–402.

[164] G. Bond, W. Hu, et al. “A Single Nucleotide Polymorphism in the MDM2 Promoter Attenuates the p53 Tumor Suppressor Pathway and Accelerates Tumor Formation in Humans”. en. In: *Cell* 119.5 (2004), pp. 591–602.

[165] S. Post, A. Quintas-Cardama, et al. “A High-Frequency Regulatory Polymorphism in the p53 Pathway Accelerates Tumor Development”. en. In: *Cancer Cell* 18.3 (2010), pp. 220–230.

[166] A. Vazquez, L. Grochola, et al. “Chemosensitivity Profiles Identify Polymorphisms in the p53 Network Genes 14-3-3τ and CD44 That Affect Sarcoma Incidence and Survival”. en. In: *Cancer Research* 70.1 (2010).

[167] T. Barnoud, J. Parris, et al. “Common genetic variants in the TP53 pathway and their impact on cancer”. en. In: *Journal of Molecular Cell Biology* 11.7 (2019), pp. 578–585.

[168] B. Vogelstein, D. Lane, et al. “Surfing the p53 network”. en. In: *Nature* 408 (2000), pp. 307–310.

[169] T. Guha and D. Malkin. “Inherited TP53 Mutations and the Li-Fraumeni Syndrome”. en. In: *Cold Spring Harb Perspect Med* 7.4 (2017).

[170] M. Tarunina and J. Jenkins. “Human p53 binds DNA as a protein homodimer but monomeric variants retain full transcription transactivation activity”. en. In: *Oncogene* 8.11 (1993), pp. 3165–3173.

[171] W. El-Deiry, S. Kern, et al. “Definition of a consensus binding site for p53”. en. In: *Nature Genetics* 1 (1992), pp. 45–49.

[172] R. Weinberg, D. Veprintsev, et al. “Comparative Binding of p53 to its Promoter and DNA Recognition Elements”. en. In: *Journal of Molecular Biology* 348.3 (2005), pp. 589–596.

[173] M. Noureddine, D. Menendez, et al. “Probing the Functional Impact of Sequence Variation on p53-DNA Interactions Using a Novel Microsphere Assay for Protein-DNA Binding with Human Cell Extracts”. en. In: *PLOS Genetics* 5.5 (2009).

[174] O. Bandele, X. Wang, et al. “Human single-nucleotide polymorphisms alter p53 sequence-specific binding at gene regulatory elements”. en. In: *Nucleic Acids Research* 39.1 (2011), pp. 178–189.

[175] A. Naqvi. “A single-nucleotide variation in a p53-binding site affects nutrient-sensitive human SIRT1 expression”. en. In: *Hum Mol Genet* 19.21 (2010), pp. 4123–33.

[176] J. Zeron-Medina. “A polymorphic p53 response element in KIT ligand influences cancer risk and has undergone natural selection”. fr. In: *Cell* 155.2 (2013), pp. 410–422.

[177] J. Kruse and W. Gu. “SnapShot: p53 Posttranslational Modifications”. en. In: *Cell* 133.5 (2008), p. 930.

[178] O. Laptenko and C. Prives. “Transcriptional Regulation by p53: One Protein, Many Possibilities”. en. In: *Cell Death Differ* 13.6 (2006), pp. 951–961.

[179] G. Stormo. “DNA binding sites: representation and discovery”. en. In: *Bioinformatics* 16.1 (2000), pp. 16–23.

[180] K. Zsebo, D. Williams, et al. “Stem cell factor is encoded at the Sl locus of the mouse and is the ligand for the c-kit tyrosine kinase receptor”. en. In: *Cell* 63.1 (1990), pp. 213–224.

[181] D. Anderson. “Alternate splicing of mRNAs encoding human mast cell growth factor and localization of the gene to chromosome 12q22-q24”. en. In: *Cell Growth Differ* (1991), pp. 373–378.

[182] M. Bedell, N. Copeland, et al. “Multiple pathways for Steel regulation suggested by genomic and sequence analysis of the murine Steel gene”. en. In: *Genetics* 142 (1996), pp. 927–934.

[183] Z. Han. “Hypoxia-inducible factor (HIF)-1 alpha directly enhances the transcriptional activity of stem cell factor (SCF) in response to hypoxia and epidermal growth factor (EGF”. en. In: *Carcinogenesis* 29 (2008), pp. 1853–1861.

[184] D. Kobi. “Genomewide analysis of POU3F2/BRN2 promoter occupancy in human melanoma cells reveals Kitl as a novel regulated target gene”. en. In: *Pigment Cell Melanoma Res* 23 (2010), pp. 404–418.

[185] J. Lennartsson and L. Ronnstrand. “Stem cell factor receptor/c-KIT: from basic science to clinical implication”. en. In: *Physiol Rev* 92 (2012), pp. 1619–1649.

[186] S. Yuzawa. “Structural basis for activation of the receptor tyrosine kinase KIT by stem cell factor”. en. In: *Cell* 130 (2007), pp. 323–334.

[187] V. Broudy. “Analysis of c-kit receptor dimerization by fluorescence resonance energy transfer”. en. In: *Blood* 91 (1998), pp. 898–906.

[188] C. Mol. “Structural basis for the autoinhibition and STI-571 inhibition of c-Kit tyrosine kinase”. en. In: *J Biol Chem* 279 (2004), pp. 31655 –31663.

[189] J. DiNitto. “. Function of activation loop tyrosine phosphorylation in the mechanism of c-Kit auto-activation and its implication in sunitinib resistance”. en. In: *J Biochem* 147 (2010), pp. 601–609.

[190] C. Corless, J. Fletcher, et al. “Biology of gastrointestinal stromal tumors”. pt. In: *Clin Oncol* 22 (2004), pp. 3813–3825.

[191] J. Desai. “Clonal evolution of resistance to imatinib in patients with metastatic gastrointestinal stromal tumors”. en. In: *Clin Cancer Res* 13.18 (2007), pp. 5398–405.

[192] G. Demetri, M. Mehren, et al. “Efficacy and safety of imatinib mesylate in advanced gastrointestinal stromal tumors”. en. In: *N Eng J Med* 347.7 (2002), pp. 472–80.

[193] N. Iqbal and N. Iqbal. “Imatinib: A Breakthrough of Targeted Therapy in Cancer”. en. In: (2014).

[194] P. Reichardt, J. Blay, et al. “Phase III study of nilotinib versus best supportive care with or without a TKI in patients with gastrointestinal stromal tumors resistant to or intolerant of imatinib and sunitinib”. en. In: *Annals of Oncology* 23.7 (2012), pp. 1680–1687.

[195] H. Wang. “The Proto-oncogene c-Kit Inhibits Tumor Growth by Behaving as a Dependence Receptor”. en. In: *Molecular Cell* 72.1 (2018), pp. 413–425.

[196] H. Siemens, R. Jackstadt, et al. “Repression of c-Kit by p53 is mediated by miR-34 and is associated with reduced chemoresistance, migration and stemness”. en. In: *Oncotarget* 4.9 (2013), pp. 1399–1415.

[197] S. Chanock. “High marks for GWAS”. en. In: *Nature Genetics* 41.7 (2009), pp. 765–766.

[198] P. Kanetsky, N. Mitra, et al. “Common variation in KITLG and at 5q31.3 predisposes to testicular germ cell cancer”. en. In: *Nat Genet* 41.7 (2009), pp. 811–815.

[199] K. Litchefield. “Polygenic susceptibility to testicular cancer: implications for personalised health care”. en. In: *British Journal of Cancer* 113 (2015), pp. 1512–1518.

[200] K. Litchfield, M. Levy, et al. “The genomic landscape of testicular germ cell tumours: from susceptibility to treatment”. en. In: *Nat Rev Urol* 13.7 (2016), pp. 409–419.

[201] K. Litchfield, M. Levy, et al. “Identification of 19 new risk loci and potential regulatory mechanisms influencing susceptibility to testicular germ cell tumor”. en. In: *Nat Genet* 49.7 (2017), pp. 1133–1140.

[202] C. Kratz, M. Greene, et al. “A stratified genetic risk assessment for testicular cancer”. en. In: *International Journal of Andrology* 34.4 (2011), pp. 98–102.

[203] C. Turnbull and N. Rahman. “Genome-wide association studies provide new insights into the genetic basis of testicular germ-cell tumour”. en. In: *International Journal of Andrology* 34.4 (2011), pp. 86–97.

[204] E. Rapley and K. Nathanson. “Predisposition alleles for Testicular Germ Cell Tumour”. en. In: *Current opinion in genetics & development* 20.3 (2010), pp. 225–230.

[205] M. Garner, M. Turner, et al. “Epidemiology of testicular cancer: An overview”. en. In: *IJC* 116.3 (2005), pp. 331–339.

[206] Y. Sheikine. “Molecular genetics of testicular germ cell tumors”. es. In: *Am J Cancer Res* 2.2 (2012), pp. 153–167.

[207] Alessandra di Pietro, Elisabeth G. E. de Vries, et al. “Testicular germ cell tumours: the paradigm of chemo-sensitive solid tumours.” eng. In: *The international journal of biochemistry & cell biology* 37.12 (Dec. 2005). Place: Netherlands, pp. 2437–2456.

[208] J. Aparicio, J. Terrasa, et al. “SEOM clinical guidelines for the management of germ cell testicular cancer (2016).” eng. In: *Clinical & translational oncology : official publication of the Federation of Spanish Oncology Societies and of the National Cancer Institute of Mexico* 18.12 (Dec. 2016), pp. 1187–1196.

[209] L. Cheng. “Testicular cancer”. en. In: *Nature Reviews Disease Priimers* 4 (2018).

[210] I. Godin. “Effects of the steel gene prod uct on mouse primordial germ cells in culture”. en. In: *Nature* 352 (1991), pp. 807–809.

[211] C. Wylie. “The biology of primordial germ cells”. en. In: *Eur Urol* 23 (1993), pp. 62–66.

[212] C. Runyan. “Steel factor controls midline cell death of primordial germ cells and is essential for their normal proliferation and migration”. en. In: *Development* 133 (2006), pp. 4861–4869.

[213] J. Oosterhuis and L. Looijenga. “Testicular germ-cell tumours in a broader perspective”. en. In: *Nature Reviews Cancer* 5 (2005), pp. 210–222.

[214] Y. Yin, DeWolf StahlB, et al. “p53-Mediated Germ Cell Quality”. en. In: *DEVELOPMENTAL BIOLOGY* 204 (1998), pp. 165–171.

[215] I. Allemand. “Testicular wild-type p53 expression in transgenic mice induces spermiogenesis alterations ranging from differentiation defects to apoptosis”. en. In: *Oncogene* 18 (1999), pp. 6521–6530.

[216] A. Taylor-Weiner, T. Zack, et al. “Genomic evolution and chemoresistance in germ-cell tumours”. fr. In: *Nature* 540.7631 (2016), pp. 114–118.

[217] K. McGowan. “Ribosomal mutations cause p53-mediated dark skin and pleiotropic effects”. en. In: *Nat Genet* 40.8 (2008), pp. 963–970.

[218] D. Murase. “The Essential Role of p53 in Hyperpigmentation of the Skin via Regulation of Paracrine Melanogenic Cytokine Receptor Signaling”. en. In: *JBC* 284 (2008), pp. 4343–4353.

[219] L. Smeenk. “Role of p53 Serine 46 in p53 Target Gene Regulation”. de. In: *PLoS ONE* 6.3 (2011), p. 17574.

[220] T. Terzian. “p53 prevents progression of nevi to melanoma predominantly through cell cycle regulation”. en. In: *Pigment Cell and Melanoma Research* 23.6 (2010), pp. 781–794.

[221] J. Fogh. “Cultivation, characterization, and identification of human tumor cells with emphasis on kidney, testis, and bladder tumors”. en. In: *Natl Cancer Inst Monogr* 49 (1978), pp. 5–9.

[222] J. Tan, S. Yang, et al. “C-kit signaling promotes proliferation and invasion of colorectal mucinous adenocarcinoma in a murine model”. en. In: *Oncogene* 6.29 (2015), pp. 27037–27048.

[223] J. Reyes-Sebastian, L. Montiel-Cervantes, et al. “Cell proliferation and inhibition of apoptosis are related to c-Kit activation in leukaemic lymphoblasts”. en. In: *Hematology* 23.8 (2018).

[224] C. Chresta, J. Masters, et al. “Hypersensitivity of Human Testicular Tumors to Etoposide-induced Apoptosis Is Associated with Functional p53 and a High Bax:Bcl-2 Ratio1”. en. In: *Cancer Research* 56 (1996), pp. 1834–1841.

[225] M. Walker. “Development and characterization of cisplatin-resistant human testicular and bladder tumour cell lines”. es. In: *Eur J Cancer* 26.6 (1990), pp. 742–747.

[226] S. Shellard, L. Hosking, et al. “Characterization of the unusual expression of cross resistance to cisplatin in a series of etoposide-selected resistant sublines of the SuSa testicular teratoma cell line”. en. In: *Biochemical Pharmacology* 47.5 (1994), pp. 775–779.

[227] D. Burden and N. Osheroff. “Mechanism of action of eukaryotic topoisomerase II and drugs targeted to the enzyme”. en. In: *Biochim.Biophys.Acta* 1400 (1998), pp. 139–154.

[228] C. Grandela, M. Pera, et al. “p53 is required for etoposide-induced apoptosis ofhuman embryonic stem cells”. en. In: *Stem Cell Research* 1 (2008), pp. 116–128.

[229] N. Karpinich. “The course of etoposide-induced apoptosis from damage to DNA and p53 activation to mitochondrial release of cytochrome c”. en. In: *J Biol Chem* 227 (2002), pp. 16547–16552.

[230] J. Han. “The relationship between cisplatin-induced apoptosis and p53, bcl-2 and bax expression in human lung cancer cells”. en. In: *Korean J Intern Med* 14.1 (1999), pp. 42–52.

[231] Q. Wei. “Activation and involvement of p53 in cisplatin-induced nephrotoxicity”. en. In: *Am J Physiol Renal Physiol* 293.4 (2007), pp. 1282–1291.

[232] A. Pietro. “Pro- and anti-apoptotic effects of p53 in cisplatin-treated human testicular cancer are cell context-dependent”. en. In: *Cell Cycle* 11.24 (2012), pp. 4552–4562.

[233] R. Koster, M. Vugt, et al. “Unravelling mechanisms of cisplatin sensitivity and resistance in testicular cancer”. fr. In: *Expert Revews in Molecular Medicine* (2013).

[234] E. Raymond, S. Faivre, et al. “Oxaliplatin: mechanism of action and antineoplastic activity”. cs. In: *Semin Oncol* 25.2 (1998), pp. 4–12.

[235] A. Francesco, A. Ruggiero, et al. “Cellular and molecular aspects of drugs of the future: oxaliplatin”. en. In: *CMLS* 59 (2002), pp. 1914–1927.

[236] J. Graham, M. Muhsin, et al. “Oxaliplatin”. en. In: *Nature Reviews Drug Discovery* 3 (2004), pp. 11–12.

[237] F. Toscano, B. Parmentier, et al. “P53 dependent and independent sensitivity to oxaliplatin of colon cancer cells”. en. In: *Biochemical Pharmacology* 74.3 (2007), pp. 392–406.

[238] C. Bokemeyer. “Combination chemotherapy with gemcitabine, oxaliplatin, and paclitaxel in patients with cisplatin-refractory or multiply relapsed germ-cell tumors: a study of the German Testicular Cancer Study Group”. en. In: *Ann Oncol* 19.3 (2008), pp. 448–53.

[239] C. Seidel. “Efficacy and safety of gemcitabine, oxaliplatin, and paclitaxel in cisplatin-refractory germ cell cancer in routine care–Registry data from an outcomes research project of the German Testicular Cancer Study Group”. en. In: *Urol Oncol* 34.4 (2016).

[240] R. Josephson. “Qualification of Embryonal Carcinoma 2102Ep As a Reference for Human Embryonic Stem Cell Research”. en. In: *Stem Cells* 25.2 (2009), pp. 437–446.

[241] P. Bouwman and J. Jonkers. “The effects of deregulated DNA damage signalling on cancer chemotherapy response and resistance”. en. In: *Nat Rev Cancer* 12.9 (2012), pp. 587–598.

[242] Y. Pommier. “Topoisomerase I inhibitors: camptothecins and beyond”. en. In: *Nature Reviews Cancer* 6 (2006), pp. 789–802.

[243] C. Tolis, G. Peters, et al. “Cell cycle disturbances and apoptosis induced by topotecan and gemcitabine on human lung cancer cell lines”. en. In: *EJC* 35.5 (1999), pp. 796–807.

[244] S. Daoud, P. Munson, et al. "Impact of p53 Knockout and Topotecan Treatment on Gene Expression Profiles in Human Colon Carcinoma Cells A Pharmacogenomic Study". en. In: *Cancer Research* 63.11 (2003), pp. 2782–2793.

[245] E. Rudolf, K. Rudolf, et al. "Camptothecin induces p53-dependent and -independent apoptogenic signaling in melanoma cells". en. In: *Apoptosis* 16.11 (2011), pp. 1165–1176.

[246] N. Valkov and D. Sullivan. "Tumor p53 status and response to topoisomerase II inhibitors". es. In: *Drug Resistance Updates* 6.1 (2003), pp. 27–39.

[247] S. Baltaci. "P53, bcl-2 and bax immunoreactivity as predictors of response and outcome after chemotherapy for metastatic germ cell testicular tumours". en. In: *BJU International* 87 (2001), pp. 661–666.

[248] M. Heinrich, D. Griffith, et al. "Inhibition of c-kit receptor tyrosine kinase activity by STI 571, a selective tyrosine kinase inhibitor". en. In: *Blood* 96.3 (2000), pp. 925–932.

[249] D. Tuveson, N. Willis, et al. "STI571 inactivation of the gastrointestinal stromal tumor c-KIT oncoprotein: biological and clinical implications". en. In: *Oncogene* 20.36 (2001), pp. 5054–5058.

[250] O. Hantschel, U. Rix, et al. "Target spectrum of the BCR-ABL inhibitors imatinib, nilotinib and dasatinib". pt. In: *Leuk Lymphoma* 49.4 (2008), pp. 615–619.

[251] M. Mehren. "Beyond imatinib: second generation c-KIT inhibitors for the management of gastrointestinal stromal tumors". en. In: *Clin Colorectal Cancer* 6 (2006), pp. 30–34.

[252] A. Galanis and M. Levis. "Inhibition of c-Kit by tyrosine kinase inhibitors". pt. In: *Haematologica* 100.3 (2015), pp. 77–79.

[253] S. Kopetz, D. Lesslie, et al. "Synergistic activity of the SRC family kinase inhibitor dasatinib and oxaliplatin in colon carcinoma cells is mediated by oxidative stress". en. In: *Cancer Res* 69.9 (2009), pp. 3842–2349.

[254] N. Aggerholm-Pedersen, C. Demuth, et al. "Dasatinib and Doxorubicin Treatment of Sarcoma Initiating Cells: A Possible New Treatment Strategy". en. In: (2016).

[255] G. Zauli, R. Voltan, et al. "Dasatinib Plus Nutlin-3 Shows Synergistic Antileukemic Activity in Both p53wild-type and p53mutated B Chronic Lymphocytic Leukemias by Inhibiting the Akt Pathway". en. In: *Clin Cancer Res* 17.4 (2011).

[256] A. Secord, D. Teoh, et al. "Dasatinib (BMS-35482) Interacts Synergistically With Docetaxel, Gemcitabine, Topotecan, and Doxorubicin in Ovarian Cancer Cells With High SRC Pathway Activation and Protein Expression". en. In: *International Journal of Gynecologic Cancer* 24 (2014), pp. 218–225.

[257] J. Chen, T. Lan, et al. "Dasatinib enhances cisplatin sensitivity in human esophageal squamous cell carcinoma (ESCC) cells via suppression of PI3K/AKT and Stat3 pathways". en. In: *Arch Biochem Biophys* 575 (2015), pp. 38–45.

[258] T. Chou. "Drug Combination Studies and Their Synergy Quantification Using the Chou-Talalay Method". en. In: *Cancer Research* 70 (2010).

[259] T. Chou and N. Martin. *CompuSyn for Drug Combinations: PC Software and User's Guide: A Computer Program for Quantitation of Synergism and Antagonism in Drug Combinations*. Paramus, NJ, 2005.

[260] S. Woldu, J. Amatruda, et al. "Testicular Germ Cell Tumor Genomics". it. In: *Curr Opin Urol* 27.1 (2017), pp. 41–47.

[261] S. Dasari and P. Tchounwou. "Cisplatin in cancer therapy: molecular mechanisms of action". en. In: *Eur J Pharmacol* 5.0 (2015), pp. 364–378.

[262] M. Pera, M. Blasco Lafita, et al. "Cultured stem-cells from human testicular teratomas: the nature of human embryonal carcinoma, and its comparison with two types of yolk-sac carcinoma". en. In: *Int J Cancer* 40.3 (1987), pp. 334–343.

[263] R. Huddart. "Programmed Cell Death in Response to Chemotherapeutic Agents in Human Germ Cell Tumour Lines". en. In: *European Journal of Cancer* 31A (1995), pp. 739–746.

[264] L. Kelland. "Establishment and Characterization of an in Vitro Model of Acquired Resistance to Cisplatin in a Human Testicular Nonseminomatous Germ Cell Line". en. In: *Cancer Research* 52 (1992), pp. 1710–1716.

[265] M. White. "Age and Cancer Risk". en. In: *Am J Prev Med* 46 (2014), pp. 7–15.

[266] F. Bray. "Interpreting the international trends in testicular seminoma and nonseminoma incidence". en. In: *Nat Clin Pract Urol* 3 (2006), pp. 532–543.

[267] C. Ruf. "Changes in epidemiologic features of testicular germ cell cancer: age at diagnosis and relative frequency of seminoma are constantly and significantly increasing". pt. In: *Urol Oncol* 32 (2014), pp. 1–6.

[268] K. Litchfield, J. Mitchell, et al. "Polygenic susceptibility to testicular cancer: implications for personalised health care". en. In: *Br J Cancer* 113.10 (2015), pp. 1512–1518.

[269] C. Le Cornet. "Testicular cancer incidence to rise by 25% by 2025 in Europe? Model-based predictions in 40 countries using population-based registry data". en. In: *Eur J Cancer* 50 (2014), pp. 831–839.

[270] R. Schaffar. "Testicular cancer in Geneva, Switzerland, 1970–2012: incidence trends, survival and risk of second cancer". en. In: *BMC Urology* 19 (2019).

[271] E. Haas. "Early development of the metabolic syndrome after chemotherapy for testicular cancer". en. In: *Ann Oncol* 24 (2013), pp. 749–755.

[272] L. Bujan. "Impact of chemotherapy and radiotherapy for testicular germ cell tumors on spermatogenesis and sperm DNA: a multicenter prospective study from the CECOS network". en. In: *Fertil Steril* 100 (2013), pp. 673–680.

[273] C. Rusner. "Risk of second primary cancers after testicular cancer in East and West Germany: a focus on contralateral testicular cancers". en. In: *Asian J Androl* 16 (2014), pp. 285–289.

[274] G. Schepisi, S. De Padova, et al. "Psychosocial Issues in Long-Term Survivors of Testicular Cancer". pt. In: *Front. Endocrinol* 10.113 (2019).

[275] B. Nitzsche, C. Gloesenkamp, et al. "Anti-tumour activity of two novel compounds in cisplatin-resistant testicular germ cell cancer". en. In: *Br J Cancer* 107.11 (2012), pp. 1853–1863.

[276] D. Koychev, K. Oechsle, et al. “Treatment of patients with relapsed and/or cisplatin-refractory metastatic germ cell tumours: an update”. en. In: *Int J Androl* 34 (2011), pp. 266–273.

[277] K. Baniel, R. Foster, et al. “Late relapse of clinical stage I testicular cancer”. es. In: *J Urol* 154 (1995), pp. 1370–1372.

[278] J. Dai, J. Gu, et al. “GWAS-identified colorectal cancer susceptibility loci associated with clinical outcomes”. en. In: *Carcinogenesis* 33.7 (2012), pp. 1327–1331.

[279] M. Menden, F. Casale, et al. “The germline genetic component of drug sensitivity in cancer cell lines”. en. In: *Nature Communications* 9 (2018).

[280] V. Hlavac, M. Kovacova, et al. “Use of Germline Genetic Variability for Prediction of Chemoresistance and Prognosis of Breast Cancer Patients”. en. In: *Cancers* 10.11 (2018).

[281] T. Soussi. “The history of p53”. en. In: *EMBO Rep* 11.11 (2010), pp. 822–826.

[282] T. Samuel, H. Weber, et al. “The G2/M regulator 14-3-3sigma prevents apoptosis through sequestration of Bax”. en. In: *J Biol Chem* 276.48 (2001), pp. 45201–45206.

[283] X. Zhang, Y. He, et al. “Rap2b, a novel p53 target, regulates p53-mediated pro-survival function”. en. In: *Cell Cycle* 12.8 (2013), pp. 1279–1291.

[284] A. Georgaklias, O. Martin, et al. “p21: A Two-Faced Genome Guardian”. it. In: *Trends in Molecular Medicine* 23.4 (2017), pp. 310–319.

[285] A. Kersemaekers, F. Mayer, et al. “Role of P53 and MDM2 in treatment response of human germ cell tumors”. en. In: *J Clin Oncol* 20.6 (2002), pp. 1551–1561.

[286] S. Lutzker, R. Matthew, et al. “A p53 dose-response relationship for sensitivity to DNA damage in isogenic teratocarcinoma cells”. it. In: *Oncogene* 20 (2001), pp. 2982–2986.

[287] X. Wang. “Linking polymorphic p53 response elements with gene expression in airway epithelial cells of smokers and cancer risk”. en. In: *Hum Genet* 133.12 (2014), pp. 1467–76.

[288] M. Bicak. “Prostate cancer risk SNP rs10993994 is a trans-eQTL for SNHG11 mediated through MSMB”. en. In: *Human Molecular Genetics* (2020).

[289] D. Menendez. “A SNP in the flt-1 promoter integrates the VEGF system into the p53 transcriptional network”. en. In: *Proc Natl Acad Sci U S A* 103.5 (2006), pp. 1406–11.

[290] D. Menendez. “A single-nucleotide polymorphism in a half-binding site creates p53 and estrogen receptor control of vascular endothelial growth factor receptor 1”. en. In: *Mol Cell Biol* 27.7 (2007), pp. 2590–600.

[291] Y. Ciribilli. “The coordinated p53 and estrogen receptor cis-regulation at an FLT1 promoter SNP is specific to genotoxic stress and estrogenic compound”. en. In: *PLoS One* 5.4 (2010).

[292] Y. Kan. “SIRT1 rs3758391 polymorphism and risk of diffuse large B cell lymphoma in a Chinese population”. en. In: *Cancer Cell Int* 18.163 (2018).

[293] Y. Lv, S. Lin, et al. “SIRT1 gene polymorphisms and risk of lung cancer”. en. In: *Cancer Manag Res* 9 (2017), pp. 381–386.

[294] L. Shao. “The inherited variations of a p53-responsive enhancer in 13q12.12 confer lung cancer risk by attenuating TNFRSF19 expression”. en. In: *Genome Biol* 20.1 (2019).

[295] D. Menendez. “p53-responsive TLR8 SNP enhances human innate immune response to respiratory syncytial virus”. en. In: *JCI* 129.11 (2019), pp. 4875–4884.

[296] T. Chou and P. Talalay. “Analysis of combined drug effects: a new look at a very old problem”. en. In: *Trends Pharmacol. Sci* 4 (1983), pp. 450–454.

[297] C. Bliss. “The toxicity of poisons applied jointly”. en. In: *Ann. Appl. Biol* 26 (1939), pp. 585–615.

[298] S. Loewe and H. Muischnek. “über Kombination swirkungen”. de. In: *Archiv. Experiment. Pathol. Pharmakol* 114 (1926), pp. 313–326.

[299] A. Zimmer. “Prediction of multidimensional drug dose responses based on measurements of drug pairs”. en. In: *Proc Natl Acad Sci U S A* 113.37 (2016), pp. 10442–10447.

[300] M. Schindler. “Theory of synergistic effects: Hill-type response surfaces as ’null-interaction’ models for mixtures”. en. In: *Theor Biol Med Model* 14.1 (2017), p. 15.

[301] B. Yadav, K. Wennerberg, et al. “Searching for Drug Synergy in Complex Dose-Response Landscapes Using an Interaction Potency Model”. en. In: *Comput Struct Biotechnol J* 13 (2015), pp. 504–513.

[302] N. Twarog, E. Stewart, et al. “BRAID: A Unifying Paradigm for the Analysis of Combined Drug Action”. en. In: *Sci Rep* 6 (2016), p. 25523.

[303] C. Meyer. “Quantifying Drug Combination Synergy along Potency and Efficacy Axes”. en. In: *Cell Systems* 8.2 (2019), pp. 97–108.

[304] W. Greco, G. Bravo, et al. “The Search for Synergy: A Critical Review From a Response Surface Perspective”. en. In: *Pharmacol Rev* 47.2 (1995), pp. 331–385.

[305] M. Berenbaum. “What is synergy?” de. In: *M.C. Berenbaum* 41 (1989), pp. 93–141.

[306] A. Vlot. “Applying synergy metrics to combination screening data: agreements, disagreements and pitfalls”. en. In: *Dru Discovery Today* 24.12 (2019), pp. 2286–2298.

[307] C. Meyer, D. Wooten, et al. “Charting the Fragmented Landscape ofDrug Synergy”. en. In: *Trends in Pharmacological Sciences* 41.4 (2020).

[308] J. Foucquier and M. Guedj. “Analysis of drug combinations: current methodological landscape”. en. In: *Pharmacol Res Perspect* 3.3 (2015).

[309] K. Han. “Synergistic drug combinations for cancer identified in a CRISPR screen for pairwise genetic interactions”. en. In: *Nature Biotechnology* 35 (2017), pp. 463–474.

[310] G. Jansen. “Chemogenomic profiling predicts antifungal synergies”. en. In: *Mol Syst Biol* 5.388 (2009).

[311] N. Yin. “Synergistic and Antagonistic Drug Combinations Depend on Network Topology”. en. In: *PLoS One* 9.4 (2014).

[312] S. Li, B. Zhang, et al. “Network target for screening synergistic drug combinations with application to traditional Chinese medicine”. en. In: *BMC Syst Biol* 5 (2011).

[313] X. Li. “Biomolecular Network-Based Synergistic Drug Combination Discovery”. en. In: (2016).

[314] M. Luo, J. Jiao, et al. “Screening drug target combinations in disease-related molecular networks”. en. In: *BMC Bioinformatics* 20 (2019).

[315] Z. Sheng. “Advances in computational approaches in identifying synergistic drug combinations”. en. In: *Brief Bioinform* 19.6 (2018), pp. 1172–1182.

[316] C. Goswami, L. Cheng, et al. “A new drug combinatory effect prediction algorithm on the cancer cell based on gene expression and dose-response curve”. en. In: *CPT Pharmacometr. Syst. Pharmacol* 4 (2015), pp. 80–90.

[317] J. Yang. “DIGRE: Drug-induced genomic residual effect model for successful prediction of multidrug effects”. en. In: *CPT Pharmacometr. Syst. Pharmacol* 4 (2015), pp. 91–97.

[318] K. Preuer. “DeepSynergy: predicting anti-cancer drug synergy with Deep Learning”. en. In: *Bioinformatics* 34.9 (2018), pp. 1538–1546.

[319] Y. Takeba, T. Kumai, et al. “Irinotecan Activates p53 With Its Active Metabolite, Resulting in Human”. en. In: *J Pharmacol Sci* 104.3 (2007), pp. 232–242.

[320] M. Deng, J. Sun, et al. “Inhibition of MCM2 enhances the sensitivity of ovarian cancer cell to carboplatin”. en. In: *Molecular Medicine Reports* 20.3 (2019), pp. 2258–2266.

[321] M. Patel. “Objective assessment of cancer genes for drug discovery”. en. In: *Nat Rev Ddrug Discov* 12.1 (2013), pp. 35–50.

[322] J. Sun, K. Zhu, et al. “A comparative study of disease genes and drug targets in the human protein interactome”. en. In: *BMC Bioinformatics* 16 (2015).

[323] A. Urruticoechea. “Recent Advances in Cancer Therapy: An Overview”. en. In: *Current Pharmaceutical Design* 16 (2010), pp. 3–10.

[324] A. Drilon, S. Siena, et al. “Safety and Antitumor Activity of the Multitargeted Pan-TRK, ROS1, and ALK Inhibitor Entrectinib: Combined Results from Two Phase I Trials (ALKA-372-001 and STARTRK-1”. en. In: *Cancer Discov* 7.4 (2017), pp. 400–409.

[325] A. Drilon, T. Laetsch, et al. “Efficacy of Larotrectinib in TRK Fusion-Positive Cancers in Adults and Children”. en. In: *N Engl J Med* 378.8 (2018), pp. 731–739.

[326] S. Paul. “How to improve R&D productivity: the pharmaceutical industry’s grand challenge”. en. In: *Nature Reviews Drug Discovery* 9 (2010), pp. 203–214.

[327] S. Frantz. “FDA publishes analysis of the pipeline problem”. en. In: *Nature Reviews Drug Discovery* 3 (2004), p. 379.

[328] Nature Medicine. “Mechanism Matters”. it. In: *Nature Medicine* 16 (2010), p. 347.

[329] A. Harrill and I. Rusyn. “Systems biology and functional genomics approaches for the identification of cellular responses to drug toxicity”. en. In: *Expert Opin. Drug Metab. Toxicol* 4.11 (2008), pp. 1379–1389.

[330] W. Heihne. “Systems toxicology: applications of toxicogenomics, transcriptomics, proteomics and metabolomics in toxicology”. fr. In: *Expert Rev. Proteomics* 2.5 (2005), pp. 767–780.

[331] Y. Cui and R. Paules. “Use of transcriptomics in understanding mechanisms of drug-induced toxicity”. nl. In: *Pharmacogenomics* 11.4 (2010), pp. 573–585.

[332] V. Kraus. “Biomarkers as drug development tools: discovery, validation, qualification and use”. en. In: *Nature Reviews Rheumatology* 14 (2018), pp. 354–362.

[333] R. Frank and R. Hargreaves. “Clinical biomarkers in drug discovery and development”. en. In: *Nature Reviews Drug Discovery* 2 (2003), pp. 566–580.

[334] P. Rolan, A. Atkinson, et al. “Use of biomarkers from drug discovery through clinical practice: Report of the Ninth European Federation of Pharmaceutical Sciences Conference on Optimizing Drug Development”. en. In: *Clinical Pharmacology and Therapeutics* 73.4 (2003), pp. 284–291.

[335] J. Lennartsson and L. Ronnstrand. “Stem Cell Factor Receptor/c-KIT: from Basic Science to Clinical Implications”. en. In: *Physiol Rev* 92 (2012), pp. 1619–1649.

[336] J. Lennartsson. “Phosphorylation of Shc by Src family kinases is necessary for stem cell factor receptor/ c-kit mediated activation of the Ras/MAP kinase pathway and c-fos induction”. en. In: *Oncogene* 18 (1999), pp. 5546–5553.

[337] B. O’Laughlin-Bunner. “Lyn is required for normal stem cell factor-induced proliferation and chemotaxis of primary hematopoietic cells”. en. In: *Blood* 98 (2001), pp. 343–350.

[338] M. Nishio. “Stem cell factor prevents Fas-mediated apoptosis of human erythroid precursor cells with Src-family kinase dependency”. en. In: *Exp Hematol* 29 (2001), pp. 19–29.

[339] A. Acaro. “Critical role for lipid raft-associated Src kinases in activation of PI3K-Akt signaling”. en. In: *Cell Signal* 19 (2007), pp. 1081–1092.

[340] R. Shivakrupa and D. Linnekin. “Lyn contributes to regulation of multiple Kit-dependent signaling pathways in murine bone marrow mast cells”. en. In: *Cell Signal* 17 (2005), pp. 103–109.

[341] M. Babaei, B. Kamalidehghan, et al. “Receptor tyrosine kinase (c-Kit) inhibitors: a potential therapeutic target in cancer cells”. en. In: *Drug Des Devel Ther* 10 (2016), pp. 2443–2459.

[342] S. Datta. “Akt phosphorylation of BAD couples survival signals to the cell-intrinsic death machinery”. en. In: *Cell* 91 (1997), pp. 231–241.

[343] Y. Zhang. “A Pan-Cancer Proteogenomic Atlasof PI3K/AKT/mTOR Pathway Alterations”. en. In: *Cancer Cel* 31 (2017), pp. 820–832.

[344] H. Serve, Y. Hsu, et al. “Tyrosine residue 719 of the c-kit receptor is essential for binding of the P85 subunit of phosphatidylinositol (PI) 3-kinase and for c-kit-associated PI 3-kinase activity in cos-1 cells”. pt. In: *J Biol Chem* 269 (1994), pp. 6026–6030.

[345] B. Manning and L. Cantley. “AKT/PKB Signaling: Navigating Downstream”. en. In: *Cell* 129.7 (2007), pp. 1261–1274.

[346] D. Sarbassov, D. Guertin, et al. “Phosphorylation and regulation of Akt/PKB by the rictor-mTOR complex”. en. In: *Science* 307 (2005), pp. 1098–1101.

[347] D. Alessi. “Characterization of a 3-phosphoinositide-dependent protein kinase which phosphorylates and activates protein kinase Balpha”. en. In: *Curr Biol* 7 (1997), pp. 261–269.

[348] M. Laplante and D. Sabatini. “mTOR sinalling at a glance”. fr. In: *Journal of Cell Science* 122 (2009), pp. 3589–3594.

[349] K. Dhandapani. “Neuroprotection by stem cell factor in rat cortical neurons involves AKT and NFkappaB”. en. In: *J Neurochem* 95 (2005), pp. 9–19.

[350] P. Blume-Jensen, R. Janknecht, et al. “The kit receptor promotes cell survival via activation of PI 3-kinase and subsequent Akt-mediated phosphorylation of Bad on Ser136”. en. In: *Curr Biol* 8 (1998), pp. 779–782.

[351] M. Engstrom, R. Karlsson, et al. “Inactivation of the forkhead transcription factor FoxO3 is essential for PKB-mediated survival of hematopoietic progenitor cells by kit ligand”. en. In: *Exp hematol* 31 (2003), pp. 316–323.

[352] L. Feng, N. Ravindranath, et al. “Stem cell factor/c-kit up-regulates cyclin D3 and promotes cell cycle progression via the phosphoinositide 3-kinase/p70 S6 kinase pathway in spermatogonia”. en. In: *J Biol Chem* 275 (2000), pp. 25572–25576.

[353] Yoko Ogawara, Shohei Kishishita, et al. “Akt enhances Mdm2-mediated ubiquitination and degradation of p53.” eng. In: *The Journal of biological chemistry* 277.24 (June 2002). Place: United States, pp. 21843–21850.

[354] Loretah Chibaya, Baktiar Karim, et al. “Mdm2 phosphorylation by Akt regulates the p53 response to oxidative stress to promote cell proliferation and tumorigenesis”. In: *Proceedings of the National Academy of Sciences* 118.4 (2021). Publisher: National Academy of Sciences _eprint: https://www.pnas.org/content/118/4/e2003193118.full.pdf. URL: `https://www.pnas.org/content/118/4/e2003193118`.

[355] M. V. Astle, K. M. Hannan, et al. “AKT induces senescence in human cells via mTORC1 and p53 in the absence of DNA damage: implications for targeting mTOR during malignancy.” eng. In: *Oncogene* 31.15 (Apr. 2012), pp. 1949–1962.

[356] Garth Hamilton, Aswin G. Abraham, et al. “AKT regulates NPM dependent ARF localization and p53mut stability in tumors.” eng. In: *Oncotarget* 5.15 (Aug. 2014), pp. 6142–6167.

[357] U. Degirmenci, M. Wang, et al. “Targeting Aberrant RAS/RAF/MEK/ERK Signaling for Cancer Therapy”. en. In: *Cells* 9.1 (2020), p. 198.

[358] C. Weber, J. Slupsky, et al. “Active Ras Induces Heterodimerization of cRaf and BRaf 1”. en. In: *Cancer Res* 61 (2001), pp. 3595–3598.

[359] J. Haling. “Structure of the BRAF-MEK Complex Reveals a Kinase Activity Independent Role for BRAF in MAPK Signaling”. en. In: *Cancer Cell* 26 (2014), pp. 402–413.

[360] J. Yuan. “Activating mutations in MEK1 enhance homodimerization and promote tumorigenesis”. en. In: *Sci Signal* 11 (2018).

[361] L. Hong, V. Munugalavadla, et al. “c-Kit-mediated overlapping and unique functional and biochemical outcomes via diverse signaling pathways”. en. In: *Mol Cell Biol* 24 (2004), pp. 1401–1410.

[362] C. Simon. “Lnk adaptor protein down-regulates specific Kit-induced signaling pathways in primary mast cells”. en. In: *Blood* 112 (2008), pp. 4039–4047.

[363] J. Rawlings, K. Rosler, et al. “The JAK/STAT signaling pathway”. en. In: *Journal of Cell Science* 117 (2004), pp. 1281–1283.

[364] C. DeBerry, S. Mou, et al. “Stat1 associates with c-kit and is activated in response to stem cell factor”. en. In: *Biochem J* 327 (1997), pp. 73–80.

[365] L. Ronnstrand. “Signal transduction via the stem cell factor receptor/c-Kit”. en. In: *Cellular and Molecular Life Sciences* 61 (2004), pp. 2535–2548.

[366] M. Yu. “The scaffolding adapter Gab2, via Shp-2, regulates kit-evoked mast cell proliferation by activating the Rac/JNK pathway”. en. In: *J Biol Chem* 281 (2006), pp. 28615–28626.

[367] L. Samayawardhena, J. Hu, et al. “Fyn kinase acts upstream of Shp2 and p38 mitogen-activated protein kinase to promote chemotaxis of mast cells towards stem cell factor”. en. In: *Cell Signal* 18 (2006), pp. 1447–1454.

[368] A. Cuadrado and A. Nebreda. “Mechanisms and Functions of p38 MAPK Signalling”. en. In: *Bioechm J* 429.3 (2010), pp. 403–417.

[369] I. Barrantes and A. Nebreda. “Roles of p38 MAPKs in Invasion and Metastasis”. en. In: *Biochem Soc Trans* 40.1 (2012), pp. 79–84.

[370] S. Maddens. “Kit signaling inhibits the sphingomyelin-ceramide pathway through PLC gamma 1: implication in stem cell factor radioprotective effect”. en. In: *Blood* 100 (2002), pp. 1294–1301.

[371] I. Plo. “Kit signaling and negative regulation of daunorubicin-induced apoptosis: role of phospholipase Cgamma”. en. In: *Oncogene* 20 (2001), pp. 6752–6763.

[372] R. Karlsson, M. Engstrom, et al. “Phosphatidylinositol 3-kinase is essential for kit ligand-mediated survival, whereas interleukin-3 and flt3 ligand induce expression of antiapoptotic Bcl-2 family genes”. en. In: *J Leukoc Biol* 74.5 (2003), pp. 923–931.

[373] S. Fulda and K. Debatin. “Extrinsic versus intrinsic apoptosis pathways in anticancer chemotherapy”. en. In: *Oncogene* 25 (2006), pp. 4798–4811.

[374] J. Amaral, J. Xavier, et al. “The Role of p53 in Apoptosis”. en. In: *Discovery Medicine* 9.45 (2010), pp. 145–152.

[375] D. Green and G. Kroemer. “The Pathophysiology of Mitochondrial Cell Death”. en. In: *Science* 305.5684 (2004), pp. 626–629.

[376] D. Speidel. “Transcription-independent p53 apoptosis: an alternative route to death”. en. In: *Trends Cell Biol* 20.1 (2010), pp. 14–24.

[377] B. Nogrady. “How cancer genomics is transforming diagnosis and treatment”. en. In: *Nature* 579 (2020), pp. 10–11.

[378] M. Berger and E. Mardis. “The emerging clinical relevance of genomics in cancer medicine”. en. In: *Nat Rev Clin Oncol* 15.6 (2018), pp. 353–365.

[379] T. Chan, M. Yarchoan, et al. “Development of tumor mutation burden as an immunotherapy biomarker: utility for the oncology clinic”. en. In: *Annals of Oncology* 30.1 (2019), pp. 44–56.

[380] J. Chang, Y. Lee, et al. “The Impact of the Cancer Genome Atlas on Lung Cancer”. en. In: *Transl Res* 166.6 (2015), pp. 568–585.

[381] M. Cieslik and A. Chinnaiyan. “Global genomics project unravels cancer’s complexity at unprecedented scale”. it. In: *Nature* 578 (2020), pp. 39–40.

[382] The ICGC/TCGA Pan-Cancer Analysis of Whole Genomes Consortium. “Pan-cancer analysis of whole genomes”. en. In: *Nature* 578 (2020), pp. 82–93.

[383] F. Iorio, T. Knijnenburg, et al. “A Landscape of Pharmacogenomic Interactions in Cancer”. en. In: *Cell* 166.3 (2016), pp. 740–754.

[384] P. Hedge, I. White, et al. “Interplay of transcriptomics and proteomics”. en. In: *Current Opinion in Biotechnology* 14.6 (2003), pp. 647–651.

[385] D. Kleinjan and V. Heyningen. “Long-Range Control of Gene Expression: Emerging Mechanisms and Disruption in Disease”. en. In: *AJHG* 76.1 (2005), pp. 8–32.

[386] B. Zhao, I. Roundtree, et al. “Post-transcriptional gene regulation by mRNA modifications”. en. In: *Nature Reviews Molecular Cell Biology* 18 (2017), pp. 31–42.

[387] R. Halbeisen, A. Galgano, et al. “Post-transcriptional gene regulation: From genome-wide studies to principles”. es. In: *Cellular and Molecular Life Sciences* 65 (2008).

[388] U. Moll and O. Petrenko. “The MDM2-p53 Interaction”. en. In: *Molecular Cancer Research* 1.14 (2003).

[389] S. Chen, J. Wu, et al. “iASPP mediates p53 selectivity through a modular mechanism fine-tuning DNA recognition”. cs. In: *PNAS* 116.35 (2019), pp. 17470–17479.

[390] Y. Pan, C. Tsai, et al. “Mechanisms of transcription factor selectivity”. en. In: *Trends Genet* 26.2 (2010), pp. 75–83.

[391] F. Murray-Zmijewski, E. Slee, et al. “A complex barcode underlies the heterogeneous response of p53 to stress”. en. In: *Nature Reviews Molecular Cell Biology* 9 (2008), pp. 702–712.

[392] R. Beckerman and C. Prives. “Transcriptional Regulation by P53”. en. In: *Cold Spring Harb Perspect Biol* 2.8 (2010).

[393] C. Castrogiovanni, B. Waterschoot, et al. “Serine 392 phosphorylation modulates p53 mitochondrial translocation and transcription-independent apoptosis”. en. In: *Cell Death and Differentiation* 25 (2018), pp. 190–203.

[394] S. Alagaratnam, G. Lind, et al. “The testicular germ cell tumour transcriptome”. en. In: *International Journal of Andrology* 34.4 (2011), pp. 133–151.

[395] E. Liu and L. Chang. “Suppression of ADAM17-mediated Lyn/Akt pathways induces apoptosis of human leukemia U937 cells”. en. In: *J Biol Chem* 285 (2010), pp. 30506–30515.

[396] J. Backer. “The regulation and function of Class III PI3Ks: novel roles for Vps34”. en. In: *Biochem J* 410.1 (2008), pp. 1–17.

[397] B. Ronan, O. Flamand, et al. “A highly potent and selective Vps34 inhibitor alters vesicle trafficking and autophagy”. en. In: *Nature Chemical Biology* 10 (2014), pp. 1013–1019.

[398] M. Noman, S. Parpal, et al. “Inhibition of Vps34 reprograms cold into hot inflamed tumors and improves anti–PD-1/PD-L1 immunotherapy”. en. In: *Science Advances* 6.8 (2020).

[399] M. Hayden and S. Ghosh. “Signaling to NF-kappaB”. da. In: *Genes Dev* 18.18 (2004), pp. 2195–2224.

[400] Q. Zhang, X. Meng, et al. “Lyn Kinase Promotes the Proliferation of Malignant Melanoma Cells through Inhibition of Apoptosis and Autophagy via the PI3K/Akt Signaling Pathway”. en. In: *J Cancer* 10.5 (2019), pp. 1197–1208.

[401] G. Hoxhaj and B. Manning. “The PI3K-AKT network at the interface of oncogenic signalling and cancer metabolism”. en. In: *Nat Rev Cancer* 20.2 (2020), pp. 74–88.

[402] D. Han, M. Huang, et al. “Lysine methylation of transcription factors in cancer”. en. In: *Cell Death and Disease* 10 (2019).

[403] K. Biggar and S. Li. “Non-histone Protein Methylation as a Regulator of Cellular Signalling and Function”. en. In: *Nat Rev Mol Cell Biol* 16.1 (2015), pp. 5–17.

[404] R. Hamamoto, V. Saloura, et al. “Critical Roles of Non-Histone Protein Lysine Methylation in Human Tumorigenesis”. en. In: *Nat Rev Cancer* 15.2 (2015), pp. 110–124.

[405] J. Guo. “AKT Methylation by SETDB1 Promotes AKT Kinase Activity and Oncogenic Functions”. en. In: *Nat Cell Biol* 21.2 (2019), pp. 226–237.

[406] P. Sanchez-Martin and M. Komatsu. “p62/SQSTM1 – steering the cell through health and disease”. en. In: *Journal of Cell Science* 131 (2018).

[407] M. Tinti. “ANIA: ANnotation and Integrated Analysis of the 14-3-3 interactome”. en. In: *Database* (2014).

[408] T. Gajewski and J. Fessler. “PAK4 as a cancer immune-evasion target”. en. In: *Nature Cancer* (2020), pp. 18–19.

[409] S. Desai, P. Pillai, et al. “PKC-ι promotes glioblastoma cell survival by phosphorylating and inhibiting BAD through a phosphatidylinositol 3-kinase pathway”. en. In: *Biochim Biophys Acta* 1813.6 (2011), pp. 1190–1197.

[410] D. Gwinn, D. Scackelford, et al. “AMPK Phosphorylation of Raptor Mediates a Metabolic Checkpoint”. en. In: *Molecular Cell* 30.2 (2008), pp. 214–226.

[411] P. Langlais, Z. Yi, et al. “The Identification of Raptor as a Substrate for p44/42 MAPK”. en. In: *Endocrinology* 152.4 (2011), pp. 1264–1273.

[412] N. Anstee, R. Bilardi, et al. “Impact of elevated anti-apoptotic MCL-1 and BCL-2 on the development and treatment of MLL-AF9 AML in mice”. en. In: *Cell Death & Differentiation* 26 (2019), pp. 1316–1331.

[413] S. Yann. “Deregulated SLC2A1 Promotes Tumor Cell Proliferation and Metastasis in Gastric Cancer”. en. In: *Int J Mol Sci* 16.7 (2015), pp. 16144–16157.

[414] J. Rathmell, C. Fox, et al. "Akt-Directed Glucose Metabolism Can Prevent Bax Conformation Change and Promote Growth Factor-Independent Survival". en. In: *CELL GROWTH AND DEVELOPMENT* 23.20 (2003), pp. 7315–7328.

[415] G. Chen, D. Park, et al. "Mcl-1 Interacts with Akt to Promote Lung Cancer Progression". en. In: *Cancer Reserach* 79.24 (2019), pp. 6126–6138.

[416] J. Wang, J. Chao, et al. "The Antiapoptotic Gene mcl-1 Is Up-Regulated by the Phosphatidylinositol 3-Kinase/Akt Signaling Pathway through a Transcription Factor Complex Containing CREB". en. In: *American Society for Microbiology Journals* 19.9 (1999), pp. 6195–6206.

[417] P. Longo, L. Laurenti, et al. "The Akt/Mcl-1 pathway plays a prominent role in mediating antiapoptotic signals downstream of the B-cell receptor in chronic lymphocytic leukemia B cells". en. In: *Blood* 111.2 (2008), pp. 846–855.

[418] K. Yu, B. Chen, et al. "Comprehensive transcriptomic analysis of cell lines as models of primary tumors across 22 tumor types". en. In: *Nature Communications* 10 (2019).

[419] S. Grille, A. Bellacosa, et al. "The Protein Kinase Akt Induces Epithelial Mesenchymal Transition and Promotes Enhanced Motility and Invasiveness of Squamous Cell Carcinoma Lines". en. In: *Cancer Research* 63.9 (2003).

[420] D. Pal, A. Tyagi, et al. "Suppression of Notch1 and AKT mediated epithelial to mesenchymal transition by Verrucarin J in metastatic colon cancer". en. In: *Cell Death & Disease* 9 (2018).

[421] M. Roshan, A. Soltani, et al. "Role of AKT and mTOR signaling pathways in the induction of epithelial-mesenchymal transition (EMT) process". en. In: *Biochimie* 165 (2019), pp. 229–234.

[422] C. Loveday, K. Litchfield, et al. "Genomic landscape of platinum resistant and sensitive testicular cancers". fr. In: *Nat Commun* 11.1 (2020).

[423] M. Ding, R. Bruick, et al. "Secreted IGFBP5 mediates mTORC1-dependent feedback inhibition of IGF-1 signalling". en. In: *Nature Cell Biology* 18 (2016), pp. 319–327.

[424] Z. He, X. Hu, et al. "P53 suppresses ribonucleotide reductase via inhibiting mTORC1". en. In: *Oncotarget* 8 (2017), pp. 41422–41431.

[425] D. Feldman. "Presence of somatic mutations within PIK3CA, AKT, RAS, and FGFR3 but not BRAF in cisplatin-resistant germ cell tumors". en. In: *Clin Cancer Res* 20.14 (2014), pp. 3712–3720.

[426] M. Das. "Knockdown of SPRY4 and SPRY4-IT1 inhibits cell growth and phosphorylation of Akt in human testicular germ cell tumours". en. In: *Sci Rep* 8 (2018).

[427] J. Selfe, N. Goddard, et al. "IGF1R signalling in testicular germ cell tumour cells impacts on cell survival and acquired cisplatin resistance". fr. In: *The Journal of Pathology* 244.2 (2018), pp. 242–253.

[428] F. Zhu. "SPANXN2 functions a cell migration inhibitor in testicular germ cell tumor cells". en. In: *PeerJ* 8 (2020).

[429] J. Selfe and J. Shipley. "IGF signalling in germ cells and testicular germ cell tumours: roles and therapeutic approaches". en. In: *Andrology* 7.4 (2019), pp. 536–544.

[430] M. Karaman, S. Herrgard, et al. "A quantitative analysis of kinase inhibitor selectivity". cs. In: *Nature Biotechnology* 26.1 (2008).

[431] P. Schmid, J. Abraham, et al. "Capivasertib Plus Paclitaxel Versus Placebo Plus Paclitaxel As First-Line Therapy for Metastatic Triple-Negative Breast Cancer: The PAKT Trial". en. In: *J Clin Oncol* 38.5 (2020), pp. 423–433.

[432] L. Smyth, K. Tamura, et al. "Capivasertib, an AKT Kinase Inhibitor, as Monotherapy or in Combination with Fulvestrant in Patients with AKT1 E17K-Mutant, ER-Positive Metastatic Breast Cancer". en. In: *Clin Cancer Res* 26.15 (2020), pp. 3947–3957.

[433] G. Shapiro, P. LoRusso, et al. "A phase Ib open-label dose escalation study of the safety, pharmacokinetics, and pharmacodynamics of cobimetinib (GDC-0973) and ipatasertib (GDC-0068". en. In: *Invest New Drugs* (2020).

[434] S. Isakoff, J. Tabernero, et al. "Antitumor activity of ipatasertib combined with chemotherapy: results from a phase Ib study in solid tumors". en. In: *Ann Oncol* 5 (2020), pp. 626–633.

[435] H. Hirai, H. Sootome, et al. "MK-2206, an Allosteric Akt Inhibitor, Enhances Antitumor Efficacy by Standard Chemotherapeutic Agents or Molecular Targeted Drugs In vitro and In vivo". en. In: *Molecular Cancer Therapeutics* 9.7 (2010), pp. 1535–1537.

[436] J. Kale, E. Osterlund, et al. "BCL-2 family proteins: changing partners in the dance towards death". en. In: *Cell Death Differ* 25.1 (2018), pp. 65–80.

[437] B. Sasi, C. Martines, et al. "Inhibition of SYK or BTK augments venetoclax sensitivity in SHP1-negative/BCL-2-positive diffuse large B-cell lymphoma". en. In: *Leukemia* 33 (2019), pp. 2416–2428.

[438] E. Pietsch, S. Sykes, et al. "The p53 family and programmed cell death". da. In: *Oncogene* 27.50 (2008), pp. 6507–6521.

[439] C. Warren, M. Wong-Brown, et al. "BCL-2 family isoforms in apoptosis and cancer". en. In: *Cell Death and Disease* 10 (2019).

[440] S. Grabow, A. Kueh, et al. "Subtle Changes in the Levels of BCL-2 Proteins Cause Severe Craniofacial Abnormalities". en. In: *Cell* 24 (2018), pp. 3285–3295.

[441] S. Korsmeyer. "Bcl-2/Bax: A Rheostat That Regulates an Anti-Oxidant Pathway and Cell Death". en. In: *Semin Cancer Biol* 4.6 (1993), pp. 327–332.

[442] K. Strauss, R. Narayan, et al. "Common Patterns of Bcl-2 Family Gene Expression in Two Traumatic Brain Injury Models". en. In: *Neurotox Res* 6.4 (2008), pp. 333–343.

[443] L. Lowthert. "Increased ratio of anti-apoptotic to pro-apoptotic Bcl2 gene-family members in lithium-responders one month after treatment initiation". en. In: *Biol Mood Anxiety Disord* 2.15 (2012).

[444] C. Dos Santos, T. McDonald, et al. "The Src and c-Kit kinase inhibitor dasatinib enhances p53-mediated targeting of human acute myeloid leukemia stem cells by chemotherapeutic agents". en. In: *Blood* 122.11 (2013), pp. 1900–1913.

[445] B. Fuchs, D. O'Connor, et al. "p53 phosphorylation mutants retain transcription activity". en. In: *Oncogene* 10.4 (1995), pp. 789–93.

[446] M. Ashcroft, M. Kubbutat, et al. "Regulation of p53 Function and Stability by Phosphorylation". en. In: *Mol Cell Biol* 19.3 (1999), pp. 1751–1758.

[447] M. Fiscella, N. Zambrano, et al. "The carboxy-terminal serine 392 phosphorylation site of human p53 is not required for wild-type activities". en. In: *Oncogene* 9.11 (1994), pp. 3249–3257.

[448] L. Flores-Lopez, M. Diaz-Flores, et al. "High glucose induces mitochondrial p53 phosphorylation by p38 MAPK in pancreatic RINm5F cells". en. In: *Molecular Biology Reports* 40 (2013), pp. 4947–4958.

[449] D. Meek, S. Simon, et al. "The p53 tumour suppressor protein is phosphorylated at serine 389 by casein kinase II". en. In: *EMBO J* 9.10 (1990), pp. 3253–3260.

[450] D. Keller, X. Zeng, et al. "A DNA damage-induced p53 serine 392 kinase complex contains CK2, hSpt16, and SSRP1". it. In: *Mol Cell* 7.2 (2001), pp. 283–292.

[451] M. Cox and D. Meek. "Phosphorylation of serine 392 in p53 is a common and integral event during p53 induction by diverse stimuli". en. In: *Cellular Signalling* 22.3 (2010), pp. 564–571.

[452] D. Meek and M. Cox. "Induction and activation of the p53 pathway: a role for the protein kinase CK2?" en. In: *Molecular and Cellular Biochemistry* 356 (2011).

[453] C. Huang. "p38 Kinase Mediates UV-induced Phosphorylation of p53 Protein at Serine 389". en. In: *The Journal of Biological Chemistry* 274 (1999).

[454] A. Cuddihy. "The double-stranded RNA activated protein kinase PKR physically associates with the tumor suppressor p53 protein and phosphorylates human p53 on serine 392 in vitro". en. In: *Oncogene* 18 (1999).

[455] P. Claudio, J. Cui, et al. "Cdk9 phosphorylates p53 on serine 392 independently of CKII". en. In: *Journal of Cellular Physiology* 208.3 (2006), pp. 602–612.

[456] M. Gabra. "IKKβ activates p53 to promote cancer cell adaptation to glutamine deprivation". en. In: *Oncogenesis* 7 (2018).

[457] P. Noy, K. Gaston, et al. "Dasatinib inhibits leukaemic cell survival by decreasing PRH/Hhex phosphorylation resulting in increased repression of VEGF signalling genes". en. In: *Leuk Res* 36.11 (2012), pp. 1434–1437.

[458] M. Sano, Y. Nakanishi, et al. "Overexpression of anti-apoptotic Mcl-1 in testicular germ cell tumours". en. In: *Histopathology* 46.5 (2005), pp. 532–539.

[459] M. Gutekunst, T. Mueller, et al. "Cisplatin Hypersensitivity of Testicular Germ Cell Tumors Is Determined by High Constitutive Noxa Levels Mediated by Oct-4". en. In: *Cancer Res* 73.5 (2013), pp. 1460–1469.

[460] J. Rosenbluh, D. Nijhawan, et al. "β-catenin driven cancers require a YAP1 transcriptional complex for survival and tumorigenesis". fr. In: *Cell* 151.7 (2012), pp. 1457–1473.

[461] E. Jokinen and J. Koivunen. "Bcl-xl and Mcl-1 are the major determinants of the apoptotic response to dual PI3K and MEK blockage". en. In: *International Journal of Oncology* 47.3 (2015), pp. 1103–1110.

[462] T. Chonghaile, K. Sarosiek, et al. "Pretreatment Mitochondrial Priming Correlates with Clinical Response to Cytotoxic Chemotherapy". en. In: *Science* 334.6059 (2011), pp. 1129–1133.

[463] J. Ryan, J. Brunelle, et al. "Heightened mitochondrial priming is the basis for apoptotic hypersensitivity of CD4+ CD8+ thymocytes". en. In: *PNAS* 107.29 (2010), pp. 12895–12900.

[464] S. Colak, C. Zimberlin, et al. "Decreased mitochondrial priming determines chemoresistance of colon cancer stem cells". en. In: *Cell Death and Differentiation* 21 (2014), pp. 1170–1177.

[465] B. Carter. "Synergistic effects of p53 activation via MDM2 inhibition in combination with inhibition of Bcl-2 or Bcr-Abl in CD34+ proliferating and quiescent chronic myeloid leukemia blast crisis cells". en. In: *Oncotarget* 6.31 (2015), pp. 30487–30499.

[466] B. Carter. "Combined inhibition of MDM2 and BCR-ABL1 tyrosine kinase targets chronic myeloid leukemia stem/progenitor cells in a murine model". en. In: *Haematologica* 105.5 (2020), pp. 1274–1284.

[467] V. Moore and A. Letai. "BH3 profiling – measuring integrated function of the mitochondrial apoptotic pathway to predict cell fate decisions". en. In: *Cancer Lett* 332.2 (2013), pp. 202–205.

[468] J. Deng, N. Carlson, et al. "BH3 Profiling Identifies Three Distinct Classes of Apoptotic Blocks to Predict Response to ABT-737 and Conventional Chemotherapeutic Agents". en. In: *Cancer Cell* 12.2 (2007), pp. 171–185.

[469] L. Yang, S. Ying, et al. "EGFR TKIs impair lysosome-dependent degradation of SQSTM1 to compromise the effectiveness in lung cancer". en. In: *Signal Transduct Target Ther* 4.25 (2019).

[470] A. Chitsazan. "Keratinocyte Cytokine Networks Associated with Human Melanocytic Nevus Development". en. In: *J Invest Dermatol* 139.1 (2019), pp. 177–185.

[471] A. Yasuda, H. Sawai, et al. "Stem cell factor/c-kit receptor signaling enhances the proliferation and invasion of colorectal cancer cells through the PI3K/Akt pathway". en. In: *Dig Dis Sci* 52.9 (2007), pp. 2292–2300.

[472] Y. Gan, Y. Wang, et al. "TDRG1 regulates chemosensitivity of seminoma TCam-2 cells to cisplatin via PI3K/Akt/mTOR signaling pathway and mitochondria-mediated apoptotic pathway". en. In: *Cancer Biol Ther* 17.7 (2016), pp. 741–750.

[473] M. Das, L. Kleppa, et al. "Functions of genes related to testicular germ cell tumour development". en. In: *Andrology* 7.4 (2019), pp. 527–535.

[474] R. Singh, Z. Fazal, et al. "Mechanisms of cisplatin sensitivity and resistance in testicular germ cell tumors". en. In: *Cancer Drug Resist* 2 (2019), pp. 580–594.

[475] R. Koster, A. Pietro, et al. "Cytoplasmic p21 expression levels determine cisplatin resistance in human testicular cancer". fr. In: *J Clin Invest* 120.10 (2010), pp. 3594–3605.

[476] M. Juliachs, C. Munoz, et al. “The PDGFRβ-AKT pathway contributes to CDDP-acquired resistance in testicular germ cell tumors”. en. In: *Clin Cancer Res* 20.3 (2014), pp. 658–667.

[477] S. Agarwal, C. Bell, et al. “p53 Deletion or Hot-spot Mutations Enhance mTORC1 Activity by Altering Lysosomal Dynamics of TSC2 and Rheb”. en. In: *Mol Cancer Res* 14.1 (2016), pp. 66–77.

[478] A. Budanov and M. Karin. “p53 target genes sestrin1 and sestrin2 connect genotoxic stress and mTOR signaling”. en. In: *Cell* 134.3 (2008), pp. 451–460.

[479] M. Peng, N. Yin, et al. “Sestrins Function as Guanine Nucleotide Dissociation Inhibitors for Rag GTPases to Control mTORC1 Signaling”. en. In: *Cell* 159.1 (2014), pp. 122–133.

[480] A. Morrison. “Sestrin2 promotes LKB1-mediated AMPK activation in the ischemic heart”. en. In: *FASEBJ* 29.2 (2015), pp. 408–417.

[481] A. Eid. “Sestrin 2 and AMPK Connect Hyperglycemia to Nox4-Dependent Endothelial Nitric Oxide Synthase Uncoupling and Matrix Protein Expression”. en. In: *Molecular and Cellular Biology* 33.17 (2013), pp. 3439–3460.

[482] T. Sanli, K. Linher-Melville, et al. “Sestrin2 Modulates AMPK Subunit Expression and Its Response to Ionizing Radiation in Breast Cancer Cells”. en. In: *PLOS ONE* 7.2 (2012).

[483] J. Kerley-Hamilton. “A p53-dominant transcriptional response to cisplatin in testicular germ cell tumor-derived human embyronal carcinoma”. es. In: *Oncogene* 24 (2005), pp. 6090–6100.

[484] American Association for Cancer Research. “AZD5363 Has Clinical Activity in Patients with AKT1-Mutant Solid Tumors”. en. In: *Cancer Discovery* 7.7 (2017). Publisher: American Association for Cancer Research.

[485] M. Song, A. Bode, et al. “AKT as a Therapeutic Target for Cancer”. en. In: *Cancer Research* 79.6 (2019).

[486] C. Saura, D. Roda, et al. “A first-in-human phase I study of the ATP-competitive AKT inhibitor ipatasertib demonstrates robust and safe targeting of AKT in patients with solid tumors”. en. In: *Cancer Discovery* 7 (2017), pp. 102–113.

[487] A. Sathe, G. Chalaud, et al. “Parallel PI3K, AKT and mTOR inhibition is required to control feedback loops that limit tumor therapy”. en. In: *PLoS one* 13.1 (2018).

[488] F. Li, J. Fraumeni, et al. “A cancer family syndrome in twenty-four kindreds”. en. In: *Cancer Res* 48.18 (1988), pp. 5358–5362.

[489] M. Olivier, D. Goldgar, et al. “Li-Fraumeni and related syndromes: correlation between tumor type, family structure, and TP53 genotype”. en. In: *Cancer Res* 63.20 (2003), pp. 6643–6650.

[490] A. Robles and C. Harris. “Clinical Outcomes and Correlates of TP53 Mutations and Cancer”. en. In: *Cold Spring Harb Perspect Biol* 2.3 (2010).

[491] A. Robles, J. Jen, et al. “Clinical Outcomes of TP53 Mutations in Cancers”. en. In: *Cold Spring Harb Perspect Med* 6.9 (2016).

[492] G. Blandino and S. Di Agostino. "New therapeutic strategies to treat human cancers expressing mutant p53 proteins". en. In: *Journal of Experimental & Clinical Cancer Research* 37 (2018).

[493] K. Vousden and C. Prives. "Blinded by the Light: The Growing Complexity of p53". en. In: *Cell* 137.3 (2009), pp. 413–431.

[494] T. Knijnenburg, L. Wang, et al. "Genomic and Molecular Landscape of DNA Damage". en. In: *Cell Reports* 23 (2018), pp. 239–254.

[495] S. Jones, A. Hancock, et al. "Overexpression of Mdm2 in mice reveals a p53-independent role for Mdm2 in tumorigenesis". da. In: *PNAS* 95.26 (1998), pp. 15608–15612.

[496] J. Momand, D. Jung, et al. "The MDM2 gene amplification database". en. In: *Nucleic Acids Res* 26.15 (1998), pp. 3453–3459.

[497] J. Martin-Caballero, J. Flores, et al. "Tumor susceptibility of p21(Waf1/Cip1)-deficient mice". en. In: *Cancer Res* 61.16 (2001), pp. 6234–6238.

[498] S. Xiong, V. Pant, et al. "Spontaneous Tumorigenesis in Mice Overexpressing the p53-Negative Regulator Mdm4". en. In: *Cancer Research* 70.8 (2010).

[499] G. Sanz, M. Singh, et al. "Inhibition of p53 inhibitors: progress, challenges and perspectives". en. In: *Journal of Molecular Cell Biology* 11.7 (2019), pp. 586–599.

[500] X. Zhou, B. Cao, et al. "Negative auto-regulators trap p53 in their web". en. In: *Journal of Molecular Cell Biology* 9.1 (2017), pp. 62–68.

[501] K. Hientz, A. Mohr, et al. "The role of p53 in cancer drug resistance and targeted chemotherapy". en. In: *Oncotarget* 8.5 (2017), pp. 8921–8946.

[502] Z. Yang, H. Shi, et al. "Darwinian Positive Selection on the Pleiotropic Effects of KITLG Explain Skin Pigmentation and Winter Temperature Adaptation in Eurasians". en. In: *Molecular Biology and Evolution* 35.9 (2018), pp. 2272–2283.

[503] S. Pechackova, K. Burdova, et al. "WIP1 phosphatase as pharmacological target in cancer therapy". en. In: *J Mol Med* 95.6 (2017), pp. 589–599.

[504] M. Athar, C. Elmets, et al. "Pharmacological Activation of p53 in Cancer Cells". en. In: *Curr Pharm Des* 17.6 (2011), pp. 631–639.

[505] K. Loveland and S. Schlatt. ". Stem cell factor and c-kit in the mammalian testis: lessons originating from Mother Nature's gene knockouts". en. In: *J Endocrinol* 153 (1997), pp. 337–334.

[506] H. Kissel. "Point mutation in kit receptor tyrosine kinase reveals essential roles for kit signaling in spermatogenesis and oogenesis without affecting other kit responses". en. In: *EMBO J* 19 (2000), pp. 1312–1326.

[507] B. Phung. "C-KIT signaling depends on microphthalmia-associated transcription factor for effects on cell proliferation". en. In: *PLoS One* 6 (2011), p. 24064.

[508] J. Huizinga. "W/kit gene required for interstitial cells of Cajal and for intestinal pacemaker activity". en. In: *Nature* 373 (1995), pp. 347–349.

[509] H. Maeda. "Requirement of c-kit for development of intestinal pacemaker system". fr. In: *Development* 116 (1992), pp. 369–375.

[510] L. Giebel and R. Spritz. “Mutation of the KIT (mast/stem cell growth factor receptor) protooncogene in human piebaldism”. en. In: *Proc Natl Acad Sci USA* 88 (1991), pp. 8696–8699.

[511] L. Sun, J. Lee, et al. “Neuronally expressed stem cell factor induces neural stem cell migration to areas of brain injury”. en. In: *J Clin Invest* 113 (2004), pp. 1364–1374.

[512] J. Lindsey. “c-Kit is essential for alveolar maintenance and protection from emphysema-like disease in mice”. en. In: *Am J Respir Crit Care Med* 183 (2011), pp. 1644–1652.

[513] M. Li. “c-kit is required for cardiomyocyte terminal differentiation”. fr. In: *Circ Res* 102 (2008), pp. 677–685.

[514] J. Matsui. “Stem cell factor/c-kit signaling promotes the survival, migration, capillary tube formation of human umbilical vein endothelial cells”. en. In: *J Biol Chem* 279 (2004), pp. 18600–18607.

[515] T. Burns, E. Bernhard, et al. “Tissue specific expression of p53 target genes suggests a key role for KILLER/DR5 in p53-dependent apoptosis in vivo”. en. In: *Oncogene* 20 (2001), pp. 4601–4612.

[516] V. Bouvard, T. Zaitchouk, et al. “Tissue and cell-specific expression of the p53-target genes: bax, fas, mdm2 and waf1/p21, before and following ionising irradiation in mice”. en. In: *Oncogene* 19 (2000), pp. 649–660.

[517] P. Fei, E. Bernhard, et al. “Tissue-specific induction of p53 targets in vivo”. en. In: *Cancer Res* 62.24 (2002), pp. 7316–7327.

[518] K. Botcheva, S. McCorkle, et al. “Distinct p53 genomic binding patterns in normal and cancer-derived human cells”. en. In: *Cell Cycle* 10.24 (2011), pp. 4237–4249.

[519] A. Hafner, L. Kublo, et al. “Identification of universal and cell-type specific p53 DNA binding”. en. In: *BMC Molecular and Cell Biology* 21.5 (2020).

[520] S. Negrini, V. Gorgoulis, et al. “Genomic instability — an evolving hallmark of cancer”. en. In: *Nature Reviews Molecular Cell Biology* 11 (2010), pp. 220–228.

[521] D. Hanahan and R. Weinberg. “Hallmarks of cancer: the next generation”. en. In: *Cell* 144.5 (2011), pp. 646–674.

[522] W. Hanel and U. Moll. “Links Between Mutant p53 and Genomic Instability”. en. In: *J Cell Biochem* 113.2 (2012), pp. 433–439.

[523] A. Taylor, J. Shih, et al. “Genomic and Functional Approaches to”. en. In: *Cancer Cell* 33 (2018), pp. 676–689.

[524] A. Gudkov and E. Komarova. “The role of p53 in determining sensitivity to radiotherapy”. en. In: *Nature reviews Cancer* 3.2 (2003), pp. 117–129.

[525] Philippe Bertheau, Elisabeth Turpin, et al. “Exquisite sensitivity of TP53 mutant and basal breast cancers to a dose-dense epirubicin-cyclophosphamide regimen.” eng. In: *PLoS medicine* 4.3 (Mar. 2007), e90.

[526] James G. Jackson, Vinod Pant, et al. “p53-mediated senescence impairs the apoptotic response to chemotherapy and clinical outcome in breast cancer.” eng. In: *Cancer cell* 21.6 (June 2012), pp. 793–806.

[527] Per E. Lønning and Stian Knappskog. "Chemosensitivity and p53; new tricks by an old dog". In: *Breast Cancer Research* 14.6 (Nov. 2012), p. 325. URL: https://doi.org/10.1186/bcr3326.

[528] A. Stengel, W. Kern, et al. "The impact of TP53 mutations and TP53 deletions on survival varies between AML, ALL, MDS and CLL: an analysis of 3307 cases". en. In: *Leukemia* 31.3 (2017), pp. 705–711.

[529] L. Donehower, T. Soussi, et al. "Integrated Analysis of TP53 Gene and Pathway Alterations in The Cancer Genome Atlas". en. In: *Cell Reports* 28.5 (2019), pp. 1370–1384.

[530] Y. Chen, J. McGee, et al. "Identification of Druggable Cancer Driver Genes Amplified across TCGA Datasets". en. In: *PLoS ONE* 9.5 (2014).

[531] K. Ohshima, K. Hatakeyama, et al. "Integrated analysis of gene expression and copy number identified potential cancer driver genes with amplification-dependent overexpression in 1,454 solid tumors". en. In: *Sci Rep* 7 (2017).

[532] J. Fletcher. "KIT Oncogenic Mutations: Biologic Insights, Therapeutic Advances, and Future Directions". en. In: *Cancer Research* 76.21 (2016).

[533] X. Shi, L. Sousa, et al. "Distinct cellular properties of oncogenic KIT receptor tyrosine kinase mutants enable alternative courses of cancer cell inhibition". en. In: *PNAS* 113.33 (2016), pp. 4784–4793.

[534] G. Monsel, N. Ortonne, et al. "c-Kit mutants require hypoxia-inducible factor 1α to transform melanocytes". fr. In: *Oncogene* 29 (2010), pp. 227–236.

[535] C. Torres-Cabala, W. Wang, et al. "Correlation between KIT expression and KIT mutation in melanoma: a study of 173 cases with emphasis on the acral-lentiginous/mucosal type". en. In: *Mod Pathol* 22.11 (2009), pp. 1446–1456.

[536] K. Isozaki, B. Terris, et al. "Germline-activating mutation in the kinase domain of KIT gene in familial gastrointestinal stromal tumors". en. In: *Am J Pathol* 158.5 (2000), pp. 1581–1585.

[537] R. White, W. Stanley, et al. "Long-term survival in 2,505 patients with melanoma with regional lymph node metastasis". en. In: *Ann Surg* 235.6 (2002), pp. 879–887.

[538] S. Bhalla, H. Kaur, et al. "Prediction and Analysis of Skin Cancer Progression using Genomics Profiles of Patients". en. In: *Scientific Reports* 9 (2019).

[539] P. Natli, M. Nicotra, et al. "Progression of human cutaneous melanoma is associated with loss of expression of c-kit proto-oncogene receptor". en. In: *Int J Cancer* 52.2 (1992), pp. 197–201.

[540] "The Cancer Genome Atlas Network". en. In: *Nature* 487 (2012), pp. 330–337.

[541] H. Davies, G. Bignell, et al. "Mutations of the BRAF gene in human cancer". en. In: *Nature* 417 (2002), pp. 949–954.

[542] I. Serebriiskii, C. Connelly, et al. "Comprehensive characterization of RAS mutations in colon and rectal cancers in old and young patients". en. In: *Nature Communications* 10 (2019).

[543] J. Neiswender, R. Kortum, et al. "KIT Suppresses BRAF V600E-Mutant Melanoma by Attenuating Oncogenic RAS/MAPK Signaling". en. In: *Cancer Research* 77.21 (2017), pp. 5820–5830.

[544] M. Sammons, T. Nguyen, et al. “Tumor suppressor p53: from engaging DNA to target gene regulation”. en. In: *Nucleic Acids Research* 48.16 (2020), pp. 8848–8869.

[545] K. Hoadley, C. Yau, et al. “Cell-of-Origin Patterns Dominate the Molecular Classification of 10,000 Tumors from 33 Types of Cancer”. en. In: *Cell* 173.2 (2018), pp. 291–304.

[546] H. Hou, D. Sun, et al. “The role of MDM2 amplification and overexpression in therapeutic resistance of malignant tumors”. en. In: *Cancer Cell Int* 19.216 (2019).

[547] H. Cao, X. Chen, et al. “The role of MDM2–p53 axis dysfunction in the hepatocellular carcinoma transformation”. en. In: *Cell Death Discovery* 6 (2020).

[548] H. Kimura, N. Yamamoto, et al. “Detection of MDM2 gene amplification in soft tissue sarcoma by FISH”. en. In: *Journal of Clinical Oncology* 32.15 (2014).

[549] M. Elnenaei, A. Gruszka-Westwood, et al. “Gene abnormalities in multiple myeloma; the relevance of TP53, MDM2, and CDKN2A”. it. In: *Haematologica* 88.5 (2003).

[550] C. Finan, A. Gaulton, et al. “The druggable genome and support for target identification and validation in drug development”. en. In: *Sci Transl Med* 9.383 (2017).

[551] A. Hopkins. “Network pharmacology: the next paradigm in drug discovery”. en. In: *Nature Chemical Biology* 4 (2008), pp. 682–690.

[552] S. Nabirotchkin, A. Peluffo, et al. “Next-generation drug repurposing using human genetics and network biology”. en. In: *Current Opinion in Pharmacology* 51 (2020), pp. 78–92.

[553] A. Butler, M. Buzhardt, et al. “A small molecule inhibitor of atypical protein kinase C signaling inhibits pancreatic cancer cell transformed growth and invasion”. en. In: *Oncotarget* 6.17 (2015), pp. 15297–15310.

[554] W. Liu, W. Du, et al. “Rational identification of a Cdc42 inhibitor presents a new regimen for long-term hematopoietic stem cell mobilization”. it. In: *Leukemia* 33 (2019), pp. 749–761.

[555] M. Florian, H. Leins, et al. “Inhibition of Cdc42 activity extends lifespan and decreases circulating inflammatory cytokines in aged female C57BL/6 mice”. en. In: *Ageing Cell* 19.9 (2020).

[556] D. Chaker, C. Mouawad, et al. “Inhibition of the RhoGTPase Cdc42 by ML141 enhances hepatocyte differentiation from human adipose-derived mesenchymal stem cells via the Wnt5a/PI3K/miR-122 pathway: impact of the age of the donor”. en. In: *Stem Cell Research & Therapy* 9 (2018).

[557] R. Bednarek, A. Selmi, et al. “Functional inhibition of F11 receptor (F11R/junctional adhesion molecule-A/JAM-A) activity by a F11R-derived peptide in breast cancer and its microenvironment”. en. In: *Breast Cancer Res Treat* 179.2 (2020), pp. 325–335.

[558] C. Yang, X. Hunag, et al. “PDK1 inhibitor GSK2334470 exerts antitumor activity in multiple myeloma and forms a novel multitargeted combination with dual mTORC1/C2 inhibitor PP242”. en. In: *Oncotarget* 8.24 (2017), pp. 39185–39197.

[559] C. Lynch and J. Milner. "Loss of one p53 allele results in four-fold reduction of p53 mRNA and protein: a basis for p53 haplo-insufficiency". en. In: *Oncogene* 25.24 (2006), pp. 3463–3470.

[560] A. Vilborg, J. Glander, et al. "The p53 target Wig-1 regulates p53 mRNA stability through an AU-rich element". en. In: *PNAS* 106.37 (2009), pp. 15756–15761.

[561] L. Haronikova, V. Olivares-Illana, et al. "The p53 mRNA: an integral part of the cellular stress response". en. In: *Nucleic Acids Research* 47.7 (2019), pp. 3257–3271.

[562] Q. Mao, Z. Chen, et al. "Prognostic role of corrected calcium levels in renal cell carcinoma: a systematic review and meta-analysis". en. In: *Int J Clin Exp Med* 11.3 (2018), pp. 2847–2855.

[563] Z. Yao, L. Deng, et al. "Concordant bone marrow involvement of diffuse large B-cell lymphoma represents a distinct clinical and biological entity in the era of immunotherapy". en. In: *Leukemia* 32.2 (2018), pp. 353–363.

[564] B. Wehrle-Haller. "The role of Kit-ligand in melanocyte development and epidermal homeostasis". en. In: *Pigment Cell Res* 163 (2003), pp. 287–296.

[565] C. Beadling, E. Jacobson-Dunlop, et al. "KIT gene mutations and copy number in melanoma subtypes". en. In: *Clin Cancer Res* 14.21 (2008), pp. 6821–6828.

[566] J. Curtin, K. Busam, et al. "Somatic activation of KIT in distinct subtypes of melanoma". en. In: *J Clin Oncol* 24.26 (2006), pp. 4340–4346.

[567] J. Guo, L. Si, et al. "Phase II, open-label, single-arm trial of imatinib mesylate in patients with metastatic melanoma harboring c-Kit mutation or amplification". en. In: *J Clin Oncol* 29.21 (2011), pp. 2904–2909.

[568] S. Woodman, J. Trent, et al. "Activity of dasatinib against L576P KIT mutant melanoma: molecular, cellular, and clinical correlates". en. In: *Mol Cancer Ther* 8 (2009), pp. 2079–2085.

[569] H. Kluger, A. Dudek, et al. "A phase 2 trial of dasatinib in advanced melanoma". en. In: *Cancer* 117.10 (2011), pp. 2202–2208.

[570] D. Minor, M. Kashani-Sabet, et al. "Sunitinib therapy for melanoma patients with KIT mutations". en. In: *Clin Cancer Res* 18.5 (2012), pp. 1457–1463.

[571] J. McGregor, C. Yu, et al. "p53 immunoreactivity in human malignant melanoma and dysplastic naevi". en. In: *Br J Dermatol* 128 (1993), pp. 606–611.

[572] N. Box, T. Vukmer, et al. "Targeting p53 in melanoma". en. In: *Pigment Cell Melanoma Res* 27.1 (2014), pp. 8–10.

[573] K. Satyamoorthy, N. Chehab, et al. "Aberrant Regulation and Function of Wild-Type p53 in". en. In: *Cell Growth and Differentiation* 11 (2000), pp. 467–474.

[574] M. Lu, H. Breyssens, et al. "Restoring p53 function in human melanoma cells by inhibiting MDM2 and cyclin B1/CDK1-phosphorylated nuclear iASPP". en. In: *Cancer Cell* 23.5 (2013), pp. 618–633.

[575] J. Loureiro, M. Abrantes, et al. "P53 in skin cancer: From a master player to a privileged target for prevention and therapy". en. In: *Biochimica et Biophysica Acta (BBA) - Reviews on Cancer* 1874.2 (2020).

[576] M. Webster, M. Fane, et al. “Paradoxical Role for Wild-Type p53 in Driving Therapy Resistance in Melanoma”. en. In: *Molecular Cell* 77.3 (2020), pp. 633–644.

[577] M. Hartmann and M. Czyz. “MITF in melanoma: mechanisms behind its expression and activity”. cs. In: *Cell Mol Life Sci* 72.7 (2015), pp. 1249–1260.

[578] B. Phung, J. Kazi, et al. “KITD816V Induces SRC-Mediated Tyrosine Phosphorylation of MITF and Altered Transcription Program in Melanoma”. en. In: *Molecular Cancer Research* 15.9 (2017).

[579] K. Montone, P. Belle, et al. “Proto-oncogene c-kit expression in malignant melanoma: protein loss with tumor progression”. en. In: *Mod Pathol* 10.9 (1997), pp. 939–944.

[580] R. Carvajal, C. Antonescu, et al. “KIT as a Therapeutic Target in Metastatic Melanoma”. en. In: *JAMA* 305.22 (2011), pp. 2327–2334.

[581] C. Miller, S. Beleza, et al. “cis-Regulatory changes in Kit ligand expression and parallel evolution of pigmentation in sticklebacks and humans”. it. In: *Cell* 131.6 (2007), pp. 1179–1189.

[582] W. Loomis. “Skin-pigment regulation of vitamin-D biosynthesis in man”. en. In: *Science* 157.3788 (1967), pp. 501–506.

[583] J. Grichnik, J. Burch, et al. “The SCF/KIT pathway plays a critical role in the control of normal human melanocyte homeostasis”. en. In: *J Invest Dermatol* 1112 (1998), pp. 233–238.

[584] Z. Huang, H. Ruan, et al. “The stem cell factor/Kit signalling pathway regulates mitochondrial function and energy expenditure”. en. In: *Nat Commun* 4282 (2014), p. 5.

[585] A. Gross and S. Katz. “Non-apoptotic functions of BCL-2 family proteins”. en. In: *Cell Death and Differentiation* 24 (2017), pp. 1348–1358.

[586] R. Perciavalle, S. Stewart, et al. “Anti-apoptotic MCL-1 localizes to the mitochondrial matrix and couples mitochondrial fusion to respiration”. en. In: *Nat Cell Biol* 14.6 (2012), pp. 573–583.

[587] A. Sharma, L. Boise, et al. “Cancer Metabolism and the Evasion of Apoptotic”. en. In: *cancers* 11 (2019).

[588] B. Boldajipour and E. Raz. “What Is Left Behind—Quality Control in Germ Cell Migration”. en. In: *Science's STKE* 2007.383 (2007).

[589] G. Bellone, A. Carbone, et al. “Aberrant activation of c-kit protects colon carcinoma cells against apoptosis and enhances their invasive potential”. en. In: *Cancer Res* 61.5 (2001), pp. 2200–2206.

[590] G. Belone, C. Smirne, et al. “KIT/stem cell factor expression in premalignant and malignant lesions of the colon mucosa in relationship to disease progression and outcomes”. en. In: *Int J oncol* 29.4 (2006), pp. 851–859.

[591] S. Yang, W. Li, et al. “KITLG is a novel target of miR-34c that is associated with the inhibition of growth and invasion in colorectal cancer cells”. en. In: *J Cell Mol Med* 18.10 (2014), pp. 2092–2102.

[592] E. Chen, T. Karl, et al. “KIT Signaling Promotes Growth of Colon Xenograft Tumors in Mice and is Upregulated in a Subset of Human Colon Cancers”. en. In: *Gastroenterology* 149.3 (2015), pp. 705–717.

[593] S. Fatrai, S. Schelven, et al. “Maintenance of Clonogenic KIT(+) Human Colon Tumor Cells Requires Secretion of Stem Cell Factor by Differentiated Tumor Cells”. en. In: *Gastroenterology* 149.3 (2015), pp. 692–704.

[594] S. Yang, W. Li, et al. “Resveratrol elicits anti-colorectal cancer effect by activating miR-34c-KITLG in vitro and in vivo”. en. In: *BMC Cancer* 15 (2015).

[595] S. Attoub, C. Rivat, et al. “The c-kit Tyrosine Kinase Inhibitor STI571 for Colorectal Cancer Therapy”. en. In: *Cancer Research* 62.17 (2002).

[596] E. Van Cutsem, A. Sobrero, et al. “Phase III CORRECT trial of regorafenib in metastatic colorectal cancer (mCRC”. en. In: *J Clin Oncol* 30 (2012).

[597] W. Samowitz, K. Curtin, et al. “PROGNOSTIC SIGNIFICANCE OF P53 MUTATIONS IN COLON CANCER AT”. en. In: *Int J Cancer* 99 (2002), pp. 597–602.

[598] M. Nakayama and M. Oshima. “Mutant p53 in colon cancer”. es. In: *J Mol Cell Biol* 11.4 (2019), pp. 267–276.

[599] M. Nakayama, C. Hong, et al. “Loss of wild-type p53 promotes mutant p53-driven metastasis through acquisition of survival and tumor-initiating properties”. en. In: *Nature Communications* 11 (2020).

[600] L. Shen, Y. Kondo, et al. “p14 methylation in human colon cancer is associated with microsatellite instability and wild-type p53”. en. In: *Gastroenterology* 124.3 (2003), pp. 626–633.

[601] J. Guinney, R. Dienstmann, et al. “The consensus molecular subtypes of colorectal cancer”. ro. In: *Nature Medicine* 21 (2015), pp. 1350–1356.

[602] L. Fricker. “Carboxypeptidase E”. en. In: *Annu Rev Physiol* 50 (1988), pp. 309–321.

[603] V. Hook and Y. Loh. “Carboxypeptidase B-like converting enzyme activity in secretory granules of rat pituitary”. en. In: *Proc Natl Acad Sci U S A* 81.9 (1984), pp. 2776–2780.

[604] D. Cool, E. Normant, et al. “Carboxypeptidase E is a regulated secretory pathway sorting receptor: genetic obliteration leads to endocrine disorders in Cpe(fat) mice”. en. In: *Cell* 88.1 (1997), pp. 73–83.

[605] J. Naggert, L. Fricker, et al. “Hyperproinsulinaemia in obese fat/fat mice associated with a carboxypeptidase E mutation which reduces enzyme activity”. en. In: *Nat Genet* 10.2 (1995), pp. 135–142.

[606] N. Cawley, J. Zhou, et al. “The carboxypeptidase E knockout mouse exhibits endocrinological and behavioral deficits”. en. In: *Endocrinology* 145.12 (2004), pp. 5807–5819.

[607] N. Cawley, T. Yanik, et al. “Obese carboxypeptidase E knockout mice exhibit multiple defects in peptide hormone processing contributing to low bone mineral density”. en. In: *Am J Physiol Endocrinol Metab* 299.2 (2010), pp. 189–197.

[608] S. Murthy, K. Pacak, et al. “Carboxypeptidase E: Elevated expression correlated with tumor growth and metastasis in pheochromocytomas and other cancers”. en. In: *Cell Mol Neurobiol* 30.8 (2010), pp. 1377–1381.

[609] X. Liang, L. Li, et al. “Upregulation of CPE promotes cell proliferation and tumorigenicity in colorectal cancer”. en. In: *BMC Cancer* 13 (2013).

[610] A. Liu, C. Shao, et al. “Downregulation of CPE regulates cell proliferation and chemosensitivity in pancreatic cancer”. en. In: *Tumour Biol* 35.12 (2014), pp. 12459–65.

[611] S. Fan, X. Li, et al. “Silencing of carboxypeptidase E inhibits cell proliferation, tumorigenicity, and metastasis of osteosarcoma cells”. en. In: *Onco Targets Ther* 9 (2016).

[612] T. Lee, S. Murthy, et al. “An N-terminal truncated carboxypeptidase E splice isoform induces tumor growth and is a biomarker for predicting future metastasis in human cancers”. en. In: *JCI* 121 (2011).

[613] S. Hareendran, X. Yang, et al. “Carboxypeptidase E-N Promotes Proliferation and Invasion of Pancreatic Cancer Cells via Upregulation of CXCR2 Gene Expression”. en. In: *Int J Mol Sci* 20.22 (2019).

[614] B. Zhile, F. Mengyu, et al. “Carboxypeptidase E down-regulation regulates transcriptional and epigenetic profiles in pancreatic cancer cell line: A network analysis”. en. In: *Cancer Biomarkers* 29.1 (2020), pp. 79–88.

[615] U. Dunzendorfer, D. Drahovsky, et al. “Clinical significance of peptide hormones LH, FSH, TSH, prolactin, HCG, parathormone, calcitonin and prostaglandin F2 alpha in kidney neoplasms”. en. In: *Z Urol Nephrol* 74.1 (1981), pp. 13–19.

[616] A. Czarnecka, M. Niedzwiedzka, et al. “Hormone signaling pathways as treatment targets in renal cell cancer”. en. In: *International Journal of Oncology* 48.6 (2016), pp. 2221–2235.

[617] L. Fricker, T. Plummer, et al. “Enkephalin convertase: Potent, selective, and irreversible inhibitors”. en. In: *Biochemical and Biophysical Research Communications* 111.3 (1983), pp. 994–1000.

[618] P. Aloy, V. Companys, et al. “The Crystal Structure of the Inhibitor-complexed Carboxypeptidase D Domain II and the Modeling of Regulatory Carboxypeptidases”. en. In: *JBC* 276 (2001), pp. 16177–16184.

[619] K. Kemphues, J. Priess, et al. “Identification of genes required for cytoplasmic localization in early C. elegans embryos”. en. In: *Cell* 52.3 (1988), pp. 311–320.

[620] S. Kim. “Cell polarity: new PARtners for Cdc42 and Rac”. en. In: *Nat Cell Biol* 2.8 (2000).

[621] G. Joberty, C. Petersen, et al. “The cell-polarity protein Par6 links Par3 and atypical protein kinase C to Cdc42”. en. In: *Nat Cell Biol* 2.8 (2000), pp. 531–539.

[622] R. Petrie, A. Doyle, et al. “Random versus directionally persistent cell migration”. en. In: *Nat Rev Mol Cell Biol* 10.8 (2009), pp. 538–549.

[623] C. Hidalgo-Carcedo, S. Hooper, et al. “Collective cell migration requires suppression of actomyosin at cell-cell contacts mediated by DDR1 and the cell polarity regulators Par3 and Par6”. en. In: *Nat Cell Biol* 13 (2011), pp. 49–58.

[624] M. Nolan, V. Aranda, et al. “The polarity protein Par6 induces cell proliferation and is overexpressed in breast cancer”. en. In: *Cancer Res* 68.20 (2008), pp. 8201–8209.

[625] H. Cunliffe, Y. Jiang, et al. “PAR6B is required for tight junction formation and activated PKCζ localization in breast cancer”. en. In: *Am J Cancer Res* 2.5 (2012), pp. 478–491.

[626] A. Viloria-Petit, L. David, et al. “A role for the TGFbeta-Par6 polarity pathway in breast cancer progression”. en. In: *Proc Natl Acad Sci USA* 106 (2009).

[627] A. Gunaratne, B. Thai, et al. “Atypical protein kinase C phosphorylates Par6 and facilitates transforming growth factor beta-induced epithelial-to-mesenchymal transition”. en. In: *Mol Cell Biol* 33 (2013), pp. 874–886.

[628] L. Ruan, Y. Shen, et al. “Roles of partitioning-defective protein 6 (Par6) and its complexes in the proliferation, migration and invasion of cancer cells”. en. In: *CEPP* 44.9 (2017), pp. 909–913.

[629] E. Marques, J. Englund, et al. “Par6G suppresses cell proliferation and is targeted by loss-of-function mutations in multiple cancers”. en. In: *Oncogene* 35.11 (2016), pp. 1486–1398.

[630] G. Calabrese, B. Bennett, et al. “Systems Genetic Analysis of Osteoblast-Lineage Cells”. en. In: *PLoS Genet* 8.12 (2012).

[631] K. Hope, S. Cellot, et al. “An RNAi Screen Identifies Msi2 and Prox1 as Having Opposite Roles in the Regulation of Hematopoietic Stem Cell Activity”. en. In: *Cell Stem Cell* 7.1 (2010), pp. 101–113.

[632] G. Carvalho, K. Poalas, et al. “Participation of the Cell Polarity Protein PALS1 to T-Cell Receptor-Mediated NF-ϰB Activation”. en. In: *PLOS ONE* 6.3 (2011).

[633] A. Chaderi, A. Daneshmanesh, et al. “ROR1 is Expressed in Diffuse Large B-Cell Lymphoma (DLBCL) and a Small Molecule Inhibitor of ROR1 (KAN0441571C”. es. In: *Induced Apoptosis of Lymphoma Cells. biomedicines* 8.6 (2020).

[634] J. Cerhan, S. Berndt, et al. “Genome-wide association study identifies multiple susceptibility loci for diffuse large B-cell lymphoma”. en. In: *Nat Genet* 46.11 (2014), pp. 1233–1238.

[635] B. Muir and L. Nunney. “The expression of tumour suppressors and proto-oncogenes in tissues susceptible to their hereditary cancers”. en. In: *BJC* 113.2 (2015), pp. 345–353.

[636] L. Shen, Q. Shi, et al. “Double agents: genes with both oncogenic and tumor-suppressor functions”. en. In: *Oncogenesis* 7 (2018).

[637] C. Hu, W. Wei, et al. “A Global View of the Oncogenic Landscape in Nasopharyngeal Carcinoma: An Integrated Analysis at the Genetic and Expression Levels”. en. In: *PLOS ONE* 7.7 (2012).

[638] H. Moon, K. Hwang, et al. “NFIB is a potential target for estrogen receptor-negative breast cancers”. en. In: *Molecular Oncology* 5.6 (2011), pp. 538–544.

[639] S. Denny, D. Yang, et al. “Nfib promotes metastasis through a widespread increase in chromatin accessibility”. en. In: *Cell* 166.2 (2016), pp. 328–342.

[640] D. Becker-Santos, K. Thu, et al. "Developmental transcription factor NFIB is a putative target of oncofetal miRNAs and is associated with tumour aggressiveness in lung adenocarcinoma". en. In: *The Journal of Pathology* 240.2 (2016), pp. 161–172.

[641] M. Fane, Y. Chhabra, et al. "NFIB mediates BRN2 driven melanoma cell migration and invasion through regulation of EZH2 and MITF". en. In: *eBioMedicine* 16 (2017), pp. 63–75.

[642] Z. Sondka, S. Bamford, et al. "The COSMIC Cancer Gene Census: describing genetic dysfunction across all human cancers". en. In: *Nature Reviews Cancer* 18 (2018), pp. 696–705.

[643] J. Tate, S. Bamfird, et al. "COSMIC: the Catalogue Of Somatic Mutations In Cancer". en. In: *Nucleic Acids Research* 47 (2018), pp. 941–947.

[644] E. Horing, P. Harter, et al. "The "go or grow" potential of gliomas is linked to the neuropeptide processing enzyme carboxypeptidase E and mediated by metabolic stress". it. In: *Acta Neuropathologica* 124 (2012), pp. 83–97.

[645] A. Noon, N. Vlatkovic, et al. "p53 and MDM2 in Renal Cell Carcinoma". es. In: *Cancer* 116.4 (2010), pp. 780–790.

[646] R. Okamura, A. Boichard, et al. "Analysis of NTRK Alterations in Pan-Cancer Adult and Pediatric Malignancies: Implications for NTRK-Targeted Therapeutics". en. In: *JCO Precision Oncology* 2 (2018).

[647] G. Robinson. "Entrectinib Shows Pediatric Potential". en. In: *Cancer Discovery* 9.7 (2019).

[648] L. Marcus, S. Lemery, et al. "FDA approval summary: pembrolizumab for the treatment of microsatellite instability-high solid tumors". en. In: *Clin. Cancer Res* 25 (2019), pp. 3753–3758.

[649] S. Bien and U. Peters. "Moving from one to many: insights from the growing list of pleiotropic cancer risk genes". en. In: *British Journal of Cancer* 120 (2019), pp. 1087–1089.

[650] T. O'Mara, J. Batra, et al. "Establishing Genetic Pleiotropy to Identify Common Pharmacological Agents for Common Diseases". pt. In: *Front Pharmacol* (2019).

[651] F. Stearns. "One Hundred Years of Pleiotropy: A Retrospective". en. In: *Genetics* 186.3 (2010), pp. 767–773.

[652] R. Kushwah, B. Guezguez, et al. "Pleiotropic roles of Notch signaling in normal, malignant, and developmental hematopoiesis in the human". pt. In: *EMBO Reports* 15.11 (2014), pp. 1128–1138.

[653] I. Lobo. "Pleiotropy: One Gene Can Affect Multiple Traits". en. In: *Nature Education* 1.1 (2008).

[654] D. Paul. "A double-edged sword". en. In: *Nature* 405 (2000).

[655] S. Sivakumaran, F. Agakov, et al. "Abundant Pleiotropy in Human Complex Diseases and Traits". fr. In: *AJHG* 89.5 (2011), pp. 607–618.

[656] N. Solovieff, C. Cotsapas, et al. "Pleiotropy in complex traits: challenges and strategies". en. In: *Nat Rev Genetic* 14.7 (2013), pp. 483–495.

[657] K. Gleason, F. Yang, et al. "Primo: integration of multiple GWAS and omics QTL summary statistics for elucidation of molecular mechanisms of trait-associated SNPs and detection of pleiotropy in complex traits". en. In: *Genome Biology* 21 (2020).

[658] H. Kacser and J. Burns. "The molecular basis of dominance". en. In: *Genetics* 97.3-4 (1981), pp. 639–666.

[659] A. Paaby and M. Rockman. "The many faces of pleiotropy". en. In: *Trends Genet* 29.2 (2013), pp. 66–73.

[660] R. Li, S. Tsaih, et al. "Structural model analysis of multiple quantitative traits". io. In: *PLOS Genetics* 2 (2006), pp. 1046–1057.

[661] Z. Su, Y. Zeng, et al. "A preliminary analysis of gene pleiotropy estimated from protein sequences". en. In: *J Exp Zool* 312 (2009), pp. 1–10.

[662] S. Pendergrass, K. Brown-Gentry, et al. "The use of phenome-wide association studies (PheWAS) for exploration of novel genotype-phenotype relationships and pleiotropy discovery". en. In: *Genet Epidemiol* 35.5 (2011), pp. 410–422.

[663] S. Pendergrass, K. Brown-Gentry, et al. "Phenome-Wide Association Study (PheWAS) for Detection of Pleiotropy within the Population Architecture using Genomics and Epidemiology (PAGE) Network". en. In: *PLoS Genetics* 9.1 (2013).

[664] K. Watanabe, S. Stringer, et al. "A global overview of pleiotropy and genetic architecture in complex traits". en. In: *Nature Genetics* 51 (2019), pp. 1339–1348.

[665] A. Shikov, R. Skitchenko, et al. "Phenome-wide functional dissection of pleiotropic effects highlights key molecular pathways for human complex traits". en. In: *Sci Rep* 10 (2020).

[666] J. Pickrell, T. Berisa, et al. "Detection and interpretation of shared genetic influences on 42 human traits". en. In: *Nat Genet* 48 (2016), pp. 709–717.

[667] K. Michailidou, S. Lindstrom, et al. "Association analysis identifies 65 new breast cancer risk loci". en. In: *Nature* 551 (2017), pp. 92–94.

[668] C. Medina-Gomez, J. Kemp, et al. "Life-Course genome-wide association study meta-analysis of total body BMD and assessment of age-specific effects". en. In: *Am J Hum Genet* 102 (2018), pp. 88–102.

[669] S. Lindstrom, H. Finucane, et al. "Quantifying the genetic correlation between multiple cancer types". en. In: *Cancer Epidemiol. Biomark. Prev* 26 (2017), pp. 1427–1435.

[670] X. Jiang, H. Finucane, et al. "Shared heritability and functional enrichment across six solid cancers". en. In: *Nature Communications* 10 (2019).

[671] P. Reyes-Uribe, M. Adrianzen-Ruesta, et al. "Exploiting TERT dependency as a therapeutic strategy for NRAS-mutant melanoma". no. In: *Oncogene* 37 (2018), pp. 4058–4072.

[672] S. Rashkin, R. Graff, et al. "Pan-cancer study detects genetic risk variants and shared genetic basis in two large cohorts". en. In: *Nature Communications* 11 (2020).

[673] H. Climente-González, C. Lonjou, et al. "Combining network-guided GWAS to discover susceptibility". en. In: (2020).

[674] Q. Deng, H. Hu, et al. "Tissue-specific microRNA expression alters cancer susceptibility conferred by a TP53 noncoding variant". en. In: *Nature Communications* 10 (2019).

[675] T. Rafnar, B. Gunnarsson, et al. "Variants associating with uterine leiomyoma highlight genetic background shared by various cancers and hormone-related traits". en. In: *Nature Commun* 9 (2018).

[676] H. Zhang, T. Ahearn, et al. "Genome-wide association study identifies 32 novel breast cancer susceptibility loci from overall and subtype-specific analyses". en. In: *Nature Genetics* 52 (2020), pp. 572–581.

[677] M. Landi, D. Bishop, et al. "Genome-wide association meta-analyses combining multiple risk phenotypes provide insights into the genetic architecture of cutaneous melanoma susceptibility". en. In: *Nature Genetics* 52 (2020), pp. 494–504.

[678] Q. Tang, Z. Su, et al. "Mutant p53 on the Path to Metastasis". en. In: *Trends in Cancer* 6.1 (2020), pp. 62–73.

[679] S. Stacey, P. Sulem, et al. "A germline variant in the TP53 polyadenylation signal confers cancer susceptibility". en. In: *Nature Genetics* 43.11 (2011), pp. 1098–1103.

[680] Z. Wang, P. Rajaraman, et al. "Further Confirmation of Germline Glioma Risk Variant rs78378222 in TP53 and Its Implication in Tumor Tissues via Integrative Analysis of TCGA Data". en. In: *Hum Mutat* 36.7 (2015), pp. 64–688.

[681] E. Powell, D. Piwnica-Worms, et al. "Contribution of p53 to metastasis". en. In: *Cancer Discov* 4.4 (2014), pp. 405–414.

[682] A. Lambert, D. Pattabiraman, et al. "Emerging Biological Principles of Metastasis". pt. In: *Cell* 168 (2017).

[683] J. Fares, M. Fares, et al. "Molecular principles of metastasis: a hallmark of cancer revisited". en. In: *Signal Transduction and Targeted Therapy* 5 (2020).

[684] T. Aes, A. Borresen, et al. "Specific P53 mutations are associated with de novo resistance to doxorubicin in breast cancer patients". en. In: *Nat Med* 2.7 (1996), pp. 811–814.

[685] M. Olivier, M. Hollstein, et al. "TP53 Mutations in Human Cancers: Origins, Consequences, and Clinical Use". en. In: *Cold Spring Harb Perspect Biol* 2.1 (2010).

[686] P. Essletzbichler, T. Konopka, et al. "Megabase-scale deletion using CRISPR/Cas9 to generate a fully haploid human cell line". en. In: *Genome Res* 24.12 (2014), pp. 2059–2065.

[687] T. Bürckstümmer, C. Banning, et al. "A reversible gene trap collection empowers haploid". en. In: *Nature Methods* 10.10 (2013).

[688] D. Grochova, J. Vankova, et al. "Analysis of transactivation capability and conformation of p53 temperature-dependent mutants and their reactivation by amifostine in yeast". en. In: *Oncogene* 27 (2008), pp. 1243–1252.

[689] S. Dell'Orso, G. Fontemaggi, et al. "ChIP-on-Chip Analysis of In Vivo Mutant p53 Binding To Selected Gene Promoters". en. In: *OMICS: A Journal of Integrative Biology* 15.5 (2011).

[690] N. Pfister and C. Prives. “Transcriptional Regulation by Wild-Type and Cancer-Related Mutant Forms of p53”. en. In: *Cold Spring Harb Perspect Med* 7 (2017). Issue: 2.

[691] M. Scian, K. Stagliano, et al. “Tumor-derived p53 mutants induce NF-kappaB2 gene expression”. it. In: *Mol Cell Biol* 25.22 (2005), pp. 10097–10110.

[692] T. Cooks, I. Pateras, et al. “Mutant p53 Prolongs NF-κB Activation and Promotes Chronic Inflammation and Inflammation-Associated Colorectal Cancer”. en. In: *Cancer Cell* 23.5 (2013).

[693] E. Pavlakis and T. Stiewe. “p53’s Extended Reach: The Mutant p53 Secretome”. es. In: *biomolecules* 10.307 (2020).

[694] L. Weisz, A. Damalas, et al. “Mutant p53 enhances nuclear factor kappaB activation by tumor necrosis factor alpha in cancer cells”. en. In: *Cancer Res* 67.6 (2007), pp. 2396–2401.

[695] H. Rahnamoun, H. Lu, et al. “Mutant p53 shapes the enhancer landscape of cancer cells in response to chronic immune signaling”. en. In: *Nature Communications* 8 (2017).

[696] H. Solomon, N. Dinowitz, et al. “Mutant p53 gain of function underlies high expression levels of colorectal cancer stem cells markers”. en. In: *Oncogene* 37 (2018), pp. 1669–1684.

[697] C. Chen, S. Zhao, et al. “The biology and role of CD44 in cancer progression: therapeutic implications”. en. In: *J Hematol Oncol* 11.64 (2018).

[698] K. Nam, S. Oh, et al. “Ablation of CD44 induces glycolysis-to-oxidative phosphorylation transition via modulation of the c-Src-Akt-LKB1-AMPKα pathway”. en. In: *Biochem J* 473.19 (2016), pp. 3013–3030.

[699] M. Lakshman, V. Subramaniam, et al. “CD44 promotes resistance to apoptosis in human colon cancer cells”. es. In: *Exp Mol Pathol* 77.1 (2004), pp. 18–25.

[700] S. Mani, W. Guo, et al. “The epithelial-mesenchymal transition generates cells with properties of stem cells”. en. In: *Cell* 133.4 (2008), pp. 704–715.

[701] C. Mandel, Y. Bai, et al. “Protein factors in pre-mRNA 3-end processing”. it. In: *Cell Mol LifeSci* 65 (2008), pp. 1099–1122.

[702] Y. Sun, Y. Zhang, et al. “Molecular basis for the recognition of the human AAUAAA polyadenylation signal”. en. In: *PNAS* 115.7 (2018).

[703] M. Wickens and P. Stephenson. “Role of the conserved AAUAAA sequence: four AAUAAA point mutants prevent messenger RNA 3’ end formation”. fr. In: *Science* 226.4678 (1984), pp. 1045–1051.

[704] R. Wang, R. Nambia, et al. “PolyA DB 3 catalogs cleavage and polyadenylation sites identified by deep sequencing in multiple genomes”. en. In: *Nucleic Acids Res* 46.1 (2018), pp. 315–319.

[705] B. Sartini, H. Wang, et al. “Pre-messenger RNA cleavage factor I (CFIm): Potential role in alternative polyadenylation during spermatogenesis”. en. In: *Biology of Reproduction* 78 (2008), pp. 472–482.

[706] C. MacDonald. “Tissue-specific mechanisms of alternative polyadenylation: Testis, brain, and beyond”. en. In: *WIREs RNA* 10.4 (2019).

[707] W. Hong, H. Ruan, et al. "APAatlas: decoding alternative polyadenylation across human tissues". en. In: *Nucleic Acids Research* 48.1 (2020), pp. 34–39.

[708] D. Di Giammartino, K. Nishida, et al. "Mechanisms and consequences of alternative polyadenylation". en. In: *Mol Cell* 43.6 (2011), pp. 853–866.

[709] W. Filipowicz, S. Bhattacharyya, et al. "Mechanisms of post-transcriptional regulation by microRNAs: are the answers in sight?" en. In: *Nature Reviews Genetics* 9 (2008), pp. 102–114.

[710] L. Lim, N. Lau, et al. "Microarray analysis shows that some microRNAs downregulate large numbers of target mRNAs". en. In: *Nature* 433 (2005), pp. 769–773.

[711] C. Nielsen, N. Shomron, et al. "Determinants of targeting by endogenous and exogenous microRNAs and siRNAs". en. In: *RNA* 13 (2007), pp. 1894–1910.

[712] G. Macedo, I. Vieria, et al. "Rare germline variant (rs78378222) in the TP53 3' UTR: Evidence for a new mechanism of cancer predisposition in Li-Fraumeni syndrome". en. In: *Cancer Genetics* 209.3 (2016), pp. 97–106.

[713] Y. Zhao, X. Li, et al. "rs78378222 polymorphism in the 3'-untranslated region of TP53 contributes to development of age-associated cataracts by modifying microRNA-125b-induced apoptosis of lens epithelial cells". en. In: *Molecular Medicine Reports* 14.3 (2016), pp. 2305–2310.

[714] W. Liu and X. Wang. "Prediction of functional microRNA targets by integrative modeling of microRNA binding and target expression data". en. In: *Genome Biology* 20 (2019).

[715] Y. Chen and X. Wang. "miRDB: an online database for prediction of functional microRNA targets". en. In: *Nucleic Acids Res* 48 (2020), pp. 127–131.

[716] S. Baker and B. Vogelstein. "p53: a tumor suppressor hiding in plain sight". en. In: *Journal of Molecular Cell Biology* 11.7 (2019), pp. 536–538.

[717] Eldad David Shulman and Ran Elkon. "Systematic identification of functional SNPs interrupting 3'UTR polyadenylation signals". In: *PLOS Genetics* 16.8 (2020). Publisher: Public Library of Science, pp. 1–19. URL: `https://doi.org/10.1371/journal.pgen.1008977`.

[718] E. Mariella, F. Marotta, et al. "The Length of the Expressed 3 UTR Is an Intermediate Molecular Phenotype Linking Genetic Variants to Complex Diseases". en. In: *Front Genet* 10.714 (2019).

[719] Z. Mao, H. Zhao, et al. "Post-Transcriptional Dysregulation of microRNA and Alternative Polyadenylation in Colorectal Cancer". en. In: *Front Genet* 11.64 (2020).

[720] Y. Wang, X. Wu, et al. "A novel TP53 variant (rs78378222 A > C) in the polyadenylation signal is associated with increased cancer susceptibility: evidence from a meta-analysis". en. In: *Oncotarget* 7.22 (2016), pp. 32854–32865.

[721] A. Guvenek and B. Tian. "Analysis of alternative cleavage and polyadenylation in mature and differentiating neurons using RNA-seq data". en. In: *Quantitative Biology* 6 (2018), pp. 253–266.

[722] J. Van Etten, M. Nyquist, et al. "Targeting a Single Alternative Polyadenylation Site Coordinately Blocks Expression of Androgen Receptor mRNA Splice Variants in Prostate Cancer". en. In: *Cancer Res* 77.19 (2017), pp. 5228–5235.

[723] Y. Huang, Y. Wu, et al. "MicroRNA-133a-3p exerts inhibitory effects on gallbladder carcinoma via targeting RBPJ". en. In: *Am J Cancer Res* 6.11 (2016), pp. 2448–2462.

[724] L. Xue, H. Li, et al. "Inhibition of Recombining Binding Protein Suppressor of Hairless (RBPJ) Impairs the Growth of Prostate Cancer". en. In: *Cellular Physiology and Biochemistry* 36 (2015), pp. 1982–1990.

[725] C. Hurtado, A. Safarova, et al. "Disruption of NOTCH signaling by a small molecule inhibitor of the transcription factor RBPJ". en. In: *Scientific Reports* 9 (2019).

[726] C. Massard, A. Azaro, et al. "First-in-human study of LY3039478, an oral Notch signaling inhibitor in advanced or metastatic cancer". en. In: *Ann Oncol* 29.9 (2018), pp. 1911–1917.

[727] Y. Okada, D. Wu, et al. "Genetics of rheumatoid arthritis contributes to biology and drug discovery". en. In: *Nature* 506 (2014), pp. 376–381.

[728] M. Rastegar-Mojarad, Z. Ye, et al. "Opportunities for drug repositioning from phenome-wide association studies". en. In: *Nature Biotechnology* 33 (2015), pp. 342–345.

[729] D. Tweddle, A. Malcolm, et al. "Evidence for the Development of p53 Mutations after Cytotoxic Therapy in a Neuroblastoma Cell Line". en. In: *Cancer Research* 61.1 (2001).

[730] I. Sturm, A. Bosanquet, et al. "Mutation of p53 and consecutive selective drug resistance in B-CLL occurs as a consequence of prior DNA-damaging chemotherapy". en. In: *Cell Death & Differentiation* 10 (2003), pp. 477–484.

[731] C. Ok, K. Patel, et al. "TP53 mutation characteristics in therapy-related myelodysplastic syndromes and acute myeloid leukemia is similar to de novo diseases". en. In: *Journal of Hematology & Oncology* 8 (2015).

[732] B. Li, S. Brady, et al. "Therapy-induced mutations drive the genomic landscape of relapsed acute lymphoblastic leukemia". en. In: *Blood* 135.1 (2020), pp. 41–55.

[733] H. Carter, R. Marty, et al. "Interaction Landscape of Inherited Polymorphisms with Somatic Events in Cancer". en. In: *Cancer Discovery* 7.4 (2017), pp. 410–423.

[734] J. Ramroop, M. Gerber, et al. "Germline Variants Impact Somatic Events during Tumorigenesis". en. In: *Trends in Genetics* 35.7 (2019), pp. 515–526.

[735] J. Jin, X. Wu, et al. "Identification of Genetic Mutations in Cancer: Challenge and Opportunity in the New Era of Targeted Therapy". en. In: *Front Oncol* 9.263 (2019).

[736] A. Toss, F. Piacentini, et al. "Genomic alterations at the basis of treatment resistance in metastatic breast cancer: clinical applications". en. In: *Oncotarget* 9.60 (2018).

[737] S. Roberts and D. Gordenin. "Hypermutation in human cancer genomes: footprints and mechanisms". en. In: *Nature Reviews Cancer* 14.12 (2014), pp. 786–800.

[738] H. Takahashi, M. Asaoka, et al. "Biologically Aggressive Phenotype and Anti-cancer Immunity Counterbalance in Breast Cancer with High Mutation Rate". en. In: *Scientific Reports* 10 (2020).

[739] A. Lau and H. So. "Turning genome-wide association study findings into opportunities for drug repositioning". en. In: *Comput Struct Biotechnol J* 18 (2020), pp. 1639–1650.

[740] D. Duffy, G. Zhu, et al. "Novel pleiotropic risk loci for melanoma and nevus density implicate multiple biological pathways". en. In: *Nature Communications* 9 (2018).

[741] M. Rothenberg, Y. Nusse, et al. "Identification of a cKit(+) colonic crypt base secretory cell that supports Lgr5(+) stem cells in mice". en. In: *Gastroenterology* 142 (2012), pp. 1195–1205.

[742] E. Kastenhuber and S. Lowe. "Putting p53 in Context". it. In: *Cell* 170 (2017).

[743] M. Ladds and S. Lain. "Small molecule activators of the p53 response". en. In: *Journal of Molecular Cell Biology* 11.3 (2019), pp. 245–254.

[744] S. Harris and A. Levine. "The p53 pathway: positive and negative feedback loops". en. In: *Oncogene* 24 (2005), pp. 2899–2908.

[745] X. Lu, O. Ma, et al. "The Wip1 Phosphatase acts as a gatekeeper in the p53-Mdm2 autoregulatory loop". en. In: *Cancer Cell* 12.4 (2007), pp. 342–254.

[746] M. Takekawa, M. Adachi, et al. "p53-inducible wip1 phosphatase mediates a negative feedback regulation of p38 MAPK-p53 signaling in response to UV radiation". en. In: *EMBO J* 19.23 (2000), pp. 6517–6526.

[747] K. Okamoto, H. Li, et al. "Cyclin G recruits PP2A to dephosphorylate Mdm2". en. In: *Mol Cell* 9.4 (2002), pp. 761–771.

[748] E. Gordon, J. Ravicz, et al. "Cell cycle checkpoint control: The cyclin G1/Mdm2/p53 axis emerges as a strategic target for broad spectrum cancer gene therapy - A review of molecular mechanisms for oncologists". en. In: *Molecular and Clinical Oncology* 9.2 (2018), pp. 115–134.

[749] M. Konopleva, G. Martinelli, et al. "MDM2 inhibition: an important step forward in cancer therapy". en. In: *Leukemia* (2020).

[750] I. Ringshausen, C. O'Shea, et al. "Mdm2 is critically and continuously required to suppress lethal p53 activity in vivo". en. In: *Cancer Cell* 10 (2006), pp. 501–514.

[751] S. Aretz, D. Stienen, et al. "Large submicroscopic genomic APC deletions are a common cause of typical familial adenomatous polyposis". en. In: *Journal of Medical Genetics* 42 (2005), pp. 185–192.

[752] H. Zeng, A. Jorapur, et al. "Bi-allelic Loss of CDKN2A Initiates Melanoma". it. In: *Cancer Cell* 34 (2018), pp. 56–68.

[753] E. Rheinbay, M. Nielsen, et al. "Analyses of non-coding somatic drivers in 2,658 cancer whole genomes". en. In: *Nature* 578 (2020), pp. 102–111.

[754] N. Zandwijk, N. Pavlakis, et al. "Safety and activity of microRNA-loaded minicells in patients with recurrent malignant pleural mesothelioma: a first-in-man, phase 1, open-label, dose-escalation study". en. In: *Lancet Oncol* 18.10 (2017), pp. 1386–1396.

[755] F. Foss, C. Querfeld, et al. “Phase 1 trial evaluating MRG-106, a synthetic inhibitor of microRNA-155, in patients with cutaneous t-cell lymphoma (CTCL”. en. In: *Journal of Clinical Oncology* 35.15 (2017), p. 7564.

[756] I. Adzhubei, S. Schmidt, et al. “A method and server for predicting damaging missense mutations”. en. In: *Nat Methods* 7.4 (2010), pp. 248–249.

[757] B. Stranger, E. Stahl, et al. “Progress and promise of genome-wide association studies for human complex trait genetics”. fr. In: *Genetics* 187.2 (2011), pp. 367–383.

[758] S. Montgomery, O. Griffith, et al. “A survey of genomic properties for the detection of regulatory polymorphisms”. en. In: *PLoS Comput Biol* 3.6 (2007).

[759] Y. Yao, Z. Liu, et al. “CERENKOV2: improved detection of functional noncoding SNPs using data-space geometric features”. en. In: *BMC Bioinformatics* 20 (2019).

[760] GTEx Consortium. “Genetic effects on gene expression across human tissues”. en. In: *Nature* 550 (2017), pp. 204–213.

[761] A. Mizuno and Y. Okada. “Biological characterization of expression quantitative trait loci (eQTLs) showing tissue-specific opposite directional effects”. en. In: *European Journal of Human Genetics* 27 (2019), pp. 1745–1756.

[762] B. Fairfax, P. Humburg, et al. “Innate immune activity conditions the effect of regulatory variants upon monocyte gene expression”. en. In: *Science* 343.6175 (2014).

[763] C. Yao, R. Joehanes, et al. “Sex- and age-interacting eQTLs in human complex diseases”. en. In: *Hum Mol Genet* 23.7 (2014), pp. 1947–1956.

[764] A. Buli, A. Brown, et al. “Gene-gene and gene-environment interactions detected by transcriptome sequence analysis in twins”. en. In: *Nat Genet* 47.1 (2015), pp. 88–91.

[765] J. Bryois, A. Buli, et al. “Time-dependent genetic effects on gene expression implicate aging processes”. en. In: *Genome Res* 27.4 (2017), pp. 545–552.

[766] N. Thomas, S. Edmiston, et al. “Inherited Genetic Variants Associated with Melanoma BRAF/NRAS Subtypes”. en. In: *J Invest Dermatol* 138.11 (2018), pp. 2398–2404.

[767] K. Crews, J. Hicks, et al. “Pharmacogenomics and individualized medicine: Translating science into practice”. en. In: *Clin Pharmacol Ther* 92.4 (2012), pp. 467–475.

[768] M. Lolkema, C. Gadellaa-van Hooijdonk, et al. “Ethical, Legal, and Counseling Challenges Surrounding the Return of Genetic Results in Oncology”. en. In: *Journal of Clinical Oncology* (2013).

[769] R. Altman. “Direct-to-consumer genetic testing: failure is not an option”. en. In: *Clin Pharmacol Ther* 86.1 (2009), pp. 15–17.

[770] A. Beaudet. “Ethical issues raised by common copy number variants and single nucleotide polymorphisms of certain and uncertain significance in general medical practice”. en. In: *Genome Med* 2.7 (2010), p. 42.

[771] G. Braverman, Z. Shapiro, et al. “Ethical Issues in Contemporary Clinical Genetics”. en. In: *Mayo Clin Proc Innov Qual Outcomes* 2.2 (2018), pp. 81–90.

[772] M. Kanehisa and S. Goto. “KEGG: Kyoto Encyclopedia of Genes and Genomes”. es. In: *Nucleic Acids Res* 28 (2000), pp. 27–30.

[773] D. Nishimura. “Biocarta”. de. In: *Biotech Software & Internet Report* 2.3 (2000).

[774] P. Thomas, M. Campbell, et al. “PANTHER: a library of protein families and subfamilies indexed by function”. en. In: *Genome Res* 13 (2003), pp. 2129–2141.

[775] Y. Liao, G. Smyth, et al. “featureCounts: an efficient general purpose program for assigning sequence reads to genomic features”. en. In: *Bioinformatics* 30.7 (2014), pp. 923–930.

[776] D. Kim, B. Langmead, et al. “HISAT: a fast spliced aligner with low memory requirements”. en. In: *Nature Methods* (2015).

[777] M. Robinson, D. McCarthy, et al. “edgeR: a Bioconductor package for differential expression analysis of digital gene expression data”. en. In: *Bioinformatics* 26.1 (2010), pp. 139–140.

[778] S. Davis, P. Charles, et al. “Expanding Proteome Coverage with CHarge Ordered Parallel Ion aNalysis (CHOPIN) Combined with Broad Specificity Proteolysis”. en. In: *J. Proteome Res* 16.3 (2017), pp. 1288–1299.

[779] S. Tyanova, T. Temu, et al. “The MaxQuant computational platform for mass spectrometry-based shotgun proteomics”. en. In: *Nature Protocols* 11 (2016), pp. 2301–2319.

[780] M. Ritchie, B. Phipson, et al. “limma powers differential expression analyses for RNA-sequencing and microarray studies”. en. In: *Nucleic Acids Research* 43.7 (2015).

[781] A. Liberzon, C. Birger, et al. “The Molecular Signatures Database (MSigDB) hallmark gene set collection”. en. In: *Cell Syst* 1.6 (2015), pp. 417–425.

[782] A. Colapeico, T. Silva, et al. “TCGAbiolinks: An R/Bioconductor package for integrative analysis of TCGA data”. en. In: *Nucleic Acids Research* (2015).

[783] C. Mermel, S. Schumacher, et al. “GISTIC2.0 facilitates sensitive and confident localization of the targets of focal somatic copy-number alteration in human cancers”. en. In: *Genome Biol* 12.4 (2011).

[784] J. Liu, T. Lichtenberg, et al. “An Integrated TCGA Pan-Cancer Clinical Data Resource to Drive High-Quality Survival Outcome Analytics”. en. In: *Cell* 173.2 (2018), pp. 400–416.

[785] S. Lopez, L. Lim, et al. “Interplay between whole-genome doubling and the accumulation of deleterious alterations in cancer evolution”. en. In: *Nature Genetics* 52 (2020), pp. 283–293.

[786] J. Korn, F. Kuruvilla, et al. “Integrated genotype calling and association analysis of SNPs, common copy number polymorphisms and rare CNVs”. en. In: *Nature Genetics* 40.10 (2008), pp. 1253–1260.

[787] S. Das, L. Forer, et al. “Next-generation genotype imputation service and methods”. en. In: *Nature Genetics* 48.10 (2016), pp. 1284–1287.

[788] B. Zhang and S. Horvath. "A General Framework for Weighted Gene Co-Expression Network Analysis". en. In: *Statistical Applications in Genetics and Molecular Biology* 4.1 (2005).

[789] P. Langfelder and S. Horvath. "WGCNA: an R package for weighted correlation network analysis". et. In: *BMC Bioinformatics* 9.559 (2008).

[790] D. Szklarczyk, A. Gable, et al. "STRING v11: protein-protein association networks with increased coverage, supporting functional discovery in genome-wide experimental datasets". en. In: *Nucleic Acids Res* 47 (2019), pp. 607–613.

[791] C. Mering, L. Jensen, et al. "STRING: known and predicted protein–protein associations, integrated and transferred across organisms". en. In: *Nucleic Acids Research* 33 (2005), pp. 433–437.

[792] R.Core Team. *R: A language and environment for statistical computing*. Vienna, 2020.

[793] T. Chou. "Theoretical basis, experimental design, and computerized simulation of synergism and antagonism in drug combination studies". en. In: *Pharmacol Rev* 58.3 (2006), pp. 621–681.

[794] P. Zhang, S. Elabd, et al. "TRIM25 has a duel function in the p53/MDM2 circuit". en. In: *Oncogene* 34.46 (2015), pp. 5729–5738.

[795] N. Ke, X. Wang, et al. "The xCELLigence system for real-time and label-free montoring of cell viability". en. In: *Methods in Molecular Biology* 740 (2011), pp. 33–43.

[796] C. Schneider, W. Rasband, et al. "NIH Image to ImageJ: 25 years of image analysis". en. In: *Nature Method* 9.7 (2012), pp. 671–675.

[797] F. Ma, B. Fuqua, et al. "A comparison between whole transcript and 3' RNA sequencing methods using Kapa and Lexogen library preparation methods". en. In: *BMC Genomics* 20 (2019).

[798] Y. Chen, A. Lun, et al. "From reads to genes to pathways: differential expression analysis of RNA-Seq experiments using Rsubread and the edgeR quasi-likelihood pipeline". en. In: *F1000Research* 5.1438 (2016).

[799] M. Robinson and A. Oshlack. "A scaling normalization method for differential expression analysis of RNA-seq data". en. In: *Genome Biology* (2010), p. 11.

[800] B. Phipsom, S. Lee, et al. "Robust hyperparameter estimation protects against hypervariable genes and improves power to detect differential expression". en. In: *Annals of Applied Statistics* 10 (2016), pp. 946–963.

[801] A. Lun, Y. Chen, et al. "It's DE-licious: a recipe for differential expression analyses of RNA-seq experiments using quasi-likelihood methods in edgeR". en. In: *Methods in Molecular Biology* 1418 (2016), pp. 391–416.